



UNIVERSIDADE FEDERAL DE MINAS GERAIS
INSTITUTO DE CIÊNCIAS EXATAS
PROGRAMA DE PÓS-GRADUAÇÃO EM QUÍMICA

GUILHERME AUGUSTO DE MELO JARDIM

**“OVERCOMING QUINONE DEACTIVATION: RHODIUM
CATALYSED C-H ACTIVATION AS A NEW GATEWAY FOR
POTENT TRYPANOCIDAL PROTOTYPES”**

BELO HORIZONTE
2018



UFMG/ICE_x/DQ. 1288^a
T. 583^a

Guilherme Augusto de Melo Jardim

**“OVERCOMING QUINONE DEACTIVATION: RHODIUM
CATALYSED C-H ACTIVATION AS A NEW GATEWAY FOR
POTENT TRYPANOCIDAL PROTOTYPES”**

Thesis presented to the
Department of Chemistry of the
Institute of Exact Sciences of the
Federal University of Minas
Gerais as a partial fulfillment for
the degree of Doctor of
Chemistry - Organic Chemistry.

Professor Adviser:

Professor Dr. Eufrânio Nunes da Silva Júnior

Belo Horizonte

2018

J371o Jardim, Guilherme Augusto de Melo.
2018 Overcoming quinone deactivation [manuscrito]: Rhodium
T Catalysed C-H activation as a new gateway for potent
trypanocidal prototypes / Guilherme Augusto de Melo
Jardim. 2018.
xxi , 222 f.: il.

Orientador: Eufrânio Nunes da Silva Júnior

Tese (doutorado) - Universidade Federal de Minas
Gerais - Departamento de Química.

1. Química orgânica - Teses 2 Quinonas- Teses
3.Catalisadores de metais de transição. 4.Chagas,
doença de - Teses I. Silva Junior, Eufrânio Nunes de
Orientador II. Título

CDU 043

UFMG

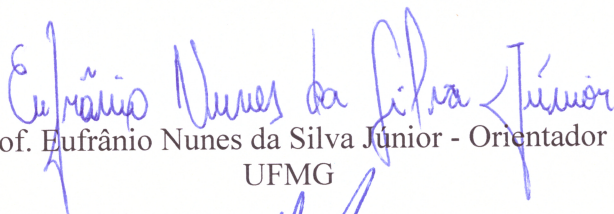
Programa de Pós-Graduação em Química
Departamento de Química - ICEX



"Overcoming Quinone Deactivation: Rhodium Catalysed C-H Activation as a New Gateway for Potent Trypanocidal Prototypes"

Guilherme Augusto de Melo Jardim

Tese aprovada pela banca examinadora constituída pelos Professores:


Prof. Eufrânio Nunes da Silva Júnior - Orientador
UFMG


Prof. Helio Gauze Bonacorso
UFSM


Prof. José Augusto Ferreira Perez Villar
UFSJ


Prof. José Dias de Souza Filho
UFMG


Prof. Adão Aparecido Sabino
UFMG

Belo Horizonte, 20 de julho de 2018.



Instituto de Ciências Exatas – DQ UFMG
PhD Thesis - Guilherme A. M. Jardim
Quote

“There is no substitute
for hard work.”

Thomas Edison



ACKNOWLEDGMENTS

To my family, my parents Fernando Antônio Jardim and Maria José Jardim and to my sister Barbara, for all the love and encouragement to be a better human being.

To Giovana, my flower, for love, support and patience.

To Professor Eufrânio Nunes da Silva Júnior, for friendship, guidance and patience.

To Professor John Bower, for receiving me in Bristol and for the wonderful opportunity.

To all the friends and co-workers of the Laboratory of Synthetic and Heterocyclic Chemistry, for all good work and assistance in the development of my research.

To all the friends and co-workers of the Bower Research Group, for receiving me as an equal and helping me to walk the path of synthetic chemistry.

To my dear friends Niall McCreanor, Giacomo Crisenza and Hugo Campello, the “Chavales” for such a good friendship, amazing times in the old World and in Brazil carnival. Our paths will meet again in the world of Chemistry.

To all members and ex-members of “Wednesday's football chemistry”, and by all liters of "barrigudinha 3x10" that we consumed together in the past years.

To Professor Luiz Cláudio Almeida Barbosa and his research group, for the friendship, support with reagents and guidance.

To Professoras Rosemeire Brondi and Rossimiriam Freitas and their respective research groups, for all support with reagents and guidance.



To all students and professors of the Department of Chemistry for all the help, and also for the high amount of reactants provided. There is a little bit of each one of you in this work.

To professors Solange de Castro and Rubem F. S. Menna-Barreto of FIOCRUZ, for the exceptional work with the biological assays.

To professor Willian Xerxes, Professor Carlos Simone, Dr. Hazel Sparkes and Dr Natalie Pridmore, for the exquisite work in X-ray crystallography. This work is much more beautiful because of you all.

To all technicians of University of Bristol Mass Spectrometry Facility and the Analytical Center of USP for the amazing work with mass spectrometry analysis.

To Professor Ricardo Alves and his student Flaviano "Valdivia" Ottoni for the help in the acquisition of infrared spectra.

To professors Jarbas Magalhães Resende and José Dias da Souza Filho, Dr. Ivana Silva Lula from the Department of Chemistry - UFMG and all technicians of the NMR facilities in School of Chemistry-University of Bristol, for the flawless work in NMR.

To all professors that evaluated this work, for helping me in the corrections and providing support.

To professor David Boothman from University of Texas, for the gently donation of deuterated benzoquinone.

To CAPES, CNPQ and the Science without Borders program, for financial support and for the opportunity to work in England.



ABSTRACT

The following manuscript encompasses all efforts in the development of a methodology that aims for the direct functionalization of the benzenoid and dicarbonyl ring of 1,4-naphthoquinones, referred to as *A-ring* and *B-ring*, respectively, via rhodium catalysed C-H activation-functionalization, and all other reactions that have been discovered during the research process. In a first approach, optimization studies were carried out to define the best reactional conditions for C5 and C2-halogenation, followed by the appliance of the optimized methodology in different naphthoquinoidal substrates. In a second part, the recently discovered C-2 halogenation/phenyl selenylation protocol was explored and the new methodology applied to a wide range of 1,4-benzoquinones. The C5-halogenation process opened way for new modifications in the *A-ring*, such as palladium cross-coupling and copper-catalysed organoyl-thiolation reactions. Finally, all new compounds were evaluated against *Trypanosoma cruzi* trypomastigote forms, with the majority of them presenting remarkable bioactivity.

Keywords: Quinones, C-H Activation, Transition Metal Catalysis, Deactivated Systems, *Trypanosoma cruzi*, Chagas Disease.



TABLE OF CONTENTS

Abstract.....	vi
Table of Contents	vii
List of abbreviations and acronyms.....	ix
List of tables	xiii
Schematics List.....	xiv
Figures List.....	xvii
1. Introduction	1
1.1. Quinones: Natural Occurrence.....	1
1.2. The Role of Quinones in Chagas Disease Therapy	9
1.3. Metal Catalyzed C-H Bond Activation.....	18
2. Motivation	29
3. Proposed Strategy	33
4. Objectives	37
4.1. General Objective	37
4.2. Specific Objectives	37
5. Results and Discussion	38
5.1. Development of a C-H Functionalization Protocol	38
5.2. Exploring Functionalization at C-2 Position.....	58
5.3. Development of Functionalization Reactions Involving the C-I bond of the Novel Quinones	67
5.3.1. Palladium Catalyzed Cross-Coupling Reactions.....	67
5.3.2. Copper Catalyzed Organoyl-Thiolation Reactions.....	70
5.4. Biological Assays.....	79
6. Conclusion	88
7. Experimental data.....	90
7.1. General experimental details.....	90
7.2. General Procedure for <i>in situ</i> Yield Analysis	91
7.3. Synthesis of Substrates and Known Compounds.....	91
7.3.1. Synthesis of Substituted Cpx Ligands.....	92
7.3.2. Synthesis of $[\text{RhCp}^{*i\text{-Pr}}\text{Cl}_2]_2$, $[\text{RhCp}^{*\text{Cy}}\text{Cl}_2]_2$ and $[\text{RhCp}^{*\text{CF}_3}\text{Cl}_2]_2$	93



UFMG

7.3.3. Synthesis of $[\text{RhCp}^*(\text{OAc})_2(\text{H}_2\text{O})]$	95
7.3.4. Synthesis of Quinoidal Substrates	96
7.4. Procedures for the Synthesis of Novel Derivatives	109
7.4.1. General Microwave Procedure for the Halogenation reactions	109
7.4.2. General Procedure for Halogenation/Selenylation at the C2-Position.....	121
7.4.3. Intermolecular Competition Experiment.....	132
7.4.4. Procedures for Cross-Coupling Reactions	133
7.4.5. Procedures for Organoyl-Thiolation and Oxidation reactions	137
7.5. Trypanocidal and Cytotoxicity Assays	152
7.5.1. Trypanocidal Assays for Halogenated/Selenylated Quinoidal Compounds	152
7.5.2. Cytotoxicity Assays for Halogenated/Selenylated Quinoidal Compounds.....	153
7.5.3. Trypanocidal Assays for Thiolated Quinoidal Compounds	154
7.5.4. Cytotoxicity Assays for Thiolated Quinoidal Compounds	154
7.6. Crystallographic Data Collection and Refinement	154
7.7. ^1H and ^{13}C NMR Spectra of Novel Compound	157

LIST OF ABBREVIATIONS AND ACRONYMS

ATP	adenosine triphosphate
IC ₅₀	half maximal inhibitory concentration
MIC	minimum inhibitory concentration
<i>T. cruzi</i>	<i>Trypanosoma cruzi</i>
IgG	immunoglobulin G
ROS	reactive oxygen species
DNA	deoxyribonucleic acid
SET	single electron transfer
E.A.C.	Ehrlich ascites carcinoma
DG	directing group
FG	functional group
CT	charge transfer
σ (C-H)	sigma carbon-hydrogen bond orbital
$d\sigma$	sigma bond d orbital
σ^*	sigma anti-bond orbital
CMD	concerted metalation-deprotonation
S _e Ar	electrophilic aromatic substitution
Rh ^{II}	rhodium (II)
σ -CAM	σ -complex-assisted metathesis
Rh ^{III} Cp* ₅	rhodium (III) pentamethylcyclopentadienyl
DCE	1,2-dichloroethane
HFIP	hexafluoro-2-propanol
TEMPO	(2,2,6,6-Tetramethylpiperidin-1-yl)oxyl
DFT	density functional theory
N-Ac-L-iso	(2S,3S)-2-acetamido-3-methylpentanoic acid
DMF	dimethyl formamide
<i>t</i> -BuOK	potassium <i>tert</i> -butoxide
<i>t</i> -BuOH	<i>tert</i> -butanol
TBAB	tetrabutylammonium bromide
μ M	micro molar



LC ₅₀	median lethal dose
NIS	<i>N</i> -iodosuccinimide
DIH	3,3-dimethyl- <i>N</i> -diiodo-hydantoin
NISac	<i>N</i> -iodosacharin
TolSO ₂ I	4-methylbenzenesulfonyl iodide
M	molar
NMR	Nuclear Magnetic Resonance
Cu(PivO) ₂	copper pivalate
DBH	3,3-dimethyl- <i>N</i> -bromo-hidantoin
Phta-Se-Ph	<i>N</i> -(phenylselenyl)phthalimide
DCH	3,3-dimethyl- <i>N</i> -dichloro-hidantoin
Phta-S-Ph	<i>N</i> -(phenylthio)phthalimide
W	Watts
NBS	<i>N</i> -bromosuccinimide
KIE	kinect isotope effect
THF	tetrahydrofuran
DMAc	dimethyl acetamide
DMSO	dimethyl sulfoxide
Cy ₂ NMe	<i>N,N</i> -Dicyclohexylmethylamine
TBAC	tetrabutylammonium chloride
SAR	structure-activity relation
CuTc	copper(I)-thiophene-2-carboxylate
TLC	thin layer chromatography
MCPA	<i>meta</i> -chloroperoxybenzoic acid
Bpy	2,2'-bipyridine
SI	selectivity index
FCC	flash column chromatography
MHz	mega Hertz
ppm	parts per million
<i>J</i>	coupling constant (Hz)
Hz	Hertz



δ	chemical shift
d	doublet
dd	double doublet
m	multiplet
q	quartet
s	singlet
t	triplet
bs	broad singlet
dt	double triplet
hept	heptet
2D	two-dimensional
DEPT135	distortionless enhancement by polarization transfer
COSY	homonuclear correlation spectroscopy spectroscopy
HMBC	heteronuclear multiple bond correlation
HSQC	heteronuclear single quantum coherence spectroscopy
1,4-DNB	1,4-dinitrobenzene
Li	lithium
Ts-OH	<i>p</i> -toluenesulfonic acid
Ms-OH	methanesulfonic acid
DDQ	2,3-Dichloro-5,6-dicyano-1,4-benzoquinone
CAN	cerium ammonium nitrate
^1H	hydrogen
^{13}C	carbon 13
I.R.	infrared spectroscopy
ν	wave number
m.p.	melting point
HRMS	high resolution mass spectrometry
EI	electronic ionization
(+) - ESI	electrospray ionization (positive mode)



Instituto de Ciências Exatas - DQ UFMG
PhD Thesis – Guilherme A. M. Jardim
List of Abbreviations and Acronyms



LIST OF TABLES

Table 1. Solvent screening.....	40
Table 2: Iodine sources investigation	41
Table 3: Variations in time, concentration and temperature.....	42
Table 4: Catalyst screening.....	44
Table 5: Salts screening	45
Table 6: Microwave optimization conditions	48
Table 7: Optimization results.....	60
Table 8: Selected optimization results.....	72
Table 9: Activity of synthetic derivatives against bloodstream trypomastigotes of <i>T. cruzi</i> (Y strain) at 37 °C and no blood, cytotoxicity to mammalian cells and Selectivity Index (SI).....	79
Table 10. Activity of synthetic derivatives against bloodstream trypomastigotes of <i>T. cruzi</i> (Y strain) at 4 °C and 5% blood	85
Table 11. Activity of synthetic thio-derivatives against bloodstream trypomastigotes of <i>T. cruzi</i> (Y strain) at 37 °C and no blood, cytotoxicity to mammalian cells and Selectivity Index (SI).....	87



SCHEMATICS LIST

Scheme 1. The bombardier beetle and its defence mechanism.....	3
Scheme 2. Schematic representation of <i>p</i> -quinone metabolism, redox cycling and production of reactive species	15
Scheme 3. Ipê tree, lapachol (1), β -lapachone (28) and α -lapachone (29), synthesis and conversion.....	16
Scheme 4. General scheme for metal catalysed C-H bond activation reactions.....	19
Scheme 5. Historical background of metal catalyzed C-H bond activation reactions.....	20
Scheme 6. Murai pioneer work and catalytic cycle investigated by Morokuma.	21
Scheme 7. Frontier orbitals interactions for electrophilic (left) and nucleophilic (right) mechanisms.	23
Scheme 8. Concerted metalation-deprotonation (CMD) pathway.....	23
Scheme 9. Electrophilic aromatic substitution ($S_{\text{E}}\text{Ar}$) pathway.....	24
Scheme 10. σ -complex-assisted metathesis (σ -CAM) pathway.	24
Scheme 11. Rhodium catalyzed double <i>ortho</i> -functionalization of phenols by Zhou and Zhu.....	25
Scheme 12. Palladium catalyzed ligand-accelerated non-directed C–H activation by Yu and co-workers.	26
Scheme 13. Ruthenium(II)-catalyzed C-H <i>para</i> -difluoromethylation of ketoximes.....	27
Scheme 14. Palladium-catalyzed tandem C–H activation/dual C–N bond formation.....	27
Scheme 15. Synthesis of 2-benzazepines via rhodium(III) C-H activation.	28
Scheme 16. Rh(III)-catalyzed cascade annulations and rosettacin (46) total synthesis.....	28
Scheme 17. A-ring construction strategy by Ji (17a) and Gao (17b) groups.....	30
Scheme 18. Oxidation strategy by Li (18a) and Zeng (18b) groups.....	31
Scheme 19. A-ring functionalization strategy by Shvartsberg and co-workers.....	31
Scheme 20. Simple modifications in juglone leading to compounds with potent trypanocidal activity. * $\text{IC}_{50}/24$ h values for the lytic activity on bloodstream trypomastigotes.....	32
Scheme 21. Strategy for the achievement of A-ring substituted naphthoquinones.	33
Scheme 22. Functionalization strategy used by Zhang and co-workers	34
Scheme 23. Deuterium labelling experiments by Zhang and co-workers.	35



Scheme 24. Equilibrium between 1,4-naphthoquinone and the metalated specie.	35
Scheme 25. Strategies for the synthesis of novel trypanocidal naphthoquinones and benzoquinones.	36
Scheme 26. Preliminary results.	38
Scheme 27. Combination of both reactions (Glorius and Chang).	39
Scheme 28. Synthesis of the $\text{Rh}^{\text{III}}\text{Cp}^{\text{X}}$ complexes.	43
Scheme 29. Synthesis of $[\text{RhCp}^{*\text{Cy}}\text{Cl}_2]_2$	43
Scheme 30. Synthesis of $[\text{RhCp}^*(\text{OAc})_2\text{H}_2\text{O}]$	44
Scheme 31. Final results for functionalization at position 2 and crystal structure of 74	46
Scheme 32. Results for functionalization at position 2 with an unsymmetrical substrate. .	46
Scheme 33. Derivatization experiments with unsymmetrical substrates 76 - 79	49
Scheme 34. Derivatization experiments with juglone (15)	50
Scheme 35. Derivatization experiments with 86 - 88	51
Scheme 36. Derivatization experiments with 48, 92 and 93	52
Scheme 37. Derivatization experiments with 57 and 59	53
Scheme 38. Further results for additional functionalization of the A-ring at position 5	54
Scheme 39. Possible activation of NIS by Cu^{2+} coordination.	55
Scheme 40. Concerted metalation-deprotonation pathway described by Jones et. al.	56
Scheme 41. Proposed mechanism governed by concerted metalation-deprotonation pathway.	57
Scheme 42. Proposed mechanism governed by electrophilic aromatic substitution.	57
Scheme 43. General hypothesis for the functionalization of 1,4-benzoquinones	59
Scheme 44. Preliminary results.	59
Scheme 45. Use of another electrophile sources.	60
Scheme 46. Use of electron-rich substrates	61
Scheme 47. Reaction with unsymmetrical substrate 117	62
Scheme 48. Reaction with unsymmetrical substrate 121	62
Scheme 49. Reactions with substrate 127	63
Scheme 50. Reaction with electron-deficient substrate 131	63
Scheme 51. KIE intermolecular competition experiment.	64
Scheme 52. Proposed mechanism governed by σ -complex-assisted metathesis pathway. .	66



Scheme 53. Unsuccessful attempts to achieve Suzuki coupling.....	68
Scheme 54. Optimization and best conditions for Stille coupling.....	69
Scheme 55. Heck cross-couplings and reaction with phenylethynylcuprate(I).....	70
Scheme 56. Initial result for the copper catalysed trifluoromethylthiolation reactions.....	71
Scheme 57. Results for reaction with substrates 80 , 97 and 89	73
Scheme 58. Experiments with substrate 81	73
Scheme 59. Experiments with substrates 64 , 90 , 100 and 144	74
Scheme 60. Oxidation reactions.....	75
Scheme 61. General reaction for benzyl, alkyl and aryl derivatives.....	75
Scheme 62. Benzyl, alkyl and aryl derivatives 152 – 157	76
Scheme 63. Oxidation reactions with substrate 158	76
Scheme 64. Inhibition experiments with TEMPO and its derivatives.....	77
Scheme 65. Experiments with the presence and absence of Cu and Ag.....	77
Scheme 66. Experiments with the presence and absence of Cu and Ag.....	78
Scheme 67. Proposed mechanism for organoyl-thiolation reaction.....	78
Scheme 68. Modifications of 56 leading to more potent and selective derivatives.....	88

TABLE OF FIGURES

Figure 1. The quinone “backbone” present in several natural products	1
Figure 2. Ubiquinone (6)	2
Figure 3. Primin (9) and 3-libocedroxythymoquinone (10)	3
Figure 4. Avarone (11) and sarubicin A (12)	4
Figure 5. Quinolidomicin A ₁ (13).....	5
Figure 6. Lawsone (14), juglone (15), pumblagin (16) and isopumblagin (17).	6
Figure 7. 3-chloroplumbagin (18), 3-bromoplumbagin (19), marinone (20) and debromomarinone (21).	7
Figure 8. Alkannin (22) and shikonin (23).	8
Figure 9. 5-methoxy-3,4- dehydroxanthomegnin (24)	9
Figure 10. Kissing bug, <i>T. cruzi</i> (trypomastigote), and the purplish swelling symptom....	10
Figure 11. Chagas disease life cycle.....	12
Figure 12. benznidazole (25), nifurtimox (26) and crystal violet (27)	13
Figure 13. Purpurin (30), (-)-2,3,3-trimethyl-2-3-dihydronaphtho[2,3- <i>b</i>]furan-4,9-quinone (31) and 7-epiclusianone (32).....	17
Figure 14. Diospyrin (33) and derivatives (34) and (35).....	17
Figure 15. Dracocephalone (36) and komaroviquinone (37).....	18
Figure 16: Iodine sources and crystal structure of 62.....	41
Figure 17: ¹ H NMR spectra (400 MHz, CDCl ₃) and deuterium NMR spectra (400 MHz, CHCl ₃) for determination of the 108/ <i>d</i> ₃ -108 ratio	65
Figure 18. Crystal structures of compounds 152, 155 and 156	76
Figure 19: Re-sealable reaction tube and microwave apparatus	110
Figure 20. ¹ H NMR spectrum (400 MHz, CDCl ₃) of compound 60	157
Figure 21. ¹³ C NMR spectrum (100 MHz, CDCl ₃) of compound 60	157
Figure 22. ¹ H NMR spectrum (400 MHz, CDCl ₃) of compound 61.	158
Figure 23. ¹³ C NMR spectrum (100 MHz, CDCl ₃) of compound 61	158
Figure 24. ¹ H NMR spectrum (400 MHz, CDCl ₃) of compound 62	159
Figure 25. ¹³ C NMR spectrum (100 MHz, CDCl ₃) of compound 62.....	159
Figure 26. ¹ H NMR spectrum (400 MHz, CDCl ₃) of compound 74.....	160
Figure 27. ¹³ C NMR spectrum (100 MHz, CDCl ₃) of compound 74.....	160



UFMG

Figure 28.	^1H NMR spectrum (400 MHz, CDCl_3) of compound 77	161
Figure 29.	^{13}C NMR spectrum (100 MHz, CDCl_3) of compound 77	161
Figure 30.	^1H NMR spectrum (400 MHz, CDCl_3) of compound 80	162
Figure 31.	^{13}C NMR spectrum (100 MHz, CDCl_3) of compound 80	162
Figure 32.	^1H NMR spectrum (500 MHz, CDCl_3) of compound 80'	163
Figure 33.	^{13}C NMR spectrum (125 MHz, CDCl_3) of compound 80'	163
Figure 34.	^1H NMR spectrum (400 MHz, CDCl_3) of compound 81	164
Figure 35.	^{13}C NMR spectrum (100 MHz, CDCl_3) of compound 81	164
Figure 36.	^1H NMR spectrum (400 MHz, CDCl_3) of compound 82	165
Figure 37.	^{13}C NMR spectrum (100 MHz, CDCl_3) of compound 82	165
Figure 38.	^1H NMR spectrum (500 MHz, CDCl_3) of compound 82'	166
Figure 39.	^{13}C NMR spectrum (125 MHz, CDCl_3) of compound 82'	166
Figure 40.	^1H NMR spectrum (400 MHz, CDCl_3) of compound 83	167
Figure 41.	^{13}C NMR spectrum (100 MHz, CDCl_3) of compound 83	167
Figure 42.	^1H NMR spectrum (500 MHz, CDCl_3) of compound 84	168
Figure 43.	^{13}C NMR spectrum (125 MHz, CDCl_3) of compound 84	168
Figure 44.	^1H NMR spectrum (400 MHz, CDCl_3) of compound 89	169
Figure 45.	^{13}C NMR spectrum (100 MHz, CDCl_3) of compound 89	169
Figure 46.	^1H NMR spectrum (400 MHz, CDCl_3) of compound 90	170
Figure 47.	^{13}C NMR spectrum (100 MHz, CDCl_3) of compound 90	170
Figure 48.	^1H NMR spectrum (400 MHz, CDCl_3) of compound 91	171
Figure 49.	^{13}C NMR spectrum (100 MHz, CDCl_3) of compound 91	171
Figure 50.	^1H NMR spectrum (500 MHz, CDCl_3) of compound 94	172
Figure 51.	^{13}C NMR spectrum (125 MHz, CDCl_3) of compound 94	172
Figure 52.	^1H NMR spectrum (500 MHz, CDCl_3) of compound 95	173
Figure 53.	^{13}C NMR spectrum (125 MHz, CDCl_3) of compound 95	173
Figure 54.	^1H NMR spectrum (400 MHz, CDCl_3) of compound 96	174
Figure 55.	^{13}C NMR spectrum (100 MHz, CDCl_3) of compound 96	174
Figure 56.	^1H NMR spectrum (500 MHz, CDCl_3) of compound 97	175
Figure 57.	^{13}C NMR spectrum (125 MHz, CDCl_3) of compound 97	175
Figure 58.	^1H NMR spectrum (400 MHz, CDCl_3) of compound 98	176
Figure 59.	^{13}C NMR spectrum (100 MHz, CDCl_3) of compound 98	176



UFMG

Figure 60.	^1H NMR spectrum (400 MHz, CDCl_3) of compound 100	177
Figure 61.	^{13}C NMR spectrum (100 MHz, CDCl_3) of compound 100	177
Figure 62.	^1H NMR spectrum (400 MHz, CDCl_3) of compound 101	178
Figure 63.	^{13}C NMR spectrum (100 MHz, CDCl_3) of compound 101	178
Figure 64.	^1H NMR spectrum (400 MHz, CDCl_3) of compound 102	179
Figure 65.	^{13}C NMR spectrum (100 MHz, CDCl_3) of compound 102	179
Figure 66.	^1H NMR spectrum (400 MHz, CDCl_3) of compound 107	180
Figure 67.	^{13}C NMR spectrum (100 MHz, CDCl_3) of compound 107	180
Figure 68.	^1H NMR spectrum (400 MHz, CDCl_3) of compound 108	181
Figure 69.	^{13}C NMR spectrum (100 MHz, CDCl_3) of compound 108	181
Figure 70.	^1H NMR spectrum (400 MHz, CDCl_3) of compound 109	182
Figure 71.	^{13}C NMR spectrum (100 MHz, CDCl_3) of compound 109	182
Figure 72.	^1H NMR spectrum (400 MHz, CDCl_3) of compound 110	183
Figure 73.	^{13}C NMR spectrum (100 MHz, CDCl_3) of compound 110	183
Figure 74.	^1H NMR spectrum (400 MHz, CDCl_3) of compound 111	184
Figure 75.	^{13}C NMR spectrum (100 MHz, CDCl_3) of compound 111	184
Figure 76.	^1H NMR spectrum (400 MHz, CDCl_3) of compound 114	185
Figure 77.	^{13}C NMR spectrum (100 MHz, CDCl_3) of compound 114	185
Figure 78.	^1H NMR spectrum (400 MHz, CDCl_3) of compound 115	186
Figure 79.	^{13}C NMR spectrum (100 MHz, CDCl_3) of compound 115	186
Figure 80.	^1H NMR spectrum (400 MHz, CDCl_3) of compound 116	187
Figure 81.	^{13}C NMR spectrum (100 MHz, CDCl_3) of compound 116	187
Figure 82.	^1H NMR spectrum (400 MHz, CDCl_3) of compounds 118 and 119	188
Figure 83.	^{13}C NMR spectrum (100 MHz, CDCl_3) of compound 118 and 119	188
Figure 84.	^1H NMR spectrum (400 MHz, CDCl_3) of compound 120	189
Figure 85.	^{13}C NMR spectrum (100 MHz, CDCl_3) of compound 120	189
Figure 86.	^1H NMR spectrum (400 MHz, CDCl_3) of compound 122	190
Figure 87.	^{13}C NMR spectrum (100 MHz, CDCl_3) of compound 122	190
Figure 88.	^1H NMR spectrum (400 MHz, CDCl_3) of compound 123	191
Figure 89.	^{13}C NMR spectrum (100 MHz, CDCl_3) of compound 123	191
Figure 90.	^1H NMR spectrum (400 MHz, CDCl_3) of compounds 124 and 125	192
Figure 91.	^{13}C NMR spectrum (100 MHz, CDCl_3) of compounds 124 and 125	192



UFMG

Figure 92. ^1H NMR spectrum (400 MHz, CDCl_3) of compound 126	193
Figure 93. ^{13}C NMR spectrum (100 MHz, CDCl_3) of compound 126	193
Figure 94. ^1H NMR spectrum (400 MHz, CDCl_3) of compound 128	194
Figure 95. ^{13}C NMR spectrum (100 MHz, CDCl_3) of compound 128	194
Figure 96. ^1H NMR spectrum (400 MHz, CDCl_3) of compound 130	195
Figure 97. ^{13}C NMR spectrum (100 MHz, CDCl_3) of compound 130	195
Figure 98. ^1H NMR spectrum (400 MHz, CDCl_3) of compound 132	196
Figure 99. ^{13}C NMR spectrum (100 MHz, CDCl_3) of compound 132	196
Figure 100. ^1H NMR spectrum (400 MHz, CDCl_3) of compound 133	197
Figure 101. ^{13}C NMR spectrum (100 MHz, CDCl_3) of compound 133	197
Figure 102. ^1H NMR spectrum (400 MHz, CDCl_3) of compound 134	198
Figure 103. ^{13}C NMR spectrum (100 MHz, CDCl_3) of compound 134	198
Figure 104. ^1H NMR spectrum (400 MHz, CDCl_3) of compound 135	199
Figure 105. ^{13}C NMR spectrum (100 MHz, CDCl_3) of compound 135	199
Figure 106. ^1H NMR spectrum (400 MHz, CDCl_3) of compound 136	200
Figure 107. ^{13}C NMR spectrum (100 MHz, CDCl_3) of compound 136	200
Figure 108. ^1H NMR spectrum (400 MHz, CDCl_3) of compound 137	201
Figure 109. ^{13}C NMR spectrum (100 MHz, CDCl_3) of compound 137	201
Figure 110. ^1H NMR spectrum (400 MHz, CDCl_3) of compound 138	202
Figure 111. ^{13}C NMR spectrum (100 MHz, CDCl_3) of compound 138	202
Figure 112. ^1H NMR spectrum (400 MHz, CDCl_3) of compound 139	203
Figure 113. ^{13}C NMR spectrum (100 MHz, CDCl_3) of compound 139	203
Figure 114. ^1H NMR spectrum (400 MHz, CDCl_3) of compound 140	204
Figure 115. ^{13}C NMR spectrum (100 MHz, CDCl_3) of compound 140	204
Figure 116. ^1H NMR spectrum (400 MHz, CDCl_3) of compound 141	205
Figure 117. ^{13}C NMR spectrum (100 MHz, CDCl_3) of compound 141	205
Figure 118. ^1H NMR spectrum (400 MHz, CDCl_3) of compound 142	206
Figure 119. ^{13}C NMR spectrum (100 MHz, CDCl_3) of compound 142	206
Figure 120. ^1H NMR spectrum (400 MHz, CDCl_3) of compound 143	207
Figure 121. ^{13}C NMR spectrum (100 MHz, CDCl_3) of compound 143	207
Figure 122. ^1H NMR spectrum (400 MHz, CDCl_3) of compound 145	208
Figure 123. ^{13}C NMR spectrum (100 MHz, CDCl_3) of compound 145	208



UFMG

Figure 124. ^1H NMR spectrum (400 MHz, CDCl_3) of compound 146	209
Figure 125. ^{13}C NMR spectrum (100 MHz, CDCl_3) of compound 146	209
Figure 126. ^1H NMR spectrum (400 MHz, CDCl_3) of compound 147	210
Figure 127. ^{13}C NMR spectrum (100 MHz, CDCl_3) of compound 147	210
Figure 128. ^1H NMR spectrum (400 MHz, CDCl_3) of compound 148	211
Figure 129. ^{13}C NMR spectrum (100 MHz, CDCl_3) of compound 148	211
Figure 130. ^1H NMR spectrum (400 MHz, CDCl_3) of compound 149	212
Figure 131. ^{13}C NMR spectrum (100 MHz, CDCl_3) of compound 149	212
Figure 132. ^1H NMR spectrum (400 MHz, CDCl_3) of compound 150	213
Figure 133. ^{13}C NMR spectrum (100 MHz, CDCl_3) of compound 150	213
Figure 134. ^1H NMR spectrum (400 MHz, CDCl_3) of compound 151	214
Figure 135. ^{13}C NMR spectrum (100 MHz, CDCl_3) of compound 151	214
Figure 136. ^1H NMR spectrum (400 MHz, CDCl_3) of compound 152	215
Figure 137. ^{13}C NMR spectrum (100 MHz, CDCl_3) of compound 152	215
Figure 138. ^1H NMR spectrum (400 MHz, CDCl_3) of compound 153	216
Figure 139. ^{13}C NMR spectrum (100 MHz, CDCl_3) of compound 153	216
Figure 140. ^1H NMR spectrum (400 MHz, CDCl_3) of compound 154	217
Figure 141. ^{13}C NMR spectrum (100 MHz, CDCl_3) of compound 154	217
Figure 142. ^1H NMR spectrum (400 MHz, CDCl_3) of compound 155	218
Figure 143. ^{13}C NMR spectrum (100 MHz, CDCl_3) of compound 155	218
Figure 144. ^1H NMR spectrum (400 MHz, CDCl_3) of compound 156	219
Figure 145. ^{13}C NMR spectrum (100 MHz, CDCl_3) of compound 156	219
Figure 146. ^1H NMR spectrum (400 MHz, CDCl_3) of compound 157	220
Figure 147. ^{13}C NMR spectrum (100 MHz, CDCl_3) of compound 157	220
Figure 148. ^1H NMR spectrum (400 MHz, CDCl_3) of compound 158	221
Figure 149. ^{13}C NMR spectrum (100 MHz, CDCl_3) of compound 158	221
Figure 150. ^1H NMR spectrum (400 MHz, CDCl_3) of compound 159	222
Figure 151. ^{13}C NMR spectrum (100 MHz, CDCl_3) of compound 159	222

1. Introduction

1.1. Quinones: Natural Occurrence

Quinones are compounds containing a fully conjugated cyclic dione. In general, quinoidal systems are structures derived from aromatic compounds by conversion of an even number of C-H into C=O groups, including heterocyclic and polycyclic analogues.¹ Despite the simplicity of the definition, the quinones are a large and heterogeneous collection of compounds, distributed in nature as a massive series of natural products, acting in biological processes of extreme importance.² Some examples include lapachol (**1**),³ streptonigrin (**2**),⁴ thiaplidiaquinone A (**3**),⁵ doxorubicin (**4**)⁶ and phylloquinone (**5**).⁷ (Figure 1).⁸

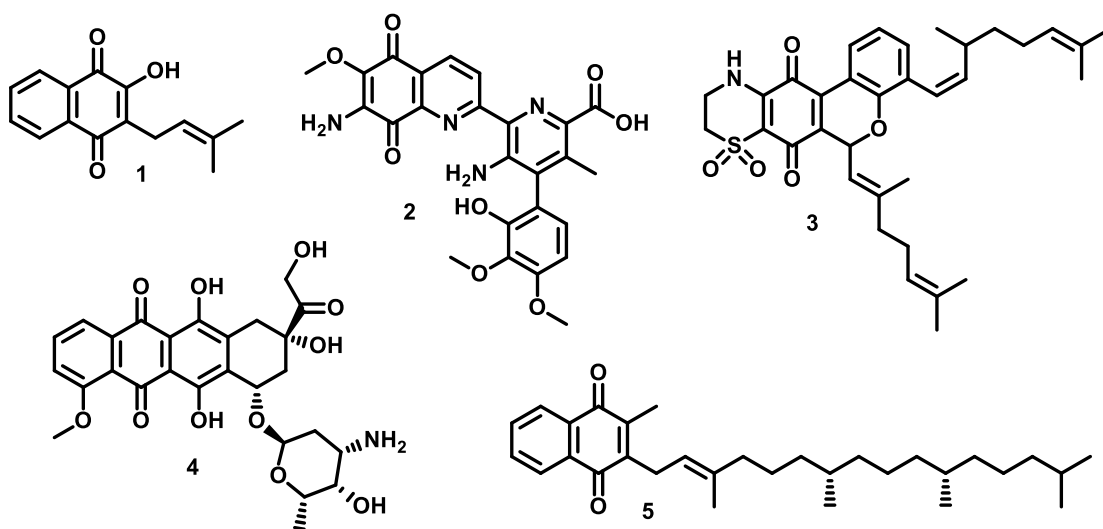


Figure 1. The quinone “backbone” present in several natural products.

1. IUPAC; *Compendium of Chemical Terminology Gold Book, Version 2.3.3*, 2014, 1220.
2. Morton, R.A.; *Biochemistry of quinones*, New York, 1965.
3. Arnaudon, G.; *Compt. Rend.*, **1858**, 46, 1152.
4. Rao, K.V.; Cullen, W.P.; *Antibiotics Annual 1959-1960*, New York, 1960.
5. Aiello, A.; Fattorusso, E.; Luciano, P.; Macho, A.; Menna, M.M.; Muñoz, E.; Antitumor effects of two novel naturally occurring terpene quinones isolated from the Mediterranean ascidian *Aplidium conicum*. *J. Med. Chem.*, **2005**, 48, 3410.
6. Blum, R.H.; Carter, S.K.; Adriamycin. A new anticancer drug with significant clinical activity. *Ann. Intern. Med.* **1974**, 80, 249.
7. Binkley, S.B.; MacCorquodale, D.W.; Thayer, S.A.; Doisy, E.A.; The isolation of vitamin K1. *J. Biol. Chem.*, **1939**, 130, 219.
8. Patai, S.; Rappaport, Z.; *The Chemistry of Quinonoid Compounds*, New York, 1988.

Due to their unique electronic properties, especially electron and proton transfer,⁹ the quinone moiety is present in a wide range of science fields such as chemistry,¹⁰ material sciences¹¹ and medicine.¹² Quinones also play an important role in cell respiration, participating as “links” between primary dehydrogenases and terminal reductases or oxidases.¹³ A notable example is ubiquinone (**6**) or coenzyme Q10, which remains in every cell of most animals, playing an essential role in the electron transport chain and, consequently, in the ATP production process¹⁴ (Figure 2).

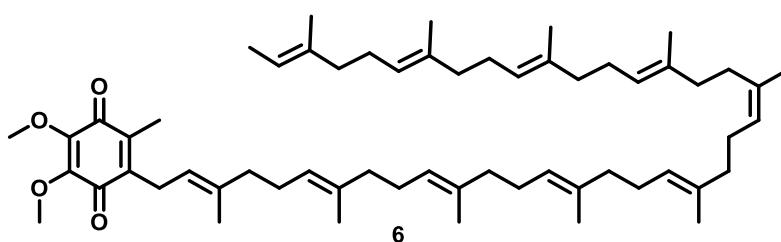


Figure 2. Ubiquinone (**6**).

The most simple sub group of the quinoidal family is known as benzoquinones. They are present mainly in insects as defensive agents,¹⁵ and plants as metabolites.¹⁶ Interesting example in insects include the secretions of the black beetles or bombardier beetles, which uses these secretions as a fine spray containing a mixture of hydroquinone (**7**) and hydrogen peroxide (H₂O₂). Both components combined with peroxidase enzymes results in the oxidation of **7** to 1,4-benzoquinone (**8**), a exothermic reaction that reach temperatures of 100 °C. 1,4-benzoquinone is also known to be particularly irritating to the eyes and respiratory system (Scheme 1).¹⁷

9. Price, C.E.; Driessen, A.J.M.; Biogenesis of membrane bound respiratory complexes in *Escherichia coli*. *Biochim. Biophys. Acta*, **2010**, *1803*, 748.

10. Thomson, R.H.; Naturally Occurring Quinones IV; Blackie Academic: London, **1997**.

11. Jesionowski, T.; Klapiszewski, L.; Kraft lignin and silica as precursors of advanced composite materials and electroactive blends. *J. Mater. Sci.*, **2014**, *49*, 1376.

12. Koyama, J.; Anti-infective quinone derivatives of recent patents. *Recent Pat. Anti-Infect. Drug Discovery*, **2006**, *1*, 113.

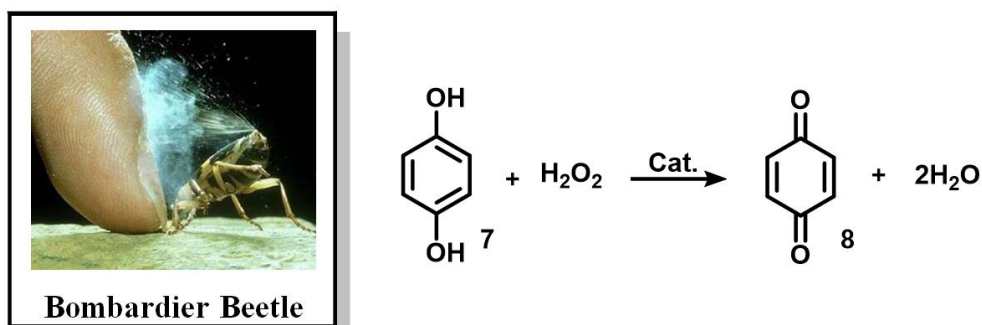
13. Adams, M.W.; Mortenson, L.E.; Chen, J.S.; Hydrogenase. *Biochim. Biophys. Acta*, **1980**, *594*, 105.

14. Ernster, L.; Dallner, G.; Biochemical, physiological and medical aspects of ubiquinone function. *Biochimica et Biophysica Acta*, **1995**, *1271*, 195.

15. Leal, W.S.; Snapshot of insect–fungus arms race. *Proc. Natl. Acad. Sci. USA*, **2015**, *112*, 8519.

16. Dayan, F.E.; Watson, S.B. Nanayakkara, N.P.D.; Biosynthesis of lipid resorcinols and benzoquinones in isolated secretory plant root hairs. *J. Exp. Bot.*, **2007**, *58*, 3263.

17. Eisner, T.; Aneshansley, D.J.; Spray aiming in the bombardier beetle: photographic evidence. *Proc. Natl. Acad. Sci. USA*, **1999**, *96*, 9705.



Scheme 1. The bombardier beetle and its defence mechanism.

Other common examples include the ornamental plant *Primula obconica*, frequently used for household decoration, famous for cause of allergic reaction in humans.¹⁸ The reason is that the secretion of the glandular hairs in the leaves are rich in primin (9), a benzoquinone which causes dermatitis,¹⁹ that is also commercialized in Brazil for the treatment of basal cell carcinoma.²⁰ Another plant, the incense cedar heartwood possesses his red/brown colour due to the existence of 3-libocedroxythymoquinone (10), a trimeric red benzoquinone (Figure 3).²¹

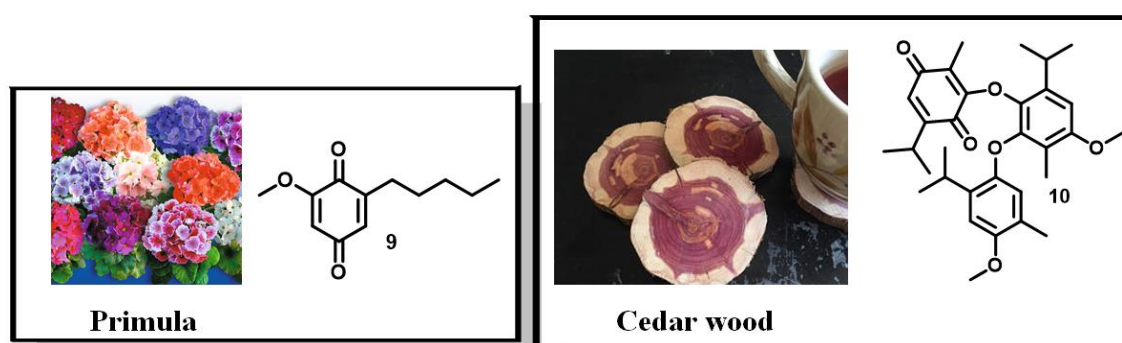


Figure 3. Primin (9) and 3-libocedroxythymoquinone (10).

18. Aplin, C.G.; Lovell, C.R.; Contact dermatitis due to hardy *Primula* species and their cultivars. *Contact Dermatitis*, **2001**, *44*, 23.

19. Zachariae, C.; Engkilde, K.; Johansen, J.D.; Menné, T.; Primin in the European standard patch test series for 20 years. *Contact Dermatitis*, **2007**, *56*, 344.

20. Bieber, L.W.; Chiappeta, A.A.; De Moraes e Souza, M.A.; Generino, M.; Neto, P.R.; Simple synthesis of primin and its analogues via lithiation of protected guaiacol. *J. Nat. Prod.*, **1990**, *53*, 706.

21. Zavarin, E.; Extractive components from incense cedar heartwood (*Libocedrus decurrens* Torrey). VI. On the occurrence of 3-Libocedroxythymoquinone. *J. Org. Chem.*, **1958**, *23*, 1198.

Benzoquinones are also present in the sea, most specifically inside some sea sponges like *Dysidea cinerea*.²² As an example, avarone (**11**) is a cytostatic agent with potent antileukemic activity both *in vitro* and *in vivo* (mice)²³ and also displays antibacterial and antifungal activities against a limited range of microorganisms.²⁴ Benzoquinones are also produced by bacteria of the *Streptomyces* gender, and molecules like sarubicin A (**12**) were isolated as red crystals from their cultures.²⁵ These benzoquinone possess antibiotic activity against common bacteria like *Micrococcus luteus* and *Alcaligenes faecalis* (Figure 4).²⁶

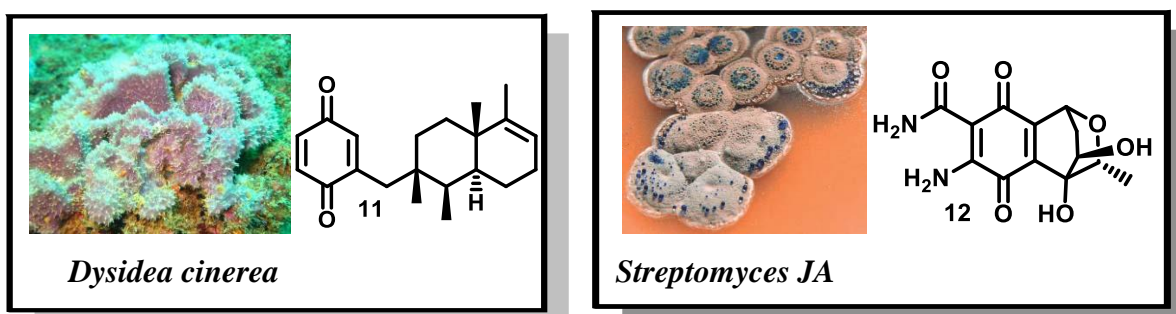


Figure 4. Avarone (**11**) and sarubicin A (**12**).

Despite the simplicity of the benzoquinone nucleus, these backbones are present in extremely complex molecules like quinolidomicin A₁ (**13**), a 60-membered macrolide isolated from the culture of *Micromonospora sp.*²⁷ This massive molecule was elucidated by Seto and co-workers in 1993 and was reported as a highly cytotoxic agent against P388 murine leukemia cells (IC₅₀^{1/24h} = 8 nM) (Figure 5).²⁸

22. Tsoukatou, M.; Maréchal, J.P.; Hellio, C.; Novaković, I.; Tufegdžic, S.; Sladić, D.; Gasić, M.J.; Clare, A.S.; Vagias, C.; Roussis, V.; Evaluation of the activity of the sponge metabolites avarol and avarone and their synthetic derivatives against fouling micro- and macroorganisms. *Molecules*, **2007**, *12*, 1022.

23. Belisario, M.A.; Maturo, M.; Avagnale, G.; De Rosa, S.; Scopacasa, F.; De Caterina, M.; In vitro effect of avarone and avarol, a quinone/hydroquinone couple of marine origin, on platelet aggregation. *Pharmacol. Toxicol.*, **1996**, *79*, 300.

24. Amigó, M.; Terencio, M.C.; Mitova, M.; Iodice, C.; Payá, M.; De Rosa, S.; Potential antipsoriatic avarol derivatives as antioxidants and inhibitors of PGE(2) generation and proliferation in the HaCaT cell line. *J. Nat. Prod.*, **2004**, *67*, 1459.

25. Takeuchi, Y.; Sudani, M.; Yoshii, E.; Total synthesis of (+-)-sarubicin A (U-58,431). *J. Org. Chem.*, **1983**, *48*, 4151.

26. Reinhardt, G.; Bradler, G.; Eckardt, D.; Tresselt, D.; Ihn, W.; isolation and characterization of sarubicin A, a new antibiotic. *J. Antibiot.*, **1980**, *33*, 787.

27. Hayakawa, Y.; Matsuoka, M.; Shin-ya, K.; Seto, H.; Quinolidomicins A₁, A₂ and B₁, novel 60-membered macrolide antibiotics. *J. Antibiot.*, **1993**, *46*, 1557.

28. Hayakawa, Y.; Shin-ya, K.; Furihata, K.; Seto, H.; Structure of a novel 60-membered macrolide, quinolidomicin A. *J. Am. Chem. Soc.*, **1993**, *115*, 3014.

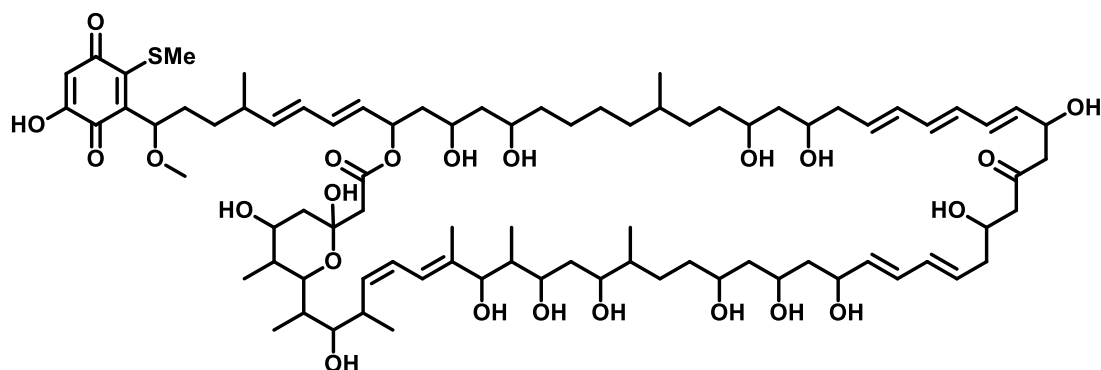


Figure 5. Quinolidomicin A₁ (**13**).

As another sub-group in the quinone family, naphthoquinones are characterized by a benzene ring fused with a benzoquinone.²⁹ These molecules occur in nature most commonly as pigments³⁰, being considered privileged structures due to their multi-bioactivity and medicinal properties.³¹ Figure 6 shows examples of two pairs of isomers (lawsone (**14**)/juglone (**15**) and pumblagin (**16**)/isopumblagin (**17**)) that are natural pigments and common building blocks in the chemistry of naphthoquinones. Lawsone (**14**) is used as a skin and hair dye for more than 5000 years and its potential as a pigment has been used in forensic sciences as a fingerprint revelator.³² Juglone (**15**) is produced by plants of the *Juglans* species to act as an allelopathic detrimental compound, a substance that inhibits the growth of other plants nearby.³³ It is also a common dye in food industry, known as C.I. Natural Brown 7.³⁴

Plumbagin (**16**) is a naphthoquinone that stands out for its pharmacological properties, showing antimicrobial,³⁵ anti-inflammatory³⁶ and neuro protective action,

29. Kumagai, Y.; Shinkai, Y.; Miura, T.; Cho, A.K.; The chemical biology of naphthoquinones and its environmental implications. *Annu. Rev. Pharmacol. Toxicol.*, **2012**, *55*, 221.

30. López, L.I.L.; Flores, S.D.N.; Belmares, S.Y.S.; Galindo, A.S.; Naphthoquinones: biological properties and synthesis of lawsone and derivatives – a structured review. *VITAE*, **2014**, *21*, 248.

31. Liu, K.K.C.; Li, J.; Sakya, S.; Synthetic approaches to the 2003 new drugs. *Mini-Rev. Med. Chem.*, **2004**, *4*, 1105.

32. Jelly, R.; Lewis, S.W.; Lennard, C.; Lim, K.F.; Almog, J.; Lawsone: a novel reagent for the detection of latent fingerprints on paper surfaces. *Chem. Commun.*, **2008**, 3513.

33. Soderquist, C.J.; Juglone and allelopathy. *J. Chem. Educ.*, **1973**, *50*, 782.

34. Bechtold, T.; Mussak, R.; Handbook of Natural Colorants. John Wiley & Sons, **2009**.

35. de Paiva, S.R.; Figueiredo, M.R.; Aragão, T.V.; Kaplan, M.A.C.; Antimicrobial activity *in vitro* of plumbagin isolated from plumbago species. *Mem. Inst. Oswaldo Cruz*, **2003**, *98*, 959.

36. Checker, R.; Sharma, D.; Sandur, S.K.; Subrahmanyam, G.; Krishnan, S.; Poduval, T.B.; Sainis, K.B.; Plumbagin inhibits proliferative and inflammatory responses of T cells independent of ROS generation but by modulating intracellular thiols. *J. Cell. Biochem.*, **2010**, *110*, 1082.

³⁷ among others. ³⁸ Anti-inflammatory properties are also found in isopumblagin (**17**), isomer of **16** (Figure 6).³⁹

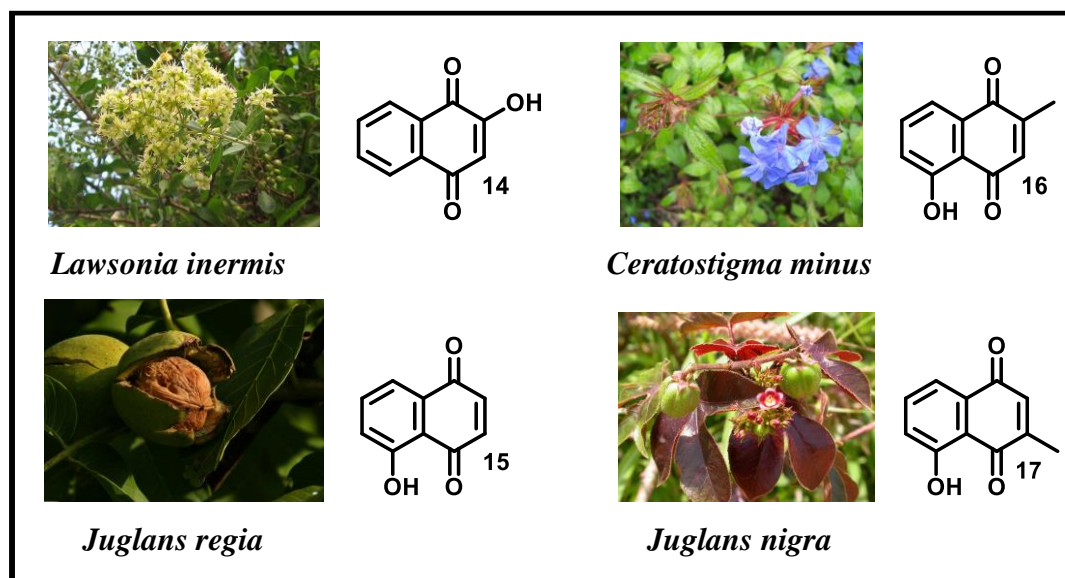


Figure 6. Lawsonsone (**14**), juglone (**15**), pumblagin (**16**) and isopumblagin (**17**).

Halogenated naphthoquinones are often rare to occur in terrestrial plants, being present mostly in marine organisms.⁴⁰ However, some coastal plants like *Diospyros maritima* produce molecules like 3-chloroplumbagin (**18**) and 3-bromoplumbagin (**19**) as secondary metabolites, possessing antifungal activity (Figure 7).⁴¹ The biodiversity of the sea is often the main source of halogenated compounds, and over the years the interests for marine compounds have grown exponentially, once the problems with the isolation and characterisation of those have been solved with new technologies.⁴² In this context, naphthoquinones like marinone (**20**) and debromomarinone (**21**) (Figure 7)

37. Son, T.G.; Camandola, S.; Arumugam, T.V.; Cutler, R.G.; Telljohann, R.S.; Mughal, M.R.; Moore, T.A.; Luo, W.; Yu, Q.S.; Johnson, D.A.; Johnson, J.A.; Greig, N.H.; Mattson, M.P.; Plumbagin, a novel Nrf2/ARE activator, protects against cerebral ischemia. *J. Neurochem.*, **2010**, *112*, 1316.

38. Ding, Y.; Chen, Z.-J.; Liu, S.; Che, D.; Vetter, M.; Chang, C.-H.; Inhibition of Nox-4 activity by plumbagin, a plant-derived bioactive naphthoquinone. *J. Phar. Pharmacol.*, **2004**, *57*, 111.

39. Gupta, S.; Ali, M.; Pillai, K.K.; Alam, M.S.; Evaluation of anti-inflammatory activity of some constituents of *Lawsonia inermis*. *Fitoterapia*, **1993**, *64*, 365.

40. Motohashi, K.; Irie, K.; Toda, T.; Matsuo, Y.; Kasai, H.; Sue, M.; Furihata, K.; Seto, H.; Studies on terpenoids produced by actinomycetes. *J. Antibiot.*, **2008**, *61*, 75.

41. Higa, M.; Ogihara, K.; Yogi, S.; Bioactive naphthoquinone derivatives from *Diospyros maritima* blume. *Chem. Pharm. Bull.*, **1998**, *46*, 1189.

42. Solanki, R.; Khanna, M.; Lal, R.; Bioactive compounds from marine actinomycetes. *Indian J. Microbiol.*, **2008**, *48*, 410,

have been isolated of bacteria of the Actinomycetales order.⁴³ These presented antibacterial activity (MIC values of 1-2 µg/mL) against several bacteria strains.⁴⁴

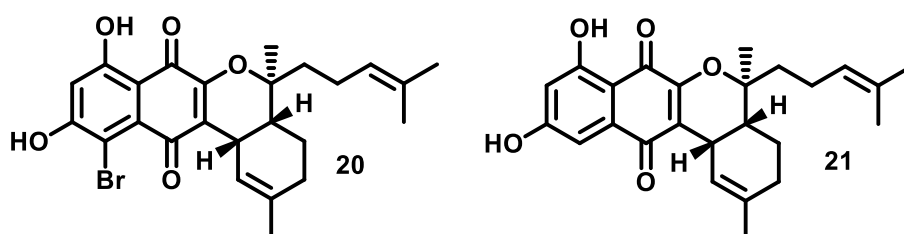
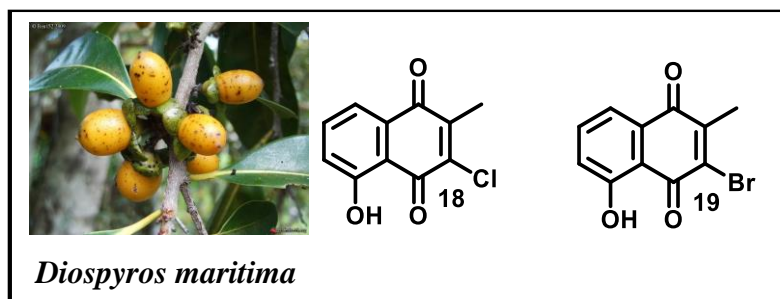


Figure 7. 3-chloroplumbagin (**18**), 3-bromoplumbagin (**19**), marinone (**20**) and debromomarinone (**21**).

As part of both European and Asian history, the enantiomeric naphthoquinone natural products alkannin (**22**) and shikonin (**23**) were the main red dyes used in both continents, being correlated only in the 20th century by the elucidation of their structures.⁴⁵ Alkannin (**22**) is founded in the roots of the plant *Alkanna tinctoria*, a common bush in all Europe, and its medicinal properties were famous in the treatment of ulcers, inflammations and burnings (Figure 8).⁴⁶

The other enantiomer shikonin (**23**) is the major constituent of the root extracts of the plant *Lithospermum erythorhizon*, and most ancient Chinese herbal texts describes its medicinal properties to be similar to **22**.⁴⁷ Several preparations that contain **23** are used until today in China, Japan and Korea in the cosmetics and dyestuff

43. Gallagher, K.A.; Rauscher, K.; Pavan loca, L.; Jensen, P.R.; Phylogenetic and chemical diversity of a hybrid-isoprenoid producing Streptomycete lineage. *Appl. Environ. Microbiol.*, **2013**, *79*, 6894.

44. Pathirana, C.; Jensen, P.R.; Fenical, W.; Marinone and debromomarinone: antibiotic sesquiterpenoid naphthoquinones of a new structure class from a marine bacterium. *Tetrahedron Lett.*, **1992**, *33*, 7663.

45. Papageorgiou, V.P.; Assimopoulou, A.N.; Couladouros, E.A.; Hepworth, D.; Nicolaou, K.C.; The chemistry and biology of alkannin, shikonin, and related naphthazarin natural products. *Angew. Chem. Int. Ed.*, **1999**, *38*, 270.

46. Culpeper, N.; The english physitian enlarged, Churchill, London, **1695**.

47. A barefoot doctor's manual (translation of a chinese instruction to certain chinese health personnel), US Government Printing Office, Washington, **1974**.

industry.⁴⁸ Nowadays, it is known that both enantiomers present wound healing properties,⁴⁹ anti-inflammatory action,⁵⁰ antitumor⁵¹ and antimicrobial activity (Figure 8).⁵²

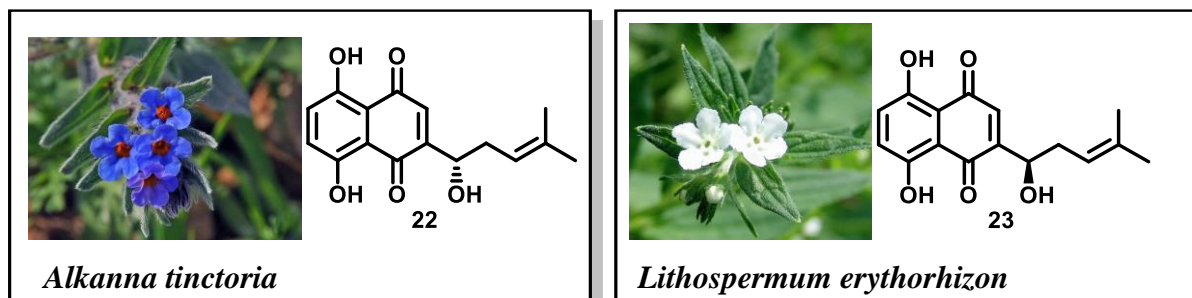


Figure 8. Alkannin (**22**) and shikonin (**23**).

Plants of the Eriocaulaceae family are widespread in the region of the Serra do Cipó, State of Minas Gerais, Brazil.⁵³ Several plants from this family are known as “everlasting plants” because they appear to be alive even for years after being harvested.⁵⁴ As a member of this family, plants of the *Paepalanthus* species are famous for produce naphthopyranone derivatives.⁵⁵ Extracted from the capitula of the plant *Paepalanthus latipes*, 5-methoxy-3,4-dehydroxanthomegnin (**24**) is an unique example of naphthoquinone with a pyrone ring due to its significant cytotoxic activity (IC₅₀ = 35.8 µg/mL) (Figure 9).⁵⁶

48. Ootani, S.; Takagishi, I.; (Pentel K.K.) *JP-B 06 336 411*, **1994**.

49. Michaelides, C.; Striglis, C.; Panayotou, P.; Ioannovich, I.; *Ann. Medit. Burns Club*, **1993**, 6, 24.

50. Hayashi, M.; *Nippon yakurigaku zasshi*, **1977**, 73, 177.

51. Driscoll, J.S.; Hazard, G.F.; Wood, H.B.Jr.; Goldin, A.Jr.; Structure-antitumor activity relationships among quinone derivatives. *Cancer Chemother. Rep. Part 2*, **1974**, 4, 1.

52. Bhakuni, D.S.; Dhar, M.L.; Dhar, M.M.; Dhawn, B.N.; Mehrotra, B.N.; Screening of Indian plants for biological activity. II. *Indian J. Exp. Biol.*, **1969**, 7, 250.

53. Giulietti, A.M.; Hensold, N.; Patterns of geographic distribution of the genera of Eriocaulaceae. *Acta. Bot. Bras.*, **1990**, 4, 133.

54. Moreira, R.R.D.; Santos, L.E.; Varella, S.D.; Varanda, E.A.; Vilegas, W.; Avaliação da atividade mutagênica do extrato etanólico bruto de *Paepalanthus latipes* (Eriocaulaceae) e dos compostos flavonóidicos 7-metoxilados relacionados. *Rev. Bras. Farmacogn.*, **2002**, 12, 11.

55. Leitão, G.G.; Leitão, S.G.; Vilegas, W.; Quick preparative separation of natural naphthopyranone with antioxidante activity by high-speed conter-current chromatography. *Z. Naturforsch.*, **2002**, 57, 1051.

56. Kitagawa, R.R.; Raddi, M.S.G.; Santos, L.C.; Vilegas, W.; A new cytotoxic naphthoquinone from *Paepalanthus latipes*. *Chem. Pharm. Bull.*, **2004**, 52, 1487.

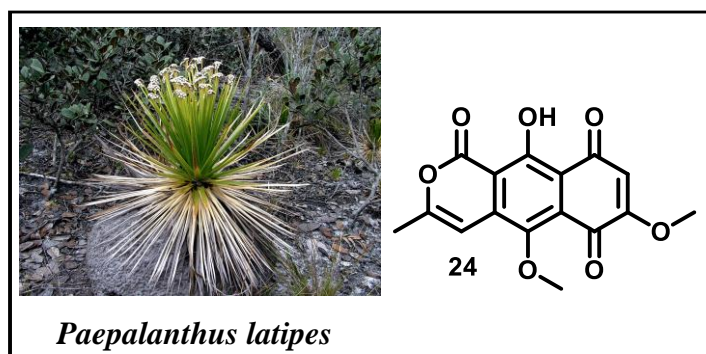


Figure 9. 5-methoxy-3,4- dehydroxanthomegnin (**24**).

1.2. The Role of Quinones in Chagas Disease Therapy

Chagas disease is a potentially life-threatening illness, also known as American trypanosomiasis, caused by the protozoan *Trypanosoma cruzi* (*T. cruzi*), and transmitted by a triatomine bug known as “kissing bug” (Figure 10).⁵⁷ Chagas disease is endemic in twenty one Latin American countries, and about six to seven million people worldwide are estimated to be infected with.⁵⁸ It was named after Carlos Justiniano Chagas, a Brazilian physician and researcher who discovered the disease in 1909.⁵⁹ Carlos Chagas is considered one of the most influent Brazilian scientist of all times, together with names like Osvaldo Cruz⁶⁰ and Cesar Lattes,⁶¹ being until today the only in history to fully describe a illness (Chagas disease: the pathogen, the vector, the hosts, the clinical manifestations and the epidemiology).⁶²

The disease presents itself in two phases, an initial acute phase that lasts for two months after infection and a chronic phase that can endure for life.⁶³ Acute phase is characterised by a high number of parasites circulating through the blood stream, but

57. WHO Fact sheet n° 340, updated march 2013. <http://www.who.int/mediacentre/factsheets/fs340/en/>; accessed in 28/09/2017.

58. Costa, J.; Peterson, A.T.; Ecological niche modeling as a tool for understanding distributions and interactions of vectors, hosts, and etiologic agents of Chagas disease. *Adv. Exp. Med. Biol.*, **2012**, 710, **59**.

59. (a) Pereira, P.C.M.; Navarro, E.C.; Challenges and perspectives of Chagas disease: a review. *J. Venom. Anim. Toxins incl. Trop. Dis.*, **2013**, 19, 34. (b) Chagas, C. Neue Trypanosomen. *Vorläufige Mitteilung Arch. Schiff. Tropenhyg.*, **1909**, 13, 120.

60. Fraga, C.; *Life and work of Oswaldo Cruz.*, Fiocruz, **2005**.

61. Caruso, F.; Marques, A.; Troper, A.; Cesar Lattes, a descoberta do méson π e outras histórias. *Ciência e Cultura*, **1984**, 36, 2066.

62. Almeida, D.F.; Carlos Chagas Filho, scientist and citizen. *An. Acad. Bras. Ciênc.*, **2000**, 72, 299.

63. Bezerra, R.C.; Neto, V.A.; *Trypanosoma cruzi*, hemocultura: uma abordagem prática. *Rev. Bras. Clín. Méd.*, **2010**, 8, 205.

symptoms are absent or unspecific, manifesting in less than 50% of people by a skin lesion or a purplish swelling of the lids of one eye (Figure 10).⁶⁴



Figure 10. Kissing bug, *T. cruzi* (trypomastigote), and the purplish swelling symptom.

If the patient is not treated in the acute phase, the disease evolves to a silent chronic phase, where symptoms can be hardly detected after years of incubation, manifesting by hearth or digestive system problems and, later on, progressive hearth failure caused by the destruction of his muscles and nervous system.⁶⁵ Diagnosis in this phase can be the detection of IgG antibodies (anti-*T. cruzi* antibodies) in the infected blood by serologic exams.⁶⁶

People and animals can become infected orally through ingesting food and drink contaminated with the faeces of a triatomine carrying kissing bug, where cases of contamination were described in Venezuela by ingestion of Guava juice, and the presence of the parasite was detected in the harvested and pressed fruits of the açai palm in the Amazon forest.⁶⁷

First occurrences of Chagas disease can be traced back to 7000 bc to 1500 ad, when mummies from Chile and Peru showed signs of the disease chronic stage.⁶⁸ The colonization of South America in 1500 by the Portuguese and Spanish were known to

64. Guerrant, R.L.; Walker, D.H.; Weller, P.F.; *American trypanosomiasis (Chagas' disease). Tropical Infectious Diseases Principles, Pathogens, & Practice*. Philadelphia: Churchill Livingstone Elsevier, **2006**.

65. Córdova, E.; Maiolo, E.; Corti, M.; Orduña, T.; Neurological manifestations of Chagas' disease. *Neurol. Res. Int.*, **2010**, *32*, 238.

66. Portela-Lindoso, A.A.B.; Shikanai-Yasuda, M.A.; Doença de Chagas crônica: do xenodiagnóstico e hemocultura à reação em cadeia da polimerase. *Rev. Saúde Pública.*, **2003**, *37*, 107.

67. Pereira, K.S.; Schmidt, F.L.; Guaraldo, A.M.; Franco, R.M.; Dias, V.L.; Passos, L.A.; Chagas' disease as a foodborne illness. *J. Food. Prot.*, **2009**, *72*, 441.

68. Aufderheide, A.C.; Salo, W.; Madden, M.; Streitz, J.; Buikstra, J.; Guhl, F.; Arriaza, B.; Renier, C.; Wittmers Jr., L.E.; Fornaciari, J.; Allison, M.; A 9,000-year record of Chagas' disease. *Proc. Natl. Acad. Sci. USA*, **2004**, *101*, 2034.

promote the spread of *T. cruzi* vector *Triatoma infestans*, which is the main domestic vector for Chagas disease until nowadays.⁶⁹ In 1835, Charles Darwin himself reported being bitten by a triatomine bug in Chile.⁷⁰

The life cycle of the disease goes as follows: a contaminated kissing bug takes a blood meal and defecates close to the wound, the parasite goes from the faeces to the blood stream of the host in his trypomastigote form (1); the trypomastigotes parasites penetrates several cells at the bite wound site, beginning their transformation to amastigotes (2); the intracellular amastigotes multiply inside the cell and transform into trypomastigotes again to be released through the blood stream again. Trypomastigotes can infect new cells and transform into amastigotes in new infection sites (3) and (4); a kissing bug can take a blood meal from the infected host, ingesting trypomastigotes (5); the parasite differentiates into epimastigote inside the insect midgut and multiplies (6) and (7); the epimastigotes differentiate again into trypomastigotes in the insect hindgut (8), contaminating the kissing bug faeces. The insect now is ready to take another blood meal and contaminate another host (Figure 11).⁷¹

The only available treatments for Chagas disease are the drugs benznidazole (**25**) and nifurtimox (**26**) (Figure 12).⁷² Those two substances are especially effective for the treatment of patients in the acute phase, with cure rates of 80% in a complete 60-day course treatment with the correct dosages.⁷³ However, for patients in the chronic phase, these two drugs are not ideal due to their severe side effects associated with long treatment time and high dosages.⁷⁴ The dye crystal violet (**27**) is a chemoprophylactic agent, used in blood banks in endemic areas to ensure the decontamination of these blood stocks, avoiding contamination by blood transfusion.⁷⁵

69. Steverding, D.; The history of Chagas disease. *Parasit. Vectors*, **2014**, *7*, 317.

70. Clayton, J.; Did Darwin have Chagas disease? *Nature*, **2010**, *465*, 4.

71. Centers for Disease Control and Prevention, updated march **2015**. <https://www.cdc.gov/parasites/chagas/biology.html>; accessed in 03/10/2017.

72. (a) <https://www.drugs.com/mmx/benznidazole.html>, accessed in 05/10/2017. (b) <https://www.drugs.com/international/nifurtimox.html>, accessed in 05/10/2017.

73. Caldas, I.V.; Talvani, A.; Caldas, S.; Caneiro, C.M.; de Lana, M.; Guedes, P.M.M.; Bahia, M.T.; Benznidazole therapy during acute phase of Chagas disease reduces parasite load but does not prevent chronic cardiac lesions. *Parasitol. Res.*, **2008**, *103*, 413.

74. Castro, J.A.; Diaz de Toranzo, E.G.; Toxic effects of nifurtimox and benznidazole, two drugs used against American trypanosomiasis (Chagas' disease). *Biomed. Environ. Sci.*, **1988**, *1*, 19.

75. Vilaseca, G.C.; Cerisola, J.A.; Olarte, J.A.; Zothner, A.; The use of Crystal violet in the prevention of the transfusional transmission of Chagas-Mazza disease. *Vox Snag.*, **1966**, *11*, 711.

Trypanosomiasis, American (Chagas disease) (*Trypanosoma cruzi*)

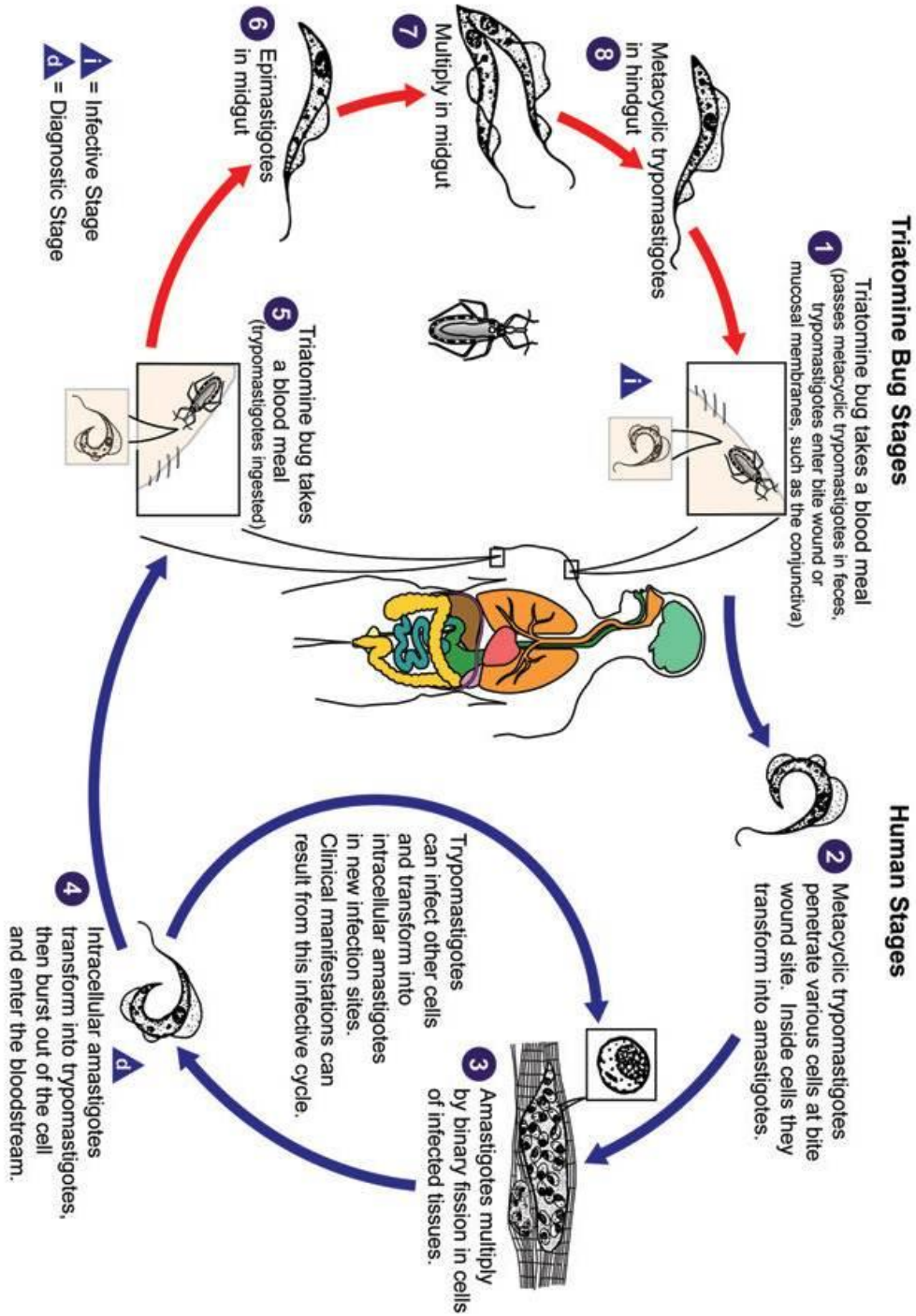


Figure 11. Chagas disease life cycle.

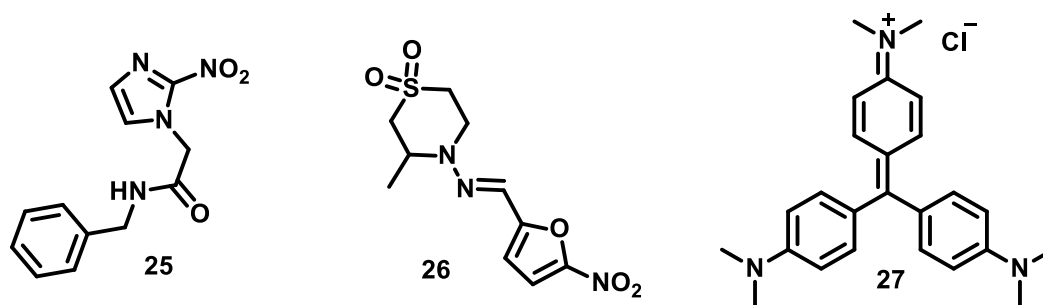


Figure 12. benznidazole (**25**), nifurtimox (**26**) and crystal violet (**27**).

Main challenges for the design and development of new drugs against *T. cruzi* lies in the fact that it is an intracellular parasite: it uses cells metabolism to produce hundreds of new parasites that, after cell implosion, release new progenies to infect surrounding tissues.⁷⁶ Other trypanosome parasites like *Leishmania* (leishmaniasis) and *Trypanosoma brucei* (sleeping sickness) remains in the blood, and are more accessible to drugs.⁷⁷

In this context, quinoidal compounds represent one of the most promising classes of molecules with trypanocidal activity.⁷⁸ Inside this group, naphthoquinones are ubiquitous in nature, presenting several forms of multi-bioactivity and medicinal properties, especially in cancer therapy⁷⁹ and against the several forms of the *T. cruzi* parasite.⁸⁰

Quinoidal structures are analogous to coenzyme Q10 (ubiquinone (**6**)), which has a wide range of functions in protozoa metabolism, mainly in the electron-transfer

76. Alves, M.J.M.; Colli, W.; *Trypanosoma cruzi*: adhesion to the host cell and intracellular survival. *IUBMB Life*, **2007**, *59*, 274.

77. Khare, S.; Nagle, A.S.; Biggart, A.; Lai, Y.H.; Liang, F.; Davis, L.C.; Barnes, S.W.; Mathison, C.J.; Myburgh, E.; Gao, M.Y.; Gillespie, J.R.; Liu, X.; Tan, J.L.; Stinson, M.; Rivera, I.C.; Ballard, J.; Yeh, V.; Groessl, T.; Federe, G.; Koh, H.X.; Venable, J.D.; Bursulaya, B.; Shapiro, M.; Mishra, P.K.; Spraggon, G.; Brock, A.; Mottram, J.C.; Buckner, F.S.; Rao, S.P.; Wen, B.G.; Walker, J.R.; Tuntland, T.; Molteni, V.; Glynn, R.J.; Supek, F.; Proteasome inhibition for treatment of leishmaniasis, Chagas disease and sleeping sickness. *Nature*, **2016**, *537*, 229.

78. Coura, J.R.; De Castro, S.L.; A critical review on Chagas Disease chemotherapy. *Mem. Inst Oswaldo Cruz*, **2002**, *97*, 3.

79. Reinicke, K.E.; Bey, E.A.; Bentle, M.S.; Pink, J.P.; Ingalls, S.T.; Hoppel, C.L.; Misico, R.I.; Arzac, G.M.; Burton, G.; Bornmann, W.G.; Sutton, D.; Gao, J.; Boothman, D.A.; Development of beta-lapachone prodrugs for therapy against human cancer cells with elevated NAD(P)H: quinone oxidoreductase 1 levels. *Clin. Cancer Res.*, **2005**, *11*, 3055.

80. Sepúlveda-Boza, S.; Cassels, B.K.; Plant metabolites active against *Trypanosoma cruzi*. *Planta Med.*, **1996**, *62*, 98.

chain.⁸¹ Quinonoid substances are expected to interfere and disrupt the parasites mitochondrial electron transport chain, explaining the broad-spectrum antiprotozoal activity of such compounds, since respiratory inhibition itself can lead to organism death.⁸²

Quinones also generate free radicals during interaction of these substances with the respiratory chain, especially reactive oxygen species (ROS) like OH[•] and O₂^{•-}.⁸³ As show in Scheme 2, quinones are reduced by cytochrome P450 reductase resulting in a reactive semiquinone radical that can bind covalently into proteins and nucleic acids, leading to enzymatic deactivation and DNA damage.⁸⁴ When aerobic conditions, especially in mitochondrial environment sets in motion, the semiquinone radical can react with oxygen by single electron transfer (SET), regenerating the quinone and producing superoxide anion O₂^{•-} in a cycle. The superoxide anion is converted to hydrogen peroxide by the action of the enzyme superoxide dismutase, which has several fates:

- . Can be converted in H₂O and O₂ by the enzyme catalase;⁸⁵
- . Undergoes in a Haber-Weiss reaction⁸⁶ to be converted to OH[•], well-known ROS specie that causes oxidative damage to macromolecules;⁸⁷
- . It reacts with glutathione peroxidase, resulting in H₂O formation.⁸⁸

81. Ellis, J.E.; Coenzyme Q homologs in parasitic protozoa as targets for chemotherapeutic attack. *Parasitol. Today.*, **1994**, *10*, 297.

82. Hudson, A.T.; Atovaquinone – a novel broad-spectrum anti-infective drug. *Parasitol. Today*, **1993**, *9*, 66.

83. Salas, C.; Tapia, R.A.; Ciudad, K.; Armstrong, V.; Orellana, M.; Kemmerling, U.; Ferreira, J.; Maya, J.D.; Morello, A.; *Trypanosoma cruzi*: activities of lapachol and α - and β -lapachone derivatives against epimastigote and trypomastigote forms. *Bioorg. Med. Chem.*, **2008**, *16*, 668.

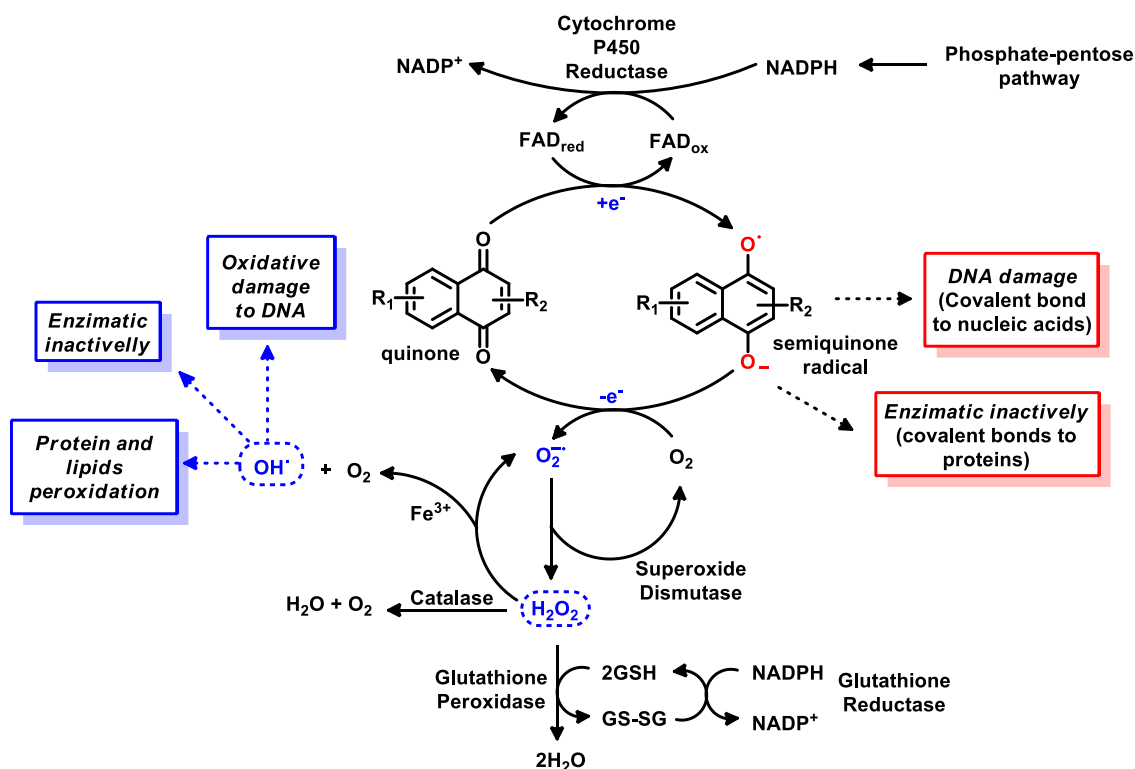
84. Jarasiene-Burinskaja, R.; Alksne, M.; Bartuskiene, V.; Voisniene, V.; Burinskij, J.; Cenas, N.; Bukelskiene, V.; Study of the cytotoxic effects of 2,5-diaziridinyl-3,6-dimethyl-1,4-benzoquinone (MEDZQ) in mouse hepatoma cells. *EXCLI Journal*, **2017**, *16*, 151.

85. Aebi, H.; “Catalase *in vitro*”. *Meth. Enzymol.*, **1984**, *105*, 121.

86. Haber, F.; Weiss, J.; Über die katalyse des hydroperoxyde. *Naturwissenschaften*, **1932**, *20*, 948.

87. Bandyopadhyay, U.; Das, D.; Banerjee, R.K.; Reactive oxygen species: oxidative damage and pathogenesis. *Curr. Sci.*, **1999**, *77*, 658.

88. Heverly-Coulson, G.S.; Boyd, R.J.; Reduction of hydrogen peroxide by glutathione peroxidase mimics: reaction mechanism and energetics. *J. Phys. Chem. A.*, **2010**, *114*, 1996.



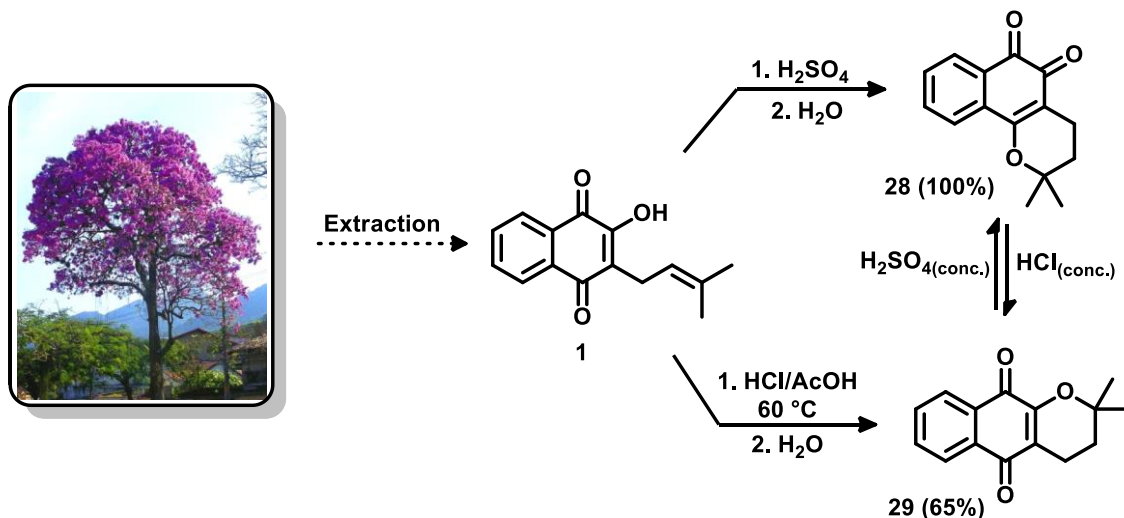
Scheme 2. Schematic representation of *p*-quinone metabolism, redox cycling and production of reactive species (adapted from reference **83**).

Lapachol (**1**) and its derivatives β -lapachone (**28**) and α -lapachone (**29**), are quinones that were originally isolated from the heartwood of trees of the Bignoniaceae family (*Tabebuia sp*) for example, the Brazilian Ipê trees.⁸⁹ The chemistry of these compounds, referred as “lapachones”, was initially investigated in the beginning of the twentieth century by the chemist Samuel Hooker, showing that β -lapachone (**28**) and α -lapachone (**29**) are found in small portions in the extraction of lapachol, but by simple acid treatment these molecules can be obtained in good to excellent yields (Scheme 3).⁹⁰ Among the three lapachones, β -lapachone (**28**) showed bioactivity against epimastigote forms of *T. cruzi* but, unfortunately, no trypanocidal effect was observed in blood

89. Hussain, H.; Krohn, K.; Uddin Ahmad, V.U.; Miana, G.A.; Greend, I.R. Lapachol: An overview. *Arkivoc*, **2007**, 2, 145.

90. Hooker, S.C.; Steyermark, A.; Conversion of *ortho* into *para*, and of *para* into *ortho* quinone derivatives. Part IV. Synthesis of furan derivatives of α - and β -naphthoquinones. *J. Am. Chem. Soc.*, **1936**, 58, 1202.

contaminated with the parasite, suggesting that β -lapachone could be inactivated either by reduction in the presence of oxyhaemoglobin.⁹¹



Scheme 3. Ipê tree, lapachol (**1**), β -lapachone (**28**) and α -lapachone (**29**), synthesis and conversion.

Among other molecules extracted from natural sources, purpurin (**30**), a trihydroxylated anthraquinone extracted from the roots of *Rubia tinctorum*, showed *in vitro* activity against trypomastigotes forms 1.5 higher than crystal violet (**27**) ($IC_{50} = 536 \pm 3 \mu M$).⁹² From a series of 1,4-naphthoquinones isolated from *Calceolaria sessilis*, (-)-2,3,3-trimethyl-2,3-dihydronaphtho[2,3-*b*]furan-4,9-quinone (**31**) showed high cytotoxicity against epimastigote strains ($IC_{50} = 2.1 \pm 0.2 \mu M$).⁹³ The polyprenylated benzoquinone 7-epiclusianone (**32**) was highly active in *in vitro* assays against trypomastigote forms of *T. cruzi*, being 29 times more active than crystal violet (**27**), being considered a promising candidate for use as a chemoprophylactic agent (Figure 13).⁹⁴

91. Pinto, A.V.; de Castro, S.L.; The trypanocidal activity of naphthoquinones: a review. *Molecules*, **2009**, *14*, 4570.

92. De Castro, S.L.; Pinto, M.C.F.R.; Pinto, A.V.; Screening of natural and synthetic drugs against *Trypanosoma cruzi*: establishing a structure/activity relationship. *Microbios*, **1994**, *78*, 83.

93. Morello, A.; Pavani, M.; Garbarino, J.A.; Chamy, M.C.; Frey, C.; Mantilla, J.; Guerrero, A.; Repetto, Y.; Ferreira, J.; Effects and mode of action of 1,4-naphthoquinones isolated from *Calceolaria sessilis* on tumoral cells and trypanosoma parasites. *Comp. Biochem. Physiol.*, **1995**, *112*, 119.

94. Alves, T.M.A.; Alves, R.O.; Romanha, A.J.; dos Santos, M.H.; Nagem, T.J.; Zani, C.L.; Biological activities of 7-epiclusianone. *J. Nat. Prod.*, **1999**, *62*, 369.

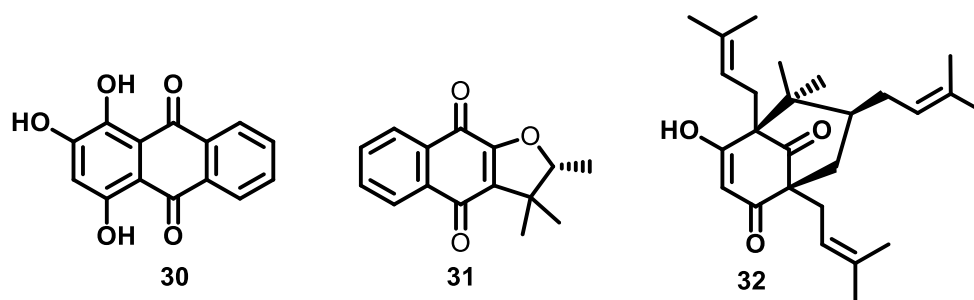


Figure 13. Purpurin (**30**), (-)-2,3,3-trimethyl-2-3-dihydronaphtho[2,3-*b*]furan-4,9-quinone (**31**) and 7-epiclusianone (**32**).

The naphthoquinone dimer diospyrin (**33**) can be isolated from the stem bark of the plant *Diospyros montana*, and is well known for his bioactivity against Ehrlich Ascites Carcinoma (E.A.C.).⁹⁵ By doing simple modifications in the A ring of these structures, derivatives **34** and **35** were synthesised and the three substances were tested *in vitro* against intracellular amastigotes and extracellular trypomastigotes forms of *T. cruzi*, showing that improvement of antitrypanosomal activities could be brought by doing simple changes in diospyrin (**33**) hydroxy group (Figure 14).⁹⁶

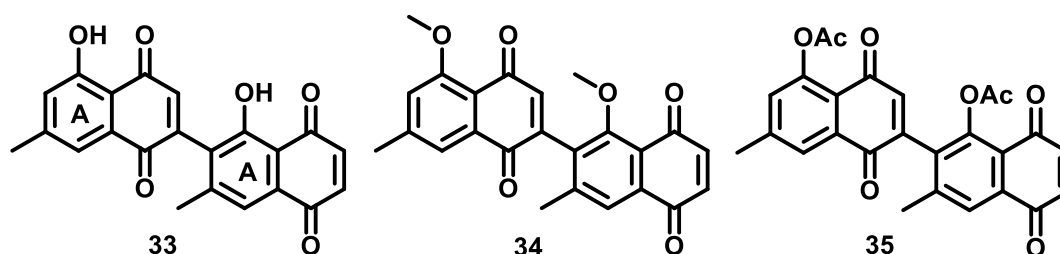


Figure 14. Diospyrin (**33**) and derivatives (**34**) and (**35**).

The plant *Dracocephalum komarovi*, called “buzbosh” by the native folk in Uzbekistan, is a common bush that grows in the West Tien Shan mountain system, being commonly consumed as a tea to treat inflammatory diseases and hypertonia.⁹⁷ Kiuchi and co-workers have founded that the plants extracts contains two major substances, dracocephalone (**36**) and komaroviquinone (**37**), that showed moderate

95. Hazra, B.; Sur, P.; Roy, D.K.; Sur, B.; Banerjee, A.; Biological activity of diospyrin towards Ehrlich Ascites Carcinoma in swiss A mice. *Planta Med.*, **1984**, *50*, 295.

96. Yardley, V.; Croft, S.; *In vitro* activity of diospyrin and derivatives against *Leishmania donovani*, *Trypanosoma cruzi* and *Trypanosoma brucei brucei*. *Phytother. Res.*, **1996**, *10*, 559.

97. Vvedenski, A.I.; Flora Uzbekistana; *Editio Academiae Scientiarum UzSSR: Tashkent*, **1961**, *5*, 313.

activity against epimastigote forms of *T. cruzi*.⁹⁸ Later on, Urade and collaborators showed that komaroviquinone (**37**) presented IC₅₀/24h values of 9 nM, which is 33 and 190 times lower than nifurtimox (**25**) and benznidazole (**26**), respectively. Furthermore, **37** showed low toxicity against KB 3-1 and HeLa human cells, making this compound one of the most promising candidate for drug development to use in Chagas disease therapy (Figure 15).⁹⁹

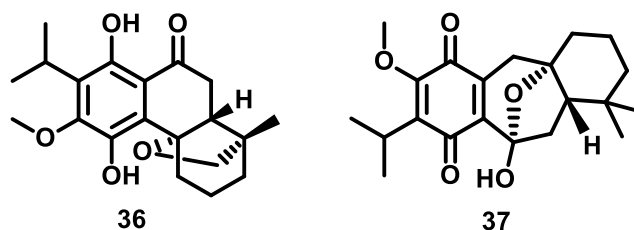


Figure 15. Dracocephalone (**36**) and komaroviquinone (**37**).

1.3. Metal Catalyzed C-H Bond Activation

The occurrence of a chemical reaction is characterized by bond cleavage, migration, substitution and addition events to form new species.¹⁰⁰ These reactional events depend on low bonds energetic values to occur. Bonds with this characteristic are known as activated bonds in organic synthesis.¹⁰¹

As consequence, the transformation of C-H bonds represents a challenge to modern synthetic chemists due to the difficulties in the development of practical, selective and efficient methodologies that undergoes this kind of process.¹⁰² The

98. Uchiyama, N.; Kiuchi, F.; Ito, M.; Honda, G.; Takeda, Y.; Khodzhimatov, O.K.; Ashurmetov, O.A.; New icetexane and 20-norabietane diterpenes with trypanocidal activity from *Dracocephalum komarovi*. *J. Nat. Prod.*, **2003**, *66*, 128.

99. Uchiyama, N.; Kabututu, Z.; Kubata, B.K.; Kiuchi, F.; Ito, M.; Nakajima-Shimada, J.; Aoki, T.; Ohkubo, K.; Fukuzumi, S.; Martin, S.Q.; Honda, G.; Urade, Y.; Antichagasic activity of komaroviquinone is due to generation of reactive oxygen species catalyzed by *Trypanosoma cruzi* old yellow enzyme. *Antimicrob. Agents Chemother.*, **2005**, *49*, 5123.

100. Azambuja, F.; Correia, C.R.D.; O desafio da ativação das ligações C-H em síntese orgânica. *Quím. Nova*, **2011**, *34*, 1779.

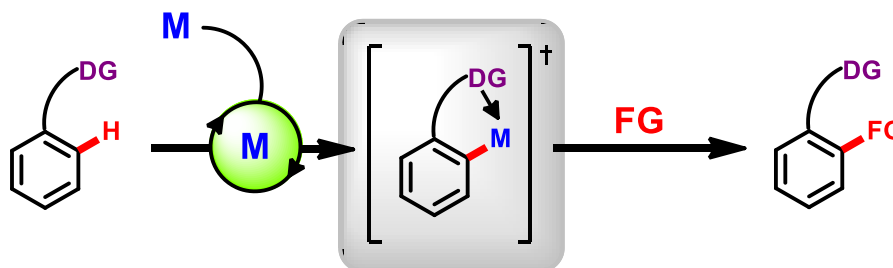
101. Shilov, A.E.; Shul'pin, G.B.; Activation of C-H bonds by metal complexes. *Chem. Rev.*, **1997**, *97*, 2879.

102. Crabtree, R.H.; Introduction to selective functionalization of C-H bonds. *Chem. Rev.*, **2010**, *110*, 575.

breaking of a C-H bond requires about 410 kJmol^{-1} of energy, meaning that this bond is thermodynamically stable and kinetically inert, considered a deactivated bond.¹⁰³

By definition, C-H bond activation is a process that occurs by direct conversion of a C-H bond into a C-R bond, without the need of previous functionalization.¹⁰⁴ As consequence, this process leads to a substantial reduction in the synthetic steps of a former synthesis.¹⁰⁵ The necessity for the development of new methodologies to provide substituted heterocycles in a practical, reliable, atom economic and “green” process, usually in an one step route, with high yields and broad scope, makes the C-H activation reactions to emerge as a powerful alternative in order to achieve these goals.¹⁰⁶

The term “metal catalysed C-H bond activation” is used to describe reactions between a C-H bond and a transition metal complex, generating discrete intermediates.¹⁰⁷ The substrates must have groups with free electron pairs to act as directing groups (DG) to coordinate with the metal and selectively activate the desirable C-H bond, an event known as metalation. Then, a functional group (FG) is transferred to the reaction site to achieve functionalization (Scheme 4).¹⁰⁸



Scheme 4. General scheme for metal catalysed C-H bond activation reactions (adapted from reference **105**).

103. Gunay, A.; Theopold, K.H.; C-H bond activations by metal oxo compounds. *Chem. Rev.*, **2010**, *110*, 1060.

104. Wencel-Delord, J.; Glorius, F.; C-H bond activation enables the rapid construction and late-stage diversification of functional molecules. *Nat Chem.*, **2013**, *5*, 369.

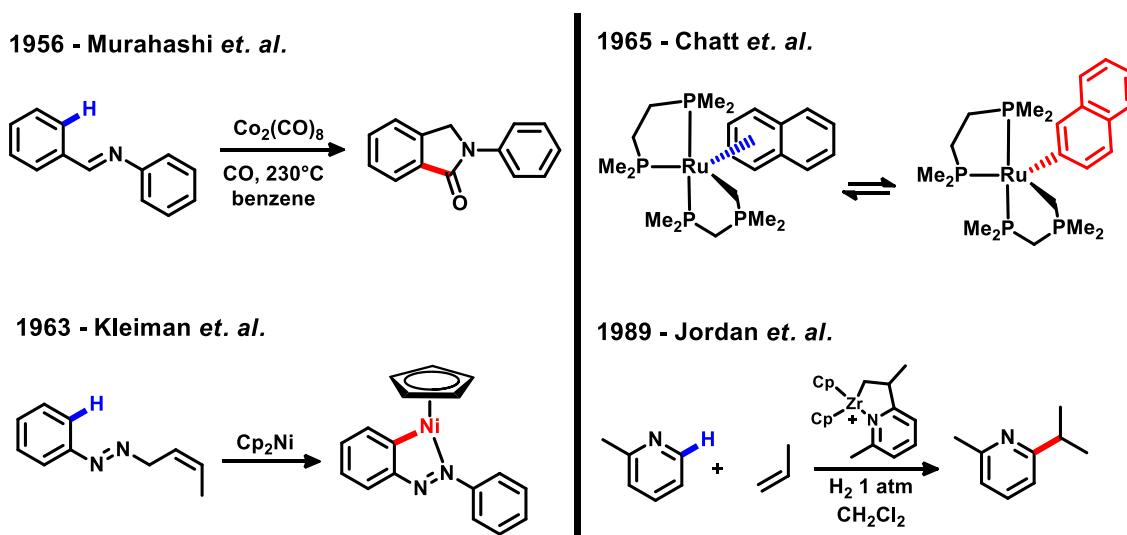
105. Ghorai, D.; Choudhury, J.; Exploring a unique reactivity of *N*-heterocyclic carbenes (NHC) in rhodium(III)-catalyzed intermolecular C-H activation/annulation. *Chem. Comm.*, **2014**, *50*, 15159.

106. Dyker, G.; *Handbook of C-H transformations: applications in organic synthesis*, Wiley-VCH: **2005**.

107. Hashiguchi, B.G.; Bischof, S.M.; Konnick, M.M.; Periana, R.A.; Designing catalysts for functionalization of unactivated C-H bonds based on the C-H activation reaction. *Acc. Chem. Res.*, **2012**, *45*, 885.

108. Chepaikin, E.G.; Homogeneous catalysis in the oxidative functionalization of alkanes in protic media. *Russ. Chem. Rev.*, **2011**, *80*, 363.

The first idea involving the use of a metal to promote C-H activation can be traced back to 1956, when Murahashi and co-workers reported a carbonyl addition/ring-closure reaction of *N*-benzylideneanilines promoted by $\text{Co}_2(\text{CO})_8$, using carbon monoxide atmosphere at high temperatures.¹⁰⁹ Almost seven years later, Kleiman and Dubeck described the preparation of cyclopentadienyl[*o*-(phenylazo)phenyl]nickel complex with a unusual C-Ni bond, probably one of the first examples of metalation involving nickel.¹¹⁰ Next, the work of Chatt and Davidson is regarded as the pioneer of metal promoted C-H activation reaction, reporting in 1965 the insertion of a Ru(0) complex in a naphthalene C-H bond.¹¹¹ At last, Jordan and collaborators described the C-H coupling of propene and α -picoline catalyzed by a zirconium complex, without the need of further functionalization (Scheme 5).¹¹²



Scheme 5. Historical background of metal catalyzed C-H bond activation reactions.

The contributions of Murai and Kakiuchi are known to mark the beginning of a long series of related works that explore the C-H activation concept, by reporting the

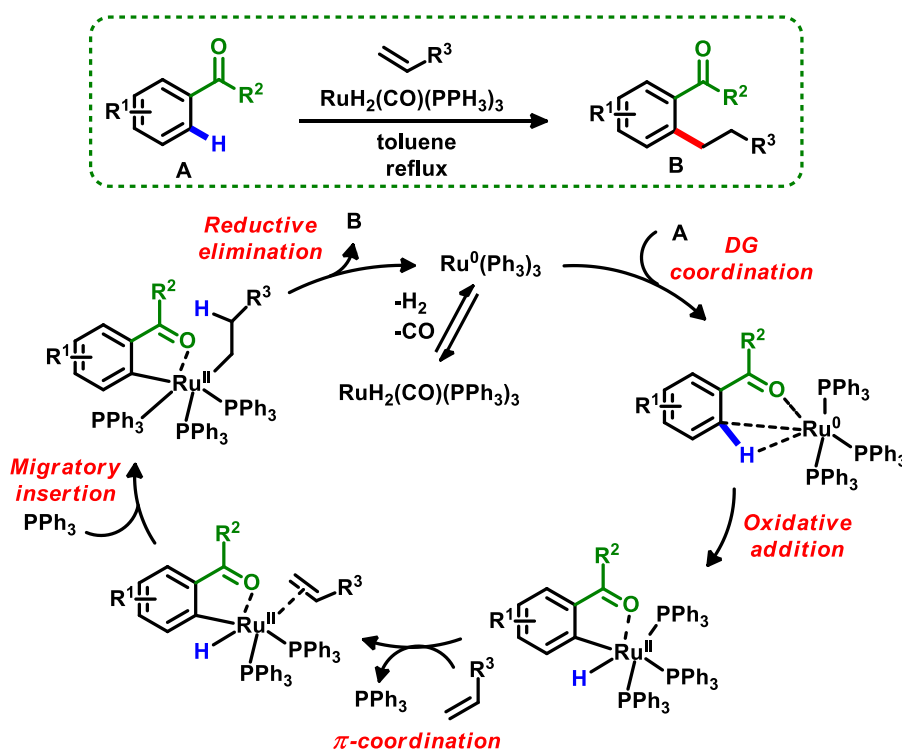
109. Murahashi, S.; Horie, S.; The reaction of azobenzene and carbon monoxide. *J. Am. Chem. Soc.*, **1956**, *78*, 4816.

110. Kleiman, J.P.; Dubeck, M.; The preparation of cyclopentadienyl[*o*-(phenylazo)phenyl]nickel. *J. Am. Chem. Soc.*, **1963**, *85*, 1544.

111. Chatt, J.; Davidson, J.M.; The tautomerism of arene and ditertiary phosphine complexes of ruthenium(0), and the preparation of new types of hydrido complexes of ruthenium(II). *J. Chem. Soc. A*, **1965**, 843.

112. Jordan, R.F.; Taylor, D.F.; Zirconium-catalyzed coupling of propene and α -picoline. *J. Am. Chem. Soc.*, **1989**, *111*, 778.

Ru(II) catalyzed insertion of olefins into C-H bonds of aromatic ketones.¹¹³ The reaction mechanism was later explored by Morokuma in 2000 and suggests that the active ruthenium specie is $\text{Ru}^0(\text{PPh}_3)_3$ (14 valence electrons), which is generated *in situ* by H_2 extrusion by heating. Then, after the initial coordination of the directing group (carbonyl), oxidative addition happens via directed nucleophilic attack of the Ru(0) specie into the *ortho*-carbon atom of the aromatic ketone. Subsequently, alkene coordination to the ruthenium center, followed by migratory insertion and reductive elimination provides the product (Scheme 6).¹¹⁴



Scheme 6. Murai pioneer work and catalytic cycle investigated by Morokuma.

113. (a) Kakiuchi, F.; Murai, S.; Catalytic C–H/olefin coupling. *Acc. Chem. Res.*, **2002**, *35*, 826. (b) Sonoda, M.; Kakiuchi, F.; Chatani, N.; Murai, S.; Ruthenium-catalyzed addition of carbon–hydrogen bonds in aromatic ketones to olefins. The effect of various substituents at the aromatic ring. *Bull. Chem. Soc. Jpn.*, **1997**, *70*, 3117. (c) Kakiuchi, F.; Sekine, S.; Tanaka, Y.; Kamatani, A.; Sonoda, M.; Chatani, N.; Murai, S.; Catalytic addition of aromatic carbon–hydrogen bonds to olefins with the aid of ruthenium complexes. *Bull. Chem. Soc. Jpn.*, **1995**, *68*, 62. (d) Murai, S.; Kakiuchi, F.; Sekine, S.; Tanaka, Y.; Kamatani, A.; Sonoda, M.; Chatani, N.; Efficient catalytic addition of aromatic carbon-hydrogen bonds to olefins. *Nature*, **1993**, *366*, 529.

114. (a) Matsubara, T.; Koga, N.; Musaev, D.G.; Morokuma, K.; Density functional study on highly *ortho*-selective addition of an aromatic C–H bond to olefins catalyzed by a $\text{Ru}(\text{H})_2(\text{CO})(\text{PR}^3)_3$ complex. *Organometallics*, **2000**, *19*, 2318. (b) Matsubara, T.; Koga, N.; Musaev, D.G.; Morokuma, K.; Density functional study on activation of *ortho*-C–H bond in aromatic ketone by Ru complex. Role of unusual five-coordinated d^6 metallacycle intermediate with agostic interaction. *J. Am. Chem. Soc.*, **1998**, *120*, 12692.

Metal promoted C-H activation/functionalization processes can be mechanistically classified in two main classes: outer and inner sphere mechanisms. The first one involves the initial insertion of a C-H bond into the ligand of a transition metal complex (outer sphere mechanism), while the second is characterized by the coordination of the C-H bond to the metal center to create an organometallic complex (inner sphere mechanism).¹¹⁵ Examples of outer sphere mechanisms are the reaction of metal-carbenes and metal-nitrenes with C-H bonds.¹¹⁶ *In order to maintain the objectivity of this manuscript, only inner sphere mechanisms will be discussed forward.*

Inner sphere mechanisms can be first classified according to the main direction of the charge transfer (CT) involved in the C-H activation step, it is important emphasizing that these charge transfers mutually contribute to weaken and eventually break the C-H bond (Scheme 7):¹¹⁷

. When the main CT occurs from the filled $\sigma(\text{C-H})$ orbital to an empty metal-based d orbital, the mechanism is classified as *electrophilic*; it happens when electron poor late transition metals with high oxidation states (Pd^{II} , Pt^{II} , Rh^{III} , Ir^{III} , Ru^{II}) are used.¹¹⁸

. If the main CT occurs from a metal-based occupied d orbital to the σ^* orbital of the C-H bond, the mechanism is classified as *nucleophilic*; it happens when electron-rich transition metal complexes with high energy $d\pi$ and $d\sigma$ orbitals (Pd^0 , Au^0 , Rh^{I} , Cu^{I} , Ru^0) are used.¹¹⁹

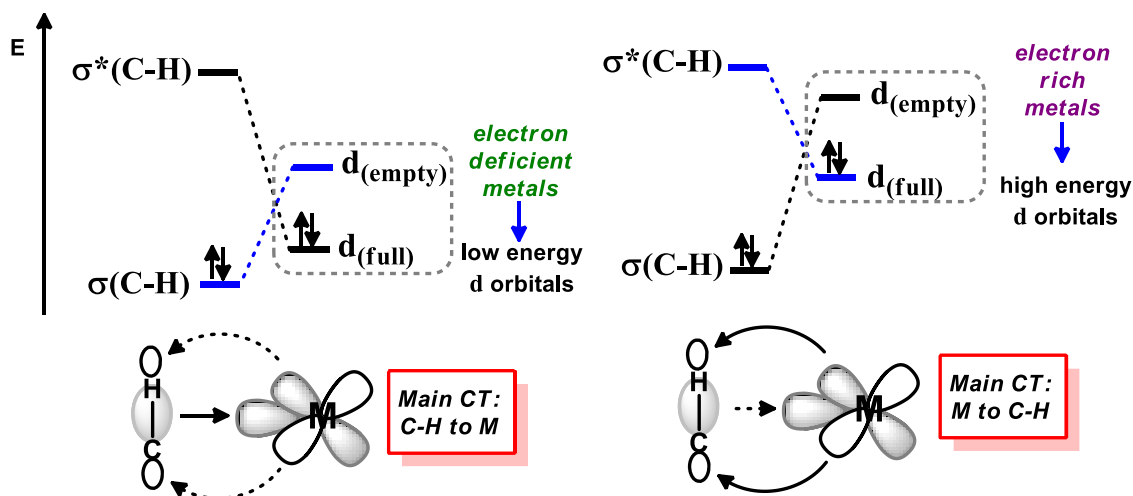
115. Roudesly, F.; Oble, J.; Poli, G.; Metal-catalyzed C-H activation/functionalization: the fundamentals. *J. Mol. Catal. A: Chem.*, **2017**, 426, 275.

116. Gutekunst, W.R.; baran, P.S.; C-H functionalization logic in total synthesis. *Chem Soc Rev.*, **2011**, 40, 1976.

117. Ess, D.H.; Goddard III, W.A.; Periana, R.A.; Electrophilic, ambiphilic, and nucleophilic C-H bond activation: understanding the electronic continuum of C-H bond activation through transition-state and reaction pathway interaction energy decompositions. *Organometallics*, **2010**, 29, 6459.

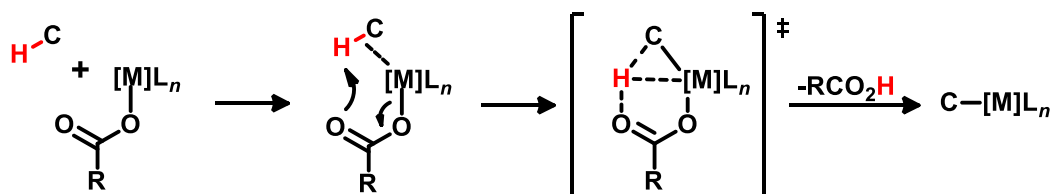
118. Davies, D.L.; Donald, S.M.A.; Al-Duaij, O.; MacGregor, S.A.; Polleth, M.; Electrophilic C-H activation at $\{\text{Cp}^*\text{Ir}\}$: ancillary-ligand control of the mechanism of C-H activation. *J. Am. Chem. Soc.*, **2006**, 128, 4210.

119. Hashiguchi, B.G.; Young, K.J.H.; Yousufuddin, M.; Goddard III, W.A.; Periana, R.A.; Acceleration of nucleophilic C-H activation by strongly basic solvents. *J. Am. Chem. Soc.*, **2010**, 132, 12542.



Scheme 7. Frontier orbitals interactions for electrophilic (left) and nucleophilic (right) mechanisms (adapted from reference **115**).

Both nucleophilic and electrophilic mechanisms can be characterized in more specific pathways, depending on the metal center, steric and electronic properties of the metal environment and the substrates involved in the transformations.¹²⁰ For example, when lone pair bearing ligands are abundant in reaction media (usually oxygen based, most commonly carboxylates), it promotes hydrogen bonding interactions between the H-C proton, increasing the C-H bond electron density and favouring metalation process (Scheme 8). This pathway can be classified as concerted metalation-deprotonation (CMD) and occurs when electron poor transition metals, electrophilic substrates and acetate salts are employed. It presents a 6 member intermediate that lowers the energy of the transition state (Scheme 8).¹²¹

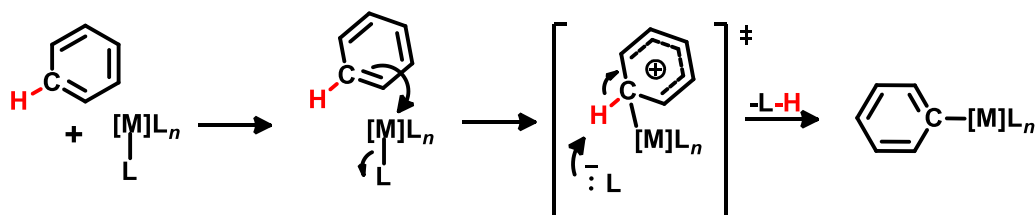


Scheme 8. Concerted metalation-deprotonation (CMD) pathway (adapted from reference **115**).

120. Gorelsky, S.I.; Lapointe, D.; Fagnou, K.; Analysis of the concerted metalation-deprotonation mechanism in palladium-catalyzed direct arylation across a broad range of aromatic substrates. *J. Am. Chem. Soc.*, **2008**, *130*, 10848.

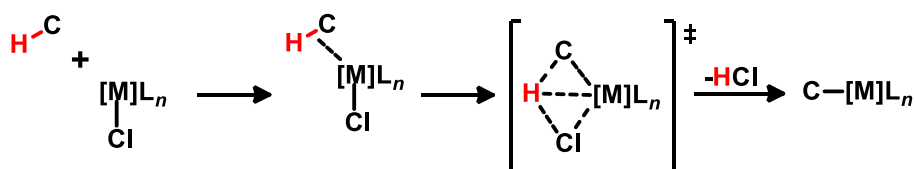
121. Davies, D.L.; Macgregor, S.A.; McMullin, C.L.; Computational studies of carboxylate-assisted C-H activation and functionalization at group 8–10 transition metal centers. *Chem. Rev.*, **2017**, *117*, 8649.

Electron poor transition metals also promote another kind of electrophilic mechanism, especially when electron rich aryl based substrates are employed.¹²² The metalation event occurs by the attack of the aromatic ring to the metal center, generating a Wheland intermediate, similar to electrophilic aromatic substitution reactions, being known as electrophilic aromatic substitution (S_eAr) (Scheme 9).¹²³



Scheme 9. Electrophilic aromatic substitution (S_eAr) pathway (adapted from reference 115).

Metal complexes with intermediate oxidation states like Rh^{II} can promote the formation of σ -complexes with C-H bonds, which undergo dynamic rearrangements to promote metalation.¹²⁴ This type of C-H bond cleavage is represented by a 4 membered transition state and can be classified as σ -complex-assisted metathesis (σ -CAM), and it is facilitated by complexes that contain back- μ -donation (Scheme 10).¹²⁵



Scheme 10. σ -complex-assisted metathesis (σ -CAM) pathway (adapted from reference 115).

122. Oxgaard, J.; Tenn, III, W.J.; Nielsen, R.J.; Periana, R.A.; Goddard, III, W.A.; Mechanistic analysis of iridium heteroatom C-H activation: evidence for an internal electrophilic substitution mechanism. *Organometallics*, **2007**, *26*, 1565.

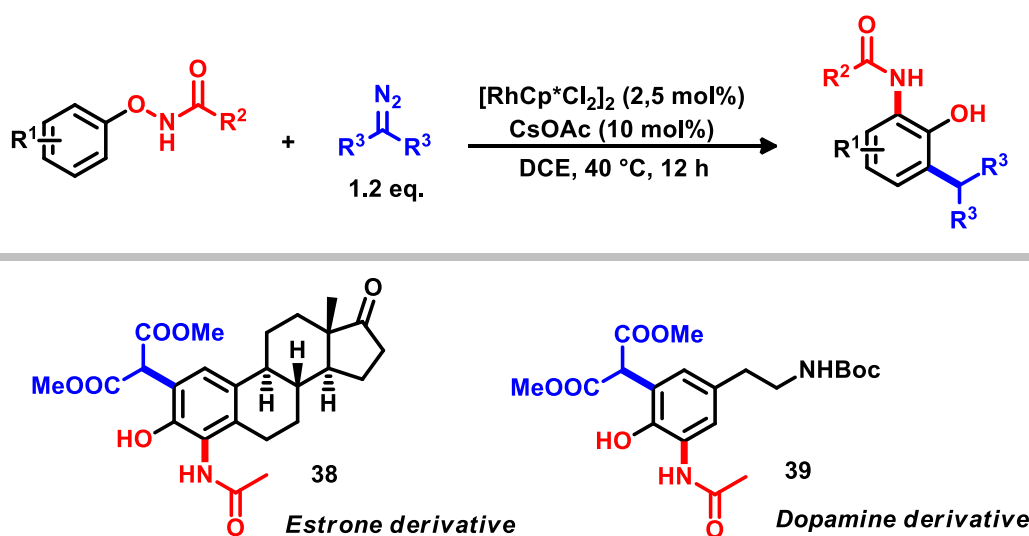
123. Stokes, B.J.; Dong, H.; Leslie, B.E.; Pumphrey, A.L.; Driver, T.G.; Intramolecular C-H amination reactions: exploitation of the $Rh_2(II)$ -catalyzed decomposition of azidoacrylates. *J. Am. Chem. Soc.*, **2007**, *129*, 7500.

124. Lin, Y.; Zhu, L.; Lan, Y.; Rao, Y.; Development of a rhodium(II)-catalyzed chemoselective $C(sp^3)$ -H oxygenation. *Chem. Eur. J.*, **2015**, *21*, 14937.

125. Perutz, R.N.; Sabo-Etienne, S.; The σ -CAM mechanism: σ complexes as the basis of σ -bond metathesis at late-transition-metal centers. *Angew. Chem. Int. Ed.*, **2007**, *46*, 2578.

Apart from the mechanistic insights, it is important to emphasize that transition-metal mediated C-H activation processes occupy a commanding position and has revolutionized the synthetic field in an unprecedented manner, especially in the late stage functionalization of natural products and, consequently, total synthesis.¹²⁶ To emphasize the importance of such transformations, some pioneer examples are illustrated next.

Zhou and Zhu have showed that double *ortho*-functionalization of phenols can be achieved by reaction of *N*-phenoxyacetamides with diazo compounds catalyzed by Rh^{III}Cp* catalyst in excellent yields. The reaction tolerates even bulky groups in the aromatic ring like isopropyl and several *N*-phenoxyacetamides were used. The robustness of the reaction was successfully proven by use of complex biologically interesting substrates like estrone (**38**) and a dopamine derivative (**39**) (Scheme 11).¹²⁷



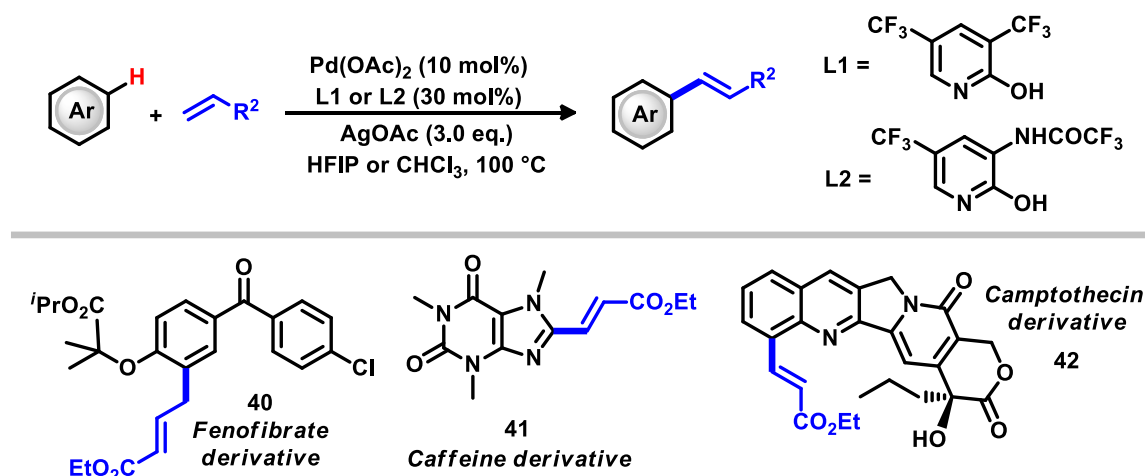
Scheme 11. Rhodium catalyzed double *ortho*-functionalization of phenols by Zhou and Zhu.

Yu and co-workers developed a milestone ligand-accelerated non-directed C–H activation protocol that enables the functionalization of a large range of electron deficient and electron rich arenes. The new reaction tolerates the use of a large range of

126. Chen, D. Y.-K.; Youn, S.W.; C-H activation: a complementary tool in the total synthesis of complex natural products. *Chem. Eur. J.*, **2012**, *18*, 9452.

127. Wu, Y.; Chen, Z.; Yang, Y.; Zhu, W.; Zhou, B.; Rh(III)-catalyzed redox-neutral unsymmetrical C-H alkylation and amidation reactions of *N*-phenoxyacetamides. *J. Am. Chem. Soc.*, **2018**, *140*, 42.

olefins, simple arenes and heterocycles, with high regioselectivity and good to excellent yields. The combination of palladium acetate and special bidentate ligands (**L1** and **L2**) provided the functionalization of natural products like fenofibrate (**40**), caffeine (derivative **41**) and camptothecin (derivative **42**) (Scheme 12).¹²⁸

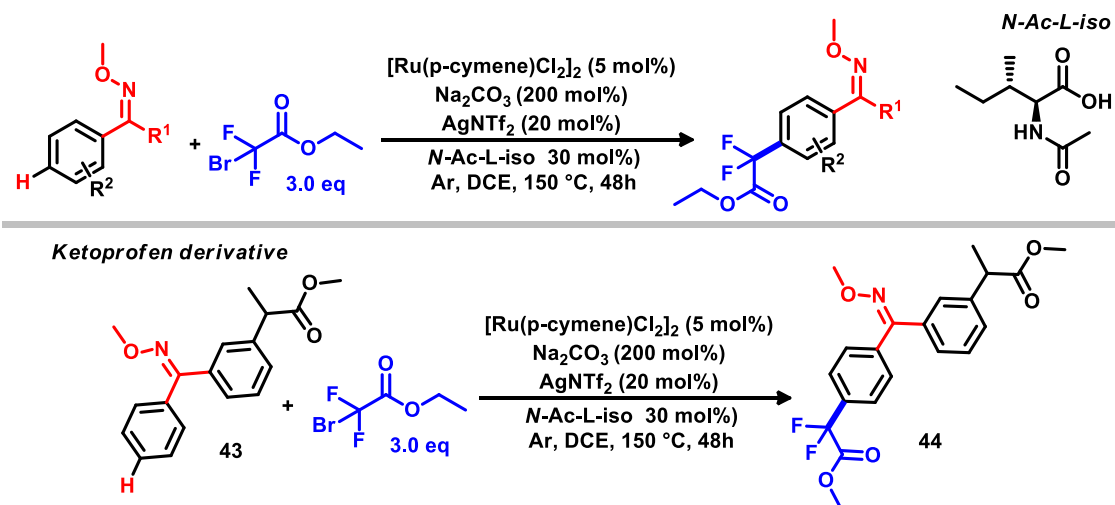


Scheme 12. Palladium catalyzed ligand-accelerated non-directed C–H activation by Yu and co-workers.

Zhao and Lan report aimed for the highly selective ruthenium(II)-catalyzed C-H difluoromethylation of ketoximes in moderate to good yields.¹²⁹ The authors have achieved *para*-regioselectivity by using a combination of substituted oxime ester as the directing group and a special amino acid *N*-Ac-L-iso derivative as the ligand. Further reactional scope investigation showed that the reaction tolerates a large quantity of different oximes, and robustness was proved by modifying a ketoprofen derivative (**43**) in moderate yield. Mechanistic studies like deuterium labelling experiments, synthesis of intermediates and radical scavenging with TEMPO, allied with DFT studies suggests that a free-radical pathway is involved in the *para*-selective difluoromethylation reaction (Scheme 13).

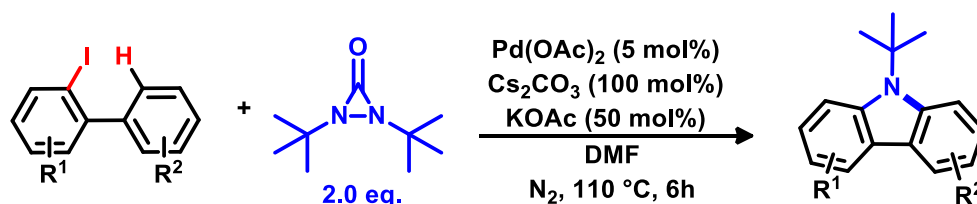
128. Wang, P.; Verma, P.; Xia, G.; Shi, J.; Qiao, J.X.; Tao, S.; Cheng, P.T.W.; Poss, M.A.; Farmer, M.E.; Yeung, K.-S.; Yu, J.-Q.; Ligand-accelerated non-directed C–H functionalization of arenes. *Nature*, **2017**, *55*, 489.

129. Yuan, C.; Zhu, L.; Zeng, R.; Lan, Y.; Zhao, Y.; Ruthenium(II)-catalyzed C-H difluoromethylation of ketoximes: tuning the regioselectivity from the *meta* to the *para* position. *Angew. Chem. Int. Ed.*, **2018**, *57*, 1277.



Scheme 13. Ruthenium(II)-catalyzed C-H *para*-difluoromethylation of ketoximes.

The synthesis of carbazoles from 2-Iodobiphenyls was described by Zhang and co-workers utilizing palladium-catalyzed C–H activation/amination with diaziridinone, in a two-step process involving a tandem C–H activation/dual C–N bond formation sequence.¹³⁰ The reactional scope of several substituted 2-Iodobiphenyls was presented in good to excellent yields (Scheme 14).

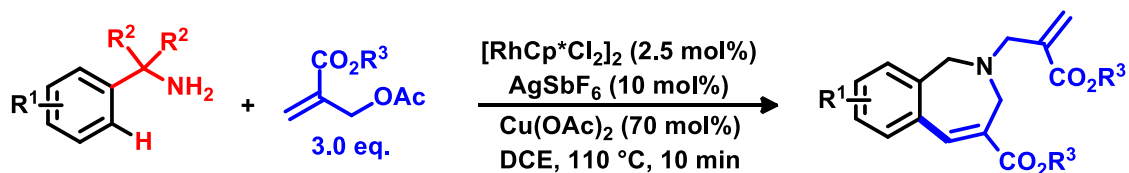


Scheme 14. Palladium-catalyzed tandem C–H activation/dual C–N bond formation.

Hong, Park and Kim reported a coupling between benzylamines and Morita-Bailys-Hillman adducts under rhodium(III) catalysis to achieve the synthesis of 2-benzazepines via C-H activation.¹³¹ The reaction proceeded smoothly over a short period of ten minutes, presenting a broad scope with yields varying from 31% to 80%, depending on the benzylamines substituents (Scheme 15).

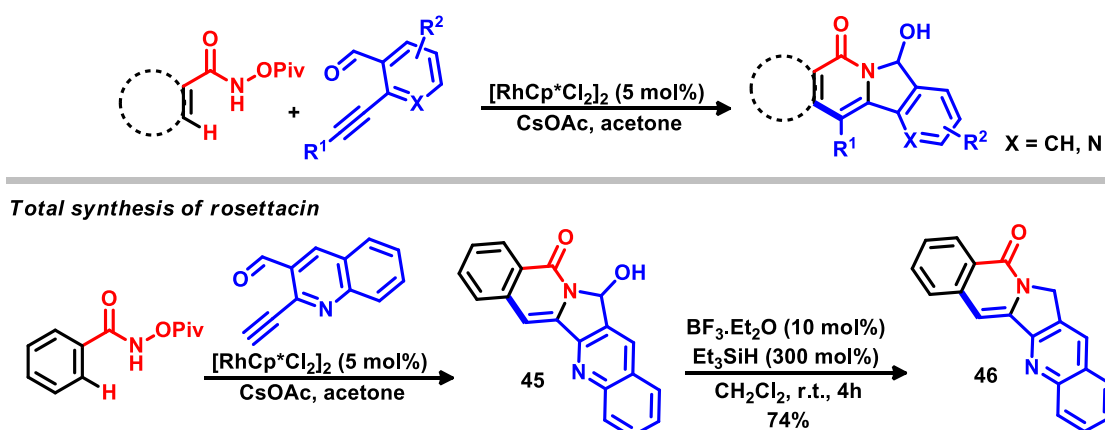
130. Shao, C.; Zhou, B.; Wu, Z.; Ji, X.; Zhang, Y.; Synthesis of carbazoles from 2-iodobiphenyls by palladium-catalyzed C–H activation and amination with diaziridinone. *Adv. Synth. Catal.*, **2018**, *360*, 887.

131. Pandey, A.K.; Han, S.H.; Mishra, N.K.; Kang, D.; Lee, S.H.; Chun, R.; Hong, S.; Park, J.S.; Kim, I.S.; Synthesis of 2-benzazepines from benzylamines and MBH adducts under rhodium(III) catalysis via C(sp²)–H functionalization. *ACS Catal.*, **2018**, *8*, 742.



Scheme 15. Synthesis of 2-benzazepines via rhodium(III) C-H activation.

Reddy and Mallesh reported the total synthesis of rosettacin (**46**) by Rh(III)-catalyzed cascade annulations via C–H activation utilizing *N*-(pivaloyloxy)-benzamides and 2-alkynyl aldehydes.¹³² The reaction involves a sequential isoquinolone formation followed by addition of NH portion to the aldehyde, leading to an unprecedented facile synthesis of 7-hydroxyisoindolo[2,1-*b*]isoquinolin-5(7*H*)-ones. Such important finding led to a total synthesis in only two steps in good yields (Scheme 16).



Scheme 16. Rh(III)-catalyzed cascade annulations and rosettacin (**46**) total synthesis.

132. Reddy, C.R.; Mallesh, K.; Rh(III)-catalyzed cascade annulations to access isoindolo[2,1-*b*]isoquinolin-5(7*H*)-ones via C–H activation: Synthesis of rosettacin. *Org. Lett.*, **2018**, *20*, 150.

2. Motivation

Over the years our research group have been concentrating efforts in the development of new strategies for the modification of natural occurring quinones, especially naphthoquinones, aiming in the achievement of more potent and selective molecules for application in the therapy of several illnesses, especially Chagas disease¹³³ and cancer.¹³⁴

Extensive literature research showed that the great majority of works related to 1,4-naphthoquinones are based on the modification of the conjugated di-carbonyl ring of these structures (referenced as *B-ring*), especially in the positions 2 and 3, by use of methodologies based in C-H functionalizations,¹³⁵ Michael additions,¹³⁶ Diels-Alder reactions¹³⁷ and halogenations.¹³⁸ Benzenoid ring modifications (referenced as *A-ring*) are often rare and represent a major challenge in quinone chemistry. A classical strategy

133. (a) de Souza, C.M.; Silva, R.C.; Fernandes, P.O.; de Souza Filho, J.D.; Duarte, H.A.; Araujo, M.H.; de Simone, C.A.; de Castro, S.L.; Menna-Barreto, R.F.S.; Demicheli, C.P.; da Silva Júnior, E.N.; Cyclometalated ruthenium complexes from naturally occurring quinones: studies on their photophysical features, computational details and trypanocidal activity. *New J. Chem.*, **2017**, *41*, 3723. (b) Bahia, S.B.B.B.; Reis, W.J.; Jardim, G.A.M.; Souto, F.T.; de Simone, C.A.; Gatto, C.C.; Menna-Barreto, R.F.S.; de Castro, S.L.; Cavalcanti, B.C.; Pessoa, C.; Araujo, M.H.; da Silva Júnior, E.N.; Molecular hybridization as a powerful tool towards multitarget quinoidal systems: synthesis, trypanocidal and antitumor activities of naphthoquinone-based 5-iodo-1,4-disubstituted-, 1,4- and 1,5-disubstituted-1,2,3-triazoles. *Med. Chem. Commun.*, **2016**, *7*, 1555. (c) Jardim, G.A.M.; Reis, W.J.; Ribeiro, M.F.; Ottoni, F.M.; Alves, R.J.; Silva, T.L.; Goulart, M.O.F.; Braga, A.L.; Menna-Barreto, R.F.S.; Salomão, K.; de Castro, S.L.; da Silva Júnior, E.N.; On the investigation of hybrid quinones: synthesis, electrochemical studies and evaluation of trypanocidal activity. *RSC Adv.*, **2015**, *5*, 78047.

134. (a) Valença, W.O.; Baiju, T.V.; Brito, F.G.; Araujo, M.H.; Pessoa, C.; Cavalcanti, B.C.; de Simone, C.A.; Jacob, C.; Namboothiri, I.N.N.; da Silva Júnior, E.N.; Synthesis of quinone-based *N*-sulfonyl-1,2,3-triazoles: chemical reactivity of Rh(II) azavinyl carbenes and antitumor activity. *Chemistry Select*, **2017**, *2*, 4301. (b) Costa, M.P.; Feitosa, A.C.S.; Oliveira, F.C.E.; Cavalcanti, B.C.; Dias, G.G.; Caetano, E.W.S.; Sales, F.A.M.; Freire, V.N.; Di Fiore, S.; Fischer, R.; Ladeira, L.O.; da Silva Júnior, E.N.; Pessoa, C.; Encapsulation of *nor*- β -lapachone into poly(D,L)-lactide-co-glycolide (PLGA) microcapsules: full characterization, computational details and cytotoxic activity against human cancer cell lines. *Med. Chem. Commun.*, **2017**, *8*, 1993. (c) Cruz, E.H.G.; Silvers, M.A.; Jardim, G.A.M.; Resende, J.M.; Cavalcanti, B.C.; Bomfim, I.S.; Pessoa, C.; de Simone, C.A.; Botteselle, G.V.; Synthesis and antitumor activity of selenium-containing quinone-based triazoles possessing two redox centres, and their mechanistic insights. *Eur. J. Med. Chem.*, **2016**, *122*, 1.

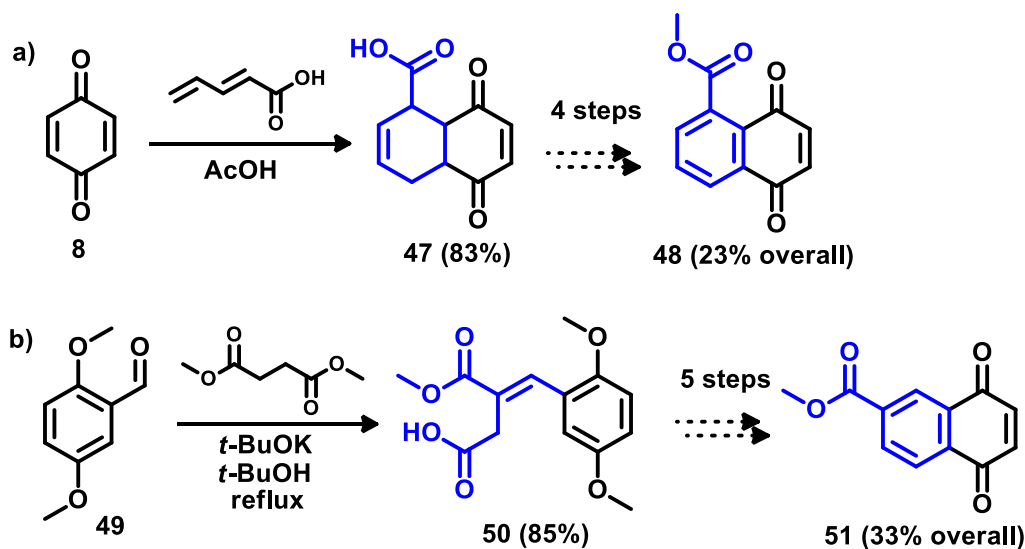
135. Lisboa, C.S.; Santos, V.G.; Vaz, B.G.; de Lucas, N.C.; Eberlin, M.N.; Garden, S.J.; C-H functionalization of 1,4-naphthoquinone by oxidative coupling with anilines in the presence of a catalytic quantity of copper(II) acetate. *J. Org. Chem.*, **2011**, *76*, 5264.

136. Yadav, J.S.; Reddy, B.V.S.; Swamy, T.; Shankar, K.S.; Green protocol for conjugate addition of amines to *p*-quinones accelerated by water. *Monatsh. Chem.*, **2008**, *139*, 1317.

137. Akinea, S.; Kusama, D.; Takatsukia, Y.; Nabeshima, T.; Synthesis of tetrafunctionalized pentiptycenequinones for construction of cyclic dimers with a cylindrical shape by boronate ester formation. *Tetrahedron Lett.*, **2015**, *56*, 4880.

138. Cheng, Y.; An, L.-K.; Wu, N.; Wang, X.-D.; Bu, X.-Z.; Huang, Z.-S.; Gu, L.-Q.; Synthesis, cytotoxic activities and structure-activity relationships of topoisomerase I inhibitors: indolizinoquinoline-5,12-dione derivatives. *Bioorg. Med. Chem.*, **2008**, *16*, 4617.

involves the full construction of the A-ring, followed by several oxidation steps. Ji and co-workers¹³⁹ constructed the A-ring starting from benzoquinone (Scheme 17a). A Diels-Alder reaction between 1,4-benzoquinone (**8**) and pentadienoic acid generated **47** in 83% yield. Several oxidation steps allowed the preparation of the A-ring substituted compound **48** in 23% overall yield. Gao *et. al.* started from the condensation between 2,5-dimethoxybenzaldehyde (**49**) and dimethyl succinate to afford **50** in 85% yield, and then alternating between reduction and oxidation steps to achieve **51** in 33% overall yield (Scheme 17b).¹⁴⁰



Scheme 17. A-ring construction strategy by Ji (17a) and Gao (17b) groups.

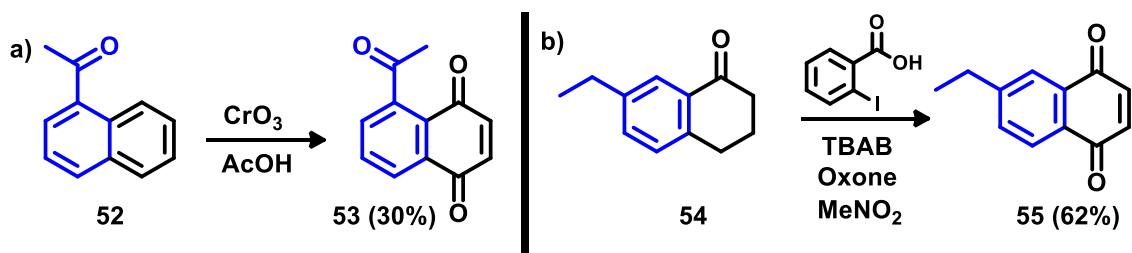
Direct oxidation of precursors was reported by Li *et. al.* (Scheme 18a), involving the oxidation of substituted naphthalenes with CrO_3 ¹⁴¹ and Zeng *et. al.* (Scheme 18b), which performed the oxidation of tetralones with Oxone[®]/2-iodobenzoic acid to achieve A-ring substituted 1,4-naphthoquinones.¹⁴² Both methods gave moderate to low yields with limited substrate scope, employing non-environmentally-friendly reagents like CrO_3 and large excesses of oxidants like Oxone[®] (Scheme 18).

139. Cai, J.; Li, Y.; Chen, J.; Wang, P.; Ji, M.; Novel and convenient synthesis of 5-benzoyl-1,4-naphthoquinone and its derivatives. *Res. Chem. Intermed.*, **2015**, *41*, 1.

140. Gust, D.; Moore, T.A.; Moore, A.; Seely, G.; Liddell, P.; Garrett, D.; Harding, L.O.; Ma, X.C.; Lee, S.; Gao, F.; A carotenoid-porphyrin-diquinone tetrad: synthesis, electrochemistry and photoinitiated electron transfer. *Tetrahedron*, **1989**, *45*, 4867.

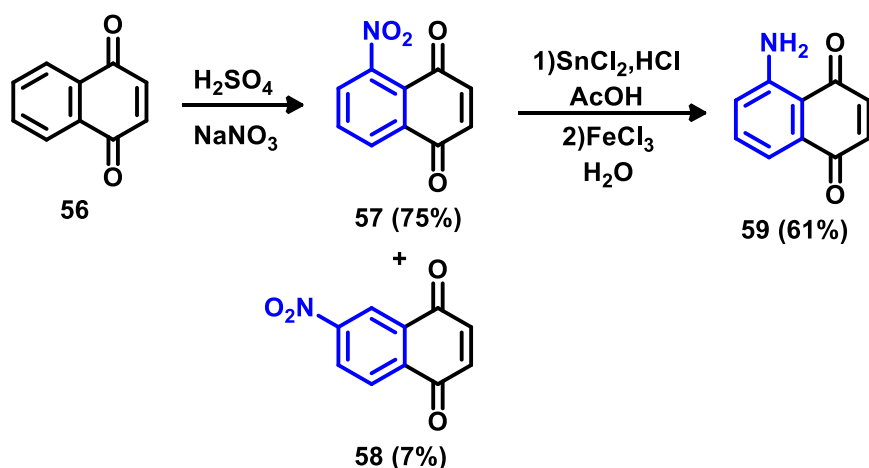
141. Bhasin, D.; Cisek, K.; Pandharkar, T.; Regan, N.; Li, C.; Pandit, B.; Linb, J.; Li, P.; Design, synthesis, and studies of small molecule STAT3 inhibitors. *Bioorg. Med. Chem. Lett.*, **2008**, *18*, 391.

142. Ren, J.; Lu, L.; Xu, J.; Yu, T.; Zeng, B.; Selective oxidation of 1-tetralones to 1,2-naphthoquinones with IBX and to 1,4-naphthoquinones with Oxone[®] and 2-iodobenzoic Acid. *Synthesis*, **2015**, *47*, 2270.



Scheme 18. Oxidation strategy by Li (18a) and Zeng (18b) groups.

A-ring functionalization by functional group interconversion was reported by Schartzberg in a three step process starting by nitration of 1,4-naphthoquinone (**56**) into 5-nitro-1,4-naphthoquinone (**57**), followed by reduction with $\text{SnCl}_2/\text{FeCl}_3$ (Scheme 19).¹⁴³

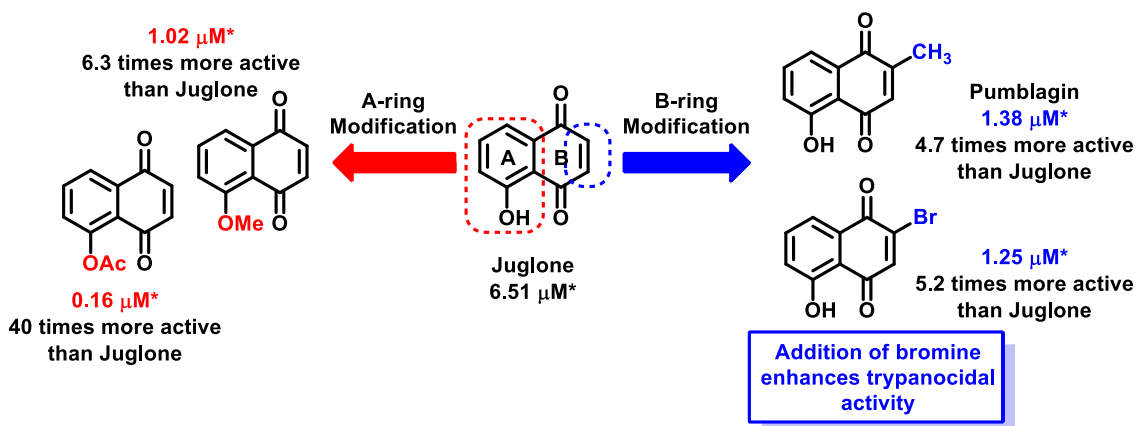


Scheme 19. A-ring functionalization strategy by Shvartsberg and co-workers.

Despite the lack of methods for direct functionalization of 1,4-naphthoquinones, the biological potential for these structures is well known, and as an example of 1,4-naphthoquinones with remarkable trypanocidal activity, the report of Salomão and co-workers can be considered a major evidence that A-ring and B-ring substituted naphthoquinones can kill *T. cruzi* and highlight the importance of synthesizing and

143. Ivashkina, N.V.; Romanov, V.S.; Moroz, A.A.; Shvartsberg, M.S.; 5-arylethynyl-1,4-naphthoquinones. *Izv. Akad. Nauk SSSR, Ser. Khim.*, **1984**, 2561.

evaluating new quinoidal compounds against parasites.¹⁴⁴ As shown in Scheme 20, in assays performed in the absence of blood and with incubation at 37 °C, several compounds presented IC₅₀ values of <2 μM against *T. cruzi*. For instance, further assays with 5-acetoxy-1,4-naphthoquinone (IC₅₀ = 0.16 μM) revealed activity against the proliferative forms of *T. cruzi*, intracellular amastigotes and epimastigotes. In experiments with this latter parasite form, this compound led to mitochondrial swelling, vacuolization, and flagellar blebbing, as well as a remarkable decrease in the mitochondrial membrane potential and a discrete increase of ROS production. Such redox dependent effects are likely reliant on the acetyl group facilitating quinone reduction, as previously demonstrated by electrochemical analysis (Scheme 20).¹⁴⁵



Scheme 20. Simple modifications in juglone leading to compounds with potent trypanocidal activity. *IC₅₀/24 h values for the lytic activity on bloodstream trypomastigotes.

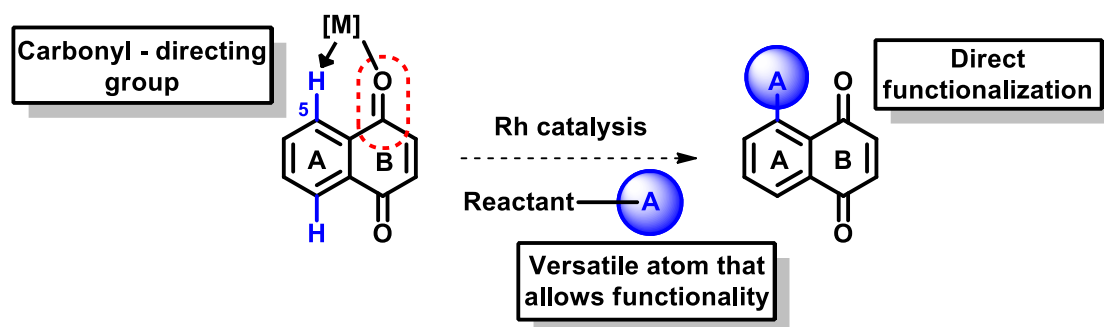
144. Salomão, K.; de Santana, N.A.; Molina, M.T.; de Castro, S.L.; Menna-Barreto, R.F.S.; *Trypanosoma cruzi* mitochondrial swelling and membrane potential collapse as primary evidence of the mode of action of naphthoquinone analogues. *BMC Microbiol.*, **2013**, *13*, 196.

145. Costa, E.O.; Molina, M.T.; de Abreu, F.C.; dos Santos Silva, F.A.; Costa, C.O.; Pinho, W.; Valentim, I.B.; Aguilera-Venegas, B.; Pérez-Cruz, F.; Norambuena, E.; Olea-Azar, C.; Goulart, M.O.F.; Electrochemical and spectroscopic investigation of bioactive naphthoquinone. *Int. J. Electrochem. Sci.*, **2012**, *7*, 6524.

3. Proposed Strategy

Due to their electron deficient character, 1,4-naphthoquinones are generally used as substrates in reactions like nucleophilic substitution¹⁴⁶ or cycloadditions¹⁴⁷ affording new substances with substituents exclusively in the B-ring. Reactions leading to substitution on the A-ring are rare. As a pioneer example, Kakiuchi and co-workers¹⁴⁸ described a ruthenium-catalysed alkylation of anthraquinones, obtaining new derivatives with substitution on the benzenoid ring.

The lack of synthetic methods dedicated to the activation of the A-ring calls for the need to develop methodologies like C-H bond activation reactions.¹⁴⁹ The strategy used in this work was based on the use of rhodium catalysts to insert versatile atoms like iodine and bromine in the position 5 of the naphthoquinoidal A-ring, providing access to new functionalization protocols (Scheme 21).



Scheme 21. Strategy for the achievement of A-ring substituted naphthoquinones.

The main difficulties observed in the execution of C-H bond activation in naphthoquinones includes: their susceptibility to reduction, high electrophilicity of the quinone ring, low nucleophilicity of the benzenoid A-ring and the weak coordination capability of the carbonyl groups in the quinoidal ring. In truth, only one protocol that

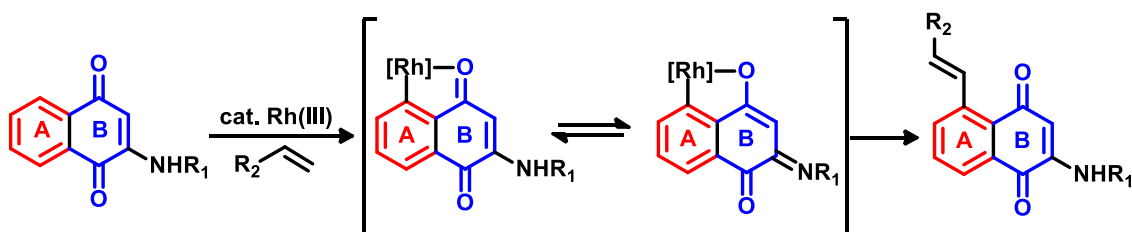
146. Bukhtoyarova, A.D.; Rybalova, T.V.; Ektova, L.V.; Amination of 5-hydroxy-1,4-naphthoquinone in the presence of copper acetate *Russ. J. Org. Chem.*, **2010**, *46*, 855.

147. Zhang, J.; Redman, N.; Litke, A.P.; Zeng, J.; Zhan, J.; Chan, K.Y.; Chang, C.-W.T.; Synthesis and antibacterial activity study of a novel class of cationic anthraquinone analogs. *Bioorg. Med. Chem.*, **2011**, *19*, 498.

148. Matsumura, D.; Kitazawa, K.; Terai, S.; Kochi, T.; Ie, Y.; Nitani, M.; Aso, Y.; Kakiuchi, F.; Short synthesis of alkyl-substituted acenes using carbonyl-directed C-H and C-O functionalization. *Org. Lett.*, **2012**, *14*, 3882.

149. Hartwig, J.F.; Larsen, M.A.; Undirected, homogeneous C-H bond functionalization: challenges and opportunities. *ACS Cent. Sci.*, **2016**, *2*, 281.

allows A-ring functionalization of 1,4-naphthoquinones was reported and discussed earlier. In this particular case, Rh(III)-catalysed vinylation was possible by improving the basicity of the carbonyl groups by inserting an amino group in the position 2 (Scheme 22).¹⁵⁰



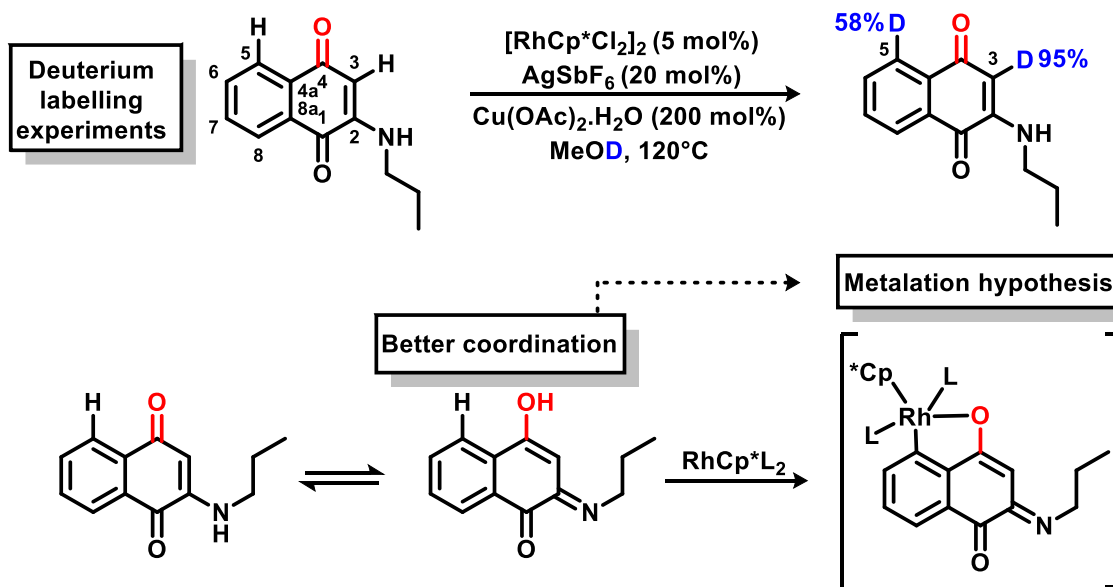
Scheme 22. Functionalization strategy used by Zhang and co-workers.

Deuterium labelling experiments reported by Zhang¹⁵¹ showed that incorporation of deuterium occurred partially in the 5- and 3- positions of the substrate, indicating a reversible path, suggesting that the cascade reaction was started by C₅-H activation. As a hypothesis discussed by the authors, a concerted metalation-deprotonation process between the Rh(III) catalytic specie and carbon 5 directed by the carbonyl group was the proposed mechanism for this reaction. These experiments demonstrated that position 5 of the benzenoid ring of 1,4-naphthoquinones can undergo metalation-deprotonation (Scheme 23).

Encouraged by these studies, and the fact that 1,4-naphthoquinones are lower homologues of bioactive molecules like lapachol (**1**) and α -lapachone (**29**) makes them ideal model systems for the development of a method designed to functionalize the A-ring of this kind of structure.

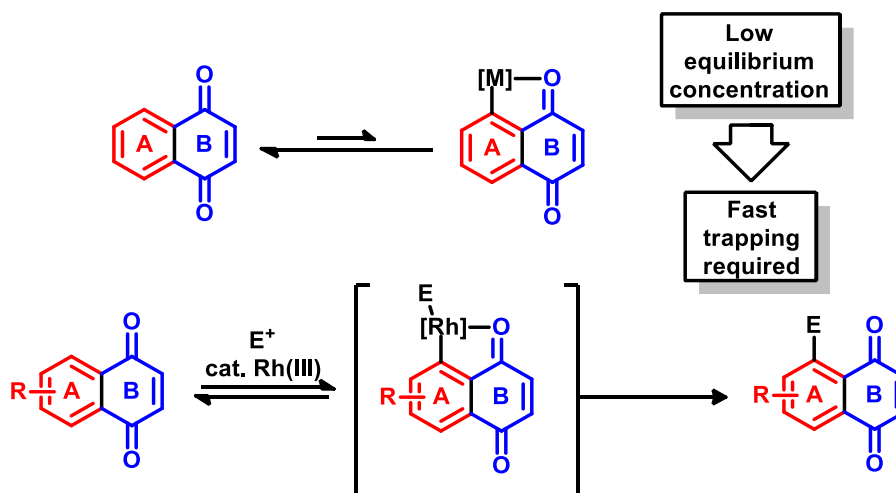
150. Zhang, C.; Wang, M.; Fan, Z.; Sun, L.-P.; Zhang, A.; Substituent-enabled oxidative dehydrogenative cross-coupling of 1,4-naphthoquinones with alkenes. *J. Org. Chem.*, **2014**, *79*, 7626.

151. Wang, M.; Zhang, C.; Sun, L.-P.; Ding, C.; Zhang, A.; Naphthoquinone-directed C-H annulation and C(sp³)-H bond cleavage: one-pot synthesis of tetracyclic naphthoxazoles. *J. Org. Chem.*, **2014**, *79*, 4553.



Scheme 23. Deuterium labelling experiments by Zhang and co-workers.

Carbonyl group *ortho*-metalation is known to be a reversible process,¹⁵² where the equilibrium depends on both the nucleophilicity of the arene and the coordinating ability of the directing group.¹⁵³ Neither of these aspects is favourable in 1,4-naphthoquinones, which requires a fast trapping of the metalated intermediate (Scheme 24).



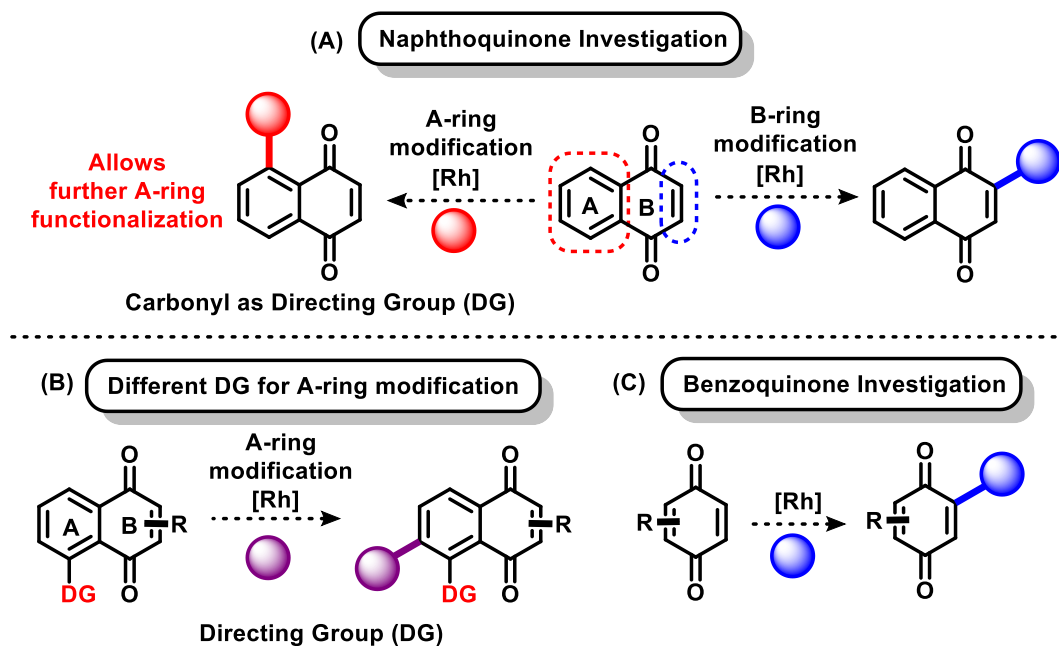
Scheme 24. Equilibrium between 1,4-naphthoquinone and the metalated specie.

152. Wang, Lu.; Spangler, J.E.; Chen, K.; Cui, P.-P.; Zhao, Y.; Sun, W.-Y.; Yu, J.-Q.; Rh(III)-catalysed C–H olefination of N-pentafluoroaryl benzamides using air as the sole oxidant. *Chem. Sci.*, **2015**, *6*, 1923.

153. Kakiuchi, F.; Murai, S.; Activation of C–H bonds: catalytic reactions. *Top. Organomet. Chem.*, **1999**, *3*, 47.

To achieve the fast trapping requirement, a highly reactive, oxidative and non-nucleophilic reactant has to be used to promote functionalization in the 5 position of the A-ring of the naphthoquinone. Electrophilic iodine sources like *N*-iodosuccinimide (NIS) and 3,3-dimethyl-*N*-diiodo-hidantoin (DIH) were promising candidates as they are commercially available and meet the requirements of the reaction. As for B-ring modification, Zhang and co-workers have proved that metalation in C-2 is possible, and functionalization in this position using electrophilic halogen sources could be performed.

We believe that this strategy, if succeeded, could open new avenues in the chemistry of quinones, once the developed protocols could also be applied to molecules with similar structures as, for example, benzoquinones. The effect of more efficient directing groups can also be investigated, as well as another electrophile sources (Scheme 25).



Scheme 25. Strategies for the synthesis of novel trypanocidal naphthoquinones and benzoquinones.

At last, all new proposed derivatives could be tested against bloodstream forms of *T. cruzi* (IC₅₀/24h) and mammalian cells (LC₅₀/24h), allowing the determination of the selectivity index (SI) derived from the ratio of LC₅₀/IC₅₀.



4. Objectives

4.1. General Objective

Development of a methodology capable of directly functionalize the benzenoid (A-ring) of 1,4-naphthoquinones utilizing transition metal catalysis and exploration of the medicinal potential of these new derivatives in the therapy of Chagas disease.

4.2. Specific Objectives

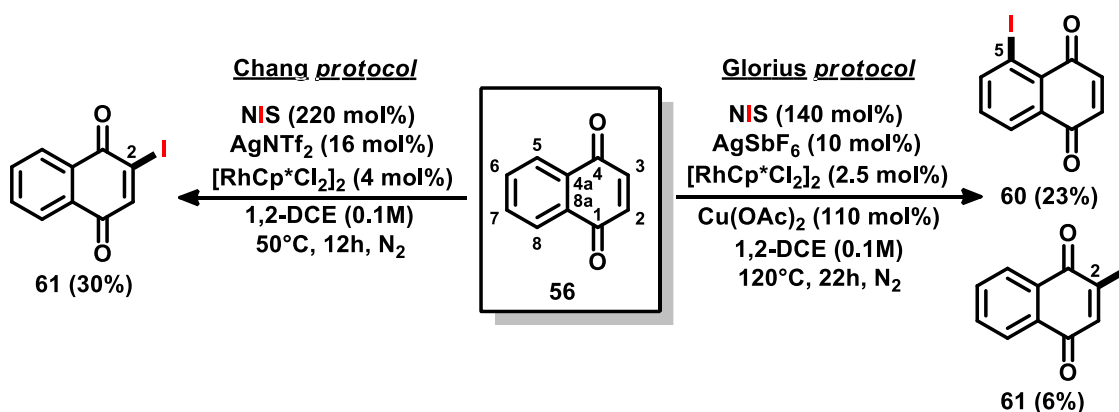
- Detailed methodological studies aiming the development of metal-catalysed C-H activation reactions between the quinoidal moiety and electrophilic halogen sources. These studies will include all the reaction variables, including different organometallic catalysts;
- Optimization of the discovered reactions will be carried out, as well as mechanistic studies seeking a plausible catalytic cycle;
- Application of the developed methodology to other quinoidal substrates;
- Development of cross-coupling protocols with the new halogenated-quinonoid derivatives.
- Development of new reactions with the new halogenated-quinonoid derivatives.
- Investigation of the biological aspects of the new derivatives in Chagas disease therapy.

5. Results and Discussion

5.1. Development of a C-H Functionalization Protocol

Attempts to find a robust methodology to perform C-H bond activation reactions in 1,4-naphthoquinone (**56**) led us to search for a methodology that was successfully performed in a similar substrate, leading to the reaction described by Glorius *et. al.* on the iodination and bromination of arenes.¹⁵⁴ This initial reaction resulted in the formation of two iodinated products in low yields, substituted in the positions 5 (**60**) and 2 (**61**), respectively (Scheme 26).

Following the same line of thought, the methodology described by Chang *et. al.* was evaluated.¹⁵⁵ This similar reaction was carried in mild conditions (50 °C), shorter reaction time (12 h) and a different additive (AgNTf₂). As an initial result, **61** was obtained in 30% yield. Unlike the first catalytic system, no copper salts were used, leading to the hypothesis that the copper acetate was somehow responsible for the regioselectivity between the positions 2 and 5 (Scheme 26). *Insertion of iodine at the current positions of the following products were confirmed by Nuclear Magnetic Resonance (NMR) techniques like ¹H, ¹³C, HSQC and HMBC. Most of the structures were also elucidated by X-ray crystallography.*

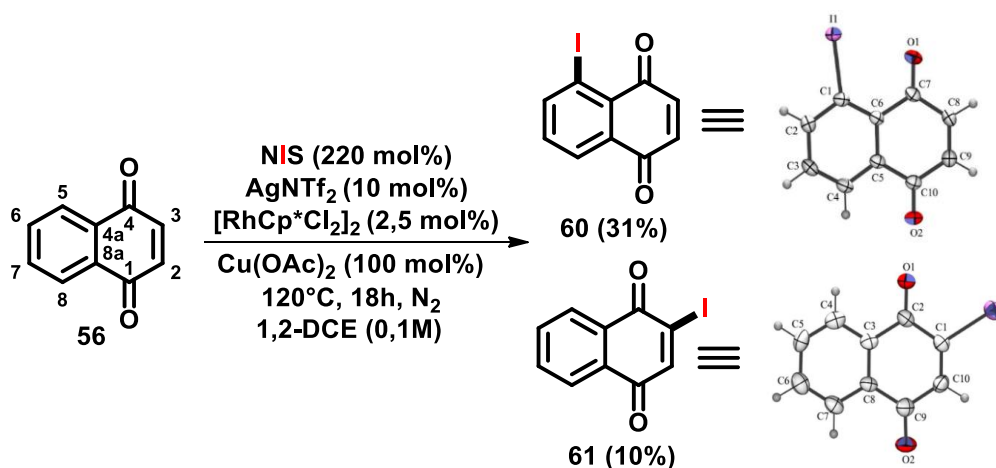


Scheme 26. Preliminary results.

154. Schröder, N.; Wencel-Delord, J.; Glorius, F.; High-yielding, versatile, and practical [Rh(III)Cp*]-catalyzed ortho bromination and iodination of arenes. *J. Am. Chem. Soc.*, **2012**, *134*, 8298.

155. Hwang, H.; Kim, J.; Jeong, J.; Chang, S.; Regioselective introduction of heteroatoms at the C-8 position of quinoline N-oxides: remote C-H activation using N-oxide as a stepping stone. *J. Am. Chem. Soc.*, **2014**, *136*, 10770.

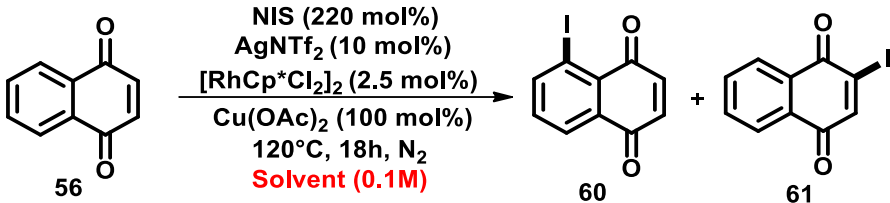
Encouraged by those two initial results, both reactions were combined in an experiment utilising $\text{Cu}(\text{OAc})_2$ and AgNTf_2 . The amount of *N*-iodosuccinimide (NIS) has set up in 220 mol% in order to investigate possible bis-iodination products and catalyst loading was maintained as low as possible (2.5 mol%). With these parameters, **60** and **61** were obtained in 31% and 10% respectively, giving 41% total yield with 3:1 regioselectivity (Scheme 27).



Scheme 27. Combination of both reactions (Glorius and Chang).

Using those as base parameters, solvent screening experiments were conducted. Results were obtained via *in situ* yield analysis technique (see experimental data). The best yield was obtained with CH_2Cl_2 . Other chlorinated solvents like 1,2-dichlorobenzene (1,2-DCB), 1,2-dichloropropane (1,2-DCP) and chloroform (CHCl_3) were also employed without satisfactory results. Use of dimethyl acetamide (DMAc), dimethyl formamide (DMF), tetrahydrofuran (THF) and acetonitrile resulted in poor yields and degradation. When conducted in water, the reaction did not occur, possibly due to poor solubility of the reactants (Table 1).

Table 1. Solvent screening.



Solvent	Yield (%) 60:61
1,2-DCE	31:10
CH₂Cl₂	39:8
DMAc	5:trace
1,2-DCB	21:5
1,2-DCP	26:8
CHCl ₃	9:2
DMF	Complex mixture
THF	10:trace
CH ₃ CN	6:trace
H ₂ O	N.R.

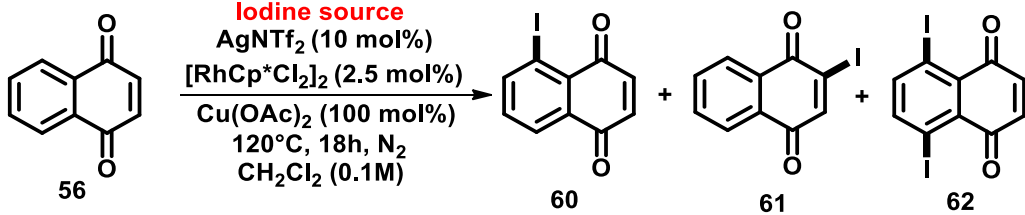
Dichloromethane was set up as the reaction solvent and several electrophilic iodine sources were investigated (Figure 16), in which commercially available sources like NIS, 3,3-dimethyl-*N*-diiodo-hydantoin (DIH) and *N*-iodosacharin (NISac) were chosen due to their previous use in several previously reported iodination protocols.¹⁵⁶ Iodine (I₂) and iodine chloride (ICl) were tested, leading to no reaction and degradation of the starting material, respectively. Diiodotriphenylphosphane (P(Ph₃)I₂)¹⁵⁷ and 4-methylbenzenesulfonyl iodide (TolSO₂I)¹⁵⁸ were synthesized and employed without success. Reaction with DIH (140 mol%) lead to the predominant formation of **61** and bis-iodinated product **62**. Use of NISac resulted in poor yields, and a gradual decrease in the amount of NIS (220 to 140 mol%) resulted in similar results (Table 2).

156. (a) Ojha, D.P.; Prabhu, K.R.; Regioselective synthesis of vinyl halides, vinyl sulfones, and alkynes: a tandem intermolecular nucleophilic and electrophilic vinylation of tosylhydrazones. *Org. Lett.*, **2015**, *17*, 18. (b) Jakab, G.; Hosseini, A.; Hausmann, H.; Schreiner, P.R.; Mild and selective organocatalytic iodination of activated aromatic compounds. *Synthesis*, **2013**, *45*, 1635. (c) Bailey, L.; Handy, S.T.; Aromatic iodination using *N*-iodosaccharin in room temperature ionic liquids. *Tetrahedron Lett.*, **2011**, *52*, 2413.

157. Issleib, V.K.; Seide, W.; Zur konstitution und solvolyse von tertiaren phosphindihalogeniden - R₃PX₂. *Z. Anorg. und Allg. Chem.*, **1956**, *288*, 201.

158. Edwards, G.L.; Muldoon, C.A.; Sinclair, D.J.; Cyclic enol ether synthesis via arenesulfonyl iodide additions to alkynols. *Tetrahedron*, **1996**, *52*, 7779.

Table 2: Iodine sources investigation.



Iodine source	Yield (%) 60:61:62
NIS – 220 mol %	39:8:0
I ₂ 120 mol %	N.R.
P(Ph ₃)I ₂ 120 mol %	N.R.
TolSO ₂ I 120 mol %	N.R.
ICl 120 mol %	Degradation
DIH – 140 mol %	4:14:10
NISac – 140 mol %	22:5:0
NIS – 180 mol %	36:9:0
NIS – 160 mol %	38:7:0
NIS – 140 mol %	37:6:0

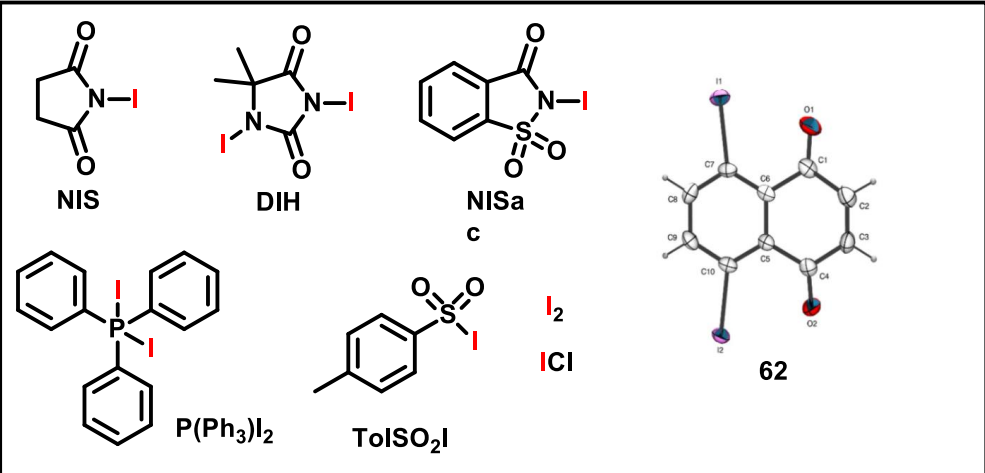


Figure 16: Iodine sources and crystal structure of **62**.

Once the best solvent and iodine source were screened, optimization of the reactional parameters was undertaken. Initially, concentration was varied in 0.05 M and 0.20 M, resulting in a decrease in the reaction yield. Same yields were observed when the reaction was carried for 18 and 48 hours, and performing the reaction for 14 and 16 hours led to lower yields. Temperature was varied in 4 different values, being observed an increasing yield at 100 °C. Fine tuning in the NIS amount (120 mol%) and catalyst loading (4 mol%) afforded the best conditions (Table 3).

Table 3: Variations in time, concentration and temperature.

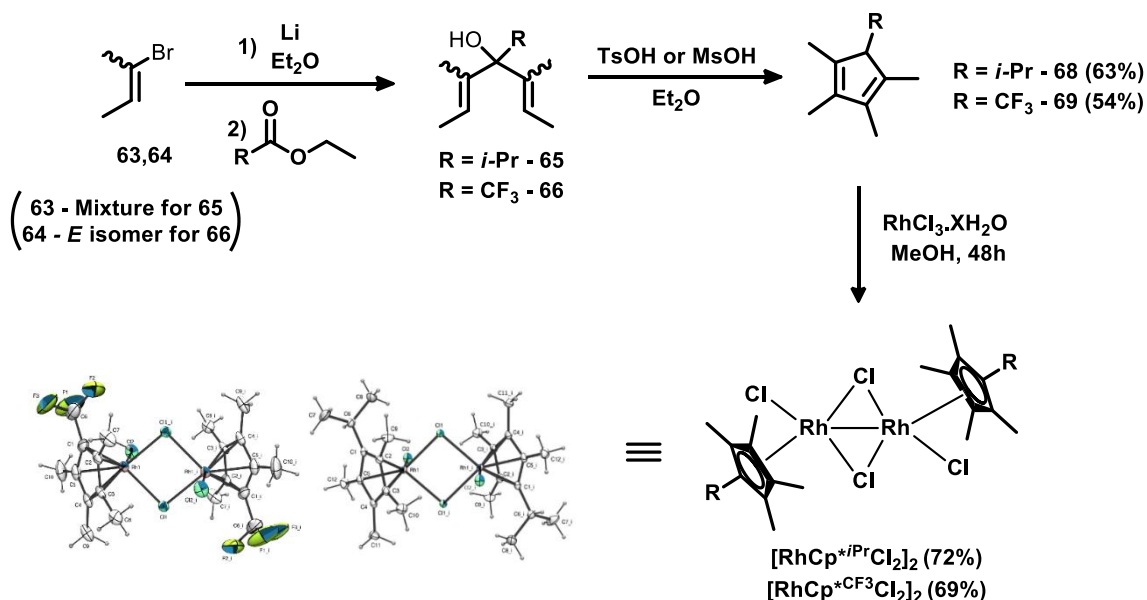
Entry	Time (h)	Temperature (°C)	Concentration (M)	Yield 60:61:62
1	18	120	0.1	37:6:0
2	18	120	0.05	22:3:0
3	18	120	0.2	30:8:0
4	14	120	0.1	21:3:0
5	16	120	0.1	38:5:0
6	24	120	0.1	38:7:0
7	48	120	0.1	38:12:0
8	18	80	0.1	23:5:0
9	18	60	0.1	12:4:0
10	18	100	0.1	41:11:0
11	18	100	0.1	44:5:0*

The reaction was performed using NIS (120 mol%), $[\text{RhCp}^\text{Cl}_2]_2$ (4 mol%) and AgNTf_2 (16 mol%).

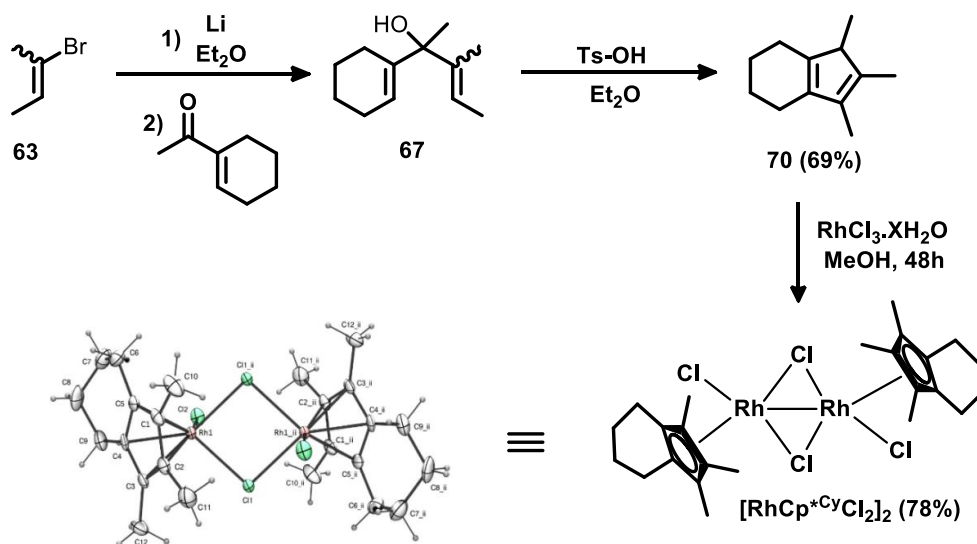
The next logical step was the investigation of different $\text{Rh}^{\text{III}}\text{Cp}^{\text{X}}$ catalysts in order to examine the electronic and hindering effects of different Cp^{X} groups. The complexes synthesis started with the lithiation of the corresponding bromo alkenes (**63** and **64**), and quenching with the proper acetates to generate the Nazarov adducts **65** - **67**, followed by an acid-promoted intramolecular pericyclic reaction to generate the Cp^{X} ligands **68** - **70**.¹⁵⁹ The complexes were obtained in good yields by reaction of the corresponding ligands with $\text{RhCl}_3 \cdot \text{XH}_2\text{O}$ in methanol. $\text{RhCp}^*(\text{OAc})_2 \cdot \text{H}_2\text{O}$ was synthesised by reaction of $[\text{RhCp}^*\text{Cl}_2]_2$ with silver acetate in dichloromethane. (Schemes 28 -30). $[\text{RhCp}^*\text{Cl}_2]_2$ and $[\text{RhCp}^t\text{Cl}_2]_2$ were obtained by commercial sources.

159. (a) Schumann, H.; Keitsch, M.R.; Winterfeld, J.; Muhle, S.; Molander, G.A.; Organometallic compounds of the lanthanides. CXXIII. Lanthanide bent-sandwich complexes with the bulky tetramethyl-iso propylcyclopentadienyl ligand—synthesis, structures and catalytic activity for the hydrosilylation of alkenes/alkynes. *J. Organomet. Chem.*, **1998**, 559, 181. (b) Gassman, P.G.; Mickelson, J.W.; Sowa, Jr., J.R.; 1,2,3,4-Tetramethyl-5-(trifluoromethyl)cyclopentadienide: a unique ligand with the steric properties of pentamethylcyclopentadienide and the electronic properties of cyclopentadienide. *J. Am. Chem. Soc.*, **1992**, 114, 6943. (c) Hastings, C.J.; Pluth, M.D.; Bergman, R.G.; Raymond, K.N.; Enzyme like catalysis of the Nazarov cyclization by supramolecular encapsulation. *J. Am. Chem. Soc.*, **2010**, 132, 6938. (d) Bosch, H.W.; Stauber, R.; Salzer, A.; Synthese bicyclischer pentaalkylcyclopentadiene und ihrer metallkomplexe. kristallstruktur von Bis(1,2,3-trimethylbicyclo[4.3.0]nonadienyl) eisen. *J. Organomet. Chem.*, **1994**, 472, 205.

The complexes were characterized by Nuclear Magnetic Resonance (NMR) and High-resolution Mass Spectrometry (HR-MS). Crystal growing techniques¹⁶⁰ were employed to achieve suitable crystals for resolution by X-Ray crystallography.

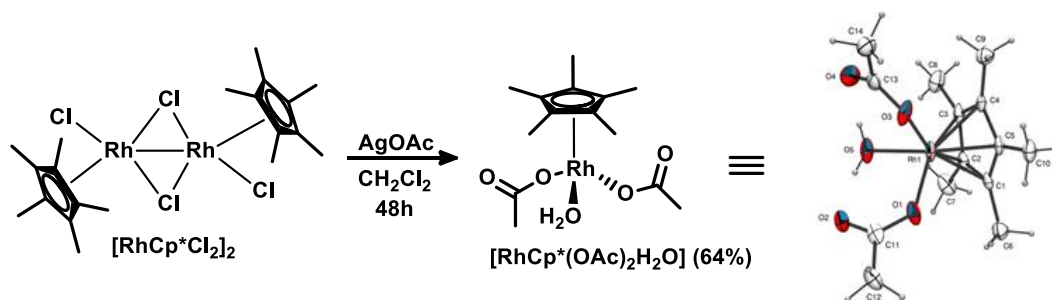


Scheme 28. Synthesis of the Rh^{III}Cp^X complexes.



Scheme 29. Synthesis of [RhCp*^{Cy}Cl₂]₂.

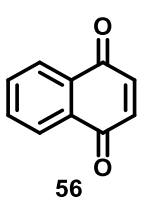
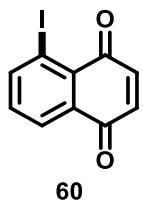
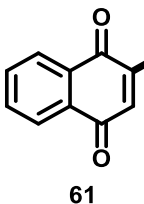
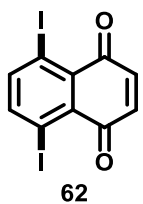
160. Jones, P.J.; Crystal growing. Reprinted from *Chemistry in Britain*, 1981, 17, 222.



Scheme 30. Synthesis of [RhCp*(OAc)₂H₂O].

Use of previous synthesised catalysts proved to be unfruitful, once the best result were still achieved with the first choice catalyst [RhCp*Cl₂]₂. It was observed that bulky catalysts like [RhCp*^{*i*-Pr}Cl₂]₂, [RhCp*^{*Cy*}Cl₂]₂ and [RhCp^{*t*}Cl₂]₂ led to similar yields when compared with their lower analogue [RhCp*Cl₂]₂. The use of the electron deficient catalyst [RhCp*^{*CF*3}Cl₂]₂ resulted in low yield, and the catalyst [RhCp*(OAc)₂H₂O] gave lower yields than [RhCp*Cl₂]₂. This acetate based complex showed to be very hygroscopic and difficult to handle. Maybe this feature collaborated for the lower yield observed, once the experiment with water led to a no reaction. Another important observation was that reaction with [RhCp^{*t*}Cl₂]₂ gave 15% yield of **61**, even with the use of Cu(OAc)₂ (Table 4).

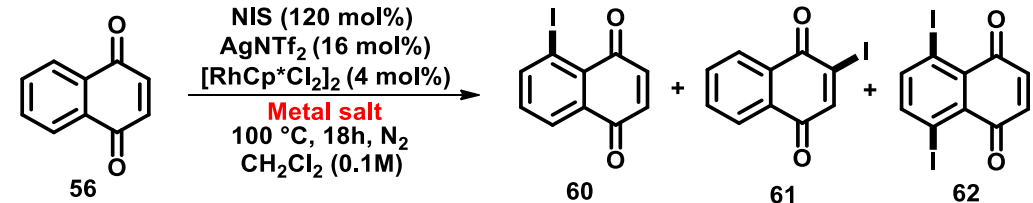
Table 4: Catalyst screening.

 56	NIS (120 mol%) AgNTf ₂ (16 mol%) [Rh] (4 mol%) Cu(OAc) ₂ (100 mol%) 100 °C, 18h, N ₂ CH ₂ Cl ₂ (0.1M)	 60	 61	 62
Catalyst (4 mol%)		Yield 60:61:62		
[RhCp*Cl ₂] ₂		44:5:0		
[RhCp* ^{<i>i</i>-Pr} Cl ₂] ₂		39:8:0		
[RhCp* ^{<i>Cy</i>} Cl ₂] ₂		33:6:0		
[RhCp ^{<i>t</i>} Cl ₂] ₂		36:15:0		
[RhCp* ^{<i>CF</i>3} Cl ₂] ₂		3:0:0		
[RhCp*(OAc) ₂ H ₂ O]		32:2:0		

In order to investigate the role of copper salts in regioselectivity at the position 5, the amount of Cu(OAc)₂ was doubled (200 mol%) and halved (50 mol%), leading to mild decrease in yield. Several copper carboxylates with electronic and hindrance variables like Cu(TFA)₂, Cu(OTf)₂ and Cu(PivO)₂ were employed, resulting in poor

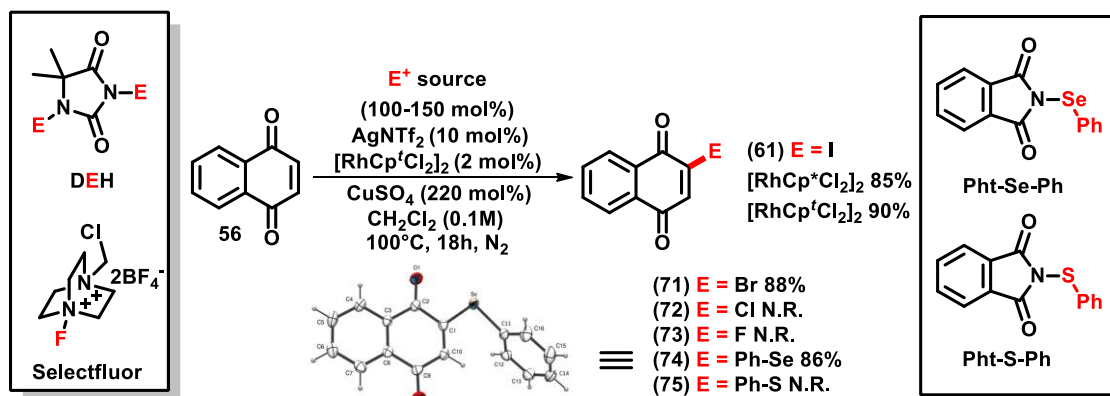
yields. For our delight, use of copper sulfate led to an exchange in regioselectivity and yield increasing. Zinc acetate afforded 36% yield with good regioselectivity. Use of sodium acetate had as consequence yield decreasing, possibly due to low solubility in dichloromethane. Investigation on the effect of copper sulphate concentration showed that 200 mol% of the salt led to better yields, and use of magnesium sulphate provided worse results when compared to copper sulfate. The use of copper sulphate heptahydrate resulted in very low yields, possible due to the effect of water in the reaction, reinforced by the fact that reaction performed using water as a solvent ended in no reaction (Table 5).

Table 5: Salts screening.

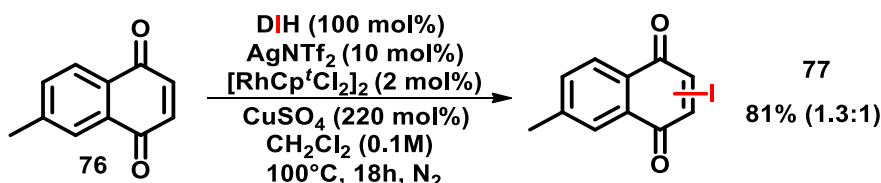
	
Salt (mol%)	Yield 60:61:62
Cu(OAc) ₂ (100)	44:5:0
Cu(OAc) ₂ (200)	41:3:0
Cu(OAc) ₂ (50)	27:8:0
Cu(PivO) ₂ (100)	16:9:0
Cu(TFA) ₂ (100)	13:10:0
Cu(OTf) ₂ (100)	8:5:0
CuSO₄ (100)	3:66:0
CuSO₄ (200)	5:78:0
MgSO ₄ (100)	3:34:0
CuSO ₄ ·7H ₂ O (100)	5:13:0
Zn(OAc) ₂ (100)	36:6:0
NaOAc (100)	10:6:0
AgOAc (100)	6:29:0

Such interesting results regarding the functionalization at position 2 led us to do some fine tuning in the reaction parameters, adjusting the catalyst amount (2 mol%) and CuSO₄ loading (220 mol%) proportionating a small increase in yield (81%). The switch of the iodine source from NIS (120 mol%) to DIH (100 mol%) led to 85% yield of **61**, with almost complete regioselectivity over **60**. Finally, use of [RhCp[†]Cl₂]₂ provided a yield of 90% of **61**.

With these optimized parameters, other electrophiles were tested. Pleasingly, bromination with 3,3-dimethyl-*N*-bromo-hidantoin (DBH) (150 mol%) and selenation with *N*-(phenylselenyl)phthalimide (Phta-Se-Ph) (120 mol%) in position 2 were achieved in 88% and 86%, respectively. There was no reaction with the use of 3,3-dimethyl-*N*-dichloro-hidantoin (DCH), selectfluor and *N*-(phenylthio)phthalimide (Phta-S-Ph) (Scheme 31). Despite the excellent yields and acceptance of three electrophile sources, the reaction proceeded with low regioselectivity when unsymmetrical substrate **76** was employed (derivative **77**) (Scheme 32).



Scheme 31. Final results for functionalization at position 2 and crystal structure of **74**.



Scheme 32. Results for functionalization at position 2 with an unsymmetrical substrate.

Derivative **61** was previously obtained in 35% by Perez and co-workers in a mixture of products, using a morpholine-iodine complex.¹⁶¹ The most previous entry for **74** involved reaction with 1,2-diphenyldisilane resulting the product in 73% yield by Ueno and co-workers, with 12% of bis-selenation. Ueno proposed a mechanism that undergoes via a nucleophilic attack of the benzeneselenolate anion on **56**.¹⁶² These facts

161. Perez, A.L.; Lamoureux, G.; Herrera, A.; Synthesis of iodinated naphthoquinones using morpholine-iodine complex. *Synth. Commun.*, **2004**, *34*, 3389.

162. Sakakibara, M.; Watanabe, Y.; Toru, T.; Ueno, Y.; New selenenylation method. Synthesis of selenonaphthoquinones and selenoquinolinequinones mediated by phenyl selenide ion. *J. Chem. Soc., Perkin Trans. 1*, **1991**, 1231.

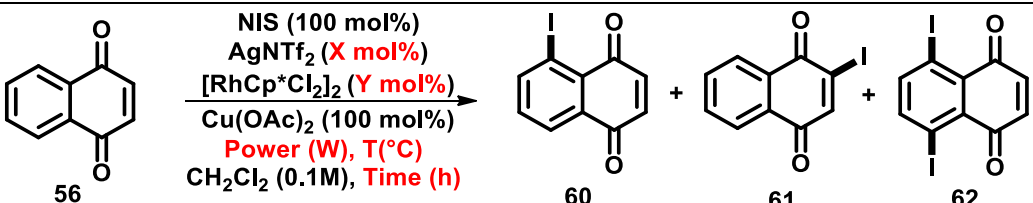
showed that the new methodology is viable to achieve selective C-2 functionalized 1,4-naphthoquinones.

Despite proceeding with good regioselectivity, efforts to improve the yield of C-5 substituted isomer **60** proved to be fruitless. Observation and careful investigation of the reaction course indicated the formation of molecular iodine in reaction medium, indicating degradation of NIS, potentially due to the high reaction temperature. In an attempt to solve this problem, microwave conditions were tested.¹⁶³ Surprisingly, 46% yield was achieved with the reactional time of two hours.

Encouraged by these results, several experiments were conducted to investigate the effect of microwave heating in the reaction. Reducing the time to one hour resulted in worst yields, and a four hours reaction time led to similar results. Raising catalyst loading (5 mol%) led to yield increasing, but 22% of bis-iodinated product **62** was observed. The microwave power was raised to 65 W, and a slight decrease in bis-iodinated product was observed with no changes in yield for main product **60**. Fine tuning of the catalyst loading afforded best results of selectivity with less catalyst quantity (3.75 mol%), but still generating a high amount of **62**. Employing nitrogen flow during the reaction course to control temperature led to better yields, and after fine tuning on both parameters (power and temperature) good regioselectivity at position 5 was achieved (15:1) in 74% total yield, with 69% yield of **60**. Extending the reaction time to either 4 or 8 hours resulted in no improvement in either yield or regioselectivity (Table 6).

163. (a) Rosana, M.R.; Tao, Y.; Stiegman, A.E.; Dudley, G.B.; On the rational design of microwave-actuated organic reactions. *Chem. Sci.*, **2012**, *3*, 1240. (b) Singh, B.K.; Kaval, N.; Tomar, S.; Van der Eycken, E.; Parmar, V.S.; Transition metal-catalyzed carbon-carbon bond formation Suzuki, Heck, and Sonogashira reactions using microwave and microtechnology. *Org. Process Res. Dev.*, **2008**, *12*, 468.

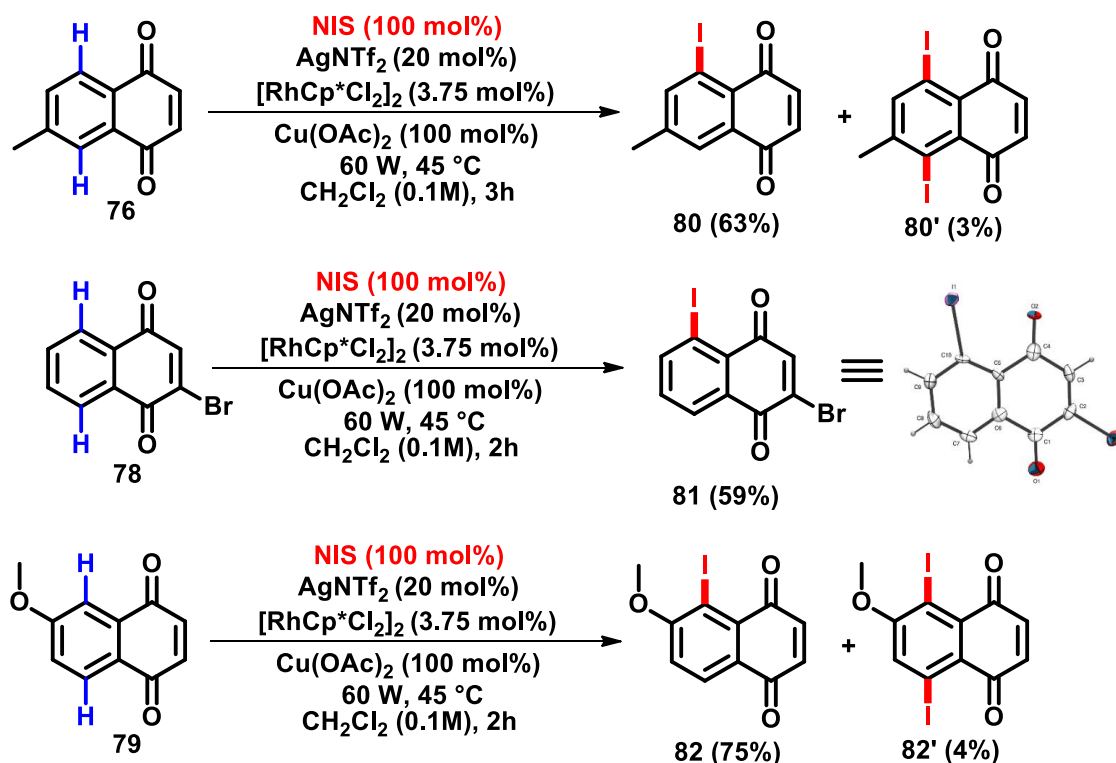
Table 6: Microwave optimization conditions.

			
[RhCp*Cl ₂] ₂ /AgNTf ₂ (mol%)	Time (h)	Power (W)/ Temperature (°C) ^a	Yield 60:61:62
2/10	2	50/50	46:7:14
2/10	1	50/50	32:4:5
2/10	4	50/50	47:9:11
5/25	2	50/50	54:3:22
5/25	2	65/50	55:2:16
4/22	2.5	65/50	54:0:14*
3.75/20	2	65/50	57:0:15
3.75/20	2	65/45	62:0:10
3.75/20	2	65/35	66:0:6
3.75/20	2	60/45	69:0:5
3.75/20	4	60/45	68:0:7
3.75/20	8	60/45	70:0:10

*The reaction was performed with NIS (120 mol%).

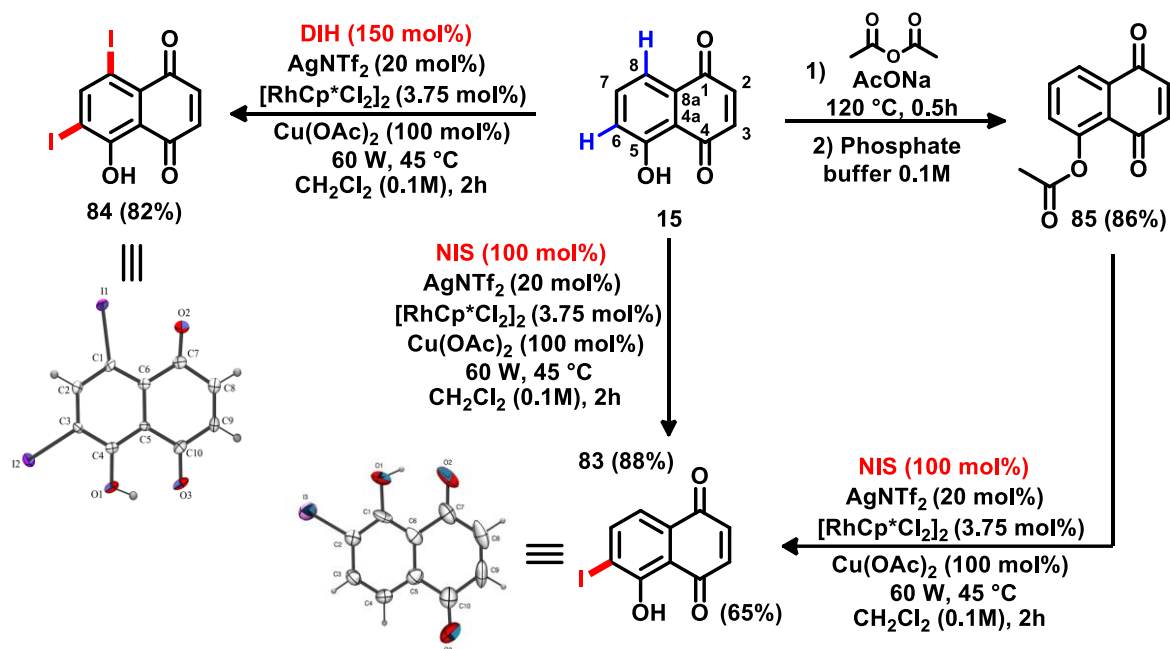
^aExternal temperature of the reaction vessel.

With the achievement of the best reaction conditions, A- and B-ring substituted 1,4-naphthoquinones were chosen to demonstrate the scope of the new methodology. First, unsymmetrical substrates **76**, **78** and **79** were chosen in order to explore the reaction behaviour. Iodination of **76** occurred in the less hindered position (derivative **80**, 63% yield), with minor occurrence of bis-iodinated product **80'** (4% yield). For **78**, high regioselectivity was observed in the reaction product **81** (59% yield), possible due to higher basicity of the carbonyl group and consequently better coordination, facilitating the metalation event. Surprisingly, iodination of **79** occurred in the most hindered position, possibly due secondary coordination of the methoxy group (derivative **82**, 75% yield), with only a minor occurrence of bis-iodinated product **82'** (4% yield) (Scheme 33).



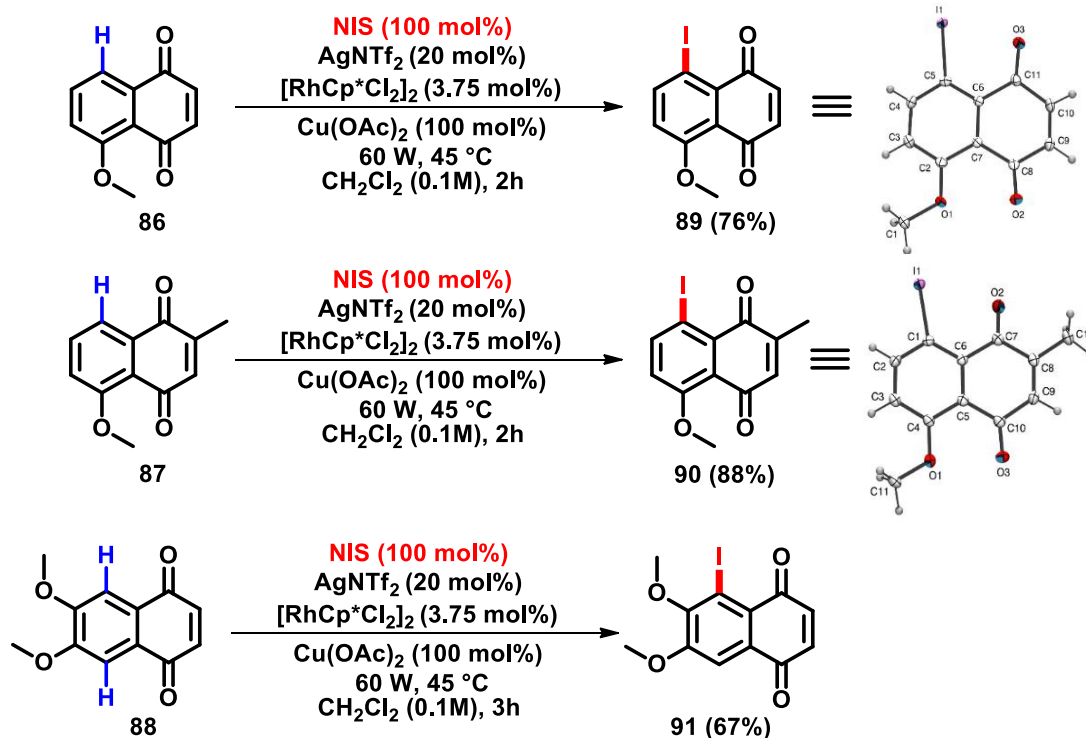
Scheme 33. Derivatization experiments with unsymmetrical substrates **76 - 79**.

Reaction with juglone (**15**) afforded **83** in 88% yield, thus iodination occurred at the position 6, and experiments without the catalyst led to no reaction. Exchanging the iodine source to DIH (100 mol%) gave a mixture of **83** and **84**, showing that the catalyst can act in both sites when an excess of iodination agent is employed. An increase in the amount of DIH to 150 mol% resulted in double iodination product **84** in 82% yield. Aiming at the investigation of a less activating group in the A-ring of **15**, protection of the hydroxyl group via reaction with acetic anhydride and sodium acetate afforded **85**, but this protecting group was not compatible with the reaction conditions, and *in situ* deprotection occurred, leading to the same product **83** (Scheme 34).



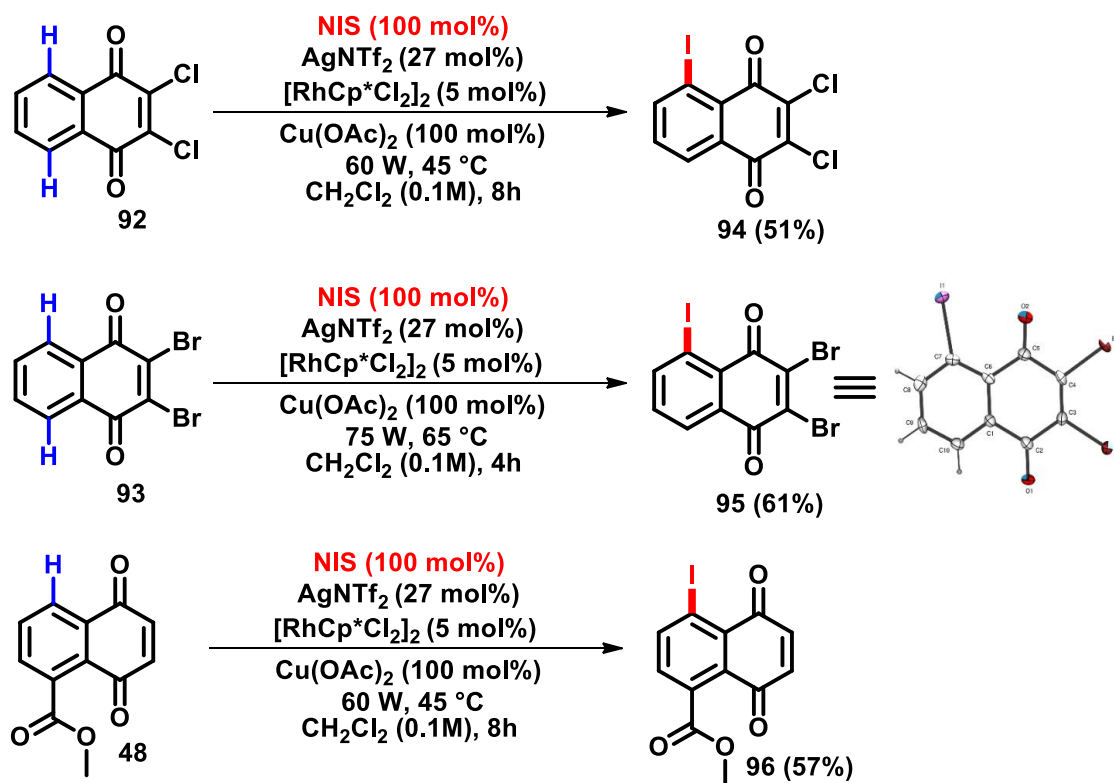
Scheme 34. Derivatization experiments with juglone (**15**).

Juglone (**15**) hydroxy group was protected with a more resistant group, affording substrate **86** in good yields (see experimental data), and the reaction proceeded with iodination at the position 5 (derivative **89**, 76% yield). Same strategy was applied to plumbagin (**16**), and derivative **90** was achieved in 88%. Use of symmetric substrate **88** resulted only in mono-iodination, and derivative **91** was achieved in 67% yield. No bis-iodination products were observed in any of those experiments (Scheme 35).



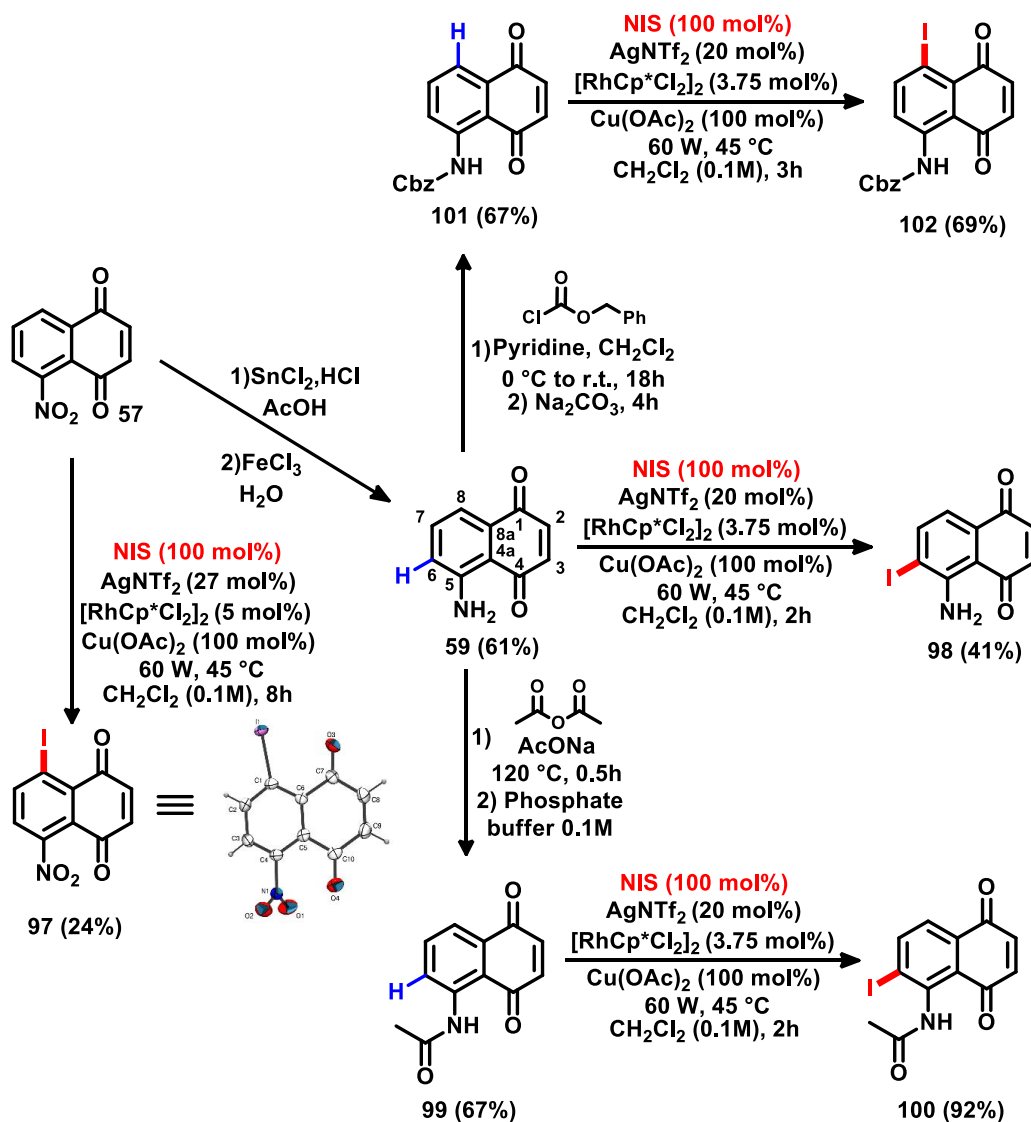
Scheme 35. Derivatization experiments with **86 - 88**.

Use of electron deficient 1,4-naphthoquinones proved to be challenging, and special conditions were applied in each case in order to maximize yields. Reaction performed on the symmetrical substrates **92** and **93** afforded low yields (derivatives **94** and **95**, 38% and 36% respectively), which led us to apply more catalyst (5 mol%), AgNTf₂ (27 mol%) and raise the reaction time (4 h). With these reactional parameters, derivative **94** was achieved in 48% yield. In case of substrate **93**, more potency (75 W) and fine tuning in temperature (65 °C) led also to yield increasing, affording derivative **95** in 61% yield. In case of substrate **48** containing a carbonyl group direct linked to the A-ring, iodination occurred at the position 5 with 57% yield with a reaction time of 8 hours (Scheme 36).



Scheme 36. Derivatization experiments with **48**, **92** and **93**.

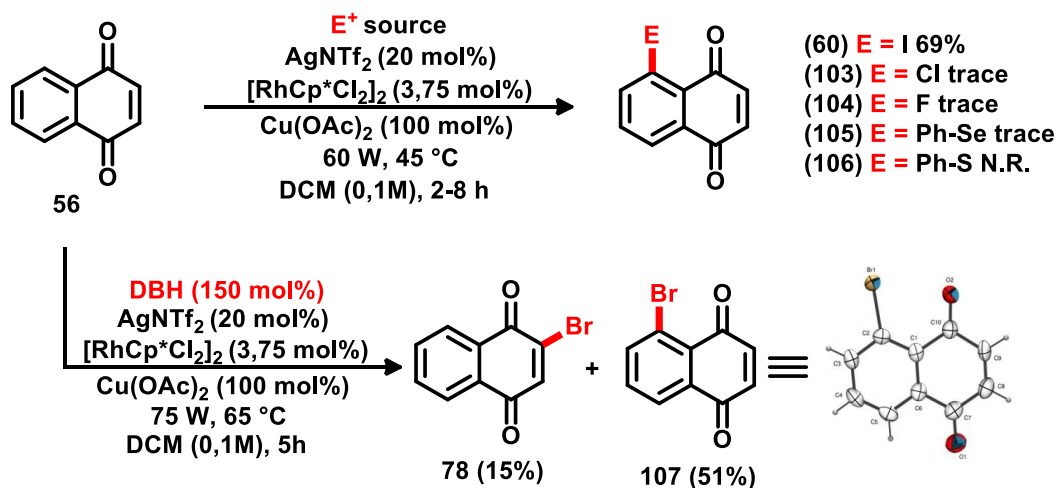
As expected, insertion of a nitro group into the A-ring caused a drastic decrease in the reaction efficiency, and derivative **97** was obtained in 24%, even with more catalyst loading (5 mol%) and a reaction time of 8 hours. After further reduction of the nitro group to amine, reaction behaviour was similar to the experiment with juglone (**15**) and derivative **98** was obtained in 41% with iodination at the position 6. However, changing the group from amine to amide (substrate **99**) afforded derivative **100** in 92% yield with iodination in the same position. Finally, protection of amine **61** with a bulkier group (substrate **101**) caused regioselectivity to change to the position 5 and derivative **102** was achieved in 69% yield (Scheme 37).



Scheme 37. Derivatization experiments with **57** and **59**.

At last, several electrophile sources were tested with the new reaction. Electrophile sources like DCH, Selectfluor and Phta-Se-Ph led to only traces of product. Use of Phta-S-Ph resulted in no reaction. Further variation of the microwave parameters and electrophile loading did not lead to satisfying improvements. Bromination attempts with NBS were more successful, resulting in 10% yield of **107** plus 5% yield of **78**. Optimization of the microwave parameters (75 W, 65 °C) and exchange of NBS by DBH afforded the best results for C-5 bromination (51%) (Scheme 38). Derivative **107**

was reported by Bhatt and group in the oxidation of naphthalenes in 15% yield plus a mixture of isomers.¹⁶⁴



Scheme 38. Further results for additional functionalization of the A-ring at position 5.

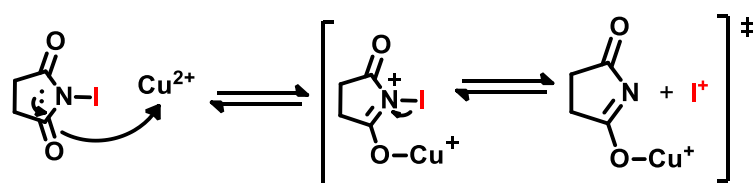
These experiments, allied with considerations of You and co-workers¹⁶⁵ led to the formulation of the following hypotheses about the reaction mechanism:

- When electron donating groups with low steric hindrance (-OH, -NH₂) are used, the metalation event often takes place at the most nucleophilic position (derivatives **83** and **98**) and the mechanism occurs via S_eAr;
- When intermediate donating groups (-OMe, NH-R) or electron-withdrawing groups (halogen, carbonyl) are used, the metalation event is governed by the directing group, and the mechanism occurs via concerted-metalation-deprotonation (CMD);
- The most effective directing group preferentially reacts first in the reaction course (carbonyl group vs amide group, derivative **100**).
- The two types of C-H bond cleavage events can be observed in the same reaction, as long as the reactional conditions permit (the two iodine insertions in derivative **84** corroborates with that hypothesis);

164. Periasam, M.; Bhatt, M.V.; A convenient method for the oxidation of polycyclic aromatic hydrocarbons to quinones. *Synthesis*, **1997**, 330.

165. Yang, Y.; Lan, J.; You, J.; Oxidative C-H/C-H coupling reactions between two (hetero)arenes. *Chem. Rev.*, **2017**, *117*, 8787.

- Groups with lone pairs that can act as electron-donor or coordinating groups (substrates **78** and **79**) can enhance the carbonyl group coordinating ability or provide additional coordination, improving reaction regioselectivity;
- When there is no electronic effects, the catalyst will prefer the less hindered position to react (derivative **80**);
- Use of $\text{Cu}(\text{OAc})_2$ is essential to achieve regioselectivity at position 5. The hypothesis that the copper ion could be acting as an oxidant is supported by previous reports.¹⁶⁶ Cu^{2+} could be also complexing with NIS and making it a better electrophilic iodine source (Scheme 39).



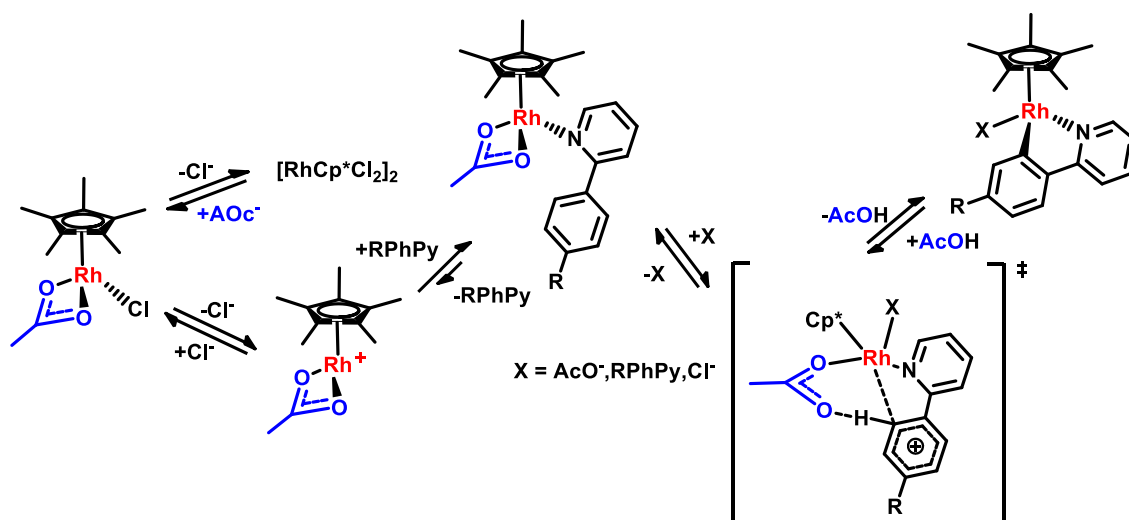
Scheme 39. Possible activation of NIS by Cu^{2+} coordination.

The role of $\text{Cu}(\text{OAc})_2$ is also indispensable in a bond cleavage event governed by a CMD pathway. In fact, advances in theoretical investigation of those mechanisms by using density functional theory (DFT) showed that $\text{Rh}^{\text{III}}\text{Cp}^{\text{X}}$ type catalysts can promote C-H bond cleavage, especially via CMD or $\text{S}_{\text{e}}\text{Ar}$, among others.¹⁶⁷ Jones et. al. also reported mechanistic insights of a CMD pathway involving acetate anions and $[\text{RhCp}^*\text{Cl}_2]_2$, where the transition state of this event involves a 6-membered transition state promoted by the acetate anion (Scheme 40).¹⁶⁸

166. Samanta, R.; Narayan, R.; Antonchick, A.P.; Rhodium(III)-catalyzed direct oxidative cross coupling at the C5 position of chromones with alkenes. *Org. Lett.*, **2012**, *14*, 6108.

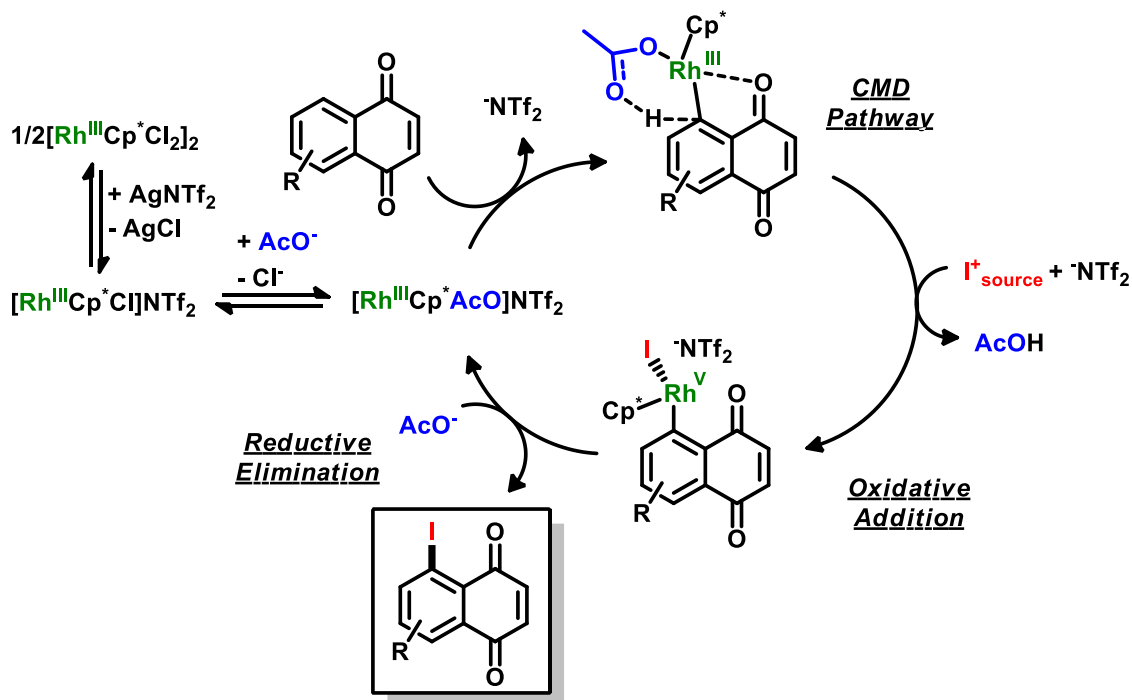
167. Qi, X.; Li, Y.; Bai, R.; Lan, Y.; Mechanism of rhodium-catalyzed C-H functionalization: advances in theoretical investigation. *Acc. Chem. Res.*, **2017**, *50*, 2799.

168. Walsh, A.P.; Jones, W.D.; Mechanistic insights of a concerted metalation-deprotonation reaction with $[\text{Cp}^*\text{RhCl}_2]_2$. *Organometallics*, **2015**, *34*, 3400.

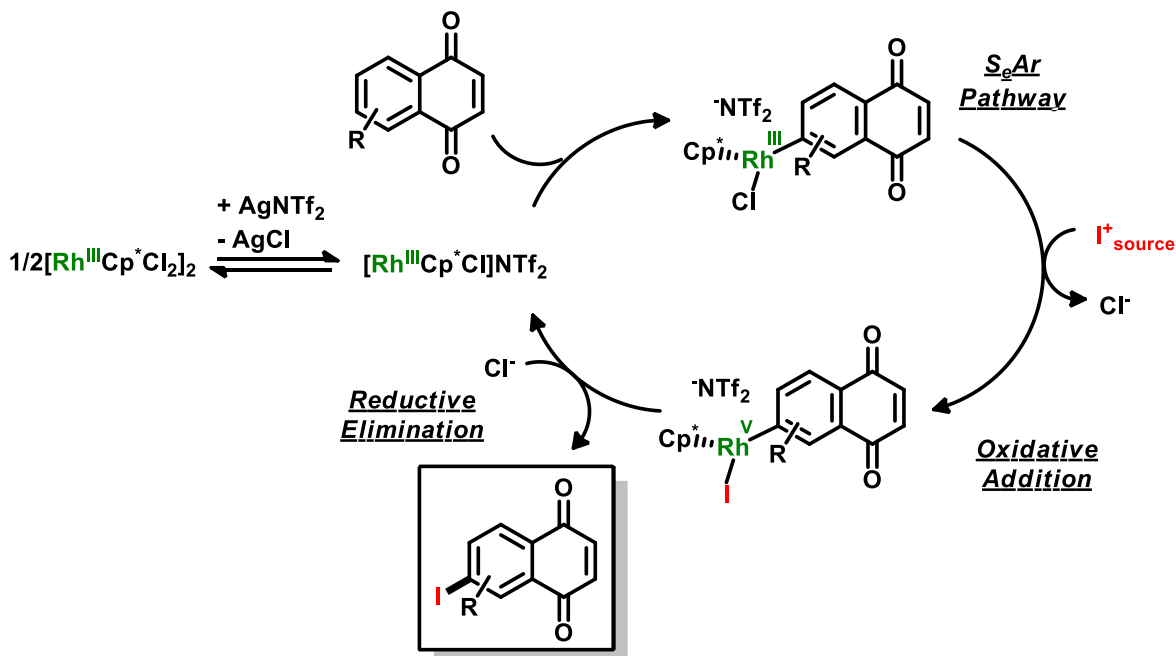


Scheme 40. Concerted metalation-deprotonation pathway described by Jones et. al.

Such observations led to the formulation of two mechanisms, one of them governed by CMD pathway and other by $S_{\text{E}}\text{Ar}$ (Schemes 41 and 42). *Note that the main metalation event was hindered for mechanism simplification, once they were broadly described in the introduction.* After metalation, it is believed that both mechanisms occurs in a similar way, governed by a simple oxidative addition – reductive elimination step. In the oxidative addition, the charge transfer undergoes between the Rh^{III} core and the electrophilic iodine, resulting in a high valence Rh^{V} complex. The iodine is then transferred to the molecule, and the electron pair of the $\text{Rh}-\text{C}$ bond is donated to the Rh^{V} specie, regenerating the catalyst.



Scheme 41. Proposed mechanism governed by concerted metalation-deprotonation pathway.



Scheme 42. Proposed mechanism governed by electrophilic aromatic substitution.

5.2. Exploring Functionalization at C-2 Position

The high yield obtained by the new C-2 functionalization reactions of **56** encouraged us to pursue new candidates with structural similarities to 1,4-naphthoquinones. There has been significant recent interest in the development of methodologies for the C–H functionalization of benzoquinones, especially as such approaches might allow analogue synthesis by late stage derivatization.¹⁶⁹

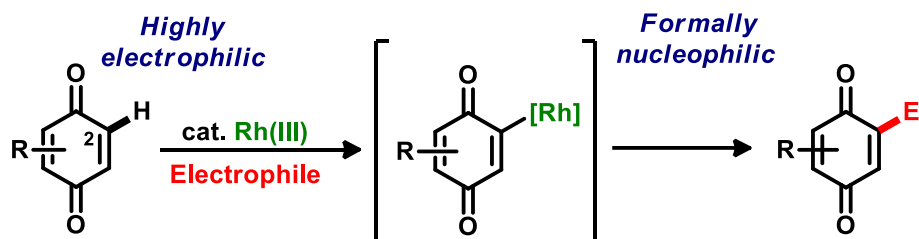
Extensive search in literature showed that catalytic halo- and hetero-functionalizations of 1,4-benzoquinones are less well developed, despite the established synthetic versatility of the products. Direct C–H halogenation of 1,4-benzoquinones is difficult, usually requiring forcing conditions or activated substrates.¹⁷⁰ Consequently, iodo- or bromo- benzoquinones are often obtained by oxidation of hydroquinone precursors, an approach that has obvious limitations.¹⁷¹

Driving by these facts, our main hypothesis is that the same C–H activation reaction performed in **56** could enable the highly electrophilic 1,4-benzoquinones C-2 position to function as a nucleophile. These kind of structure is considered more challenging than **56** because it possess multiple competing sites for C–H functionalization and are considerably more electrophilic than naphthoquinones, thereby rendering the prospect of the proposed unpoled processes uncertain (Scheme 43).

169. (a) Yang, W.; Wang, J.; Wei, Z.; Zhang, Q.; Xu, X.; Kinetic control of Rh(III)-catalyzed annulation of C–H bonds with quinones: chemoselective synthesis of hydrophenanthridinones and phenanthridinones. *J. Org. Chem.*, **2016**, *81*, 1675. (b) Zhou, T.; Li, L.; Li, B.; Song, H.; Wang, B.; Direct synthesis of N-H carbazoles via iridium(III)-catalyzed intramolecular C–H amination. *Org. Lett.*, **2015**, *17*, 4204. (c) Shaaban, S.; Jolit, A.; Petkova, D.; Maulide, N.; A family of low molecular-weight, organic catalysts for reductive C–C bond formation. *Chem. Commun.*, **2015**, *51*, 13902.

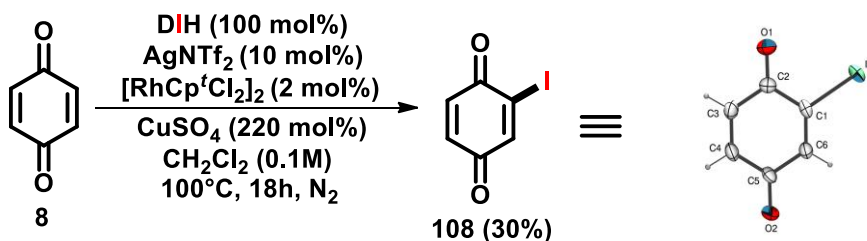
170. (a) Atkinson, R. C.; de la Mare, P. B. D.; Larsen, D. S.; The kinetics and mechanisms of additions to olefinic substances. Part 16. Addition of halogens to 1,4-benzoquinone and to 1,4-naphthoquinone, and dehydrohalogenation of the resulting adducts. *J. Chem. Soc., Perkin Trans. 2*, **1983**, *2*, 271. (b) Bansal, V.; Kanodia, S.; Thapliyal, P. C.; Khanna, R. N.; Microwave induced selective bromination of 1,4-quinones and coumarins. *Synth. Commun.*, **1996**, *26*, 887. (c) Kamigata, N.; Satoh, T.; Yoshida, M.; Reaction of benzeneselenenyl chloride with olefins in the presence of a Lewis acid. A novel one step vinylic chlorination. *Bull. Chem. Soc. Jpn.*, **1988**, *61*, 449.

171. (a) Dohi, T.; Nakae, T.; Takenaga, N.; Uchiyama, T.; Fukushima, K.; Fujioka, H.; Kita, Y.; μ -oxo-bridged hypervalent iodine(III) compound as an extreme oxidant for aqueous oxidations. *Synthesis*, **2012**, *44*, 1183. (b) Ali, M. H.; Welker, A.; York, C.; A facile and selective procedure for oxidation of hydroquinones using silica gel supported catalytic cerium(IV) ammonium nitrate. *Synthesis*, **2015**, *47*, 3207. (c) Kvalnes, D. E.; An optical method for the study of reversible organic oxidation–reduction systems. II. Halogenated benzoquinones. *J. Am. Chem. Soc.*, **1934**, *56*, 667.



Scheme 43. General hypothesis for the functionalization of 1,4-benzoquinones.

Our first attempt consisted in react 1,4-benzoquinone (**8**) with DIH (100 mol%) using the same reactional parameters developed earlier. For our delight, reaction was carried out in 30% yield and no bis-iodination products were observed (Scheme 43).



Scheme 44. Preliminary results.

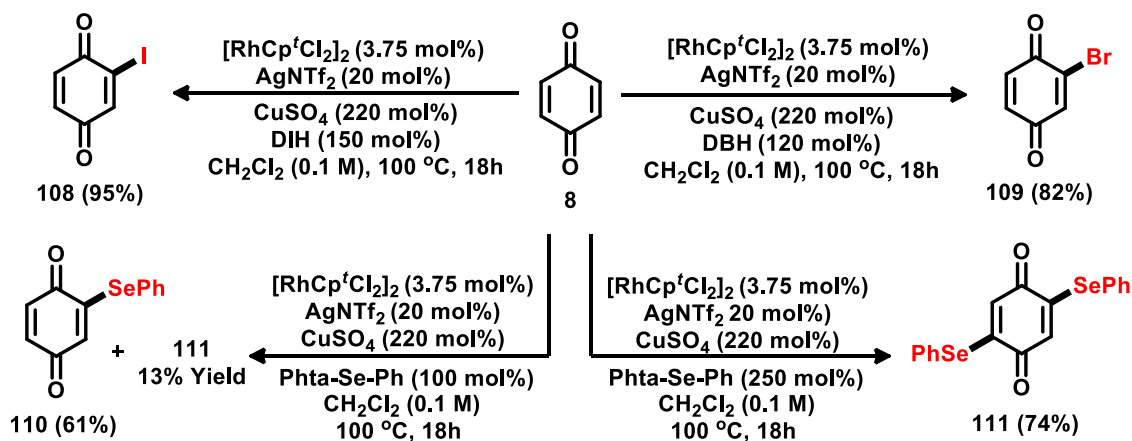
a

Next, a battery of reactions was performed in order to optimize yield. The results were detailed in Table 7. Previous synthesised rhodium pre-catalysts with different Cp-based ligands were screened, but none of them showed significant improvement in reaction yield. In order to investigate the effect of CuSO_4 in the system, a reaction was carried without this reactant, resulting in yield decrease (20%). Surprisingly, fine tuning in catalyst loading (3.75 mol%) resulted in yield increasing and **108** was obtained in 83%. Exchanging the iodine source to NIS (100 mol% and 150 mol%) using the new amount of catalyst led only yield decreasing. Alternate metal sulfate additives, such as $\text{Cu}(\text{OAc})_2$, $\text{Cu}(\text{OTf})_2$ and MgSO_4 were less effective, even with a raise in the amount of DIH (150 mol%). A reaction was carried in lower temperature (80 °C) with different amounts of DIH (100 and 150 mol%), resulting in yield decreasing (40% and 46%, respectively). Finally, the best result was achieved by raising the amount of DIH (150 mol%) with the temperature of 100 °C (Table 7).

Table 7: Optimization results.

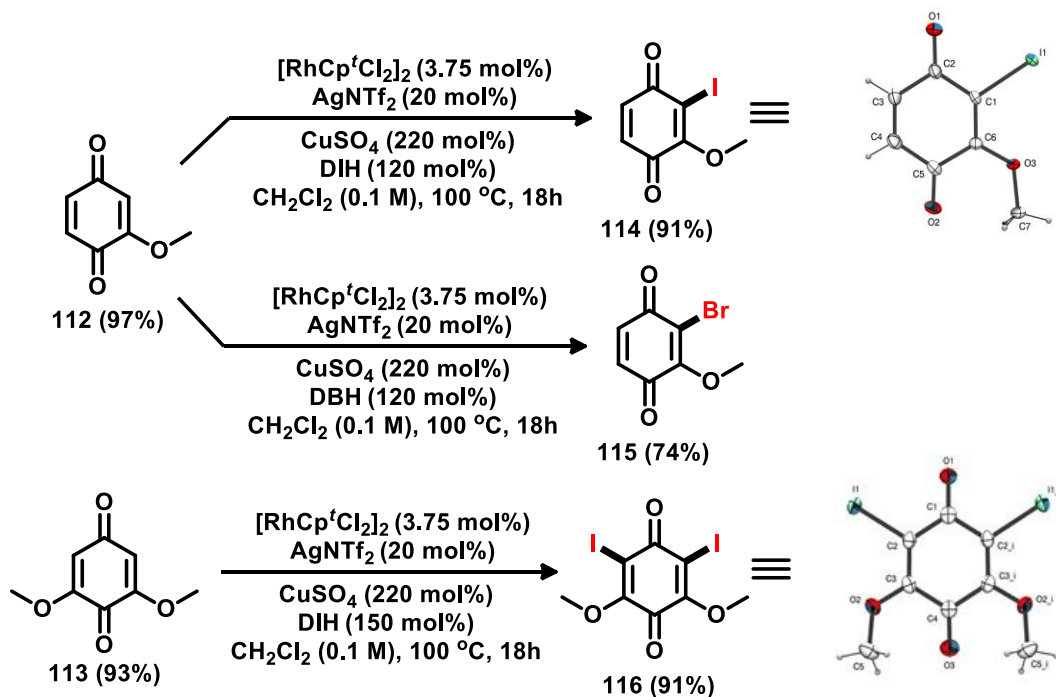
Rh source (mol%)	AgNTf ₂ (mol%)	Additive (220 mol%)	I ⁺ source (mol%)	Temp. (°C)	Yield (%)
[RhCp ^t Cl ₂] ₂ (2)	10	CuSO ₄	DIH (100)	100	30
[RhCp [*] Cl ₂] ₂ (2)	10	CuSO ₄	DIH (100)	100	24
[RhCp ^{*CF₃} Cl ₂] ₂ (2)	10	CuSO ₄	DIH (100)	100	2
[RhCp ^{*i-Pr} Cl ₂] ₂ (2)	10	CuSO ₄	DIH (100)	100	7
[RhCp ^t Cl ₂] ₂ (2)	10	none	DIH (100)	100	20
[RhCp ^t Cl ₂] ₂ (3.75)	20	CuSO ₄	DIH (100)	100	83
[RhCp ^t Cl ₂] ₂ (3.75)	20	CuSO ₄	NIS (100)	100	33
[RhCp ^t Cl ₂] ₂ (3.75)	20	CuSO ₄	NIS (150)	100	42
[RhCp ^t Cl ₂] ₂ (3.75)	20	MgSO ₄	DIH (100)	100	21
[RhCp ^t Cl ₂] ₂ (3.75)	20	MgSO ₄	DIH (150)	100	32
[RhCp ^t Cl ₂] ₂ (3.75)	20	Cu(OAc) ₂	DIH (150)	100	10
[RhCp ^t Cl ₂] ₂ (3.75)	20	Cu(OTf) ₂	DIH (150)	100	mixture
[RhCp ^t Cl ₂] ₂ (3.75)	20	CuSO ₄	DIH (100)	80	40
[RhCp ^t Cl ₂] ₂ (3.75)	20	CuSO ₄	DIH (150)	80	46
[RhCp^tCl₂]₂ (3.75)	20	CuSO₄	DIH (150)	100	95

With the best reactional conditions in hand, we sought functionalizations using other highly reactive electrophiles. Electrophile sources like DCH, Selectfluor and Phta-S-Ph resulted in no reaction. Pleasingly, using DBH (120 mol%) in place of DIH, we found that bromination of **8** proceeded smoothly to afford **109** in 82% yield. With the selenium-containing electrophile source Phta-Se-Ph, compound **110** was prepared in 61% yield, accompanied by a 13% yield of bis-selenated product **111**. Increasing the loading of Phta-Se-Ph to 250 mol% enabled the selective generation of bis-functionalization adduct **111** in 74% yield (Scheme 45).



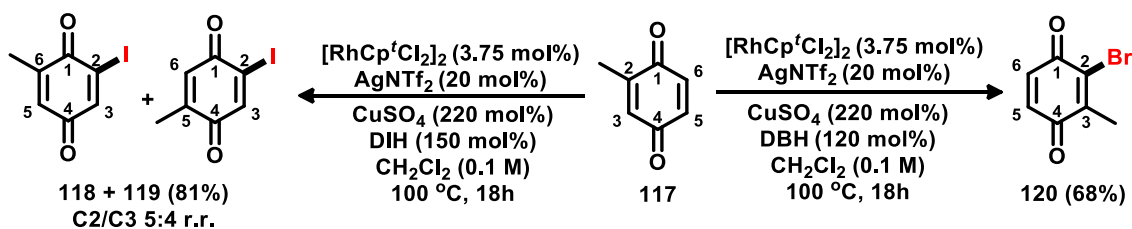
Scheme 45. Use of another electrophile sources.

Next, electron rich substrates **112** and **113** were employed in order to investigate the effects of electron donating groups. As expected, iodination happened in the electronically more activated position (derivatives **114** and **115**, 91% and 74% yield, respectively). For substrate **113**, double-iodination occurred providing derivative **116** in excellent yield (Scheme 46).



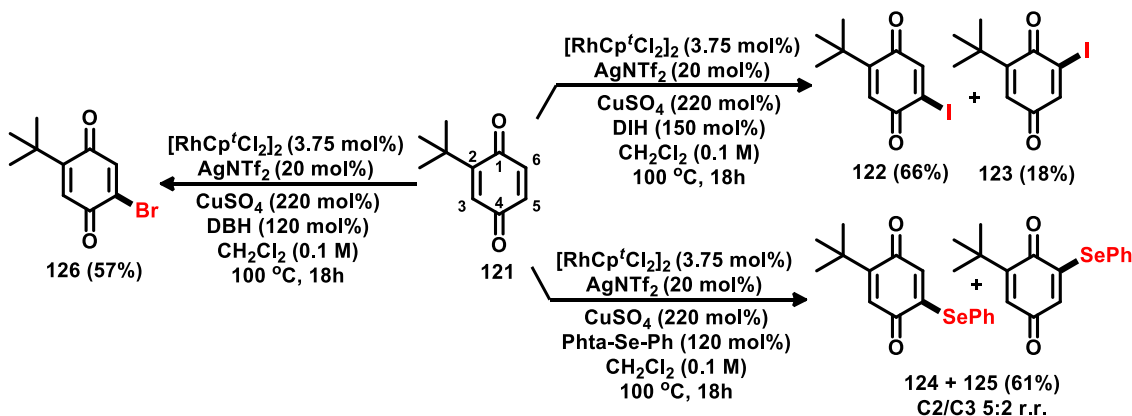
Scheme 46. Use of electron-rich substrates.

Aiming the investigation of steric hindrance effect, methyl-substituted benzoquinone (**117**) was submitted to reaction conditions. For the iodination reaction, functionalization occurred on the side opposite the C6-methyl group as a major product, but iodination product at position 5 was also detected. Both derivatives **118** and **119** were obtained in 81% yield as an inseparable mixture of regioisomers (C2/C3 5:4 r.r.). When DBH was used, bromination occurred in the most electron-rich and most hindered position C3, delivering derivative **120** in 68% yield (Scheme 47).



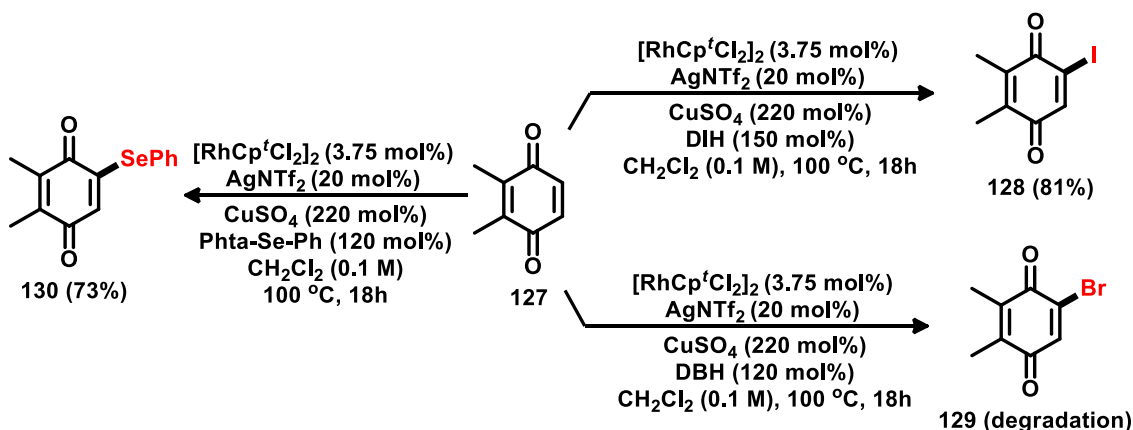
Scheme 47. Reaction with unsymmetrical substrate **117**.

As expected, regioselectivity was higher for substrate **121**, which possess a bulkier *tert*-butyl substituent, and iodination of this substrate occurred mostly in the less hindered position (derivative **122**, 66% yield). Derivative **123** was also isolated in 18% yield, resulting in a regioisomeric ratio (r.r.) of 3:1. Use of Phta-Se-Ph resulted in a mixture of inseparable isomers in the purification conditions, and derivatives **124** and **125** were obtained in 61% with regioisomeric ratio of 5:2 (C2/C3). Surprisingly, bromination of the same substrate resulted in one product (derivative **126**, 57% yield) with traces of another product, possibly the other regioisomer (determined by TLC) (Scheme 48).



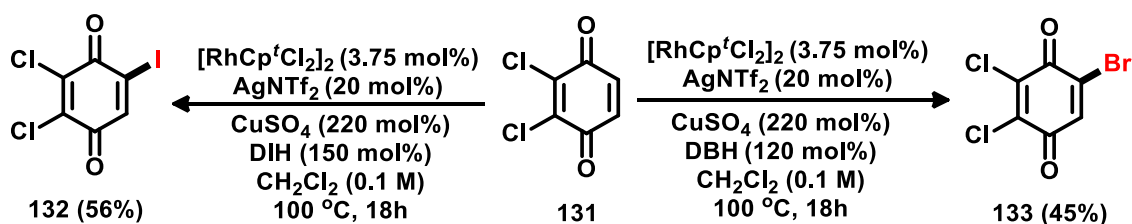
Scheme 48. Reaction with unsymmetrical substrate **121**.

The mono-functionalization protocol was extended to double-substituted benzoquinones. Iodination and phenyl-selenation reactions were carried out in substrate **127**, affording derivatives **128** and **130** in good yields. Curiously, bromination of **127** led to the formation of unstable product **129**; this product suffered degradation and couldn't been isolated (Scheme 49).



Scheme 49. Reactions with substrate **127**.

As expected, the process was less efficient for systems possessing electron-withdrawing substituents. For example, iodination of 2,3-dichloro system **131** provided adduct **132** in 56% yield. For the bromination reaction, even a lower yield was obtained (derivative **133**, 45%) (Scheme 50).



Scheme 50. Reaction with electron-deficient substrate **131**.

Even with a complete scope of derivatives provided by the development and application of iodination, bromination and phenyl-selenation reactions in naphthoquinones and benzoquinones, the idea of a plausible mechanism was still far from being predicted. Encouraged by that fact, a Kinetic isotope effect (KIE) experiment was conducted in order to provide some mechanistic insights about the rate-determining step of C-H activation reaction at C-2 position.

KIEs effects measurements is considered one of the most powerful and common techniques for studying reaction mechanisms.¹⁷² Such experiments can provide critical information about which bonds are broken and formed at different stages of the

172. Anslyn, E.V.; Dougherty, D.A.; *Modern Physical Organic Chemistry*, University Science Books, Sausalito, **2006**.

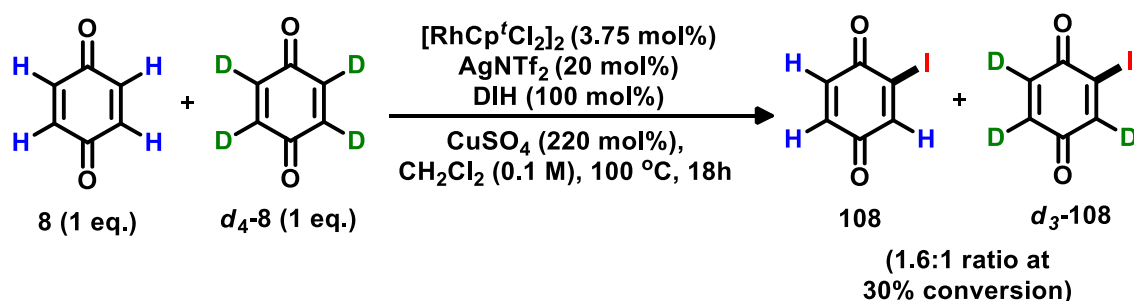
reaction, giving in some cases even properties about the transition state of the process.¹⁷³ It is considered one of the most suited experiment for mechanistic studies of C-H bond functionalization because C-H bonds rarely undergo exchange in the absence of an external reagent or catalyst (in comparison with N-H and O-H bonds).¹⁷⁴

KIE effects are commonly measured via three main experiments:¹⁷⁵

- KIE determined from two parallel reactions;
- KIE determined from an intermolecular competition;
- KIE determined from an intramolecular competition.

In this work, only KIE determined from an intermolecular competition was carried out.

In our KIE intermolecular competition experiment, both substrates (1,4-benzoquinone (**8**) and *d*₄-1,4-benzoquinone (*d*₄-**8**)) were present in the same vessel and competed in the reaction for a limited amount of DIH. KIE is calculated from the relative amount of products formed by functionalization of a C-H versus a C-D bond (Scheme 51). The experiment was monitored via ¹H and deuterium NMR (Figure 17).



Scheme 51. KIE intermolecular competition experiment.

173. Kwart, H.; Temperature dependence of the primary kinetic hydrogen isotope effect as a mechanistic criterion. *Acc. Chem. Res.*, **1982**, *15*, 401.

174. Yu, J.-Q.; Shi, Z.; *C-H Activation*, Springer, Berlin, **2010**.

175. Simmons, E.M.; Hartwig, J.F.; On the interpretation of deuterium kinetic isotope effects in C-H bond functionalizations by transition-metal complexes. *Angew. Chem. Int. Ed.*, **2012**, *51*, 3066.

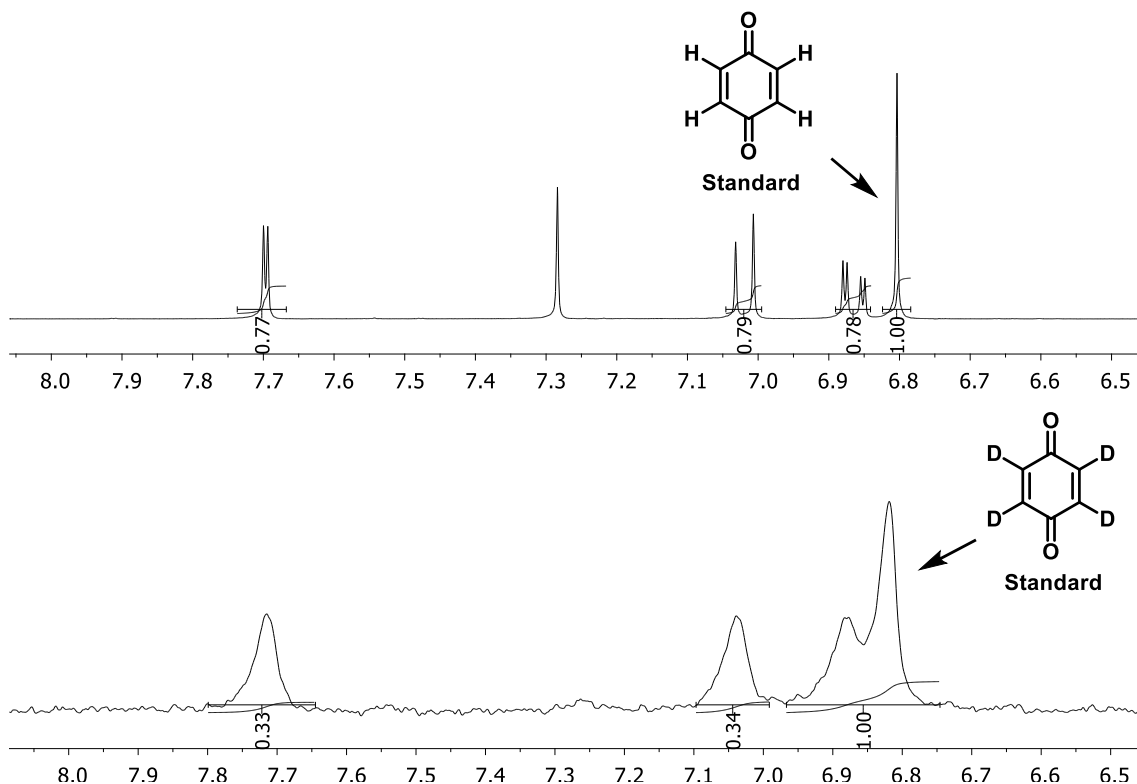


Figure 17: ¹H NMR spectra (400 MHz, CDCl₃) and deuterium NMR spectra (400 MHz, CHCl₃) for determination of the **108/d₃-108** ratio (Benzoquinone (6.9 mg) and *d*₄-benzoquinone (6.9 mg) were used as standards).

A small value of KIE = 1.6 was obtained. According to Hartwig and Simmons,¹⁷⁵ a KIE value of this magnitude infer that C-H bond cleavage is not happening during the rate determining step, which make us believe in the following hypothesis:

- C-H bond cleavage could be occurring after another step, such as the catalyst formation by the breaking of the pre-catalyst (rhodium pre-catalysts are well described in literature, and a great majority of reports shows the breaking of these dimers promoted by temperature and/or use of a silver additive), or an oxidative addition event between the electrophilic iodine source and the catalyst.

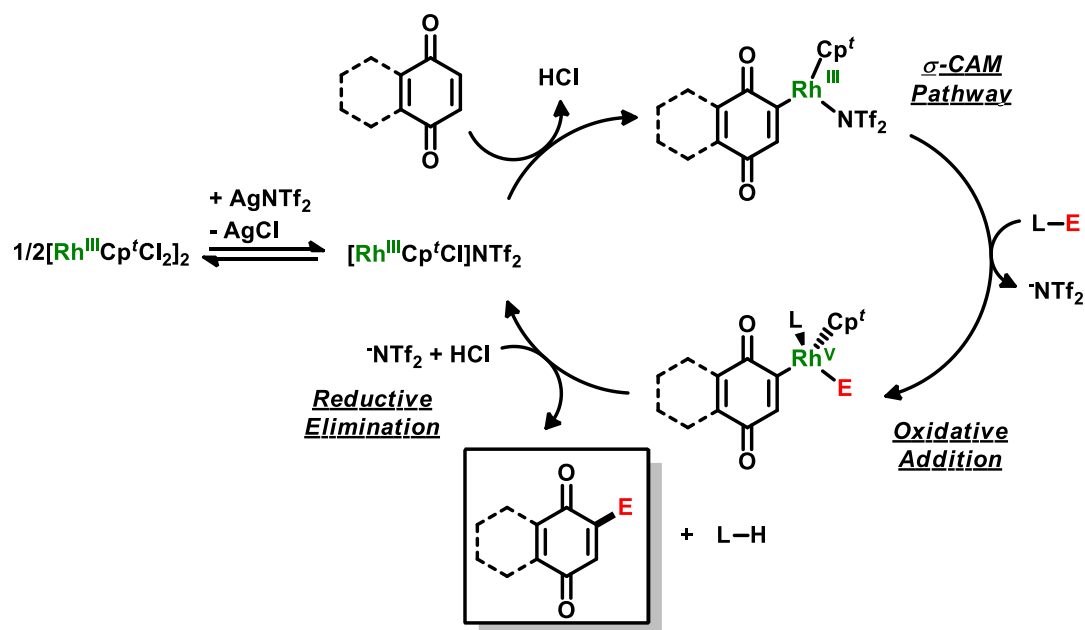
The use of CuSO₄ is justified by:

- Act as a Lewis acid, either enhancing the reactivity of the electrophile and/or sequestering the leaving group derived by-product ((halo)-5,5-dimethylhydantoin, phenylselenol).

- Act as a drying agent, once water has proved to quench the reaction.

Such considerations are not enough to construct a full mechanism based on concrete data, once open flask experiments were not possible to be performed due the nature of the reaction (these reactions were all carried out in sealed tube and inert atmosphere). But, either way, a possible mechanism for this reaction was proposed based on the current facts and hypothesis.

The mechanism starts with the formation of the active catalyst species, followed by the metalation event, which could occur via σ -complex-assisted metathesis (σ -CAM). Next, an oxidative addition between the electrophilic specie L-E and the benzoquinone complex takes place, followed by the reductive elimination to regenerate the catalyst and deliver the functionalized benzoquinone (Scheme 52).



Scheme 52. Proposed mechanism governed by σ -complex-assisted metathesis pathway.

5.3. Development of Functionalization Reactions Involving the C-I bond of the Novel Quinones

5.3.1. Palladium Catalysed Cross-Coupling Reactions

The successful iodination of the A-ring of naphthoquinones with a versatile atom like iodine made possible the further functionalization of these structures which already known protocols as for example, palladium cross-coupling reactions.¹⁷⁶ Such methodologies have been successfully employed in a wide range of natural products to achieve late stage C-C bond formations for over 40 years.¹⁷⁷

In principle, iodination at C-5 position should enable new ways for further functionalization of 1,4-naphthoquinones. However, due to inaccessibility of these A-ring substituted compounds, palladium catalysed cross-coupling involving the benzenoid ring have not been developed. Reported examples showed that the quinonoid moiety can act as an oxidant for palladium,¹⁷⁸ proving that the use of these kinds of molecules as substrates for palladium cross-coupling remains a challenge goal.

As a first attempt, a reported Suzuki protocol for electron deficient substrates was tested,¹⁷⁹ resulting in substrate decomposition. Microwave-assisted Suzuki reactions were also tested without success, leading to the same complex mixture of products (Warning: microwave assisted Suzuki reactions have to be performed in proper microwave vessels).¹⁸⁰ Variations in the catalyst, base and solvent were employed, but such variations resulted in a complex mixture of products. Use of catalyst Pd(*d*^f-bpf)Cl₂ led to only traces of product, and solvent screen failed to improve yield (Scheme 53).

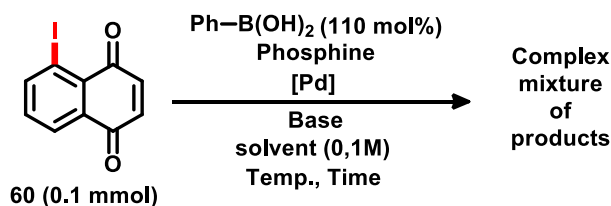
176. https://www.nobelprize.org/nobel_prizes/chemistry/laureates/2010/advanced-chemistryprize2010.pdf accessed in 25/01/2017.

177. Seechurn, C.C.C.J.; Kitching, M.O.; Colacot, T.J.; Snieckus, V.; Palladium-catalyzed cross coupling: A historical contextual perspective to the 2010 Nobel Prize. *Angew. Chem. Int. Ed.*, **2012**, *51*, 5062.

178. (a) Fujiwara, Y.; Domingo, V.; Seiple, I.B.; Gianatassio, R.; Del Bel, M.; Baran, P.S.; Practical C–H functionalization of quinones with boronic acids. *J. Am. Chem. Soc.*, **2011**, *133*, 3292. (b) Walker, S.E.; Jordan-Hore, J.A.; Johnson, D.G.; Macgregor, S.A.; Lee, A.-L.; Palladium-catalyzed direct C–H functionalization of benzoquinone. *Angew. Chem. Int. Ed.*, **2014**, *53*, 13876.

179. Kim, Y.M.; Yu, S.; Palladium(0)-catalyzed amination, Stille coupling, and Suzuki coupling of electron-deficient aryl fluorides. *J. Am. Chem. Soc.*, **2003**, *125*, 1696.

180. Sharma, A.K.; Gowdahalli, K.; Krzeminski, J.; Amin, S.; Microwave-assisted Suzuki cross coupling reaction, a key step in the synthesis of polycyclic aromatic hydrocarbons and their metabolites. *J. Org. Chem.*, **2007**, *72*, 8987.



Attempts: All conditions led to a complex mixture of products!

Dioxane/H ₂ O (10:1) Pd(OAc) ₂ (4%) K ₂ CO ₃ (125%) 250 W, 20 min	THF Pd(PPh ₃) ₄ (3%) Na ₂ CO ₃ (300%) Relux, 24 h	THF Pd(dba) ₃ (1%) KF (300%) P(<i>t</i> -Bu) ₃ (2%) r.t., 24 h	THF Pd(dba) ₃ (1%) K ₃ PO ₄ (200%) P(<i>t</i> -Bu) ₃ (2%) r.t., 24 h
--	---	---	---

With this condition, traces of product were detected!	<div style="border: 1px dashed black; padding: 5px; display: inline-block;"> CH₃CN/H₂O (10:1) Pd(d^t-bpf)Cl₂ (1.5 mol%) Na₂CO₃ (150 mol%) 60 °C, 24 h </div>	Solvent screening →	-THF -Methanol -Toluene -DMF -DMAc	traces of product
		→		

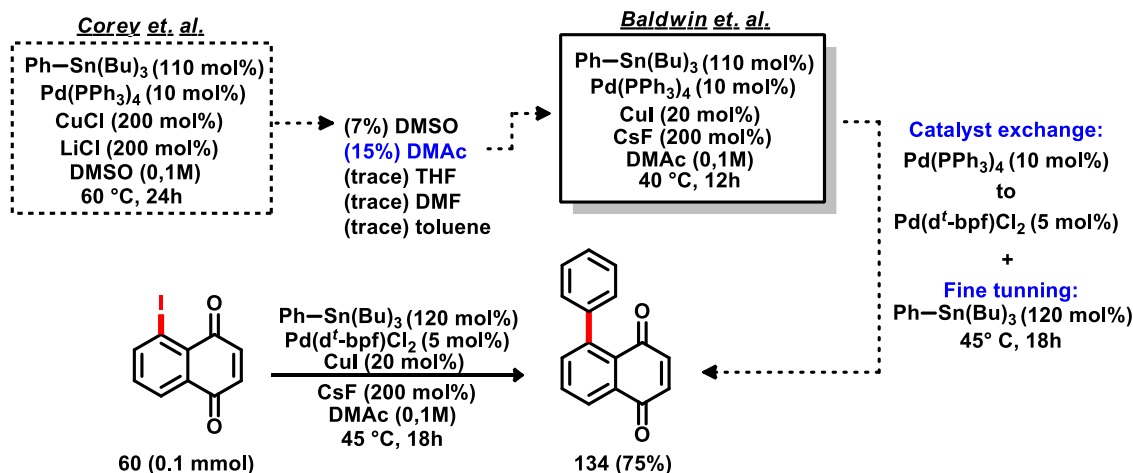
Scheme 53. Unsuccessful attempts to achieve Suzuki coupling.

Investigation on alternative cross couplings led to experiments employing Stille reaction protocol.¹⁸¹ Initial attempts followed a procedure by Corey et. al.¹⁸² providing derivative **134** in 7% yield. Solvent screening was conducted, and DMAc proved to be the best one. Next, methodology described by Baldwin and co-workers¹⁸³ was employed with DMAc as solvent, resulting in 25% yield of **134**. Use of catalyst (Pd(d^t-bpf)Cl₂) instead of Pd(PPh₃)₄ provided further major improvements (56% yield), and after fine-tuning in the reagent loading, temperature and reaction time, Stille coupling was performed in mild conditions providing **134** in 75% yield (Scheme 54).

181. Stille, J.K.; Palladium catalyzed coupling of organotin reagents with organic electrophiles. *Pure Appl. Chem.*, **1985**, *57*,1771.

182. Han, X.; Stoltz, B.M.; Corey, E.J.; Cuprous chloride accelerated Stille reactions. A general and effective coupling system for sterically congested substrates and for enantioselective synthesis. *J. Am. Chem. Soc.*, **1999**, *121*, 7600.

183. Mee, S.P.H.; Lee, V.; Baldwin, J.E.; Stille coupling made easier - the synergic effect of copper(I) salts and the fluoride ion. *Angew. Chem. Int. Ed.*, **2004**, *43*, 1132.



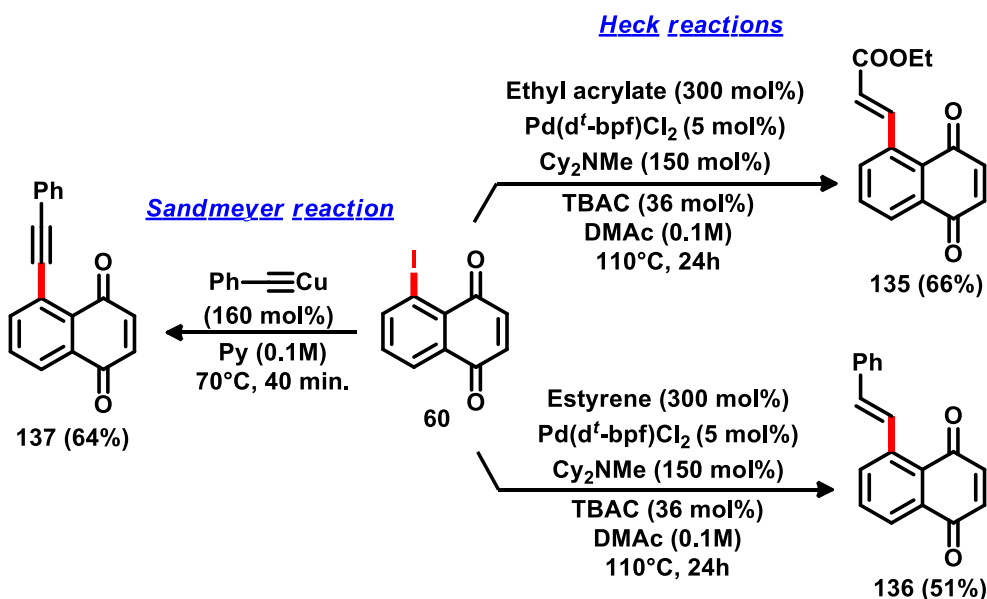
Scheme 54. Optimization and best conditions for Stille coupling.

The next reaction investigated was Heck cross-coupling. Encouraged by the results obtained by the previous palladium-catalysed cross-coupling reactions, further investigation in the literature identified a robust method described by Sweeney and co-workers¹⁸⁴ that uses previous successful reactants like Pd(d^t-bpf)Cl₂, DMAc and mild conditions to promote C-C bond formation between halogenated arenes and olefins. Use of this methodology afforded product **135** in 54% yield. With fine tuning in the reagent loading and temperature, yield could be raised to 66% yield. Use of styrene as olefin source resulted in product **136** in 51% yield (Scheme 55).

Further attempts in promote Sonogashira cross-coupling (experiments were conducted in the same conditions noted by the authors)¹⁸⁵ also led to a mixture of products in all cases, similar to the results for Suzuki experiments. Still, achievement of the Sonogashira-like product **137** in good yield was possible following the procedure described by Shvartsberg and co-workers, using stoichiometric amounts of (phenylethynyl)copper in a Sandmeyer reaction (Scheme 55).¹⁴³

184. Murray, P.M.; Bower, J.F.; Cox, D.K.; Galbraith, E.K.; Parker, J.S.; Sweeney, J.B.; A robust first-pass protocol for the Heck-Mizoroki reaction. *Org. Process Res. Dev.*, **2013**, *17*, 397.

185. (a) Uргаonkar, S.; Verkade, J.G.; Ligand-, copper-, and amine-free Sonogashira Reaction of aryl iodides and bromides with terminal alkynes. *J. Org. Chem.*, **2004**, *69*, 5752. (b) Richards, J.J.; Melander, C.; Synthesis of a 2-aminoimidazole library for antibiofilm screening utilizing the sonogashira reaction. *J. Org. Chem.*, **2008**, *73*, 5191. (c) Dolliver, D.D.; Bhattarai, B.T.; Pandey, A.; Lanier, M.L.; Bordelon, A.S.; Adhikari, S.; Dinser, J.A.; Flowers, P.F.; Wills, V.S.; Schneider, C.L.; Shaughnessy, K.H.; Moore, J.N.; Raders, S.M.; Snowden, T.S.; McKim, A.S.; Fronczek, F.R.; Stereospecific Suzuki, Sonogashira, and Negishi coupling reactions of *N*-alkoxyimidoyl iodides and bromides. *J. Org. Chem.*, **2013**, *78*, 3676.



Scheme 55. Heck cross-couplings and reaction with phenylethynylcuprate(I).

5.3.2. Copper Catalysed Organoyl-Thiolation Reactions

In our pursuit for another reactions with C-5 iodinated naphthoquinones, the methodology described by Liu and Ye¹⁸⁶ involving the copper-catalyzed trifluoromethylthiolation of aryl halides attracted our attention due to its mild conditions and high yields. Among the well-known functional groups in chemistry, -SCF₃ and -CF₃ have attracted attention because of their importance in pharmaceutical and agrochemical industries.¹⁸⁷ Sulfur-containing naphthoquinones are also quite interesting in medicinal chemistry,¹⁸⁸ and the synthesis of a family of A-ring substituted compounds aiming structure-activity relation (SAR) investigation could open new avenues in this field.

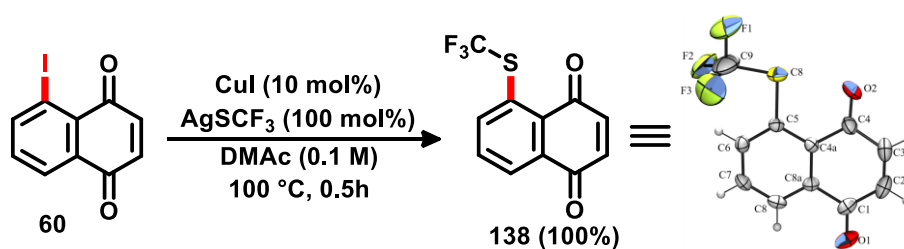
As a first attempt, C-5 iodinated 1,4-naphthoquinone **60** was reacted with silver trifluoromethylthiolate (AgSCF₃) in room temperature to afford only traces of product

186. Xu, J.; Mu, X.; Chen, P.; Ye, J.; Liu, G.; Copper-catalyzed trifluoromethylthiolation of aryl halides with diverse directing groups. *Org. Lett.*, **2014**, *16*, 3942.

187. (a) Li, M.; Zhou, B.; Xue, X.-S.; Cheng, J.-P.; *J. Org. Chem.*, **2017**, *82*, 8697. (b) Purser, S.; Moore, P.R.; Swallow, S.; Gouverneur, V.; *Chem. Soc. Rev.*, **2008**, *37*, 320.

188. (a) Heldreth, B.; Turos, E.; Microbiological properties and modes of action of organosulfur-based anti-infectives. *Curr. Med. Chem. - Anti-Infective Agents*, **2005**, *4*, 295. (b) Huang, M.-H.; Wu, S.-N.; Chen, C.-P.; Shen, A.-Y.; Inhibition of Ca²⁺-activated and voltage-dependent K⁺ currents by 2-mercaptophenyl-1,4-naphthoquinone in pituitary GH₃ cells contribution to its antiproliferative effect. *Life Sciences*, **2002**, *70*, 1185. (c) Tandon, V.K.; Singh, R.V.; Yadava, D.B.; Synthesis and evaluation of novel 1,4-naphthoquinone derivatives as antiviral, antifungal and anticancer agents. *Bioorg. Med. Chem.*, **2004**, *14*, 2901.

138. The use of high temperature (100 °C) produced the desired product in 39% yield with no other by-products observed (as for example, functionalization at the position 2 of the naphthoquinone). Next, we decided to investigate the effectiveness of a copper source in this reaction and, pleasingly, the experiments revealed impressive results. The use of 10 mol% of CuI at 100°C delivered **138** in 100% yield in a reaction time of 0.5 hour (Scheme 56).



Scheme 56. Initial result for the copper catalysed trifluoromethylthiolation reactions.

These preliminary reactional parameters were tested in the series of previously described iodinated 1,4-naphthoquinones. In general, yield decreasing was observed in most examples, fact that encouraged us to investigate another sources of Cu^I.

For this new study, CuBr was used in the same amount (10 mol%), being less effective. Further refinement aiming to minimize the amount of CuI and reaction time afforded **138** in 90% yield with 5 mol% of copper in 0.5 hour. Exchanging CuI for Cu(OAc)₂ in the same conditions gave only and yield of 16%.

We insisted on the investigation of an alternative Cu^I-salt for a quantitative preparation of **138**, and copper(I)-thiophene-2-carboxylate (CuTc) was the perfect candidate for being a well-known agent able to promote diverse reactions, for instance, Ullmann¹⁸⁹ and Liebeskind–Srogl¹⁹⁰ coupling. CuTc is a powerful salt for this reaction, probably due to its ability to allow internal coordination from the sulfur atom to the metal and/or due to an inherent ability of the carboxylate to work as a ligand to stabilize the oxidative addition product.¹⁸⁹

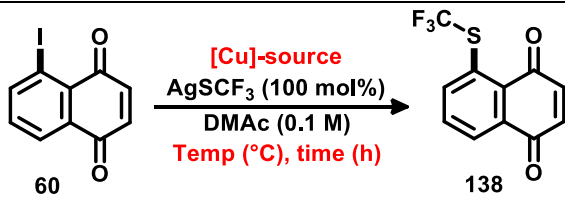
Reaction conducted using CuTc (10 mol%) for 24 hours resulted in 24% yield. Raising the temperature to 50 °C gave afforded full conversion for the product in 24

189. Zhang, S.; Zhang, D.; Liebeskind, L.S.; Ambient temperature, Ullmann-like reductive coupling of aryl, heteroaryl, and alkenyl halides. *J. Org. Chem.*, **1997**, *62*, 2312.

190. Liebeskind, L.S.; Srogl, J.; Thiol ester–boronic acid Coupling. A mechanistically unprecedented and general ketone synthesis. *J. Am. Chem. Soc.*, **2000**, *122*, 11260.

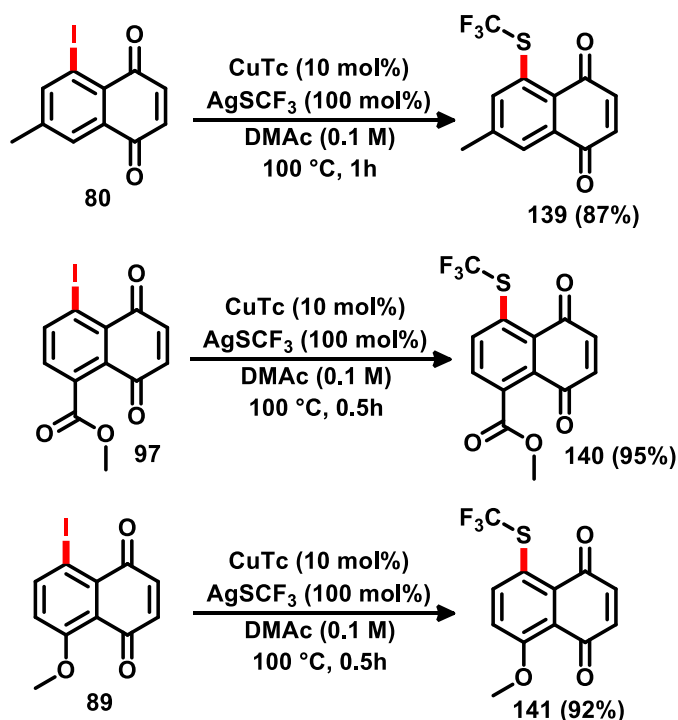
hours, but the yield dropped to 64% in a reaction time of 0.5 hour. Raising the temperature to 100 °C resulted in full conversion again, even reducing the reaction time to 0.5 hour. Best conditions were achieved with fine tuning in catalyst loading (5 mol%), once decreasing the loading even more (4.5 mol%) resulted in yield decrease (Table 8).

Table 8: Selected optimization results.



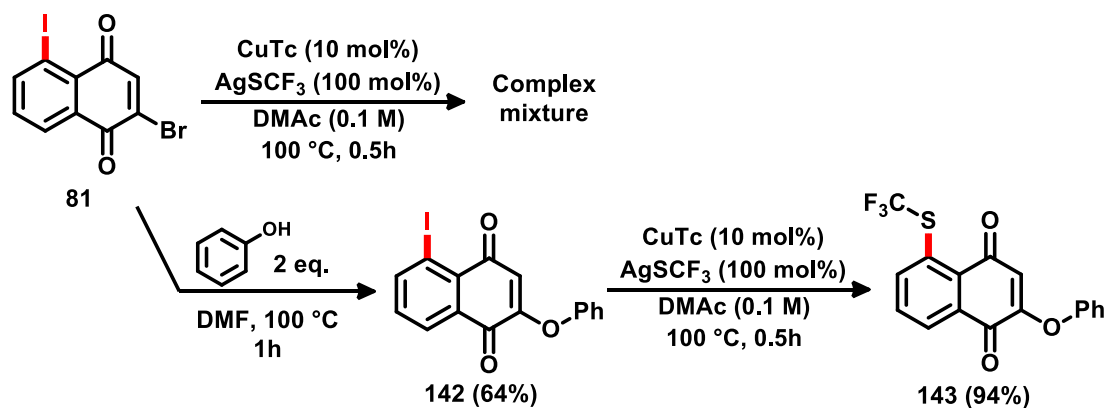
[Cu]-source (mol%)	Time (h)	Temperature (°C)	Yield (%)
none	24	r.t.	trace
none	24	100	39
CuI (10)	0.5	100	100
CuBr (10)	0.5	100	81
CuI (5)	0.5	100	90
Cu(OAc) ₂ (10)	0.5	100	16
CuTc (10)	24	r.t.	24
CuTc (10)	24	50	10
CuTc (10)	0.5	50	64
CuTc (10)	1	100	100
CuTc (10)	0.5	100	100
CuTc (5)	0.5	100	100
CuTc (4.5)	0.5	100	91

For the reactional scope, several previous synthesised C-5 iodinated naphthoquinones were chosen based on their substitution patterns. All reactions presented good to excellent yields, with some minor exceptions. The reaction showed robustness with substituents like methyl (**80**), -COOMe (**96**) and methoxy (**89**), and derivatives **139**, **140** and **141** where synthesised in good to excellent yields with no side-products observed. (Scheme 57).



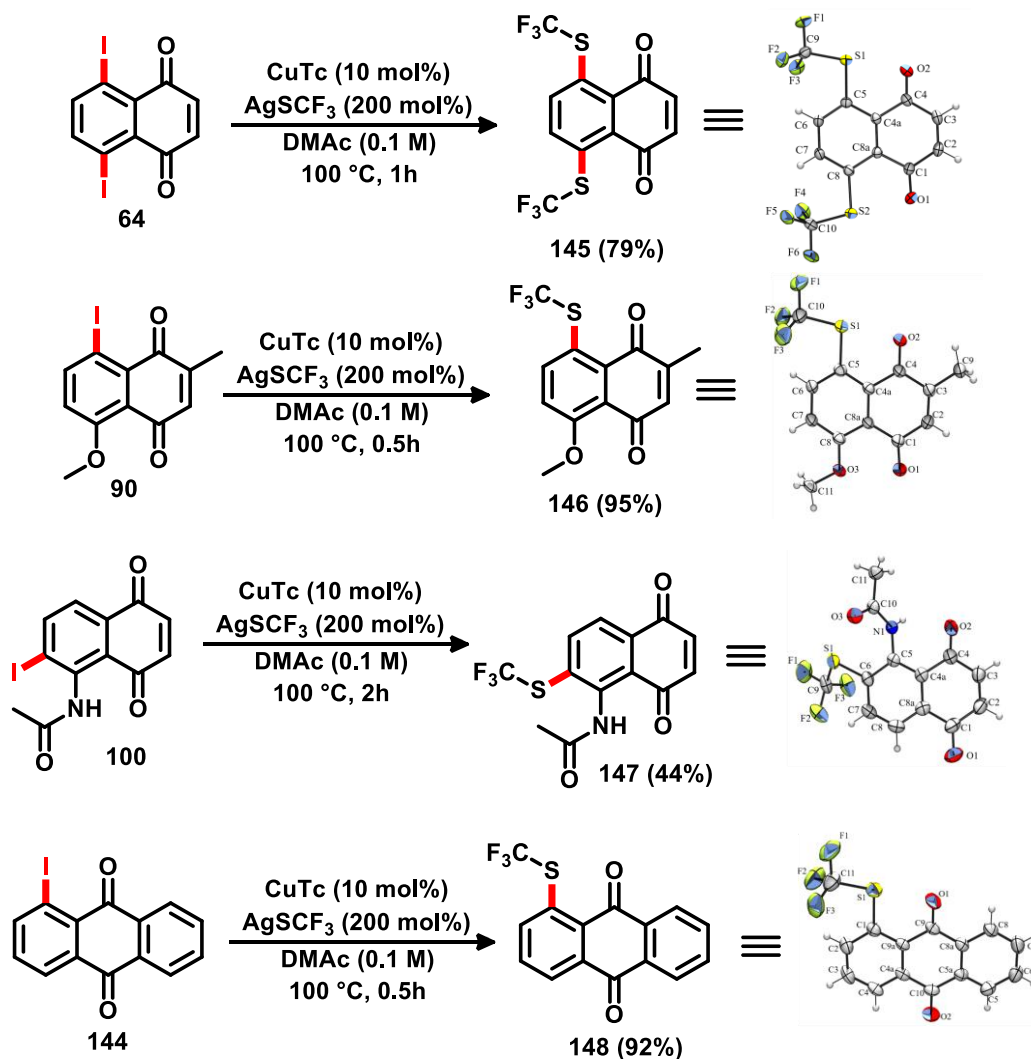
Scheme 57. Results for reaction with substrates **80**, **97** and **89**.

Next, substrate **81** was tested in order to comprehend the reactional behaviour of a molecule with two halogens in the same backbone. Surprisingly, the reaction resulted in a complex mixture of products. The bromine atom was substituted by a phenyl-ether substituent by reaction of **81** with phenol in DMF at $100\text{ }^\circ\text{C}$, affording **142** in 64% yield. Copper-catalysed trifluoromethylation performed in this substrate resulted in derivative **143** in 94% yield (Scheme 58).



Scheme 58. Experiments with substrate **81**.

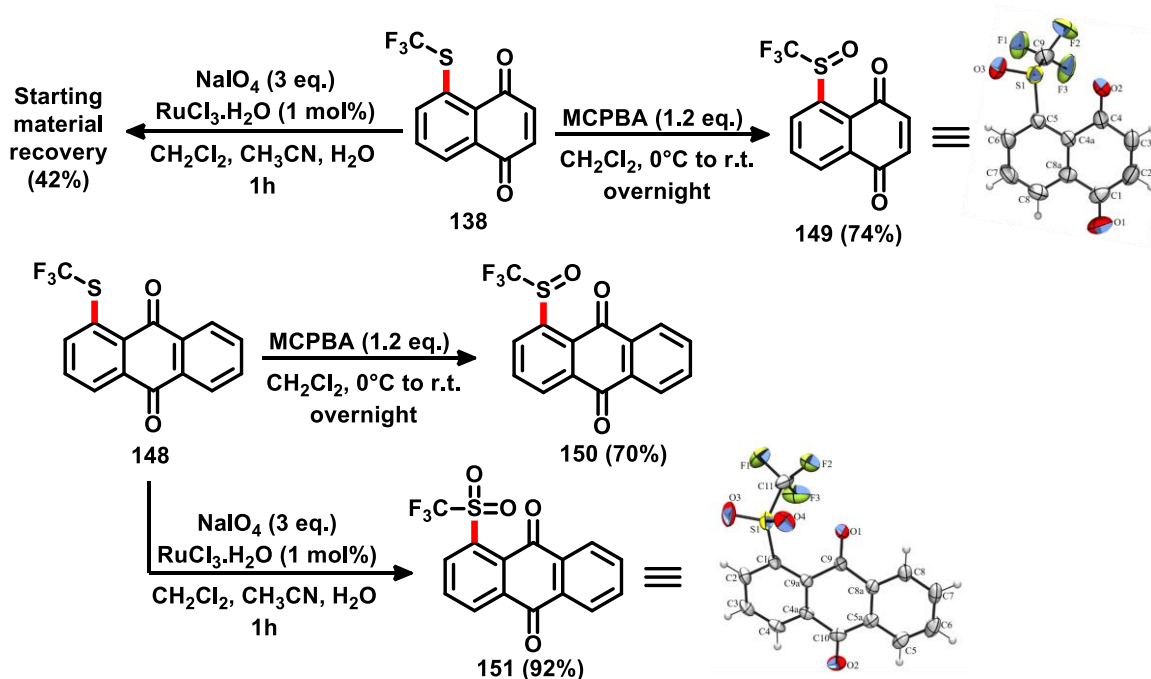
Derivatives **145**, **146** and **148** were also obtained in good to excellent yields. Only one compound was prepared in moderate yield (derivative **147**, 44%) probably due to degradation of the starting material under the reactional conditions, once a complex mixture of products was also detected by TLC. Even with a longer reaction time of 6h, was not possible to optimize the reactional parameters (Scheme 59).



Scheme 59. Experiments with substrates **64**, **90**, **100** and **144**.

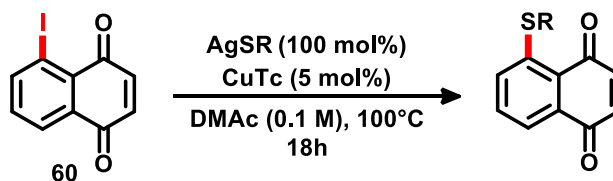
Further modifications in the –SCF₃ portions were carried out in **138** and **148**, by oxidising the sulfur atom into S^{IV} and S^{VI} using oxidants like *meta*-chloroperoxybenzoic acid (MCPA) and a system consisted of catalytic RuCl₃.H₂O and NaIO₄, methodology

described by Su.¹⁹¹ Oxidation of **138** and **148** with MCPBA provided derivatives **149** and **150** in 74% and 70% yield, respectively. Oxidation with RuCl₃.H₂O/NaIO₄ applied to **138** led only to starting material recovery. The same oxidation was performed in **148**, affording derivative **151** in excellent yield (Scheme 60).



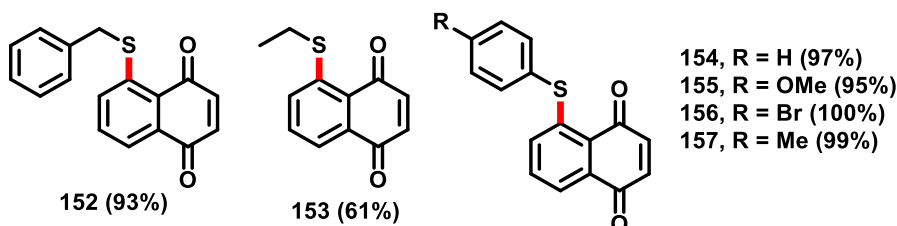
Scheme 60. Oxidation reactions.

The versatility of the organoyl-thiolation process was also studied by using different AgSR-salts for preparing new sulfur-containing quinones. With the iodinated quinone **60** in hands the respective sulphides **152** – **157** were prepared in excellent yields with exception of compound **153**, synthesized in 61% yield. It was noted that with these kinds of silver salts, other than AgSCF₃, a longer reaction time was necessary to achieve the best yields, and the reactions were carried out overnight (Schemes 61 and 62).



Scheme 61. General reaction for benzyl, alkyl and aryl derivatives.

191. Su, W.; An efficient method for the oxidation of sulfides to sulfones *Tetrahedron Lett.*, **1994**, 35, 4955.



Scheme 62. Benzyl, alkyl and aryl derivatives **152** – **157**.

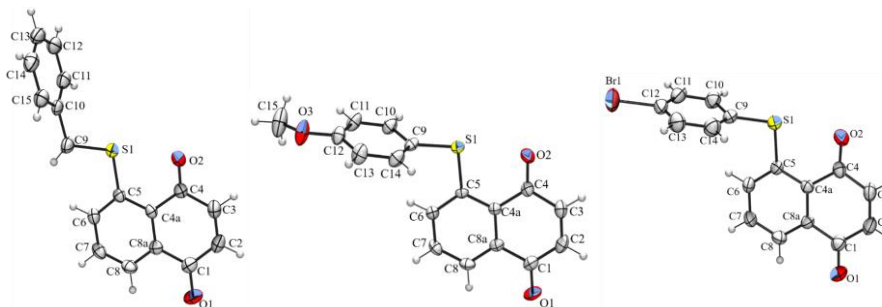
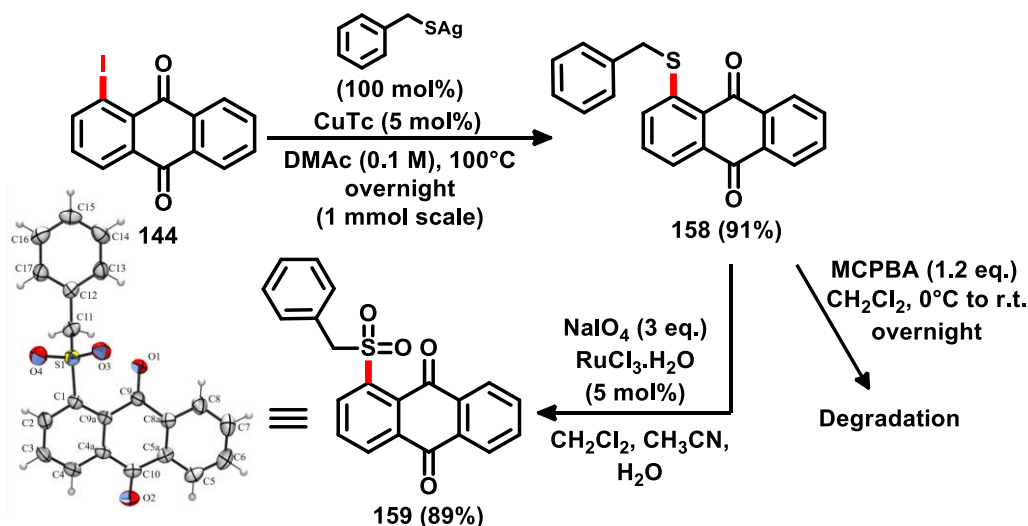


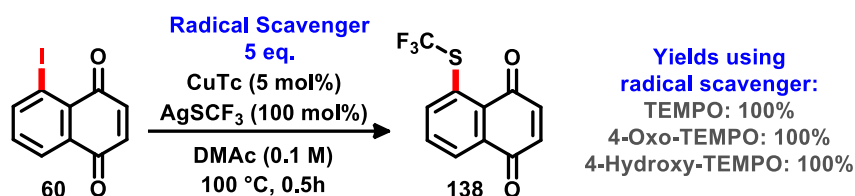
Figure 18. Crystal structures of compounds **152**, **155** and **156**.

Compound **144** was chosen for a 1 mmol-scale reaction, affording derivative **158** in excellent yield. This compound was subjected to the same oxidation protocols of the quinone–SCF₃ derivatives, resulting in degradation when MCPBA was used. **158** was successfully oxidised using with RuCl₃.H₂O/NaIO₄ generating derivative **159** in 89% yield (Scheme 63).



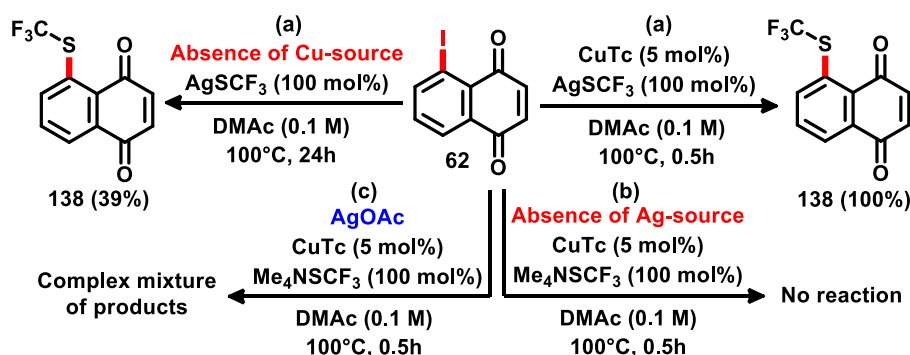
Scheme 63. Oxidation reactions with substrate **158**.

Exploratory reactions aiming to formulate a proposed mechanism for the organoyl-thiolation process were conducted. As suggested by Szabó group,¹⁹² $\cdot\text{CF}_3$ radicals may be involved in the reaction of C-H trifluoromethylation of quinones. TEMPO, which is a well-known radical scavenger, was used to evaluate the presence of radicals in those reactions. Aware of this information, we have accomplished inhibition experiments with TEMPO, 4-Oxo-TEMPO and 4-Hydroxy-TEMPO. In all cases, quinone **138** was obtained in 100% yield indicating that the reaction does not proceed via a radical mechanism (Scheme 64).



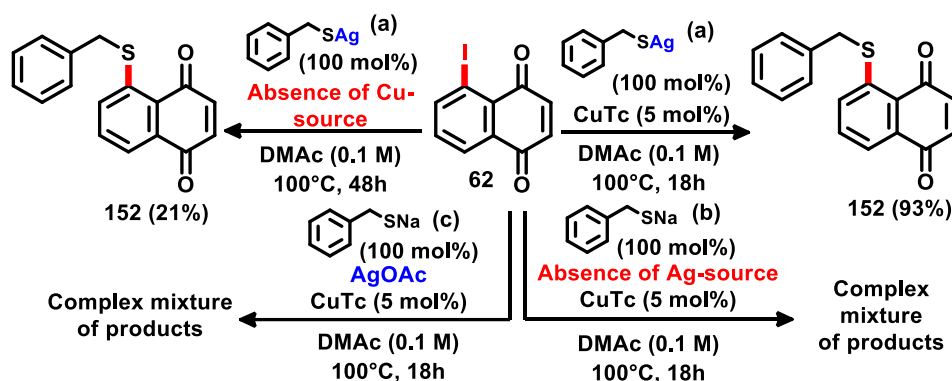
Scheme 64. Inhibition experiments with TEMPO and its derivatives.

Subsequently, we have considered three experiments: (a) Presence and absence of Cu-source, (b) Absence of Ag-source and (c) Absence of AgSR (Schemes 65 for **138** and 66 for **152**). These experiments have indicated that CuTc and AgSR are essential for forming **138** and **152** since the absence of Cu-source affords them in only 39% and 21% yields, respectively. Without Ag-salt, no reaction was observed in relation to **138** and in the case of **152**, a complex mixture of products was observed. Finally, the replacement of the Ag- and S-salts led to a complex mixture of products in both cases.



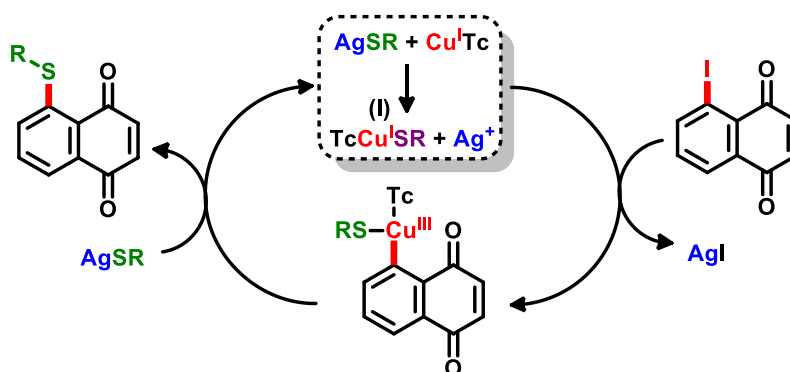
Scheme 65. Experiments with the presence and absence of Cu and Ag.

192. Ilchenko, N.O.; Janson, P.G.; Szabó, K.J.; Copper-mediated C–H trifluoromethylation of quinones. *Chem. Commun.*, **2013**, *49*, 6614.



Scheme 66. Experiments with the presence and absence of Cu and Ag.

Based on our observations, a proposed mechanism was formulated and described. The mechanism starts with complexation between the readily available organosulfur anion and the copper complex to generate active species $\text{TcCu}^{\text{I}}\text{SR}$ plus a free Ag^+ cation, in a similar event to a Liebeskind–Srogl coupling.¹⁹⁰ Another -SR source ($\text{Me}_4\text{N}^+\text{SCF}_3^-$ and PhCH_2SNa) led to a complex mixture of products, even with the prior addition of another silver salt (AgOAc), which leads us to believe that ion exchange between the thio-silver salts and the $\text{Cu}^{\text{I}}\text{Tc}$ catalytic species is fundamental. In fact, air-stable ligated copper-thiolate complexes like $(\text{bpy})\text{Cu}^{\text{I}}\text{SCF}_3$ were broadly described.¹⁹³ Finally, an oxidative addition event generates the metalated specie and silver iodide. Reductive elimination of the Cu^{III} complex affords the desired functionalized naphthoquinone and regenerates the active Cu^{I} species for the next catalytic cycle (Scheme 67).



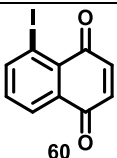
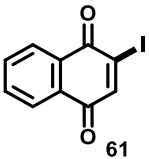
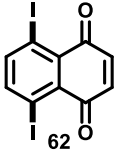
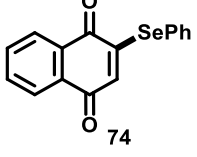
Scheme 67. Proposed mechanism for organoyl-thiolation reaction.

193. Weng, Z.; He, W.; Chen, C.; Lee, R.; Tan, D.; Lai, Z.; Kong, D.; Yuan, Y.; Huang, K.-W.; An air-stable copper reagent for nucleophilic trifluoromethylthiolation of aryl halides. *Angew. Chem. Int. Ed.*, **2013**, *52*, 1548.

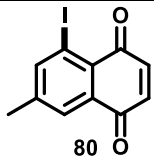
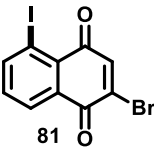
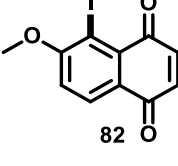
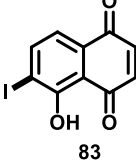
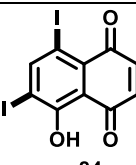
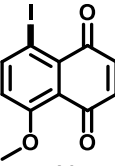
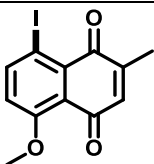
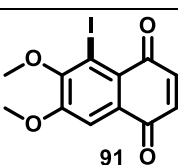
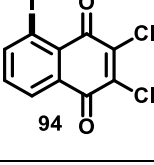
5.4. Biological Assays

The potential of selected compounds were evaluated against bloodstream forms of *Trypanosoma cruzi* (IC₅₀/24h) and mammalian cells (LC₅₀/24h), allowing the determination of the selectivity index (SI) derived from the ratio of LC₅₀/IC₅₀ (Table 9). Benznidazole (Bz) and nifurtimox (Nif) are the current drugs used to treat Chagas disease. The efficiency of these drugs is related to the phase of the disease and their effectiveness is reduced in advanced stages of the infection. In this sense, the limited curative capacity in chronic phases and high toxic effects make necessary the development of new trypanocidal drugs.¹⁹⁴ *The following results were performed at 37 °C, which is considered the host temperature and no blood.*

Table 9: Activity of synthetic derivatives against bloodstream trypomastigotes of *T. cruzi* (Y strain) at 37 °C and no blood, cytotoxicity to mammalian cells and Selectivity Index (SI).

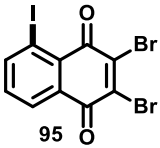
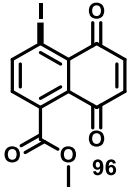
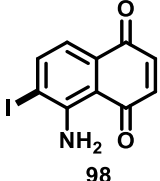
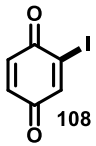
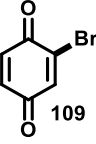
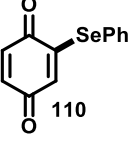
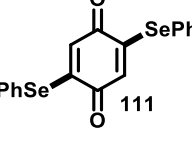
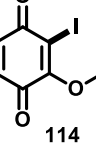
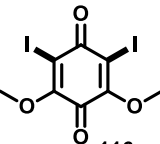
Compounds	IC ₅₀ / 24h (μM)	LC ₅₀ / 24h (μM)	SI
	0.59 ± 0.08	11.49 ± 0.54	19.5
	1.79 ± 0.37	14.72 ± 2.68	8.2
	0.22 ± 0.07	12.93 ± 1.43	28.8
	1.13 ± 0.22	12.67 ± 0.70	11.2

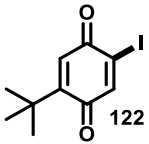
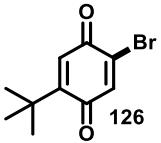
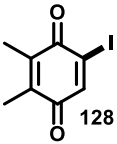
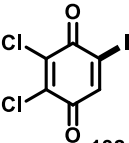
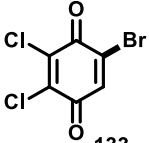
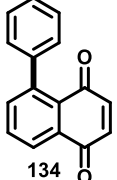
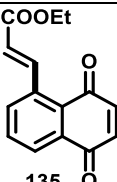
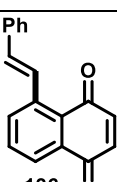
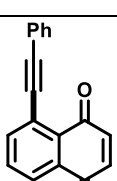
¹⁹⁴ Salomao, K.; Menna-Barreto, R.F.S.; de Castro, S.L.; Stairway to heaven or hell? Perspectives and limitations of Chagas disease chemotherapy. *Curr. Top. Med. Chem.*, **2016**, *16*, 2266.

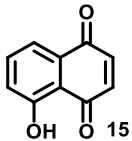
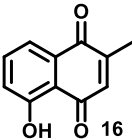
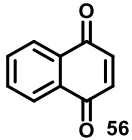
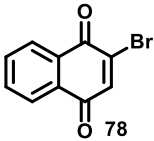
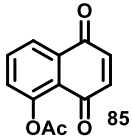
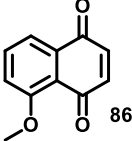
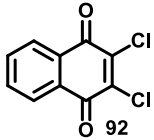
 80	0.49 ± 0.04	12.09 ± 0.24	24.7
 81	1.38 ± 0.57	12.15 ± 0.15	8.8
 82	1.17 ± 0.23	14.19 ± 3.21	12.1
 83	42.0 ± 3.11	>100	>4.6
 84	24.8 ± 4.49	>100	>5.1
 89	3.54 ± 0.71	13.59 ± 0.79	3.8
 90	7.57 ± 0.56	51.88 ± 10.42	6.9
 91	1.62 ± 0.34	12.16 ± 0.16	7.5
 94	7.26 ± 1.41	27.83 ± 5.17	3.8



UFMG

 95	2.25 ± 0.48	11.82 ± 0.37	5.3
 96	1.61 ± 0.44	13.94 ± 0.21	8.7
 98	0.56 ± 0.05	13.12 ± 1.16	23.4
 108	20.77 ± 8.31	86.02 ± 2.99	4.1
 109	21.54 ± 5.83	34.35 ± 2.46	1.6
 110	15.95 ± 3.52	13.78 ± 4.37	0.86
 111	83.42 ± 9.08	>100	>1.2
 114	23.95 ± 7.08	32.62 ± 9.71	1.4
 116	1.94 ± 0.51	27.71 ± 1.22	1.3

	12.77 ± 1.61	35.93 ± 4.92	2.8
	14.09 ± 2.32	42.30 ± 4.67	3.0
	10.07 ± 3.26	15.40 ± 3.87	1.5
	26.99 ± 4.30	>100	>3.7
	15.40 ± 1.34	>100	>6.5
	1.24 ± 0.31	12.67 ± 0.10	10.2
	6.03 ± 1.19	12.65 ± 0.26	2.1
	0.19 ± 0.08	11.87 ± 0.43	62.5
	2.20 ± 0.33	12.49 ± 0.23	5.7

 15	6.51 [*]	>10 [*]	>1.5 [*]
 16	1.38 [*]	>10 [*]	>7.2 [*]
 56	0.79 [*]	8 [*]	10.1 [*]
 78	1.37 [*]	>10 [*]	>7.3 [*]
 85	0.16 [*]	10 [*]	62.5 [*]
 86	1.02 [*]	>10 [*]	>9.8 [*]
 92	2,17 [*]	>10 [*]	>4,6 [*]
benznidazole	9.68 ± 2.35	>4000	>413.2

*Values were calculated from previous published work (Salomão et. al.; *BMC Microbiology*, **2013**, *13*, 196).

Compounds **60** and **62** showed significant activity against the parasite with IC₅₀ values of 0.59 and 0.22 μM, respectively, low toxicity for the mammalian cell, and an SI higher than 19 (*the reference drug use in this studies was benznidazole* (IC₅₀/24h = 9.68 ± 2.35 μM)). When compared with starting product **56** (IC₅₀ = 0.79 μM, SI 10.1), it's clear that the iodination strategy generated more potent and less toxic compounds. Di-iodinated naphthoquinone **62** was obtained as a by-product (*vide supra*) in poor yield (5%) and further optimization of its preparation will be necessary.

C-2 functionalization may be a good general strategy for preparing bioactive compounds, since naphthoquinones substituted at C-2 with iodine (**61** $IC_{50} = 1.79 \mu\text{M}$, SI 8.2) and selenium (**74**, $IC_{50} = 1.13 \mu\text{M}$, SI 11.2) were 5.4 and 8.5 times more active than benznidazole, respectively. It is important to notice that insertion of a selenium atom contributed to an increase in selectivity. Compound **80** ($IC_{50} = 0.49 \mu\text{M}$, SI 24.7) combine a methyl group with an iodine substituent, showed important activity, being around 20 times more active than benznidazole. Compounds **81**, **82** and **91** also exhibited good $IC_{50}/24\text{h}$ values ($<2 \mu\text{M}$).

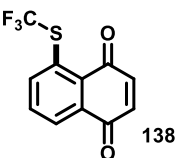
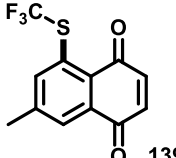
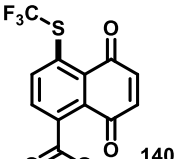
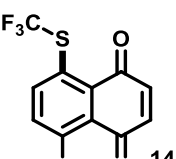
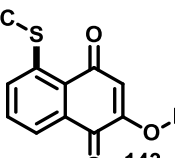
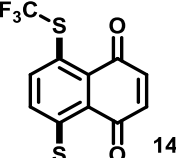
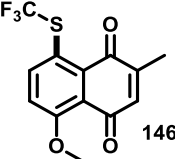
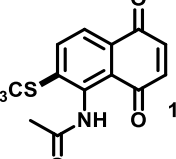
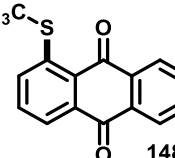
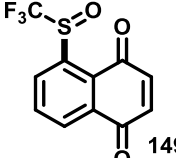
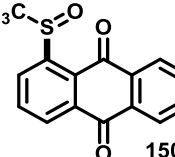
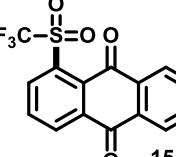
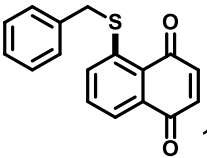
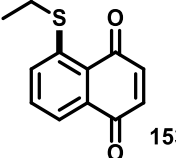
The iodination of juglone (**15**) resulted in a decrease in the activity [**83** (42.0/SI >4.6), and **84** (24.8/SI >5.1)], and a slightly decrease was also observed with the iodination of **86** [**89** (3.54/SI >3.8)]. Electron-deficient halogenated compounds **94** ($IC_{50} = 7.26 \pm 1.41 \mu\text{M}$, SI 3.8) and **95** ($IC_{50} = 2.25 \pm 0.48$, SI 5.3) presented decreased values in activity, when compared to their structural analogues **56** and **92**. Compound **96** showed good activity ($<2 \mu\text{M}$), and the combination of an amine with iodine substituent (compound **98**, $IC_{50} = 0.56 \mu\text{M}$, SI = 23.4) proved to be highly efficient.

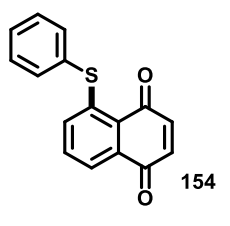
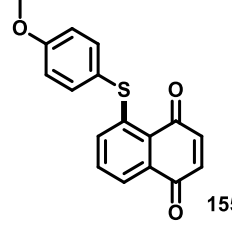
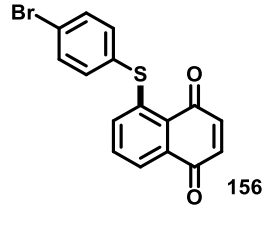
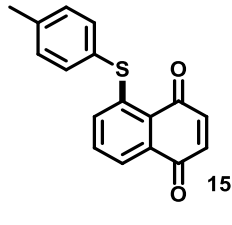
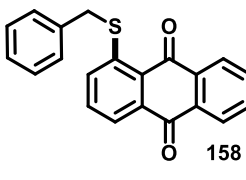
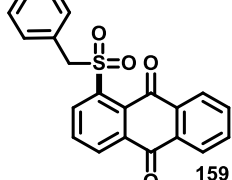
All benzoquinones presented IC_{50} values between 83 to $10 \mu\text{M}$, with the exception of **113** that showed interesting trypanocidal activity, with an IC_{50} value of less than $2 \mu\text{M}$. This compound is easily obtained from commercially available benzoquinone in just one-step.

The most active compound was **136**, with an $IC_{50}/24\text{h} = 0.19 \mu\text{M}$, is 50 times more active than benznidazole, with an SI of 62.5. Although the studies described here are preliminary, it is worth noting that the combination of a practical synthetic route, high in vitro trypanocidal activity and low toxicity to mammalian cells, makes **136** a very attractive hybrid quinone in the search for better trypanocides.

Next, The potential of the sulfur-substituted benzenoid 1,4-naphthoquinones as trypanocidal analogues has been investigated by screening them against trypomastigote forms of *Trypanosoma cruzi* (Table 10). *The following results were performed at 4°C , which is considered the temperature of blood banks and 5% blood.*

Table 10. Activity of synthetic derivatives against bloodstream trypomastigotes of *T. cruzi* (Y strain) at 4 °C and 5% blood.

Compounds	IC ₅₀ / 24h	Compounds	IC ₅₀ / 24h
 138	41.2 ± 3.5	 139	67.3 ± 5.5
 140	34.5 ± 6.3	 141	41.9 ± 5.8
 143	54.4 ± 5.5	 145	240.1 ± 14.8
 146	>1000.0	 147	32.7 ± 4.1
 148	>1000.0	 149	67.3 ± 6.1
 150	>1000.0	 151	>1000.0
 152	14.3 ± 0.9	 153	31.3 ± 2.4

	12.4 ± 2.2		7.6 ± 0.3
	6.6 ± 0.8		2.5 ± 0.3
	64.9 ± 5.9		36.3 ± 2.2
benznidazole	$103.6 \pm 0.6^*$		

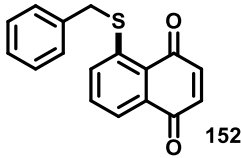
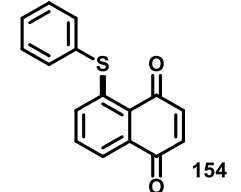
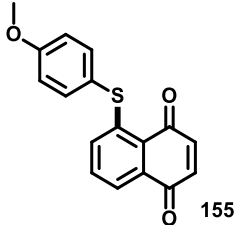
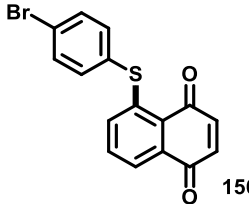
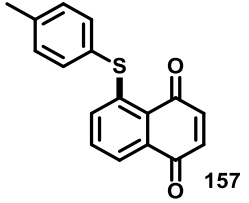
* Value from previous published work (Pinto et. al., *Eur. J. Med. Chem.*, **2008**, *43*, 1774.).

Only four compounds were not active against the parasite with $IC_{50}/24h > 1000 \mu M$ (compounds **146**, **148**, **150** and **151**). Trifluoromethylthiolated naphthoquinones **138** – **141**, **143** and **147** showed potent activity against *T. cruzi* with $IC_{50}/24h$ in the range of 67.3 to 32.7 μM , with special attention to compounds **140** ($IC_{50} = 34.5 \mu M$) and **147** ($IC_{50} = 32.7 \mu M$). In comparison to the standard drug, benznidazole ($IC_{50} = 103.6 \mu M$), **140** and **147** are 3.0 and 3.1-fold, respectively, more active.

Finally, **152-159** were also evaluated against the parasite. From this family, all compounds were more active than benznidazole, with IC_{50} values ranging from 64 to 2.5. Compound **157** with $IC_{50} = 2.5 \mu M$ was almost 41 times more active than Bz. In these conditions, these compounds could be applied as chemoprophylactic agents to treat contaminated blood in blood banks endemic areas.

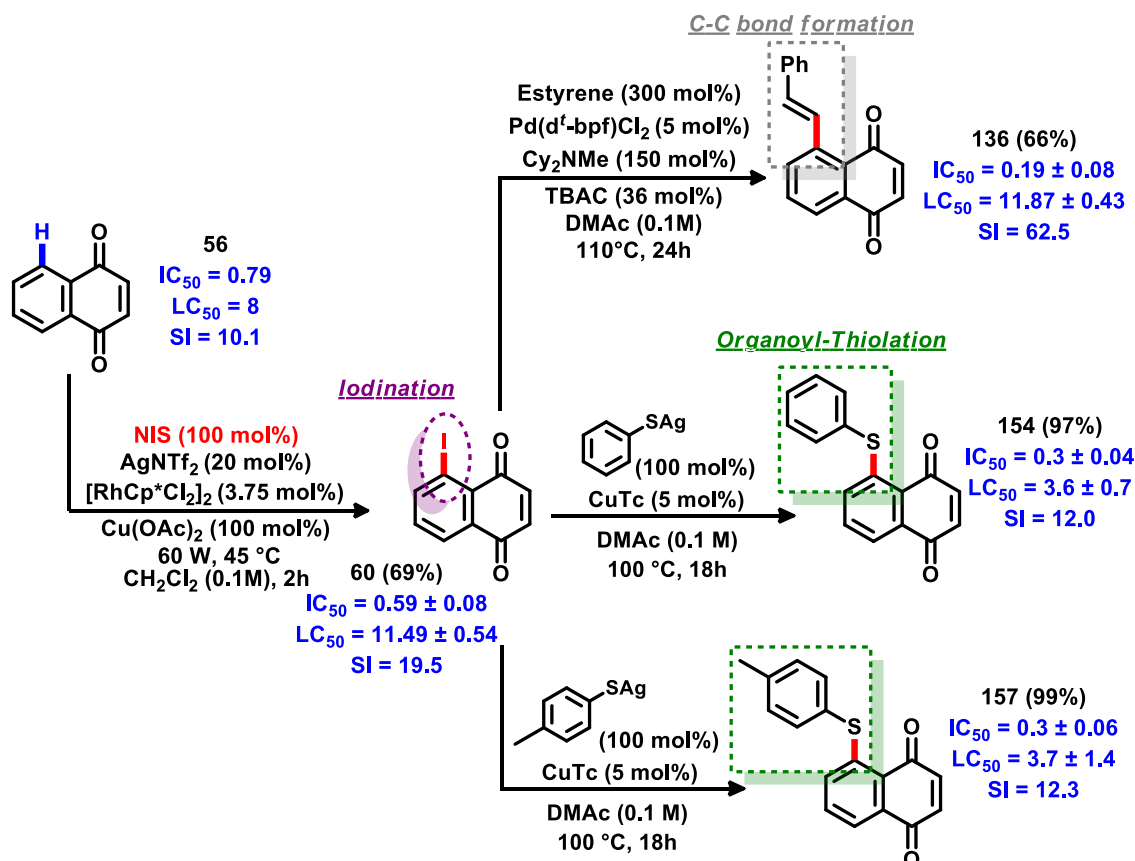
The most active compounds in the previous conditions (4 °C and 5% blood) were tested again in the host temperature conditions (37 °C). The cytotoxicity to mammalian cells and Selectivity Index (SI) were also calculated. Results are shown in Table 11.

Table 11. Activity of synthetic thio-derivatives against bloodstream trypomastigotes of *T. cruzi* (Y strain) at 37 °C and no blood, cytotoxicity to mammalian cells and Selectivity Index (SI).

Compounds	IC ₅₀ / 24h	LC ₅₀ / 24h	SI
 152	1.1 ± 0.2	10.5 ± 0.2	9.5
 154	0.3 ± 0.04	3.6 ± 0.7	12.0
 155	1.3 ± 0.03	3.3 ± 0.3	2.5
 156	1.9 ± 0.03	6.0 ± 1.0	3.2
 157	0.3 ± 0.06	3.7 ± 1.4	12.3
benznidazole	9.68 ± 2.35	>4000	>413.2

In those conditions, **152**, **154** – **157** were all more active than benznidazole, with compounds **154** and **157**, being 32 more active than the standard drug. These compounds, along with **136**, can be considered the most active quinones ever synthesized. The modification of A-ring of 1,4-naphthoquinones proved to be a valid strategy in order to achieve more active and selective naphthoquinoidal hybrids. Scheme

68 shows the modification evolution starting in **56**, emphasizing the success of the developed reaction in the achievement of more potent and selective derivatives.



Scheme 68. Modifications of **56** leading to more potent and selective derivatives.

6. Conclusion

- Efficient, valuable and practical methodologies for modification of the A-ring of naphthoquinoidal substrates using rhodium-catalyzed C-H iodination processes have been developed and optimized, mechanistic insights were made;
- With the optimized reactions, the scope of the transformation was achieved, generating 19 examples of A-ring iodination and 1 example of A-ring bromination;
- B-ring rhodium-catalyzed C-H iodination reaction was also developed, and the methodology was extended to functionalize benzoquinones, generating a total of 21 examples of iodination, bromination and phenyl-selenation; mechanistic studies and insights were conducted;

- The successful synthesis of **60** opened the way for the exploration of valuable palladium cross-coupling reactions at the A-ring, showing both the difficulties and best conditions for obtaining novel C-C bond formation derivatives, in a total of 4 examples;
- The A-ring functionalization of naphthoquinones with iodine also turned possible the development of copper-catalysed organoyl-thiolation reactions, from the optimization to the synthesis of 17 novel compounds, as well as mechanistic studies and insights;
- Oxidation reactions were also carried out, originating 4 new compounds;
- 51 compounds were evaluated against *T. cruzi* (Y strain) in different conditions, three novel derivatives **136**, **154** and **157** can be considered a quinone milestone in Chagas therapy, and further studies will be carried on in order to evaluate the potency of these compounds as new trypanocidal drugs.

This work is a detailed collection manuscript of 4 already published reports (see appendix 1 for the articles):

- *Chem. Sci.*, **2016**, 7, 3780; Impact Factor = 9.1
- *Org. Lett.*, **2016**, 18, 4454; Impact Factor = 6.6
- *Eur. J. Med. Chem.*, **2017**, 136, 406; Impact Factor = 4.5
- *Org. Biomol. Chem.*, **2018**, 16, 1686; Impact Factor = 3.6

Literature research has inspired the writing of a recently accepted review article:

- *Da Silva Júnior, E.N.; Jardim, G.; Liang, Y.-F.; da Silva, R.G.; Ackermann, L.; Weakly-coordinating N-oxide and carbonyl groups for metal-catalyzed C-H activation: The special case of A-ring functionalization. Chem. Commun.*, **2018**, 54, 7398; Impact Factor = 6.3

Also, 1 patent have been deposited claiming the rights for the synthetic methodology and biological activities of the new compounds (see appendix 1 for the patent document):

- *BR10201800866, 2018, Brasil.*

7. Experimental Data

7.1. General Experimental Details

Starting materials sourced from commercial suppliers were used as received unless otherwise stated. All reagents requiring purification were purified using standard laboratory techniques according to methods published by Perrin, Armarego, and Perrin.¹⁹⁴ Catalytic reactions were run under an atmosphere of dry nitrogen or argon; glassware, syringes and needles were either flame dried immediately prior to use or placed in an oven (200 °C) for at least 2 h and allowed to cool either in a desiccator or under an atmosphere of nitrogen or argon; liquid reagents, solutions or solvents were added via syringe through rubber septa. All optimization reactions were filtered through a sinter funnel charged with a pad of celite and silica for copper removal. Coupling partners for the Heck and Stille reactions were distilled before use. Anhydrous solvents were obtained by distillation using standard procedures or by passage through drying columns supplied by Anhydrous Engineering Ltd. Anhydrous dichloromethane (CH₂Cl₂) was purged with argon for 10 minutes prior use. Flash column chromatography (FCC) was performed using silica gel (Aldrich 40-63 μm, 230-400 mesh). Thin layer chromatography (TLC) was performed using aluminium backed 60 F254 silica plates. Visualization was achieved by UV fluorescence or a basic KMnO₄ solution and heat. Proton nuclear magnetic resonance spectra (¹H NMR) were recorded using a Varian 400 MHz, Varian 500 MHz (University of Bristol) and Bruker Advance DRX 400 (Federal University of Minas Gerais). ¹³C NMR spectra were recorded at 100 MHz or 125 MHz as stated. Chemical shifts (δ) are given in parts per million (ppm). Peaks are described as singlets (s), doublets (d), double doublets (dd), triplets (t) double triplets (dt), quartets (q), heptets (hept) and multiplets (m). ¹H and ¹³C NMR spectra were referenced to the appropriate residual solvent peak or TMS peak. Coupling constants (*J*) are quoted to the nearest 0.5 Hz. All assignments of NMR spectra were based on 2D NMR data (DEPT135, COSY, HSQC and HMBC). *In situ* yields¹⁹⁵ were determined by employing 1,4-dinitrobenzene (1,4-DNB) as an internal standard. Mass

194. Perrin, D.D.; Armarego, W.L.F.; Perrin, D.R.; Purification of laboratory chemicals, 2nd ed., Pergamon, Oxford, **1980**.

195. Rundlöf, T.; Mathiassona, M.; Bekiroglub, S.; Hakkarainen, B.; Bowdenc, T.; Arvidsson, T. Survey and qualification of internal standards for quantification by ¹H NMR spectroscopy. *J. Pharm. and Biomed. Anal.*, **2010**, *52*, 645.

spectra were recorded using a Brüker Daltonics FT-ICRMS Apex 4e 7.0T FT-MS (ESI⁺ mode) and Shimadzu GCMS QP2010+ (EI mode). Infrared spectra were recorded on a Perkin Elmer Spectrum One FTIR spectrometer as thin films or solids compressed on a diamond plate. Melting points were determined using Stuart SMP30 melting point apparatus and are uncorrected.

7.2. General Procedure for *in situ* Yield Analysis

After conclusion of the reaction, solvent was removed by reduced pressure and CH₃Cl (5 mL) was added to the reactional vessel. The mixture was filtered through a sinter funnel with a pad of silica and celite and collected in a 25 mL round bottom flask. Additional CH₃Cl (5 mL) was used to wash the reactional vessel and the sinter funnel. The CH₃Cl was removed by reduced pressure and the crude product was submitted to high vacuum for 30 minutes. A known mass of 1,4-dinitrobenzene (1,4-DNB) (never bigger than 20.0 mg) was added to a volumetric flask (1 mL). The volume of the flask was completed with deuterated solvent of choice. Then, 50 μL of the internal standard solution is transferred to the flask containing the crude product. The flask was charged with 450 μL of the same deuterated solvent used in the preparation of the internal standard and the total volume of 500 μL was transferred to a NMR tube. After ¹H spectra acquisition, the internal standard peak (1,4-DNB = 8.44 ppm) was integrated to 1. Then, a *non-overlapping sample peak* was integrated and the value was substituted in the following equation:

$$\left\{ \left[\frac{\left(\text{amount of I.S. (mg)} \right) \times \left(\text{volume of I.S. solution (50 } \mu\text{L)} \right)}{\left(\text{I.S. molecular weight (168.11 for 1,4-DNB)} \right)} \right] \times 4^* \right\} \times \left[\frac{\left(\text{integration value of the non-overlapping sample peak} \right)}{\left(\text{concentration of substrate} \right)} \right] \times 100 = \text{Yield (\%)}$$

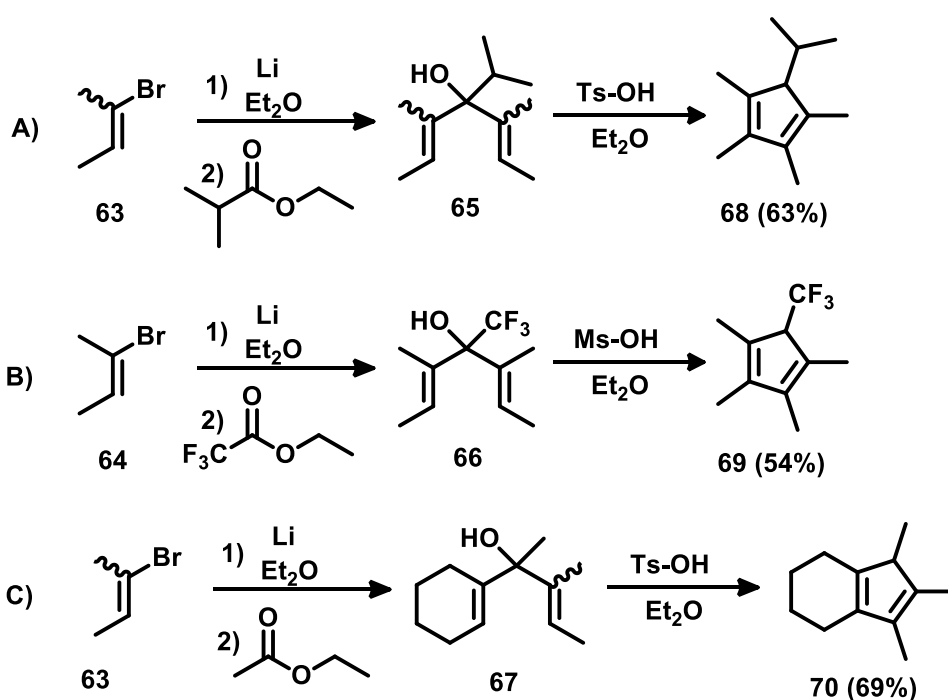
* The equation is multiplied by 4 because 1,4-DNB have 4 hydrogens.

7.3. Synthesis of Substrates and Known Compounds

1,4-naphthoquinone (**56**) and 1,4-benzoquinone (**8**) were purchased from Alfa Aesar, purified via reduced pressure sublimation using a cold finger sublimation

apparatus (50 °C, 0.9 mbar) and stored in a glovebox to prevent contact with moisture. All commercially available naphthoquinones, benzoquinones and further commercial chemicals were purchased from Sigma Aldrich, Alfa Aesar, Strem Chemicals and Santa Cruz Biotechnology. $[\text{RhCp}^*\text{Cl}_2]_2$, $[\text{RhCp}^1\text{Cl}_2]_2$, $\text{Pd}(\text{d}^t\text{bpf})\text{Cl}_2$ and CuTc were purchased from Sigma Aldrich. *The synthesis of the substrates will be showed in the order of the manuscript.*

7.3.1. Synthesis of Substituted Cp^x Ligands



A 100 mL 2-necked round-bottomed flask equipped with a magnetic stir bar and a reflux condenser was charged with lithium wire (44.8 mmol, 310 mg, cut into 1 cm lengths) and dry diethyl ether (1.5 mL). An initial portion of 2-bromo-2-butene (10.0 mmol, 1.0 mL, mixture of isomers, reaction A), (10.0 mmol, 1.0 mL, pure *E*-isomer, reaction B), (5.0 mmol, 0.5 mL, mixture of isomers, reaction C), was added to the stirred solution via syringe dropwise over the course of several minutes. At this point, the reaction initiated, as indicated by the evolution of heat and bubbling. Additional dry diethyl ether (15 mL) was added, and additional 2-bromo-2-butene (13.0 mmol, 1.3 mL, reactions A and B), (7.5 mmol, 0.65 mL, reaction C) was added slowly to keep the reaction at reflux. After the addition was complete, stirring was continued for an

additional 1h. The reaction mixture was then cooled to 0 °C in an ice bath and ethyl isopropylate (reaction A, 11.2 mmol, 1.5 mL), ethyl trifluoroacetate (reaction B, 11.2 mmol, 1.3 mL) or 1-(cyclohex-1-en-1-yl)ethan-1-one (reaction C, 11.2 mmol, 1.5 mL) diluted in dry diethyl ether (2 mL) was added dropwise. The reaction mixture was poured into saturated aqueous NH₄Cl (30 mL) and extracted with diethyl ether (5 × 20 mL). The combined organic layers were dried over Na₂SO₄, and the solvent was removed under reduced pressure to obtain the Nazarov adducts as yellow oils. *The products were used without further purification in the next step.* Under inert atmosphere the crude Nazarov adducts were added quickly via syringe to a solution of *p*-toluenesulfonic acid (reaction A and C, 10.0 mmol, 1.90 g) or methanesulfonic acid (reaction B, 92.5 mmol, 6 mL) in diethyl ether (15 mL). The mixture was stirred for 1h after which it was quenched with saturated aqueous Na₂CO₃ (30 mL). The organic layer was separated and the aqueous phase was extracted with diethyl ether (3 × 50 mL). The combined organic layers were dried over Na₂SO₄, and the solvent was removed by reduced pressure. The crude products were purified via reduced pressure distillation. **5-isopropyl-1,2,3,4-tetramethylcyclopenta-1,3-diene (68)**: 1.16 g, 63% yield, distilled at 78 °C, 10 mBar as a colorless oil; **HRMS(EI⁺)**: 164.1566 [M]⁺. Cald. for [C₁₂H₂₀]: 164.1565; ¹H NMR analysis showed a mixture of 3 isomers.

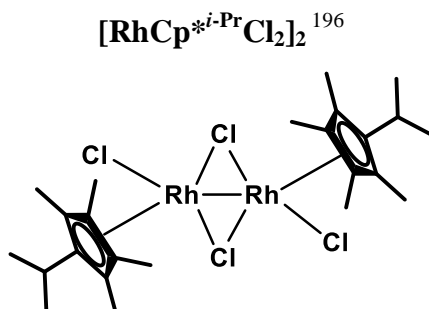
1,2,3,4-tetramethyl-5-(trifluoromethyl)cyclopenta-1,3-diene (69): 1.15 g, 54% yield, distilled at 86 °C, 10 mBar as a light yellow oil; **HRMS(EI⁺)**: 190.0965 [M]⁺. Cald. for [C₁₀H₁₃F₃]: 190.0969; ¹H NMR analysis showed a mixture of 2 major isomers.

1,2,3-trimethyl-4,5,6,7-tetrahydro-1H-indene (70): 1.24 g, 69% yield, distilled at 90 °C, 10 mBar as a yellow oil; **HRMS(EI⁺)**: 162.1396 [M]⁺. Cald. for [C₁₂H₁₈]: 162.1409; ¹H NMR analysis showed a mixture of 2 isomers.

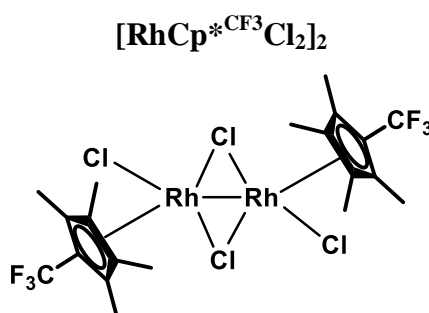
7.3.2. Synthesis of [RhCp*^{*i*-Pr}Cl₂]₂, [RhCp*^{*Cy*}Cl₂]₂ and [RhCp*^{*CF*₃}Cl₂]₂:

A 100 ml reaction tube was charged with RhCl₃.XH₂O (1.00 mmol, 209 mg), the corresponding diene (1.50 mmol) and methanol (50 mL). The tube was sealed with a screw cap and the mixture was heated at 75 °C for 48h. The mixture was cooled to room temperature and methanol was removed under reduced pressure to yield the crude product, which was washed sequentially with pentane (50 mL) and dry diethyl ether (3

× 50 mL). The resulting crystalline powder was dried under high vacuum overnight. Recrystallization from petroleum ether/chloroform afforded analytically pure crystals for characterization by single crystal X-ray diffraction.



The product was obtained by the general procedure described above. Reaction with 5-isopropyl-1,2,3,4-tetramethylcyclopenta-1,3-diene (**68**) (1.50 mmol, 246 mg) afforded $[\text{RhCp}^{*i\text{-Pr}}\text{Cl}_2]_2$ (484 mg, 72% yield) as deep red crystals; **m.p.** (°C) = 250.0 (degradation) (Petrol/ CHCl_3); **HRMS** (EI^+): 671.9831 $[\text{M}]^+$. Cald. for $[\text{C}_{24}\text{H}_{38}\text{Cl}_4\text{Rh}_2]$: 671.9838; **¹H NMR** (500 MHz, CDCl_3) δ : 2.57 (hept, $J = 7.1$ Hz, 2H), 1.69 (s, 12H), 1.57 (s, 12H), 1.26 (d, $J = 7.1$ Hz, 6H); **¹³C NMR** (125 MHz, CDCl_3) δ : 97.5 (d, $J^{\text{Rh-C}} = 8.9$ Hz), 95.2 (d, $J^{\text{Rh-C}} = 10.0$ Hz), 94.0 (d, $J^{\text{Rh-C}} = 9.1$ Hz), 24.9, 20.6, 10.4, 9.5.

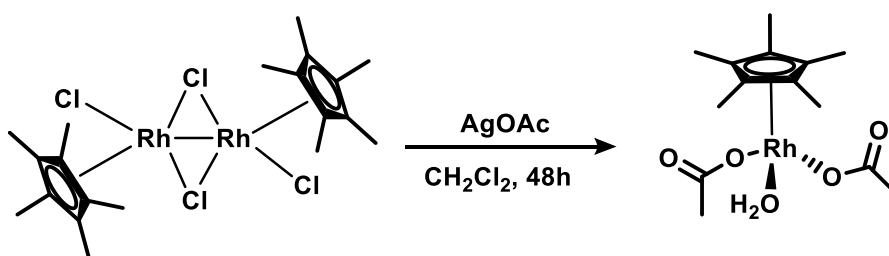


The product was obtained by the general procedure described above. Reaction with 1,2,3,4-tetramethyl-5-(trifluoromethyl)cyclopenta-1,3-diene (**69**) (1.50 mmol, 285 mg) afforded $[\text{RhCp}^{*\text{CF}_3}\text{Cl}_2]_2$ (499 mg, 69% yield) as purple crystals; **m.p.** (°C) = 250.0 (degradation) (Petrol/ CHCl_3); **HRMS** (EI^+): 723.8639 $[\text{M}]^+$. Cald. for

196. Romanov-Michailidis, F.; Sedillo, K.F.; Neely, J.M.; Rovis, T.; Expedient access to 2,3-dihydropyridines from unsaturated oximes by Rh(III)-catalyzed C–H activation. *J. Am. Chem. Soc.*, **2015**, *137*, 8892.

[C₂₀H₂₄Cl₄F₆Rh₂]: 723.8646; ¹H NMR (500 MHz, CDCl₃) δ: 1.93 (q, *J*^{F-H} = 0.9 Hz, 12H), 1.74 (s, 12H); ¹³C NMR (125 MHz, CDCl₃) δ: 124.2 (q, *J*^{F-C} = 274.1 Hz, CF₃), 101.4 (d, *J*^{Rh-C} = 8.1 Hz), 97.3 (d, *J*^{Rh-C} = 8.1 Hz), 10.1 (q, *J*^{F-C} = 2.2 Hz), 9.5; ¹⁹F NMR (400 MHz, CDCl₃) δ: -54.8 (s, 3F).

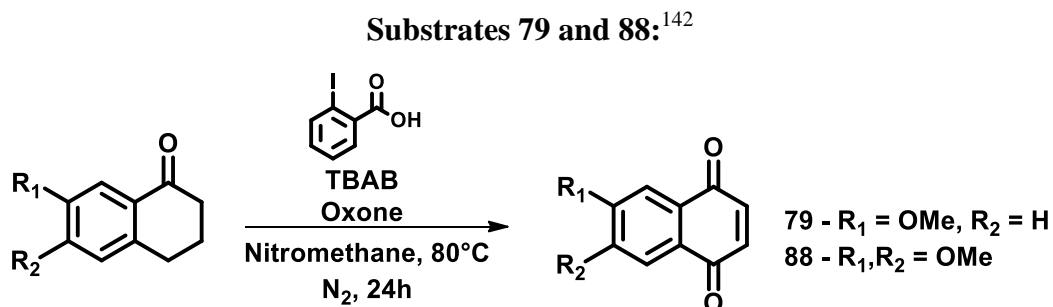
7.3.3. Synthesis of [RhCp^{*}(OAc)₂(H₂O)]¹⁹⁷



A 50 mL 2-necked round-bottomed flask equipped with a magnetic stir bar was charged with [RhCp^{*}Cl₂]₂ (0.77 mmol, 473 mg) and silver acetate (3.74 mmol, 625 mg). The flask was evacuated, flushed with N₂ and CH₂Cl₂ (30 mL) was added via syringe. The reaction mixture was stirred at room temperature for 48h. The mixture was then filtered and the solvent was removed under reduced pressure. The resulting gummy solid was washed with pentane (50 mL) and dried under vacuum overnight to afford [RhCp^{*}(OAc)₂(H₂O)] (239 mg, 64% yield) as a deep orange gummy solid. Recrystallization from petroleum ether/chloroform afforded analytically pure crystals for characterization; **m.p.** (°C) = 250.0 (degradation) (Petrol/CHCl₃); **HRMS (EI⁺):** 374.0589 [M]⁺. Cald. for [C₁₄H₂₃O₅Rh]: 374.0601; ¹H NMR (500 MHz, CDCl₃) δ: 1.91 (s, 6H), 1.65 (s, 15H); ¹³C NMR (125 MHz, CDCl₃) δ: 181.2, 98.4 (d, *J*^{Rh-C} = 7.4 Hz), 90.9 (d, *J*^{Rh-C} = 9.7 Hz), 24.1, 8.8.

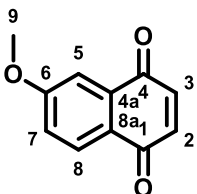
197. Boyer, P.M.; Roy, C.P.; Bielski, J.M.; Merola, J.S.; Pentamethylcyclopentadienylrhodium bis-carboxylates: monohapto carboxylate coordination, dihapto carboxylate coordination, and water coordination to Cp^{*}Rh. *Inorg. Chim. Acta*, **1996**, *245*, 7.

7.3.4. Synthesis of Quinoidal Substrates



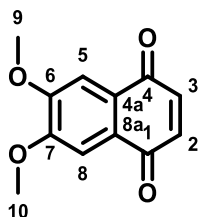
To an oven dried re-sealable reaction tube were added the corresponding α -tetralone (1.00 mmol), 2-iodobenzoic acid (0.20 mmol, 59.2 mg), tetrabutylammonium bromide (0.05 mmol, 15.3 mg) and Oxone (5.00 mmol, 3.10 g). The flask was placed under a N₂ atmosphere and nitromethane (10 mL) was added via syringe. The reaction was heated at 80 °C for 24h, cooled to room temperature, filtered through a pad of celite and the solvent was removed under reduced pressure. The crude product was purified by FCC, under the conditions noted.

6-Methoxy-1,4-naphthoquinone (79)



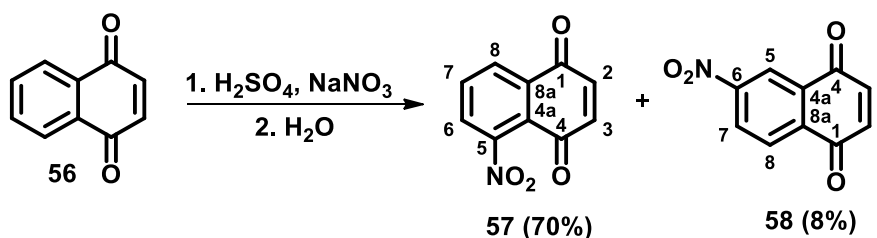
7-Methoxy-3,4-dihydronaphthalen-1(2H)-one (1.00 mmol, 176 mg) was used. Purification by FCC (hexane/ethyl acetate 5:1) afforded **79** (128 mg, 68% yield) as a yellow powder; **m.p.** (°C) = 112.8-113.1 (Petrol/CH₂Cl₂); **¹H NMR (400 MHz, CDCl₃)** δ : 8.02 (d, J = 8.8 Hz, 1H), 7.50 (d, J = 1.7 Hz, 1H), 7.21 (dd, J = 8.7, 2.4 Hz, 1H), 6.94 (d, J = 10.4 Hz, 1H), 6.93 (d, J = 10.4 Hz, 1H) 3.95 (s, 3H); **¹³C NMR (100 MHz, CDCl₃)** δ : 185.2, 184.1, 164.1, 139.0, 138.2, 133.9, 128.9, 125.5, 120.5, 109.6, 55.9.

6,7-Dimethoxy-1,4-naphthoquinone (**88**)



6,7-Dimethoxy-3,4-dihydronaphthalen-1(2*H*)-one (1.00 mmol, 206 mg) was used. Purification by FCC (hexane/ethyl acetate 5:1) afforded **88** (137 mg, 63% yield) as an orange powder; **m.p.** (°C) = 231.3-231.9 (Petrol/CH₂Cl₂); ¹H NMR (400 MHz, CDCl₃) δ : 7.48 (s, 2H), 6.87 (s, 2H), 4.01 (s, 6H); ¹³C NMR (100 MHz, CDCl₃) δ : 184.5, 153.5, 138.3, 126.7, 107.8, 56.5.

5-Nitro-1,4-naphthoquinone (**57**) and 6-Nitro-1,4-naphthoquinone (**58**)¹⁴³

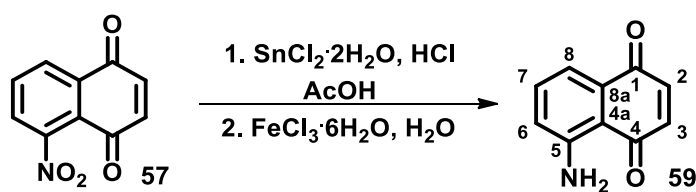


1,4-Naphthoquinone (**56**) (25.3 mmol, 4.00 g) was added portionwise, over 10 minutes, to vigorously stirred concentrated sulfuric acid (50 ml) at 0 °C. A solution of NaNO₃ (164 mmol, 14.0 g) in concentrated sulfuric acid (16 mL) was then added over 3 minutes. The ice bath was removed and the mixture was stirred at room temperature for 1h. The reaction mixture was then heated at 40 °C for 20 minutes, cooled to room temperature, and the resulting orange solution was poured onto ice (250 g). The resulting yellow precipitate was filtered, washed with water and dried under vacuum. The crude product was dissolved in CH₂Cl₂ (50 mL) and filtered through a pad of silica gel. The filtrate was concentrated under reduced pressure and the residue was crystallized from hexane/CH₂Cl₂ (5:1). The crystals were washed with pentane (50 mL) to afford the product as a mixture of isomers (4.00 g, 78% yield, 8:1 *ortho:meta*, determined by ¹H NMR analysis). The isomers were separated by FCC (petrol/ethyl acetate 10:1).

5-nitro-1,4-naphthoquinone (57): 3.49 g, 68% yield as yellow needles; **m.p.** (°C) = 166.5-167.1 (Petrol/CH₂Cl₂); **¹H NMR (400 MHz, CDCl₃)** δ : 8.29 (dd, $J = 7.8, 1.3$ Hz, 1H), 7.91 (t, $J = 7.9$ Hz, 1H), 7.74 (dd, $J = 7.9, 1.3$ Hz, 1H), 7.06 (d, $J = 10.4$ Hz, 1H), 7.02 (d, $J = 10.4$ Hz, 1H); **¹³C NMR (100 MHz, CDCl₃)** δ : 182.6, 181.3, 148.3, 139.1, 138.1, 134.7, 132.7, 128.9, 127.5, 122.9.

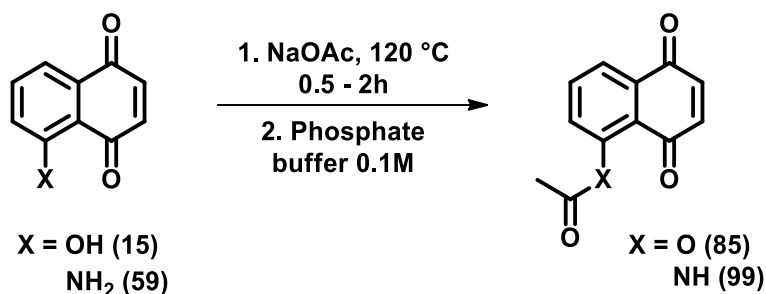
6-nitro-1,4-naphthoquinone (58): 360 mg, 7% yield as light yellow needles; **m.p.** (°C) = 147.1-148.2 (Petrol/CH₂Cl₂); **¹H NMR (400 MHz, CDCl₃)** δ : 8.89 (d, $J = 2.3$ Hz, 1H), 8.57 (dd, $J = 8.2, 2.4$ Hz, 1H), 8.30 (d, $J = 8.1$ Hz, 1H), 7.15 (d, $J = 10.5$ Hz, 1H), 7.12 (d, $J = 10.6$ Hz, 1H); **¹³C NMR (100 MHz, CDCl₃)** δ : 183.2, 182.7, 151.1, 139.2, 138.9, 135.2, 133.0, 128.4, 128.0, 121.8.

5-Amino-1,4-naphthoquinone (59)¹⁴³



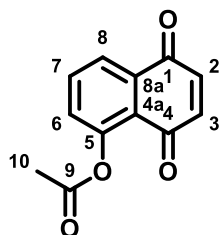
A solution of **57** (5.00 mmol, 1.02 g) in AcOH (35 mL) was heated at 50 °C in a 250 mL round bottom flask. Then, a solution of SnCl₂·2H₂O (26.6 mmol, 6.00 g) in concentrated HCl (10 mL) was added. The mixture was heated at 70 °C for 40 minutes and cooled to room temperature. A solution of FeCl₃·6H₂O (32.2 mmol, 8.70 g) in cold H₂O (10 mL) was added and stirring was continued for 30 minutes. The mixture was poured onto ice (100 g) and rested at 4 °C overnight. The resulting precipitate was filtered, washed with water and dried under reduced pressure to afford **59** (528 mg, 61% yield) as purple crystals; **m.p.** (°C) = 189.1-190.4 (Petrol/CH₂Cl₂); **¹H NMR (400 MHz, CDCl₃)** δ : 7.47-7.39 (m, 2H), 6.98-6.92 (m, 1H), 6.88 (d, $J = 10.3$ Hz, 1H), 6.84 (d, $J = 10.3$ Hz, 1H), 6.67 (s, 2H); **¹³C NMR (100 MHz, CDCl₃)** δ : 187.1, 185.4, 150.1, 140.6, 137.3, 134.6, 132.9, 123.2, 117.0, 112.3.

Substrates 85 and 99



A solution of naphthoquinone (1.00 mmol) and sodium acetate (12.4 mmol, 1.02 g) in acetic anhydride (3.5 mL) was stirred at 120 °C for 2h. The mixture was quenched with phosphate buffer (pH = 7.4, 7 mL) and extracted with CH_2Cl_2 (3 x 10 mL). The combined organic layers were dried with Na_2SO_4 and the solvent was removed by reduced pressure. The crude product was purified by FCC, under the conditions noted.

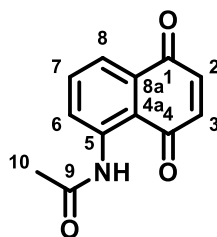
5,8-dioxo-5,8-dihydronaphthalen-1-yl acetate (85)¹⁹⁸



Purification by FCC (hexane/ethyl acetate 5:1) afforded **85** (186 mg, 86% yield) as a yellow powder; **m.p.** (°C) = 154.8-155.6 (Petrol/ CH_2Cl_2); **¹H NMR (400 MHz, CDCl_3)** δ : 8.12 (dd, $J = 7.8, 1.2$ Hz, 1H), 7.78 (t, $J = 7.6$ Hz, 1H), 7.48 (dd, $J = 7.7, 1.3$ Hz, 1H), 7.00 (d, $J = 10.4$ Hz, 1H), 6.96 (d, $J = 10.3$ Hz, 1H), 2.50 (s, 3H); **¹³C NMR (100 MHz, CDCl_3)** δ : 204.2, 184.8, 184.1, 143.5, 138.6, 134.2, 132.1, 130.6, 128.5, 127.3, 30.7.

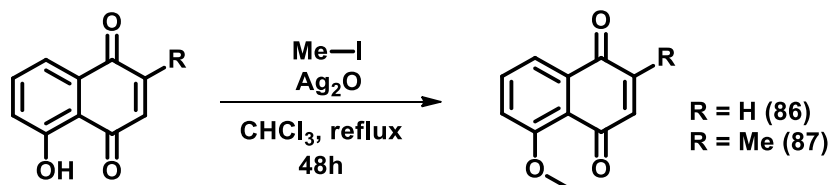
198. Montenegro, R.C.; Araújo, A.J.; Molina, M.T.; Filho, J.D.B.M.; Rocha, D.D.; López-Montero, E.; Goulart, M.O.F.; Bento, E.S.; Alves, A.P.N.N.; Pessoa, C.; de Moraes, M.O.; Costa-Lotufo, L.V.; Cytotoxic activity of naphthoquinones with special emphasis on juglone and its 5-*O*-methyl derivative. *Chem. Biol. Interact.*, **2010**, *184*, 439.

N-(5,8-dioxo-5,8-dihydronaphthalen-1-yl)acetamide (**99**)¹⁹⁹



Purification by FCC (hexane/ethyl acetate 19:1) afforded **99** (144 mg, 67% yield) as an orange powder; **m.p.** (°C) = 171.8-172.9 (Petrol/CH₂Cl₂); ¹H NMR (400 MHz, CDCl₃) δ: 11.81 (s, 1H), 9.04 (dd, *J* = 8.1, 1.3 Hz, 1H), 7.78 (dd, *J* = 7.6, 1.3 Hz, 1H), 7.69 (t, *J* = 8.1 Hz, 1H), 6.92 (d, *J* = 10.3 Hz, 1H), 6.88 (d, *J* = 10.3 Hz, 1H), 2.27 (s, 3H). ¹³C NMR (100 MHz, CDCl₃) δ: 189.0, 184.4, 169.9, 141.3, 139.8, 139.8, 137.9, 135.7, 132.1, 125.9, 121.8, 115.9, 25.6.

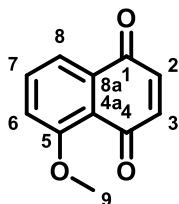
Substrates **86** and **87**



To a solution of the corresponding naphthoquinone (1.00 mmol) in CHCl₃ (30 mL) was added Ag₂O (2.00 mmol, 463 mg) and iodomethane (2.00 mmol, 125 μL). The reaction was then heated at reflux for 48h. After cooling to room temperature, the mixture was filtered through a pad of celite and the solvent was removed under reduced pressure. The crude product was purified by FCC, under the conditions noted.

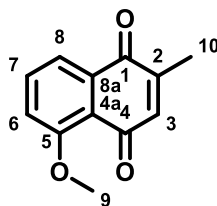
199. de Oliveira, K.T.; Millera, L.Z.; McQuade, D.T.; Exploiting photooxygenations mediated by porphyrinoid photocatalysts under continuous flow conditions. *RSC Adv.*, **2016**, 6, 12717.

5-Methoxy-1,4-naphthoquinone (**86**)²⁰⁰



5-Hydroxy-1,4-naphthoquinone (**15**) (1.00 mmol, 174 mg) was used. Purification by FCC (hexane/ethyl acetate 5:1) afforded **86** (137 mg, 73% yield) as yellow crystals; **m.p.** (°C) = 181.7-181.9 (Petrol/CH₂Cl₂); ¹H NMR (400 MHz, CDCl₃) δ: 7.77-7.60 (m, 2H), 7.29 (d, *J* = 8.0 Hz, 1H), 6.84 (s, 2H), 3.98 (s, 3H); ¹³C NMR (100 MHz, CDCl₃) δ: 185.2, 184.3, 159.6, 140.9, 136.2, 135.0, 134.0, 119.7, 119.1, 117.9, 56.5.

5-Methoxy-2-methyl-1,4-naphthoquinone (**87**)²⁰¹



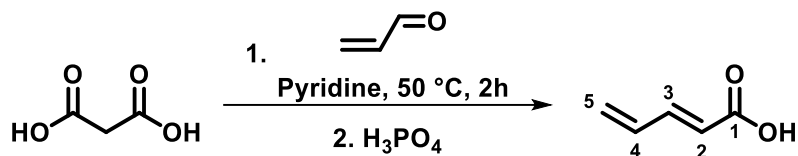
5-Hydroxy-2-methyl-1,4-naphthoquinone (**16**) (1.00 mmol, 188 mg) was used. Purification by FCC (hexane/ethyl acetate 5:1) afforded **87** (158 mg, 78% yield) as yellow crystals; **m.p.** (°C) = 94.8-95.1 (Petrol/CH₂Cl₂); ¹H NMR (400 MHz, CDCl₃) δ: 7.75 (d, *J* = 7.7 Hz, 1H), 7.65 (t, *J* = 8.4 Hz, 1H), 7.28 (d, *J* = 8.4 Hz, 1H), 6.73 (s, 1H), 4.00 (s, 3H), 2.13 (s, 3H); ¹³C NMR (100 MHz, CDCl₃) δ: 185.7, 184.4, 159.4, 145.4, 137.9, 134.6, 134.4, 120.0, 119.4, 117.7, 56.5, 15.8.

200. Tietze, L.F.; Güntner, C.; Gericke, K.M.; Schuberth, I.; Bunkoczi, G.; A Diels–Alder reaction for the total synthesis of the novel antibiotic antitumor agent mensacarcin. *Eur. J. Org. Chem.*, **2005**, 2459.

201. Bendiabdellah, Y.; Rahman, K.M.; Uranchimeg, B.; Nahar, K.S.; Antonow, D.; Shoemaker, R.H.; Melillo, G.; Zinzalla, G.; Thurston, D.E.; Tetracycline analogues with a selective inhibitory effect on HIF-1α. *Med. Chem. Commun.*, **2014**, 5, 923.

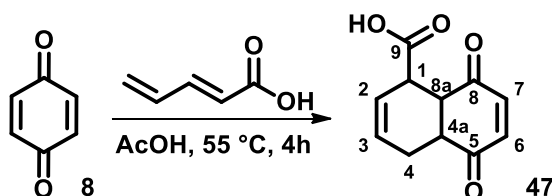
Substrate 48

Penta-2,4-dienoic acid²⁰²



Malonic acid (288 mmol, 30.0 g) was added portion wise to pyridine (50 mL). Once all the malonic acid has dissolved, acrylaldehyde (21 mL, 315 mmol) was added dropwise over 3 minutes. The mixture was heated at 55 °C for 2 h. After cooling to 4 °C, the pH was adjusted to 3 with H₃PO₄ (85% in H₂O). The mixture was extracted with diethyl ether (3 x 50 mL), dried with Na₂SO₄ and the solvent was removed under reduced pressure. The crude product was recrystallized from petroleum ether to afford penta-2,4-dienoic acid (15.3 g, 54% yield) as a pale yellow powder; **m.p.** (°C) = 66.5-68.3 (Petrol/CH₂Cl₂); ¹H NMR (400 MHz, CDCl₃) δ: 11.8 (s, 1H), 7.36 (q, *J* = 15.6 Hz, 1H), 6.56-6.39 (m, 1H), 5.92 (d, *J* = 15.6 Hz, 1H), 5.67 (dd, *J* = 16.9, 1.0 Hz, 1H), 5.56 (d, *J* = 9.8, 1H); ¹³C NMR (100 MHz, CDCl₃) δ: 172.6, 147.1, 134.5, 126.8, 121.3.

5,8-Dioxo-1,4,4a,5,8,8a-hexahydronaphthalene-1-carboxylic acid (49)¹³⁹

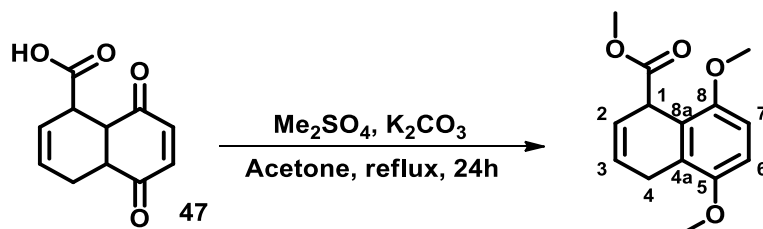


Penta-2,4-dienoic acid (102 mmol, 10.0 g) and **8** (95.0 mmol, 10.3 g) were dissolved in acetic acid (100 mL). The solution was heated at 55 °C for 4h. After cooling to room temperature, the solvent was removed under reduced pressure and the crude product was suspended in ethanol (100 mL) and filtered. The precipitate was washed with water (50 mL), ethanol (100 mL) and diethyl ether (50 mL) and dried under reduced pressure to afford **47** (8.80 g, 45%) as a silver powder; **m.p.** (°C) = 153.5-155.0 (Petrol/CH₂Cl₂); ¹H NMR (400 MHz, DMSO-*d*₆) δ: 12.3 (s, 1H), 6.76 (d, *J* = 10.2 Hz, 1H), 6.65 (d, *J* = 10.2 Hz, 1H), 6.02 (d, *J* = 9.6 Hz, 1H), 5.62-5.59 (m, 1H), 4.04 (t, *J* = 5.1 Hz, 1H),

²⁰². Bergman, J.; Romero, I.; Synthesis of 2-ethynyl-4(3H)quinazolinone and 2-(1,3-butadienyl)-4(3H)quinazolinone (HP-3742HP). *Arkivoc*, **2009**, 6, 191.

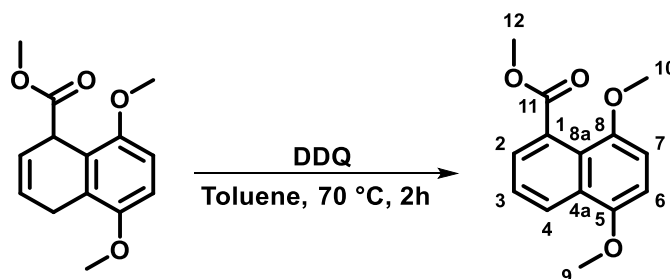
3.27-3.16 (m, 1H), 2.23-2.15 (m, 1H), 2.08-1.86 (m, 1H); ^{13}C NMR (100 MHz, DMSO-*d*₆) δ : 200.7, 198.3, 173.8, 172.8, 140.2, 138.7, 125.0, 124.5, 48.3, 47.2, 25.9.

Methyl 5,8-dimethoxy-1,4-dihydronaphthalene-1-carboxylate¹³⁹



Compound **47** (14.6 mmol, 3.01 g) and K_2CO_3 (79.7 mmol, 11.0 g) were suspended in acetone (40 mL). To this solution was added dimethyl sulphate (4.0 mL) dropwise over 5 minutes. The mixture was then heated to reflux for 24h. After cooling to room temperature, the precipitate was filtered, washing with acetone, and the filtrate was evaporated under reduced pressure to afford methyl 5,8-dimethoxy-1,4-dihydronaphthalene-1-carboxylate (3.22 g, 89% yield) as a colourless powder. The product was used without further purification; **m.p.** ($^\circ\text{C}$) = 99.5-101,3 (Acetone); ^1H NMR (400 MHz, CDCl_3) δ : 6.73 (dd, $J = 8.8, 2.0$ Hz, 1H), 6.69 (dd, $J = 8.8, 2.0$ Hz, 1H), 6.08 (d, $J = 10.1$ Hz, 1H), 5.91 (d, $J = 7.8$ Hz, 1H), 4.54-4.46 (m, 1H), 3.80 (s, 3H), 3.76 (s, 3H), 3.69 (s, 3H), 3.44-3.20 (m, 2H); ^{13}C NMR (100 MHz, CDCl_3) δ : 173.4, 151.0, 150.8, 126.8, 124.5, 122.2, 121.8, 108.3, 107.5, 55.8, 55.6, 52.1, 42.3, 24.5.

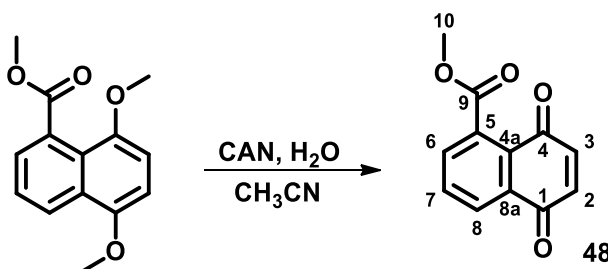
Methyl 5,8-dimethoxy-1-naphthoate²⁰³



203. Newman, M.S.; Choudhary, A.R.; The lithiation of 1,4-dimethoxynaphthalene and carboxylation of the products. *Org. Prep. Proced. Int.*, **1989**, *21*, 359.

Methyl 5,8-dimethoxy-1,4-dihydronaphthalene-1-carboxylate (11.5 mmol, 2.86 g) and DDQ (13.2 mmol, 2.99 g) were dissolved in toluene (30 mL). The mixture was heated at 70 °C for 2h. The mixture was cooled to room temperature and solvent was removed under reduced pressure. The residue was dissolved in CH₂Cl₂ (50 mL), washed sequentially with aqueous NaOH (100 mL, 0.5 M) and saturated aqueous Na₂SO₃ (100 mL), and dried with Na₂SO₄. The organic portion was concentrated under reduced pressure and the crude product was purified by FCC (hexane/ethyl acetate 10:1) to afford methyl 5,8-dimethoxy-1-naphthoate (2.04 g, 72% yield) as an off-white solid; **m.p.** (°C) = 104.5-104.9 (CH₂Cl₂); ¹H NMR (400 MHz, CDCl₃) δ: 8.31 (dd, *J* = 7.7, 2.1 Hz, 1H), 7.53-7.42 (m, 2H), 6.80 (d, *J* = 8.4 Hz, 1H), 6.75 (d, *J* = 8.4 Hz, 1H), 3.97 (s, 3H), 3.96 (s, 3H), 3.90 (s, 3H); ¹³C NMR (100 MHz, CDCl₃) δ: 172.0, 149.8, 148.6, 129.3, 126.6, 125.2, 124.8, 123.7, 122.4, 106.0, 104.1, 56.8, 55.8, 52.3.

Methyl 5,8-dioxo-5,8-dihydronaphthalene-1-carboxylate (48)²⁰⁴

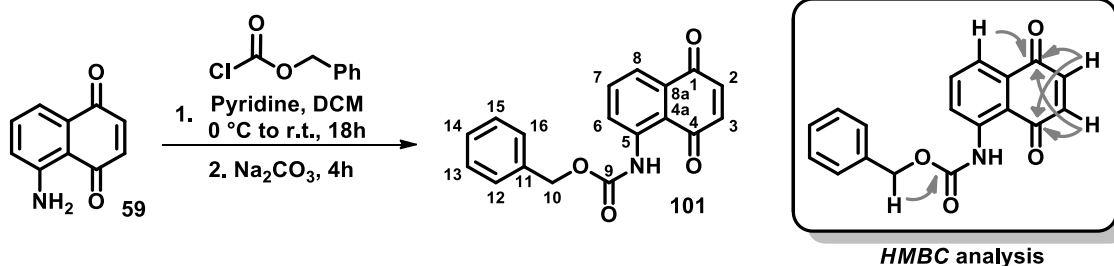


Methyl 5,8-dimethoxy-1-naphthoate (4.00 mmol, 985 mg) was dissolved in acetonitrile (15 mL) and the solution was cooled to 4 °C. A solution of cerium ammonium nitrate (12.4 mmol, 6.80 g) in water (15 mL) was then added dropwise over 1 minute. The mixture was stirred at room temperature for 30 minutes prior to extraction with ethyl acetate (50 mL). The organic layer was dried with Na₂SO₄ and evaporated under reduced pressure. Purification of the residue by FCC (hexane/ethyl acetate 19:1) afforded **48** (761 mg, 88% yield) as yellow crystals; **m.p.** (°C) = 92.3-93.0 (Petrol/CH₂Cl₂); ¹H NMR (400 MHz, CDCl₃) δ: 8.17 (dd, *J* = 7.8, 1.3 Hz, 1H), 7.79 (t, *J* = 7.7 Hz, 1H), 7.68 (dd, *J* = 7.8, 1.3 Hz, 1H), 6.98 (d, *J* = 10.5 Hz, 1H), 6.97 (d, *J* =

²⁰⁴ Koike, T.; Tanabe, M.; Takeuchi, N.; Tobinaga, S.; Aminodienylesters. I : the cycloaddition reactions of tert-aminodienylester with α, β-unsaturated carbonyl compounds, styrenes, and quinones. *Chem. Pharm. Bull.*, **1997**, *45*, 243.

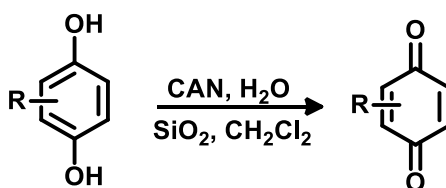
10.5 Hz, 1H), 3.98 (s, 3H); ^{13}C NMR (100 MHz, CDCl_3) δ : 172.0, 149.8, 148.6, 129.3, 126.6, 125.2, 124.8, 123.7, 122.4, 106.0, 104.1, 56.8, 55.8, 52.3.

Benzyl (5,8-dioxo-5,8-dihydropthalen-1-yl)carbamate (101)



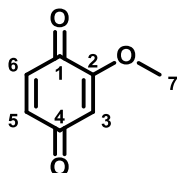
To a solution of **59** (1.00 mmol, 173 mg) in CH_2Cl_2 (10 ml) was added pyridine (1.30 mmol, 105 μL). The reaction was cooled to 0 °C and a solution of benzyl chloroformate (1.00 mmol, 143 μL) in CH_2Cl_2 (5.0 mL) was added over 30 minutes. The resulting mixture was warmed to room temperature and stirred for further 18h. Saturated aqueous Na_2CO_3 (10 mL) was added and the mixture was stirred for another 4h. The organic layer was separated, dried with anhydrous Na_2SO_4 and concentrated under reduced pressure. Purification of the residue by FCC (hexane/EtOAc 10:1) afforded **101** (197 mg, 64% yield) as an orange powder; **m.p** (°C) = 117.2-117.9 (Petrol/ CH_2Cl_2); **IR** (solid, cm^{-1}) ν : 3253 (m) 2927 (w), 1730 (s), 1579 (s), 1256 (s), 743 (m); **HRMS** (ESI^+): 330.0740 $[\text{M}+\text{Na}]^+$. Cald. for $[\text{C}_{18}\text{H}_{13}\text{NNaO}_4]^+$: 330.0737; ^1H NMR (400 MHz, CDCl_3) δ : 11.44 (s, N-H), 8.84 (d, $J = 8.5$ Hz, C6-H), 7.78 (d, $J = 6.3$ Hz, C8-H), 7.71 (t, $J = 8.5$ Hz, C7-H), 7.51-7.30 (m, C(12-16)-H), 6.93 (d, $J = 10.3$ Hz, C2-H), 6.90 (d, $J = 10.3$ Hz, C3-H), 5.25 (s, C10-H₂); ^{13}C NMR (100 MHz, CDCl_3) δ : 188.6 (C4), 184.5 (C1), 153.6 (C9), 141.6 (C5), 140.0 (C3), 137.8 (C2), 135.8 (C11), 135.5 (C7), 132.3 (C8a), 128.6 (C12, C16), 128.4 (C14), 128.3 (C13, C15), 124.6 (C6), 121.2 (C8), 115.8 (C4a), 67.3 (C10).

Substrates 112 and 127



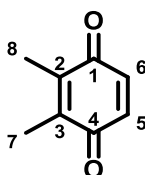
A 100-mL round-bottomed flask was charged with 6 g of silica gel and fitted with a rubber septum. A solution of 2.75 g of CAN (5.00 mmol) in 2.5 mL of water was added dropwise via syringe while the content of the flask was in vigorous stirring. After the addition of the aqueous solution of CAN was complete, stirring of the silica gel continued for 5 minutes, until a free-flowing yellow solid was obtained. CH₂Cl₂ (25 mL) was added to the flask. Hydroquinone (2.00 mmol) dissolved in 2 mL of CH₂Cl₂ was added to the mixture. After 15 minutes, the reaction mixture was filtered through a sintered-glass funnel. The solid was washed with about 75 mL of CH₂Cl₂. Removing the solvent with reduced pressure afforded pure benzoquinones.

2-Methoxy-1,4-benzoquinone (**112**)²⁰⁵



2-methoxy-1,4-hidroquinone (2.00 mmol, 280 mg) was used. Compound **112** (267.9 mg, 97% yield) was obtained as a yellow powder without further purification; **m.p.** (°C) = 133.8-134.1 (Petrol/CH₂Cl₂); **HRMS (EI⁺)**: 138.0311 [M]⁺. Cald. for [C₇H₆O₃]: 138.0317; **¹H NMR (400 MHz, CDCl₃)** δ : 6.69 (s, 2H), 5.92 (s, 1H), 3.81 (s, 3H); **¹³C NMR (100 MHz, CDCl₃)** δ : 187.4, 181.7, 158.6, 137.2, 134.4, 107.7, 56.2.

2,3-Dimethyl-1,4-benzoquinone (**127**)²⁰⁵



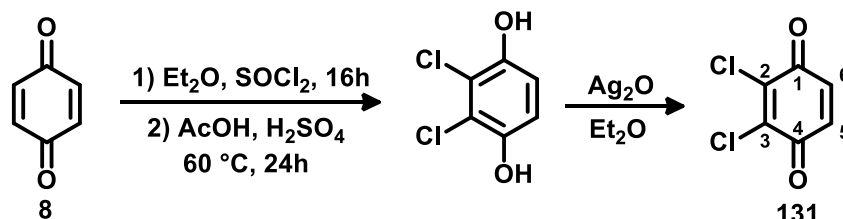
2,3-dimethyl-1,4-hidroquinone²⁰⁶ (2.00 mmol, 332 mg) was used. Compound **127** (1.68 g, 90% yield) was obtained as yellow crystals without further purification; **m.p.** (°C) =

205. Ali, M.H.; Niedbalski, M.; Bohnert, G.; Bryant, D.; Silica-gel-supported ceric ammonium nitrate (CAN): A simple and efficient solid-supported reagent for oxidation of oxygenated aromatic compounds to quinones. *Synth. Comm.*, **2006**, *36*, 1751.

206. Boufatah, N.; Gellis, A.; Maldonado, J.; Vanelle, P; Efficient microwave-assisted synthesis of new sulfonylbenzimidazole-4,7-diones: heterocyclic quinones with potential antitumor activity. *Tetrahedron*, **2004**, *60*, 9137.

54.9-56.4 (Petrol/CH₂Cl₂); **HRMS (EI⁺)**: 136.0569 [M]⁺. Cald. for [C₈H₈O₂]: 136.0524; **¹H NMR (400 MHz, CDCl₃)** δ: 6.70 (s, 2H), 2.01 (s, 6H); **¹³C NMR (100 MHz, CDCl₃)** δ: 187.4, 141.0, 136.2, 12.2.

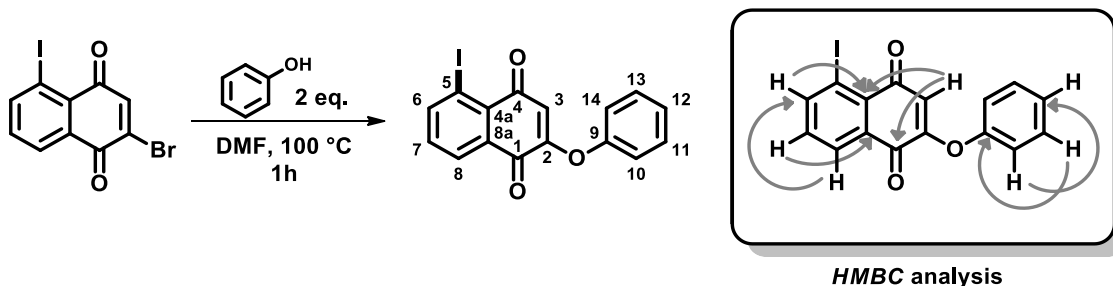
2,3-Dichloro-1,4-benzoquinone (131)²⁰⁷



A suspension of **8** (4.32 g, 40.0 mmol) in dry Et₂O (35 mL) was treated with SO₂Cl₂ (6.5 mL, 80.0 mmol), and stirred for 16 h at 25 °C. The mixture was cooled in an ice bath and filtered. The collected solid was washed with cold Et₂O (10 mL), and dried in vacuo. A suspension of the solid in AcOH (20 mL) was treated with concentrated H₂SO₄ (2 mL), stirred for 24 h at 60 °C, and poured into ice. The mixture was extracted with Et₂O (2 × 100 mL) and combined organic layers were washed with brine, dried over MgSO₄, filtered, and evaporated. The product was used without further purification. A solution of 2,3-Dichloro-1,4-hydroquinone (3.00 g, 17.0 mmol) in Et₂O (250 mL) was treated with Ag₂O (9.70 g, 42.0 mmol) for 30 min at 25 °C. The mixture was filtered and the solvent was evaporated. Purification of the residue by FCC (hexane/EtOAc 9:1) afforded **131** (1.79 g, 60% yield) as yellow crystals; **m.p.** (°C) = 102.9-103.7 (Petrol/CH₂Cl₂); **HRMS (EI⁺)**: 175.9421 [M]⁺. Cald. for [C₆H₂Cl₂O₂]: 175.9432; **¹H NMR (400 MHz, CDCl₃)** δ: 6.97 (s, 2H); **¹³C NMR (100 MHz, CDCl₃)** δ: 177.4, 141.2, 136.1.

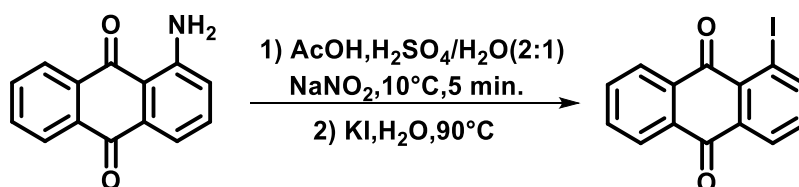
207. Pochorovski, I.; Boudon, C.; Gisselbrecht, J. P.; Ebert, M. O.; Schweizer, W. B.; Diederich, F.; Quinone-based, redox-active resorcin[4]arene cavitands. *Angew. Chem. Int. Ed.*, **2012**, *51*, 262.

5-iodo-2-phenoxy-1,4-naphthoquinone (142)²⁰⁸



The product was obtained using a reported procedure, with minor modifications. To a solution of 2-bromo-5-iodo-1,4-naphthoquinone (72.4 mg, 0.20 mmol) in DMF (1 mL) was added phenol (37.6 mg, 0.40 mmol). The reaction was heated at 100 °C and kept under stirring for 1 h. The mixture was then washed with brine (10 mL) and extracted with CH₂Cl₂ (10 mL). The organic phase was dried with Na₂SO₄ and submitted to purification by FCC (toluene) affording product **142** (48.1 mg, 64% yield) as an orange solid; **m.p.** (°C) = 166.9-167.3 (Petrol/CH₂Cl₂); **IR (solid, cm⁻¹)** ν : 2920 (w), 1648 (s), 1113 (s), 804 (s); **MS (EI⁺)**: 375.9 [M]⁺. Cald. for [C₁₆H₉IO₃]: 375.9; **¹H NMR (400 MHz, CDCl₃)** δ : 8.38 (dd, *J* = 7.7, 1.1 Hz, C6-H), 8.28 (dd, *J* = 7.7, 1.1 Hz, C8-H), 7.46 (t, *J* = 7.9 Hz, C7-H, C12-H), 7.38 – 7.30 (m, C11-H, C13-H), 7.13 (d, *J* = 7.7 Hz, C10-H, C14-H), 6.02 (s, C3-H). **¹³C NMR (100 MHz, CDCl₃)** δ : 183.2 (C4), 179.3 (C1), 159.3 (C2), 152.8 (C8a), 149.0 (C6), 148.2 (C9), 133.5 (C11), 130.7 (C7,C4a), 128.1 (C8), 127.5 (C12), 126.9 (C13), 121.2 (C10,C14), 114.7 (C3), 92.5 (C5).

1-Iodoanthracene-9,10-dione (144)¹⁴³



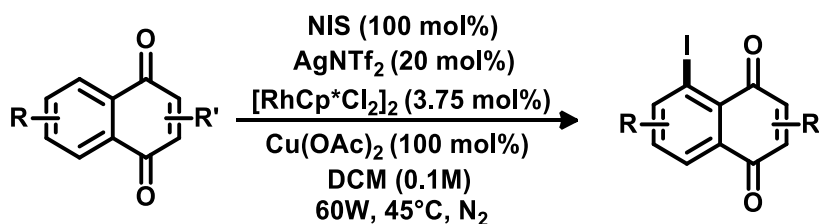
To a solution of 1-aminoanthracene-9,10-dione (670 mg, 2.99 mmol) in 30 mL of diluted H₂SO₄ (16 mL of concentrated H₂SO₄ and 8 mL of water), AcOH (20 mL) was

208. Bolognesi, M.L.; Lizzi, F.; Perozzo, R.; Brun, R.; Cavalli, A.; Synthesis of a small library of 2-phenoxy-1,4-naphthoquinone and 2-phenoxy-1,4-antraquinone derivatives bearing anti-trypanosomal and anti-leishmanial activity. *Bioorg. Med. Chem. Lett.*, **2008**, *18*, 2272.

gradually added. The solution was filtered to remove precipitated solids and 80 mL of water was added. The solution was cooled to 10 °C and diazotized with a solution of 600 mg of NaNO₂ in 1 mL of water. The diazonium solution was quickly poured into a solution of 3.00 g of KI in 80 mL of water at 90 °C and vigorously stirred. The formed precipitate was filtered, washed with water and dried. Purification by FCC (toluene/EtOAc 3:1) afforded iodinated product **144** (1.10 g, 72% yield) as a deep orange solid; ¹H NMR (400 MHz, CDCl₃) δ: 8.41 (q, *J* = 7.8 Hz, 2H), 8.33 (d, *J* = 7.2 Hz, 1H), 8.26 (d, *J* = 8.5 Hz, 1H), 7.85 – 7.75 (m, 2H), 7.39 (t, *J* = 7.8 Hz, 1H). ¹³C NMR (100 MHz, CDCl₃) δ: 182.1, 181.7, 148.9, 136.1, 134.8, 134.2, 134.1, 134.0, 132.8, 132.5, 128.6, 128.0, 127.00, 93.4.

7.4. Procedures for the Synthesis of Novel Derivatives

7.4.1. General Microwave Procedure for the Halogenation reactions

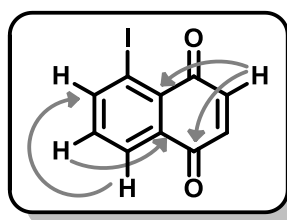
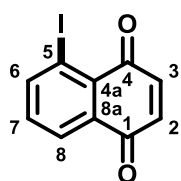


In a glovebox, an oven dried re-sealable reaction tube was charged with the corresponding naphthoquinone (0.10 mmol), [RhCp*Cl₂]₂ (3.75 mol%, 2.3 mg), silver bis(trifluoromethanesulfonyl)imide (20 mol%, 7.8 mg), *N*-iodosuccinimide (100 mol%, 22.5 mg) and anhydrous copper acetate (100 mol%, 18.2 mg). The tube was removed from the glovebox and an inert atmosphere was maintained. Anhydrous CH₂Cl₂ (1.0 mL) was added via syringe and the tube was sealed. The mixture was irradiated in a CEM Discover microwave apparatus in open flask mode (60 W) and the nitrogen flow was adjusted to maintain a reaction temperature of 45 °C. After cooling, the reaction mixture was filtered through a pad of celite and concentrated under reduced pressure. The residue was purified by FCC, under the conditions noted.



Figure 19: Re-sealable reaction tube and microwave apparatus.

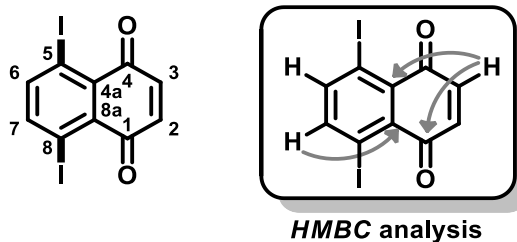
5-Iodo-1,4-naphthoquinone (60)



HMBC analysis

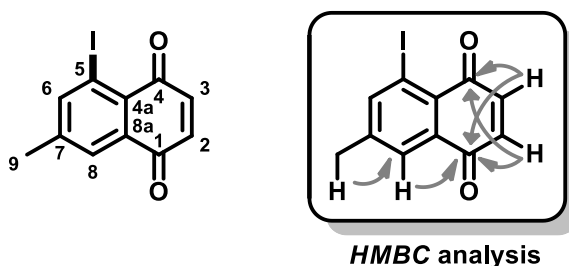
The product was obtained by the general microwave procedure described above. The reaction was conducted for 2h and purification by FCC (toluene) afforded iodinated product **60** (19.6 mg, 69% yield) as red crystals; **m.p.** (°C) = 167.8-168.6 (Petrol/CH₂Cl₂); **IR (solid, cm⁻¹)** ν : 3071 (w), 1665 (s), 1318 (m), 782 (m); **HRMS (EI⁺)**: 283.9335 [M]⁺. Cald. for [C₁₀H₅IO₂]: 283.9334; **¹H NMR (400 MHz, CDCl₃)** δ : 8.36 (d, $J = 7.8$ Hz, C6-H), 8.14 (d, $J = 7.8$ Hz, C8-H), 7.35 (t, $J = 7.8$ Hz, C7-H), 7.02 (d, $J = 10.3$ Hz, C3-H), 6.94 (d, $J = 10.3$ Hz, C2-H); **¹³C NMR (100 MHz, CDCl₃)** δ : 183.6 (C1), 183.2 (C4), 148.2 (C6), 139.7 (C2), 137.1 (C3), 134.3 (C8a), 133.7 (C7), 130.7 (C4a), 127.6 (C8), 92.7 (C5-I).

5,8-Diiodo-1,4-naphthoquinone (62)



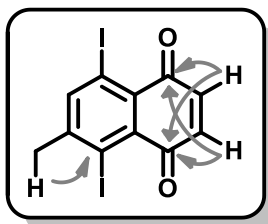
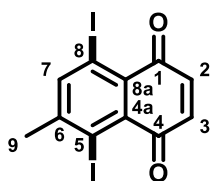
In addition to **60**, bis-iodinated by-product **62** (2.0 mg, 5% yield) was obtained as deep red crystals; **m.p.** (°C): 161.8-162.3 (Petrol/CH₂Cl₂); **IR** (solid, cm⁻¹) ν : 2922 (w), 1660 (s), 1051 (m), 820 (m); **HRMS** (EI⁺): 409.8290 [M]⁺. Cald. for [C₁₀H₄I₂O₂]: 409.8301; **¹H NMR** (400 MHz, CDCl₃) δ : 7.94 (s, C6-H, C7-H), 6.99 (s, C2-H, C3-H); **¹³C NMR** (101 MHz, CDCl₃) δ : 182.3 (C1, C4), 147.7 (C6, C7), 138.0 (C2, C3), 133.0 (C4a, C8a), 93.8 (C5-I, C8-I).

5-Iodo-7-methyl-1,4-naphthoquinone (80)



The product was obtained by the general microwave procedure described above. The reaction was conducted for 3h and purification by FCC (toluene) afforded iodinated product **80** (18.8 mg, 63% yield) as a deep orange powder; **m.p.** (°C) = 127.1-128.4 (Petrol/CH₂Cl₂); **IR** (solid, cm⁻¹) ν : 2923 (w), 1665 (s), 1313 (m), 844 (m); **HRMS** (EI⁺): 297.9491 [M]⁺. Cald. for [C₁₀H₅IO₂]: 297.9492; **¹H NMR** (400 MHz, CDCl₃) δ : 8.17 (d, *J* = 1.8 Hz, C6-H), 7.92 (d, *J* = 1.8 Hz, C8-H), 6.97 (d, *J* = 10.3 Hz, C3-H), 6.89 (d, *J* = 10.3 Hz, C2-H), 2.42 (s, C9-H₃); **¹³C NMR** (100 MHz, CDCl₃) δ : 183.9 (C1), 182.9 (C4), 148.6 (C6), 145.1 (C7), 139.8 (C3), 136.9 (C2), 133.9 (C8a), 128.4 (C4a), 128.2 (C8), 93.0 (C5-I), 21.1 (C9).

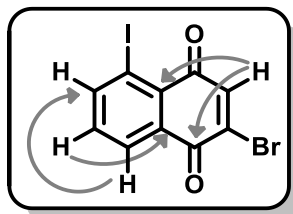
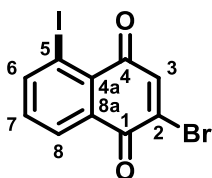
5,8-Diiodo-6-methyl-1,4-naphthoquinone (80')



HMBC analysis

In addition to **80**, a C5/8 bis-iodinated by-product **80'** (1.3 mg, 3% yield) was obtained as a deep orange powder; **m.p.** (°C) = 178.2-179.5 (Petrol/CH₂Cl₂); **IR (solid, cm⁻¹)** ν : 2987 (w), 1663 (s), 1047 (m), 854 (m); **HRMS (EI⁺)**: 423.8456 [M]⁺. Cald. for [C₁₁H₆I₂O₂]: 423.8457; **¹H NMR (500 MHz, CDCl₃)** δ : 8.24 (s, C7-H), 6.97 (d, *J* = 10.2 Hz, C3-H), 6.93 (d, *J* = 10.2 Hz, C2-H), 2.61 (s, C9-H3); **¹³C NMR (125 MHz, CDCl₃)** δ : 183.6 (C4), 182.2 (C1), 151.2 (C6), 147.3 (C7), 138.2 (C3), 137.5 (C2), 134.1 (C4a), 130.7 (C8a), 101.5 (C5-I), 93.1 (C8-I), 30.6 (C9).

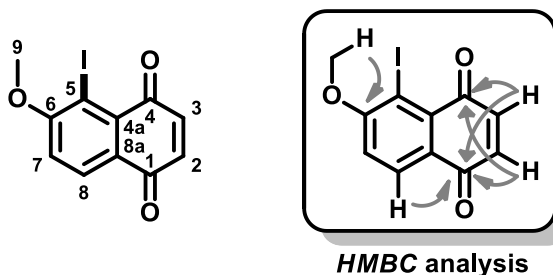
2-Bromo-5-iodo-1,4-naphthoquinone (81)



HMBC analysis

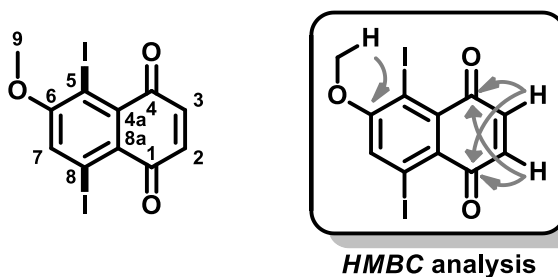
The product was obtained by the general microwave procedure described above. The reaction was conducted for 2h and purification by FCC (toluene) afforded iodinated product **81** (21.4 mg, 59% yield) as orange crystals; **m.p** (°C) = 159.5-160.6 (Petrol/CH₂Cl₂); **IR (solid, cm⁻¹)** ν : 2923 (w), 1677 (s), 1232 (m), 1062 (m); **HRMS (EI⁺)**: 361.8454 [M]⁺. Cald. for [C₁₀H₅IO₂]: 361.8439; **¹H NMR (400 MHz, CDCl₃)** δ : 8.40 (d, *J* = 7.2 Hz, C6-H), 8.25 (d, *J* = 7.7 Hz, C8-H), 7.55 (s, 1H), 7.38 (t, *J* = 7.8 Hz, C7-H); **¹³C NMR (101 MHz, CDCl₃)** δ : 180.5 (C4), 177.0 (C1), 148.7 (C6), 141.2 (C3), 137.9 (C2), 133.8 (C7), 133.6 (C8a), 130.5 (C4a), 128.9 (C8), 93.3 (C5-I).

5-Iodo-6-methoxy-1,4-naphthoquinone (**82**)



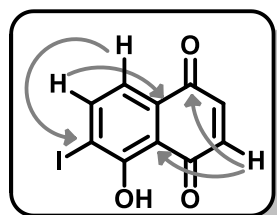
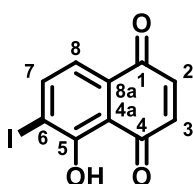
The product was obtained by the general microwave procedure described above. The reaction was conducted for 2h and purification by FCC (toluene) afforded iodinated product **82** (23.6 mg, 75% yield) as orange crystals; **m.p.** (°C) = 213.6-214.8 (Petrol/CH₂Cl₂); **IR (solid, cm⁻¹)** ν : 2988 (w), 1662 (s), 1279 (m), 1020 (m); **HRMS (ESI⁺)**: 336.9344 [M+Na]⁺. Cald. for [C₁₁H₇IO₃Na]⁺: 336.9332; **¹H NMR (400 MHz, CDCl₃)** δ : 8.16 (d, *J* = 8.6 Hz, C8-H), 7.12 (d, *J* = 8.6 Hz, C7-H), 6.99 (d, *J* = 10.2 Hz, C3-H), 6.88 (d, *J* = 10.2 Hz, C2-H), 4.03 (s, C9-H₃); **¹³C NMR (101 MHz, CDCl₃)** δ : 184.0 (C4), 183.0 (C1), 163.2 (C6), 139.7 (C3), 136.9 (C2), 133.0 (C4a), 129.9 (C8), 127.8 (C8a), 113.6 (C7), 87.2 (C5-I), 57.2 (C9).

5,8-Diiodo-6-methoxy-1,4-naphthoquinone (**82'**)



In addition to **82**, a C5/8 bis-iodinated by-product **82'** (1.8 mg, 4% yield) was obtained as a brown powder; **m.p** (°C) = 244.3-245.5 (Petrol/CH₂Cl₂); **IR (solid, cm⁻¹)** ν : 3337 (w), 1657 (s), 1307 (m), 1048 (m); **HRMS (EI⁺)**: 439.8403. Cald. for [C₁₁H₆I₂O₃]: 439.8406; **¹H NMR (500 MHz, CDCl₃)** δ : 7.71 (s, C7-H), 6.99 (d, *J* = 10.2 Hz, C2-H), 6.93 (d, *J* = 10.2 Hz, C3-H), 4.05 (s, C9-H₃); **¹³C NMR (125 MHz, CDCl₃)** δ : 183.3 (C1), 181.5 (C4), 161.8 (C6), 138.0 (C3), 137.9 (C2), 134.9 (C4a), 127.9 (C7), 126.2 (C8a), 95.2 (C8-I), 89.2 (C5-I), 57.5 (C9).

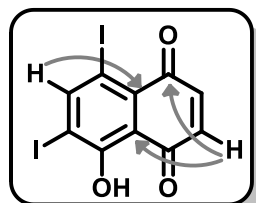
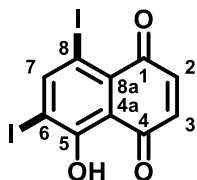
5-hydroxy-6-iodo-1,4-naphthoquinone (83)



HMBC analysis

The product was obtained by the general microwave procedure described above. The reaction was conducted for 2h and purification by FCC (toluene) afforded iodinated product **83** (26.4 mg, 88% yield) as red crystals; **m.p.** (°C) = 179.8-180.1 (Petrol/CH₂Cl₂); **IR (solid, cm⁻¹)** ν : 3021 (w), 1698 (s), 1270 (m), 830 (m); **HRMS (EI⁺)**: 299.9280 [M]⁺. Cald. for [C₁₀H₅IO₃]: 299.9283; **¹H NMR (400 MHz, CDCl₃)** δ : 12.73 (s, O-H), 8.15 (d, *J* = 8.0 Hz, C6-H), 7.33 (d, *J* = 8.0 Hz, C5-H), 6.96 (s, C2-H, C3-H); **¹³C NMR (100 MHz, CDCl₃)** δ : 190.0 (C4), 183.8 (C1), 160.1 (C5), 146.1 (C7), 139.8 (C3), 138.0 (C2), 131.5 (C8a), 120.1 (C8), 114.2 (C4a), 94.9 (C6-I).

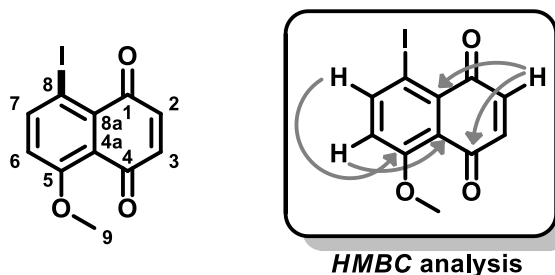
5-hydroxy-6,8-diiodo-1,4-naphthoquinone (84)



HMBC analysis

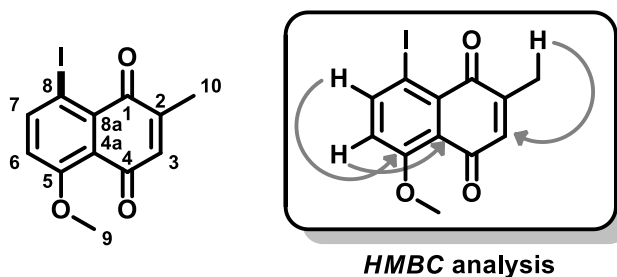
The product was obtained by the general microwave procedure described above, with minor modifications [DIH (150 mol%, 56.9 mg)]. The reaction was conducted for 2h and purification by FCC (toluene) afforded bis-iodinated product **84** (34.9 mg, 82% yield) as purple crystals; **m.p.** (°C) = 164.3-165.8 (Petrol/CH₂Cl₂); **IR (solid, cm⁻¹)** ν : 3002 (w), 1613 (s), 1211 (m), 911 (m); **HRMS (EI⁺)**: 425.8241 [M]⁺. Cald. for [C₁₀H₄I₂O₃]: 425.8250; **¹H NMR (500 MHz, CDCl₃)** δ : 13.54 (s, O-H), 8.80 (s, C7-H), 7.04 (d, *J* = 10.2 Hz, C2-H), 6.96 (d, *J* = 10.2 Hz, C3-H); **¹³C NMR (125 MHz, CDCl₃)** δ : 189.2 (C4), 182.0 (C1), 161.7 (C5), 158.5 (C7), 140.4 (C2), 136.5 (C3), 130.0 (C8a), 115.8 (C4a), 96.0 (C6-I), 83.0 (C8-I).

5-Iodo-8-methoxy-1,4-naphthoquinone (**89**)



The product was obtained by the general microwave procedure described above. The reaction was conducted for 2h and purification by FCC (toluene) afforded iodinated product **89** (23.9 mg, 76% yield) as red crystals; **m.p.** (°C) = 184.6-185.4 (Petrol/CH₂Cl₂); **IR (solid, cm⁻¹)** ν : 2924 (w), 1656 (s), 1285 (m), 1026 (m); **HRMS (ESI⁺)**: 314.9518 [M+H]⁺. Cald. for [C₁₁H₈IO₃]⁺: 314.9518; **¹H NMR (400 MHz, CDCl₃)** δ : 8.27 (d, $J = 9.0$ Hz, C6-H), 7.00 (d, $J = 9.0$ Hz, C7-H), 6.91 (d, $J = 10.2$ Hz, C3-H), 6.82 (d, $J = 10.2$ Hz, C2-H), 3.99 (s, C9-H₃); **¹³C NMR (100 MHz, CDCl₃)** δ : 183.6 (C4), 183.3 (C1), 160.4 (C8), 148.8 (C6), 139.2 (C2), 136.9 (C3), 132.4 (C4a), 122.4 (C8a), 118.8 (C7), 81.6 (C5-I), 56.7 (C9).

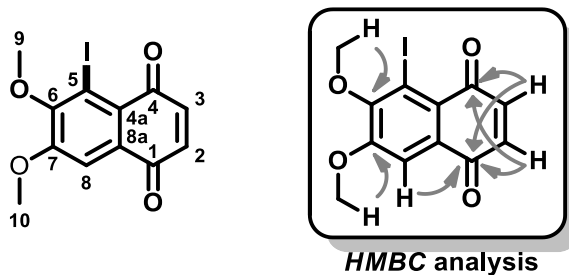
8-Iodo-5-methoxy-2-methyl-1,4-naphthoquinone (**90**)



The product was obtained by the general microwave procedure described above. The reaction was conducted for 2h and purification by FCC (toluene/EtOAc 97:3) afforded iodinated product **90** (28.9 mg, 88% yield) as red crystals; **m.p.** (°C) = 163.5-163.9 (Petrol/CH₂Cl₂); **IR (solid, cm⁻¹)** ν : 2978 (w), 1647 (s), 1223 (m), 962 (m); **HRMS (ESI⁺)**: 350.9492 [M+Na]⁺. Cald. for [C₁₂H₉IO₃Na]⁺: 350.9489; **¹H NMR (400 MHz, CDCl₃)** δ : 8.17 (d, $J = 9.0$ Hz, C7-H), 6.91 (d, $J = 9.0$ Hz, C6-H), 6.63 (s, C3-H), 3.93 (s, C9-H₃), 2.11 (s, C10-H₃); **¹³C NMR (100 MHz, CDCl₃)** δ : 184.2 (C1), 182.9 (C4),

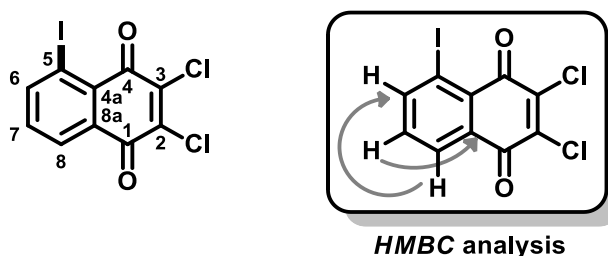
160.1 (C5), 148.4 (C7), 146.1 (C2), 136.4 (C3), 132.7 (C8a), 122.3 (C4a), 118.6 (C6), 81.8 (C8-I), 56.7 (C9), 16.3 (C10).

5-Iodo-6,7-dimethoxy-1,4-naphthoquinone (91)



The product was obtained by the general microwave procedure described above. The reaction was conducted for 3h and purification by FCC (toluene) afforded iodinated product **91** (23.1 mg, 67% yield) as an orange powder; **m.p** (°C) = 167.4-168.6 (Petrol/CH₂Cl₂); **IR (solid, cm⁻¹)** ν : 2924 (w), 1567 (s), 1316 (m), 1035 (m); **HRMS (ESI⁺)**: 366.9438 [M+Na]⁺. Cald. for [C₁₂H₉IO₄Na]⁺: 366.9450; **¹H NMR (400 MHz, CDCl₃)** δ : 7.64 (s, C8-H), 6.94 (d, *J* = 10.2 Hz, C3-H), 6.86 (d, *J* = 10.2 Hz, C2-H), 4.02 (s, C10-H₃), 3.90 (s, C9-H₃); **¹³C NMR (100 MHz, CDCl₃)** δ : 183.4 (C1), 182.7 (C4), 155.6 (C7), 154.2 (C6), 140.1 (C3), 136.2 (C2), 131.6 (C8a), 125.4 (C4a), 110.5 (C8), 93.6 (C5-I), 60.6 (C9), 56.5 (C10).

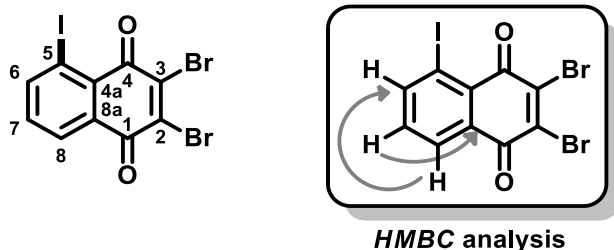
2,3-Dichloro-5-iodo-1,4-naphthoquinone (94)



The product was obtained by the general microwave procedure described above, with minor modifications [AgNTf₂ (27 mol%, 10.5 mg), [RhCp*Cl₂]₂ (5 mol%, 3.1 mg)]. The reaction was conducted for 8h and purification by FCC (toluene) afforded iodinated product **94** (20.3 mg, 51% yield) as orange crystals; **m.p.** (°C) = 194.2-195.6 (Petrol/CH₂Cl₂); **IR (solid, cm⁻¹)** ν : 3070 (w), 1676 (s), 1149 (m), 723 (m); **HRMS (EI⁺)**: 351.8555 [M]⁺. Cald. for [C₁₀H₅IO₂]: 351.8538; **¹H NMR (500 MHz, CDCl₃)** δ :

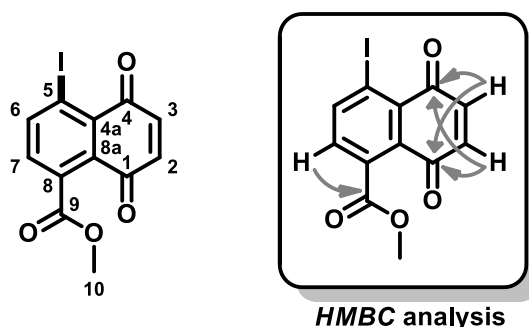
8.44 (d, $J = 7.9$ Hz, C6-H), 8.28 (d, $J = 7.7$ Hz, C8-H), 7.41 (t, $J = 7.8$ Hz, C7-H); ^{13}C NMR (125 MHz, CDCl_3) δ : 175.0 (C1), 174.2 (C4), 149.1 (C6), 144.0 (C3), 142.1 (C2), 134.2 (C7), 133.5 (C8a), 130.1 (C4a), 128.8 (C8), 94.5 (C5-I).

2,3-Dibromo-5-iodo-1,4-naphthoquinone (95)



The product was obtained by the general microwave procedure described above, with minor modifications [AgNTf_2 (27 mol%, 10.5 mg), $[\text{RhCp}^*\text{Cl}_2]_2$ (5 mol%, 3.1 mg), 65°C and 75W]. The reaction was conducted for 4h and purification by FCC (toluene) afforded iodinated product **95** (26.9 mg, 61% yield) as orange crystals; **m.p.** ($^\circ\text{C}$): 185.2-186.8 (Petrol/ CH_2Cl_2); **IR (solid, cm^{-1}) ν :** 2923 (w), 1674 (s), 1231 (m), 719 (m); **HRMS (EI^+):** 439.7540. Cald. for $[\text{C}_{10}\text{H}_3\text{IBr}_2\text{O}_2]$: 439.7545; ^1H NMR (400 MHz, CDCl_3) δ : 8.42 (d, $J = 7.9$ Hz, C6-H), 8.26 (d, $J = 7.7$ Hz, C8-H), 7.38 (t, $J = 7.8$ Hz, C7-H); ^{13}C NMR (100 MHz, CDCl_3) δ : 174.9 (C1), 174.1 (C4), 148.9 (C6), 143.2 (C3), 140.7 (C2), 134.1 (C7), 133.3 (C8a), 130.1 (C4a), 129.3 (C8), 94.9 (C5-I).

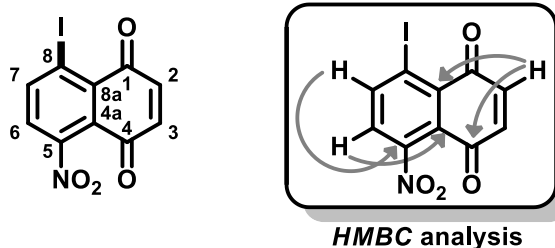
5-Iodo-8-methylcarboxylate-1,4-naphthoquinone (96)



The product was obtained by the general microwave procedure described above, with minor modifications [AgNTf_2 (27 mol%, 10.5 mg), $[\text{RhCp}^*\text{Cl}_2]_2$ (5 mol%, 3.1 mg)]. The reaction was conducted for 8h and purification by FCC (toluene) afforded iodinated product **96** (19.5 mg, 57% yield) as an orange powder; **m.p.** ($^\circ\text{C}$) = 123.9-124.7

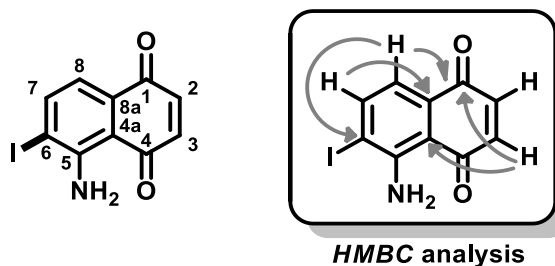
(Petrol/CH₂Cl₂); **IR (solid, cm⁻¹)** ν : 2922 (w), 1731 (s), 1667 (s), 1322 (m), 1078 (s); **HRMS (EI⁺)**: 341.9388 [M]⁺. Cald. for [C₁₂H₇IO₄]: 341.9389; **¹H NMR (400 MHz, CDCl₃)** δ : 8.42 (d, $J = 8.2$ Hz, C6-H), 7.27 (d, $J = 8.2$ Hz, C7-H), 7.05 (d, $J = 10.3$ Hz, C3-H), 6.95 (d, $J = 10.3$ Hz, C2-H), 3.97 (s, C10-H₃); **¹³C NMR (100 MHz, CDCl₃)** δ : 182.8 (C1), 182.4 (C4), 169.0 (C9), 148.0 (C6), 139.4 (C3), 137.2 (C2), 134.9 (C8), 131.9 (C7), 131.4 (C8a), 131.0 (C4a), 94.1 (C5-I), 53.2 (C10).

5-Iodo-8-nitro-1,4-naphthoquinone (97)



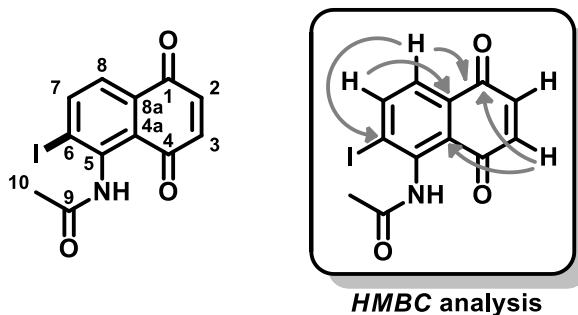
The product was obtained by the general microwave procedure described above, with minor modifications [AgNTf₂ (27 mol%, 10.5 mg), [RhCp*Cl₂]₂ (5 mol%, 3.1 mg)]. The reaction was conducted for 8h and purification by FCC (toluene) afforded iodinated product **97** (7.89 mg, 24% yield) as deep orange crystals; **m.p.** (°C) = 174.6-175.5 (Petrol/CH₂Cl₂); **IR (solid, cm⁻¹)** ν : 2922 (w), 1679 (s), 1540 (m), 1311 (m); **HRMS (EI⁺)**: 328.9190 [M]⁺. Cald. for [C₁₀H₄NIO₄]: 328.9185; **¹H NMR (400 MHz, CDCl₃)** δ : 8.55 (d, $J = 8.4$ Hz, C6-H), 7.36 (d, $J = 8.4$ Hz, C7-H), 7.12 (d, $J = 10.2$ Hz, C3-H), 7.02 (d, $J = 10.2$ Hz, C2-H); **¹³C NMR (100 MHz, CDCl₃)** δ : 181.3 (C4), 180.3 (C1), 149.0 (C6), 139.2 (C3), 137.5 (C2), 133.9 (C8), 131.4 (C4a), 127.1 (C7), 125.2 (C8a), 95.2 (C5-I).

5-amino-6-iodo-1,4-naphthoquinone (98)



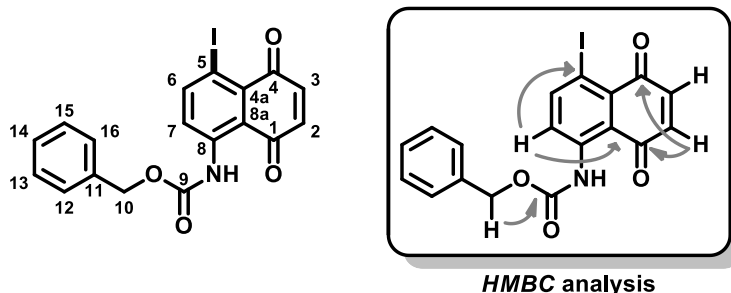
The product was obtained by the general microwave procedure described above. The reaction was conducted for 2h and purification by FCC (toluene) afforded iodinated product **98** (12.3 mg, 41% yield) as deep purple crystals; **m.p.** (°C) = 181.2-182.9 (Petrol/CH₂Cl₂); **IR (solid, cm⁻¹)** ν : 3078 (w), 1720 (s), 1380 (m), 923 (m); **HRMS (EI⁺)**: 298.9433 [M]⁺. Cald. for [C₁₀H₆INO₂]: 298.9443; **¹H NMR (400 MHz, CDCl₃)** δ : 8.03 (d, *J* = 8.0 Hz, C7-H), 7.15 (d, *J* = 8.0 Hz, C8-H), 6.90 (d, *J* = 10.3 Hz, C3-H), 6.86 (d, *J* = 10.3 Hz, C2-H); **¹³C NMR (100 MHz, CDCl₃)** δ : 186.65 (C4), 184.97 (C1), 149.21 (C5), 144.79 (C7), 140.05 (C3), 137.20 (C2), 132.92 (C8a), 117.45 (C8), 111.89 (C4a), 95.06 (C6-I).

***N*-(2-iodo-5,8-dioxo-5,8-dihydronaphthalen-1-yl)acetamide (100)**



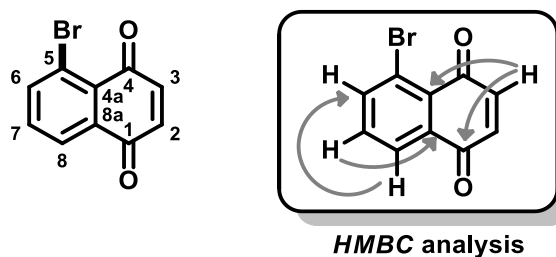
The product was obtained by the general microwave procedure described above. The reaction was conducted for 2h and purification by FCC (toluene) afforded iodinated product **100** (31.4 mg, 92% yield) as a pale yellow solid; **m.p.** (°C) = 203.8-204.9 (Petrol/CH₂Cl₂); **IR (solid, cm⁻¹)** ν : 2991 (w), 1658 (s), 1223 (m), 780 (m); **HRMS (EI⁺)**: 340.9521 [M]⁺. Cald. for [C₁₂H₈INO₃]: 340.9549; **¹H NMR (400 MHz, CDCl₃)** δ : 9.29 (s, N-H), 8.30 (d, *J* = 8.2 Hz, C7-H), 7.69 (d, *J* = 8.3 Hz, C8-H), 6.96 (d, *J* = 10.3 Hz, C2-H), 6.90 (d, *J* = 10.3 Hz, C3-H), 2.28 (s, C10-H₃); **¹³C NMR (100 MHz, CDCl₃)** δ : 186.55 (C4), 183.84 (C1), 168.68 (C9), 145.54 (C7), 140.29 (C5), 139.77 (C6-I), 139.48 (C3), 137.60 (C2), 132.52 (C8a), 125.56 (C8), 124.6(C4a) 24.48 (C10).

Benzyl (4-iodo-5,8-dioxo-5,8-dihydronaphthalen-1-yl)carbamate (**102**)



The product was obtained by the general microwave procedure described above. The reaction was conducted for 3h and purification by FCC (toluene) afforded iodinated product **102** (29.9 mg, 69% yield) as a red powder; **m.p.** (°C) = 121.4-122.5 (Petrol/CH₂Cl₂); **IR (solid, cm⁻¹)** ν : 2922 (w), 1679 (s), 1540 (m), 1311 (m); **HRMS (EI⁺)**: 432.9820 [M]⁺. Cald. for [C₁₈H₁₂NIO₄]: 432.9811; **¹H NMR (500 MHz, CDCl₃)** δ : 11.74 (s, N-H), 8.53 (d, *J* = 9.2 Hz, C7-H), 8.29 (d, *J* = 9.2 Hz, C6-H), 7.52-7.30 (m, C12,13,14,15,16-H), 6.98 (d, *J* = 10.2 Hz, C2-H), 6.86 (d, *J* = 10.2 Hz, C3-H), 5.25 (s, C-H); **¹³C NMR (125 MHz, CDCl₃)** δ : 187.7 (C4), 183.0 (C1), 153.5 (C9), 149.5 (C6), 142.8 (C8), 138.4 (C2), 138.3 (C3), 135.6 (C11), 131.1 (C4a), 128.6 (C12, C16), 128.5 (C14), 128.4 (C13, C15), 124.9 (C7), 118.0 (C8a), 85.4 (C5-I), 67.5 (C10).

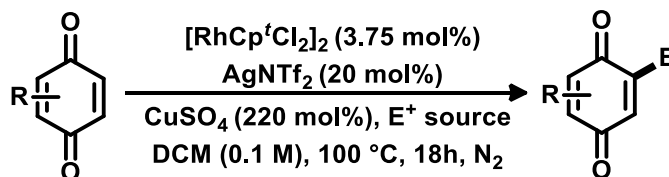
5-Bromo-1,4-naphthoquinone (**107**)



The product was obtained by the general microwave procedure described above, with minor modifications [1,3-dibromo-5,5-dimethylhydantoin (DBH) (150 mol%, 42.9 mg), 65°C and 75W]. The reaction was conducted for 5h and purification by FCC (toluene) afforded brominated product **107** (12.1 mg, 51% yield) as yellow crystals; **m.p.** (°C): 153.9-154.8 (Petrol/CH₂Cl₂); **IR (solid, cm⁻¹)** ν : 3069 (w), 1667 (s), 1319 (m), 779 (m); **HRMS (EI⁺)**: 235.9479 [M]⁺. Cald. for [C₁₀H₅BrO₂]: 235.9473; **¹H NMR (400 MHz, CDCl₃)** δ : 8.12 (dd, *J* = 8.0, 1.3 Hz, C8-H), 7.99 (dd, *J* = 8.1, 1.3 Hz, C6-H), 7.54 (t, *J*

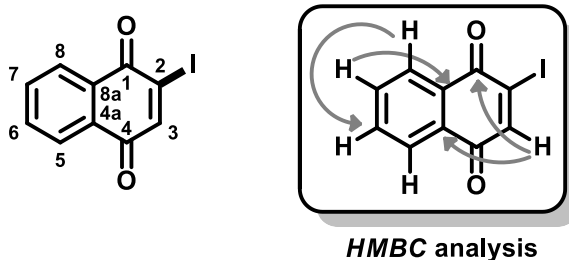
= 8.0 Hz, C7-H), 6.99 (d, $J = 10.3$ Hz, C3-H), 6.94 (d, $J = 10.3$ Hz, C2-H); ^{13}C NMR (100 MHz, CDCl_3) δ : 183.7 (C1), 183.3 (C4), 141.0 (C6), 140.1 (C3), 136.7 (C2), 134.6 (C8a), 133.7 (C7), 129.0 (C4a), 126.7 (C8), 121.9 (C5-Br).

7.4.2. General Procedure for Halogenation/Selenylation at the C2-Position



In a glovebox, an oven dried re-sealable tube was charged with the corresponding quinone (0.10 mmol), $[\text{RhCp}^*\text{Cl}_2]_2$ (3.75 mol%, 2.6 mg), silver bis(trifluoromethanesulfonyl)imide (20 mol%, 7.8 mg), the electrophile source (see below) and anhydrous copper sulfate (220 mol%, 34.9 mg). The tube was removed from the glovebox and an inert atmosphere was maintained. Anhydrous CH_2Cl_2 (1.0 mL) was added via syringe and tube was sealed. The mixture was heated at 100 °C for 18h. After cooling, the mixture was filtered through a pad of celite and purified by FCC, under the conditions noted.

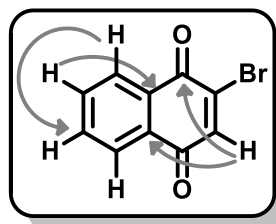
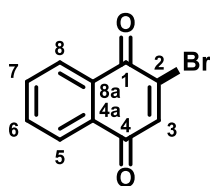
2-Iodo-1,4-naphthoquinone (61)



The product was obtained by the general halogenation/selenylation procedure described above, with minor modifications [AgNTf_2 (10 mol%, 3.8 mg), $[\text{RhCp}^*\text{Cl}_2]_2$ (2 mol%, 1.4 mg)], using 1,3-diiodo-5,5-dimethylhydantoin (DIH) (100 mol%, 37.9 mg) and a reaction time of 18h. Purification by FCC (hexane/ethyl acetate 99:1) afforded iodinated product **61** (26 mg, 90% yield) as orange crystals; **m.p.** (°C): 111.4-112.9 (Petrol/ CH_2Cl_2); **IR** (solid, cm^{-1}) ν : 3043 (w), 1671 (s), 1652 (s), 1320 (m); **HRMS**

(Et^+): 283.9326 $[\text{M}]^+$. Cald. for $[\text{C}_{10}\text{H}_5\text{IO}_2]$: 283,9334; $^1\text{H NMR}$ (400 MHz, CDCl_3) δ : 8.18 (d, $J = 7.0$ Hz, C8-H), 8.09 (d, $J = 9.1$ Hz, C5-H), 7.91 (s, C3-H), 7.83 – 7.72 (m, C7-H, C6-H); $^{13}\text{C NMR}$ (100 MHz, CDCl_3) δ : 182.0 (C4), 178.8 (C1), 148.4 (C3), 134.3 (C6), 134.0 (C7), 131.7 (C4a), 129.7 (C8a), 128.2 (C8), 127.0 (C5), 123.0 (C2-I).

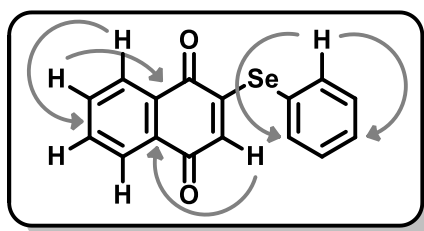
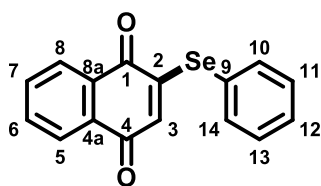
2-Bromo-1,4-naphthoquinone (71)²⁰⁹



HMBC analysis

The product was obtained by the general halogenation/selenylation procedure described above, with minor modifications [AgNTf_2 (10 mol%, 3.8 mg), $[\text{RhCp}^*\text{Cl}_2]_2$ (2 mol%, 1.4 mg)], using 1,3-dibromo-5,5-dimethylhydantoin (DBH) (150 mol%, 42.9 mg) and a reaction time of 18h. Purification by FCC (hexane/ethyl acetate 98:2) afforded brominated product **71** (21 mg, 88% yield) as light yellow crystals; **m.p.** ($^\circ\text{C}$) = 130.8–131.6 (Petrol/ CH_2Cl_2); $^1\text{H NMR}$ (400 MHz, CDCl_3) δ : 8.16 (dd, $J = 5.9, 3.1$ Hz, 1H), 8.07 (dd, $J = 5.9, 3.0$ Hz, 1H), 7.83 – 7.70 (m, 2H), 7.51 (s, 1H); $^{13}\text{C NMR}$ (100 MHz, CDCl_3) δ : 182.4, 177.8, 140.3, 140.1, 134.4, 134.1, 131.7, 130.9, 127.8, 126.9.

2-(phenylselanyl)-1,4-naphthoquinone (74)



HMBC analysis

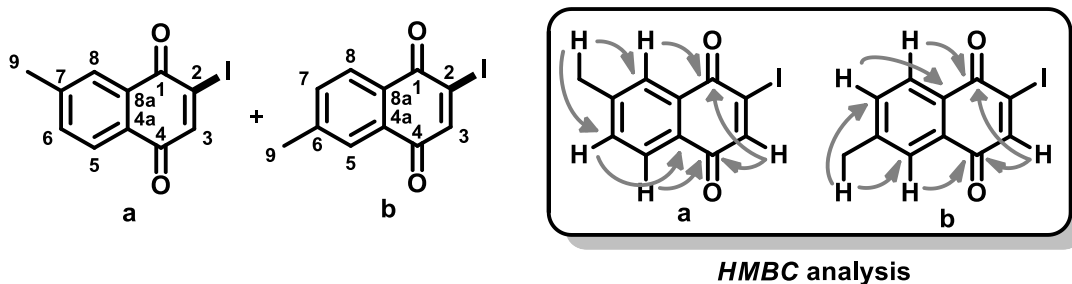
The product was obtained by the general halogenation/selenylation procedure described above, with minor modifications [AgNTf_2 (10 mol%, 3.8 mg), $[\text{RhCp}^*\text{Cl}_2]_2$ (2 mol%, 1.4 mg)], using *N*-phenyl selenium phthalimide (120 mol %, 36.2 mg) and a reaction

²⁰⁹. Creceley, R.W.; Creceley, K.M.; Goldstein, J.H.; The PMR spectral parameters of some 2- and 2,3-substituted naphthoquinones and their relation to electronic structures. *J. Mol. Spectrosc.*, **1969**, 32, 407.

time of 18h. Purification by FCC (toluene) afforded product **74** (26.9 mg, 86% yield) as orange crystals; **m.p.** (°C) = 152.8-153.7 (Petrol/CH₂Cl₂); **IR (solid, cm⁻¹)** ν : 2930 (w), 1664 (s), 1296 (m), 690 (s); **HRMS (EI⁺)**: 313.9848 [M⁺]. Cald. for [C₁₆H₁₀SeO₂]: 313.9846; **¹H NMR (400 MHz, CDCl₃)** δ : 8.14 (dd, *J* = 7.2, 1.9 Hz, C8-H), 8.03 (dd, *J* = 6.1, 1.9 Hz, C5-H), 7.82 – 7.67 (m, C6-H, C7-H), 7.68 – 7.61 (m, C10-H, C14-H), 7.57 – 7.42 (m, C11-H, C12-H, C13-H), 6.40 (s, C3-H); **¹³C NMR (100 MHz, CDCl₃)** δ : 183.0 (C1), 181.7 (C4), 157.0 (C2), 137.1 (C10, C14), 134.3 (C6), 133.3 (C7), 132.8 (C3), 132.3 (C4a), 131.6 (C8a), 130.4 (C11, C13), 130.2 (C12), 126.9 (C8), 126.7 (C5), 124.4 (C9).

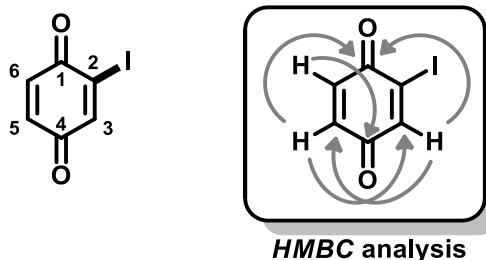
2-Iodo-7-methyl-1,4-naphthoquinone and 2-Iodo-6-methyl-1,4-naphthoquinone

(77)



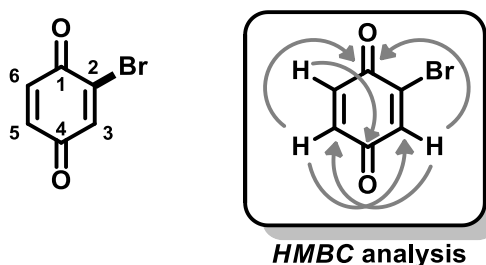
The products were obtained by the general halogenation/selenylation procedure described above, with minor modifications [AgNTf₂ (10 mol%, 3.8 mg), [RhCp⁺Cl₂]₂ (2 mol%, 1.4 mg)], using 1,3-diiodo-5,5-dimethylhydantoin (DIH) (100 mol %, 37.9 mg) and a reaction time of 18h. Purification by FCC (hexane/ethyl acetate 99:1) afforded iodinated product **77** as a mixture of isomers **a** and **b** (23.0 mg, 81% yield, 1.3:1 **a**:**b**) as a yellow powder; **HRMS (EI⁺)**: 297.9477 [M]⁺. Cald. for [C₁₁H₇IO₂]: 297.9491; **¹H NMR (400 MHz, CDCl₃)** δ : 8.05 (d, *J* = 7.9 Hz, C8-H for **b**), 7.99 – 7.92 (m, C5-H, C8-H for **a**), 7.87 – 7.83 (m, C5-H, C3-H for **b** + C3-H for **a**), 7.56 (d, *J* = 7.8 Hz, C6-H for **a**), 7.52 (d, *J* = 8.2 Hz, C7-H for **b**), 2.50 (s, C9-H₃ for **b** + C9-H₃ for **a**); **¹³C NMR (100 MHz, CDCl₃)** δ : 182.3 (C4, **b**), 181.9 (C4, **a**), 179.0 (C1, **a**), 178.5 (C1, **b**), 148.5 (C3, **a**), 148.2 (C3, **b**), 145.7 (C7, **a**), 145.3 (C7, **b**), 135.0 (C6, **a**), 134.7 (C6, **b**), 131.6 (C5, **b**), 129.6 (C4a, **a**), 129.5 (C4a, **b**), 128.5 (C8, **a**), 128.4 (C8, **b**), 127.4 (C8a for **b**, C8a for **a**), 127.2 (C5, **a**), 123.4 (C2-I, **b**), 122.7 (C2-I, **a**), 21.9 (C9, **b** and **a**).

2-Iodo-1,4-benzoquinone (108)



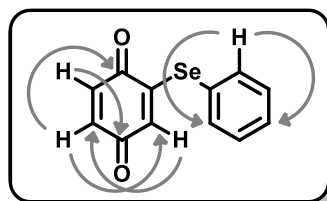
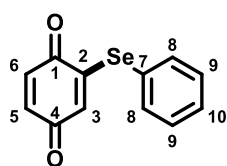
The product was obtained by the general halogenation/selenylation procedure described above using 1,3-diiodo-5,5-dimethylhydantoin (DIH) (150 mol%, 56.9 mg) and a reaction time of 18 h. Purification by FCC (toluene) afforded product **108** (22 mg, 95% yield) as orange crystals; **m.p.** (°C) = 58.3-58.9 (Petrol/CH₂Cl₂); **IR (solid, cm⁻¹)** ν : 3042 (w), 1644 (s), 1269 (s), 914 (s); **HRMS (EI⁺)**: 233.9174 [M]⁺. Cald. for [C₆H₃IO₂]: 233.9178; **¹H NMR (400 MHz, CDCl₃)** δ : 7.67 (d, J = 2.4 Hz, C3-H), 7.00 (d, J = 10.0 Hz, C6-H), 6.84 (dd, J = 10.1, 2.4 Hz, C5-H); **¹³C NMR (100 MHz, CDCl₃)** δ : 184.0 (C4), 180.2 (C1), 146.1 (C3), 136.6 (C5), 134.56 (C6), 119.6 (C2).

2-Bromo-1,4-benzoquinone (109)



The product was obtained by the general halogenation/selenylation procedure described above using 1,3-dibromo-5,5-dimethylhydantoin (DBH) (120 mol%, 34.3 mg) and a reaction time of 18 h. Purification by FCC (toluene) afforded product **109** (15.3 mg, 82% yield) as yellow crystals; **m.p.** (°C) = 54.5-55.1 (Petrol/CH₂Cl₂); **IR (solid, cm⁻¹)** ν : 3042 (w), 1661 (s), 1276 (s), 967 (s); **HRMS (EI⁺)**: 185.9312 [M]⁺. Cald. for [C₆H₃BrO₂]: 185.9316; **¹H NMR (400 MHz, CDCl₃)** δ : 7.29 (d, J = 2.4 Hz, C3-H), 6.96 (d, J = 10.1 Hz, C6-H), 6.82 (dd, J = 10.1, 2.4 Hz, C5-H); **¹³C NMR (100 MHz, CDCl₃)** δ : 184.55 (C4), 179.17 (C1), 138.12 (C3), 137.50 (C2), 136.63 (C5), 135.79 (C6).

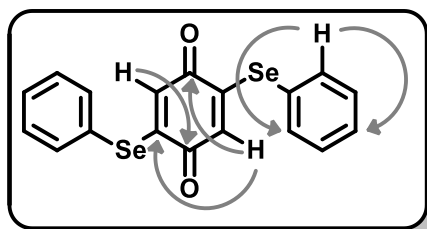
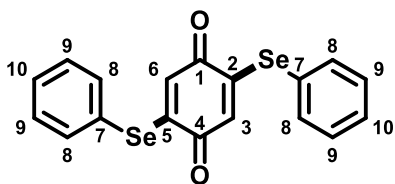
2-(Phenylselanyl)-1,4-benzoquinone (110)



HMBC analysis

The product was obtained by the general halogenation/selenylation procedure described above using *N*-phenyl selenium phthalimide (100 mol%, 30.2 mg) and a reaction time of 18 h. Purification by FCC (toluene) afforded product **110** (16.0 mg, 61% yield) as a red powder; **m.p.** (°C) = 100.4-101.1 (Petrol/CH₂Cl₂); **IR (solid, cm⁻¹)** ν : 2921 (w), 1631 (s), 1279 (m), 967 (s); **HRMS (EI⁺)**: 263.9682 [M]⁺. Cald. for [C₁₂H₈SeO₂]: 263.9690; **¹H NMR (400 MHz, CDCl₃)** δ : 7.64-7.53 (m, C8-H, C12-H), 7.53-7.39 (m, C9-H, C10-H, C11-H), 6.85 (d, *J* = 10.0 Hz, C6-H), 6.68 (dd, *J* = 10.0, 2.4 Hz, C5-H), 6.15 (d, *J* = 2.4 Hz, C3-H); **¹³C NMR (100 MHz, CDCl₃)** δ : 184.8 (C1), 184.1 (C4), 154.5 (C2), 137.5 (C5), 137.0 (C8), 135.9 (C6), 130.5 (C3), 130.4 (C9), 130.2 (C10), 123.9 (C7). Compound **111** was eluted first and obtained (5.4 mg, 13% yield) as an orange powder. The data for this compound are given at the end of the next procedure.

2,5-Bis(phenylselanyl)-1,4-benzoquinone (111)

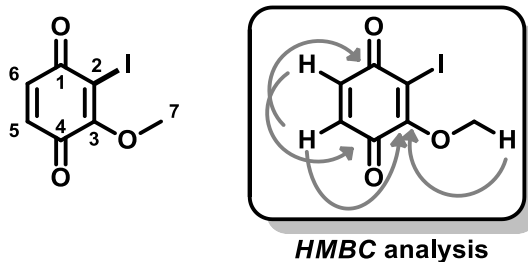


HMBC analysis

The product was obtained by the general halogenation/selenylation procedure described above using *N*-phenyl selenium phthalimide (250 mol%, 75.5 mg) and a reaction time of 18 h. Purification by FCC (toluene) afforded product **111** (30.9 mg, 74% yield) as an orange powder; **m.p.** (°C) = 230.3-231.0 (Petrol/CH₂Cl₂); **IR (solid, cm⁻¹)** ν : 3055 (w), 1634 (s), 1546 (m), 990 (s); **HRMS (ESI⁺)**: 420.9263 [M+H]⁺. Cald. for [C₁₈H₁₃Se₂O₂]: 420.9244; **¹H NMR (400 MHz, CDCl₃)** δ : 7.63-7.53 (m, C8-H), 7.54-7.39 (m, C9-H,

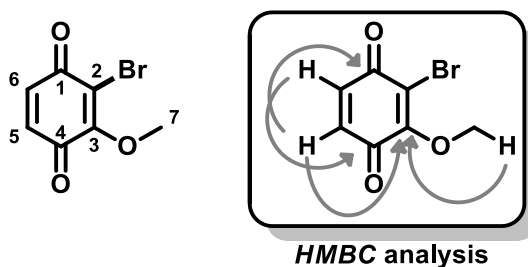
C10-H), 6.21 (s, C3-H, C6-H); ^{13}C NMR (100 MHz, CDCl_3) δ : 181.38 (C1, C4), 157.1 (C2, C5), 136.9 (C8), 130.4 (C9), 130.2 (C10), 129.4 (C3, C6), 124.1 (C7).

2-Iodo-3-methoxy-1,4-benzoquinone (114)



The product was obtained by the general halogenation/selenylation procedure described above using 1,3-diiodo-5,5-dimethylhydantoin (DIH) (120 mol%, 45.5 mg) and a reaction time of 18 h. Purification by FCC (toluene) afforded product **114** (24.0 mg, 91% yield) as orange crystals; **m.p.** ($^{\circ}\text{C}$) = 98.1-99.9 (Petrol/ CH_2Cl_2); **IR (solid, cm^{-1})** ν : 3027 (w), 1698 (s), 1354 (s), 991 (s); **HRMS (EI^+)**: 261.9493 $[\text{M}]^+$. Cald. for $[\text{C}_7\text{H}_5\text{IO}_3]$: 263.9283; ^1H NMR (400 MHz, CDCl_3) δ : 6.91 (d, $J = 10.0$ Hz, C6-H), 6.67 (d, $J = 10.0$ Hz, C5-H), 4.21 (s, C7-H₃); ^{13}C NMR (100 MHz, CDCl_3) δ : 181.73 (C1), 179.36 (C4), 161.43 (C3), 135.10 (C6), 134.66 (C5), 100.93 (C2), 61.67 (C7).

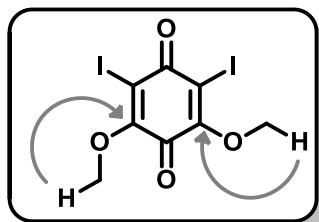
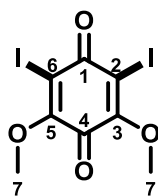
2-Bromo-3-methoxy-1,4-benzoquinone (115)



The product was obtained by the general halogenation/selenylation procedure described above using 1,3-dibromo-5,5-dimethylhydantoin (DBH) (120 mol%, 34.3 mg) and a reaction time of 18 h. Purification by FCC (toluene) afforded product **115** (16.1 mg, 74% yield) as an orange powder; **m.p.** ($^{\circ}\text{C}$) = 85.7-86.3 (Petrol/ CH_2Cl_2); **IR (solid, cm^{-1})** ν : 2960 (w), 1651 (s), 1555 (s), 1092 (s); **HRMS (EI^+)**: 215.9410 $[\text{M}]^+$. Cald. for $[\text{C}_7\text{H}_5\text{BrO}_3]$: 215.9422; ^1H NMR (400 MHz, CDCl_3) δ : 6.87 (d, $J = 10.0$ Hz, C6-H),

6.68 (d, $J = 10.1$ Hz, C5-H), 4.21 (s, C7-H₃); ¹³C NMR (100 MHz, CDCl₃) δ : 180.8 (C4), 180.3 (C1), 157.0 (C3), 135.8 (C6), 134.6 (C5), 118.5 (C2), 61.6 (C7).

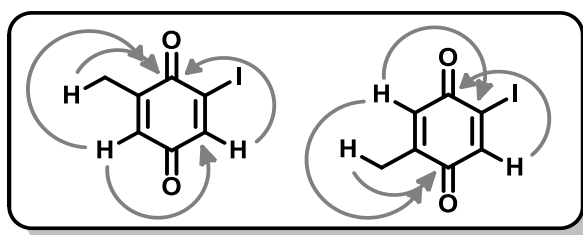
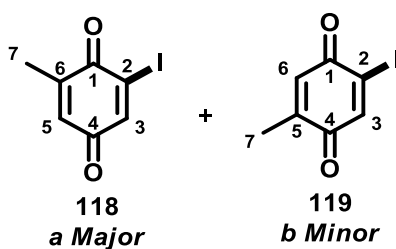
2,6-Diiodo-3,5-dimethoxy-1,4-benzoquinone (116)



HMBC analysis

The product was obtained by the general halogenation/selenylation procedure described above using 1,3-diiodo-5,5-dimethylhydantoin (DIH) (150 mol%, 56.9 mg) and a reaction time of 18 h. Purification by FCC (toluene) afforded product **116** (38.1 mg, 91% yield) as deep red crystals; **m.p.** (°C) = 160.2-160.9 (Petrol/CH₂Cl₂); **IR (solid, cm⁻¹)** ν : 2947 (w), 1667 (s), 1266 (s), 924 (s); **HRMS (EI⁺)**: 419.8349 [M]⁺. Cald. for [C₈H₆I₂O₄]: 419.8355; ¹H NMR (400 MHz, CDCl₃) δ : 4.16 (s, C7-H₆); ¹³C NMR (100 MHz, CDCl₃) δ : 175.2 (C1), 171.2 (C4), 160.4 (C2, C6), 98.1 (C3, C5), 61.6 (C7).

2-Iodo-6-methyl-1,4-benzoquinone (118) and 2-Iodo-5-methyl-1,4-benzoquinone (119)

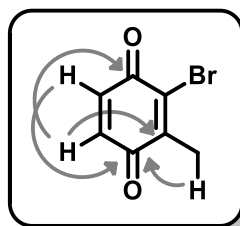
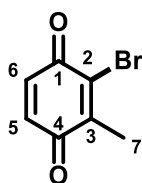


HMBC analysis

The product was obtained by the general halogenation/selenylation procedure described above using 1,3-diiodo-5,5-dimethylhydantoin (DIH) (150 mol%, 56.9 mg) and a reaction time of 18 h. Purification by FCC (toluene) afforded products **118** and **119** (mixture of isomers, 5:4/a:b) (20 mg, 81% yield) as an orange powder; **HRMS (EI⁺)**: 247.9326 [M]⁺. Cald. for [C₇H₅IO₂]: 247.9334; ¹H NMR (500 MHz, CDCl₃) δ : 7.64 (d, $J = 1.4$ Hz, C3b-H), 7.59 (dd, $J = 2.4, 1.5$ Hz, C3a-H), 6.84 (t, $J = 1.6$ Hz, C6b-H),

6.66 (dt, $J = 2.4, 1.5$ Hz, C5a-H), 2.14 (t, $J = 1.5$ Hz, C7a-H₃), 2.07 (t, $J = 1.5$ Hz, C7b-H₃); ¹³C NMR (125 MHz, CDCl₃) δ : 184.6 (C4b), 184.5 (C4a), 180.8 (C1a), 180.4 (C1b), 146.4 (C5b), 146.2 (C3a), 146.1 (C3b), 144.6 (C6a), 133.5 (C5a), 131.4 (C6b), 119.7 (C2-Ib), 119.3 (C2-Ia), 17.3 (C7a), 15.8 (C7b).

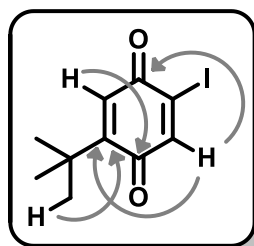
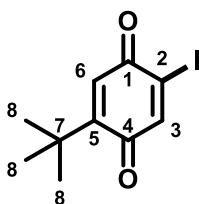
2-Bromo-3-methyl-1,4-benzoquinone (120)



HMBC analysis

The product was obtained by the general halogenation/selenylation procedure described above using 1,3-dibromo-5,5-dimethylhydantoin (DBH) (120 mol%, 34.3 mg) and a reaction time of 18 h. Purification by FCC (toluene) afforded product **120** (13.7 mg, 68% yield) as a yellow powder; **m.p.** (°C) = 55.1-56.7 (Petrol/CH₂Cl₂); **IR** (solid, cm⁻¹) ν : 2987 (w), 1596 (s), 1233 (s), 870 (s); **HRMS** (EI⁺): 199.9461 [M]⁺. Cald. for [C₇H₅BrO₂]: 199.9473; ¹H NMR (400 MHz, CDCl₃) δ : 6.92 (d, $J = 10.0$ Hz, C6-H), 6.81 (d, $J = 10.0$ Hz, C5-H), 2.23 (s, C7-H₃); ¹³C NMR (100 MHz, CDCl₃) δ : 183.9 (C4), 179.1 (C1), 146.2 (C3), 136.3 (C5), 136.1 (C2), 135.8 (C6), 16.9 (C7).

2-Iodo-5-(tert-butyl)-1,4-benzoquinone (122)

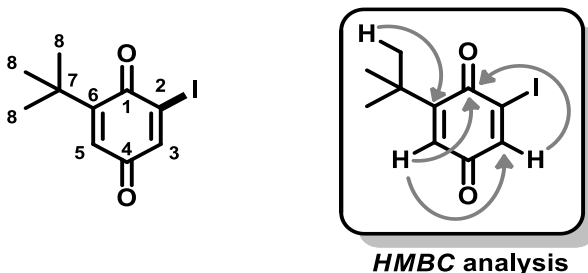


HMBC analysis

The product was obtained by the general halogenation/selenylation procedure described above using 1,3-diiodo-5,5-dimethylhydantoin (DIH) (120 mol%, 45.5 mg) and a reaction time of 18 h. Purification by FCC (toluene) afforded product **122** (19.2 mg, 66% yield) as a deep yellow solid; **m.p.** (°C) = 70.5-71.0 (Petrol/CH₂Cl₂); **IR** (solid,

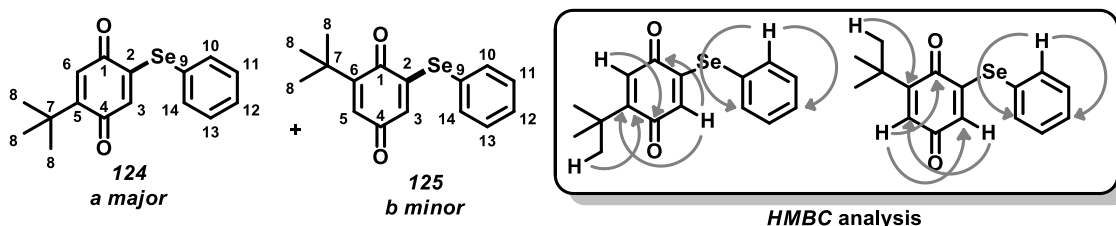
cm^{-1}) ν : 2960 (s), 1651 (s), 1180 (s), 1009 (s); **HRMS (EI⁺)**: 289.9798 [M]⁺. Cald. for [C₁₀H₁₁IO₂]: 289.9804; **¹H NMR (400 MHz, CDCl₃)** δ : 7.54 (s, C3-H), 6.81 (s, C6-H), 1.27 (s, C8-H₉); **¹³C NMR (100 MHz, CDCl₃)** δ : 184.2 (C4), 181.3 (C1), 156.6 (C5), 147.9 (C3), 129.8 (C6), 117.5 (C2), 35.5 (C7), 29.0 (C8).

2-Iodo-6-(*tert*-butyl)-1,4-benzoquinone (123)



Continued elution afforded product **123** (5.2 mg, 18% yield) as a deep yellow solid; **m.p.** (°C) = 71.8-72.9 (Petrol/CH₂Cl₂); **IR (solid, cm⁻¹)** ν : 2965 (s), 1689 (s), 1218 (s), 1124 (s); **HRMS (EI⁺)**: 289.9807 [M]⁺. Cald. for [C₁₀H₁₁IO₂]: 289.9804; **¹H NMR (400 MHz, CDCl₃)** δ : 7.59 (d, *J* = 2.4 Hz, C3-H), 6.65 (d, *J* = 2.4 Hz, C5-H), 1.28 (s, C8-H₉); **¹³C NMR (100 MHz, CDCl₃)** δ : 185.3 (C4), 179.9 (C1), 155.1 (C6), 145.1 (C3), 131.9 (C5), 122.7 (C2), 36.2 (C7), 29.1 (C8).

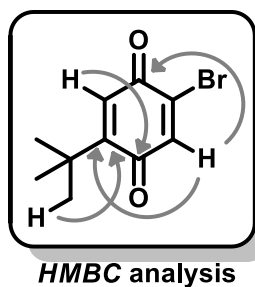
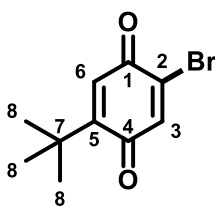
5-(*Tert*-butyl)-2-(phenylselanyl)-1,4-benzoquinone (124) and 6-(*Tert*-butyl)-2-(phenylselanyl)-1,4-benzoquinone (125)



The product was obtained by the general halogenation/selenylation procedure described above using *N*-phenyl selenium phthalimide (120 mol %, 36.2 mg) and a reaction time of 18h. Purification by FCC (toluene) afforded products **124** and **125** (mixture of isomers, 5:2/*a*:*b*) (19.5 mg, 61% yield) as a red powder; **HRMS (EI⁺)**: 321.0405 [M+H]⁺. Cald. for [C₁₆H₁₇O₂Se]: 321.0393; **¹H NMR (400 MHz, CDCl₃)** δ : 7.65 - 7.58 (m, 5H), 7.52 - 7.41 (m, 5H), 6.69 (s, C3a-H), 6.52 (d, *J* = 2.4 Hz C3b-H), 6.11 (d, *J* =

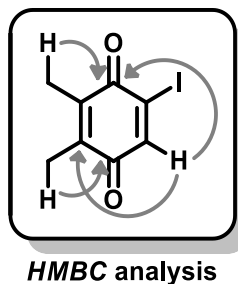
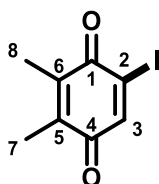
2.4 Hz, C6b-H), 6.07 (s, C6a-H), 1.32 (s, C8b-H₉), 1.27 (s, C8a-H₉); ¹³C NMR (125 MHz, CDCl₃) δ: 185.7 (C1a), 185.0 (C4b), 184.8 (C1b), 184.3 (C4a), 157.2 (C5a), 155.8 (C6a) 152.0 (C6b), 137.0 (C11a, C12a, C13a), 132.6 (C3a), 132.5 (C3b), 130.9 (C10b, C14b), 130.3 (C11b, C12b, C13b, C9a), 130.1 (C9b) 130.0 (C10a, C14a), 129.7 (C5b), 124.7 (C2b), 124.1 (C2a), 35.4 (C7a,C7b), 29.3 (C8a), 29.2 (C8b).

2-Bromo-5-(*tert*-butyl)-1,4-benzoquinone (126)



The product was obtained by the general halogenation/selenylation procedure described above using 1,3-dibromo-5,5-dimethylhydantoin (DBH) (120 mol%, 34.3 mg) and a reaction time of 18 h. Purification by FCC (toluene) afforded product **126** (13.9 mg, 57% yield) as a yellow powder; **m.p.** (°C) = 100.2-101.1 (Petrol/CH₂Cl₂); **IR (solid, cm⁻¹)** ν: 2963 (s), 1654 (s), 1013 (s), 733 (s); **HRMS (EI⁺)**: 241.9932 [M]⁺. Cald. for [C₁₀H₁₁BrO₂]: 241.9942; ¹H NMR (400 MHz, CDCl₃) δ: 7.19 (s, C3-H), 6.78 (s, C6-H), 1.28 (s, C8 -H₉); ¹³C NMR (100 MHz, CDCl₃) δ: 184.7 (C4), 180.4 (C1), 156.7 (C5), 139.9 (C3), 135.7 (C2), 130.9 (C6), 35.5 (C7), 29.1 (C8).

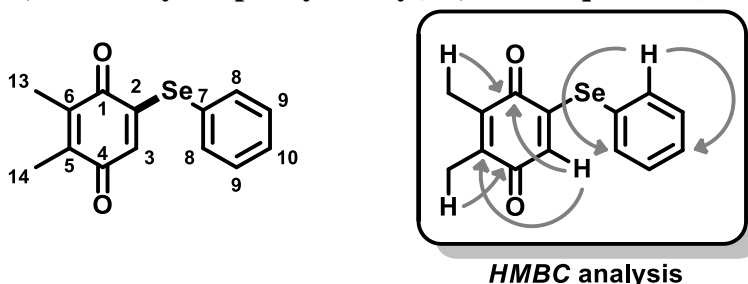
2-Iodo-5,6-dimethyl-1,4-benzoquinone (128)



The product was obtained by the general halogenation/selenylation procedure described above using 1,3-diiodo-5,5-dimethylhydantoin (DIH) (150 mol%, 56.9 mg) and a reaction time of 18 h. Purification by FCC (toluene) afforded product **128** (21.2 mg,

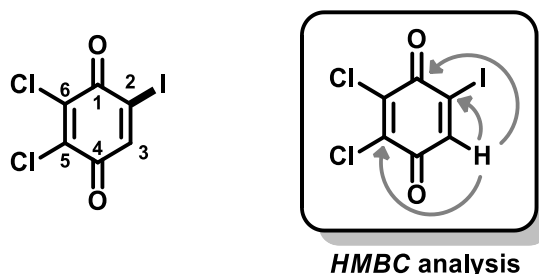
81% yield) as a red oil; **IR** (solid, cm^{-1}) ν : 2921 (w), 1638 (s), 1236 (s), 838 (s); **HRMS** (EI^+): 261.9493 $[\text{M}]^+$. Cald. for $[\text{C}_8\text{H}_7\text{IO}_2]$: 261.9491; ^1H NMR (400 MHz, CDCl_3) δ : 7.59 (s, C3-H), 2.10 (d, $J = 1.2$ Hz, C8-H₃), 2.02 (d, $J = 1.2$ Hz, C7-H₃); ^{13}C NMR (100 MHz, CDCl_3) δ : 184.4 (C4), 180.4 (C1) 145.9 (C3), 141.4 (C5), 140.0 (C6), 119.1 (C2), 13.8 (C8), 12.5 (C7).

2,3-Dimethyl-5-(phenylselanyl)-1,4-benzoquinone (130)



The product was obtained by the general halogenation/selenylation procedure described above using *N*-phenyl selenium phthalimide (120 mol%, 36.2 mg) and a reaction time of 18 h. Purification by FCC (toluene) afforded product **130** (21.3 mg, 73% yield) as red crystals; **m.p.** ($^{\circ}\text{C}$) = 98.1-99.0 (Petrol/ CH_2Cl_2); **IR** (solid, cm^{-1}) ν : 2930 (w), 1634 (s), 1236 (m), 746 (s); **HRMS** (EI^+): 292.0006 $[\text{M}]^+$. Cald. for $[\text{C}_{14}\text{H}_{12}\text{SeO}_2]$: 292.0003; ^1H NMR (500 MHz, CDCl_3) δ : 7.62-7.54 (m, C8-H), 7.51-7.37 (m, C9-H, C10-H), 6.11 (s, C3-H), 2.06 (s, C13-H₃), 1.99 (s, C14-H₃); ^{13}C NMR (125 MHz, CDCl_3) δ : 184.9 (C1), 184.2 (C4), 153.6 (C2), 141.9 (C6), 140.5 (C5), 137.0 (C8), 130.5 (C3), 130.2 (C9), 129.9 (C10), 124.5 (C7), 12.4 (C13, C14).

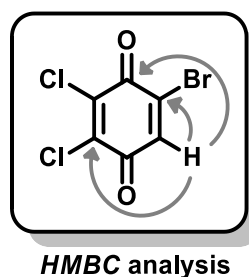
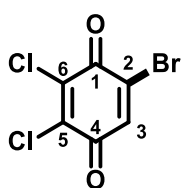
2-Iodo-5,6-dichloro-1,4-benzoquinone (132)



The product was obtained by the general halogenation/selenylation procedure described above using 1,3-diiodo-5,5-dimethylhydantoin (DIH) (150 mol%, 56.9 mg) and a

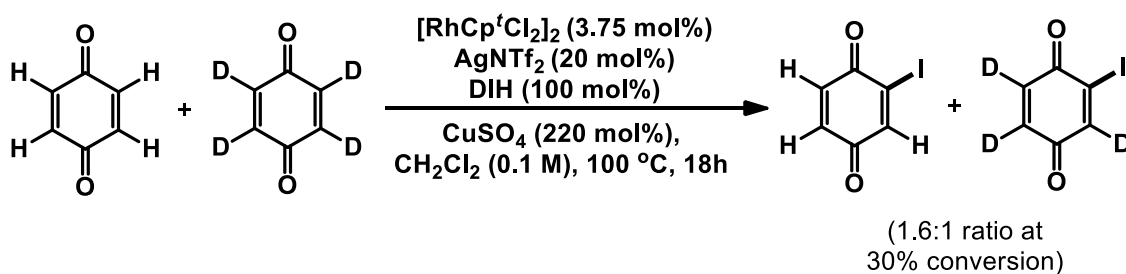
reaction time of 18 h. Purification by FCC (toluene) afforded product **132** (16.9 mg, 56% yield) as yellow crystals; **m.p.** (°C) = 162.8-163.5 (Petrol/CH₂Cl₂); **IR (solid, cm⁻¹)** ν : 2973 (w), 1667 (s), 1046 (m), 881 (s); **HRMS (EI⁺)**: 301.8402 [M]⁺. Cald. for [C₆HICl₂O₂]: 301.8398; **¹H NMR (400 MHz, CDCl₃)** δ : 7.83 (s, C3-H); **¹³C NMR (100 MHz, CDCl₃)** δ : 175.3 (C4), 171.9 (C1), 145.2 (C3), 141.6 (C5), 138.2 (C6), 117.4 (C2).

2-Bromo-5,6-dichloro-1,4-benzoquinone (133)



The product was obtained by the general halogenation/selenylation procedure described above using 1,3-dibromo-5,5-dimethylhydantoin (DBH) (120 mol%, 34.3 mg) and a reaction time of 18 h. Purification by FCC (toluene) afforded product **133** (11.5 mg, 45% yield) as yellow crystals; **m.p.** (°C) = 153.9-155.1 (Petrol/CH₂Cl₂); **IR (solid, cm⁻¹)** ν : 2970 (w), 1671 (s), 1187 (m), 1052 (s); **HRMS (EI⁺)**: 253.8542 [M]⁺. Cald. for [C₆HBrCl₂O₂]: 253.8537; **¹H NMR (400 MHz, CDCl₃)** δ : 7.46 (s, C3-H); **¹³C NMR (100 MHz, CDCl₃)** δ : 175.3 (C4), 171.0 (C1), 141.4 (C5), 140.1 (C6), 137.4 (C3), 136.6 (C2).

7.4.3. Intermolecular Competition Experiment



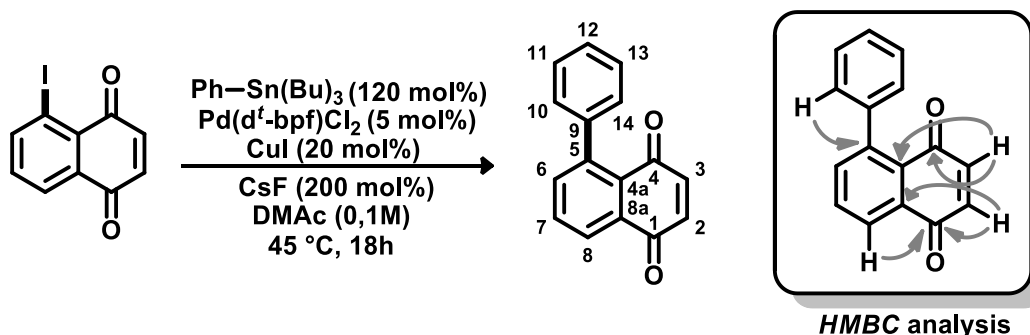
In a glovebox, an oven dried re-sealable tube was charged with 1,4-benzoquinone (**8**) (0.10 mmol), d₄-benzoquinone (**d₄-8**) (0.10 mmol), [RhCp^{*}Cl₂]₂ (3.75 mol%, 2.6 mg),

silver bis(trifluoromethanesulfonyl)imide (20 mol%, 7.8 mg), DIH (100 mol%) and anhydrous copper sulfate (220 mol%, 34.9 mg). The tube was removed from the glovebox and an inert atmosphere was maintained. Anhydrous CH₂Cl₂ (1.0 mL) was added via syringe and tube was sealed. The mixture was heated at 100 °C for 18h. After cooling, the mixture was filtered through a pad of celite and purified by FCC (toluene).

7.4.4. Procedures for Cross-Coupling Reactions

Stille coupling

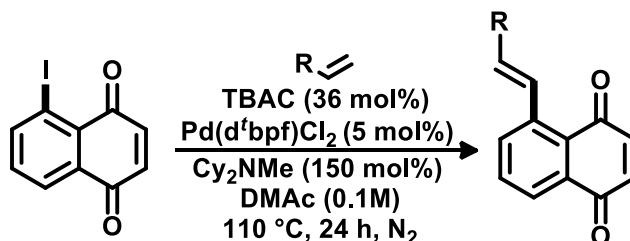
5-Phenyl-1,4-naphthoquinone (**134**)



An oven dried re-sealable tube was charged with **134** (0.10 mmol, 28.4 mg), Pd(d^tbpf)Cl₂ (5 mol%, 3.7 mg), CuI (20 mol%, 4.0 mg) and CsF (200 mol%, 30.0 mg). After achievement of inert atmosphere by N₂ purge, PhSnBu₃ (0.12 mmol, 40.0 μL) and *N,N*-dimethylacetamide (1.0 mL) were added via syringe. The tube was sealed and the mixture was heated at 45 °C for 18h. After cooling, the solvent was removed under reduced pressure. The residue was dissolved in CH₂Cl₂ (5 mL) and filtered through a pad of celite. The filtrate was concentrated under reduced pressure and the residue was purified by FCC (hexane/EtOAc 5:1) to afford **134** (17.6 mg, 75% yield) as an orange powder; **m.p.** (°C) = 165.5-166.9 (Petrol/CH₂Cl₂); **IR** (solid, cm⁻¹) **v**: 3050 (w), 1658 (s), 1279 (s), 698 (s); **HRMS** (EI⁺): 234.0672 [M]⁺. Cald. for [C₁₆H₁₀O₂]: 234.0681; **¹H NMR** (400 MHz, CDCl₃) **δ**: 8.17 (dd, *J* = 7.8, 1.3 Hz, C8-H), 7.73 (t, *J* = 7.8 Hz, C7-H), 7.56 (dd, *J* = 7.8, 1.3 Hz, C6-H), 7.48 – 7.36 (m, C11-H, C12-H, C13-H), 7.29 – 7.21 (m, C10-H, C14-H), 6.94 (d, *J* = 10.3 Hz, C2-H), 6.82 (d, *J* = 10.3 Hz, C3-H); **¹³C NMR** (100 MHz, CDCl₃) **δ**: 185.2 (C4), 185.1 (C1), 143.7 (C5), 141.0 (C9), 140.3

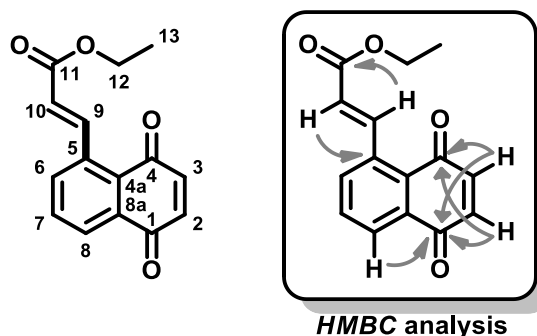
(C3), 137.5 (C6), 137.0 (C2), 133.2 (C8a), 132.8 (C7), 129.1 (C4a), 128.1 (C10, C11, C13, C14), 127.4 (C12), 126.4 (C8).

Heck reactions



A oven dried re-sealable tube was charged with **60** (0.10 mmol, 28.4 mg), Pd(d^tbpf)Cl₂ (5 mol%, 3.7 mg) and tetrabutylammonium chloride (TBAC) (36 mol%, 10.0 mg). The tube was purged with N₂ and the corresponding olefin (0.30 mmol), Cy₂NMe (150 mol%, 32.0 μL) and *N,N*-dimethylacetamide (1.0 mL) were added via syringe. The tube was sealed and the mixture was heated at 110 °C for 24h. After cooling, the solvent was removed under reduced pressure. The residue was dissolved in CH₂Cl₂ (5 mL) and filtered through a pad of celite. The filtrate was concentrated and the residue was purified by FCC, under the conditions noted.

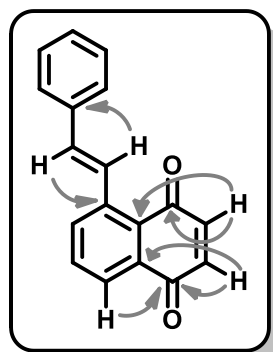
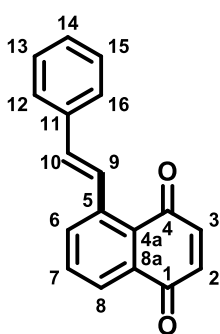
Ethyl (*E*)-3-(5,8-dioxo-5,8-dihydronaphthalen-1-yl)acrylate (**135**)



The product was obtained using ethyl acrylate (0.30 mmol, 32.6 μL) and a reaction time of 24h. Purification by FCC (hexane/EtOAc 5:1) afforded **135** (17.8 mg, 66% yield) as a yellow powder; **m.p.** (°C) = 133.8-134.9 (Petrol/CH₂Cl₂); **IR** (solid, cm⁻¹) *v*: 2909 (w), 1717 (s), 1654 (s), 1322 (m), 1193 (m), 773 (m); **HRMS** (ESI⁺): 279.0629 [M+Na]⁺. Cald. for [C₁₅H₁₂NaO₄]⁺: 279.0628; **¹H NMR** (400 MHz, CDCl₃) *δ*: 8.59 (d, *J* = 15.9 Hz, C9-H), 8.17 (dd, *J* = 7.2, 1.9 Hz, C8-H), 7.87 – 7.68 (m, C6-H, C7-H),

6.96 (s, C2-H, C3-H), 6.27 (d, $J = 15.9$ Hz, C10-H), 4.30 (q, $J = 7.1$ Hz, C12-H₂), 1.36 (t, $J = 7.1$ Hz, C13-H₃). ¹³C NMR (100 MHz, CDCl₃) δ : 186.2 (C4), 184.6 (C1), 166.2 (C11), 144.0 (C9), 140.0 (C3), 137.2 (C2), 137.2 (C8a), 134.1 (C6), 133.6 (C7), 133.1 (C5), 129.0 (C4a), 128.1 (C8), 122.8 (C10), 60.7 (C12), 14.3 (C13).

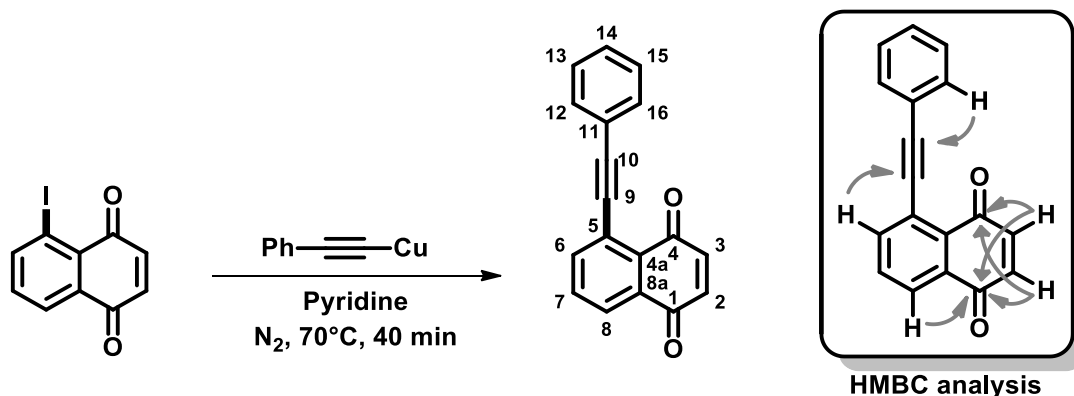
(E)-5-styrylnaphthalene-1,4-dione (136)



HMBC analysis

The product was obtained using styrene (0.30 mmol, 35 μ L) and a reaction time of 24h. Purification by FCC (hexane/EtOAc 8:1) afforded **136** (13.3 mg, 51% yield) as a red powder; **m.p.**($^{\circ}$ C): 140.8–141.9; **IR** (solid, cm^{-1}) ν : 2956 (w), 1717 (s), 1632 (s), 1278 (m), 1100 (m), 790 (m); **HRMS**(EI⁺): 260.0822. Cald. for [C₁₈H₁₂O₂]⁺: 260.0837; **¹H NMR** (500 MHz, CDCl₃) δ : 8.30 (d, $J = 16.1$ Hz, C9-H), 8.10 (dt, $J = 7.6, 1.2$ Hz, C8-H), 7.98 (dd, $J = 7.9, 0.8$ Hz, C6-H), 7.72 (t, $J = 7.8$ Hz, C7-H), 7.62 – 7.60 (m, 2H), 7.43 – 7.37 (m, 2H), 7.35 – 7.29 (m, 1H), 7.06 (d, $J = 16.2$ Hz, C10-H), 6.95 (d, $J = 1.0$ Hz, C2-H, C3-H). ¹³C NMR (125 MHz, CDCl₃) δ : 187.0 (C4), 185.2 (C1), 140.5 (C2), 140.2 (C5), 137.1 (C8a), 136.9 (C3), 133.5 (C10), 133.5 (C6), 133.3 (C7), 128.8 (C13, C15), 128.3 (C14), 127.9 (C4a), 127.7 (C9), 127.1 (C12, C16), 126.5 (C8).

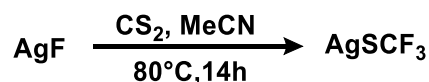
5-(Phenylethynyl)-1,4-naphthoquinone (**137**)



A oven dried re-sealable tube was charged with **60** (0.10 mmol, 28.4 mg) and (phenylethynyl)copper (0.16 mmol, 26.4 mg). The tube was purged with N_2 and pyridine (1.0 mL) was added via syringe. The tube was sealed and the mixture was heated at 70°C for 40 minutes. The mixture was cooled to room temperature and extracted with ether (10 mL). The organic extract were combined, dried with anhydrous Na_2SO_4 and concentrated under reduced pressure. Purification of the residue by FCC (toluene) afforded **137** (16.5 mg, 64% yield) as a green powder; **m.p.** ($^\circ\text{C}$) = 101.8-102.9 (Petrol/ CH_2Cl_2); **IR (solid, cm^{-1})** ν : 3059 (w), 1667 (s), 1289 (m), 756 (m); **HRMS (EI⁺)**: 258.0685 $[\text{M}]^+$. Cald. for $[\text{C}_{18}\text{H}_{10}\text{IO}_2]$: 258.0681; **^1H NMR (400 MHz, CDCl_3)** δ : 8.10 (d, $J = 7.8$ Hz, C8-H), 7.93 (d, $J = 7.8$ Hz, C6-H), 7.76 – 7.65 (m, C12-H, C16-H, C7-H), 7.45 – 7.34 (m, (C13-H, C14-H, C15-H), 7.00 (d, $J = 10.3$ Hz, C3-H), 6.96 (d, $J = 10.3$ Hz, C2-H); **^{13}C NMR (101 MHz, CDCl_3)** δ : 184.6 (C1), 183.8 (C4), 139.9 (C3), 139.7 (C6), 137.2 (C2), 132.9 (C8a), 132.7 (C7), 132.1 (C12, C16), 131.4 (C4a), 129.0 (C14), 128.4 (C13, C15), 126.6 (C8), 123.0 (C5), 123.0 (C11), 95.8 (C10), 88.3 (C9).

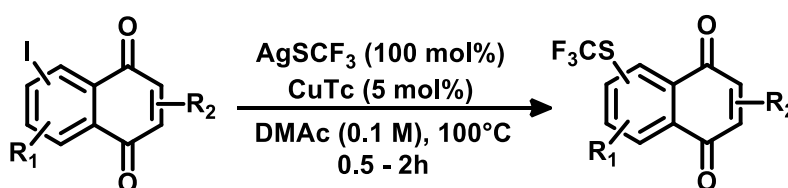
7.4.5. Procedures for Organoyl-Thiolation and Oxidation reactions

Synthesis of AgSCF_3 ²¹⁰



To an oven dried 30 mL Schlenk flask equipped with a stir bar 2.50 g (19.7 mmol) of dry AgF was added. The flask was evacuated and refilled with Argon (three times) until inert atmosphere was achieved. 15 mL of dry MeCN was injected into the flask followed by 2.5 mL of CS₂. The flask was then placed into a pre-heated at 80 °C oil bath with efficient stirring. After 14 h, the reaction mixture was black, and the mixture was allowed to cool to room temperature. MeCN and the excess of CS₂ were removed under reduced pressure to produce a black residue, which was then dissolved in EtOAc and filtered through a pad of celite. The solvent was once again removed under reduced pressure and the resulting yellow solid was dissolved in a minimum amount of MeCN to produce a clear yellow solution. 30 mL of Et₂O was carefully layered on top of the yellow solution. The flask was placed in a freezer set to -10°C for 24 h to produce off-white crystals. The crystals were collected by filtration, dried under vacuum, affording AgSCF₃ (1.25 g, 5.98 mmol, 90%). **m.p.** (°C) = 224.8-225.9 (degrades) (Et₂O/CH₃CN).

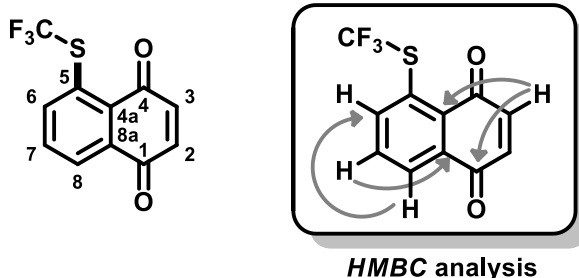
General procedure for the trifluoromethylthiolation reactions:



An oven dried re-sealable reaction tube was charged with the corresponding iodinated quinone (0.10 mmol), AgSCF₃ (0.10 mmol, 20.8 mg) and CuTc (5 mol%, 0.8 mg). Anhydrous DMAc (1.0 mL) was added and the tube was sealed. The mixture was heated at 100 °C for 0.5 – 2 h. After cooling and solvent removal by reduced pressure, the residue was purified by FCC, under the conditions noted.

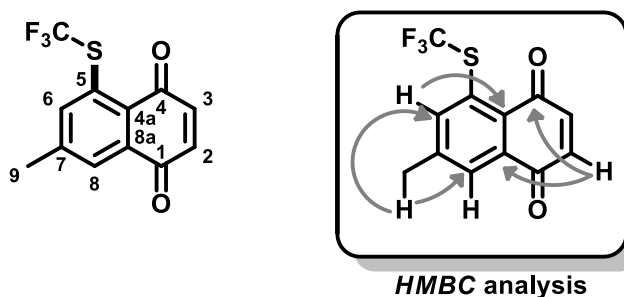
210. (a) Teverovskiy, G.; Surry, D.S.; Buchwald, S.L.; Pd-catalyzed synthesis of Ar-SCF₃ compounds under mild conditions *Angew. Chem. Int. Ed.*, **2011**, *50*, 7312. (b) Clark, J.H.; Jones, C.H.; Kybett, A.P.; McClinton, M.A.; Miller, J.M.; Bishop, D.; Blade, R.J.; The introduction of SCF₃ into aromatic substrates using CuSCF₃ and alumina-supported CuSCF₃. *J. Fluorine Chem.*, **1990**, *48*, 249.

5-((Trifluoromethyl)thio)-1,4-naphthoquinone (138)



The product was obtained by the general trifluoromethylthiolation procedure, described above with a reaction time of 0.5 h. Purification by FCC (toluene) afforded product **138** (25.8 mg, 100% yield) as yellow crystals; **m.p.** (°C) = 116.3-117.1 (Petrol/CH₂Cl₂); **IR (solid, cm⁻¹)** ν : 2923 (m), 1657 (s), 1107 (s), 776 (m); **HRMS (ESI⁺)**: 259.0028 [M+H]⁺. Cald. for [C₁₁H₆F₃O₂S]⁺: 259.0035; **¹H NMR (400 MHz, CDCl₃)** δ : 8.07 (d, *J* = 7.6 Hz, C8-H), 7.97 (d, *J* = 8.2 Hz, C6-H), 7.76 (t, *J* = 8.0 Hz, C7-H), 7.03 (d, *J* = 10.3 Hz, C3-H), 6.99 (d, *J* = 10.3 Hz, C2-H). **¹³C NMR (100 MHz, CDCl₃)** δ : 185.6 (C4), 184.0 (C1), 139.1 (C3), 138.0 (C2), 134.0 (C7), 133.8 (C8a), 132.4 (q, *J* = 3.1 Hz, C6), 131.2 (C5), 128.5 (C4a), 128.1 (C-F₃), 125.8 (C8).

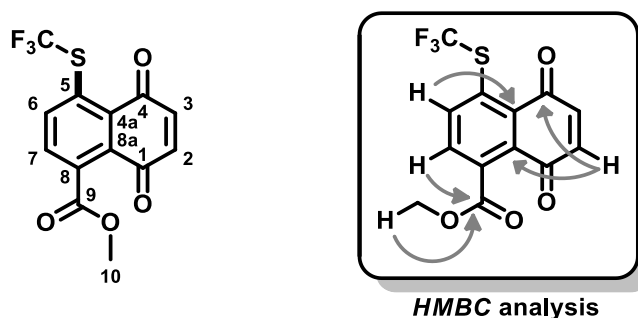
7-methyl-5-((trifluoromethyl)thio)-1,4-naphthoquinone (139)



The product was obtained by the general trifluoromethylthiolation procedure described above with a reaction time of 1.0 h. Purification by FCC (toluene) afforded product **139** (23.7 mg, 95% yield) as yellow crystals; **m.p.** (°C) = 122.1-123.5 (Petrol/CH₂Cl₂); **IR (solid, cm⁻¹)** ν : 1645 (s), 1334 (m), 1107 (s), 842 (m); **HRMS (ESI⁺)**: 273.0279 [M+H]⁺. Cald. for [C₁₂H₈F₃O₂S]⁺: 273.0192; **¹H NMR (400 MHz, CDCl₃)** δ : 7.89 (s, C8-H), 7.76 (s, C6-H), 7.01 (d, *J* = 10.3 Hz, C3-H), 6.97 (d, *J* = 10.3 Hz, C2-H), 2.56 (s, C9-H₃). **¹³C NMR (100 MHz, CDCl₃)** δ : 185.3 (C4), 184.4 (C1), 145.6 (C7), 139.2

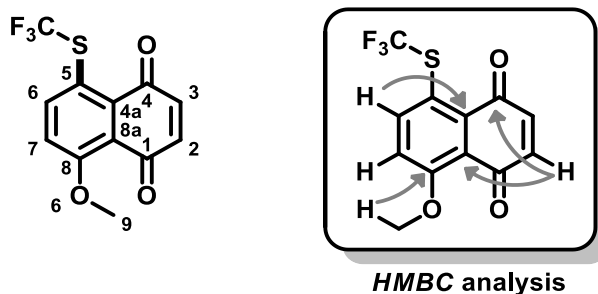
(C3), 137.8 (C2), 134.0 (q, $J = 2.3$ Hz, C5), 133.6 (C8a), 132.7 (q, $J = 3.4$ Hz, C6), 128.1 (C-F₃), 126.6 (C8), 126.3 (C4a), 22.4 (C9).

Methyl 1,4-dioxo-5-((trifluoromethyl)thio)-1,4-dihydronaphthalene-8-carboxylate
(140)



The product was obtained by the general trifluoromethylthiolation procedure described above with a reaction time of 0.5 h. Purification by FCC (toluene) afforded product **140** (30.0 mg, 95% yield) as a green-yellow solid; **m.p.** (°C) = 85.5-86.3 (Petrol/CH₂Cl₂); **IR (solid, cm⁻¹)** ν : 2923 (w), 1648 (s), 1113 (s), 807 (s); **HRMS (ESI⁺)**: 338.9904 [M+Na]⁺. Cald. for [C₁₃H₇F₃O₄SNa]⁺: 338.9909; **¹H NMR (400 MHz, CDCl₃)** δ : 7.98 (d, $J = 8.3$ Hz, C6-H), 7.66 (d, $J = 8.3$ Hz, C7-H), 7.04 (d, $J = 10.3$ Hz, C3-H), 6.99 (d, $J = 10.3$ Hz, C2-H), 3.98 (s, C10-H₃). **¹³C NMR (100 MHz, CDCl₃)** δ : 185.0 (C1), 183.1 (C4), 168.8 (C9), 138.6 (C3), 138.2 (C2), 136.2 (C4a), 133.0 (C8a), 132.4 (C7), 131.9 (q, $J = 3.2$ Hz, C6), 131.1 (C8), 128.6 (C5), 127.8 (C-F₃), 53.4 (C10).

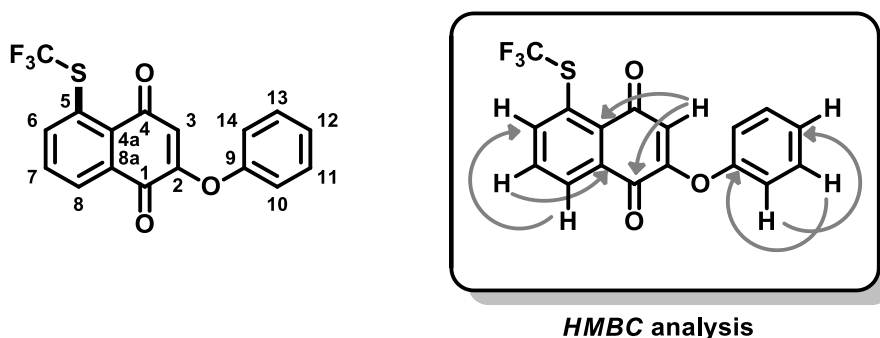
8-Methoxy-5-((trifluoromethyl)thio)-1,4-naphthoquinone (141)



The product was obtained by the general trifluoromethylthiolation procedure described above with a reaction time of 0.5 h. Purification by FCC (toluene) afforded product **141** (26.5 mg, 92% yield) as an orange solid; **m.p.** (°C) = 142.3-143.9 (Petrol/CH₂Cl₂); **IR**

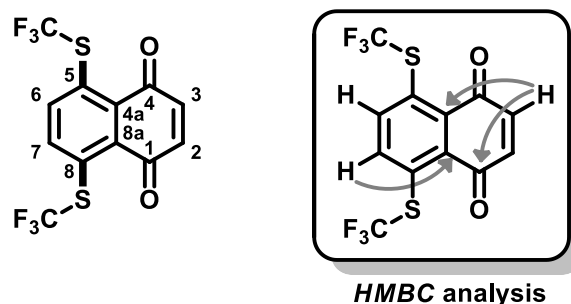
(solid, cm^{-1}) ν : 2926 (w), 1648 (s), 1113 (s), 807 (m); **HRMS (ESI⁺)**: 289.0134 [M+H]⁺. Calcd. for [C₁₂H₈F₃O₃S]⁺: 289.0141; **¹H NMR (400 MHz, CDCl₃)** δ : 7.84 (d, J = 9.3 Hz, C6-H), 7.29 (d, J = 9.3 Hz, C7-H), 6.84 (d, J = 10.2 Hz, C2-H), 6.79 (d, J = 10.2 Hz, C3-H), 3.95 (s, C9-H₃). **¹³C NMR (100 MHz, CDCl₃)** δ : 185.7 (C4), 183.4 (C1), 159.0 (C8), 139.9 (C3), 136.1 (C2), 134.3 (q, J = 3.3 Hz, C6), 131.3 (C5), 128.2 (C-F₃), 124.4 (C8a), 121.0 (C4a), 118.8 (C7), 56.8 (C9).

2-Phenoxy-5-((trifluoromethyl)thio)-1,4-naphthoquinone (143)



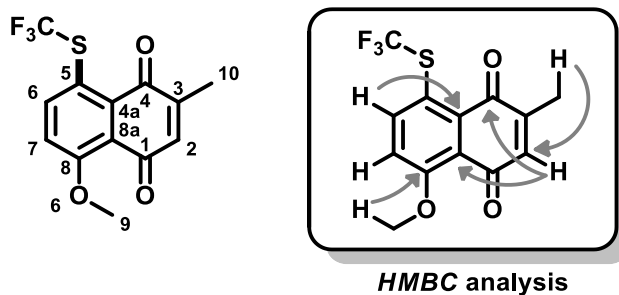
The product was obtained by the general trifluoromethylthiolation procedure described above with a reaction time of 0.5 h. Purification by FCC (toluene) afforded product **143** (32.9 mg, 94% yield) as an yellow solid; **m.p.** (°C) = 100.9-101.3 (Petrol/CH₂Cl₂); **IR** (solid, cm^{-1}) ν : 2923 (w), 1645 (s), 1113 (s), 854 (m); **HRMS (ESI⁺)**: 373.0104 [M+Na]⁺. Calcd. for [C₁₇H₉F₃O₃SNa]⁺: 373.0117; **¹H NMR (400 MHz, CDCl₃)** δ : 8.17 (d, J = 8.2 Hz, C8-H), 7.96 (d, J = 8.2 Hz, C6-H), 7.74 (t, J = 8.2 Hz, C7-H), 7.47 (t, J = 7.9 Hz, C11-H, C13-H), 7.33 (t, J = 7.5 Hz, C12-H), 7.13 (d, J = 7.7 Hz, C10-H, C14-H), 5.98 (s, C3-H). **¹³C NMR (100 MHz, CDCl₃)** δ : 185.5 (C4), 178.8 (C1), 159.7 (C2), 152.5 (C5), 133.3 (C7), 132.8 (C8a), 132.4 (q, J = 3.5 Hz, C6), 130.5 (C11, C13), 127.8 (C4a) 126.8 (C12), 125.8 (C8), 120.9 (C10, C14), 113.4 (C-F₃).

5,8-Bis((trifluoromethyl)thio)-1,4-naphthoquinone (145)



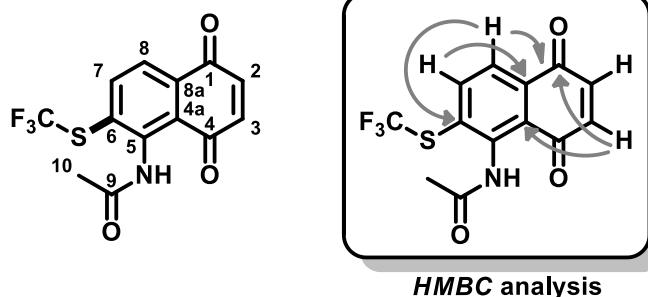
The product was obtained by the general trifluoromethylthiolation procedure described above with a reaction time of 1.0 h. Purification by FCC (toluene) afforded product **145** (28.3 mg, 79% yield) as orange crystals; **m.p.** (°C) = 132.5-133.9 (Petrol/CH₂Cl₂); **IR** (solid, cm⁻¹) ν : 1645 (s), 1337 (w), 1069 (s), 750 (m); **HRMS** (ESI⁺): 358.9626 [M+H]⁺. Calcd. for [C₁₂H₅F₆O₂S₂]⁺: 358.9630; **¹H NMR** (400 MHz, CDCl₃) δ : 8.00 (s, C6-H, C7-H), 7.09 (s, C2-H, C3-H). **¹³C NMR** (100 MHz, CDCl₃) δ : 184.6 (C1, C4), 137.8 (C2, C3), 133.8 (q, *J* = 2.2 Hz, C5, C8), 131.7 (q, *J* = 3.0 Hz, C6, C7), 129.5 (C4a, C8a), 127.6 (C-F₃).

8-methoxy-2-methyl-5-((trifluoromethyl)thio)-1,4-naphthoquinone (146)



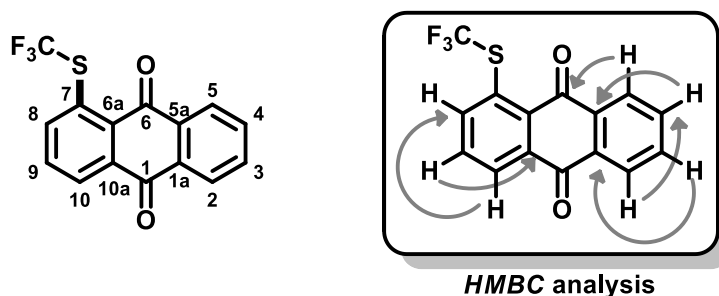
The product was obtained by the general trifluoromethylthiolation procedure described above with a reaction time of 0.5 h. Purification by FCC (toluene) afforded product **146** (28.7 mg, 95% yield) as an orange powder; **m.p.** (°C) = 174.4-175.9 (Petrol/CH₂Cl₂); **IR** (solid, cm⁻¹) ν : 1645 (s), 1236 (m), 1092 (s), 810 (m); **HRMS** (ESI⁺): 325.0124 [M+Na]⁺. Calcd. for [C₁₃H₉F₃O₃SNa]⁺: 325.0117; **¹H NMR** (400 MHz, CDCl₃) δ : 7.90 (d, *J* = 9.3 Hz, C6-H), 7.35 (d, *J* = 9.3 Hz, C7-H), 6.75 (s, C2-H), 4.03 (s, C9-H₃), 2.16 (s, C10-H₃). **¹³C NMR** (100 MHz, CDCl₃) δ : 186.5 (C4), 183.4 (C1), 158.7 (C8), 145.5 (C3), 137.1 (C2), 133.9 (q, *J* = 3.1 Hz, C6), 131.4 (C4a), 128.2 (C-F₃), 124.4 (q, *J* = 2.2 Hz, C5), 121.2 (C8a), 118.6 (C7), 56.7 (C9), 15.7 (C10).

***N*-(1,4-Dioxo-6-((trifluoromethyl)thio)-1,4-dihydronaphthalen-5-yl)acetamide (147)**



The product was obtained by the general trifluoromethylthiolation procedure described above with a reaction time of 2.0 h. Purification by FCC (toluene) afforded product **147** (13.9 mg, 44% yield) as yellow crystals; **m.p.** (°C) = 116.3-117.1 (Petrol/CH₂Cl₂); **IR (solid, cm⁻¹)** ν : 3309 (w), 1668 (s), 1651 (s), 1098 (s), 842 (s); **HRMS (ESI⁺)**: 338.0060 [M+Na]⁺. Cald. for [C₁₃H₈F₃O₃NSNa]⁺: 338.0069; **¹H NMR (400 MHz, CDCl₃)** δ : 10.74 (s, N-H), 8.14 (d, *J* = 8.2 Hz, C7-H), 8.00 (d, *J* = 8.2 Hz, C8-H), 7.01 (d, *J* = 10.3 Hz, C2-H), 6.97 (d, *J* = 10.3 Hz, C3-H), 2.34 (s, C10-H₃). **¹³C NMR (100 MHz, CDCl₃)** δ : 187.9 (C4), 183.5 (C1), 170.2 (C9), 140.5 (q, *J* = 1.1 Hz, C7), 140.4 (C6), 139.9 (C3), 138.0 (C2), 133.4 (C8a), 130.1 (C5), 127.7 (C-F₃), 123.8 (C8), 121.7 (C4a), 24.2 (C10).

1-((trifluoromethyl)thio)anthracene-9,10-dione (148)



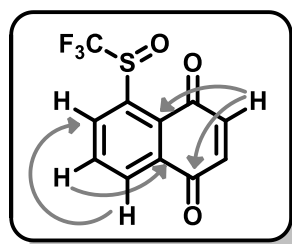
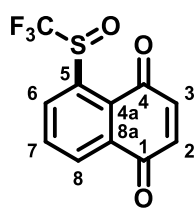
The product was obtained by the general trifluoromethylthiolation procedure described above with a reaction time of 0.5 h. Purification by FCC (toluene) afforded product **148** (28.3 mg, 92% yield) as yellow crystals; **m.p.** (°C) = 174.7-175.1 (Petrol/CH₂Cl₂); **IR (solid, cm⁻¹)** ν : 1671 (w), 1274 (m), 1098 (s), 698 (s); **HRMS (ESI⁺)**: 331.0011 [M+Na]⁺. Cald. for [C₁₅H₇F₃O₂SNa]⁺: 331.0011; **¹H NMR (400 MHz, CDCl₃)** δ : 8.27 (d, *J* = 7.5 Hz, C2-H, C5-H, C10-H), 7.99 (d, *J* = 8.2 Hz, C8-H), 7.84 – 7.75 (m, C3-H, C4-H, C9-H). **¹³C NMR (100 MHz, CDCl₃)** δ : 184.1 (C6), 182.3 (C1), 135.0 (q, *J* =

2.6 Hz, C7), 134.8 (C3), 134.7 (C4), 134.1 (C9), 133.4 (C10a), 132.7 (C1a), 132.4 (q, $J = 3.1$ Hz, C8), 131.3 (C5a), 130.0 (C6a), 128.2 (C-F₃), 127.7 (C5), 127.4 (C2), 126.4 (C10).

General procedure for oxidation with MCPBA²¹¹

To a solution of the corresponding quinone (0.10 mmol) in CH₂Cl₂ (3.0 mL) was added MCPBA (0.15 mmol, 25.8 mg) at 0°C, under inert atmosphere. The reaction was allowed to warm to room temperature and kept under stirring for 18 h. The mixture was then washed with a saturated solution of NaHCO₃ (10 mL) and extracted with CH₂Cl₂ (10 mL). The organic phase was dried with Na₂SO₄ and submitted to purification by FCC, under the conditions noted.

5-((Trifluoromethyl)sulfinyl)-1,4-naphthoquinone (149)

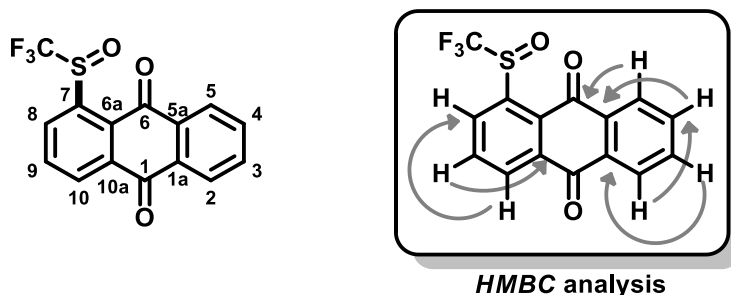


HMBC analysis

Purification by FCC (toluene) afforded product **149** (20.3 mg, 74% yield) as yellow crystals; **m.p.** (°C) = 101.3-102.5 (Petrol/CH₂Cl₂); **IR** (solid, cm⁻¹) ν : 2926 (w), 1657 (s), 1300 (m), 1072 (s); **HRMS** (ESI⁺): 296.9802 [M+Na]⁺. Cald. for [C₁₁H₅F₃O₃SNa]⁺: 296.9804; **¹H NMR** (400 MHz, CDCl₃) δ : 8.60 (d, $J = 7.9$ Hz, C6-H), 8.35 (d, $J = 7.7$ Hz, C8-H), 8.08 (t, $J = 7.8$ Hz, C7-H), 7.09 (d, $J = 10.3$ Hz, C2-H), 7.05 (d, $J = 10.3$ Hz, C3-H). **¹³C NMR** (100 MHz, CDCl₃) δ : 185.5 (C4), 183.4 (C1), 140.5 (q, $J = 2.8$ Hz, C5), 139.3 (C2), 138.2 (C3), 135.0 (C7), 133.2 (C8a), 131.0 (C6), 130.8 (C4a), 130.6 (C8), 123.6 (C-F₃).

²¹¹. Yang, J.-J.; Kirchmeier, R.L.; Shreeve, J.M.; New electrophilic trifluoromethylating agents. *J. Org. Chem.*, **1998**, *63*, 2656.

1-((trifluoromethyl)sulfinyl)anthracene-9,10-dione (**150**)

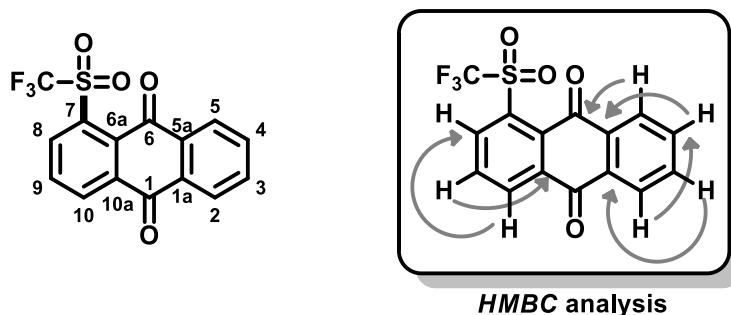


Purification by FCC (toluene) afforded product **150** (22.7 mg, 70% yield) as yellow crystals; **m.p.** (°C) = 217.9-218.1 (Petrol/CH₂Cl₂); **IR** (solid, cm⁻¹) ν : 2923 (w), 1657 (s), 1303 (m), 1072 (s); **HRMS** (ESI⁺): 346.9972 [M+Na]⁺. Cald. for [C₁₅H₇F₃O₃SNa]⁺: 346.9960; **¹H NMR** (400 MHz, CDCl₃) δ : 8.68 (d, J = 7.8 Hz, C8-H), 8.59 (d, J = 7.8 Hz, C10-H), 8.34 (dd, J = 7.2, 1.8 Hz, C2-H), 8.30 (dd, J = 7.2, 1.8 Hz, C5-H), 8.12 (t, J = 7.8 Hz, C9-H), 7.92 – 7.84 (m, C3-H, C4-H). **¹³C NMR** (100 MHz, CDCl₃) δ : 183.9 (C6), 181.7 (C1), 141.4 (q, J = 2.8 Hz, C7), 135.5 (C9), 135.1 (C4), 135.0 (C3), 133.0 (C10a), 132.5 (C6a), 132.4 (C5a), 131.4 (C10), 131.2 (C8), 127.9 (C2), 127.8 (C5), 127.1 (C1a), 123.7 (C-F₃).

General procedure for oxidation with RuCl₃.H₂O/NaIO₄¹⁹¹

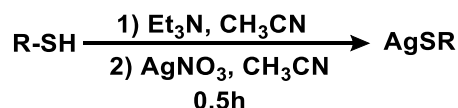
To a solution of the corresponding quinone (0.10 mmol) in H₂O/CH₃CN/CH₂Cl₂ (2:1:1, 4.0 mL) was added RuCl₃.H₂O (5 mol%, 1.1 mg). The mixture was kept under vigorous stirring, and NaIO₄ (63.9 mg, 0.30 mmol) was added. The mixture was allowed to stir for 1 h, washed with a saturated solution of NaHCO₃ (10 mL) and extracted with CH₂Cl₂ (10 mL). The organic phase was dried with Na₂SO₄ and submitted to purification by FCC under the conditions noted.

1-((trifluoromethyl)sulfonyl)anthracene-9,10-dione (**151**)



Purification by FCC (toluene) afforded product **151** (31.3 mg, 92% yield) as yellow crystals; **m.p.** (°C) = 214.9-216.0 (Petrol/CH₂Cl₂); **IR** (solid, cm⁻¹) ν : 2923 (w), 1685 (m), 1190 (s), 704 (s); **HRMS** (ESI⁺): 362.9913 [M+Na]⁺. Cald. for [C₁₅H₇F₃O₄SNa]⁺: 362.9909; **¹H NMR** (400 MHz, CDCl₃) δ : 8.77 (dd, *J* = 7.9, 1.0 Hz, C10-H), 8.73 (dd, *J* = 7.9, 1.0 Hz, C8-H), 8.37 – 8.31 (m, C2-H), 8.32 – 8.26 (m, C5-H), 8.06 (t, *J* = 7.9 Hz, C9-H), 7.93 – 7.81 (m, 2H). **¹³C NMR** (100 MHz, CDCl₃) δ : 181.2 (C6), 180.9 (C1), 138.5 (C8), 136.1 (C10a), 135.3 (C4), 135.1 (C3), 134.8 (C10), 134.7 (C6a), 134.1 (C9), 133.6 (C5a), 132.2 (C1a), 128.2 (C2), 127.5 (C5), 122.6 (C7), 119.1 (C-E₃).

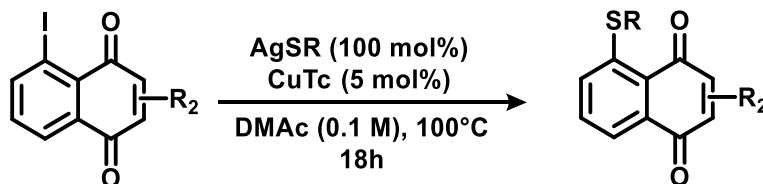
General procedure for the synthesis of AgSR salts:²¹²



A 50 mL round bottom flask was charged with the corresponding thiol (2.00 mmol), Et₃N (2.00 mmol, 279 μ L) and acetonitrile (5.0 mL). The mixture was stirred and a solution of AgNO₃ (339.7 mg, 2.00 mmol) in acetonitrile (10 mL) was added dropwise. The suspension was vigorously stirred for 30 min, and the resulting solid was filtered, washed with acetonitrile (30 mL) and dried under reduced pressure. Yields for all AgSR salts were quantitative.

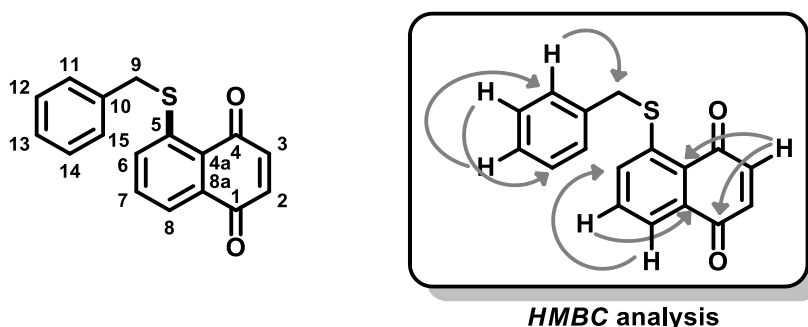
212. (a) Baena, M.J.; Espinet, P.; Lequerica, M.C.; Levelut, A.M.; Mesogenic behavior of silver thiolates with layered structure in the solid state: covalent soaps. *J. Am. Chem. Soc.*, **1992**, *114*, 4182. (b) Dance, I.G.; Fisher, K.J.; Banda, R.M.H.; Scudder, M.L.; Layered structure of crystalline compounds silver thiolates (AgSR). *Inorg. Chem.*, **1991**, *30*, 183.

General procedure for the thiolation reactions:



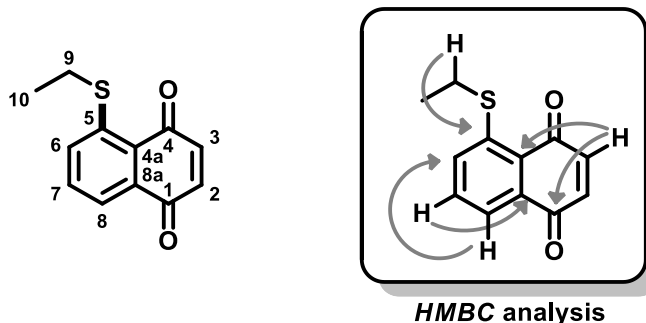
An oven dried re-sealable reaction tube was charged with the corresponding iodinated quinone (0.10 mmol), AgSR salt (0.10 mmol) and CuTc (5 mol%, 0.8 mg). Anhydrous DMAc (1.0 mL) was added and the tube was sealed. The mixture was heated at 100 °C for 18 h. After cooling and solvent removal by reduced pressure, the residue was purified by FCC, under the conditions noted.

5-(Benzylthio)-1,4-naphthoquinone (152)



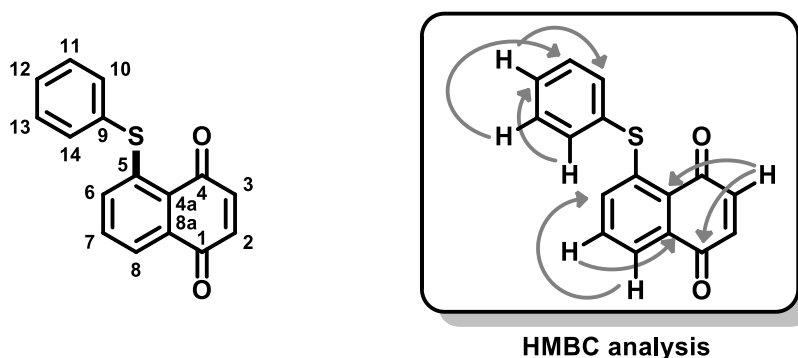
The product was obtained by the general thiolation procedure described above. (Benzylthio)silver (0.10 mmol, 23.1 mg) was used. Purification by FCC (toluene) afforded product **152** (26.0 mg, 93% yield) as red crystals; **m.p.** (°C) = 183.9-185.1 (Petrol/CH₂Cl₂); **IR** (solid, cm⁻¹) ν : 3053 (w), 1648 (m), 1136 (s), 773 (s); **HRMS** (ESI⁺): 281.6030 [M+H]⁺. Cald. for [C₁₇H₁₃O₂S]⁺: 281.0631; **¹H NMR** (400 MHz, CDCl₃) δ : 7.88 (d, *J* = 7.3 Hz, C8-H), 7.66 (d, *J* = 8.0 Hz, C6-H), 7.59 (t, *J* = 7.8 Hz, C7-H), 7.45 (d, *J* = 7.3 Hz, C11-H, C15-H), 7.34 (t, *J* = 7.3 Hz, C10-H, C14-H), 7.31 – 7.26 (m, C13-H), 6.96 (d, *J* = 10.2 Hz, C3-H), 6.90 (d, *J* = 10.2 Hz, C2-H), 4.23 (s, C9-H₂). **¹³C NMR** (100 MHz, CDCl₃) δ : 185.5 (C4), 185.1 (C1), 144.78 (C5), 139.9 (C3), 137.0 (C2), 135.6 (C10), 134.0 (C8a), 133.1 (C7), 130.2 (C6), 129.3 (C11, C15), 129.0 (C12, C14), 127.9 (C13), 127.5 (C4a), 123.2 (C8), 37.28 (C9).

5-(Ethylthio)-1,4-naphthoquinone (153)



The product was obtained by the general thiolation procedure described above. (Ethylthio)silver (0.10 mmol, 16.9 mg) was used. Purification by FCC (toluene) afforded product **153** (13.3 mg, 61% yield) as a red solid; **m.p.** (°C) = 140.5-142.0 (Petrol/CH₂Cl₂); **IR (solid, cm⁻¹)** ν : 2932 (m), 1648 (m), 1291 (s), 773 (s); **HRMS (ESI⁺)**: 219.0642 [M+H]⁺. Calcd. for [C₁₂H₁₁O₂S]⁺: 219.0474; **¹H NMR (400 MHz, CDCl₃)** δ : 7.87 (dd, J = 5.8, 2.6 Hz, C8-H), 7.66 – 7.58 (m, C6-H, C7-H), 6.96 (d, J = 10.2 Hz, C3-H), 6.90 (d, J = 10.2 Hz, C2-H), 3.01 (q, J = 7.4 Hz, C9-H₂), 1.44 (t, J = 7.4 Hz, C10-H₃). **¹³C NMR (100 MHz, CDCl₃)** δ : 185.5 (C4), 185.1 (C1), 145.1 (C5), 140.1 (C3), 136.9 (C2), 134.1 (C8a), 133.0 (C7), 129.9 (C6), 127.5 (C4a), 122.9 (C8), 26.0 (C9), 13.1 (C10).

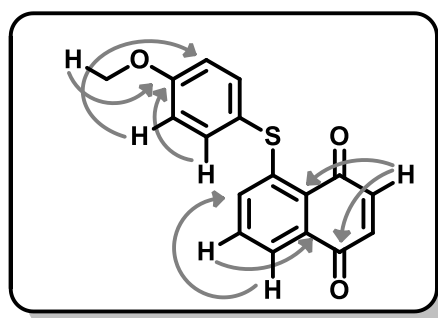
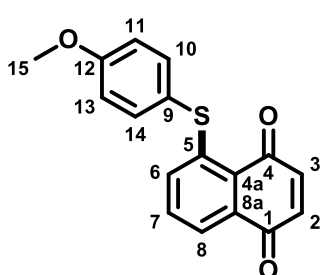
5-(Phenylthio)-1,4-naphthoquinone (154)



The product was obtained by the general thiolation procedure described above. (Phenylthio)silver (0.10 mmol, 21.7 mg) was used. Purification by FCC (toluene) afforded product **154** (25.8 mg, 97% yield) as a red solid; **m.p.** (°C) = 157.3-158.0 (Petrol/CH₂Cl₂); **IR (solid, cm⁻¹)** ν : 2926 (m), 1636 (m), 1133 (s), 744 (s); **HRMS**

(ESI⁺): 267.0470 [M+H]⁺. Cald. for [C₁₅H₁₁O₂S]⁺: 267.0474; ¹H NMR (400 MHz, CDCl₃) δ: 7.84 (d, *J* = 7.5 Hz, C8-H), 7.60 (m, C10-H, C14-H), 7.54 – 7.44 (m, C11-H, C12-H, C13-H), 7.39 (t, *J* = 7.9 Hz, C7-H), 7.11 – 6.97 (m, C3-H, C6-H), 6.94 (d, *J* = 10.3 Hz, C2-H). ¹³C NMR (100 MHz, CDCl₃) δ: 185.5 (C4), 185.0 (C1), 146.0 (C5), 139.9 (C3), 137.3 (C2), 136.3 (C10, C14), 133.7 (C8a), 132.9 (C7), 131.9 (C6), 131.5 (C9), 130.3 (C11, C13), 130.1 (C12), 126.8 (C4a), 123.7 (C8).

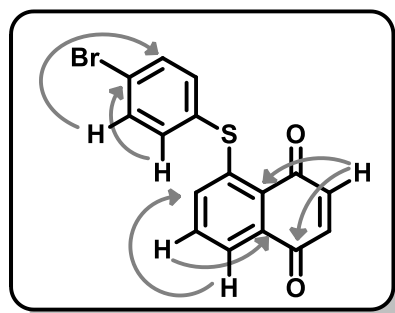
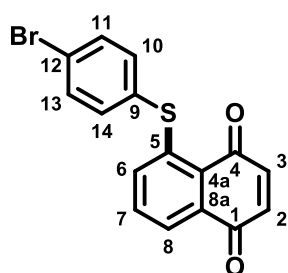
5-((*para*-Methoxyphenyl)thio)-1,4-naphthoquinone (155)



HMBC analysis

The product was obtained by the general thiolation procedure described above. ((4-Methoxyphenyl)thio)silver (0.10 mmol, 24.7 mg) was used. Purification by FCC (toluene) afforded product **155** (28.1 mg, 95% yield) as a red solid; **m.p.** (°C) = 165.0–166.0 (Petrol/CH₂Cl₂); **IR** (solid, cm⁻¹) *v*: 2920 (w), 1651 (m), 1245 (s), 779 (s); **HRMS** (ESI⁺): 319.0393 [M+Na]⁺. Cald. for [C₁₇H₁₂O₃SNa]⁺: 319.0399; ¹H NMR (400 MHz, CDCl₃) δ: 7.83 (d, *J* = 7.5 Hz, C8-H), 7.50 (d, *J* = 8.7 Hz, C10-H, C14-H), 7.39 (t, *J* = 7.9 Hz, C7-H), 7.08 – 6.97 (m, C3-H, C6-H, C11-H, C13-H), 6.93 (d, *J* = 10.3 Hz, C2-H), 3.87 (s, C15-H₃). ¹³C NMR (100 MHz, CDCl₃) δ: 185.5 (C4), 185.1 (C1), 161.3 (C12), 147.1 (C5), 139.9 (C3), 137.9 (C10, C14), 137.3 (C2), 133.7 (C8a), 132.8 (C7), 131.7 (C6), 126.6 (C4a), 123.5 (C8), 121.9 (C9), 115.9 (C11, C13), 55.7 (C15).

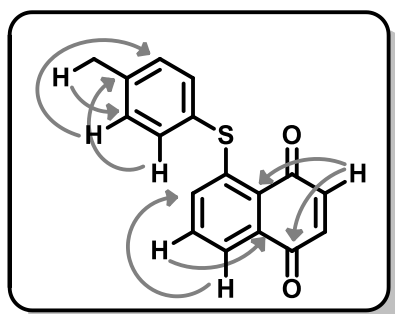
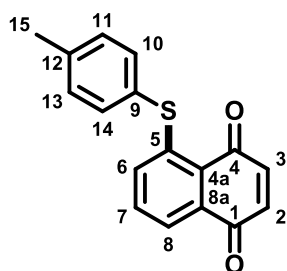
5-((*para*-Bromophenyl)thio)-1,4-naphthoquinone (156)



HMBC analysis

The product was obtained by the general thiolation procedure described above. ((4-Bromophenyl)thio)silver (0.10 mmol, 29.6 mg) was used. Purification by FCC (toluene) afforded product **156** (34.5 mg, 100% yield) as a red solid; **m.p.** (°C) = 178.9-179.6 (Petrol/CH₂Cl₂); **IR (solid, cm⁻¹)** ν : 1645 (m), 1334 (m), 1265 (m), 779 (m); **HRMS (ESI⁺)**: 344.9595 [M+H]⁺. Cald. for [C₁₆H₁₀BrO₂S]⁺: 344.9579; **¹H NMR (400 MHz, CDCl₃)** δ : 7.86 (d, *J* = 8.3 Hz, C8-H), 7.61 (d, *J* = 8.4 Hz, C10-H, C14-H), 7.47 – 7.41 (m, C7-H, C11-H, C13-H), 7.05 - 7.03 (m, C3-H, C6-H), 6.95 (d, *J* = 10.3 Hz, C2-H). **¹³C NMR (100 MHz, CDCl₃)** δ : 185.5 (C4), 184.9 (C1), 145.1 (C5), 139.8 (C3), 137.8 (C11, C13), 137.4 (C2), 133.7 (C8a), 133.5 (C10, C14), 133.1 (C7), 131.7 (C6), 130.8 (C12), 126.9 (C4a), 124.9 (C9), 123.9 (C8).

5-((*para*-Methylphenyl)thio)-1,4-naphthoquinone (157)

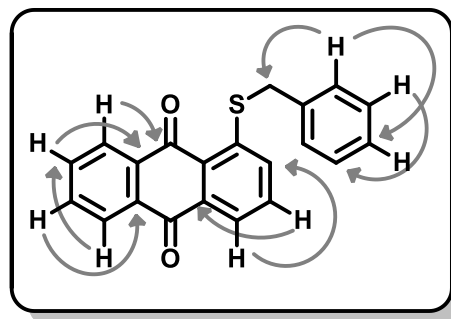
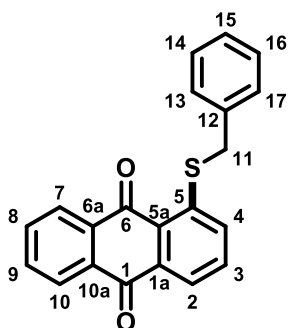


HMBC analysis

The product was obtained by the general thiolation procedure described above. ((4-Methoxyphenyl)thio)silver (0.10 mmol, 24.7 mg) was used. Purification by FCC (toluene) afforded product **157** (27.7 mg, 99% yield) as a red solid; **m.p.** (°C) = 162.4-163.1 (Petrol/CH₂Cl₂); **IR (solid, cm⁻¹)** ν : 2909 (w), 1645 (m), 1334 (s), 782 (m);

HRMS (ESI⁺): 281.0626 [M+H]⁺. Calcd. for [C₁₇H₁₃O₂S]⁺: 281.0631; **¹H NMR (400 MHz, CDCl₃)** δ: 7.83 (d, *J* = 8.2 Hz, C8-H), 7.47 (d, *J* = 8.0 Hz, C10-H, C14-H), 7.39 (t, *J* = 7.9 Hz, C7-H), 7.29 (d, *J* = 7.9 Hz, C11-H, C13-H), 7.10 – 6.96 (m, C3-H, C6-H), 6.93 (d, *J* = 10.3 Hz, C2-H), 2.43 (s, C15-H₃). **¹³C NMR (100 MHz, CDCl₃)** δ: 185.5 (C4), 185.1 (C1), 146.5 (C5), 140.4 (C12), 139.9 (C3), 137.3 (C2), 136.3 (C10, C14), 133.7 (C8a), 132.8 (C7), 131.8 (C6), 131.1 (C11, C13), 127.9 (C9), 126.7 (C4a), 123.6 (C8), 21.6 (C15).

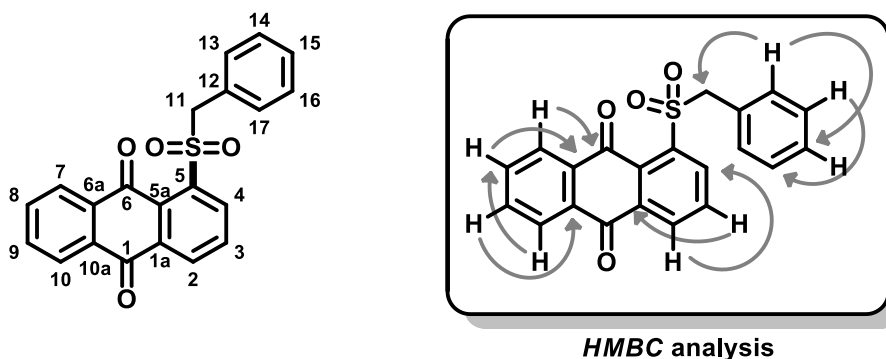
1-(benzylthio)anthracene-9,10-dione (158)



HMBC analysis

The product was obtained by the general thiolation procedure described above. (Benzylthio)silver (0.10 mmol, 23.1 mg) was used. Purification by FCC (toluene) afforded product **158** (30.0 mg, 91% yield) as a light orange solid; **m.p.** (°C) = 250.7-251.1 (Petrol/CH₂Cl₂); **IR (solid, cm⁻¹)** ν: 2923 (m), 1668 (m), 1271 (m), 704 (s); **HRMS (ESI⁺):** 331.0781 [M+H]⁺. Calcd. for [C₂₁H₁₅O₂S]⁺: 331.0787; **¹H NMR (400 MHz, CDCl₃)** δ: 8.31 (dd, *J* = 7.4, 1.4 Hz, C7-H), 8.27 (dd, *J* = 7.4, 1.4 Hz, C10-H), 8.13 (d, *J* = 7.8 Hz, C2-H), 7.82 – 7.71 (m, C8-H, C9-H, C15-H), 7.65 (t, *J* = 7.8 Hz, C3-H), 7.48 (d, *J* = 7.2 Hz, C13-H, C17-H), 7.35 (t, *J* = 7.3 Hz, C14-H, C16-H), 7.30 (d, *J* = 7.2 Hz, C4-H), 4.26 (s, C11-H₂). **¹³C NMR (100 MHz, CDCl₃)** δ: 183.8 (C6), 183.3 (C1), 145.5 (C5), 135.7 (C13), 135.3 (C1a), 134.7 (C10a), 134.6 (C9), 134.2 (C17), 133.9 (C8), 133.3 (C3), 132.8 (C6a), 130.3 (C15), 130.0 (C12), 129.4 (C14), 129.0 (C16), 128.9 (C5a), 127.8 (C7), 127.7 (C4), 127.1 (C10), 123.8 (C2), 37.7 (C11).

1-(benzylsulfonyl)anthracene-9,10-dione (159)



The product was obtained by the general procedure for oxidation with $\text{RuCl}_3 \cdot \text{H}_2\text{O} / \text{NaIO}_4$ described above. Purification by FCC (toluene) afforded product **159** (32.2 mg, 89% yield) as a yellow solid; **m.p.** ($^\circ\text{C}$) = 241.3-242.1 (Petrol/ CH_2Cl_2); **IR (solid, cm^{-1})** ν : 1680 (m), 1303 (s), 1110 (m), 692 (s); **HRMS (ESI⁺)**: 363.0680 [$\text{M} + \text{H}^+$]. Calcd. for $[\text{C}_{21}\text{H}_{15}\text{O}_4\text{S}]^+$: 363.0686; **^1H NMR (400 MHz, CDCl_3)** δ : 8.55 (d, $J = 8.9$ Hz, C10-H), 8.36 (d, $J = 8.7$ Hz, C7-H), 8.29 (d, $J = 7.0$ Hz, C2-H), 8.18 (d, $J = 6.8$ Hz, C4-H), 7.93 – 7.82 (m, C8-H, C9-H), 7.73 (t, $J = 7.8$ Hz, C3-H), 7.40 – 7.31 (m, C13-H, C17-H), 7.28 – 7.26 (m, C14-H, C15-H, C16-H), 5.27 (s, C11-H₂). **^{13}C NMR (100 MHz, CDCl_3)** δ : 183.6 (C6), 182.0 (C1), 140.1 (C5), 138.1 (C8), 135.7 (C1a), 134.7 (C9), 134.6 (C10a), 134.3 (C6a), 133.3 (C3), 132.6 (C10), 132.4 (C5a), 131.3 (C13, C17), 129.1 (C15), 128.9 (C14, C16), 128.5 (C12), 128.0 (C7), 127.3 (C2), 62.6 (C11).

General procedure for the synthesis of Me_4NSCF_3 :²¹³

The original procedure was used with minor modifications. 343 mg of elemental sulfur (10.7 mmol) was dissolved in 80 mL of THF at room temperature under inert atmosphere, followed by the addition of 1.9 mL of trifluoromethyltrimethylsilane (1.83 g, 12.9 mmol). The solution was subsequently cooled to -60 $^\circ\text{C}$ and 1.00 g of tetramethylammonium fluoride (10.7 mmol) was added under argon flow to the stirred mixture. The reaction was stirred for 13 h, while allowing it to warm to room temperature. An off-white to orange solid was subsequently filtered and washed with

213. Matheis, C.; Krause, T.; Bragioni, V.; Goossen, L.J.; Trifluoromethylthiolation and trifluoromethylselenolation of α -diazo esters catalyzed by copper. *Chem. Eur. J.*, **2016**, 22, 12270.

THF (30 mL) and diethyl ether (30 mL). The obtained solid was suspended in minimum amount of acetonitrile, filtered, washed with THF (30 mL) and diethyl ether (30 mL) and dried in vacuo. Me₄NSCF₃ was obtained (1.50 g, 80% yield) as a white powder. **m.p.** (°C) = 153.8-155.1, 194.2-194.9 (Et₂O/CH₃CN).

General procedure for the synthesis of sodium phenylmethanethiolate:²¹⁴

The original procedure was used with minor modifications. A solution of phenylmethanethiol (4.84 g, 39.0 mmol) in 5.0 mL of Et₂O was added to a stirring suspension of sodium (0.45 g, 19.5 mmol) in 20 mL of Et₂O. Stirring was continued until sodium could no longer be seen. The white solid product was filtered and washed with hexane to remove phenylmethanethiol and dried under reduced pressure to give sodium phenylmethanethiolate (2.56 g, 90% yield) as a white powder. **m.p.** (°C) = 70.8-72.1 (EtOH).

7.5. Trypanocidal and Cytotoxicity Assays

Animals

Albino Swiss mice were employed for the trypanocidal and cytotoxicity assays, in accordance to the guidelines of the Colégio Brasileiro de Experimentação Animal (COBEA), and these were performed under biosafety conditions. All animal experimentation procedures were approved by the Comissão de Ética em Experimentação Animal (CEUA/Fiocruz), license LW 16/13.

7.5.1. Trypanocidal Assays for Halogenated/Selenylated Quinoidal Compounds

The experiments were performed with the Y strain of *T. cruzi*.²¹⁵ Stock solutions of the compounds were prepared in dimethyl sulfoxide (DMSO), with the final concentration of the latter in the experiments never exceeding 0.1%. Preliminary experiments showed

214. Bio, M.; Nkepan, G.; You, Y.; Click and photo-unclick chemistry of aminoacrylate for visible light-triggered drug release. *Chem. Commun.*, **2012**, 48, 6517.

215. Silva, L.H.P.; Nussenzweig, V.; Sobre uma cepa de *Trypanosoma cruzi* altamente virulenta para o camundongo branco. *Folia Clin. Biol.*, **1953**, 20, 191.

De Castro, S.L.; Pinto, M.C.; Pinto, A.V.; Screening of natural and synthetic drugs against *Trypanosoma cruzi*. 1. Establishing a structure/activity relationship. *Microbios*, **1994**, 78, 83.

that at concentrations of up to 0.5%, DMSO has no deleterious effect on the parasites.²¹⁶ Bloodstream trypomastigotes were obtained from infected Albino Swiss mice at the peak of parasitemia by differential centrifugation. The parasites were re-suspended to a concentration of 10×10^6 cells/mL in DMES medium. This suspension (100 μ L) was added to the same volume of each of the compounds, which had been previously prepared at twice the desired final concentrations. The incubation was performed in 96-well microplates (Nunc Inc., Rochester, USA) at 37 °C for 24 h. Benznidazole (Lafepe, Brazil), the standard drug for treatment of chagasic patients, was used as control. Cell counts were performed in a Neubauer chamber, and the activity of the compounds corresponding to the concentration that led to 50% lysis of the parasites was expressed as the IC₅₀/24h.

7.5.2. Cytotoxicity Assays for Halogenated/Selenylated Quinoidal Compounds

The cytotoxicity assays were performed using primary cultures of peritoneal macrophages obtained from Albino Swiss mice. For the experiments, 2.5×10^4 cells in 200 μ L of RPMI-1640 medium (pH 7.2 plus 10% foetal bovine serum and 2 mM glutamine) were added to each well of a 96-well microtiter plate and incubated for 24 h at 37 °C. The treatment of the cultures was performed in fresh supplemented medium (200 μ L/well) for 24 h at 37 °C. After this period, 110 μ L of the medium was discarded and 10 μ L of PrestoBlue (Invitrogen) was added to complete the final volume of 100 μ L. Thus, the plate was incubated for 2 h and the measurement was performed at 560 and 590 nm, as recommended by the manufacturer. The results were expressed as the difference in the percentage of reduction between treated and untreated cells being the LC₅₀ value, corresponding to the concentration that leads to damage of 50% of the mammalian cells.²¹⁷

216. De Castro, S.L.; Pinto, M.C.; Pinto, A.V.; Screening of natural and synthetic drugs against *Trypanosoma cruzi*. 1. Establishing a structure/activity relationship. *Microbios*, **1994**, *78*, 83.

217. Jardim, A.M.J.; Reis, W.J.; Ribeiro, M.F.; Ottoni, F.M.; Alves, R.J.; Silva, T.L.; Goulart, M.O.F.; Braga, A.L.; Menna-Barreto, R.F.S.; Salomão, K.; de Castro, S.L.; da Silva Júnior, E.N.; On the investigation of hybrid quinones: synthesis, electrochemical studies and evaluation of trypanocidal activity. *RSC Adv.*, **2015**, *5*, 78047.

7.5.3. Trypanocidal Assays for Thiolated Quinoidal Compounds

Bloodstream trypomastigotes (Y strain) were obtained at the peak of parasitaemia from infected albino mice, isolated by differential centrifugation and re-suspended in RPMI medium (10^7 parasites/mL) in the presence of 10% of mouse blood. This suspension (100 μ L) was added in the same volume of each compound previously prepared at twice the desired final concentrations in 96-well microplates and incubated at 4 °C for 24 h. Alternatively, trypomastigotes were also re-suspended in absence of mouse blood and incubated at 37 °C for 24 h. Parasites counts were performed in Neubauer chamber and the trypanocidal activity was expressed as $IC_{50}/24$ h, corresponding to the concentration that leads to lysis of 50% of the parasites. Stock solutions of the compounds were prepared in dimethyl sulfoxide (DMSO), with the final concentration of the latter in the experiments never exceeding 0.1%.

7.5.4. Cytotoxicity Assays for Thiolated Quinoidal Compounds

Swiss mice peritoneal macrophages were re-suspended in RPMI, added to 24-well plates (10^5 cells/well) and maintained for 24 h at 37°C. The cultures were then washed with phosphate buffered saline (PBS, pH 7.2) and treated with the compounds in medium without phenol red (200 μ L/well) for 24 h at 37°C. After this period, 110 μ L of the medium was discarded and 10 μ L of PrestoBlue (Invitrogen) was added to complete the final volume of 100 μ L. Thus, the plate was incubated for 2 h and the measurement was performed at 560 and 590 nm, as recommended by the manufacturer. The results were expressed as the difference in the percentage of reduction between treated and untreated cells being the $LC_{50}/24$ h value, corresponds to the concentration that leads to damage of 50% of the mammalian cells.

7.6. Crystallographic Data Collection and Refinement

X-ray diffraction data collections on single crystals of all compounds were performed with an Oxford-Diffraction GEMINI-Ultra using Mo-K α radiations (0.71073 Å) and on an Enraf-Nonius Kappa-CCD diffractometer (95 mm CCD camera on k-goniostat) using graphite monochromated MoK α radiation (0.71073 Å), both at room temperature

(293 K). Data integration and scaling of the reflections for all compounds were performed with the *CRYSTALIS* suite.²¹⁸ Final unit cell parameters were based on the fitting of all reflections positions. Analytical absorption corrections and the space group identification were performed using *CRYSTALIS* suite. The structures of all compounds were solved by direct methods using the *SUPERFLIP* program.²¹⁹ For each compound, the positions of all atoms could be unambiguously assigned on consecutive difference Fourier maps. Refinements were performed using *SHELXL*²²⁰ based on F^2 through full-matrix least square routine. All non-hydrogen atoms were refined with anisotropic atomic displacement parameters. All hydrogen atoms were located in difference maps and included as fixed contributions according to the riding model.²²¹ Molecular graphics were obtained with ORTEP3²²² in association with POV-Ray software.²²³ All structures were deposited in the Cambridge Crystallographic Data Centre²²⁴

CCDC numbers concerning the crystal structures presented in this work are:

[RhCp^{*i*-Pr}Cl₂]₂ . CCDC 1441685

[RhCp^{CF₃}Cl₂]₂ . CCDC 1441684

[RhCp^{*}(OAc)₂(H₂O)] - CCDC 1441683

5-Iodo-1,4-naphthoquinone (60) - CCDC 1441686

5,8-Diiodo-1,4-naphthoquinone (62) - CCDC 1441693

2-(phenylselanyl)-1,4-naphthoquinone (74) - CCDC 1505108

2-Iodo-1,4-benzoquinone (61) - CCDC 1505106

2-Bromo-5-iodo-1,4-naphthoquinone (81) - CCDC 1441690

5-hydroxy-6-iodo-1,4-naphthoquinone (83) - CCDC 1526294

5-hydroxy-6,8-diiodo-1,4-naphthoquinone (84) - CCDC 1526293

5-Iodo-8-methoxy-1,4-naphthoquinone (89) - CCDC 1441687

8-Iodo-5-methoxy-2-methyl-1,4-naphthoquinone (90) - CCDC 1441688

218. CrysAlisPro Software system, Rigaku Corporation: Oxford, UK, 2015.

219. Palatinus, L.; Chapuis, G.; *J. Appl. Crystallogr.*, 2007, 40, 786.

220. Sheldrick, G.M.; *Acta Cryst.*, 2015, 71, 3.

221. Johnson, C.K.; *ORTEP, Crystallographic Computing*; F. R. Ahmed Ed.: Copenhagen, Denmark, 1971, 217.

222. Farrugia, L.J.; *J. Appl. Cryst.*, 2012, 45, 849.

223. Persistence of Vision Raytracer, Persistence of Vision, Pty. Ltd.: Williamstown, Australia, 2004.

224. <https://www.ccdc.cam.ac.uk/>



- 2,3-Dibromo-5-iodo-1,4-naphthoquinone (95)** - CCDC 1441691
5-Iodo-8-nitro-1,4-naphthoquinone (97) - CCDC 1441689
5-Bromo-1,4-naphthoquinone (107) - CCDC 1441694
2-Iodo-1,4-naphthoquinone (108) - CCDC 1441692
2-Iodo-3-methoxy-1,4-benzoquinone (114) - CCDC 1505107
2,6-Diiodo-3,5-dimethoxy-1,4-benzoquinone (116) - CCDC 1526364
5-((Trifluoromethyl)thio)-1,4-naphthoquinone (138) – CCDC 1586329
5,8-Bis((trifluoromethyl)thio)-1,4-naphthoquinone (145) – CCDC 1586323
8-methoxy-2-methyl-5-((trifluoromethyl)thio)-1,4-naphthoquinone (146) – CCDC 1586328
N-(1,4-Dioxo-6-((trifluoromethyl)thio)-1,4-dihydronaphthalen-5-yl)acetamide (147)
– CCDC 1586321
1-((trifluoromethyl)thio)anthracene-9,10-dione (148) – CCDC 1586325
5-((Trifluoromethyl)sulfinyl)-1,4-naphthoquinone (149) – CCDC 1586747
1-((trifluoromethyl)sulfonyl)anthracene-9,10-dione (151) – CCDC 1586748
5-(Benzylthio)-1,4-naphthoquinone (152) – CCDC 1586326
5-((para-Methoxyphenyl)thio)-1,4-naphthoquinone (155) – CCDC 1586322
5-((para-Bromophenyl)thio)-1,4-naphthoquinone (156) – CCDC 1586324
1-(benzylsulfonyl)anthracene-9,10-dione (159) – CCDC 1586327

7.7. ^1H and ^{13}C NMR Spectra of Novel Compounds

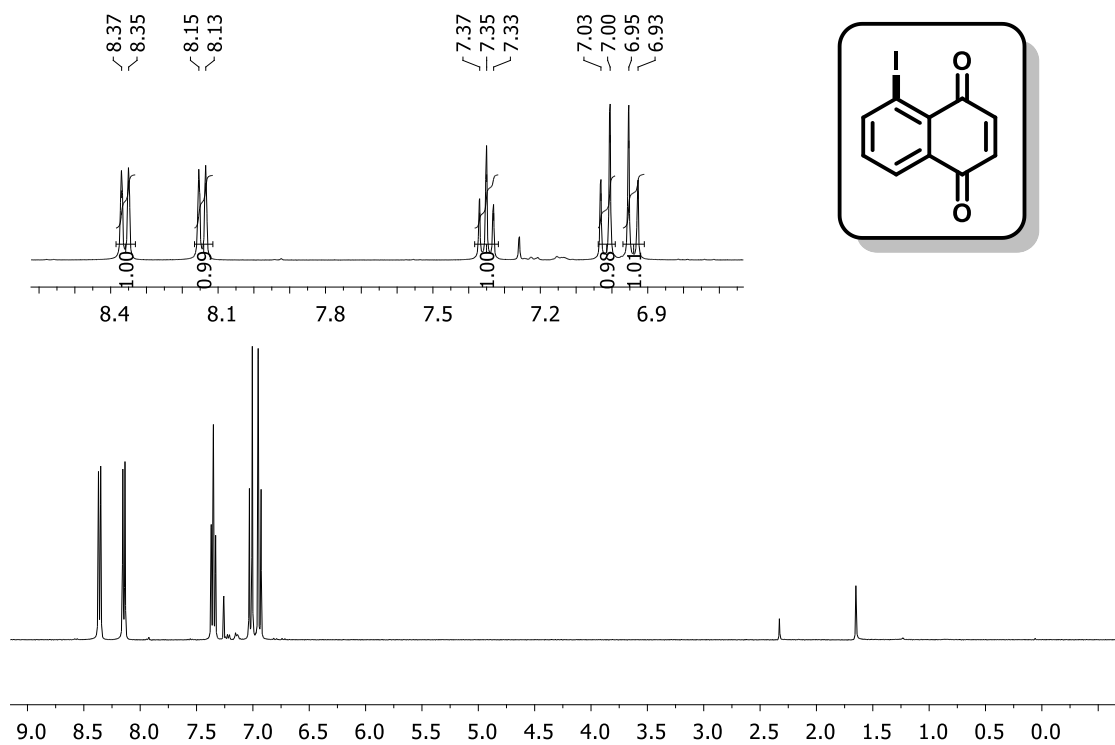


Figure 20. ^1H NMR spectrum (400 MHz, CDCl_3) of compound **60**.

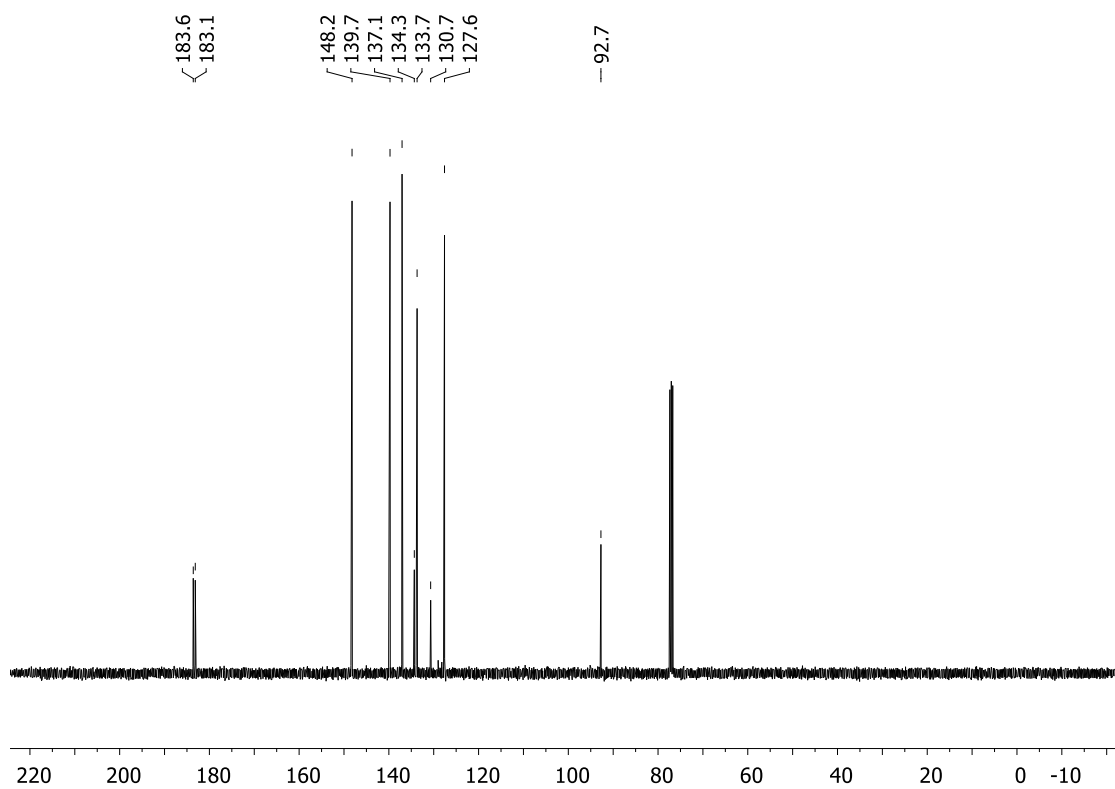


Figure 21. ^{13}C NMR spectrum (100 MHz, CDCl_3) of compound **60**.

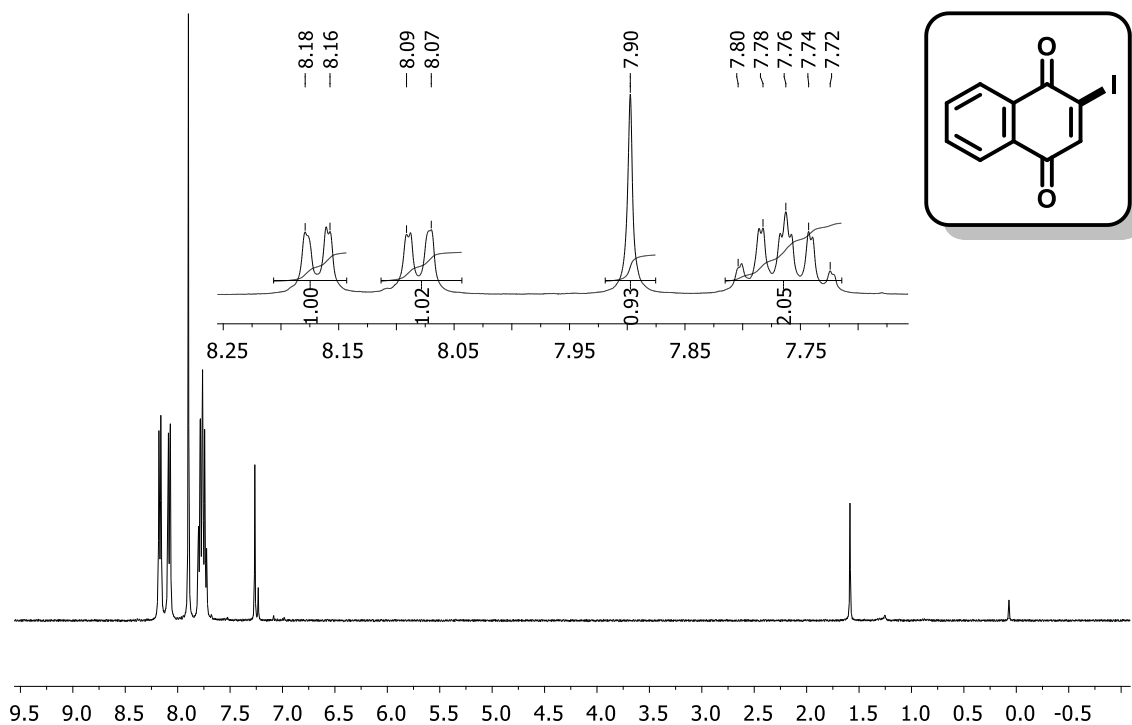


Figure 22. ¹H NMR spectrum (400 MHz, CDCl₃) of compound **61**.

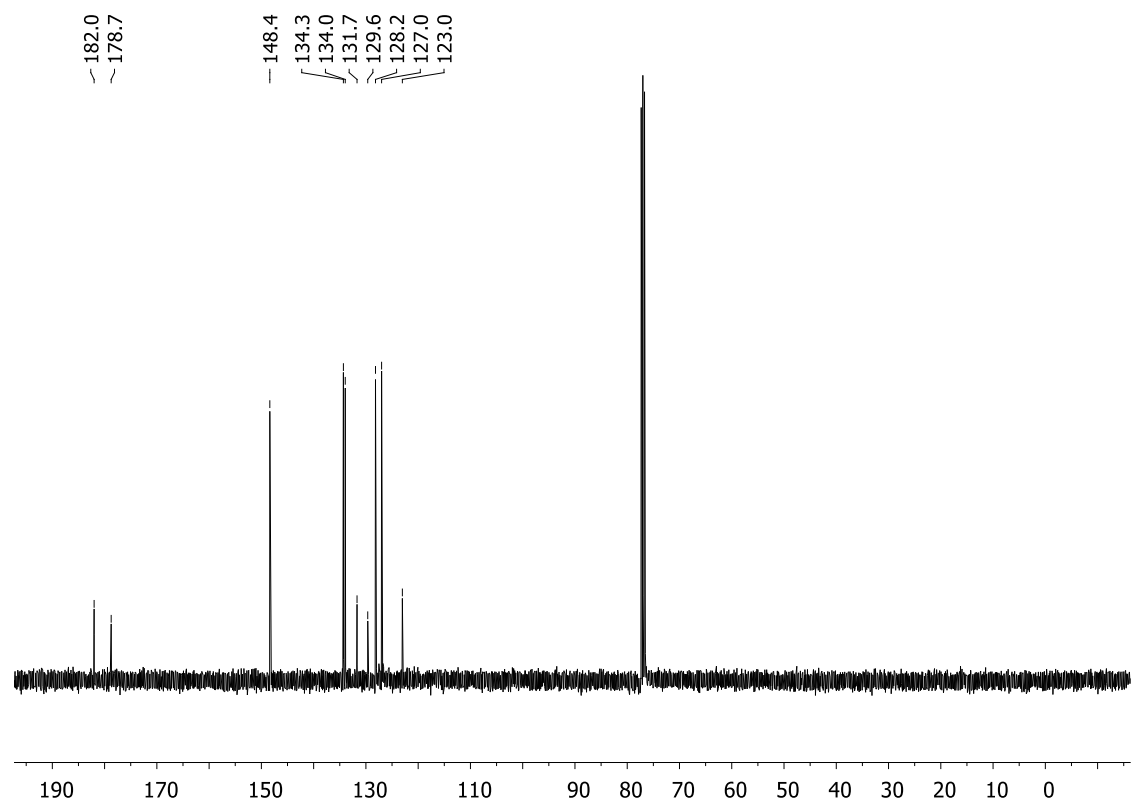


Figure 23. ¹³C NMR spectrum (100 MHz, CDCl₃) of compound **61**.

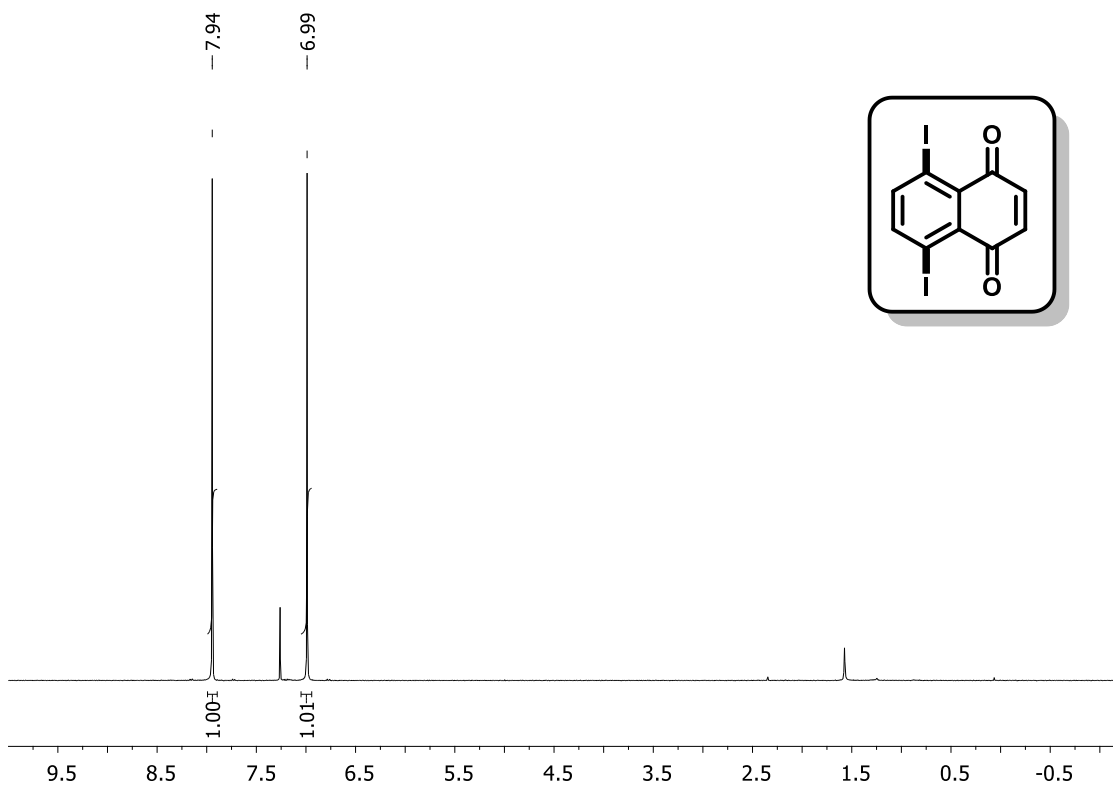


Figure 24. ¹H NMR spectrum (400 MHz, CDCl₃) of compound **62**.

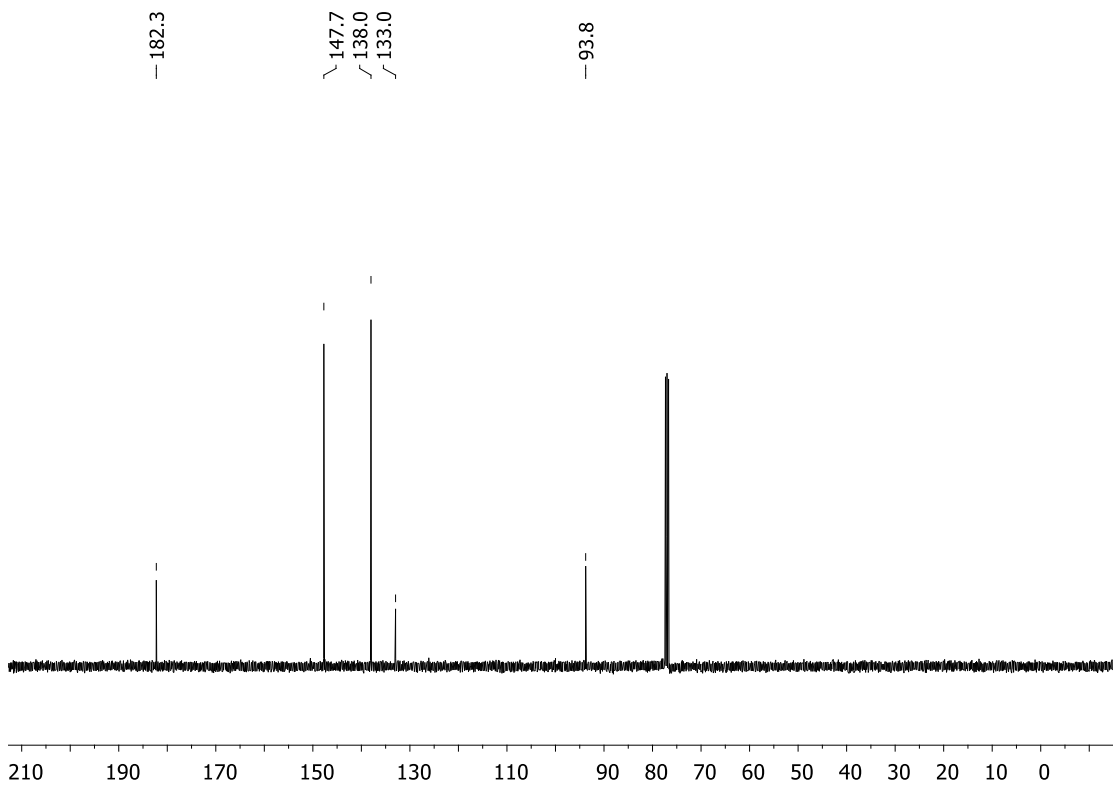


Figure 25. ¹³C NMR spectrum (100 MHz, CDCl₃) of compound **62**.

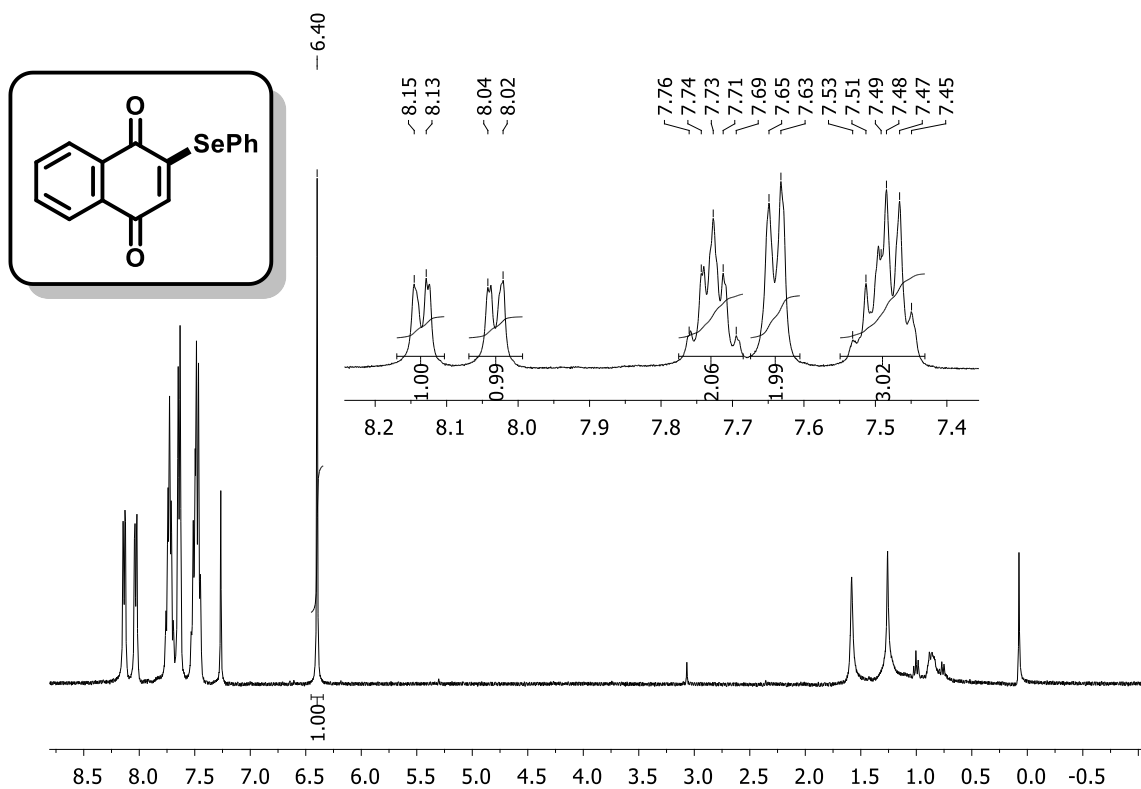


Figure 26. ¹H NMR spectrum (400 MHz, CDCl₃) of compound 74.

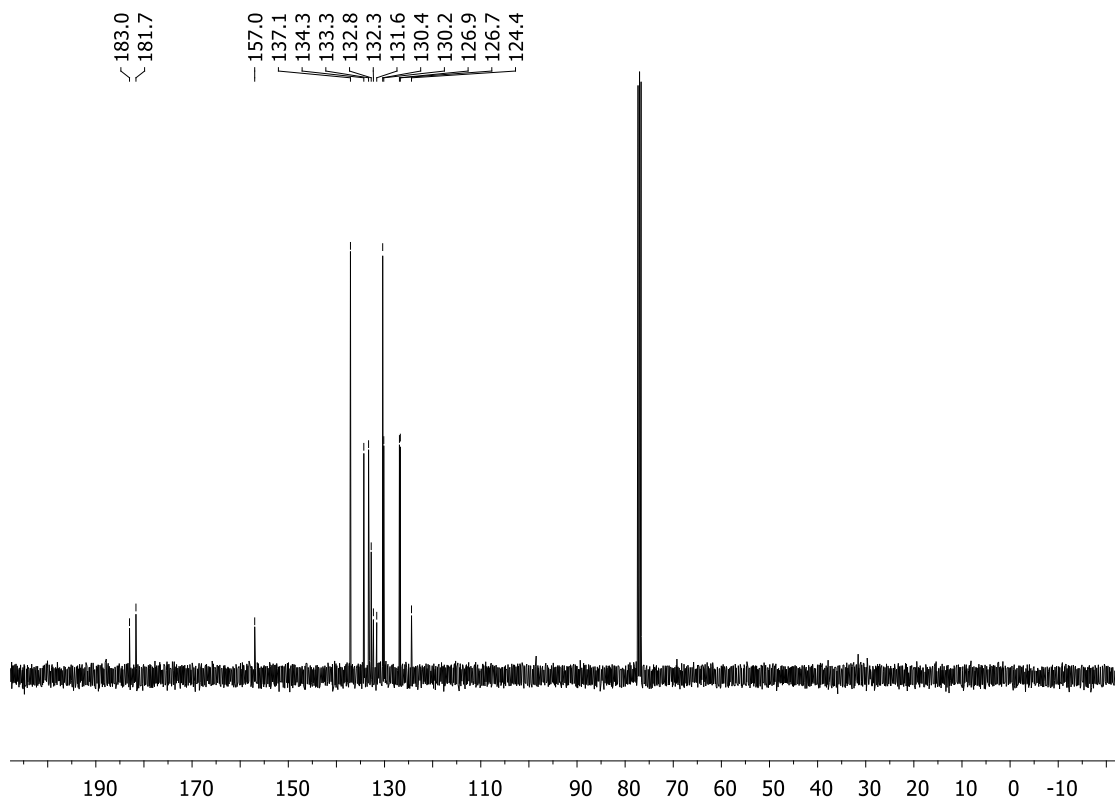


Figure 27. ¹³C NMR spectrum (100 MHz, CDCl₃) of compound 74.

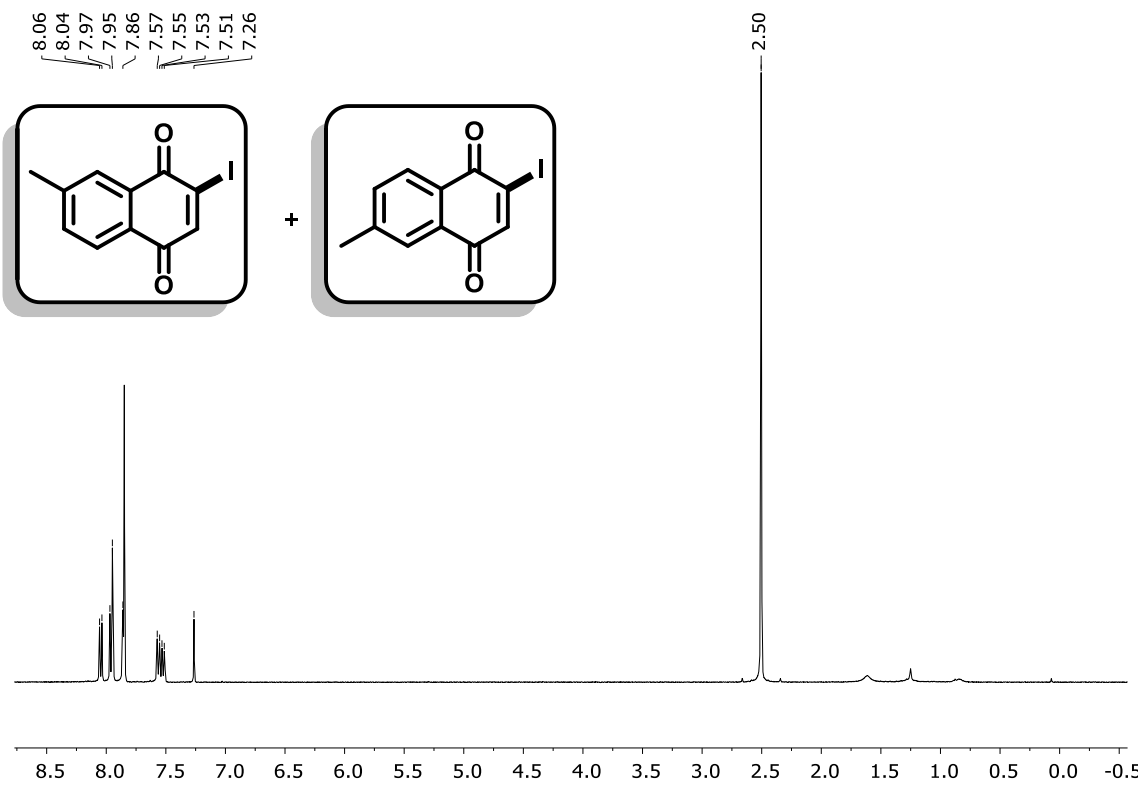


Figure 28. ¹H NMR spectrum (400 MHz, CDCl₃) of compound **77**.

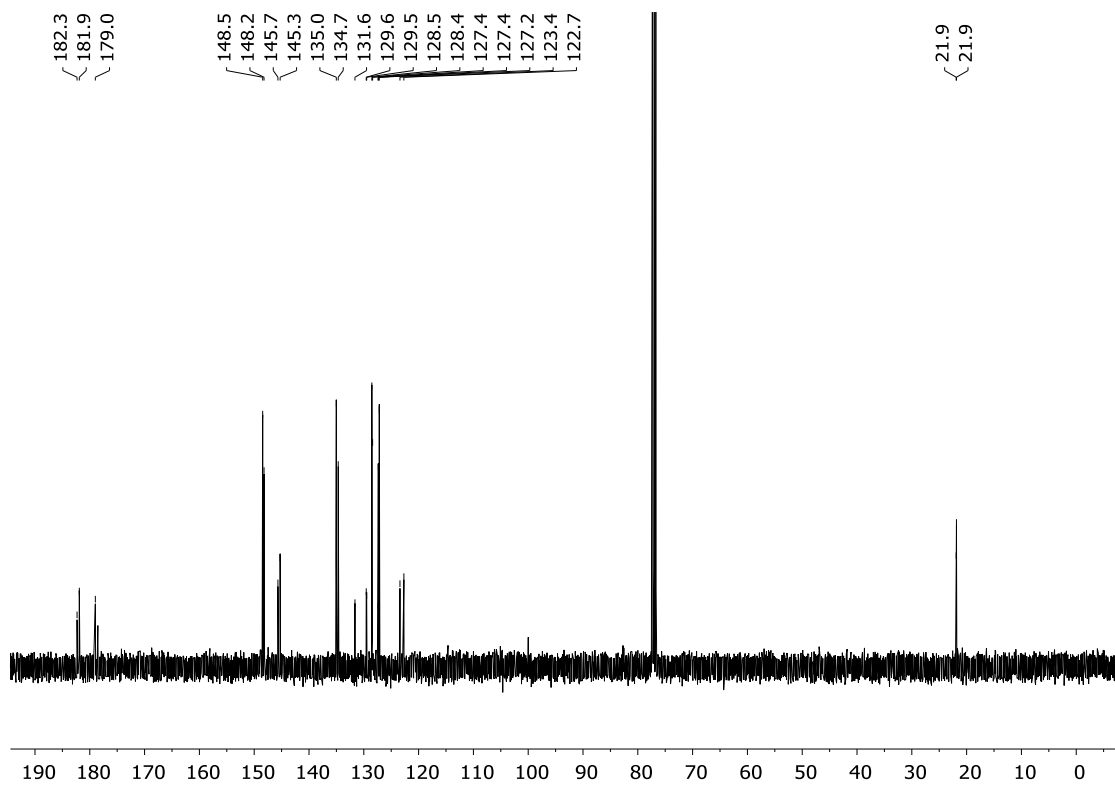


Figure 29. ¹³C NMR spectrum (100 MHz, CDCl₃) of compound **77**.

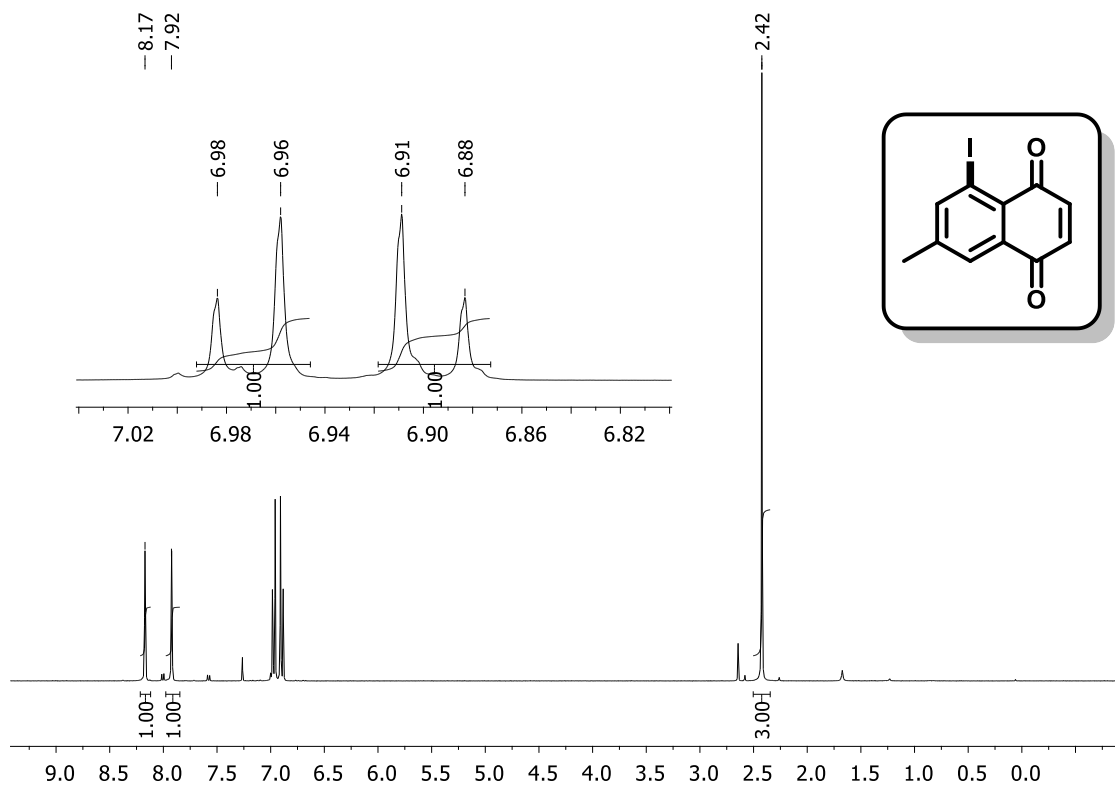


Figure 30. ¹H NMR spectrum (400 MHz, CDCl₃) of compound **80**.

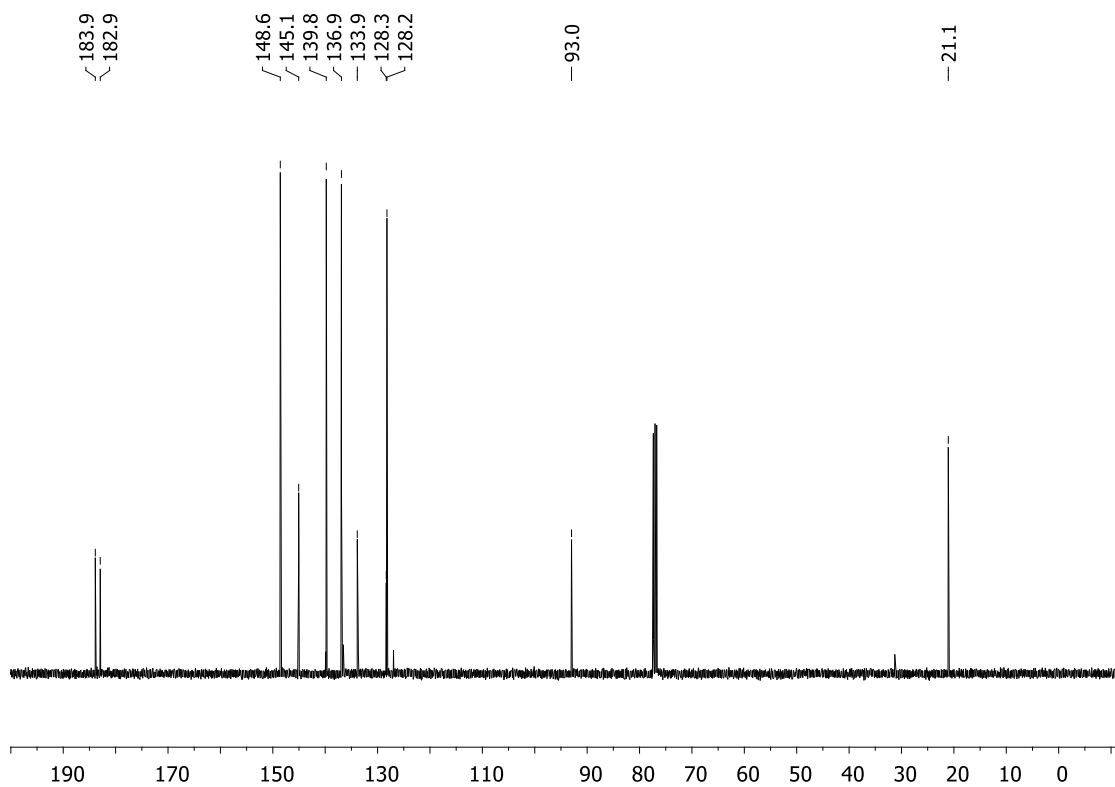


Figure 31. ¹³C NMR spectrum (100 MHz, CDCl₃) of compound **80**.

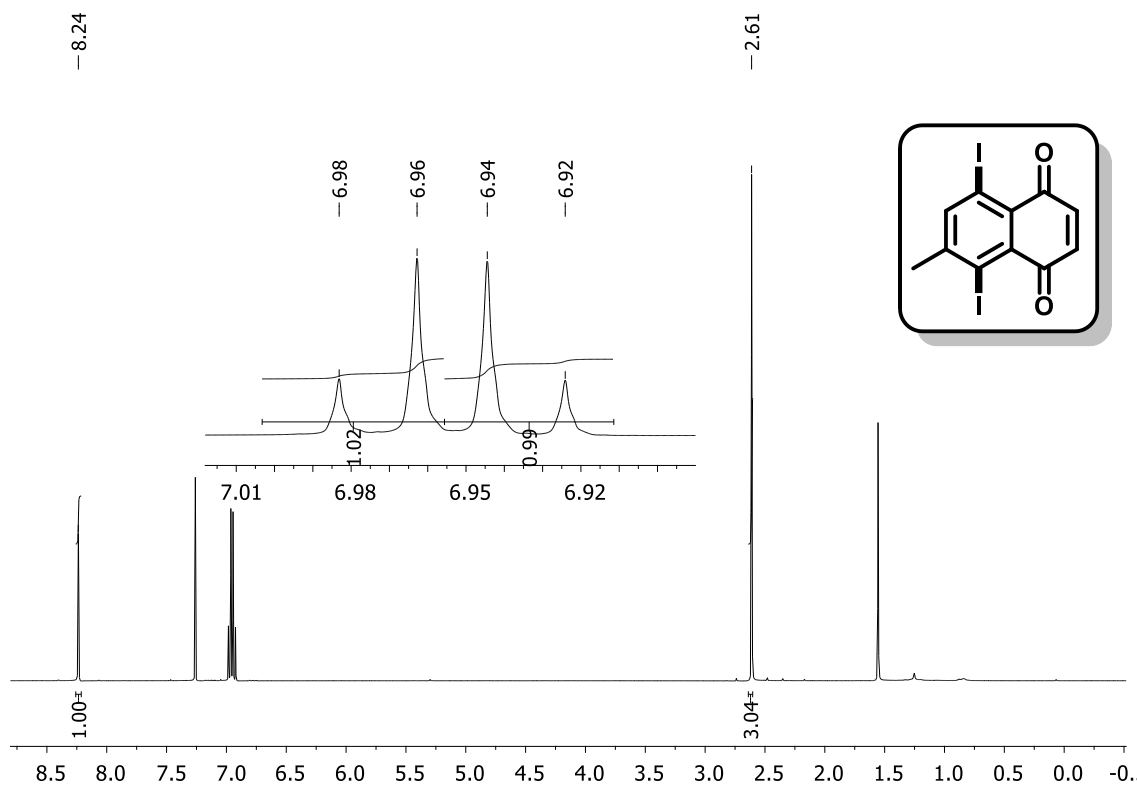


Figure 32. ^1H NMR spectrum (500 MHz, CDCl_3) of compound **80'**.

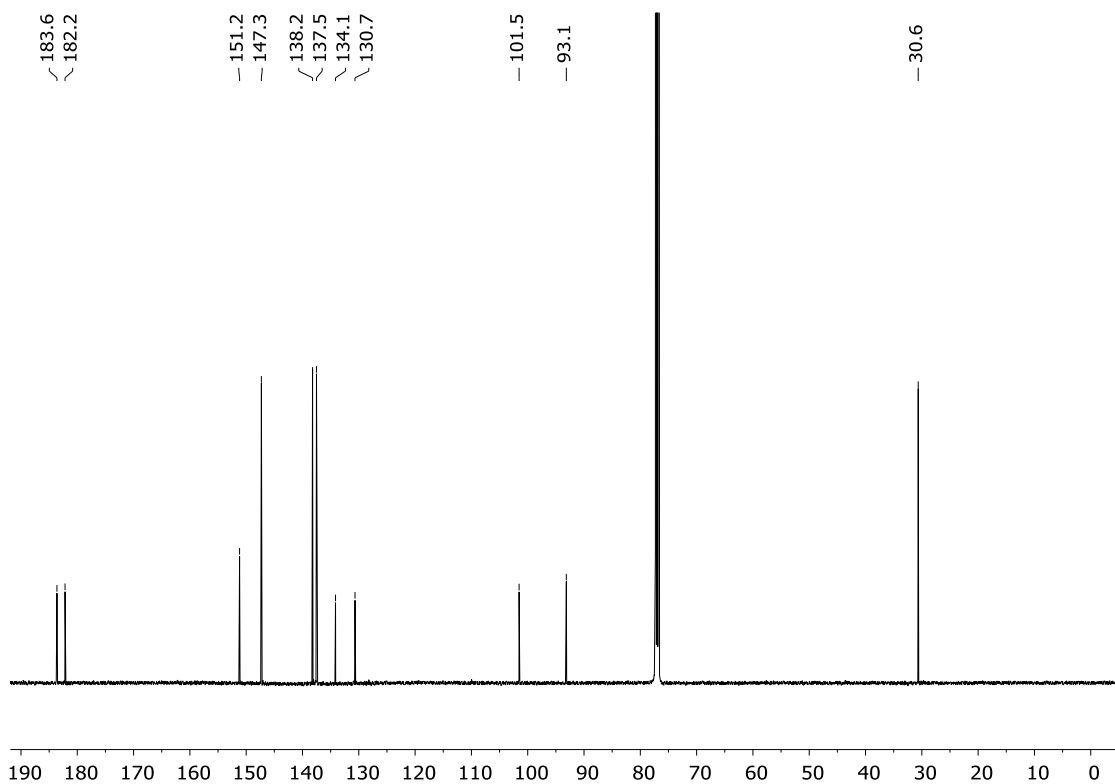


Figure 33. ^{13}C NMR spectrum (125 MHz, CDCl_3) of compound **80'**.

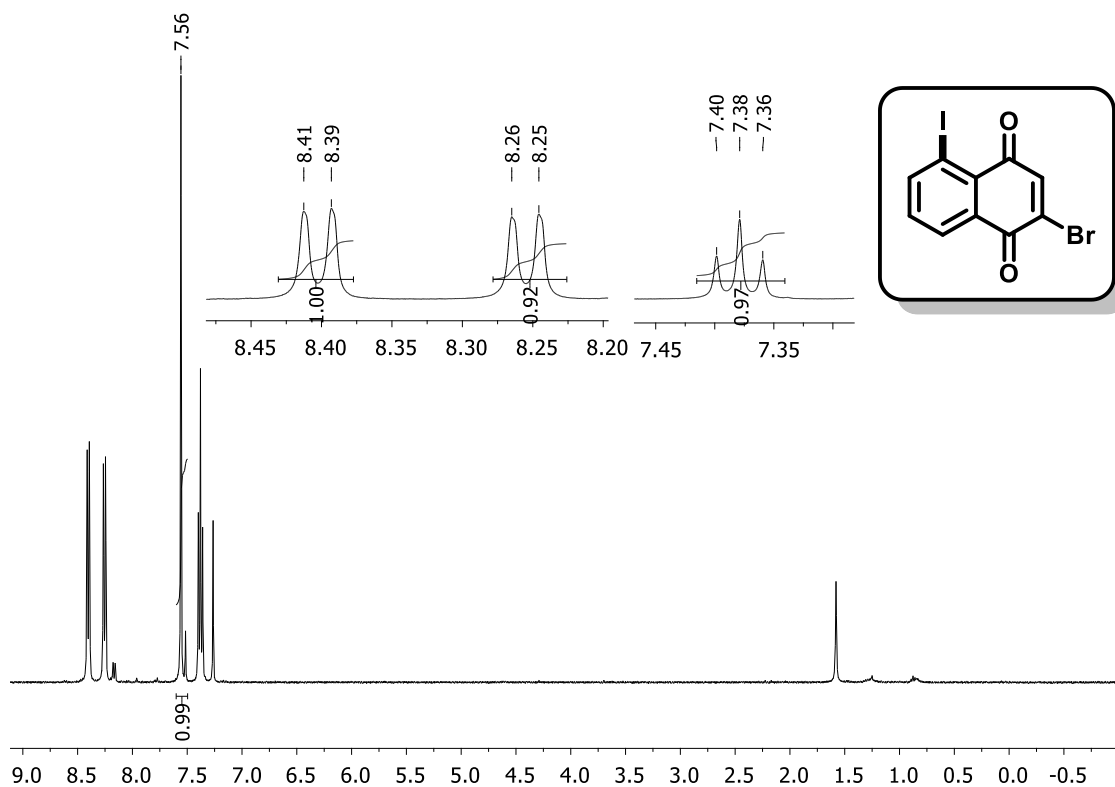


Figure 34. ^1H NMR spectrum (400 MHz, CDCl_3) of compound **81**.

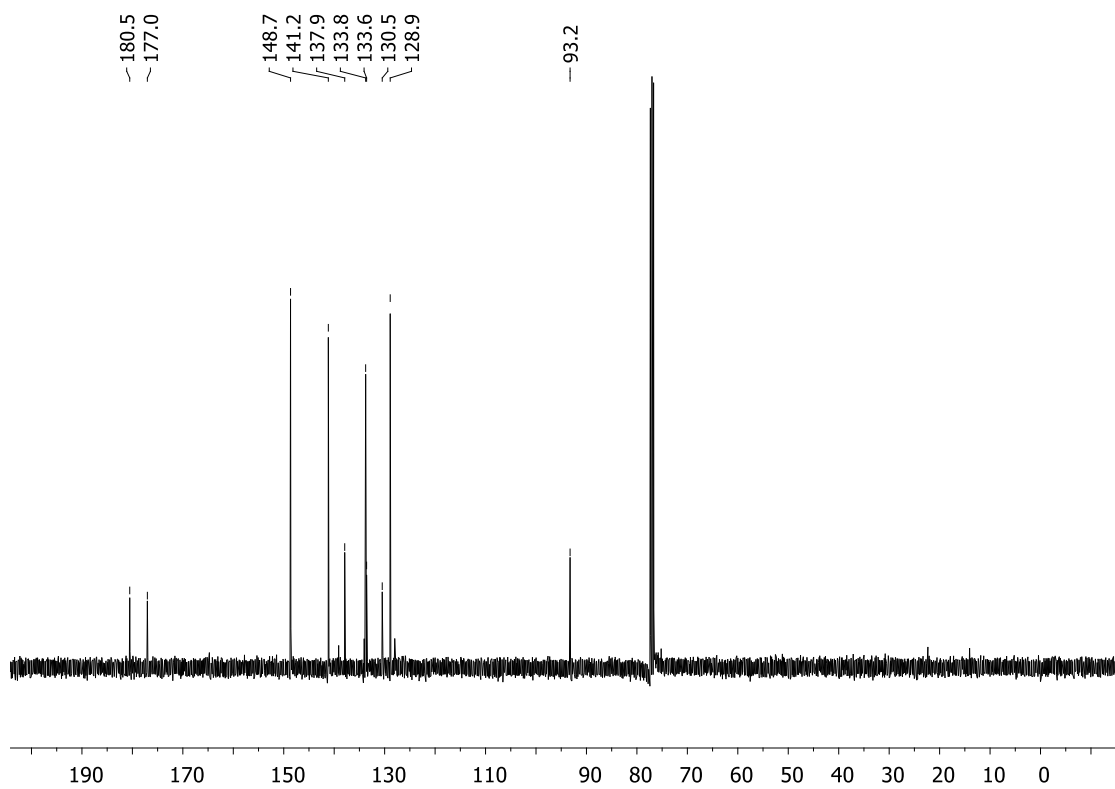


Figure 35. ^{13}C NMR spectrum (100 MHz, CDCl_3) of compound **81**.

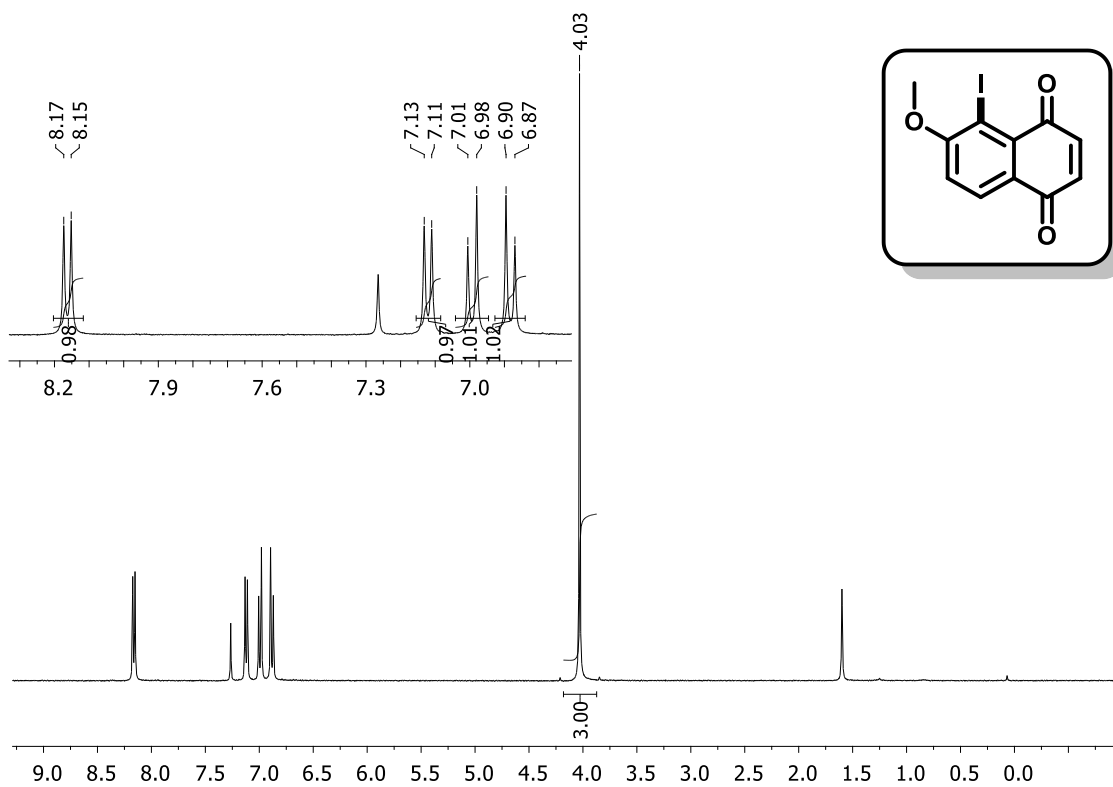


Figure 36. ¹H NMR spectrum (400 MHz, CDCl₃) of compound **82**.

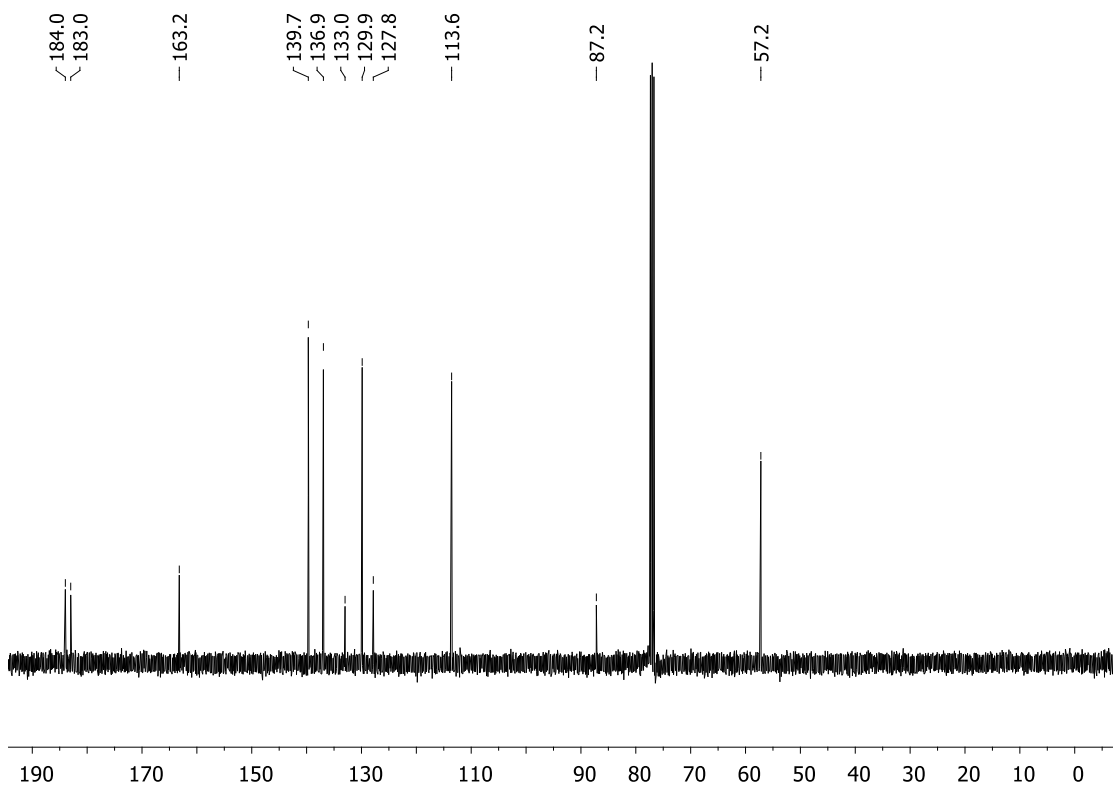


Figure 37. ¹³C NMR spectrum (100 MHz, CDCl₃) of compound **82**.

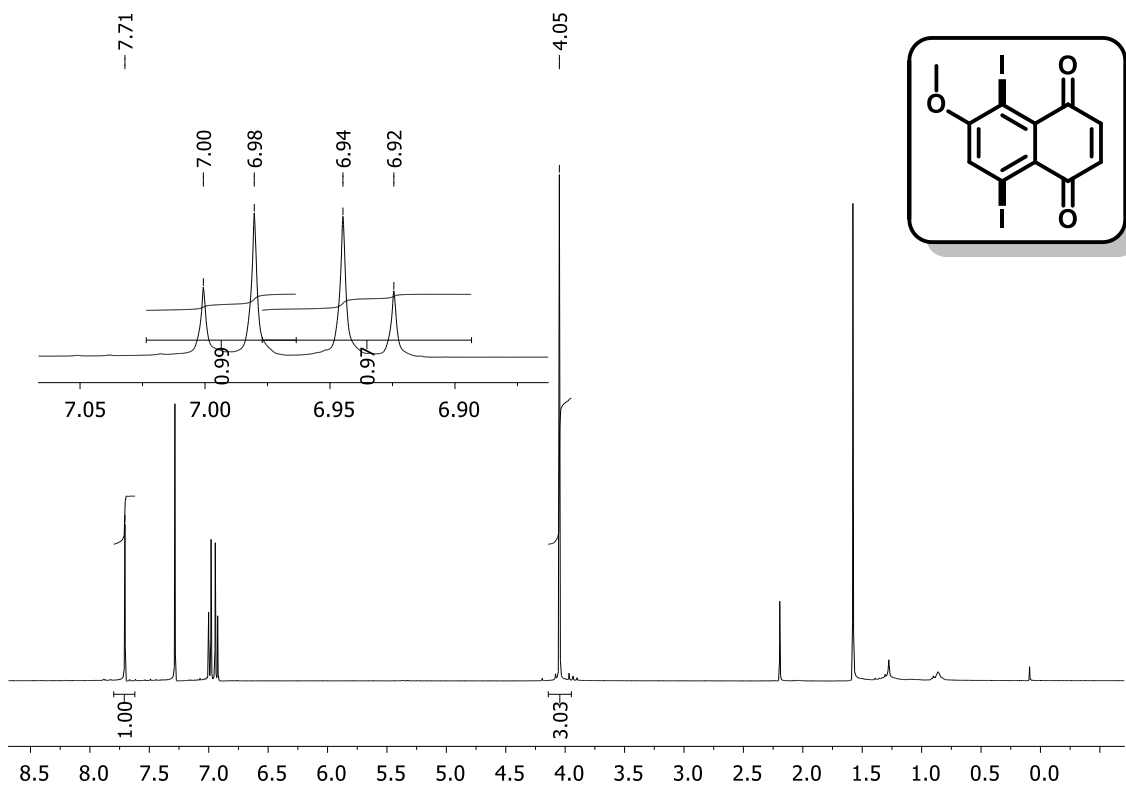


Figure 38. ^1H NMR spectrum (500 MHz, CDCl_3) of compound **82'**.

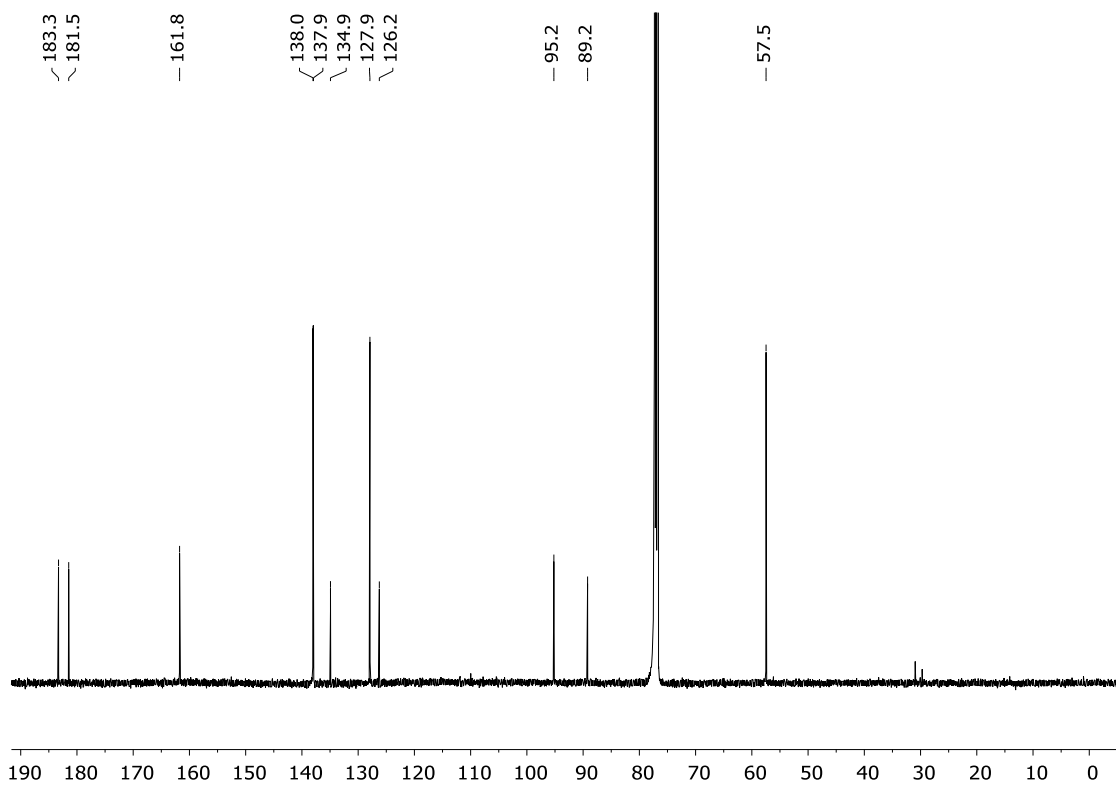


Figure 39. ^{13}C NMR spectrum (125 MHz, CDCl_3) of compound **82'**.

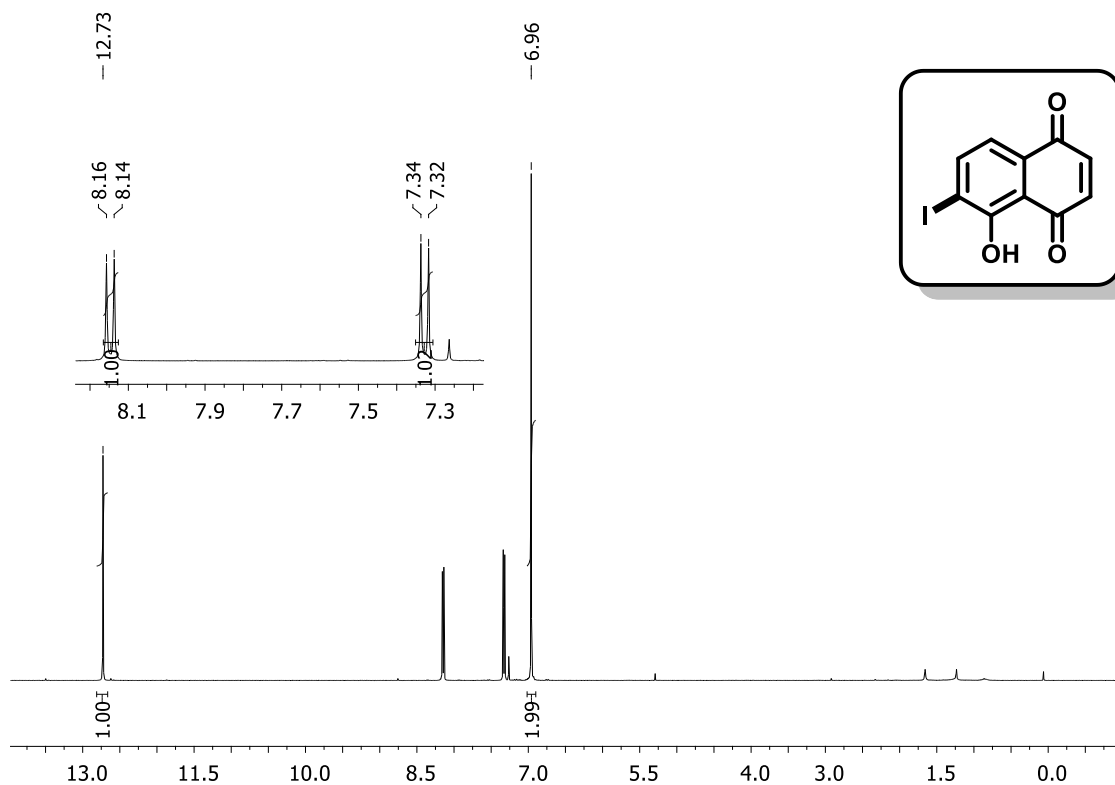


Figure 40. ¹H NMR spectrum (400 MHz, CDCl₃) of compound **83**.

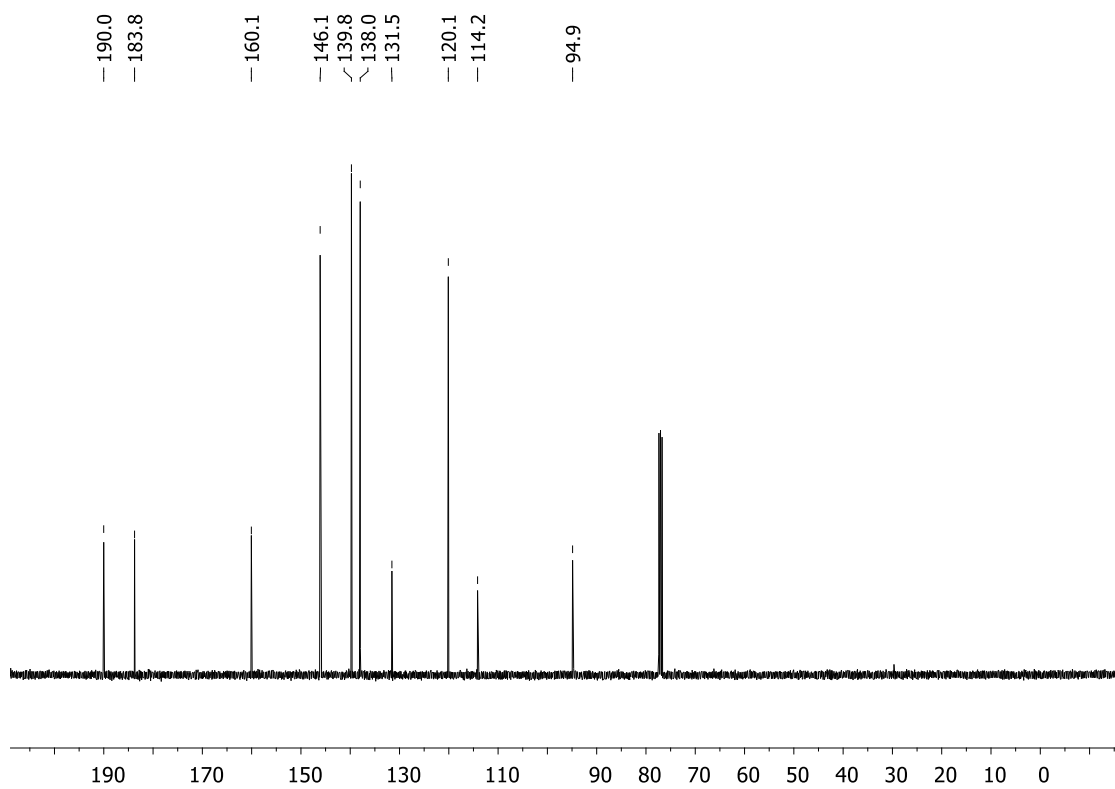


Figure 41. ¹³C NMR spectrum (100 MHz, CDCl₃) of compound **83**.

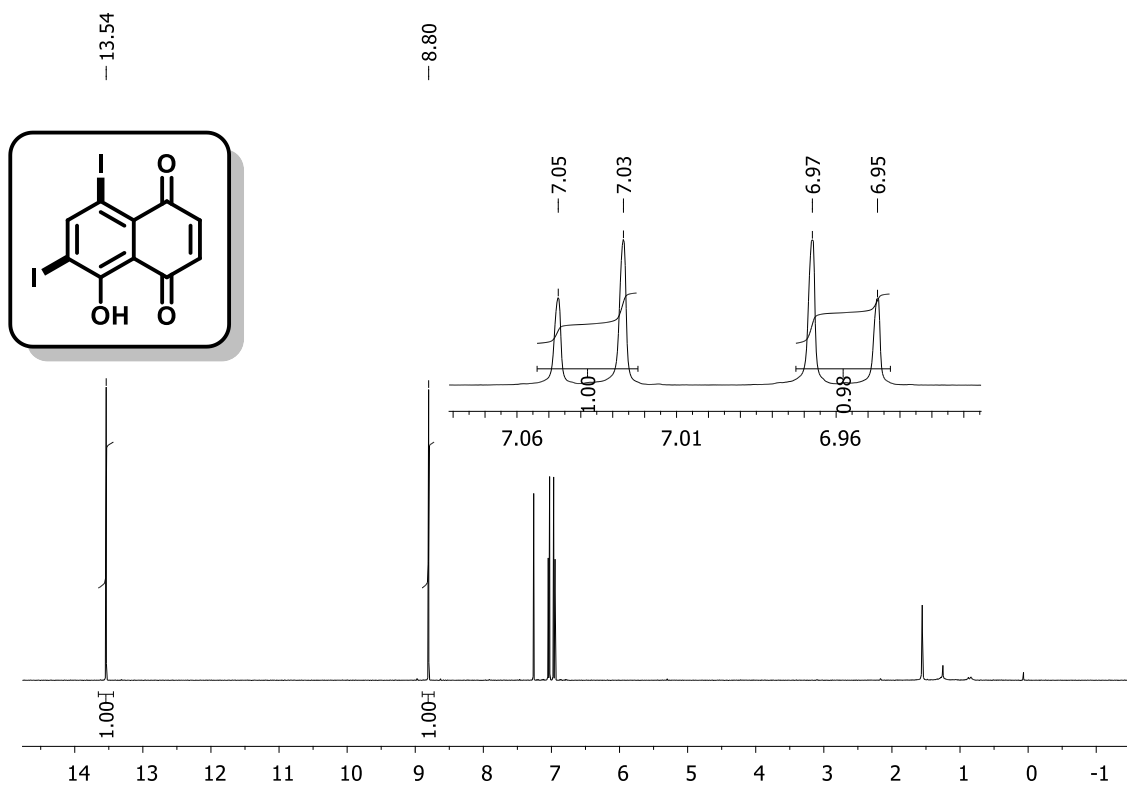


Figure 42. ¹H NMR spectrum (500 MHz, CDCl₃) of compound **84**.

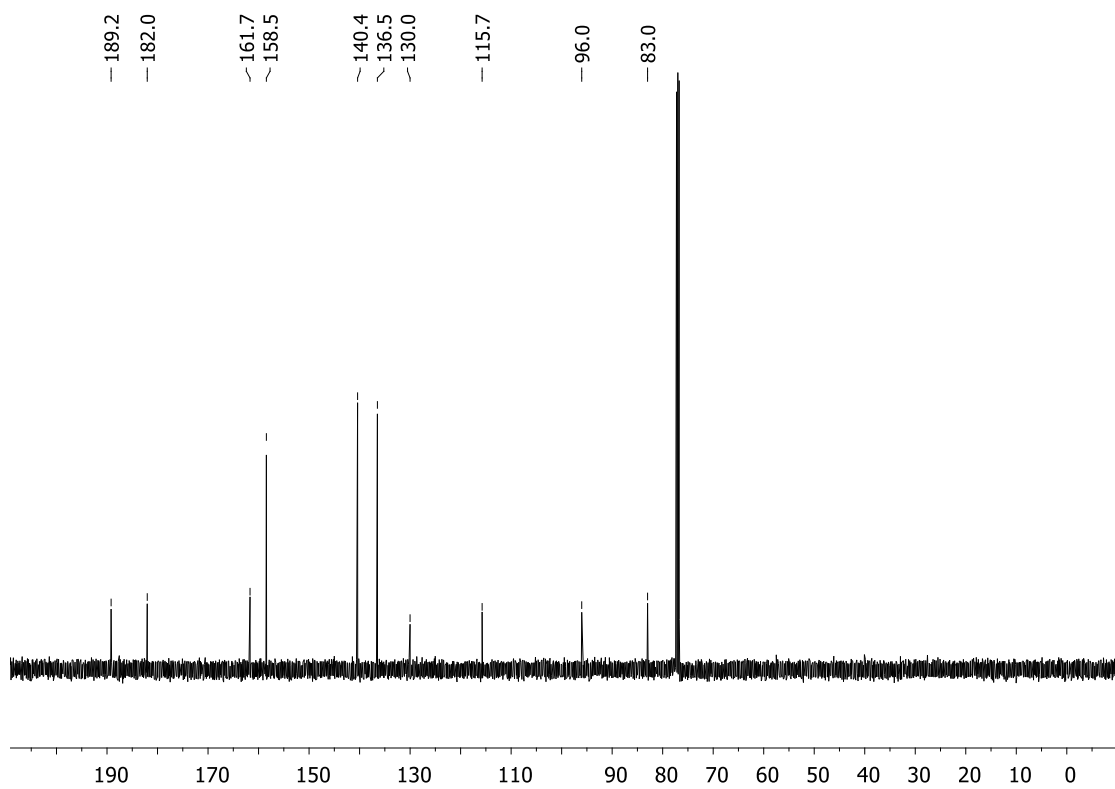


Figure 43. ¹³C NMR spectrum (125 MHz, CDCl₃) of compound **84**.

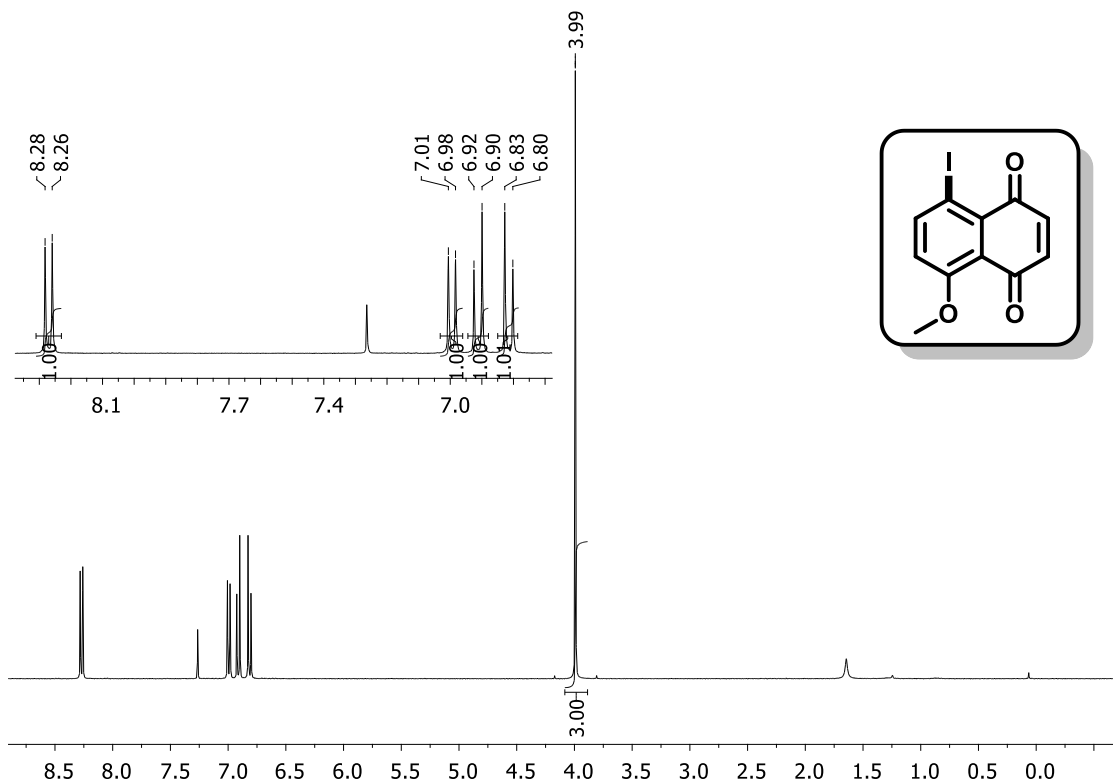


Figure 44. ¹H NMR spectrum (400 MHz, CDCl₃) of compound **89**.

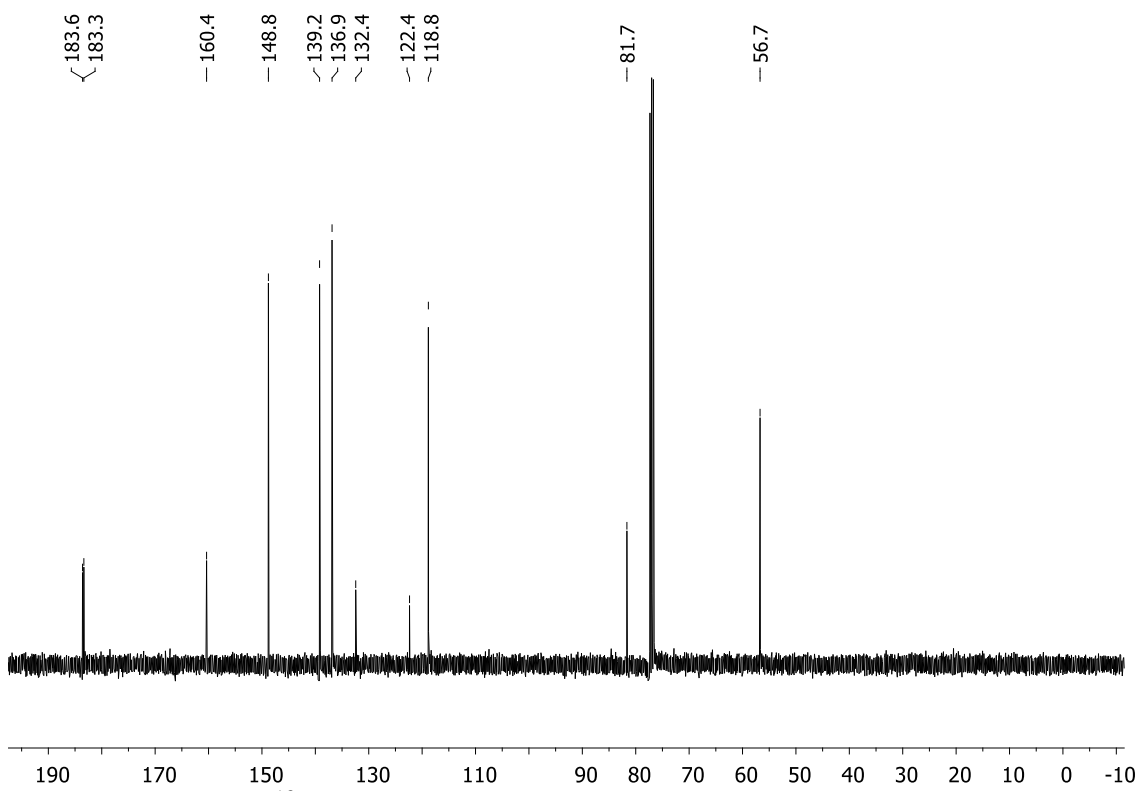


Figure 45. ¹³C NMR spectrum (100 MHz, CDCl₃) of compound **89**.

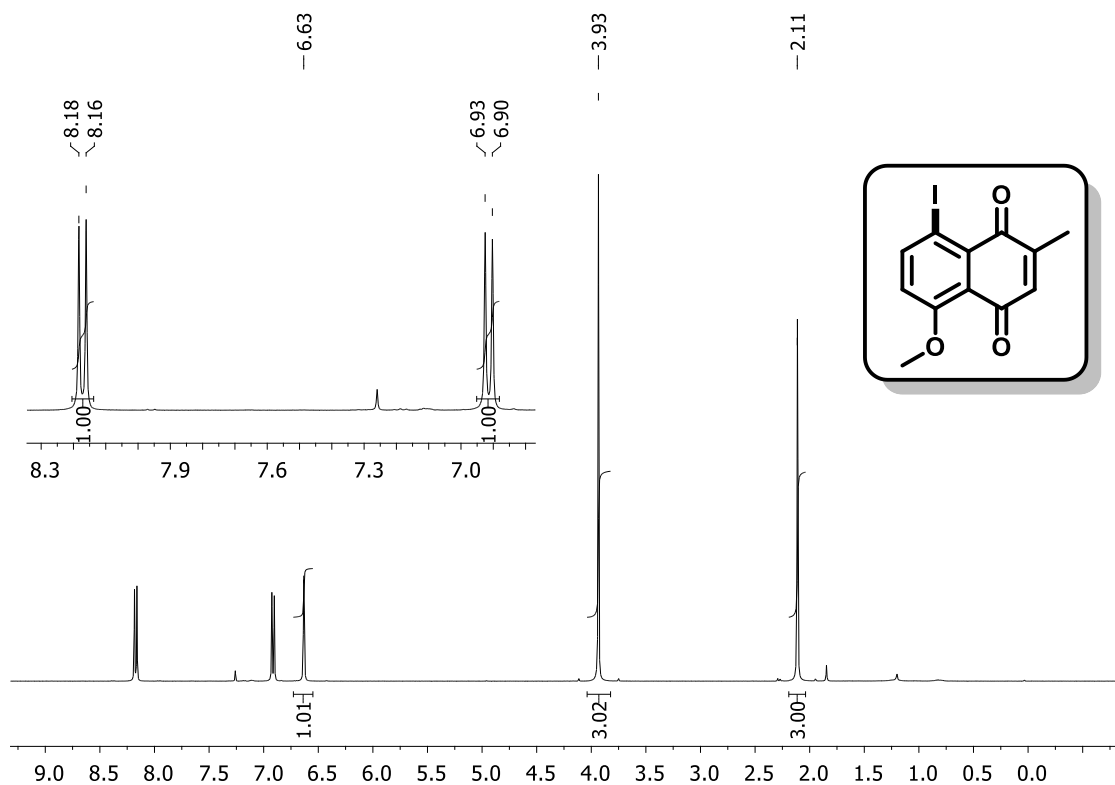


Figure 46. ¹H NMR spectrum (400 MHz, CDCl₃) of compound **90**.

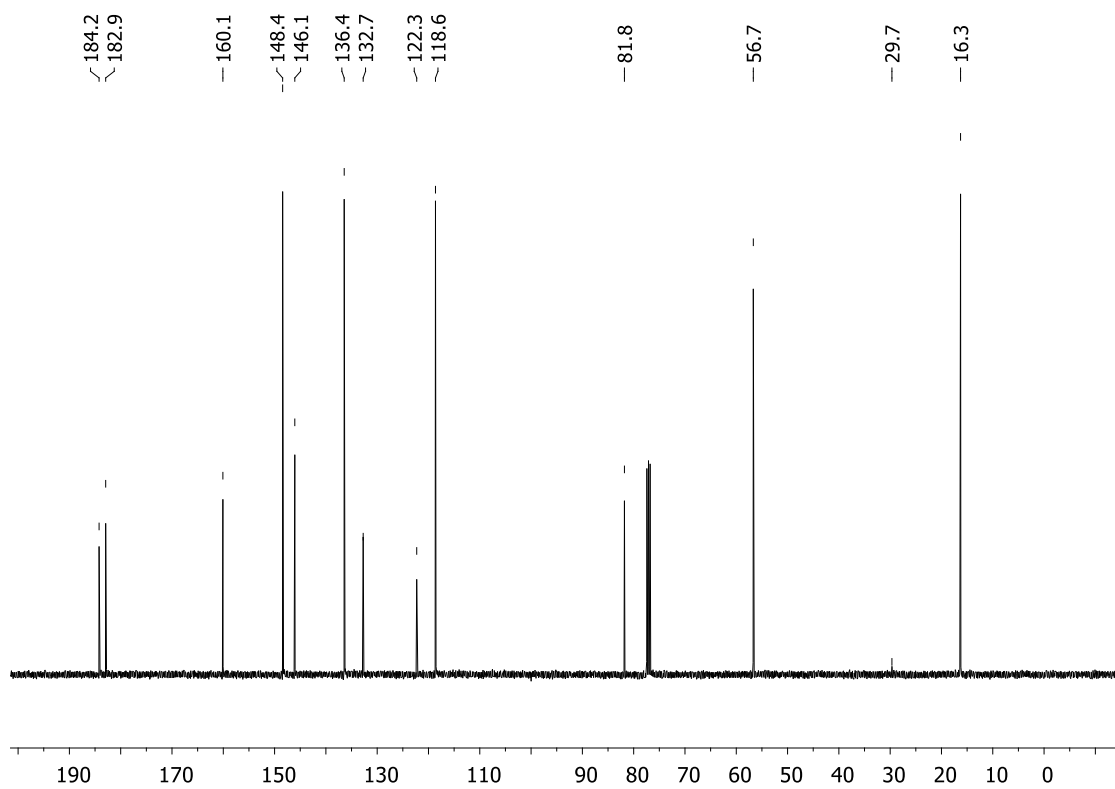


Figure 47. ¹³C NMR spectrum (100 MHz, CDCl₃) of compound **90**.

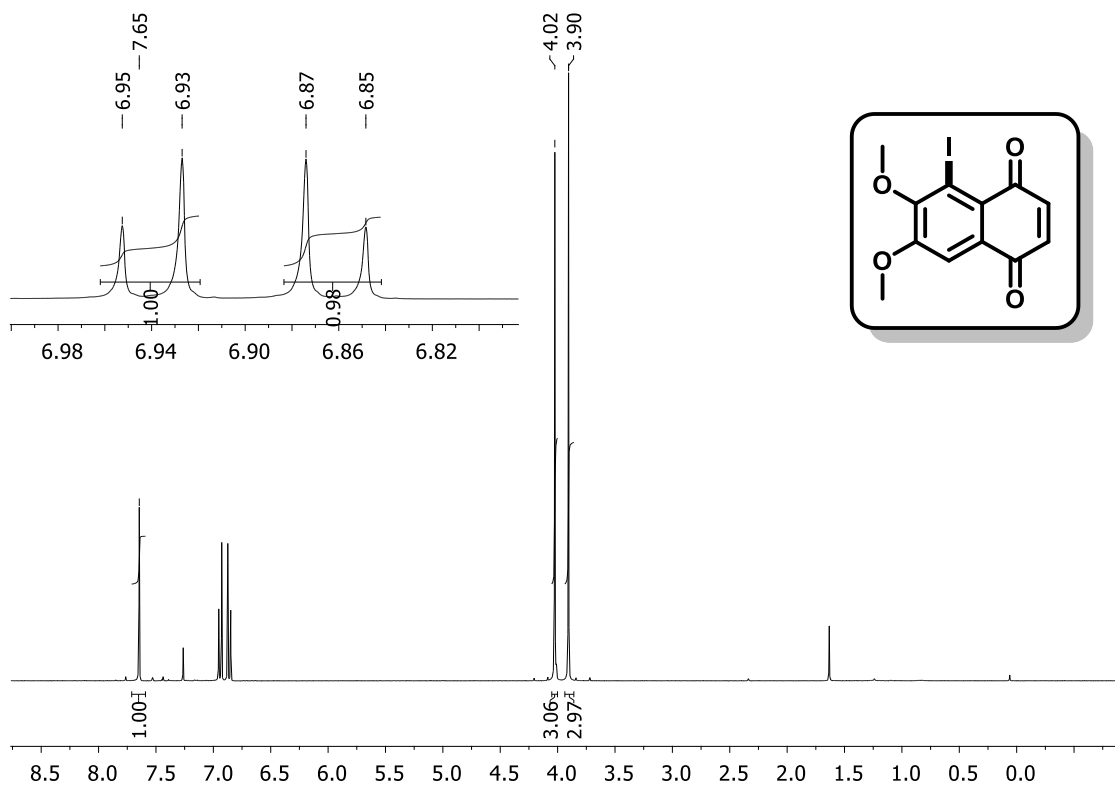


Figure 48. ¹H NMR spectrum (400 MHz, CDCl₃) of compound **91**.

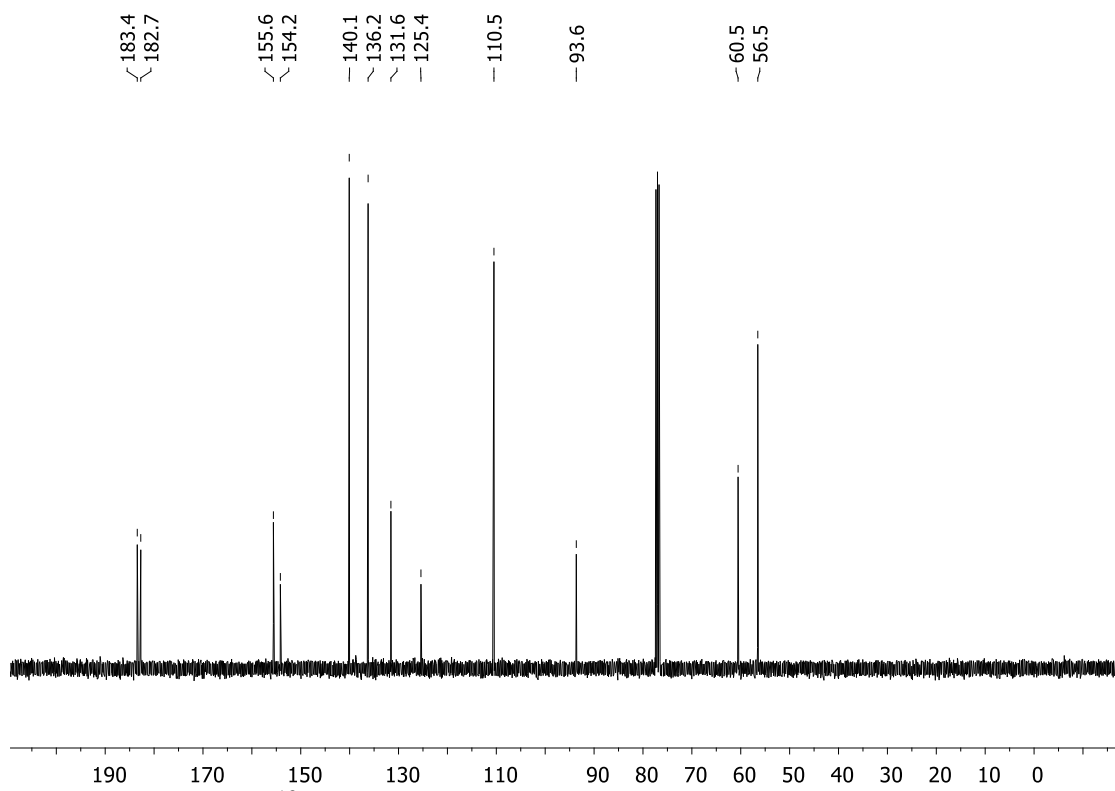


Figure 49. ¹³C NMR spectrum (100 MHz, CDCl₃) of compound **91**.

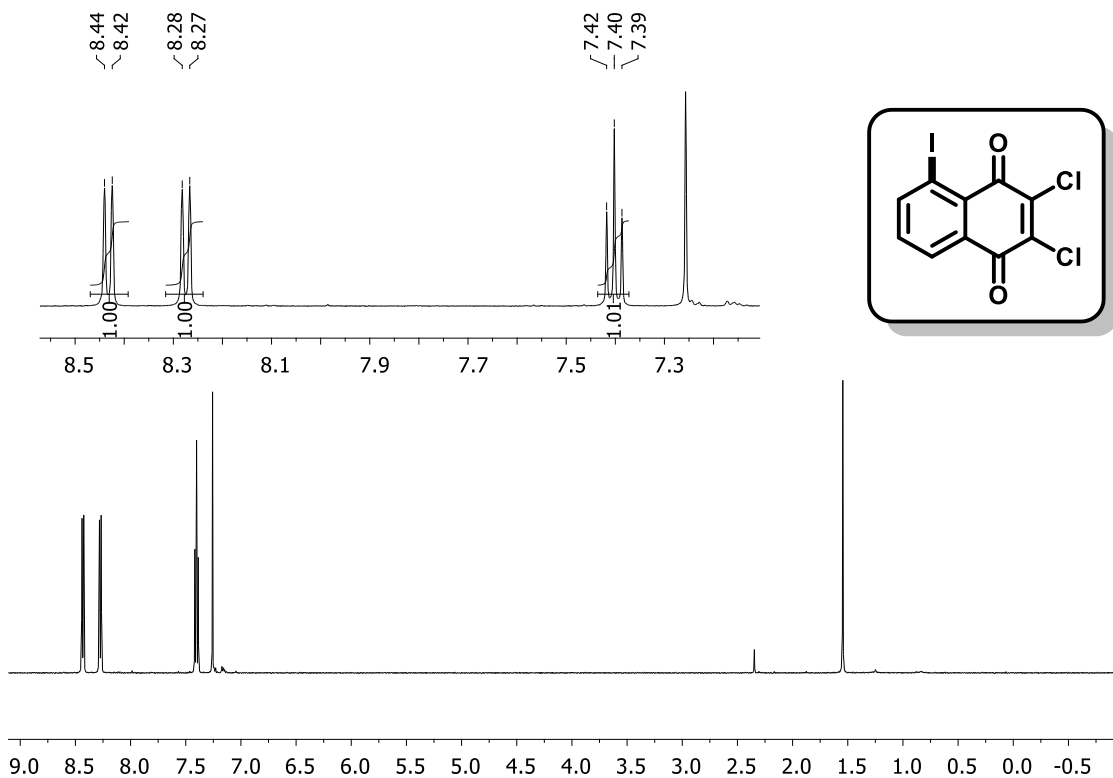


Figure 50. ¹H NMR spectrum (500 MHz, CDCl₃) of compound **94**.

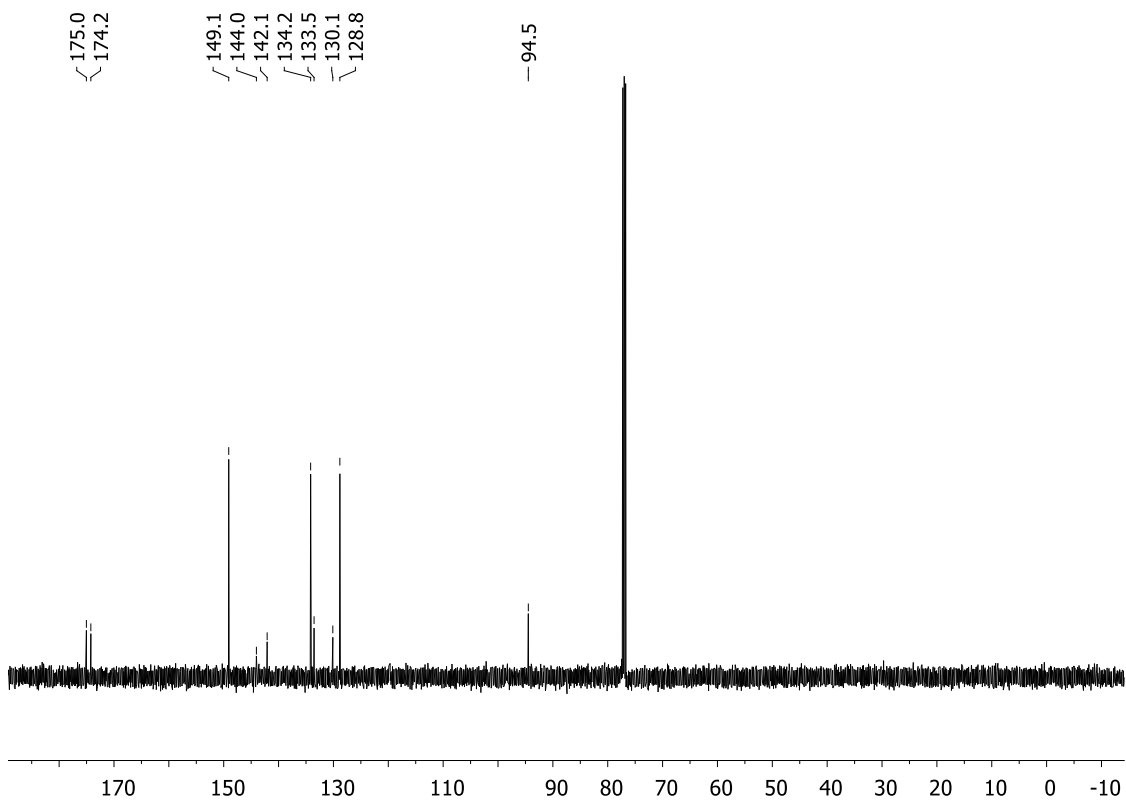


Figure 51. ¹³C NMR spectrum (125 MHz, CDCl₃) of compound **94**.

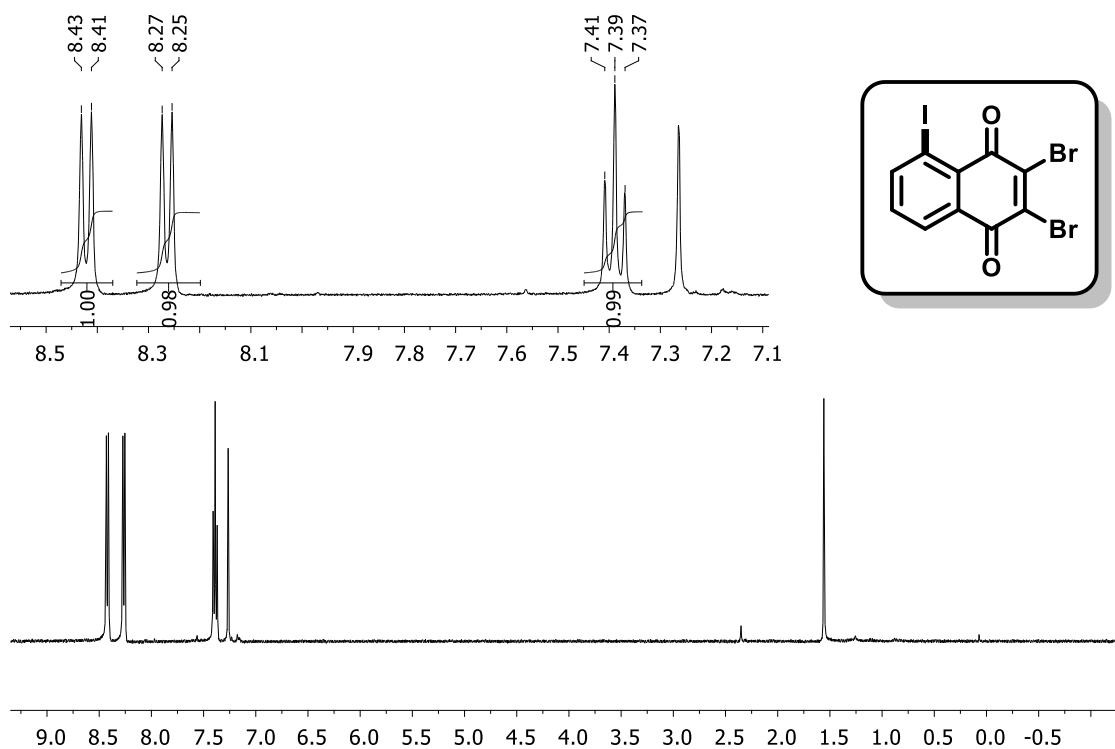


Figure 52. ¹H NMR spectrum (500 MHz, CDCl₃) of compound **95**.

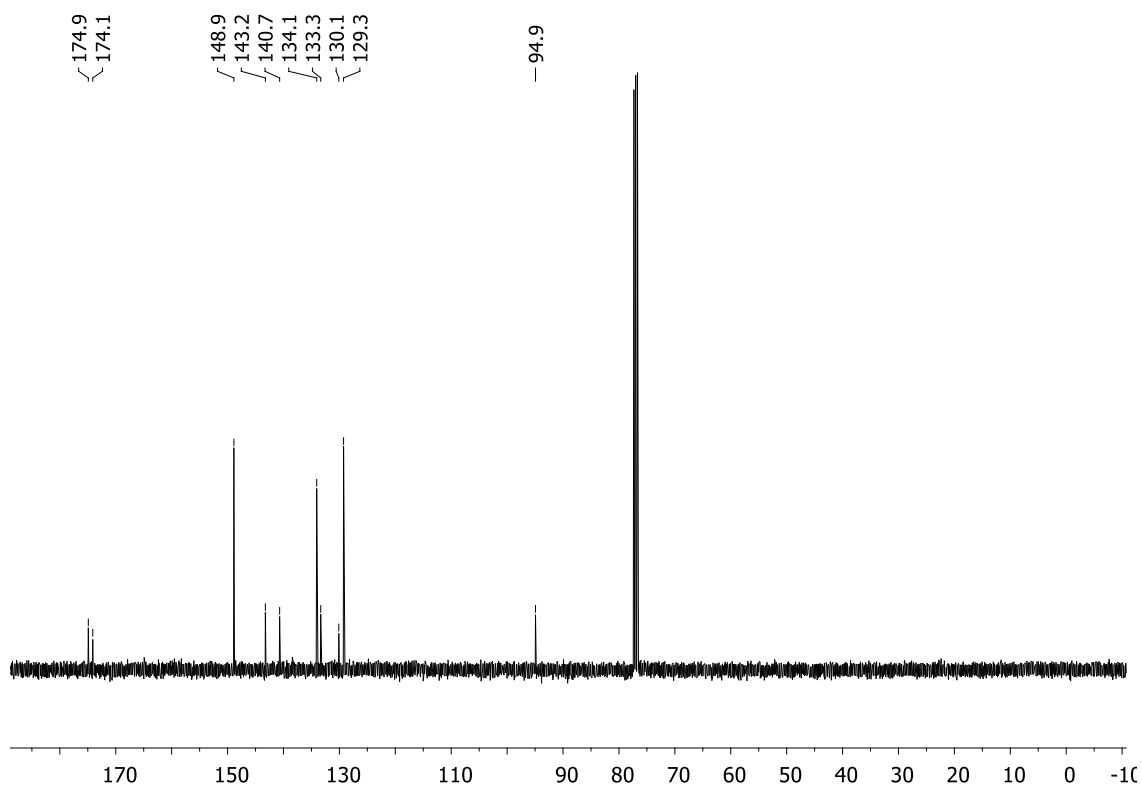


Figure 53. ¹³C NMR spectrum (125 MHz, CDCl₃) of compound **95**.

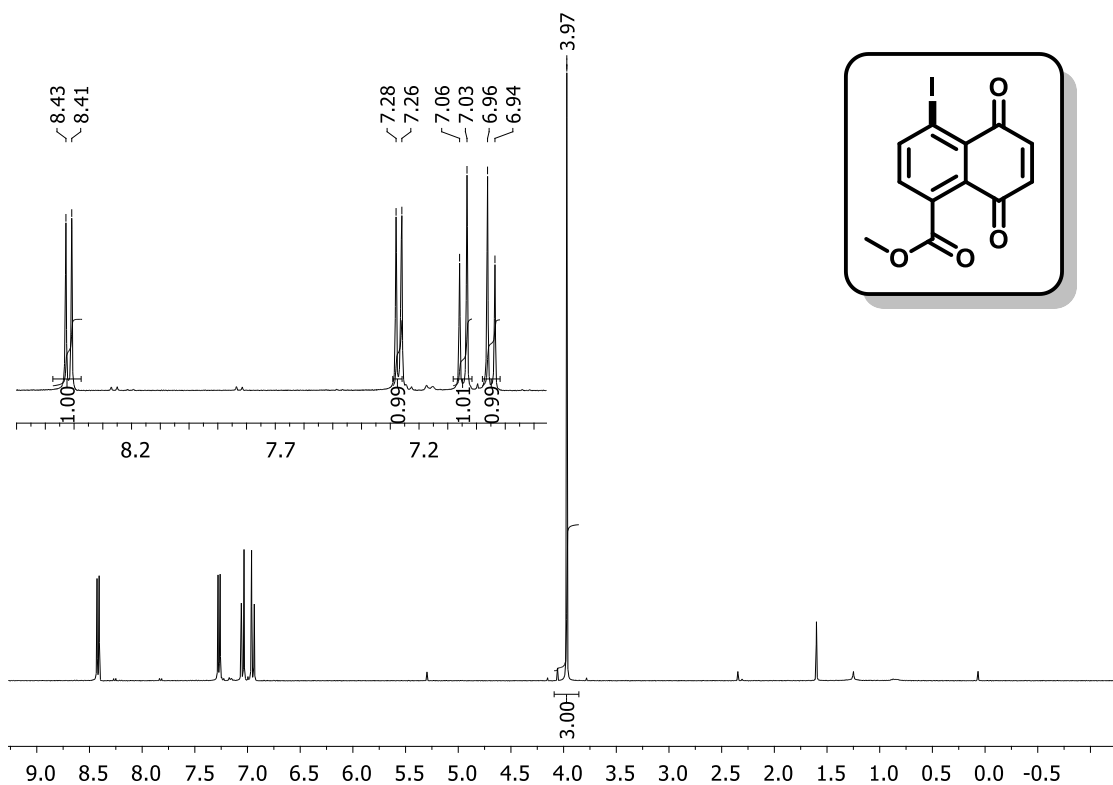


Figure 54. ¹H NMR spectrum (400 MHz, CDCl₃) of compound **96**.

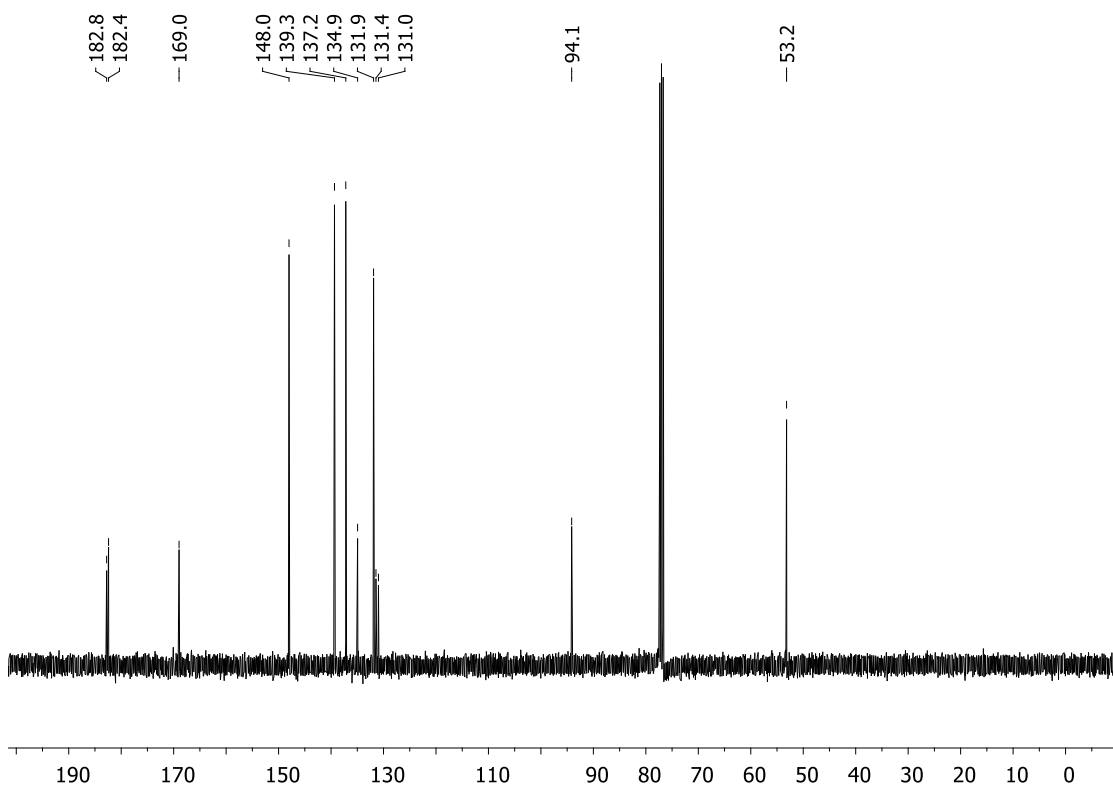


Figure 55. ¹³C NMR spectrum (100 MHz, CDCl₃) of compound **96**.

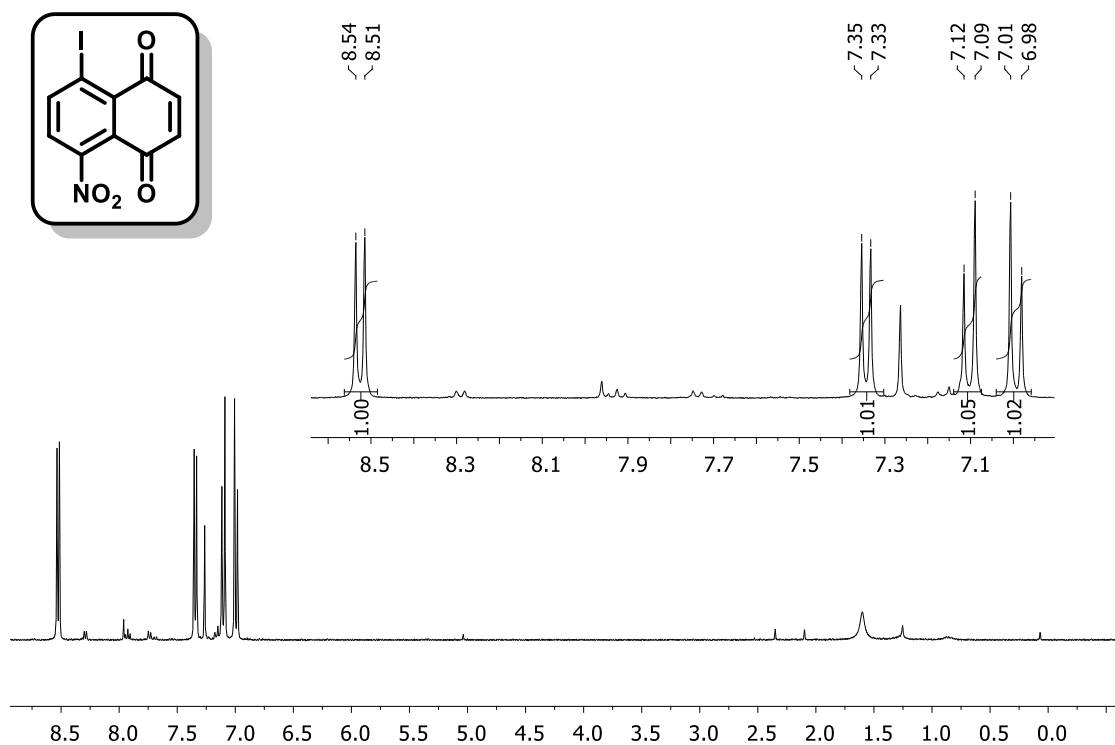


Figure 56. ¹H NMR spectrum (500 MHz, CDCl₃) of compound **97**.

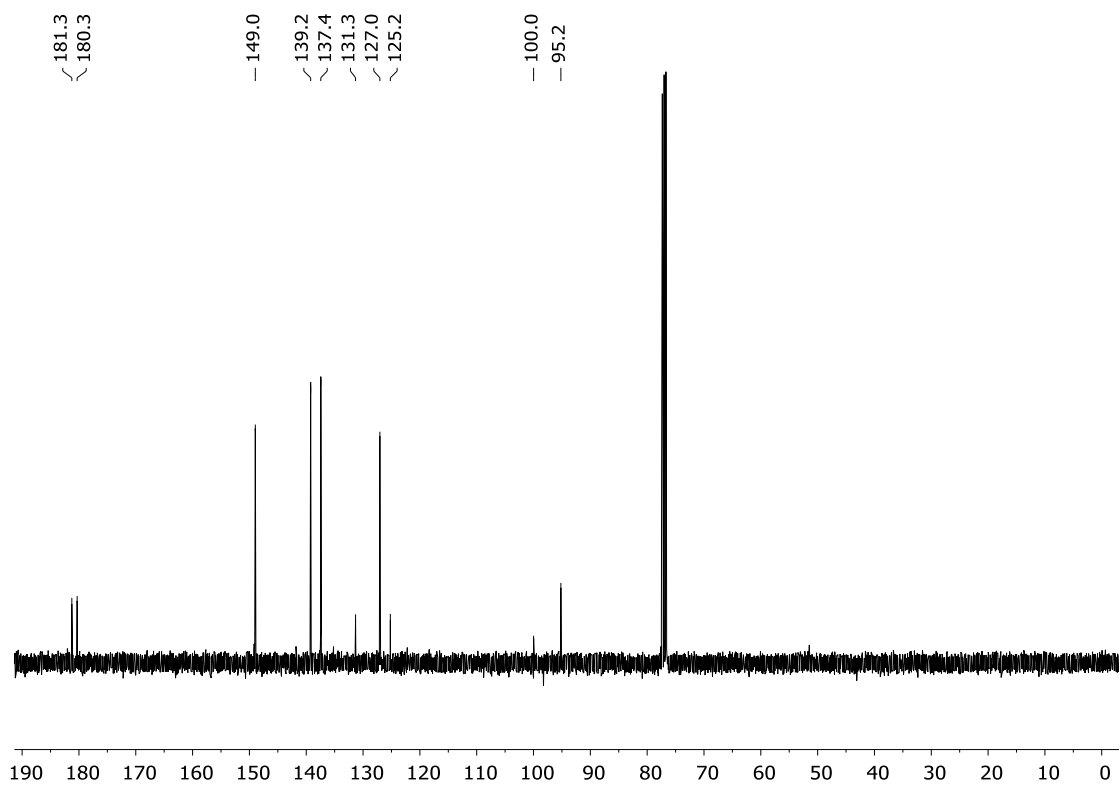


Figure 57. ¹³C NMR spectrum (125 MHz, CDCl₃) of compound **97**.

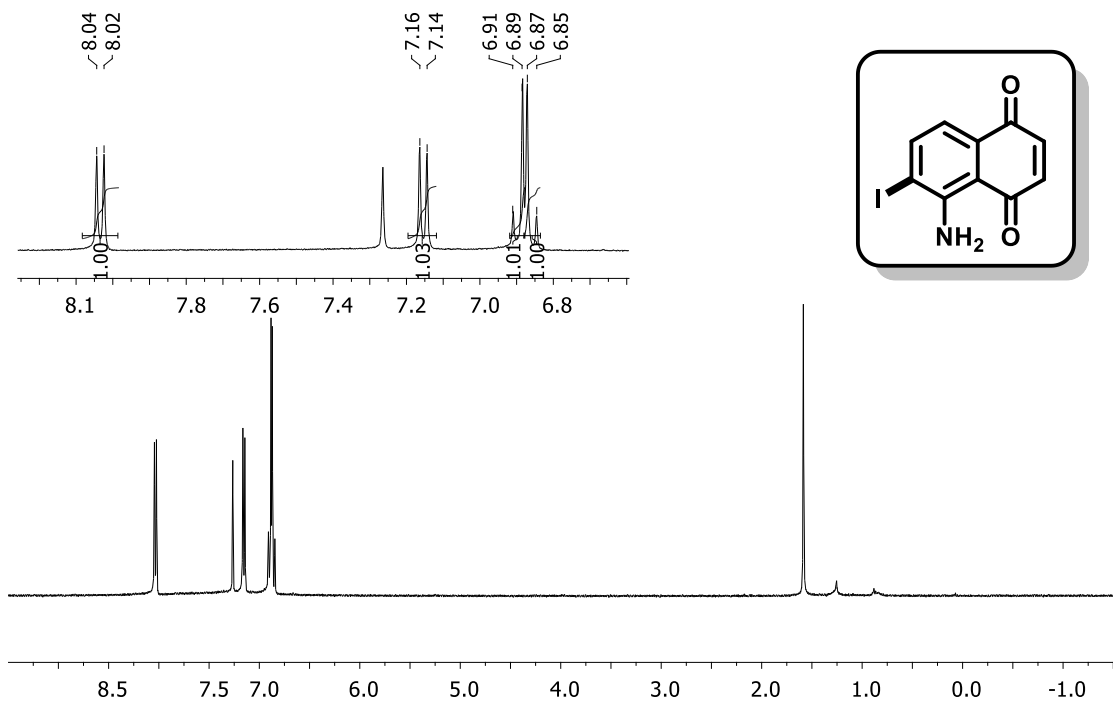


Figure 58. ¹H NMR spectrum (400 MHz, CDCl₃) of compound **98**.

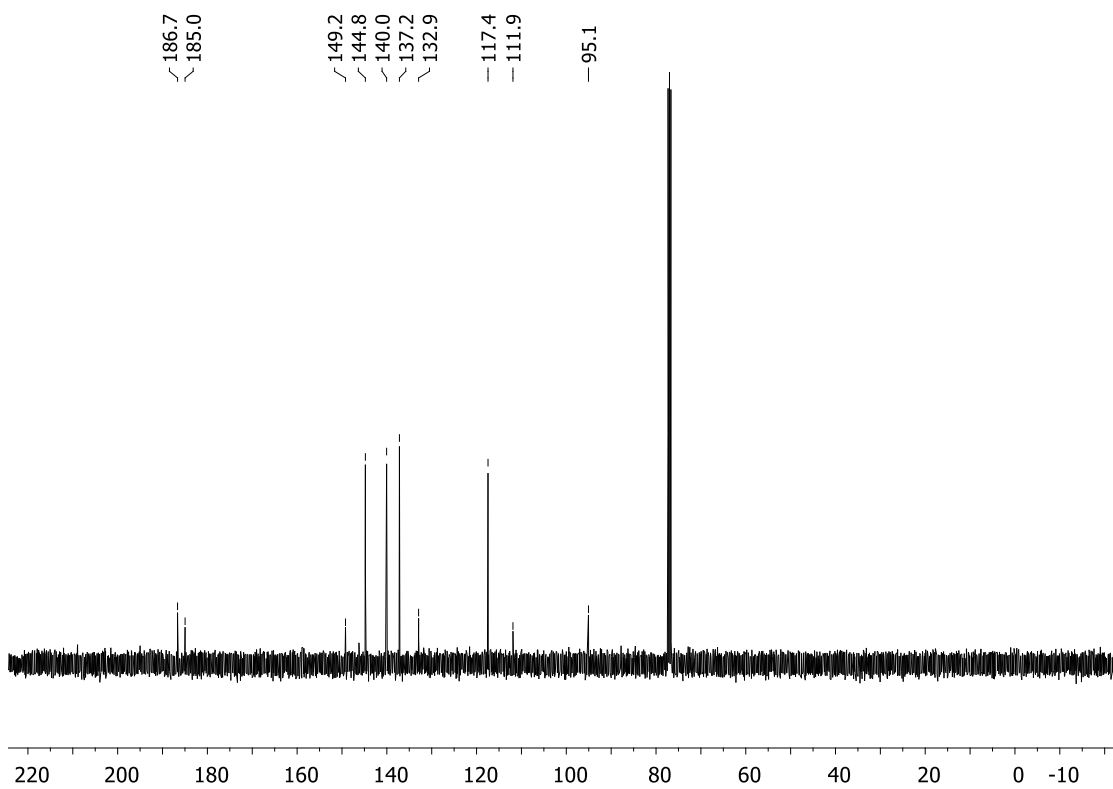


Figure 59. ¹³C NMR spectrum (100 MHz, CDCl₃) of compound **98**.

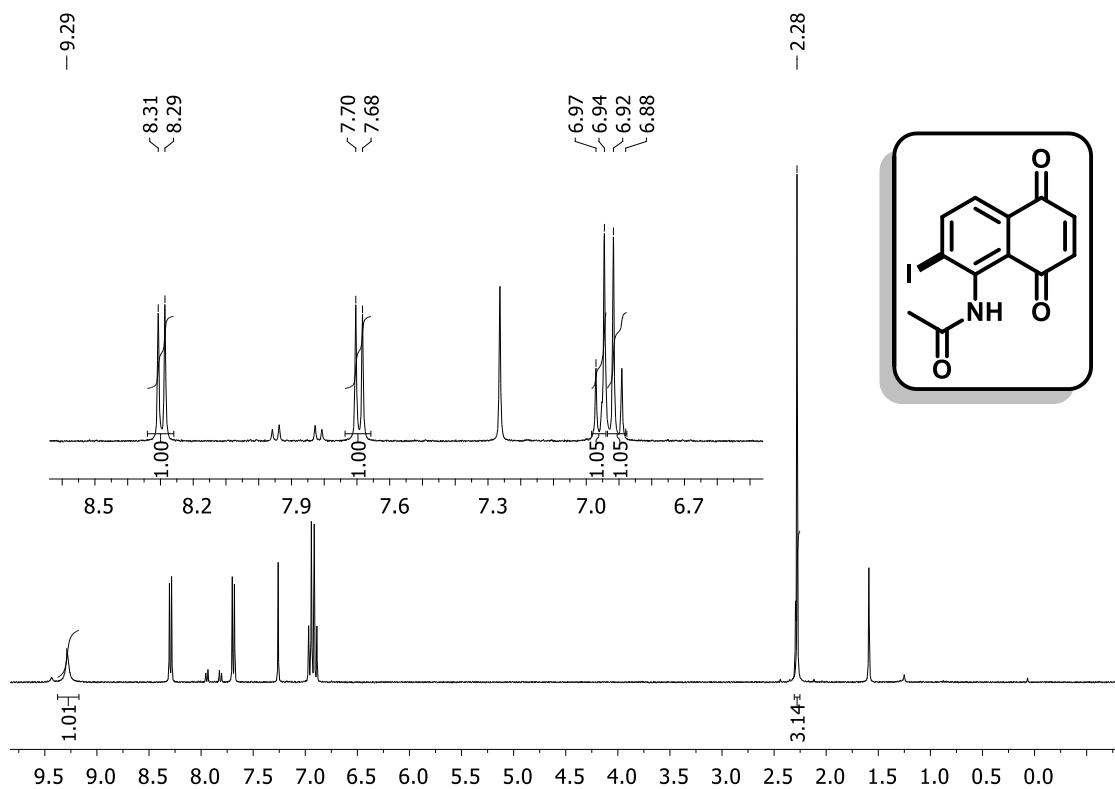


Figure 60. ^1H NMR spectrum (400 MHz, CDCl_3) of compound **100**.

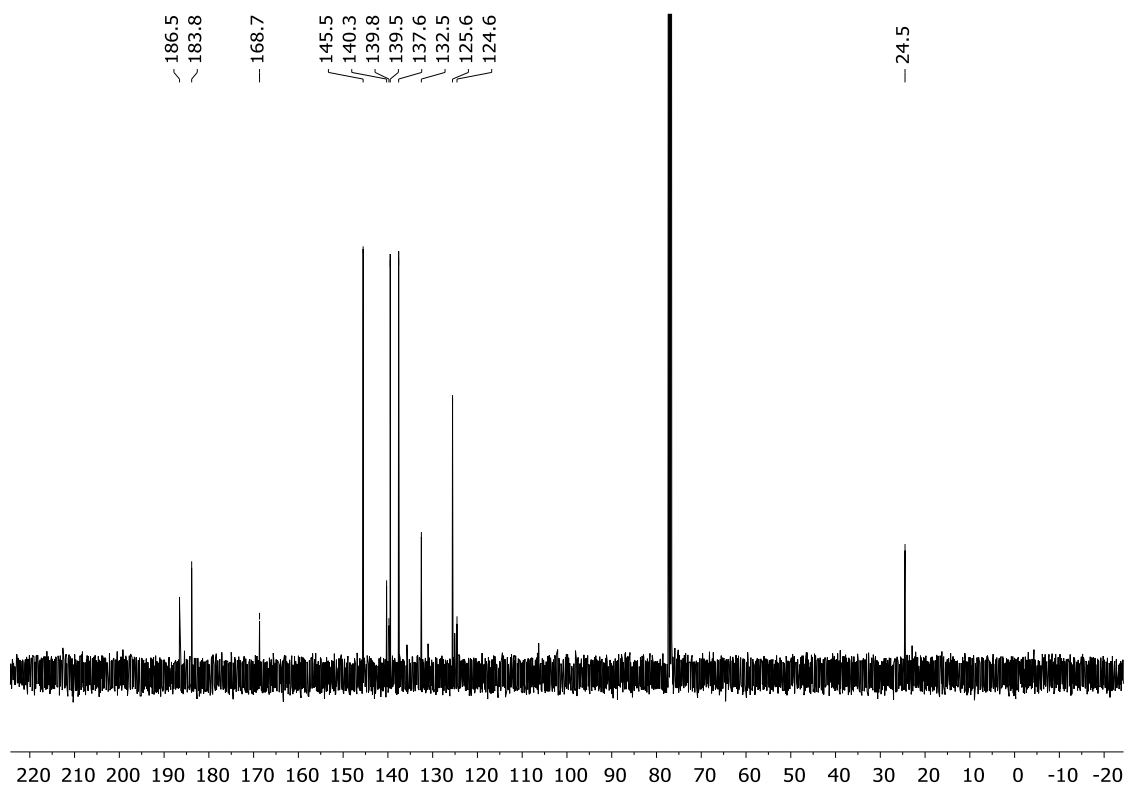


Figure 61. ^{13}C NMR spectrum (100 MHz, CDCl_3) of compound **100**.

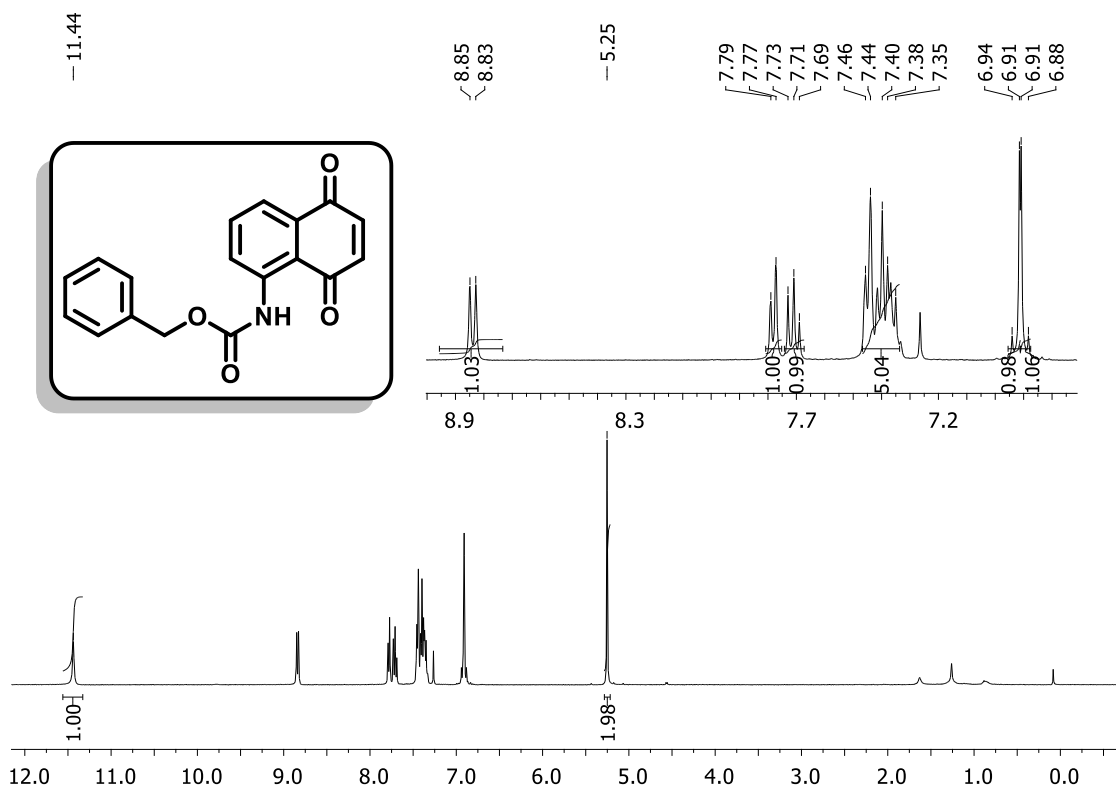


Figure 62. ¹H NMR spectrum (400 MHz, CDCl₃) of compound 101.

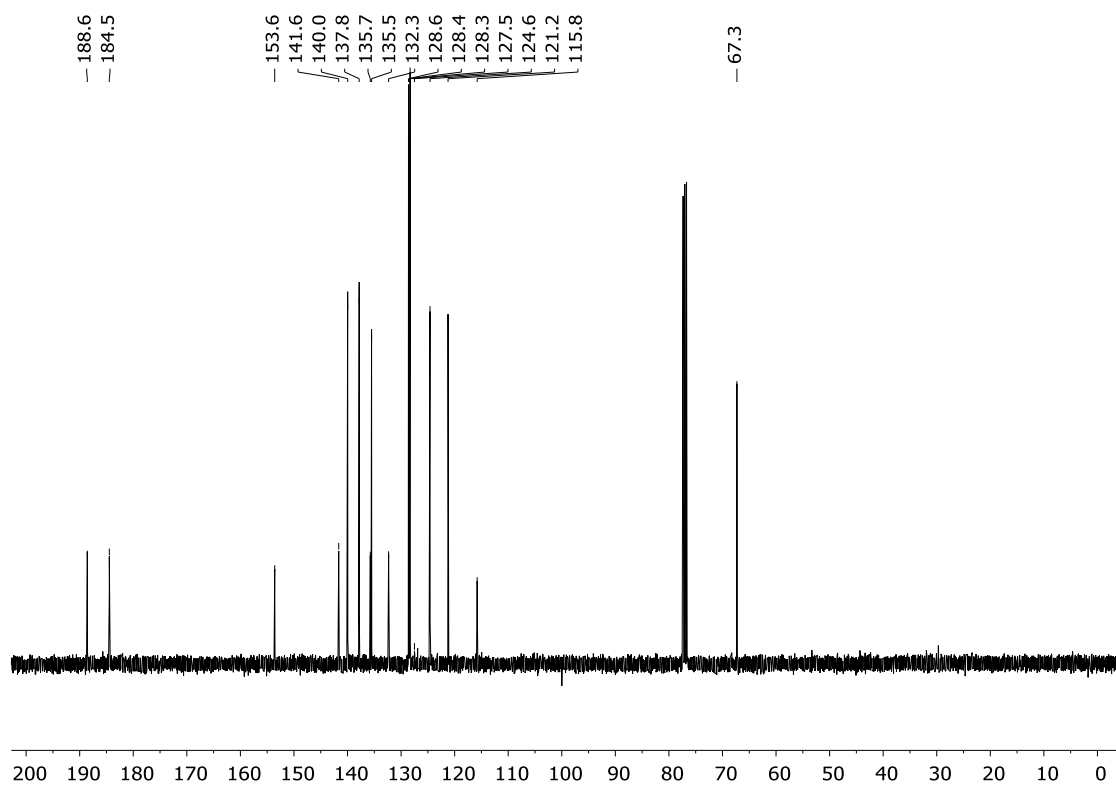


Figure 63. ¹³C NMR spectrum (100 MHz, CDCl₃) of compound 101.

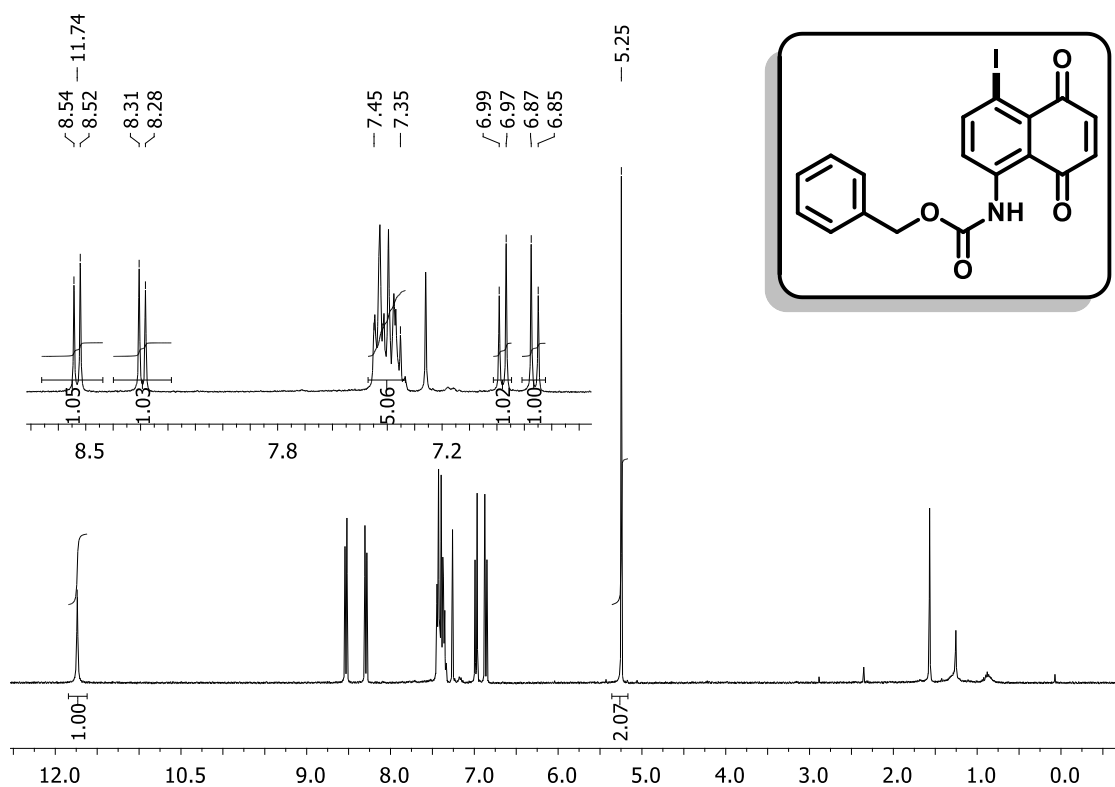


Figure 64. ¹H NMR spectrum (400 MHz, CDCl₃) of compound **102**.

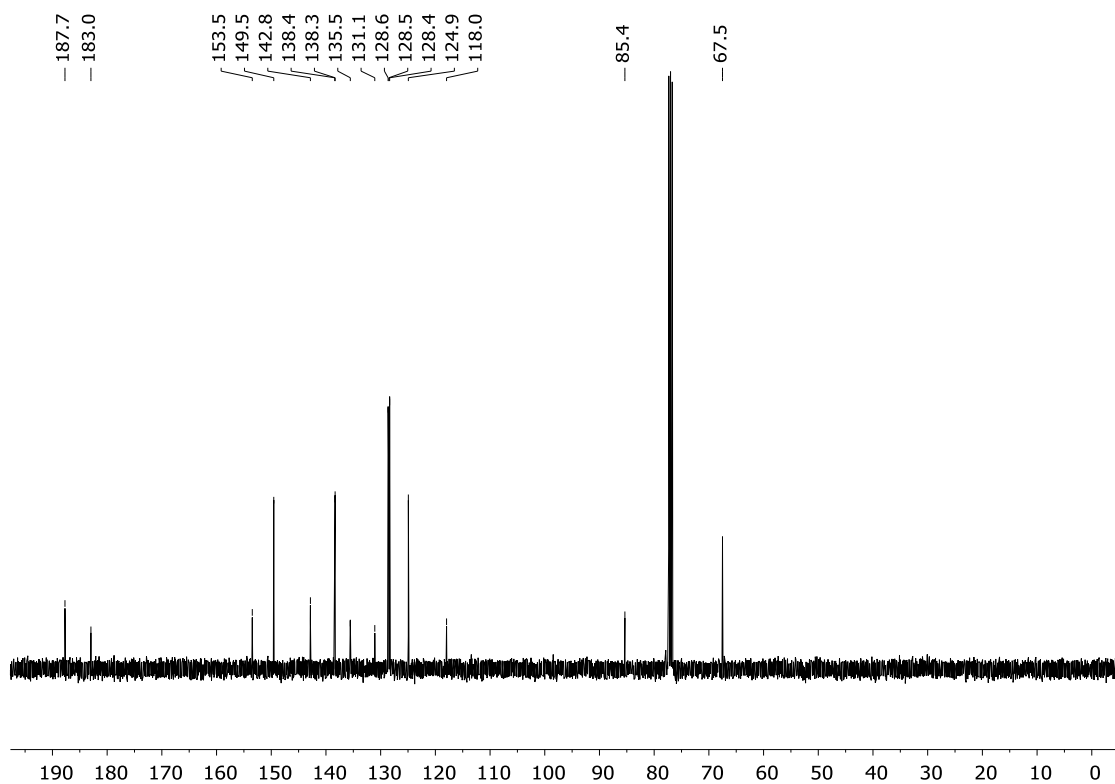


Figure 65. ¹³C NMR spectrum (100 MHz, CDCl₃) of compound **102**.

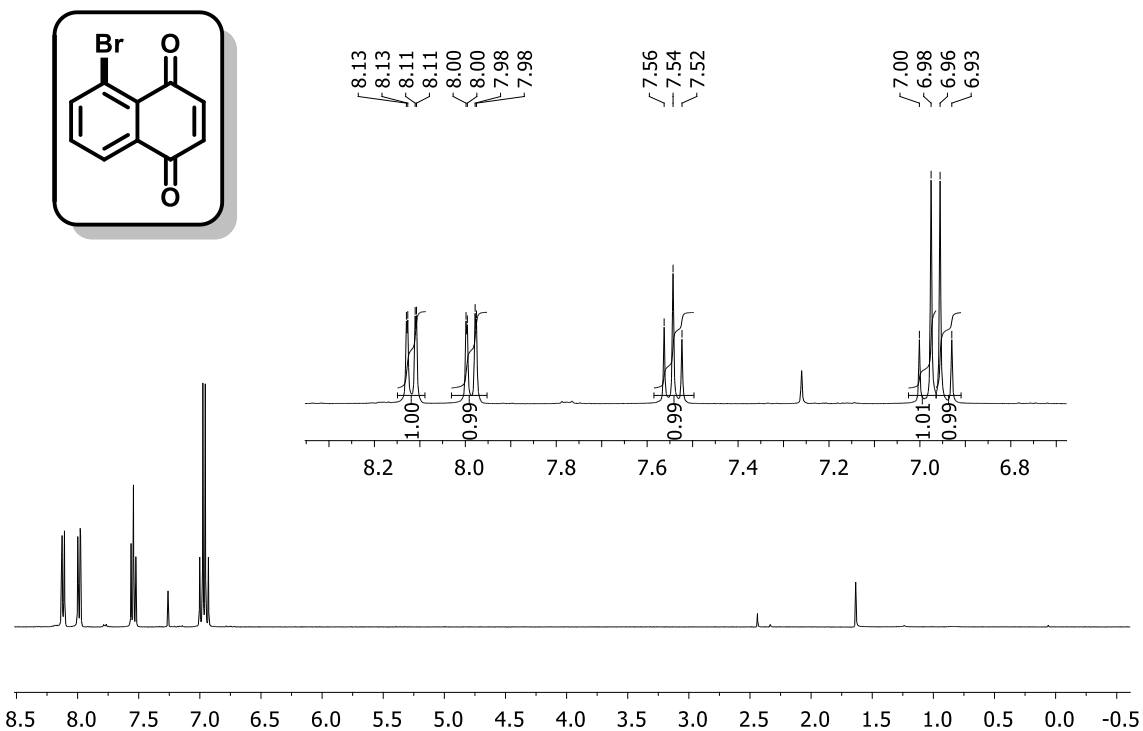


Figure 66. ¹H NMR spectrum (400 MHz, CDCl₃) of compound 107.

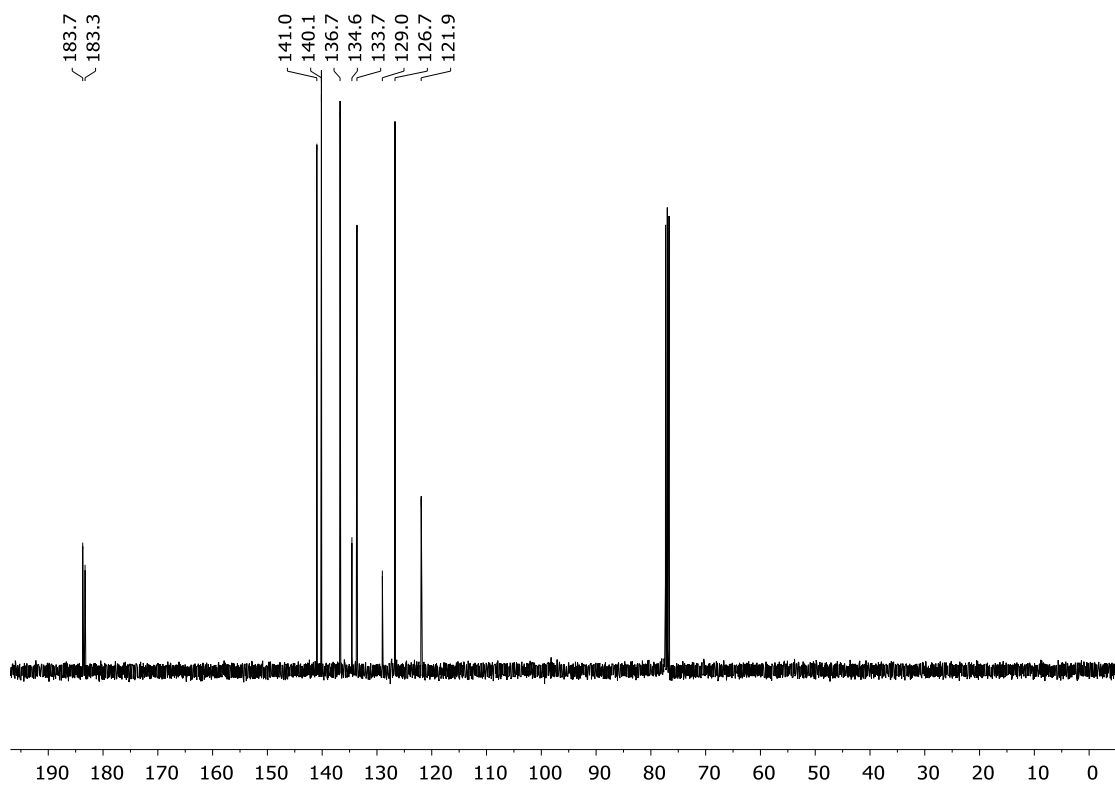


Figure 67. ¹³C NMR spectrum (100 MHz, CDCl₃) of compound 107.

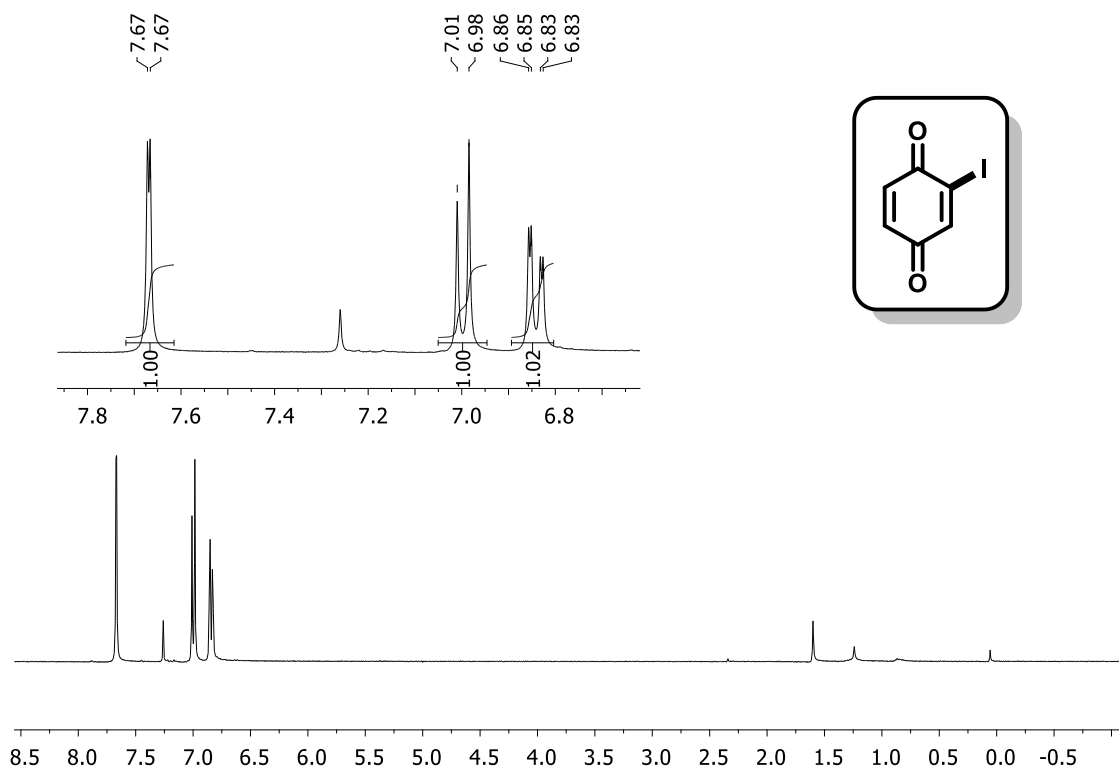


Figure 68. ¹H NMR spectrum (400 MHz, CDCl₃) of compound 108.

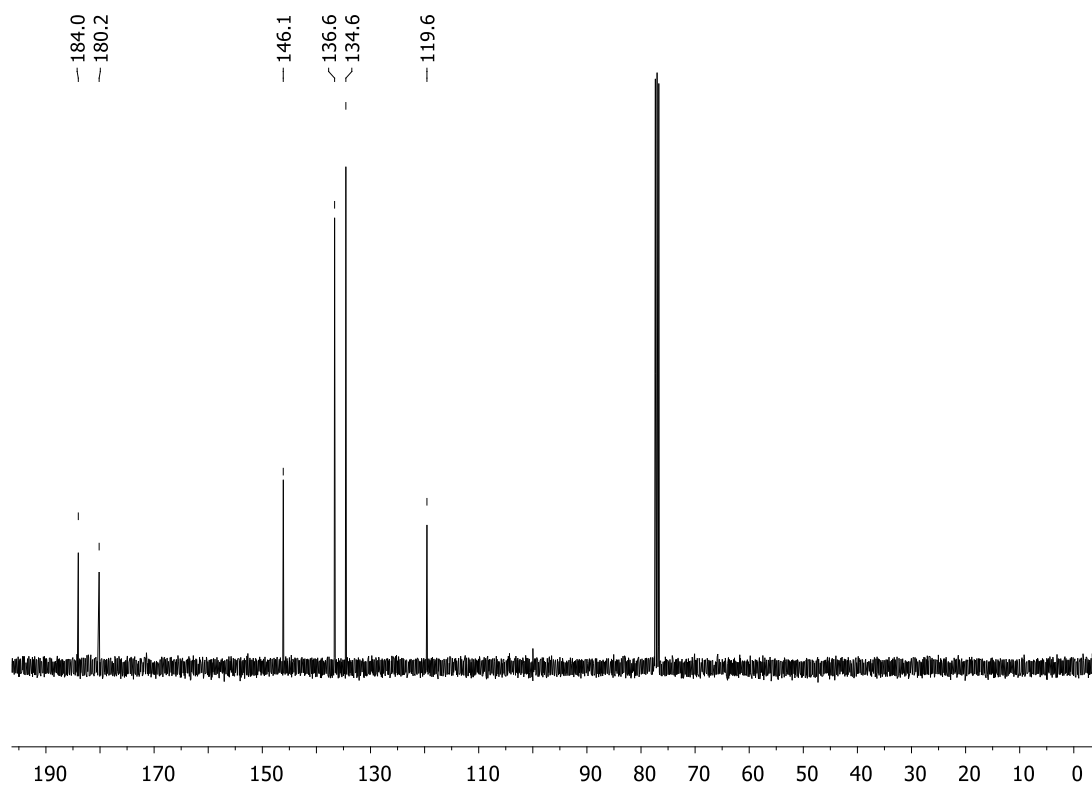


Figure 69. ¹³C NMR spectrum (100 MHz, CDCl₃) of compound 108.

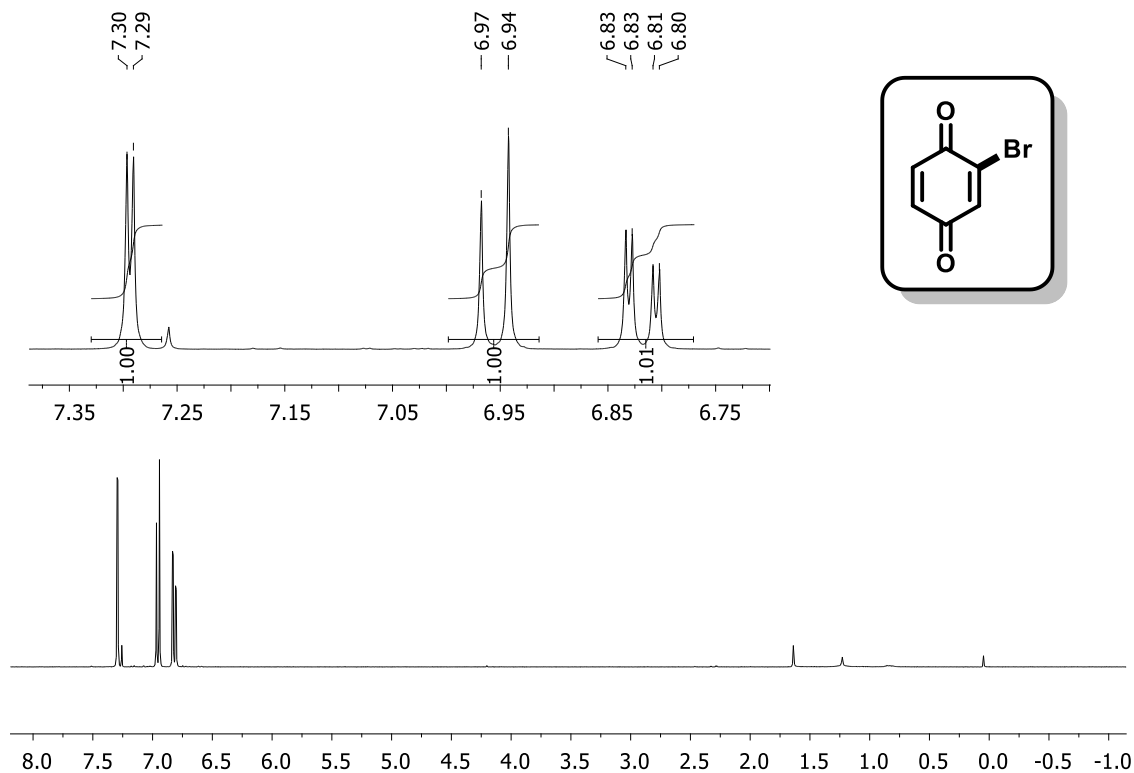


Figure 70. ^1H NMR spectrum (400 MHz, CDCl_3) of compound **109**.

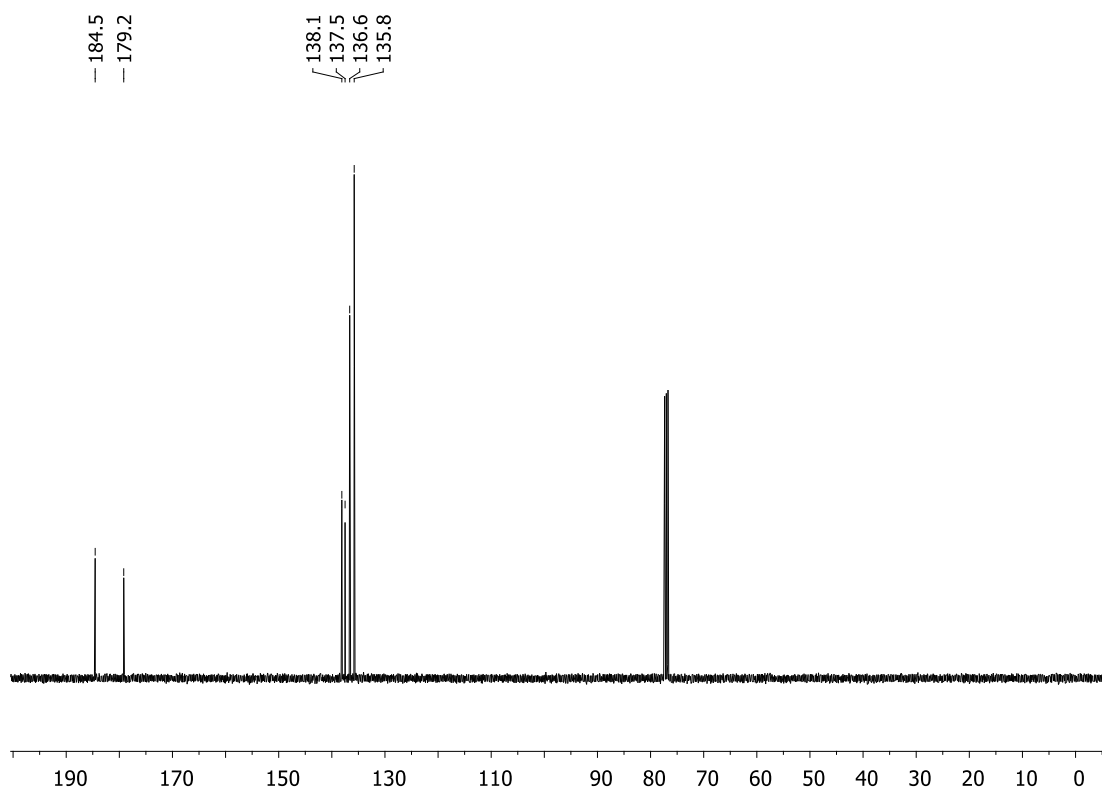


Figure 71. ^{13}C NMR spectrum (100 MHz, CDCl_3) of compound **109**.

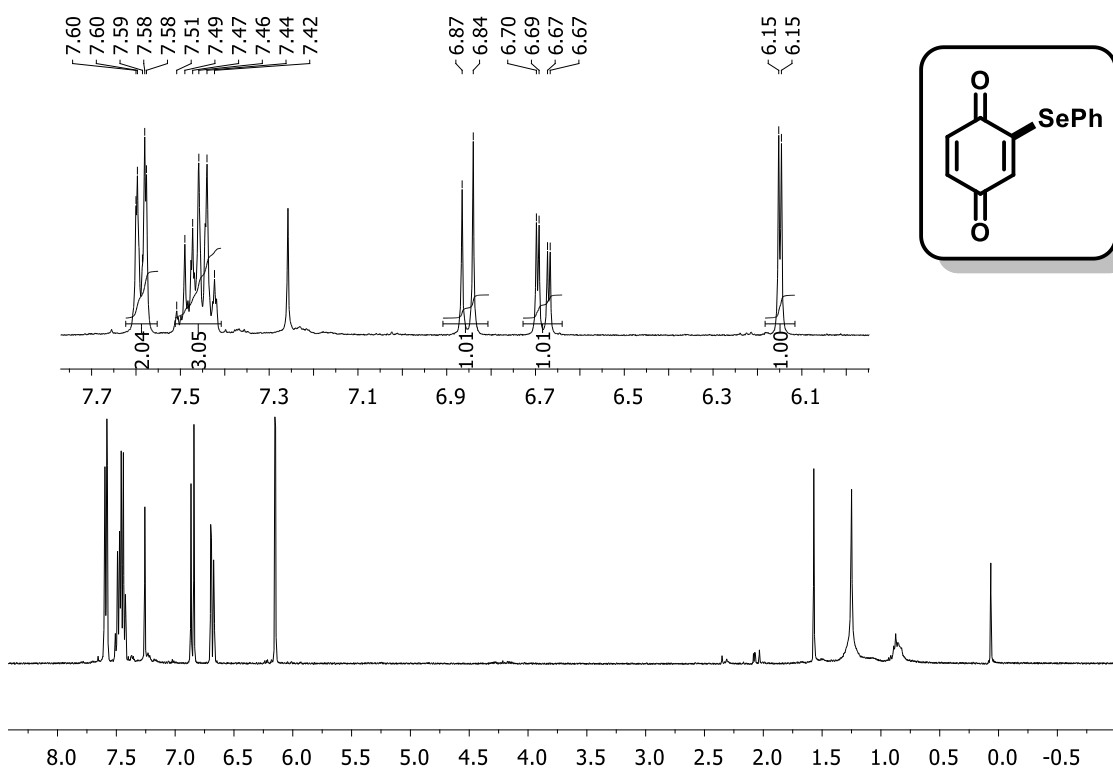


Figure 72. ¹H NMR spectrum (400 MHz, CDCl₃) of compound **110**.

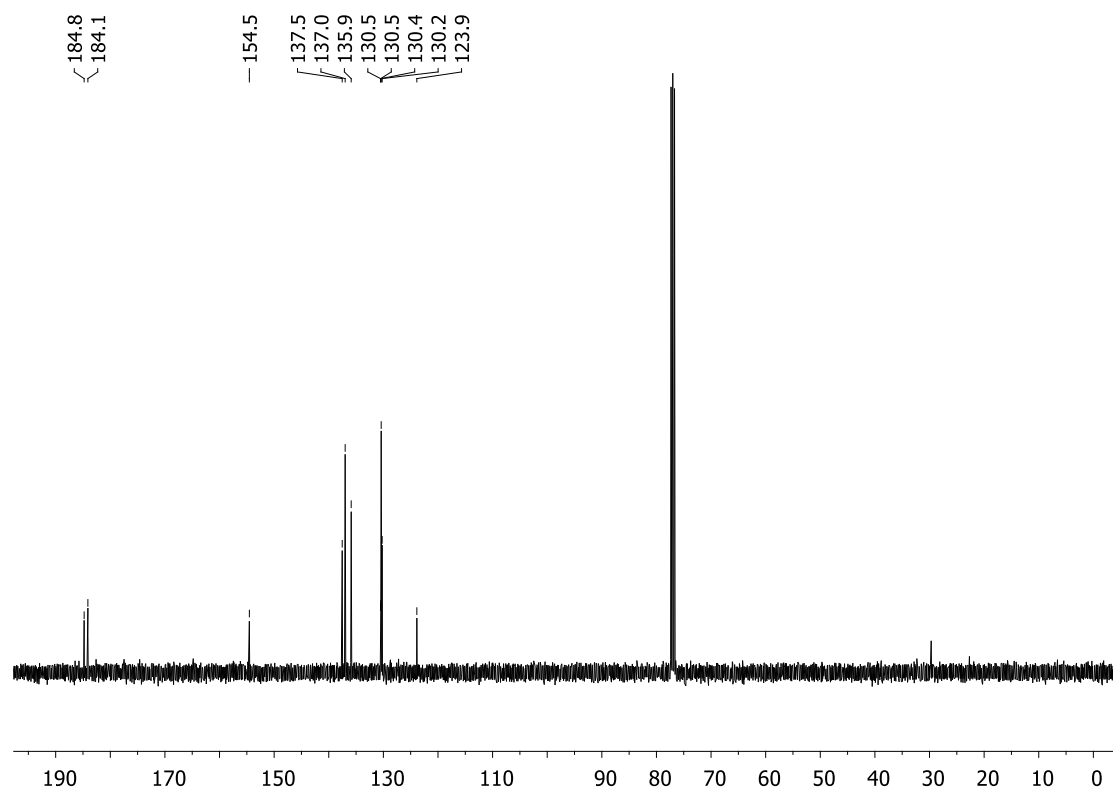


Figure 73. ¹³C NMR spectrum (100 MHz, CDCl₃) of compound **110**.

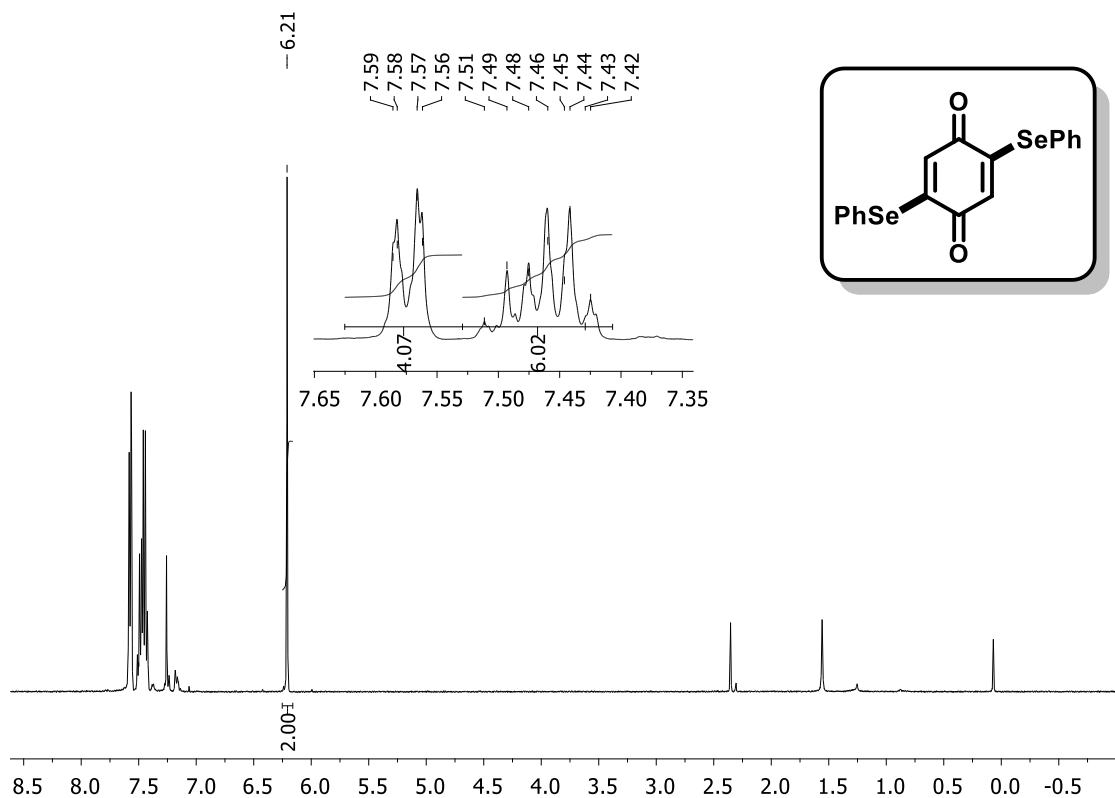


Figure 74. ^1H NMR spectrum (400 MHz, CDCl_3) of compound **111**.

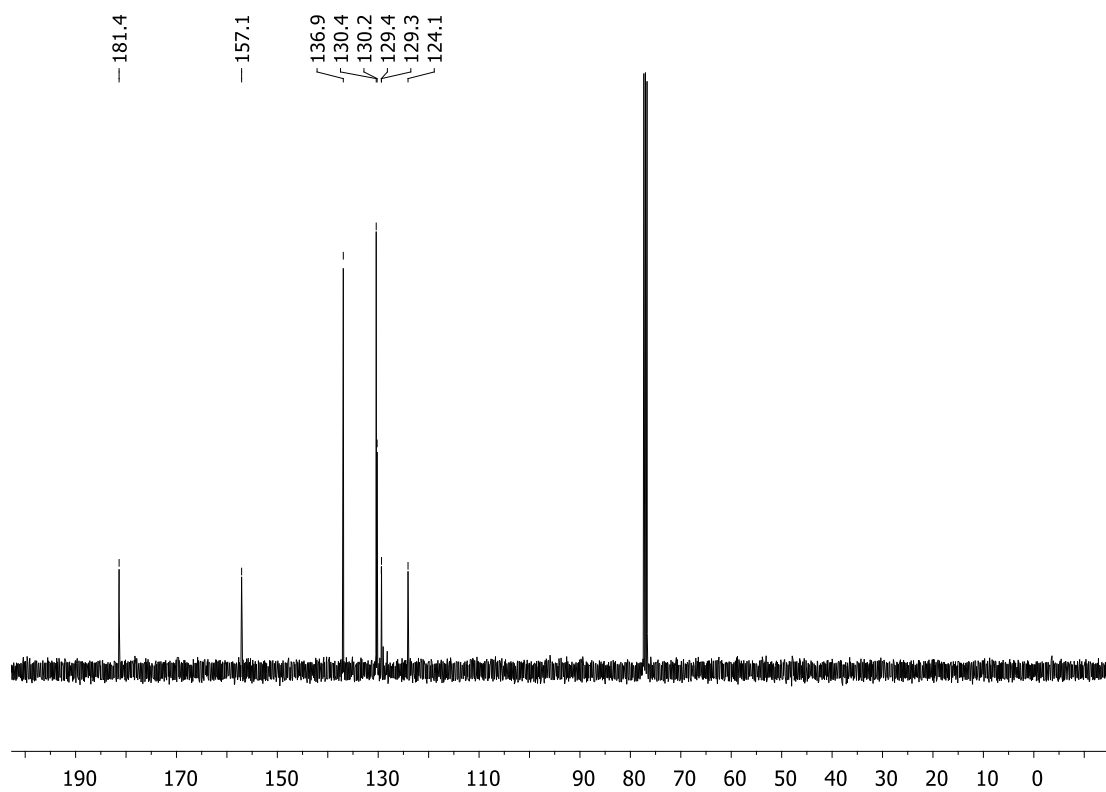


Figure 75. ^{13}C NMR spectrum (100 MHz, CDCl_3) of compound **111**.

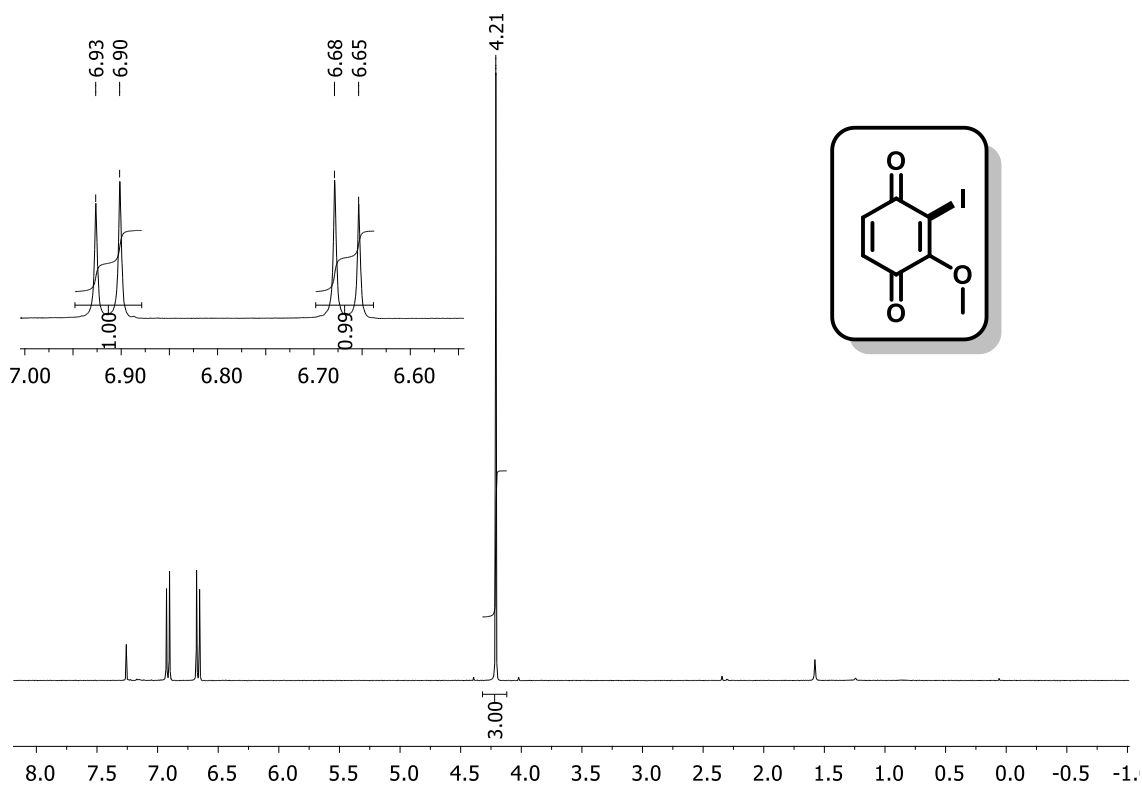


Figure 76. ^1H NMR spectrum (400 MHz, CDCl_3) of compound **114**.

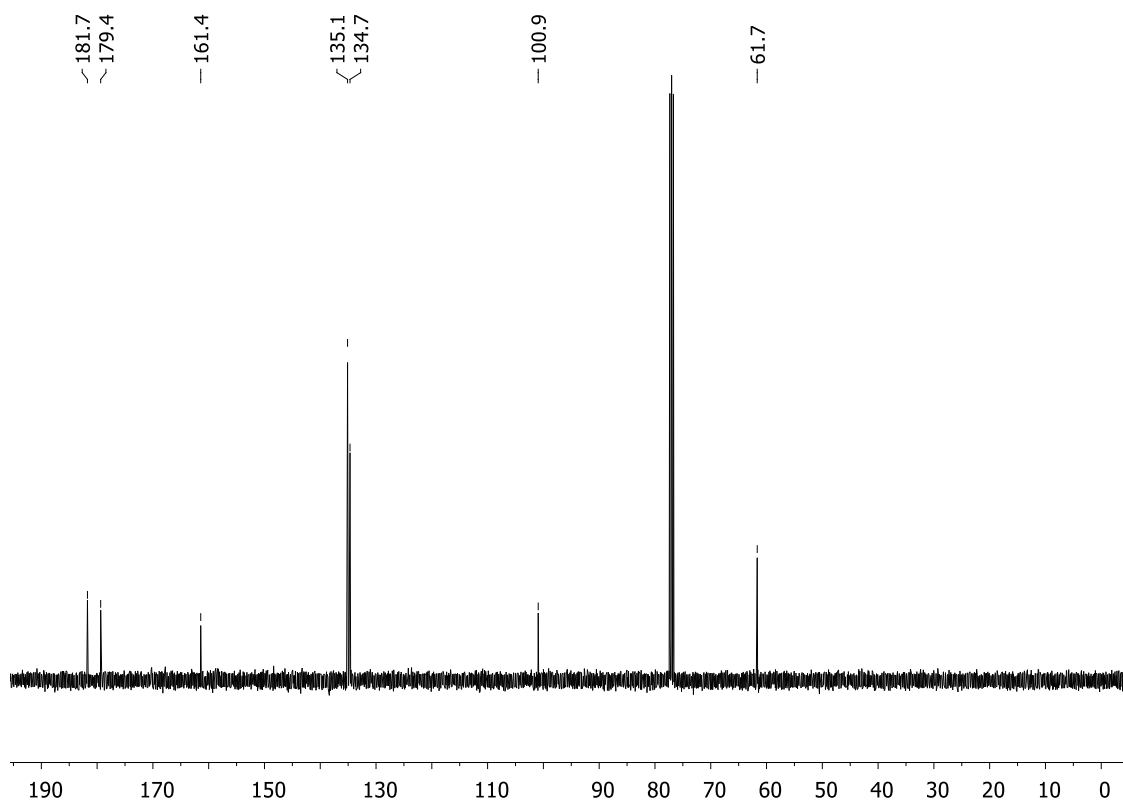


Figure 77. ^{13}C NMR spectrum (100 MHz, CDCl_3) of compound **114**.

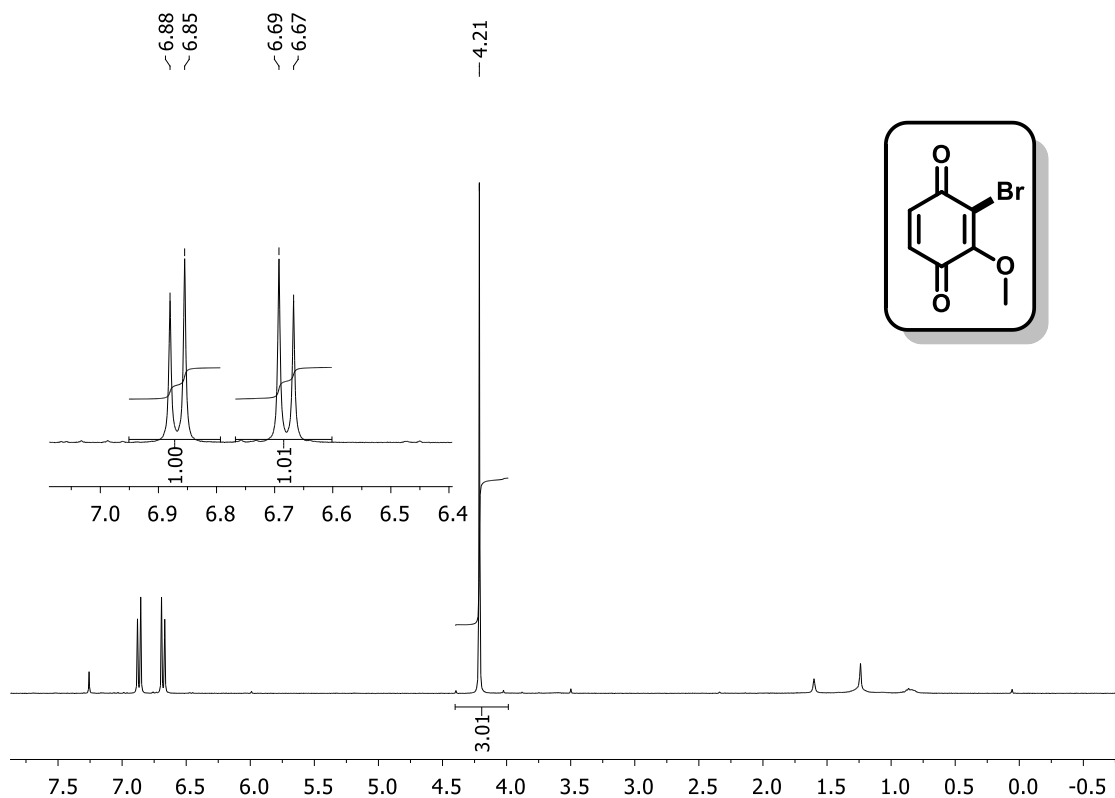


Figure 78. ¹H NMR spectrum (400 MHz, CDCl₃) of compound **115**.

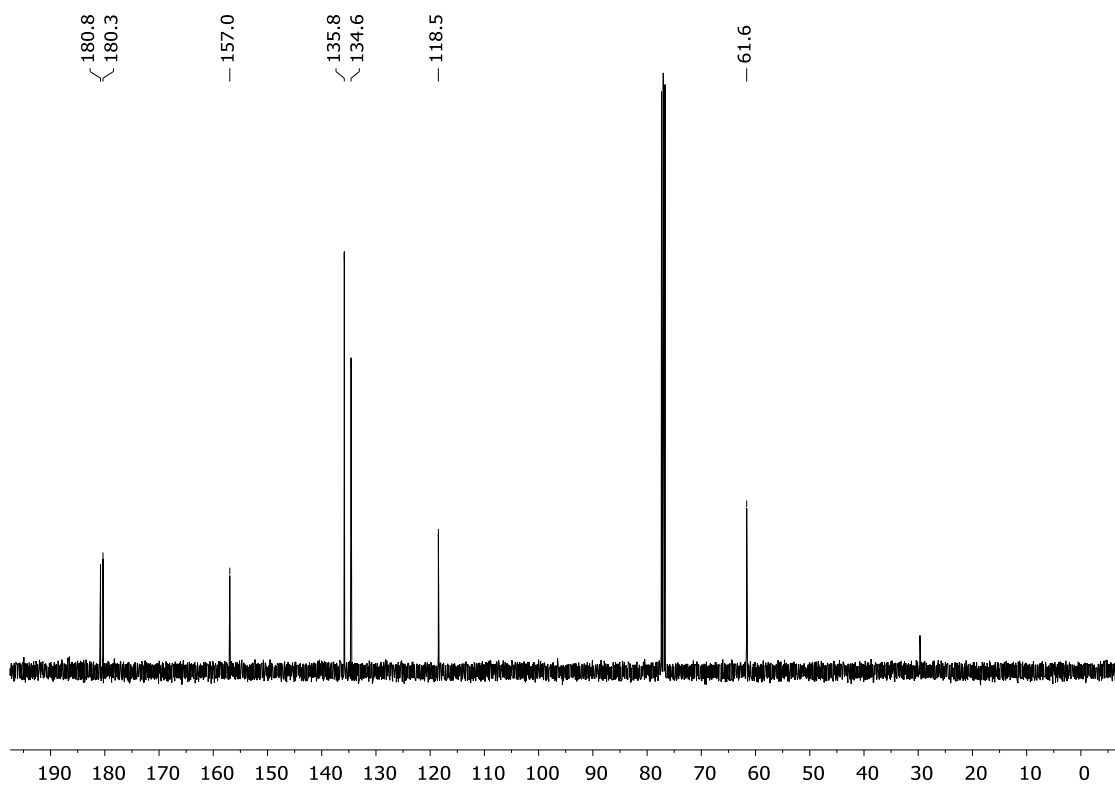


Figure 79. ¹³C NMR spectrum (100 MHz, CDCl₃) of compound **115**.

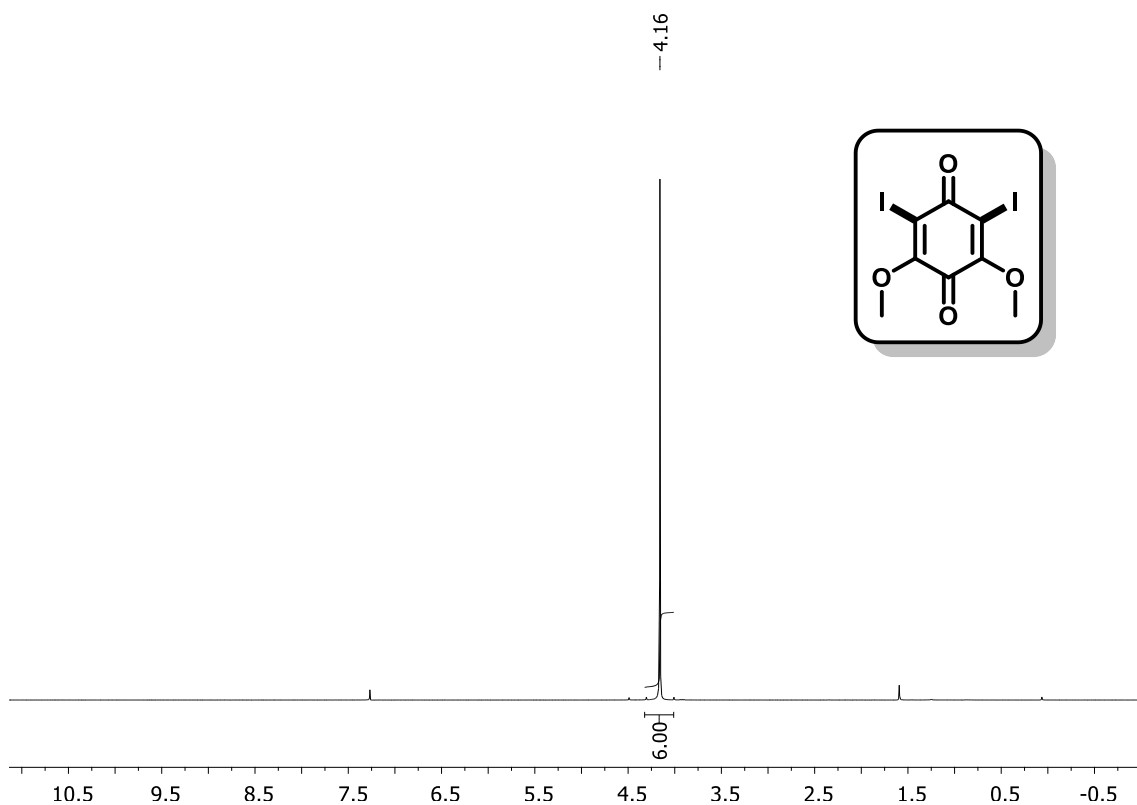


Figure 80. ¹H NMR spectrum (400 MHz, CDCl₃) of compound **116**.

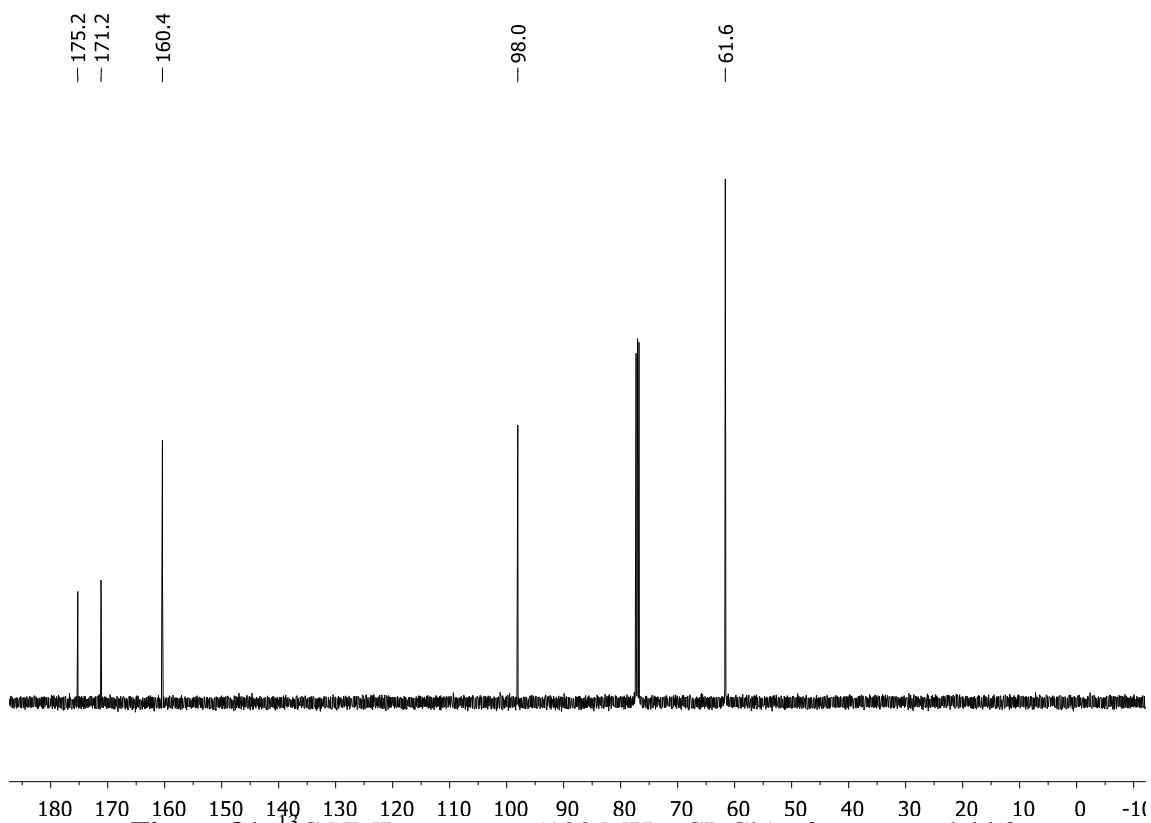


Figure 81. ¹³C NMR spectrum (100 MHz, CDCl₃) of compound **116**.

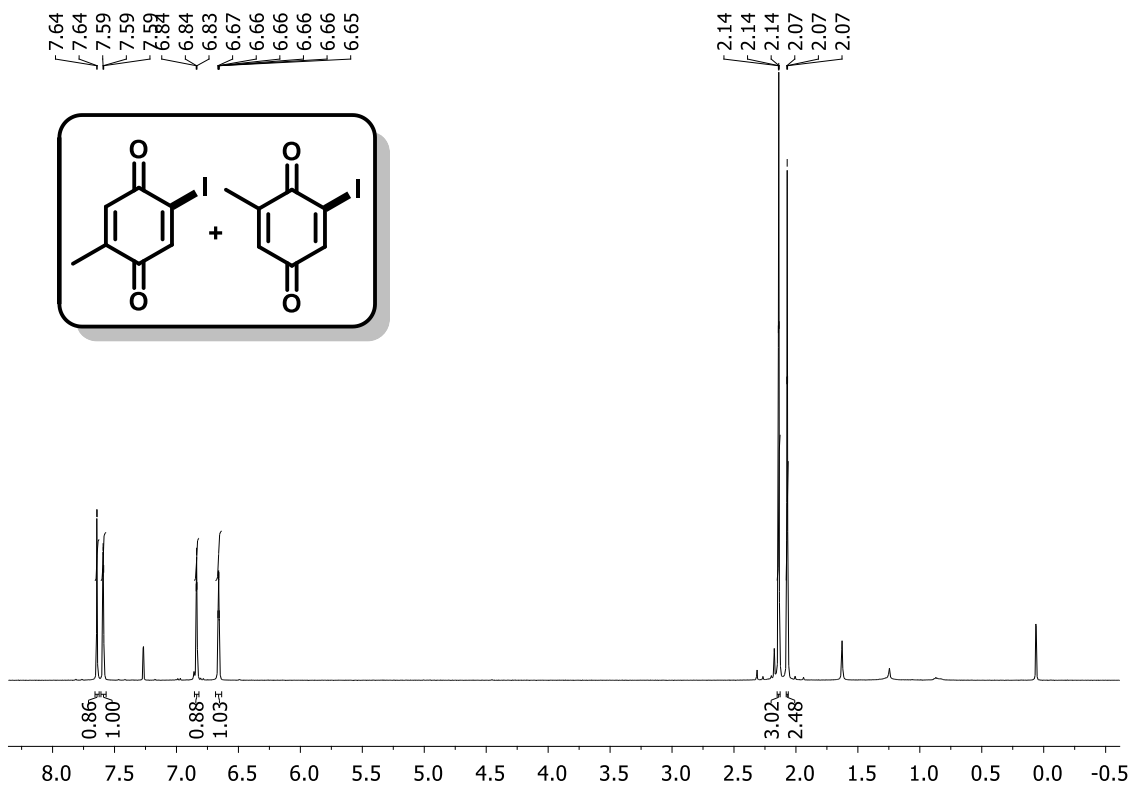


Figure 82. ^1H NMR spectrum (400 MHz, CDCl_3) of compounds 118 and 119.

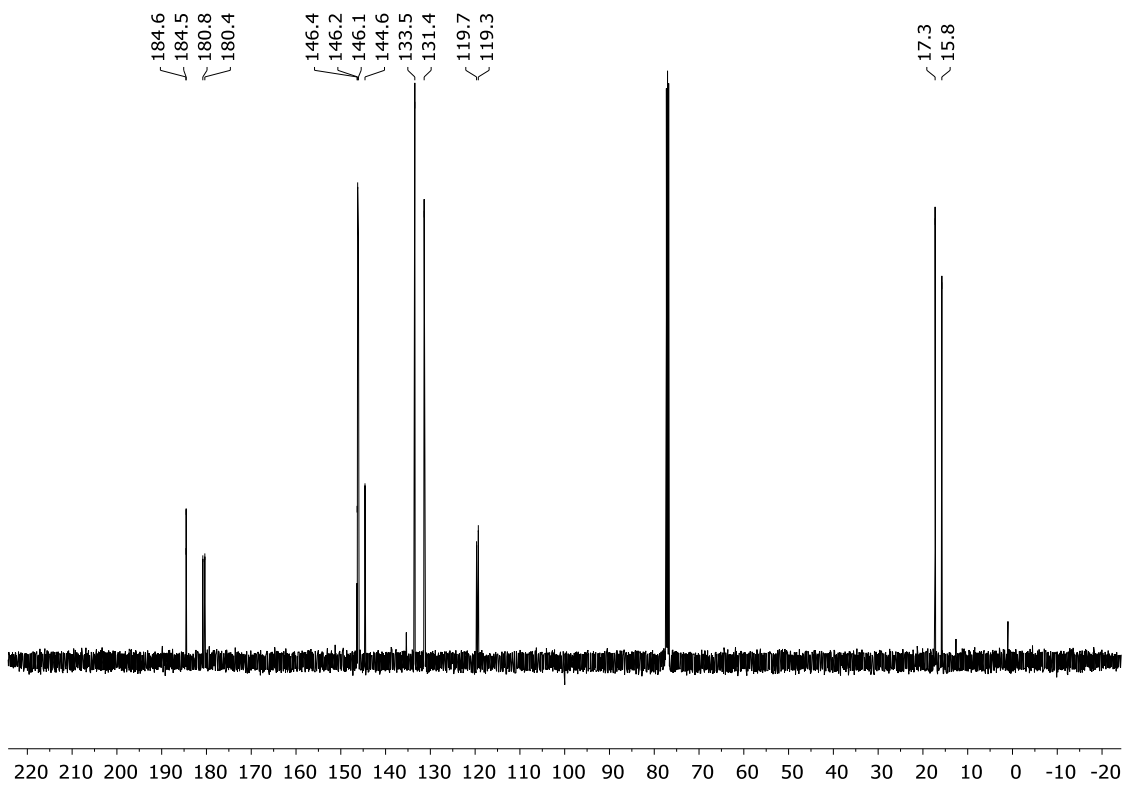


Figure 83. ^{13}C NMR spectrum (100 MHz, CDCl_3) of compound 118 and 119.

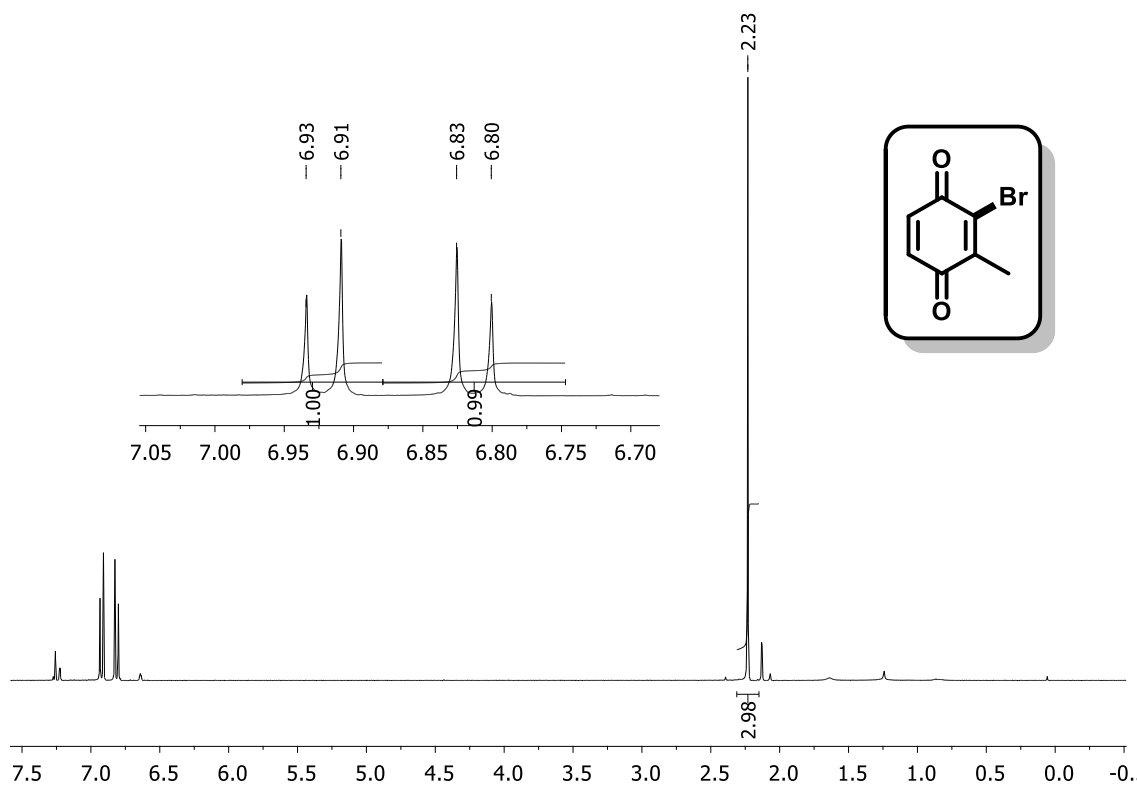


Figure 84. ¹H NMR spectrum (400 MHz, CDCl₃) of compound **120**.

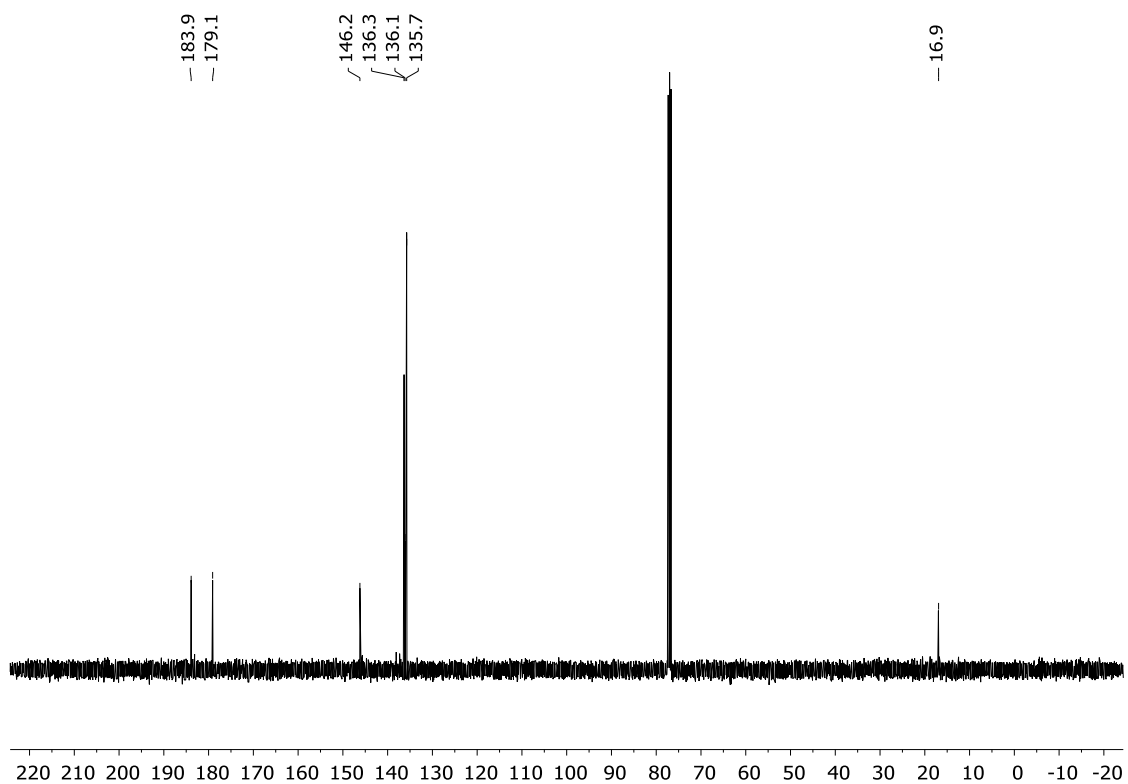


Figure 85. ¹³C NMR spectrum (100 MHz, CDCl₃) of compound **120**.

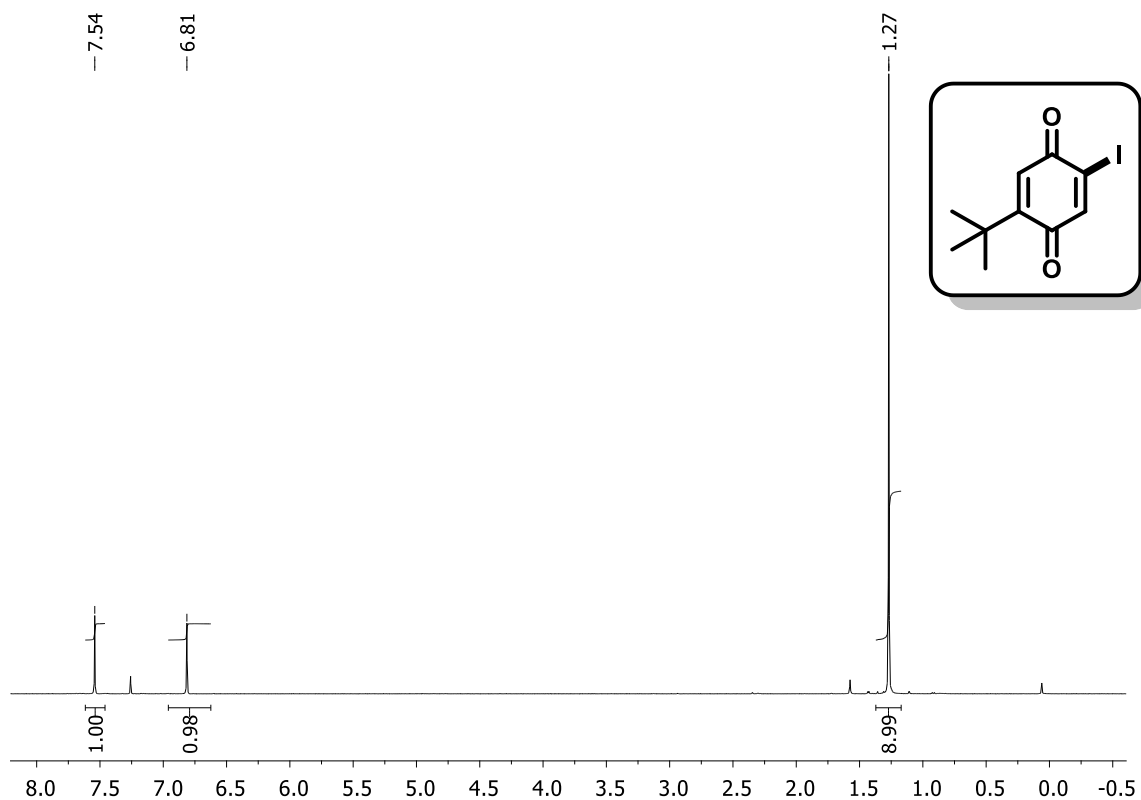


Figure 86. ¹H NMR spectrum (400 MHz, CDCl₃) of compound **122**.

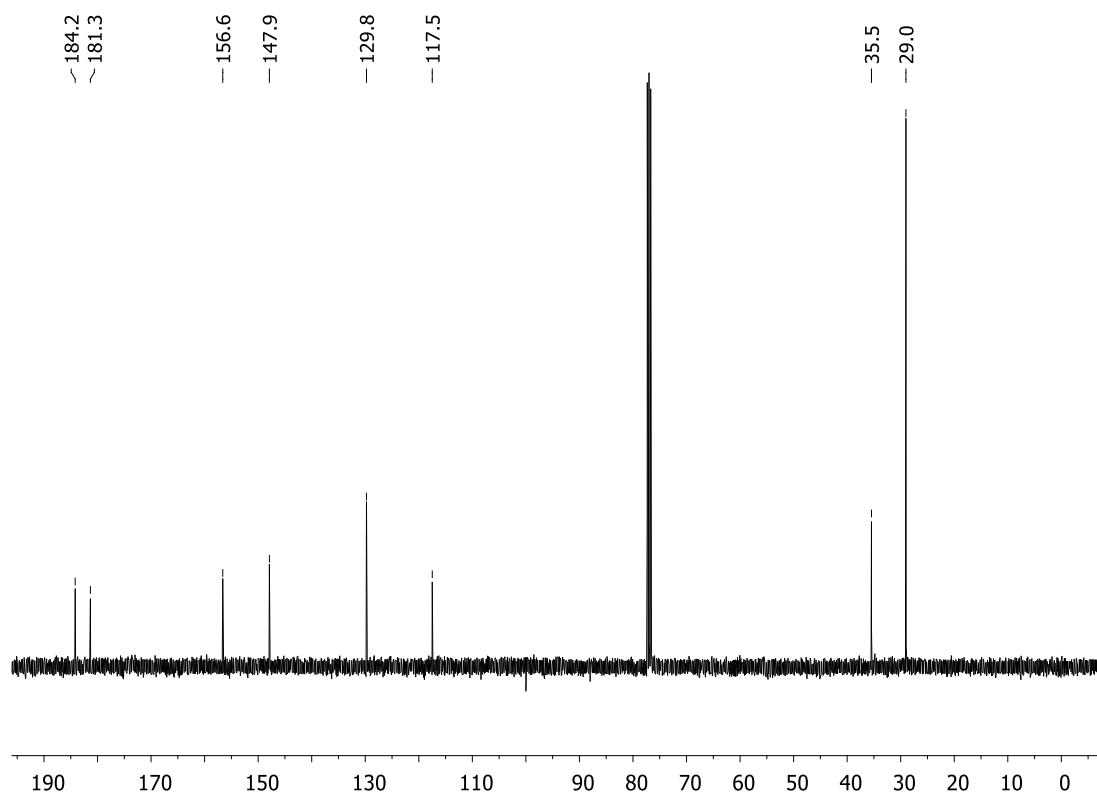


Figure 87. ¹³C NMR spectrum (100 MHz, CDCl₃) of compound **122**.

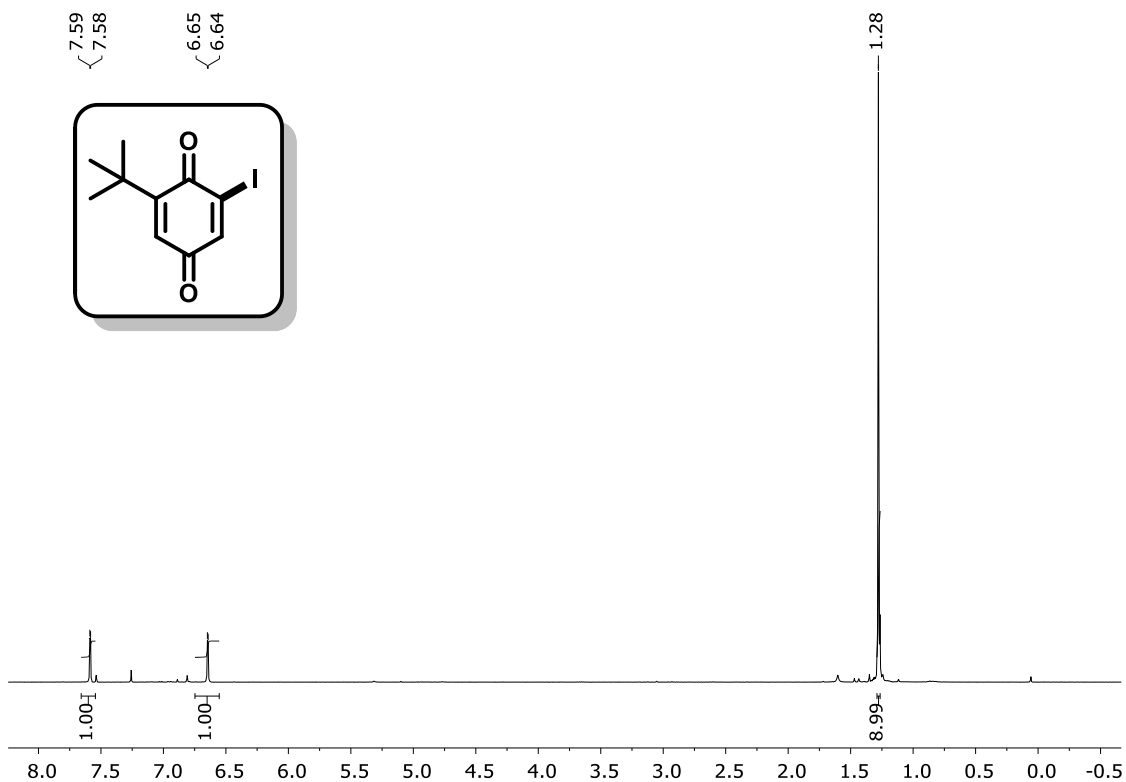


Figure 88. ^1H NMR spectrum (400 MHz, CDCl_3) of compound **123**.

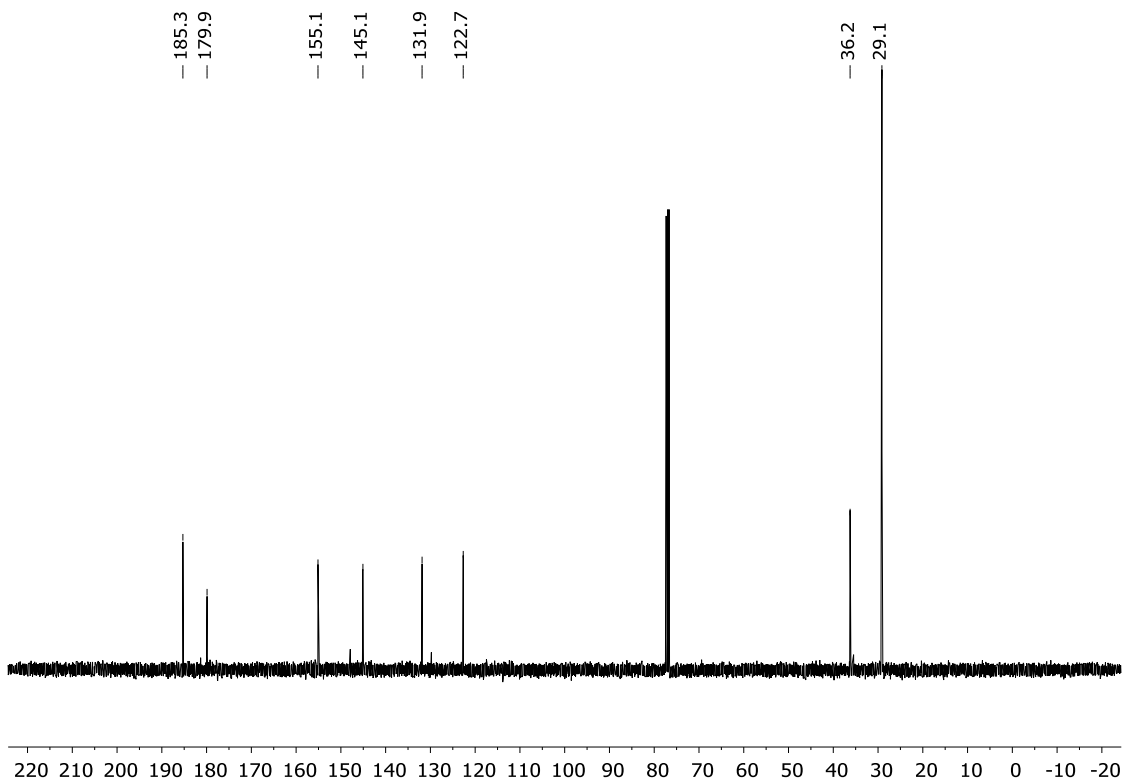


Figure 89. ^{13}C NMR spectrum (100 MHz, CDCl_3) of compound **123**.

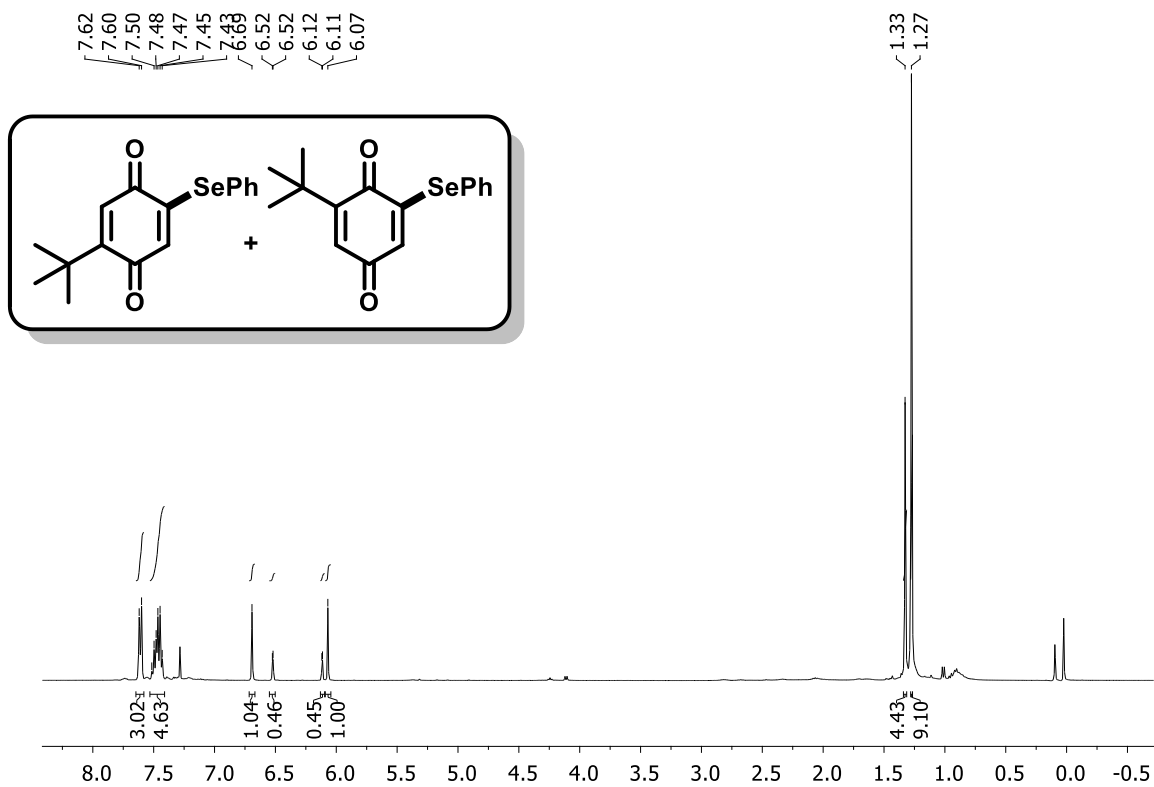


Figure 90. ¹H NMR spectrum (400 MHz, CDCl₃) of compounds **124** and **125**.

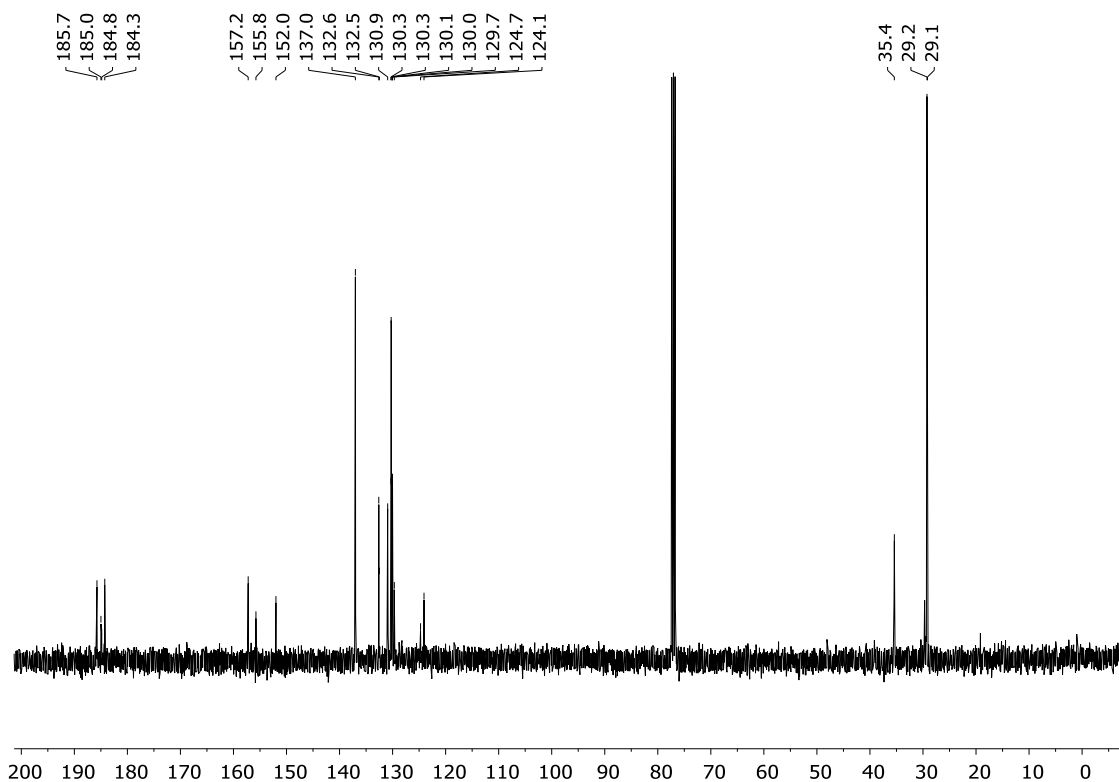


Figure 91. ¹³C NMR spectrum (100 MHz, CDCl₃) of compounds **124** and **125**.

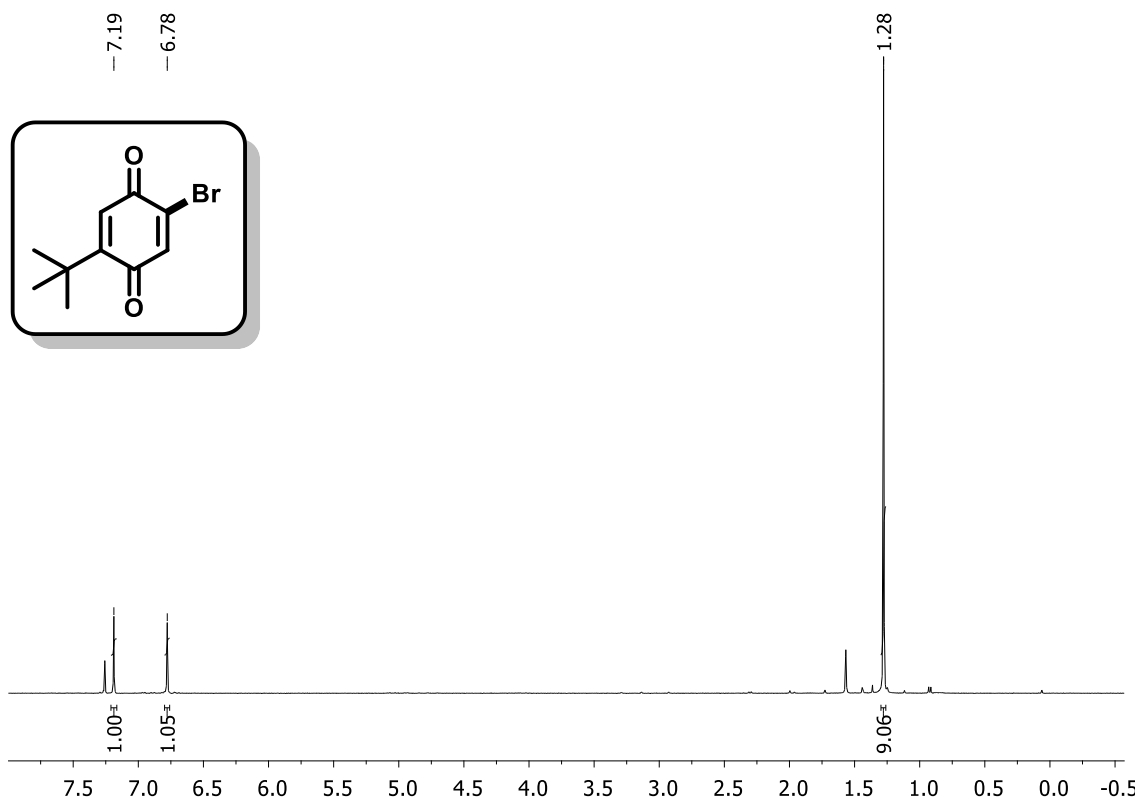


Figure 92. ¹H NMR spectrum (400 MHz, CDCl₃) of compound **126**.

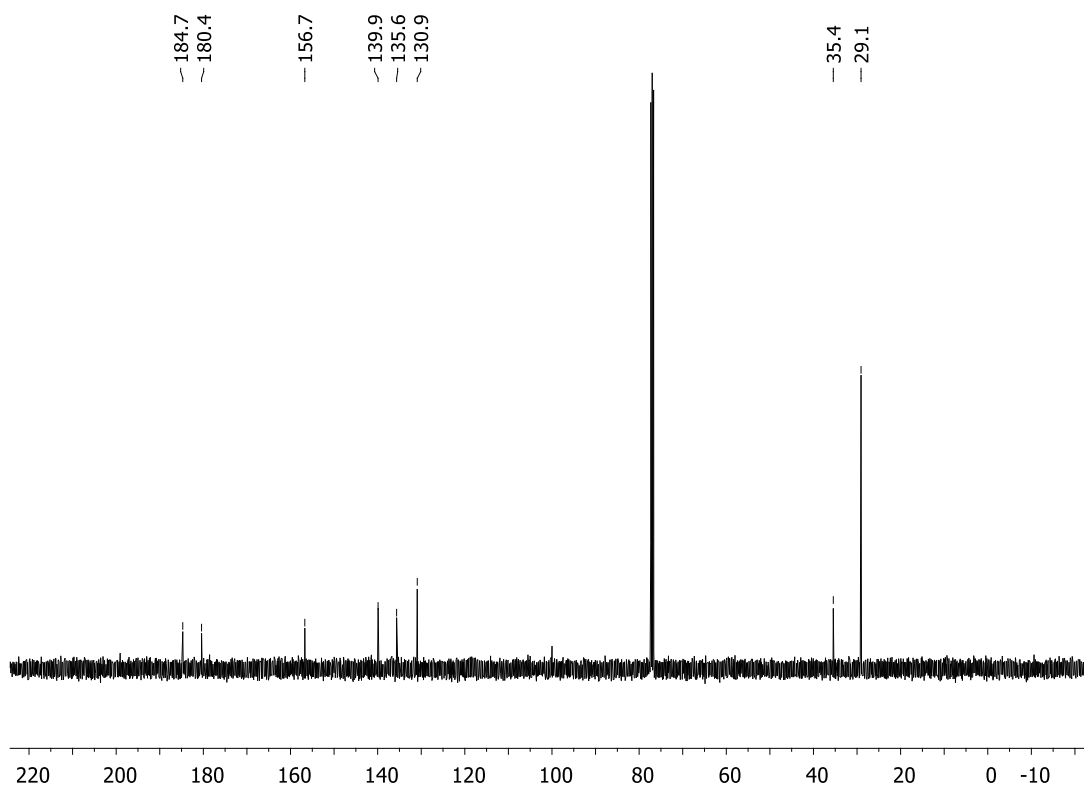


Figure 93. ¹³C NMR spectrum (100 MHz, CDCl₃) of compound **126**.

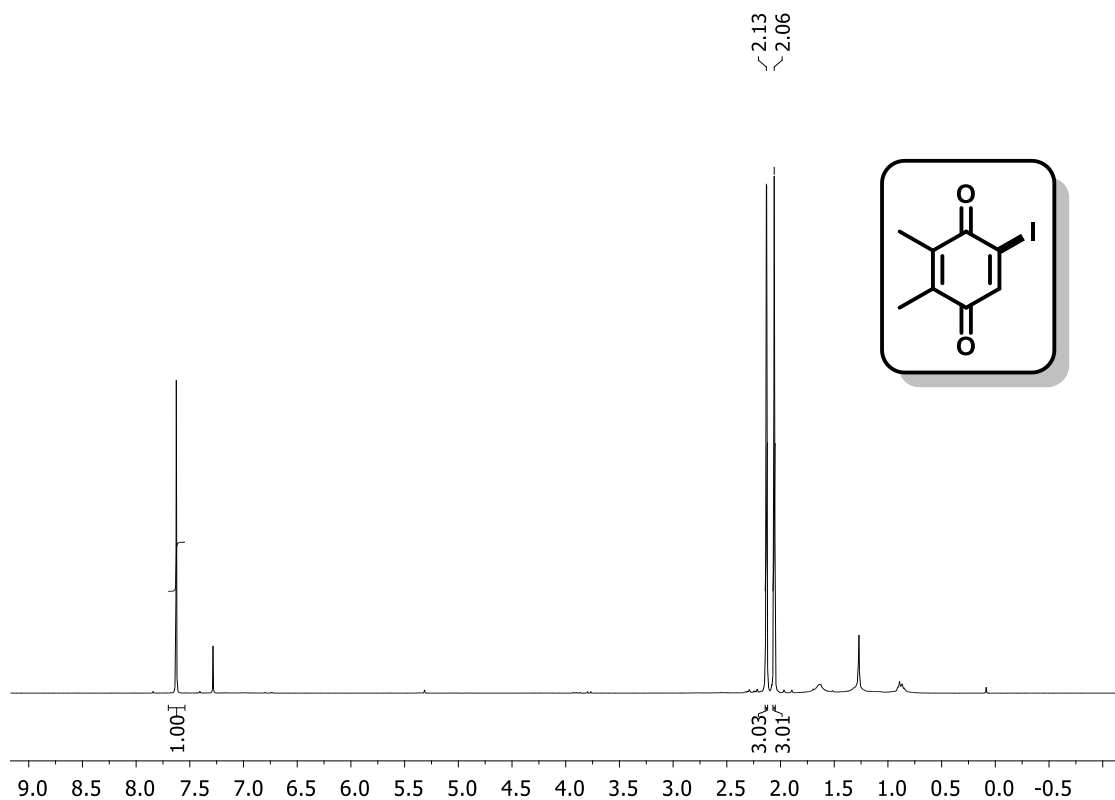


Figure 94. ¹H NMR spectrum (400 MHz, CDCl₃) of compound **128**.

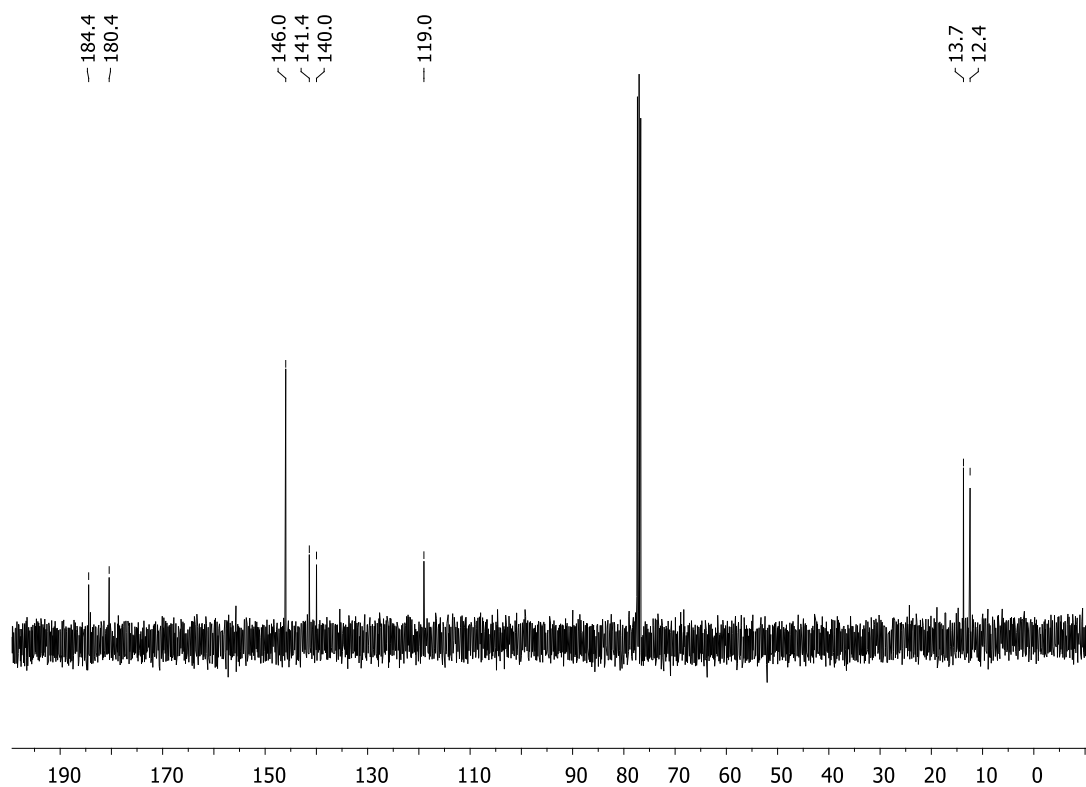


Figure 95. ¹³C NMR spectrum (100 MHz, CDCl₃) of compound **128**.

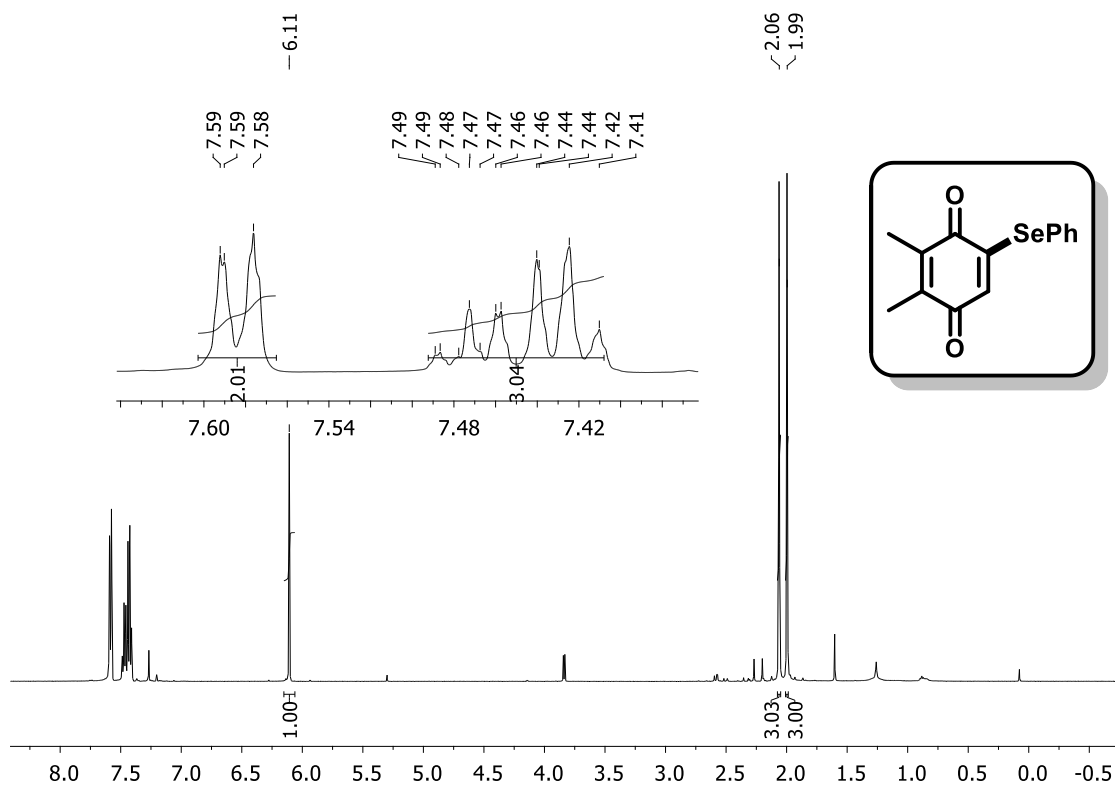


Figure 96. ¹H NMR spectrum (400 MHz, CDCl₃) of compound **130**.

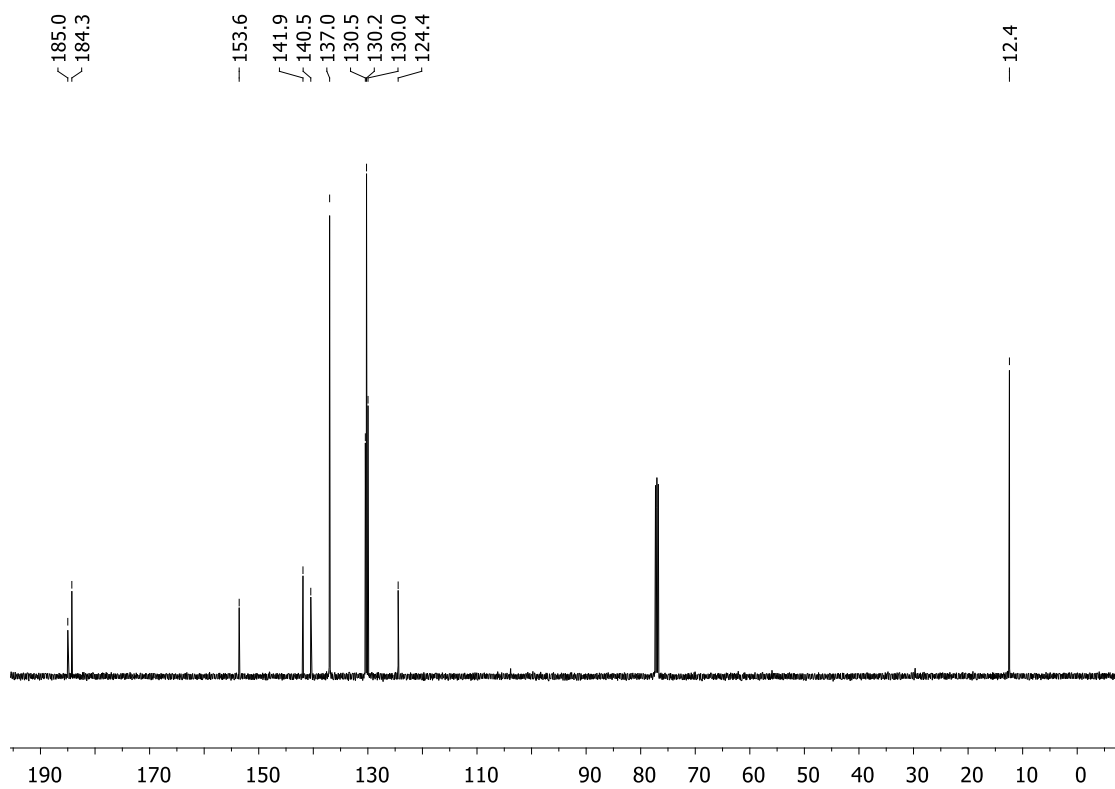


Figure 97. ¹³C NMR spectrum (100 MHz, CDCl₃) of compound **130**.

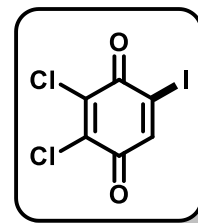
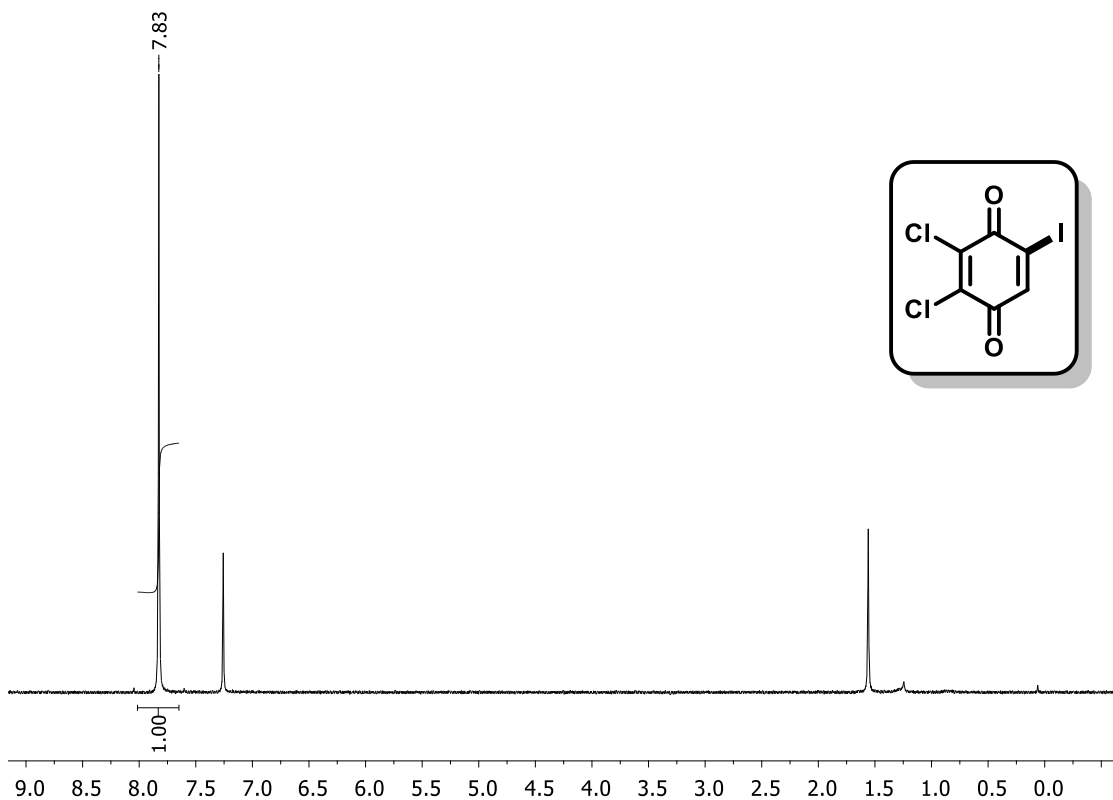


Figure 98. ¹H NMR spectrum (400 MHz, CDCl₃) of compound 132.

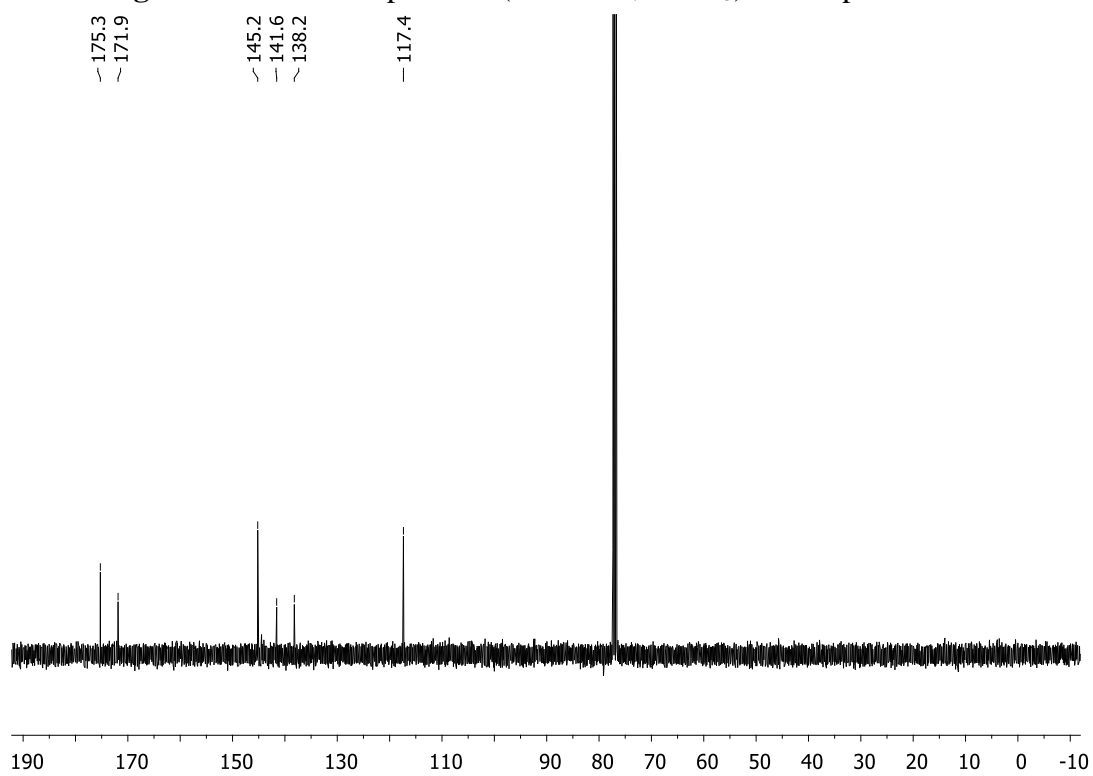


Figure 99. ¹³C NMR spectrum (100 MHz, CDCl₃) of compound 132.

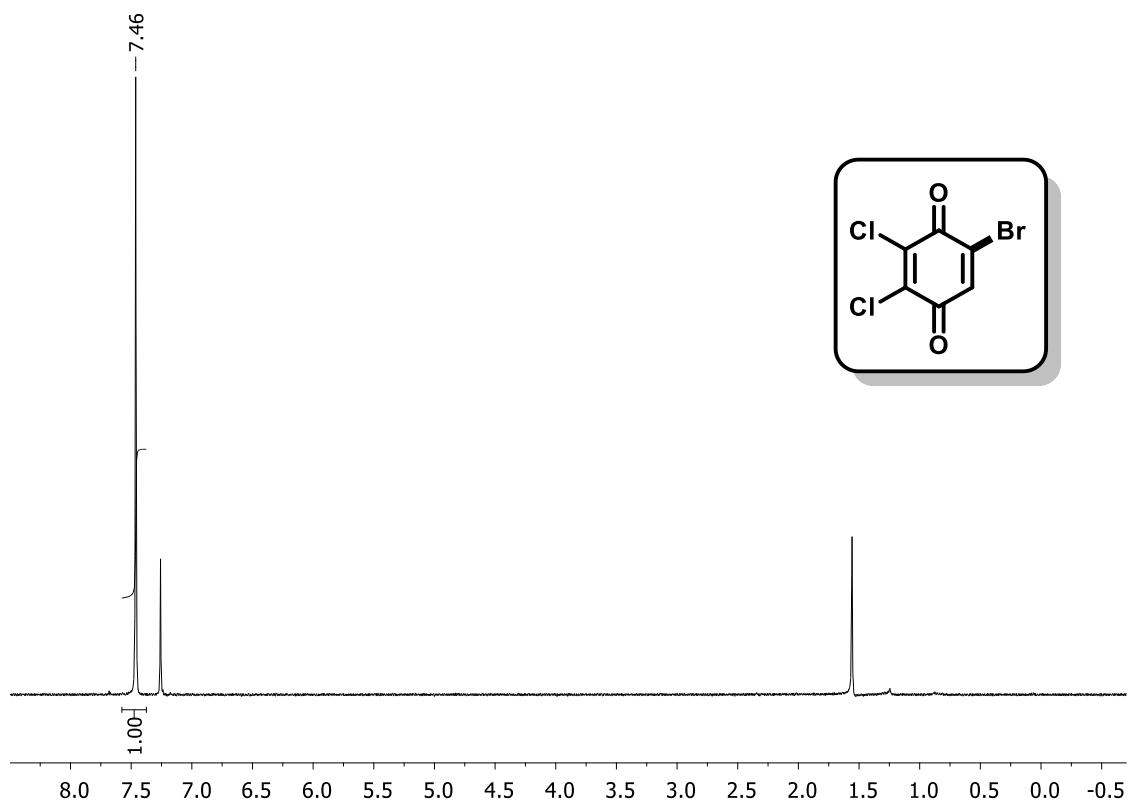


Figure 100. ¹H NMR spectrum (400 MHz, CDCl₃) of compound 133.

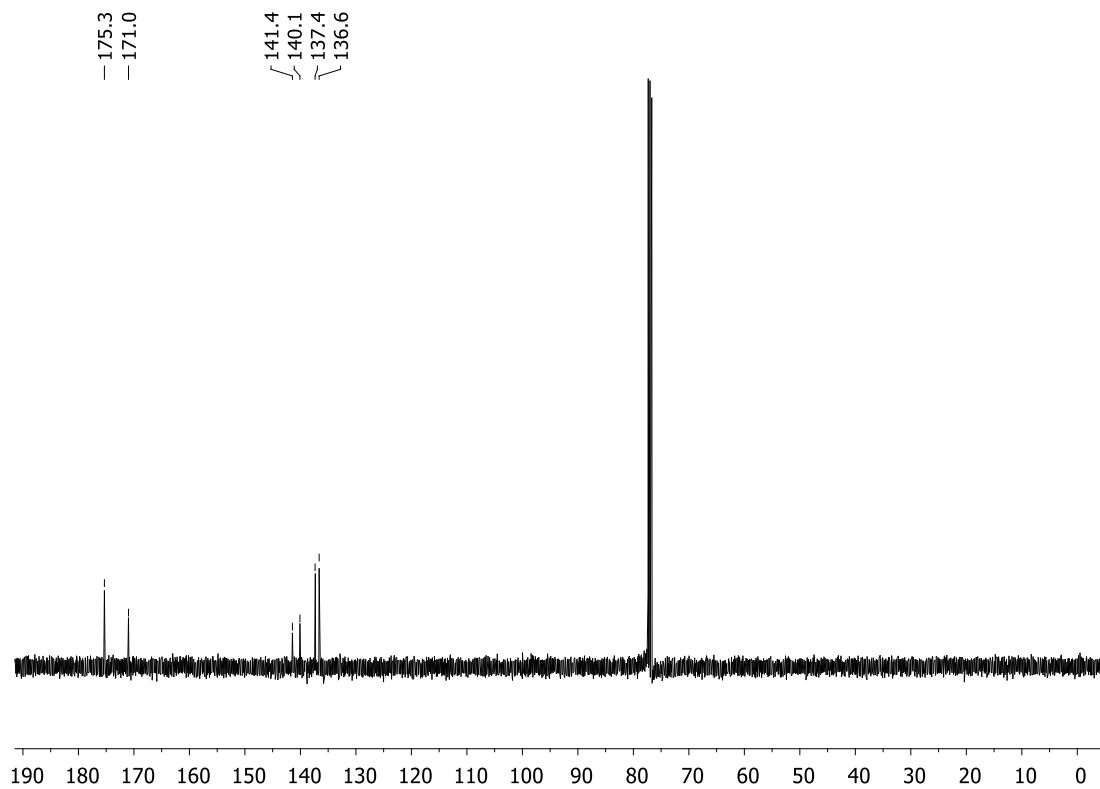


Figure 101. ¹³C NMR spectrum (100 MHz, CDCl₃) of compound 133.

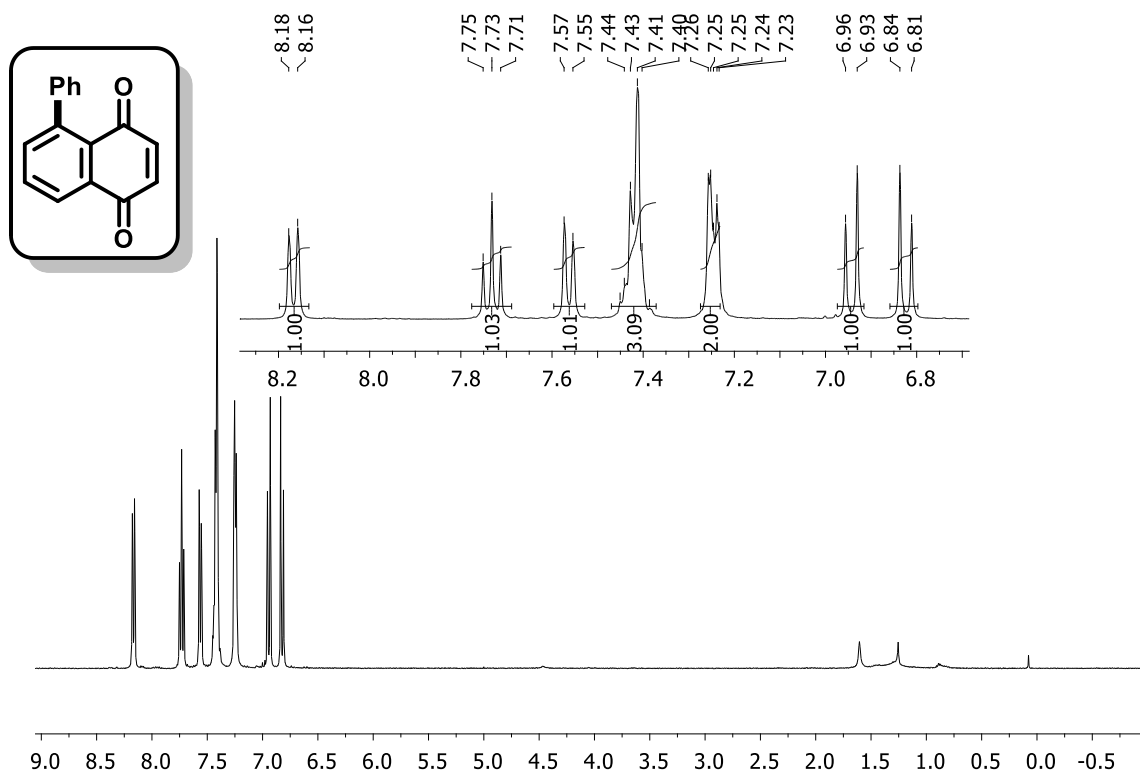


Figure 102. ¹H NMR spectrum (400 MHz, CDCl₃) of compound **134**.

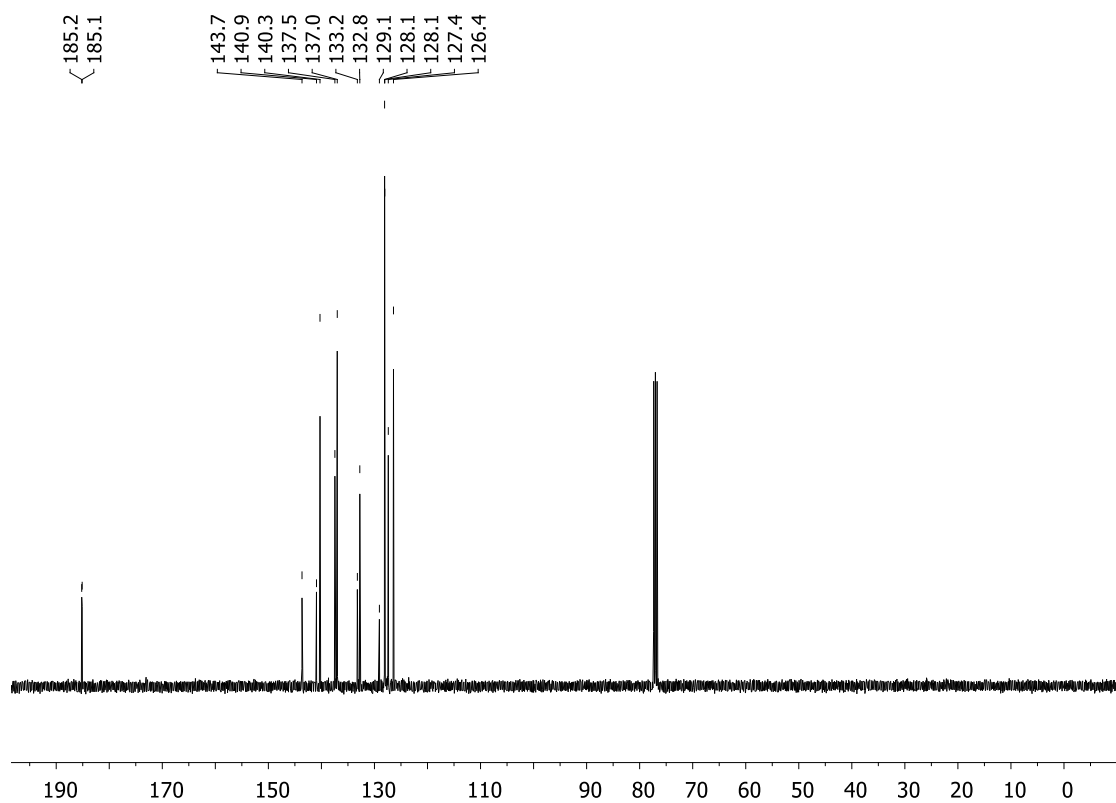


Figure 103. ¹³C NMR spectrum (100 MHz, CDCl₃) of compound **134**.

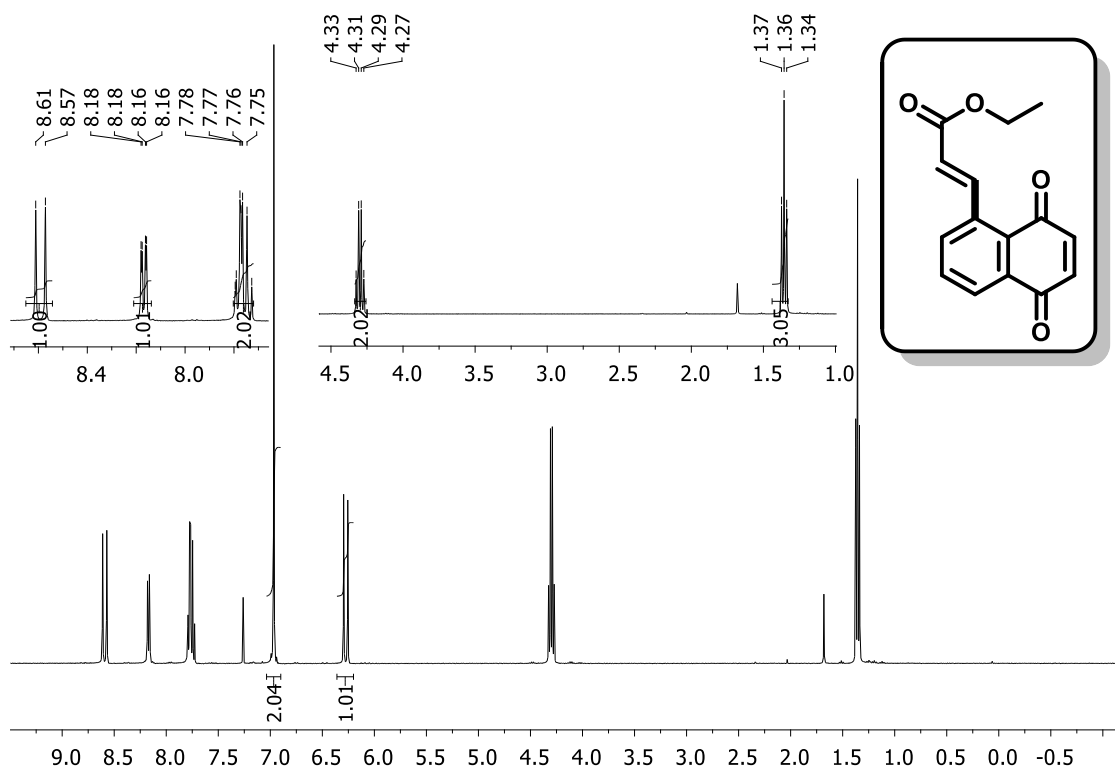


Figure 104. ¹H NMR spectrum (400 MHz, CDCl₃) of compound **135**.

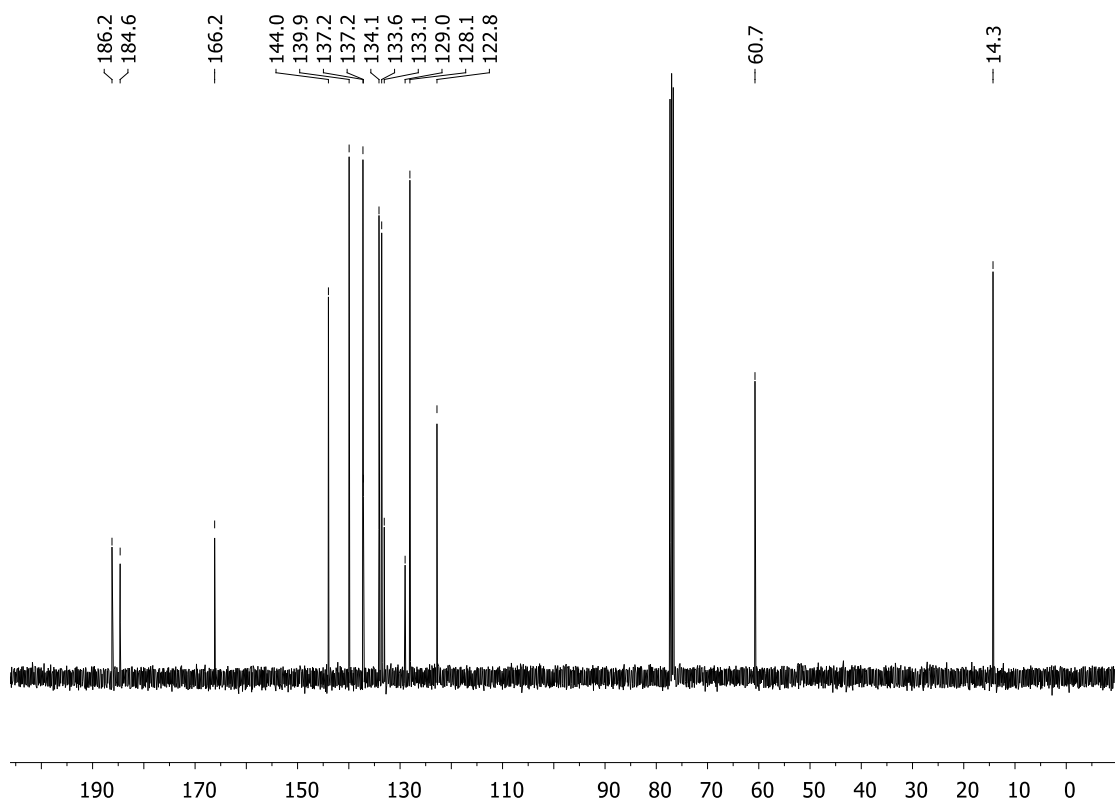


Figure 105. ¹³C NMR spectrum (100 MHz, CDCl₃) of compound **135**.

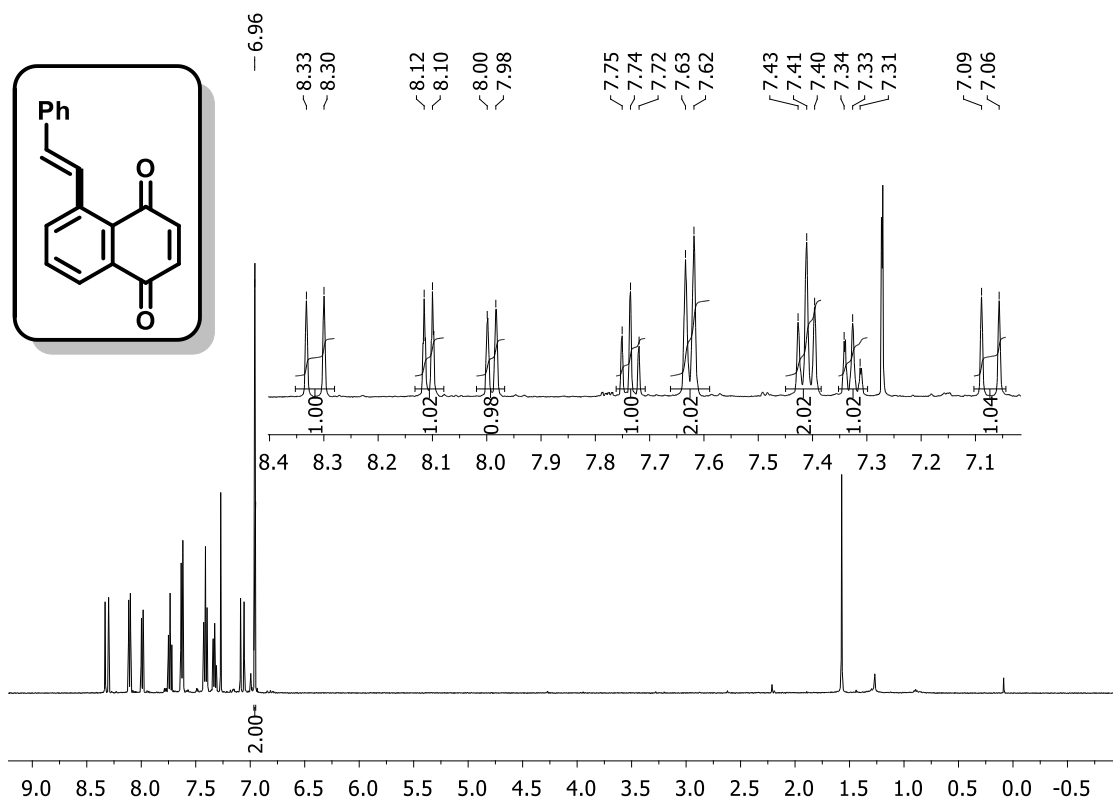


Figure 106. ¹H NMR spectrum (400 MHz, CDCl₃) of compound **136**.

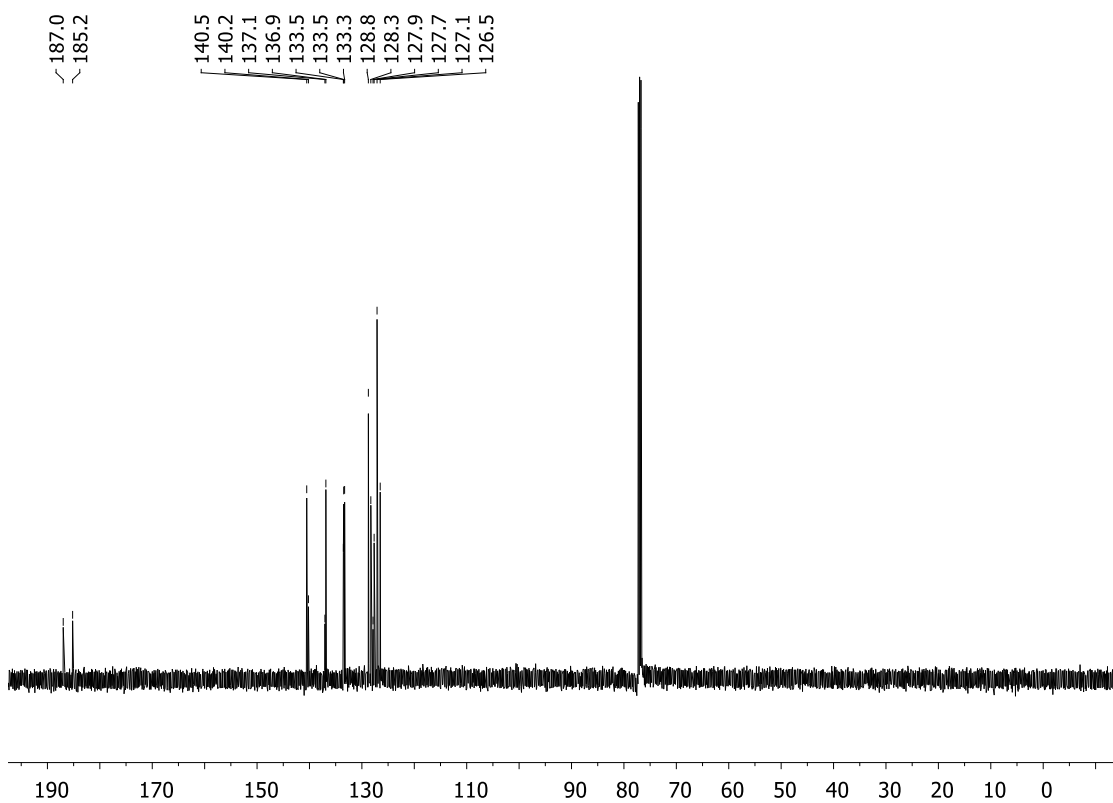


Figure 107. ¹³C NMR spectrum (100 MHz, CDCl₃) of compound **136**.

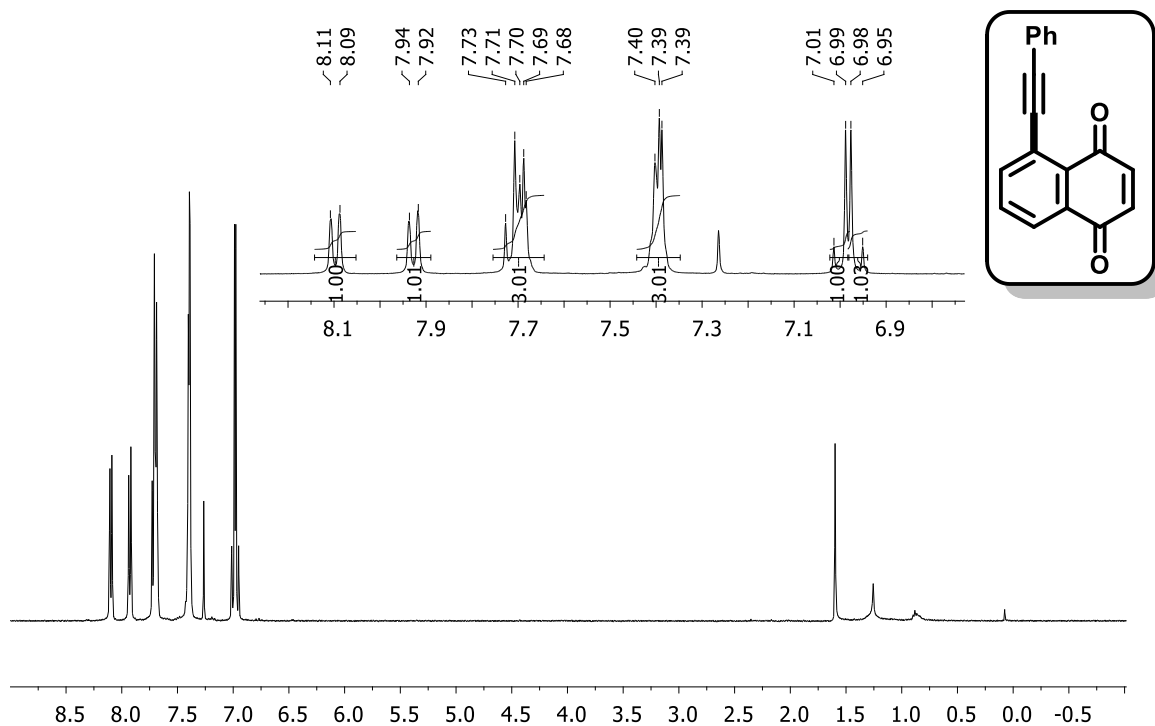


Figure 108. ¹H NMR spectrum (400 MHz, CDCl₃) of compound **137**.

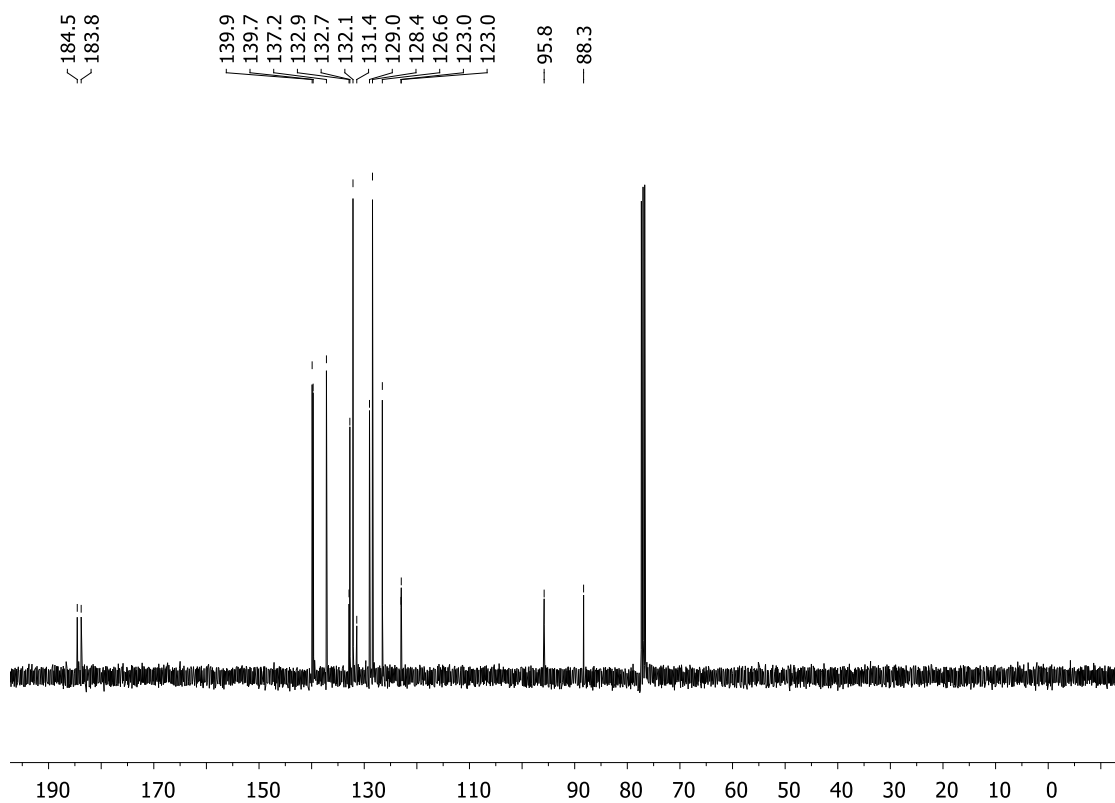


Figure 109. ¹³C NMR spectrum (100 MHz, CDCl₃) of compound **137**.

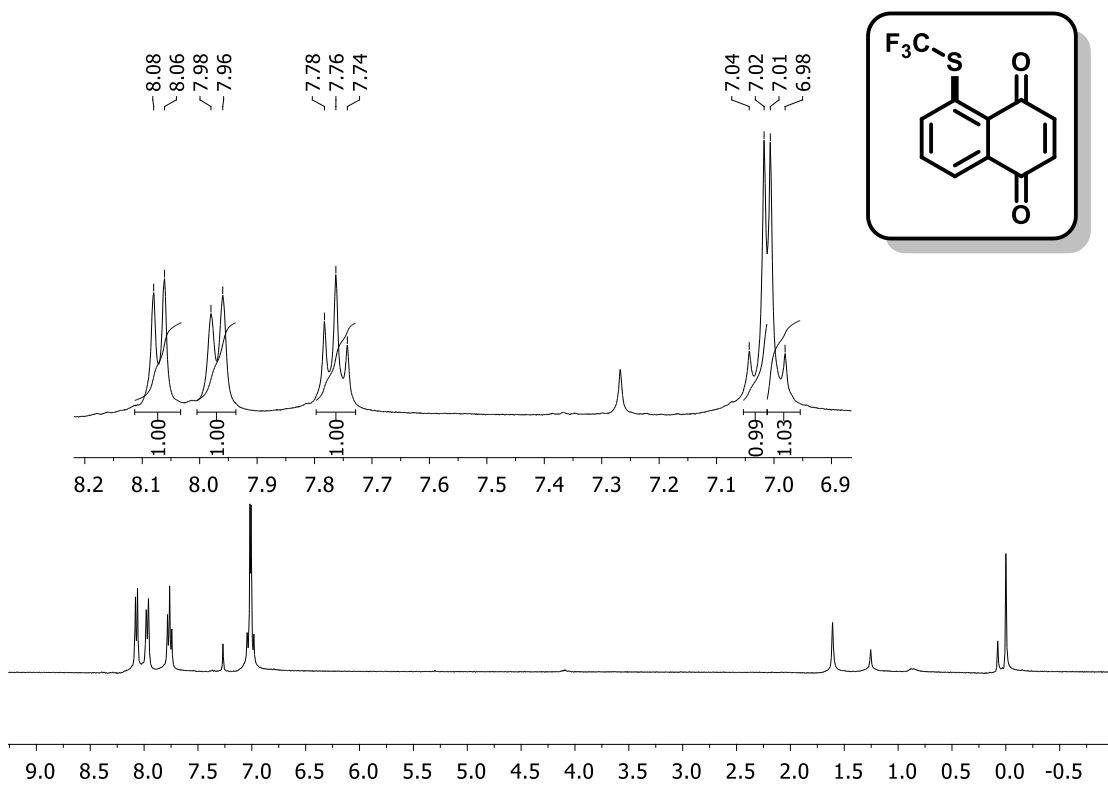


Figure 110. ¹H NMR spectrum (400 MHz, CDCl₃) of compound **138**.

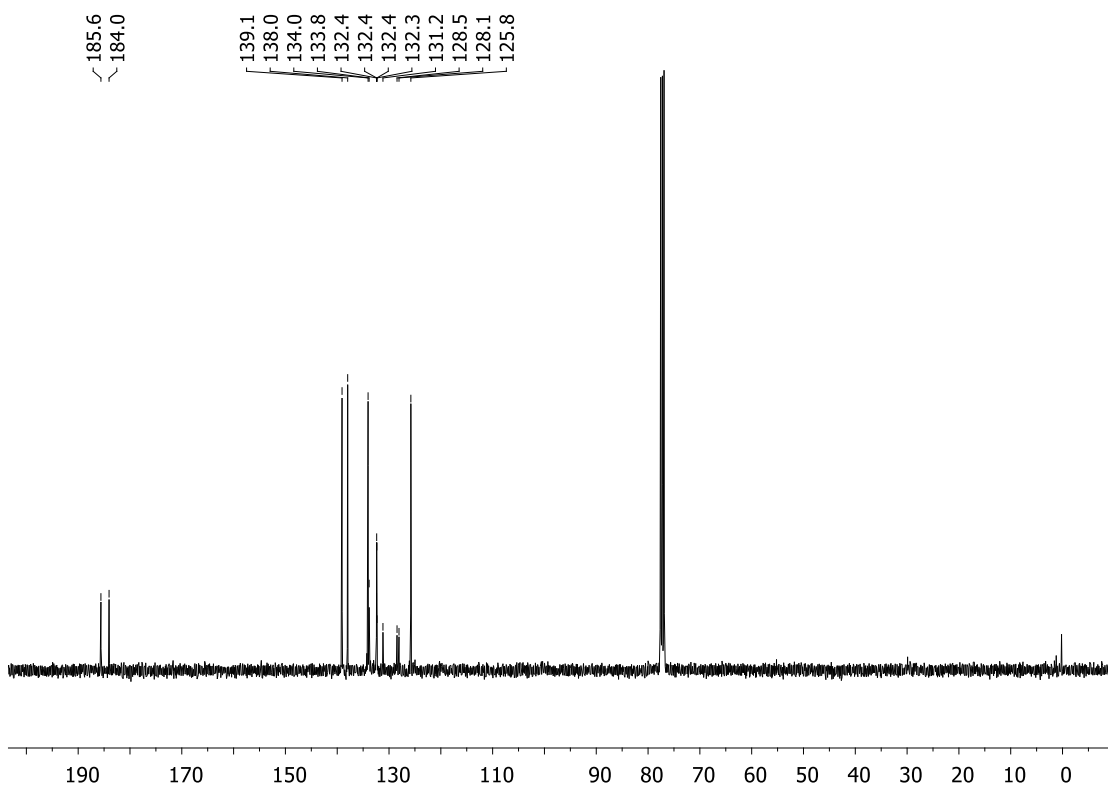


Figure 111. ¹³C NMR spectrum (100 MHz, CDCl₃) of compound **138**.

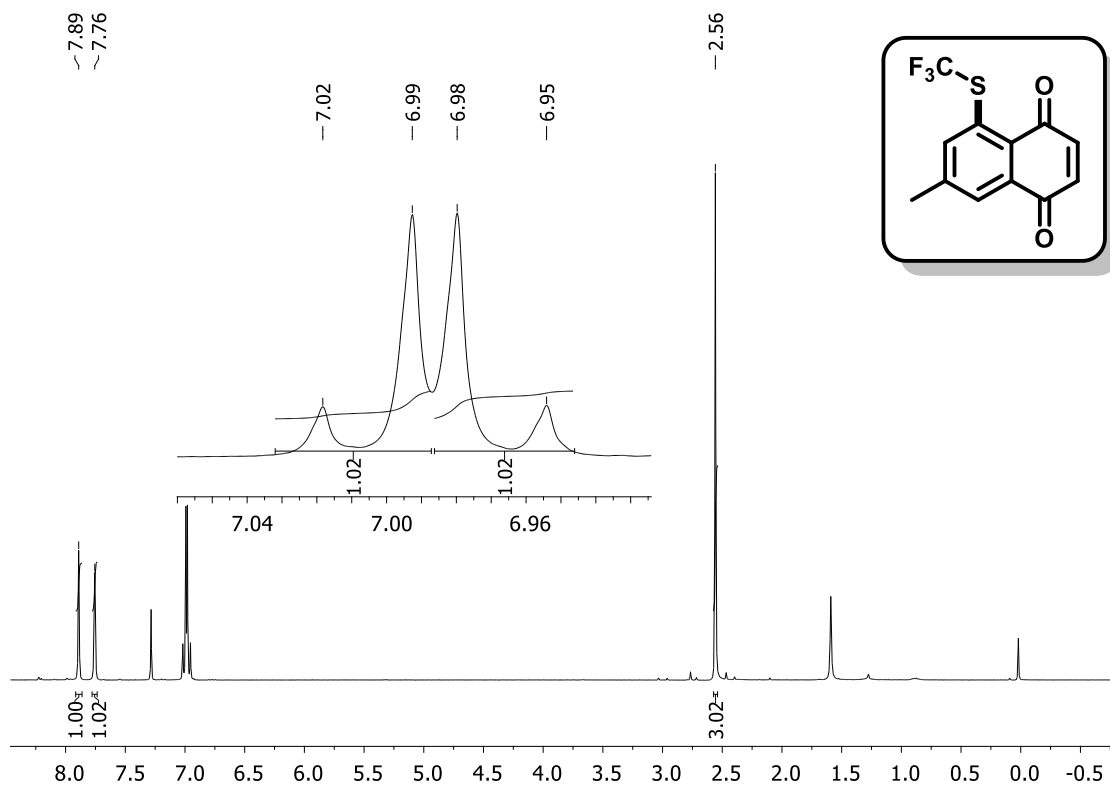


Figure 112. ¹H NMR spectrum (400 MHz, CDCl₃) of compound 139.

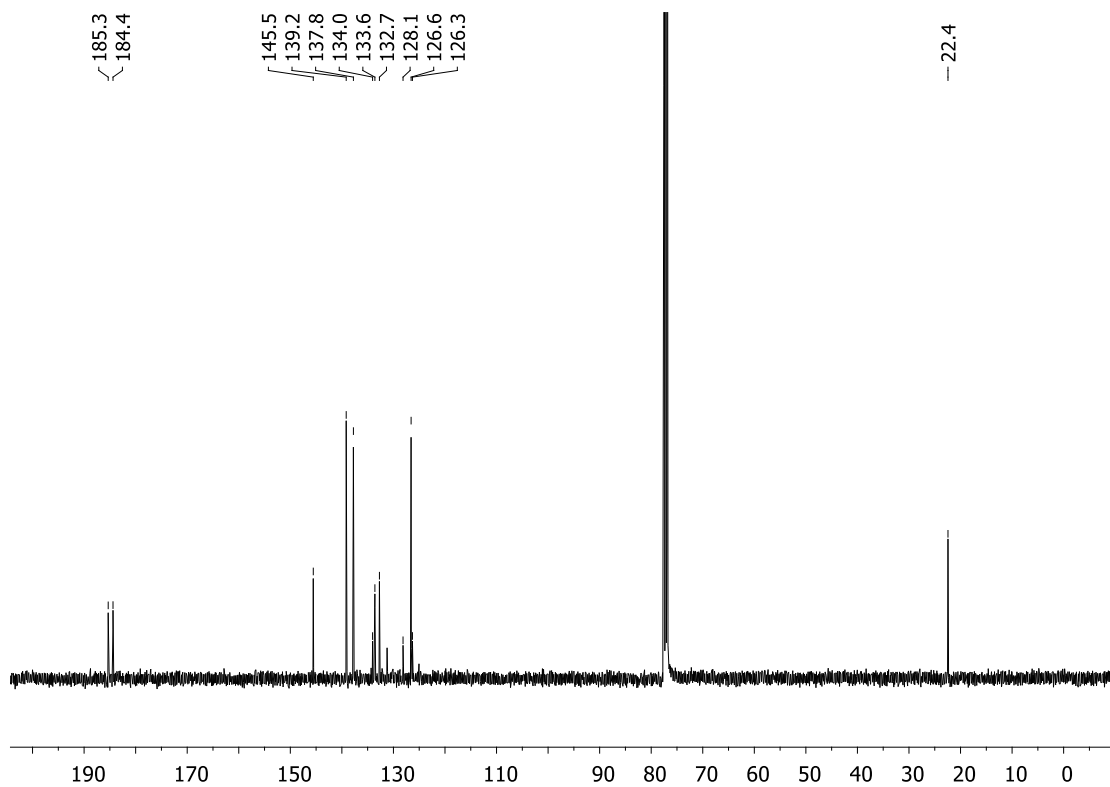


Figure 113. ¹³C NMR spectrum (100 MHz, CDCl₃) of compound 139.

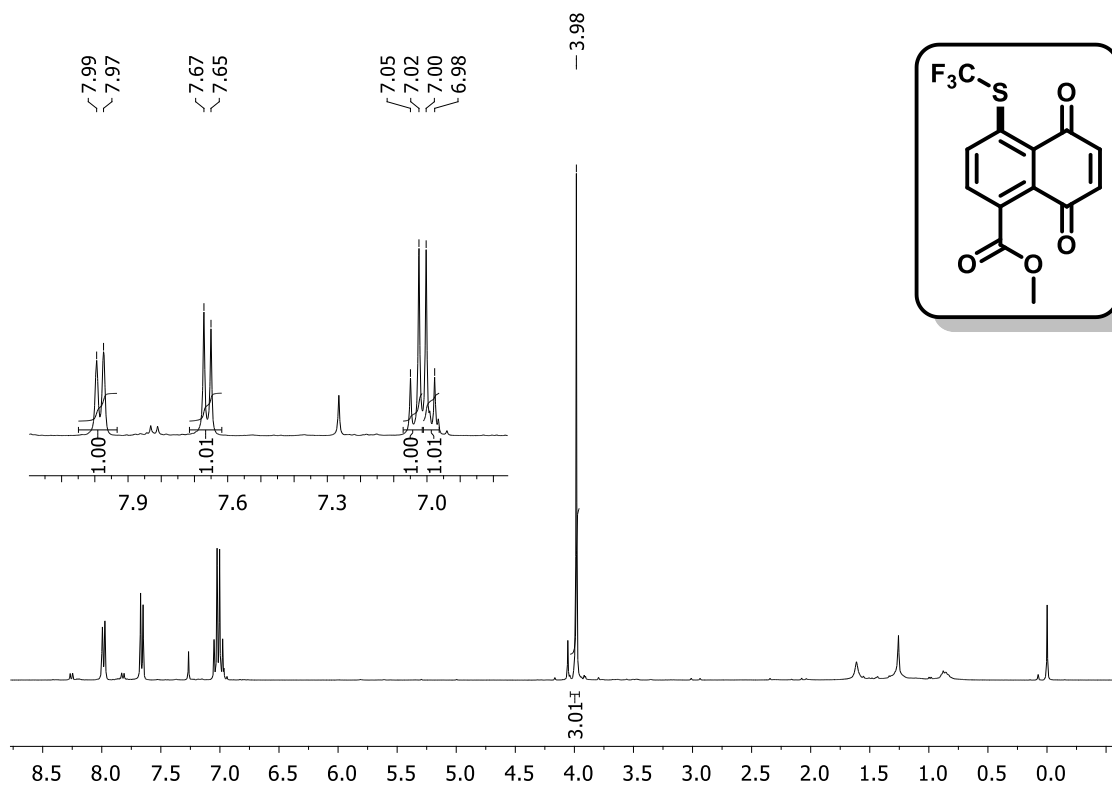


Figure 114. ¹H NMR spectrum (400 MHz, CDCl₃) of compound 140.

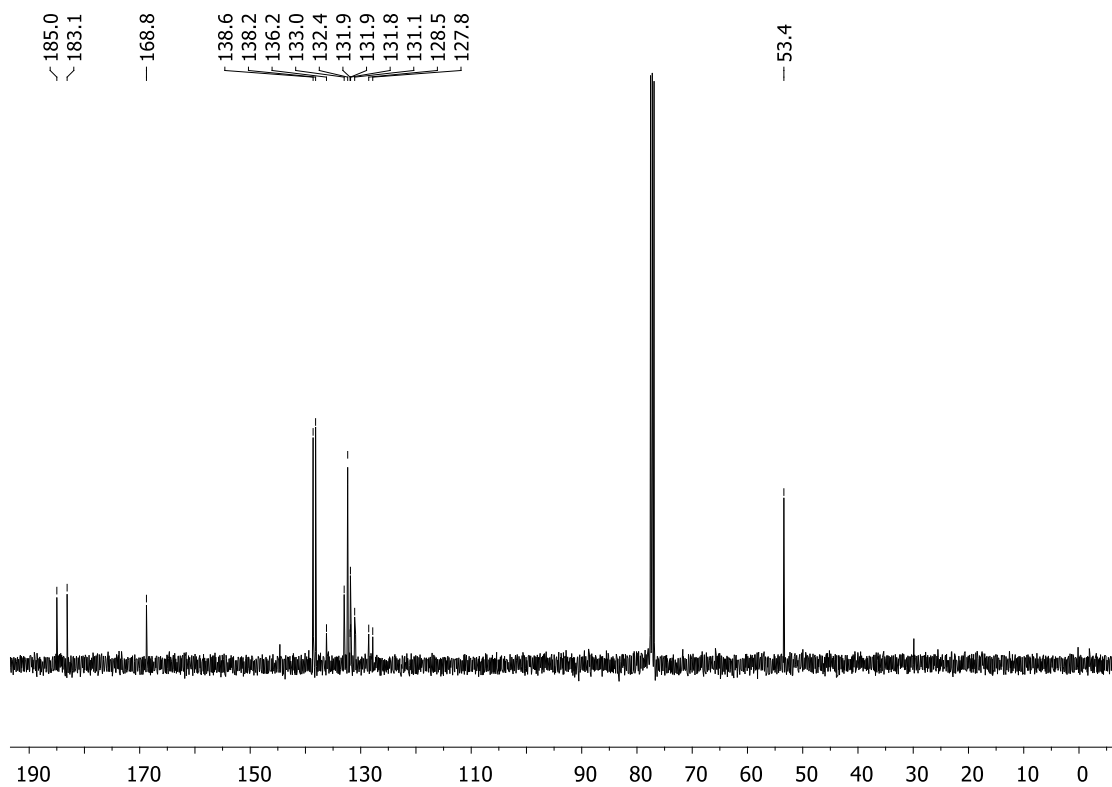


Figure 115. ¹³C NMR spectrum (100 MHz, CDCl₃) of compound 140.

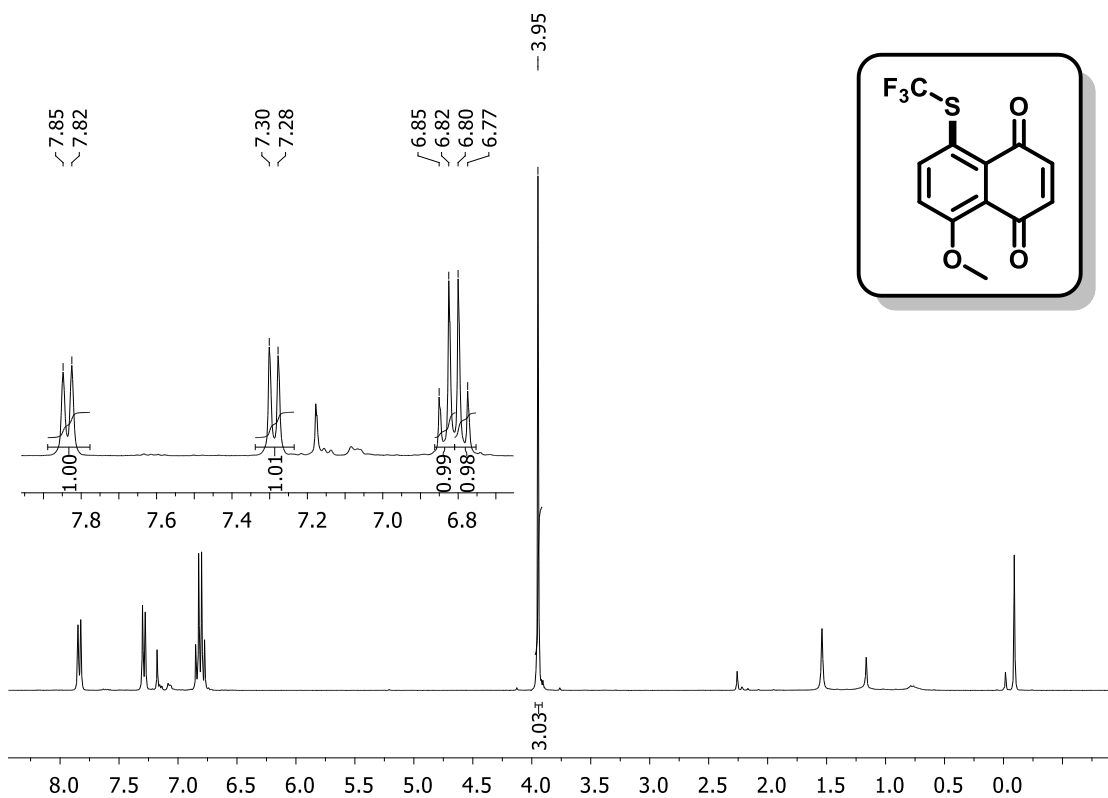


Figure 116. ¹H NMR spectrum (400 MHz, CDCl₃) of compound **141**.

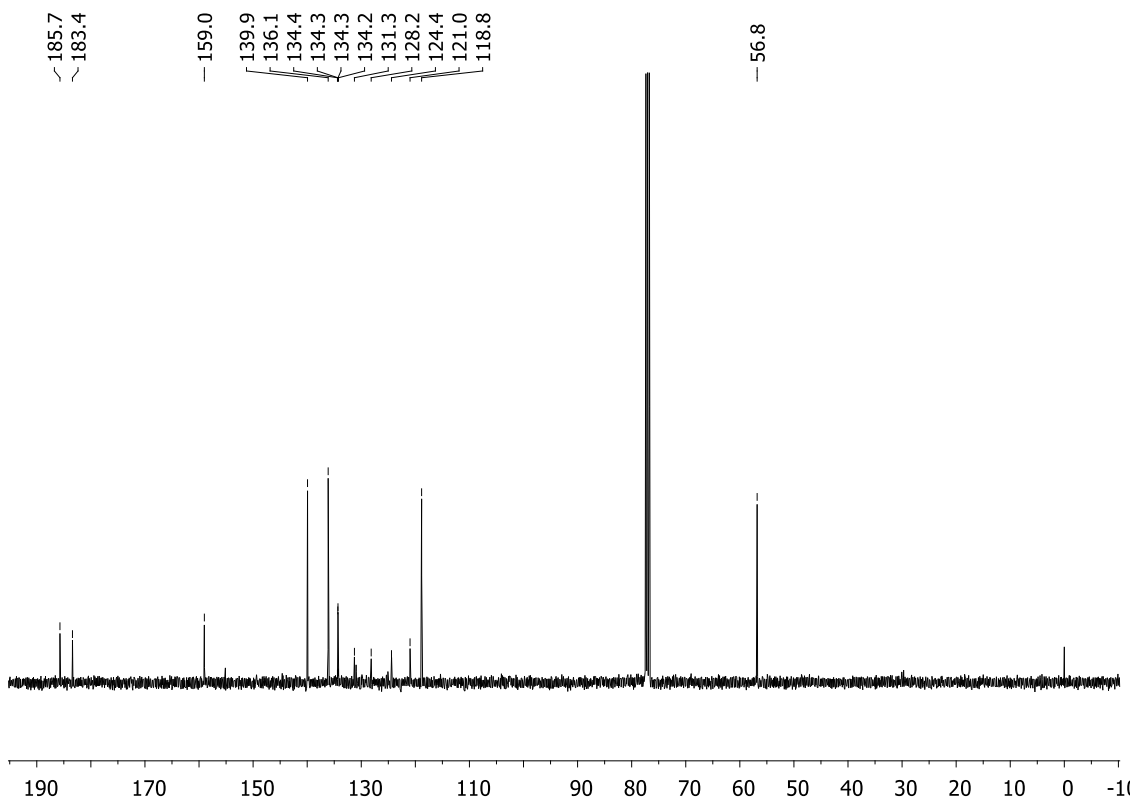


Figure 117. ¹³C NMR spectrum (100 MHz, CDCl₃) of compound **141**.

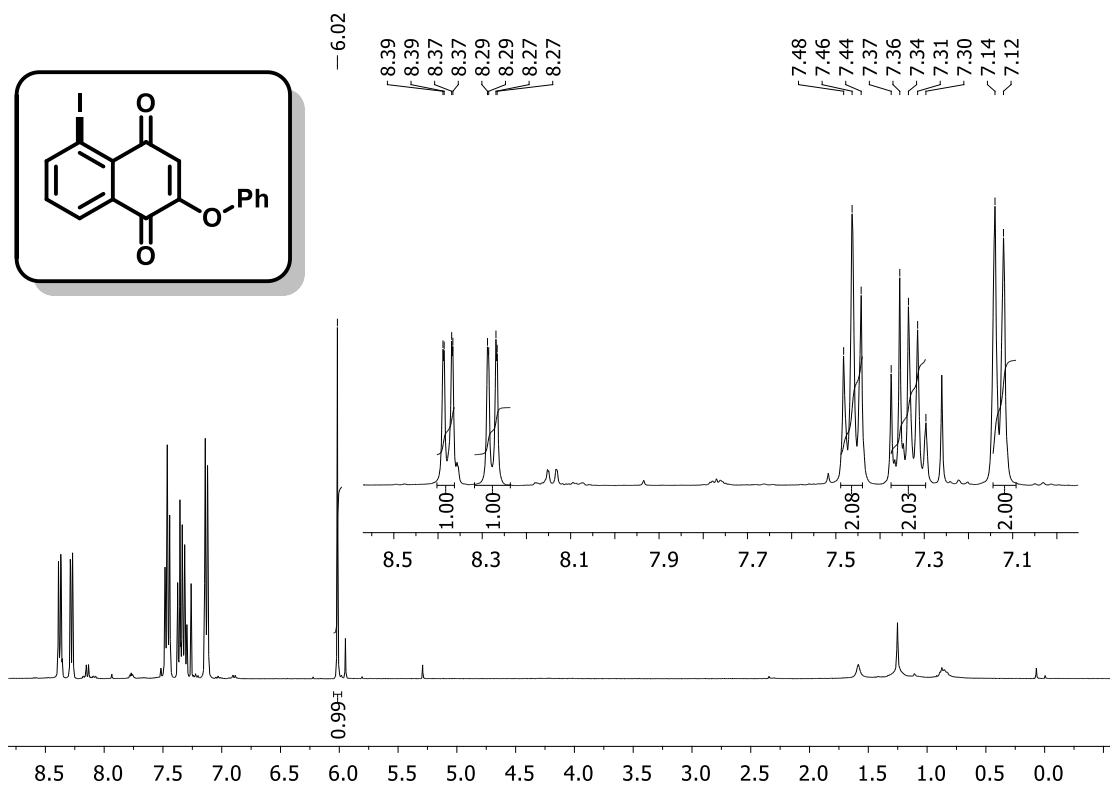


Figure 118. ¹H NMR spectrum (400 MHz, CDCl₃) of compound 142.

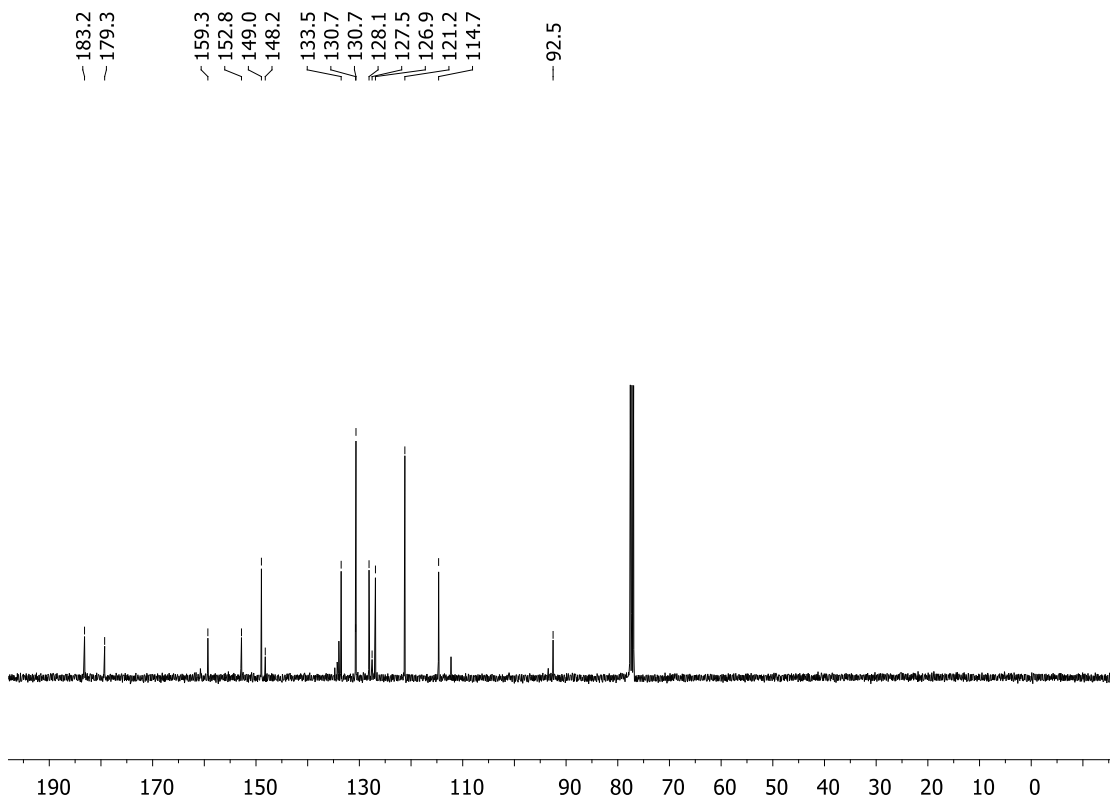


Figure 119. ¹³C NMR spectrum (100 MHz, CDCl₃) of compound 142.

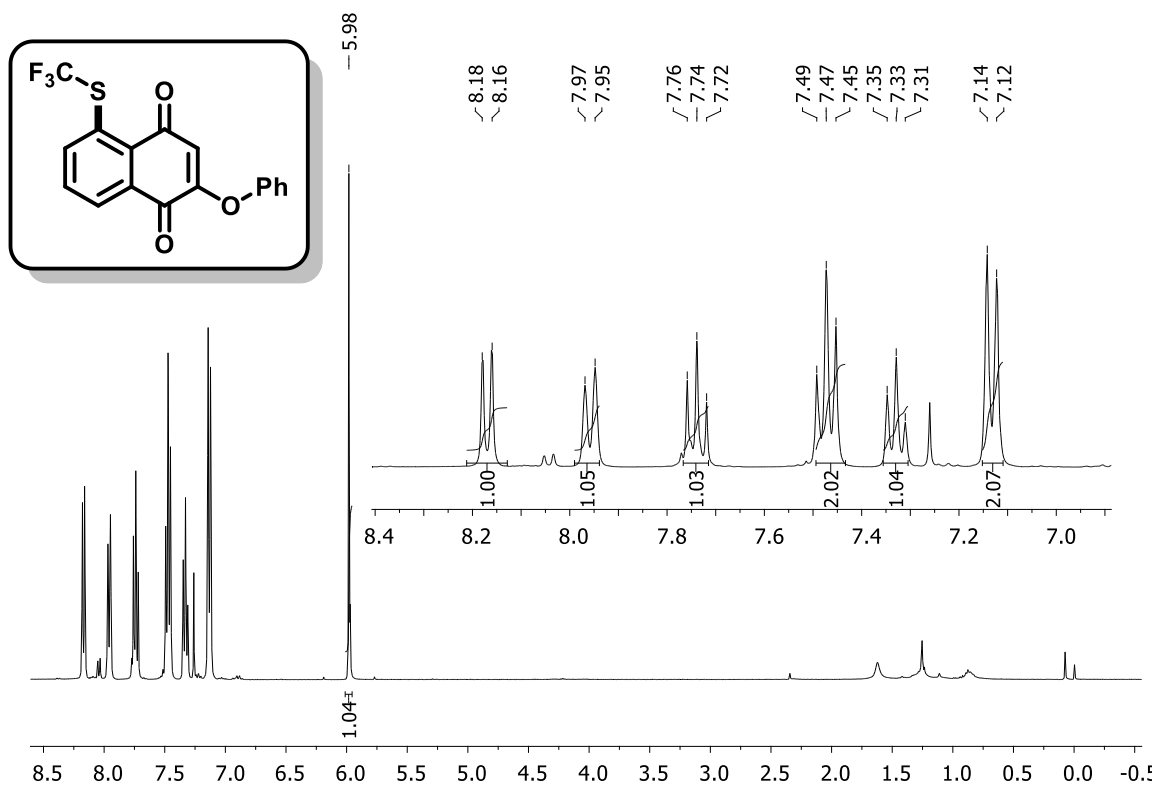


Figure 120. ¹H NMR spectrum (400 MHz, CDCl₃) of compound 143.

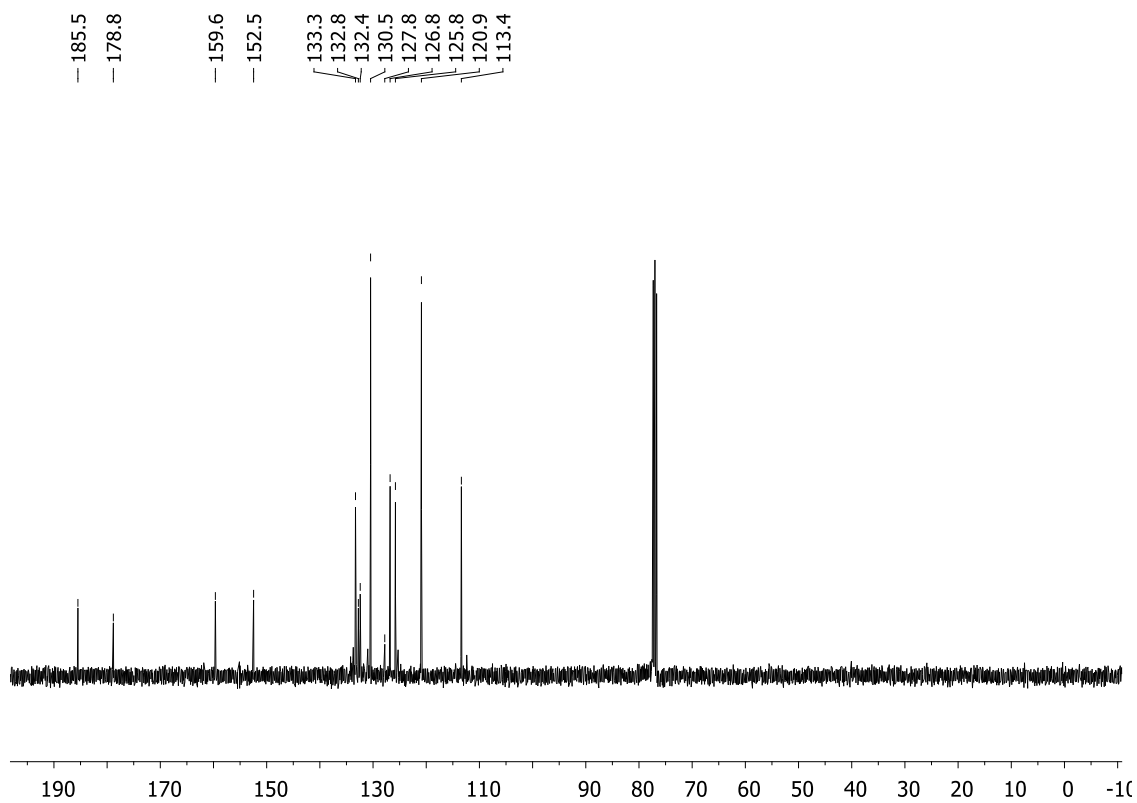


Figure 121. ¹³C NMR spectrum (100 MHz, CDCl₃) of compound 143.

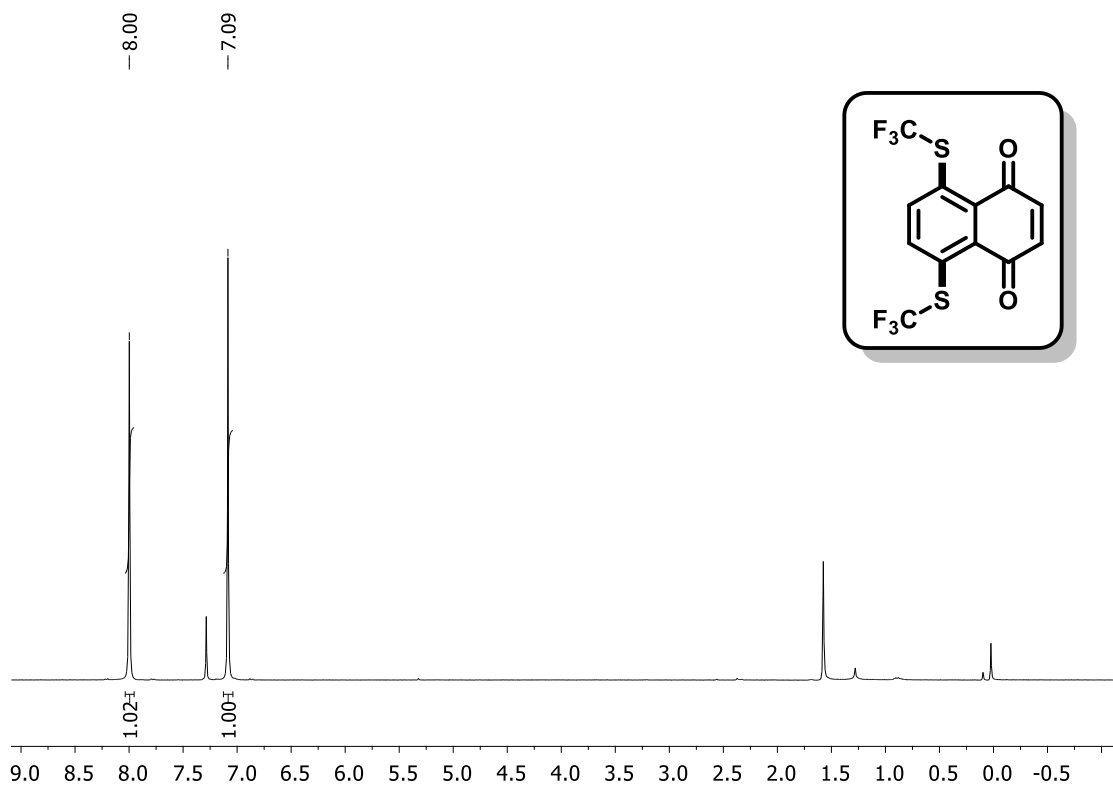


Figure 122. ¹H NMR spectrum (400 MHz, CDCl₃) of compound 145.

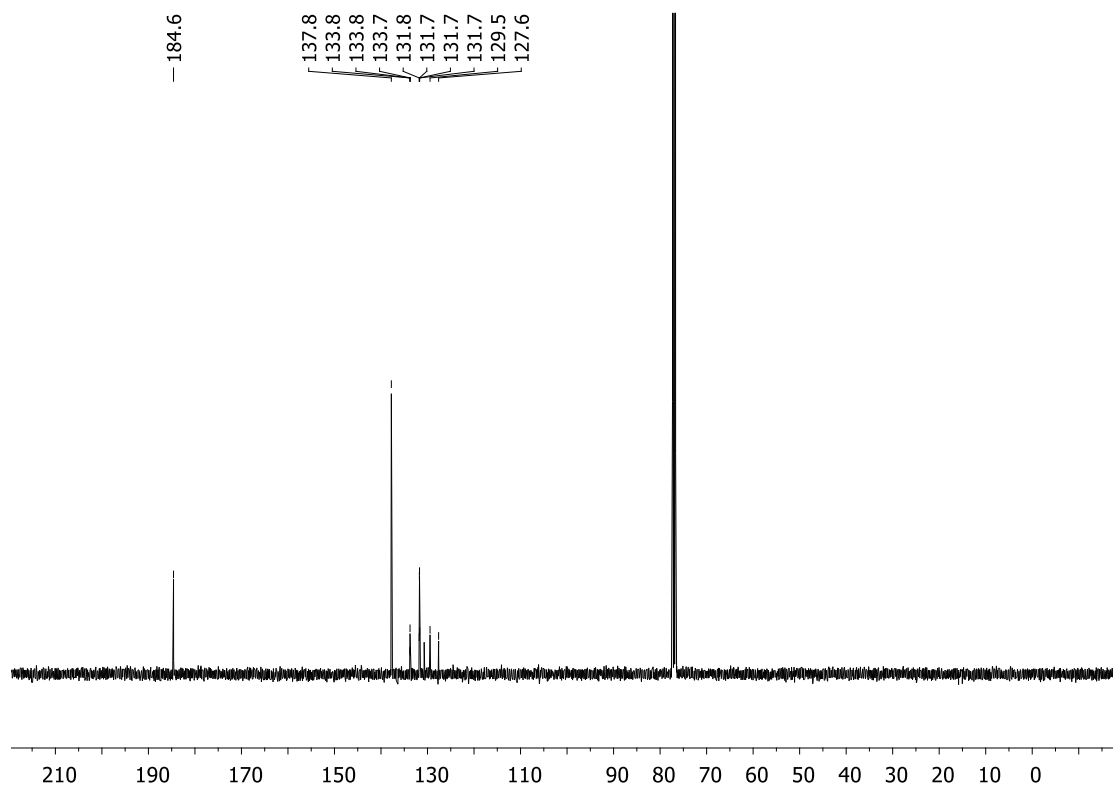


Figure 123. ¹³C NMR spectrum (100 MHz, CDCl₃) of compound 145.

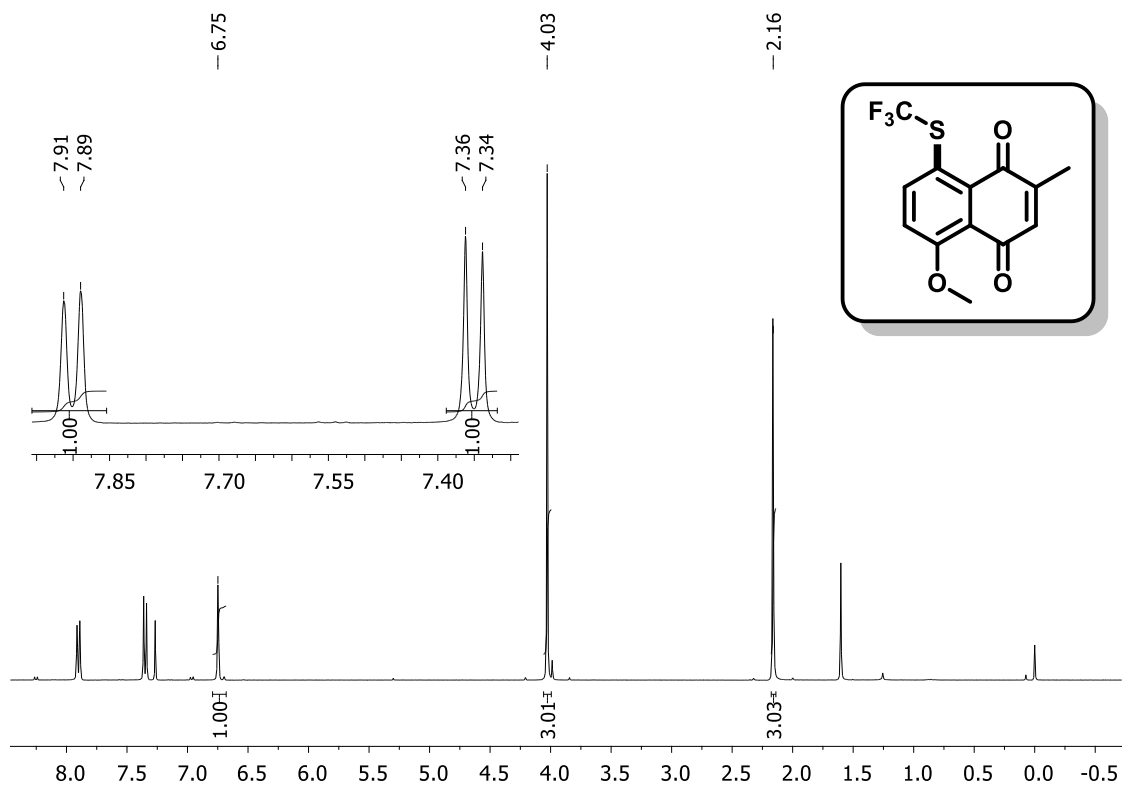


Figure 124. ¹H NMR spectrum (400 MHz, CDCl₃) of compound 146.

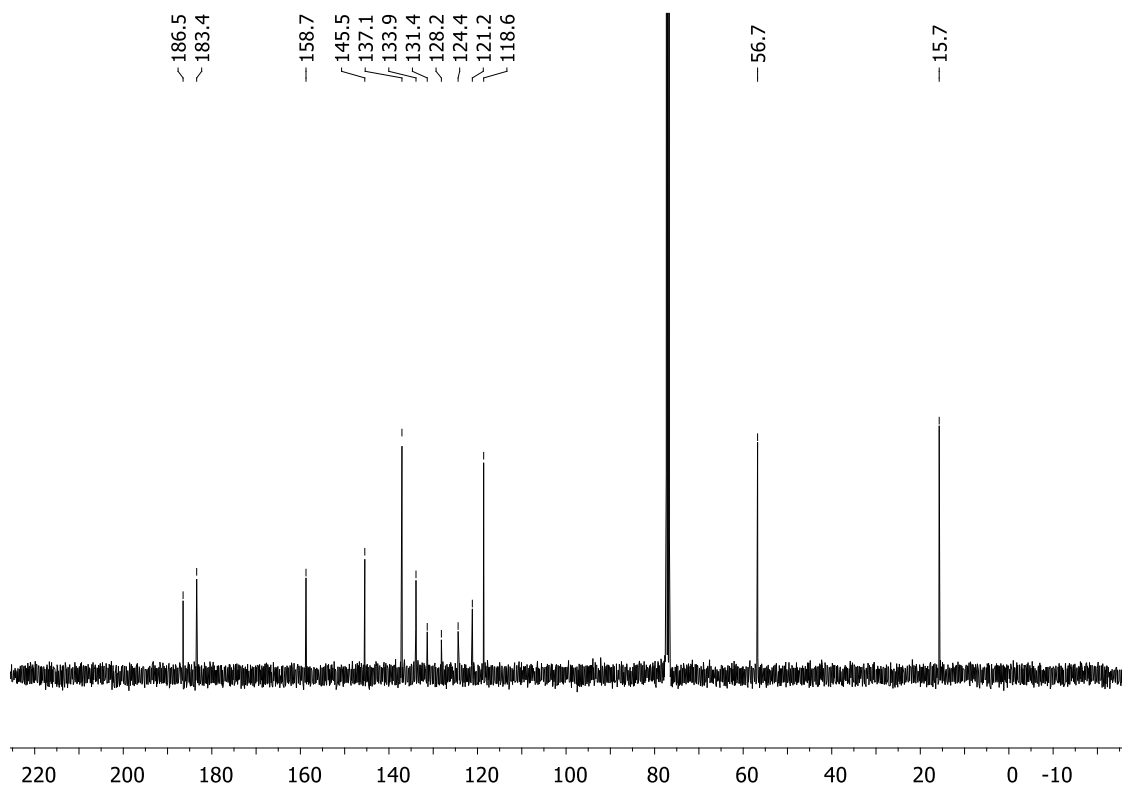


Figure 125. ¹³C NMR spectrum (100 MHz, CDCl₃) of compound 146.

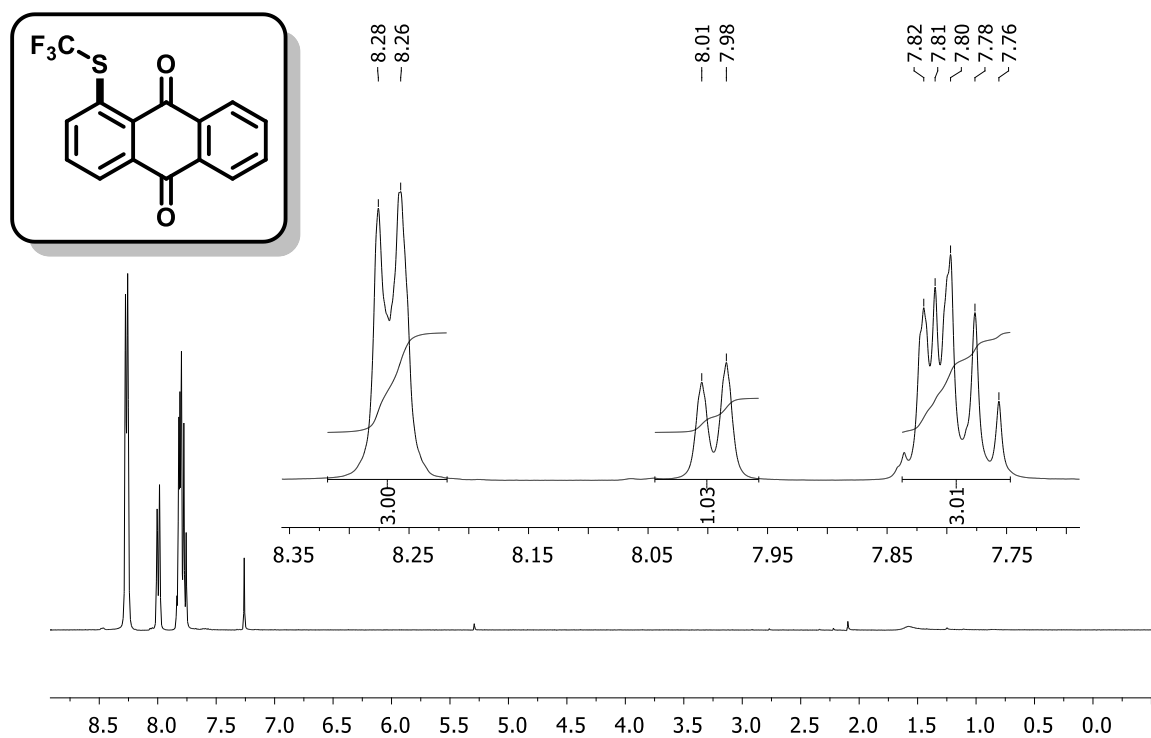


Figure 128. ¹H NMR spectrum (400 MHz, CDCl₃) of compound **148**.

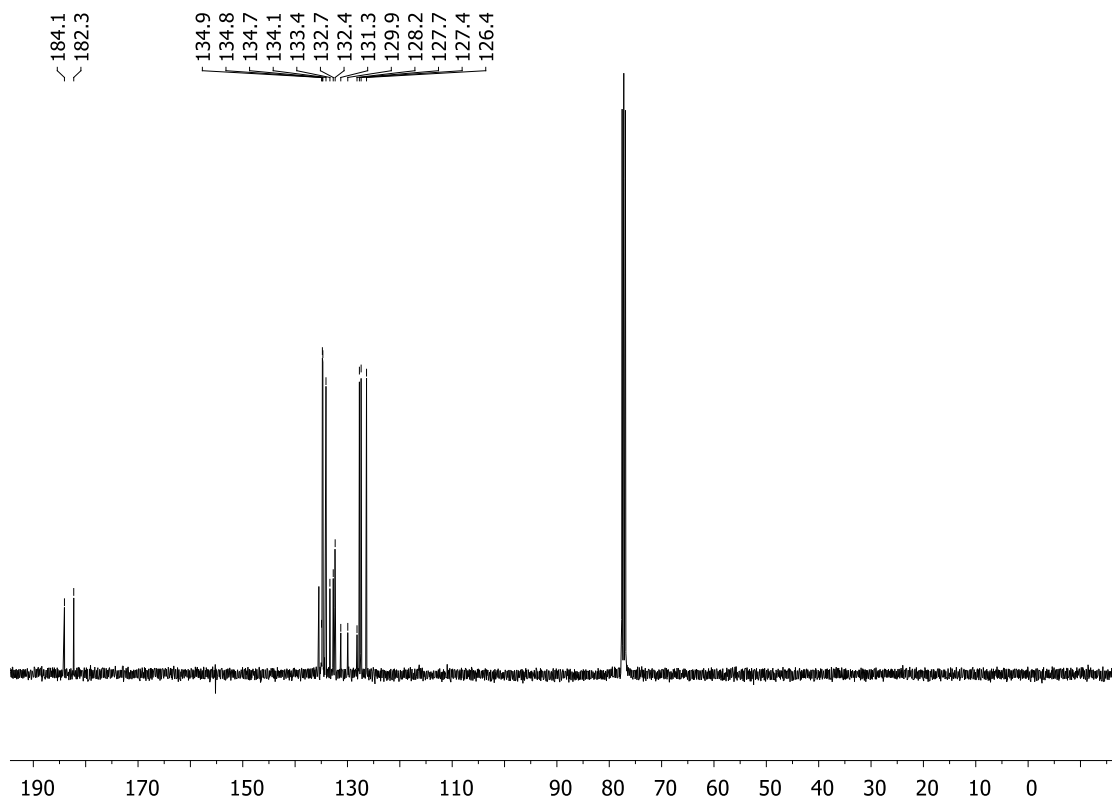


Figure 129. ¹³C NMR spectrum (100 MHz, CDCl₃) of compound **148**.

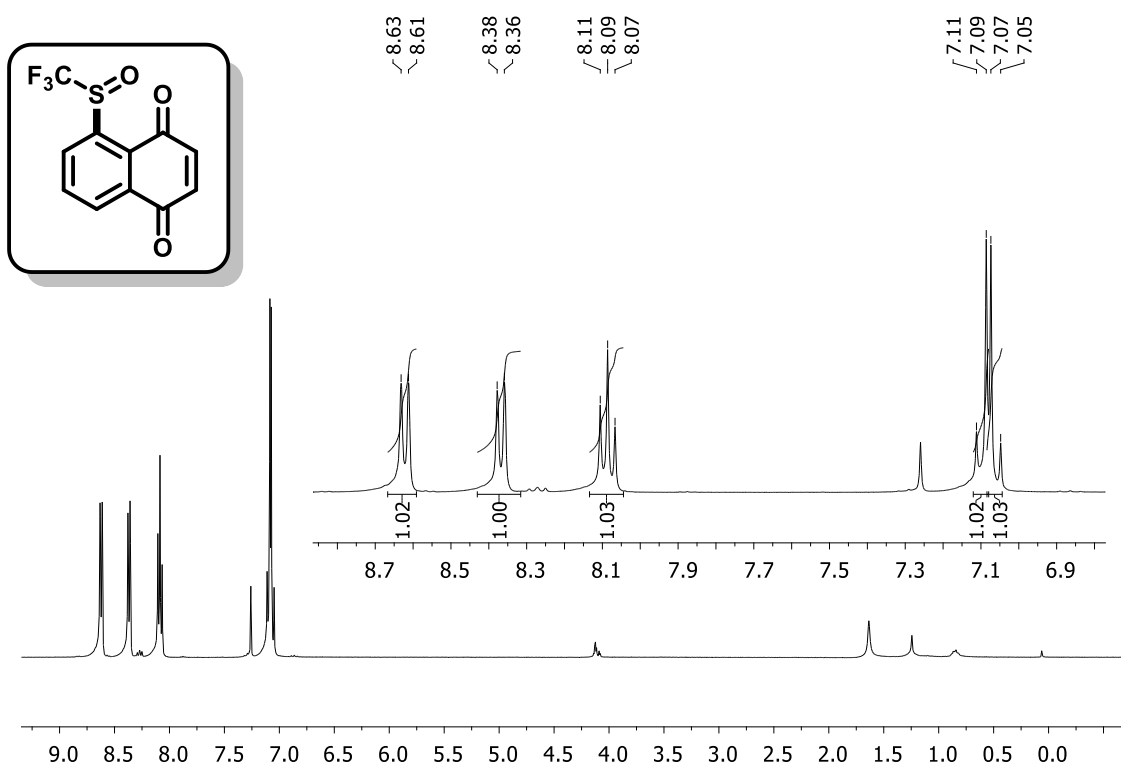


Figure 130. 1H NMR spectrum (400 MHz, $CDCl_3$) of compound **149**.

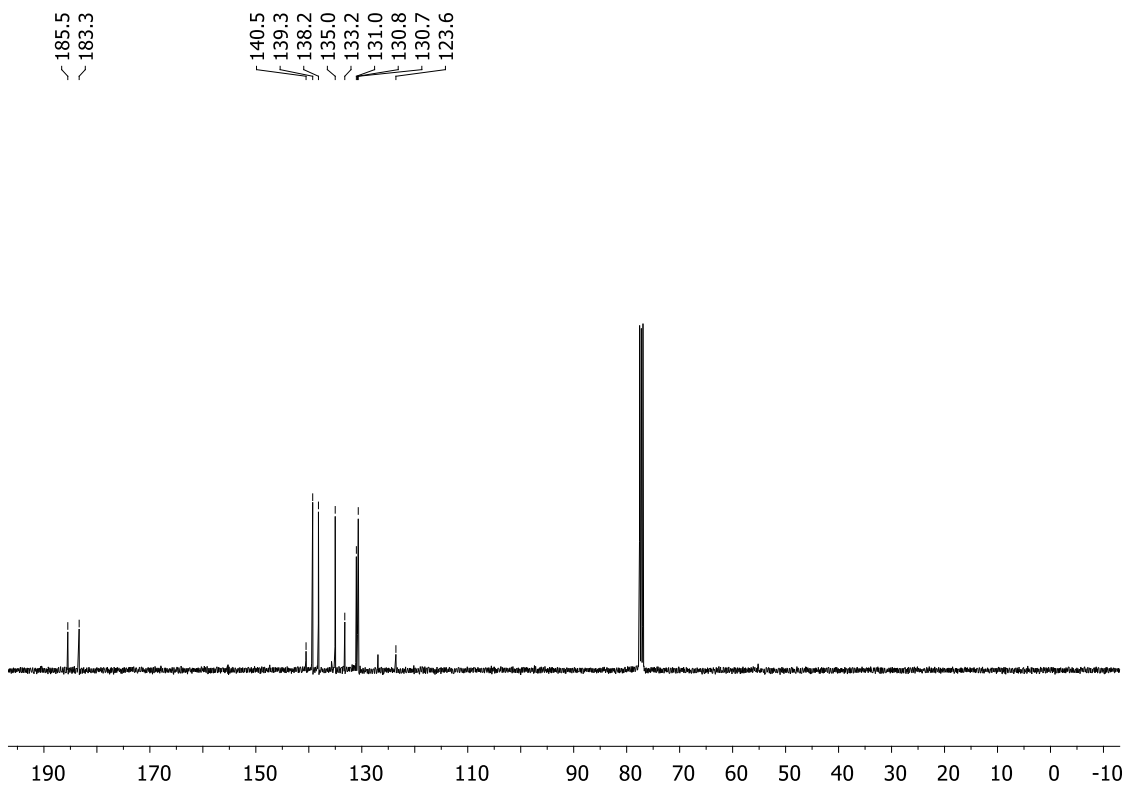


Figure 131. ^{13}C NMR spectrum (100 MHz, $CDCl_3$) of compound **149**.

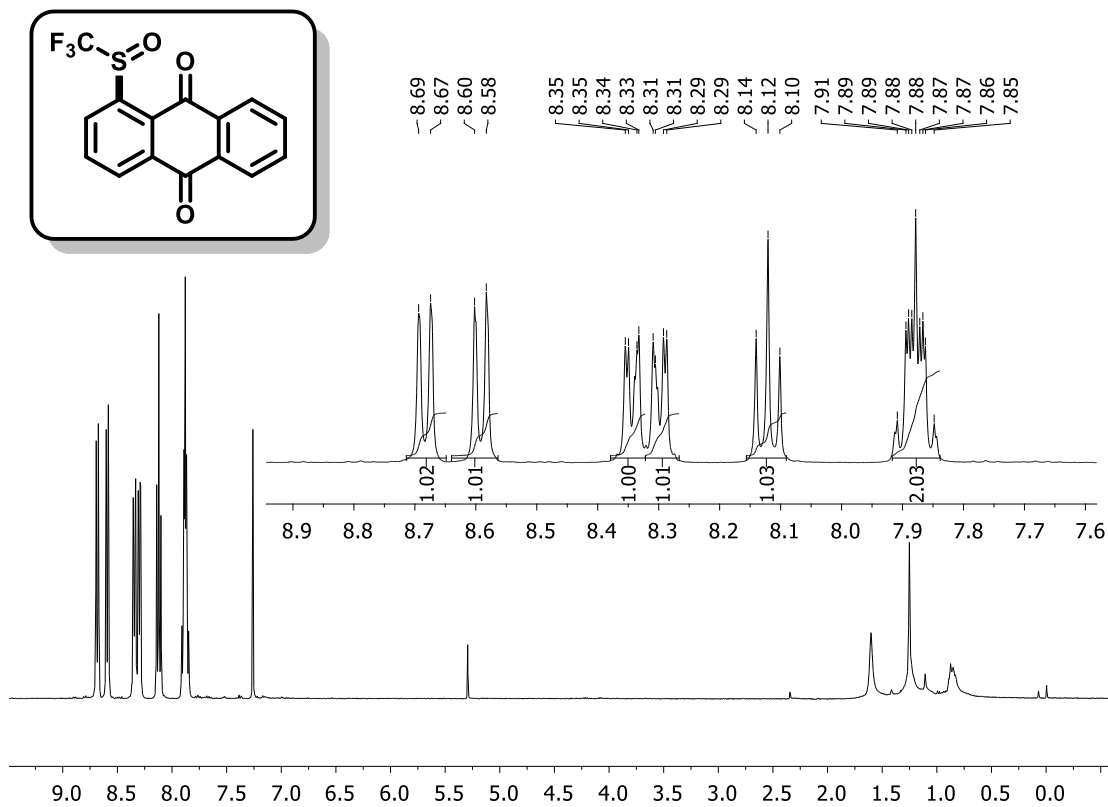


Figure 132. ¹H NMR spectrum (400 MHz, CDCl₃) of compound 150.

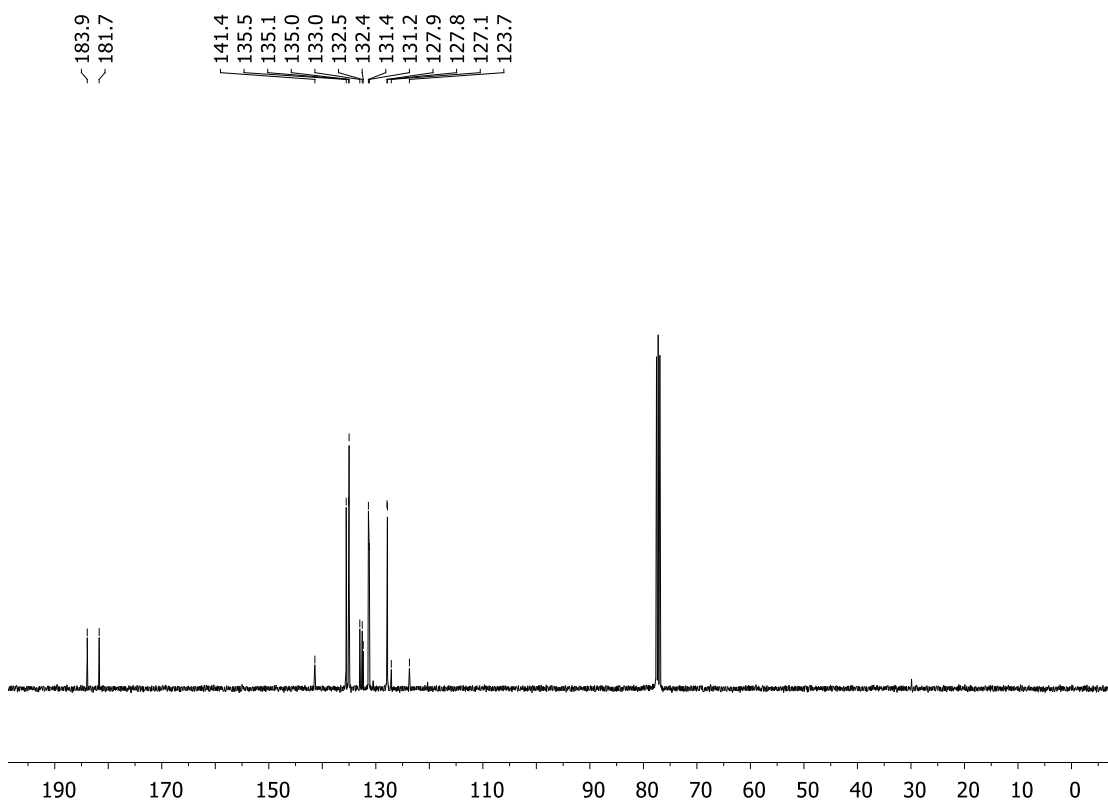


Figure 133. ¹³C NMR spectrum (100 MHz, CDCl₃) of compound 150.

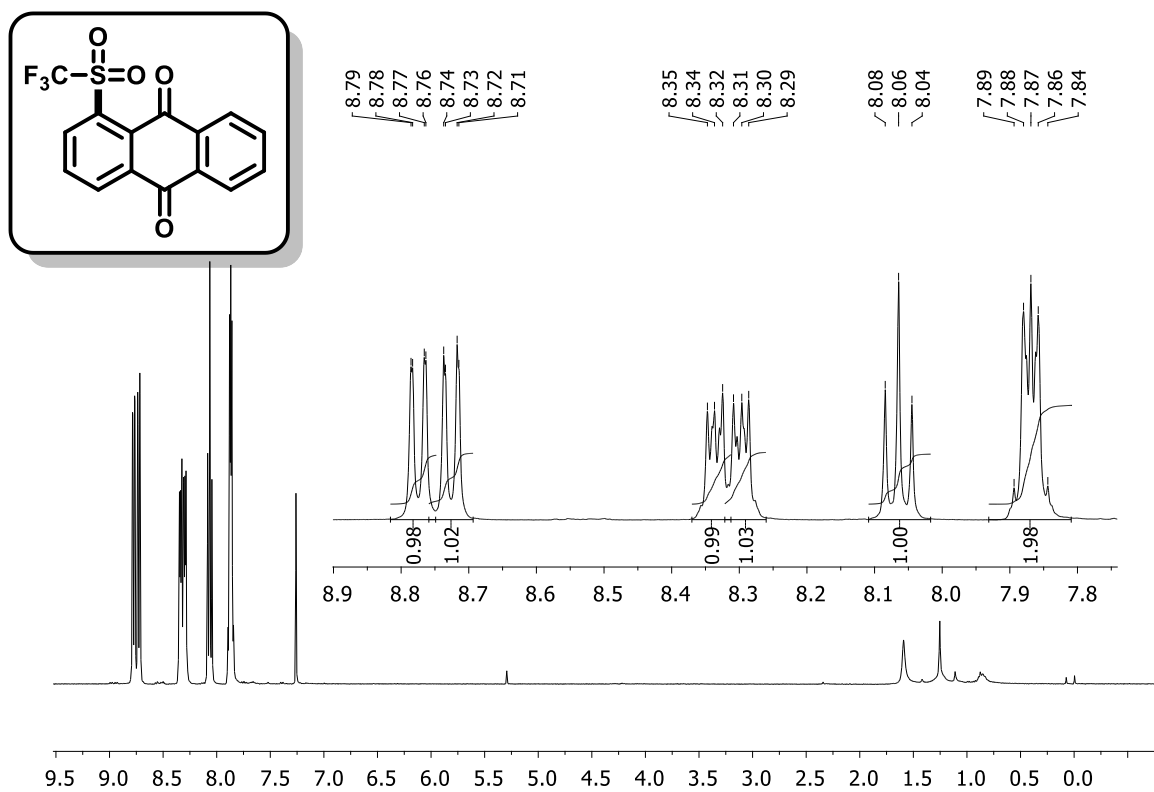


Figure 134. ¹H NMR spectrum (400 MHz, CDCl₃) of compound 151.

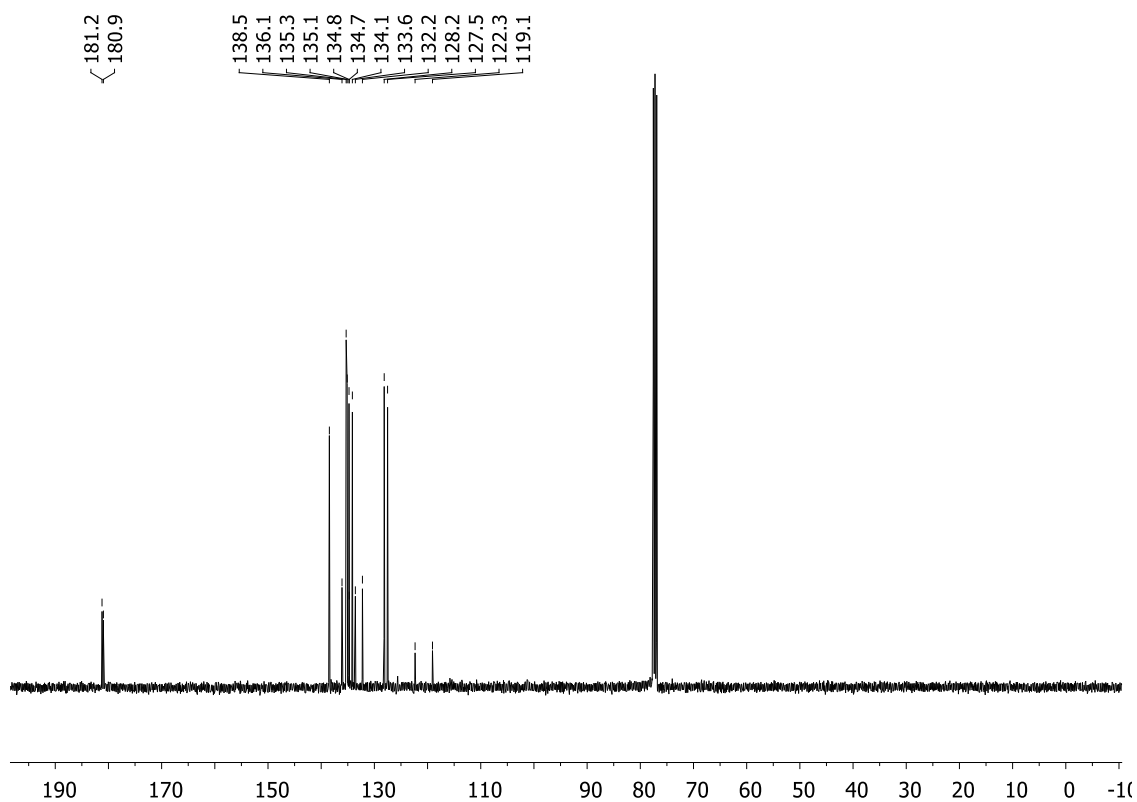


Figure 135. ¹³C NMR spectrum (100 MHz, CDCl₃) of compound 151.

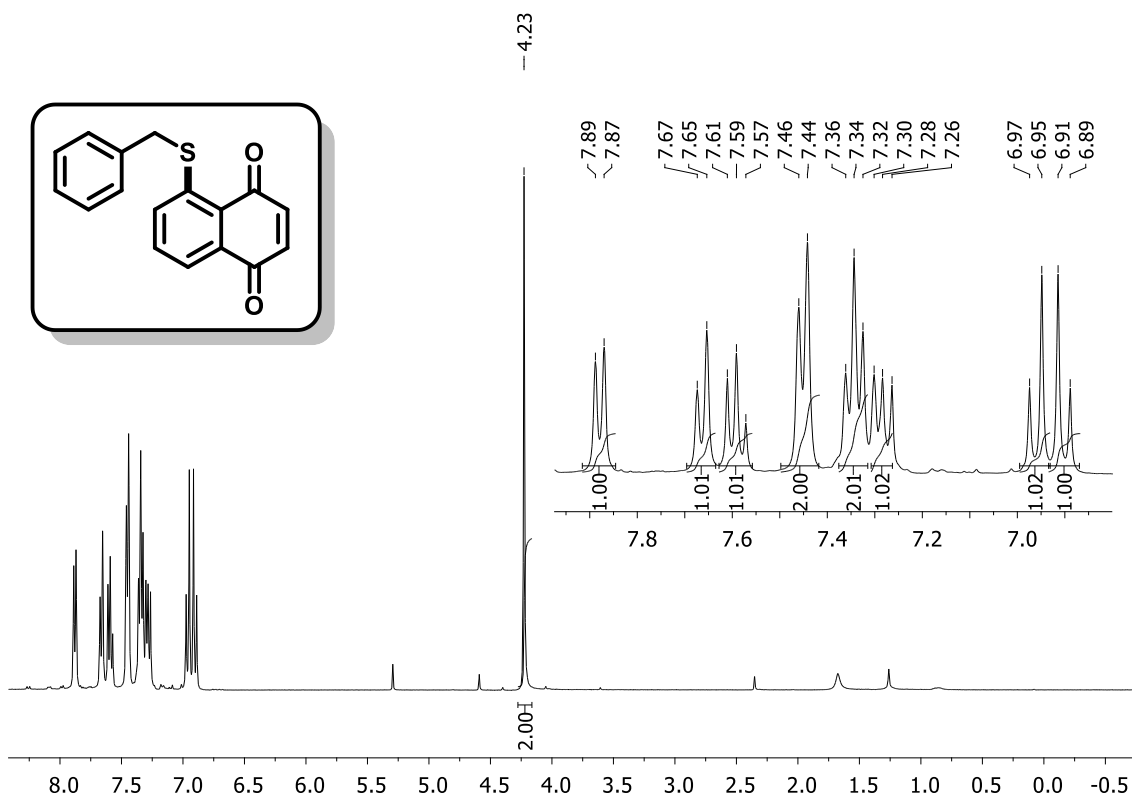


Figure 136. ¹H NMR spectrum (400 MHz, CDCl₃) of compound **152**.

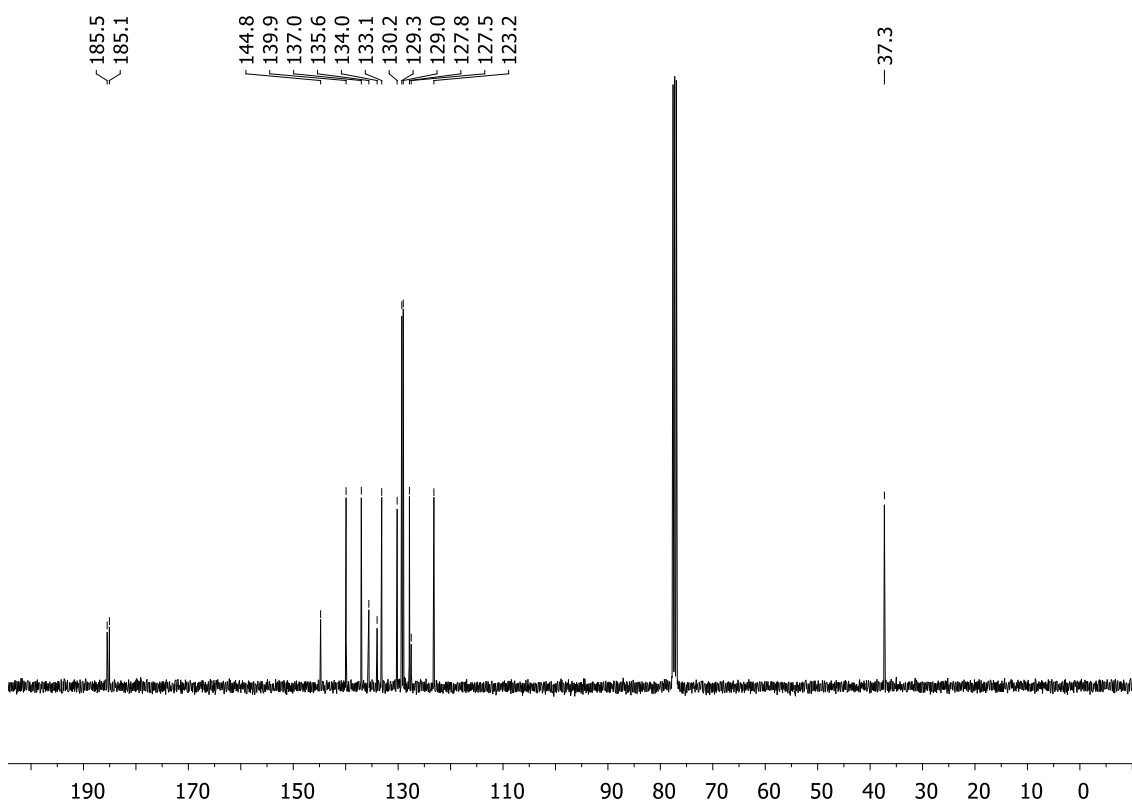


Figure 137. ¹³C NMR spectrum (100 MHz, CDCl₃) of compound **152**.

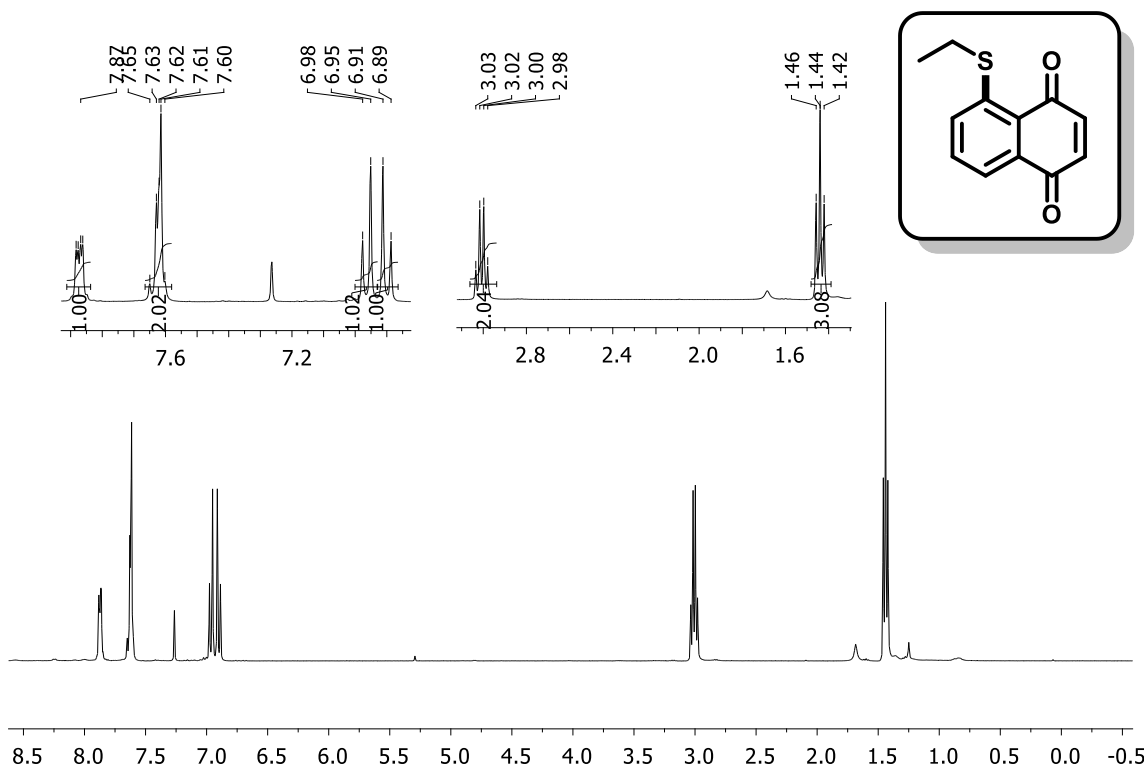


Figure 138. ¹H NMR spectrum (400 MHz, CDCl₃) of compound **153**.

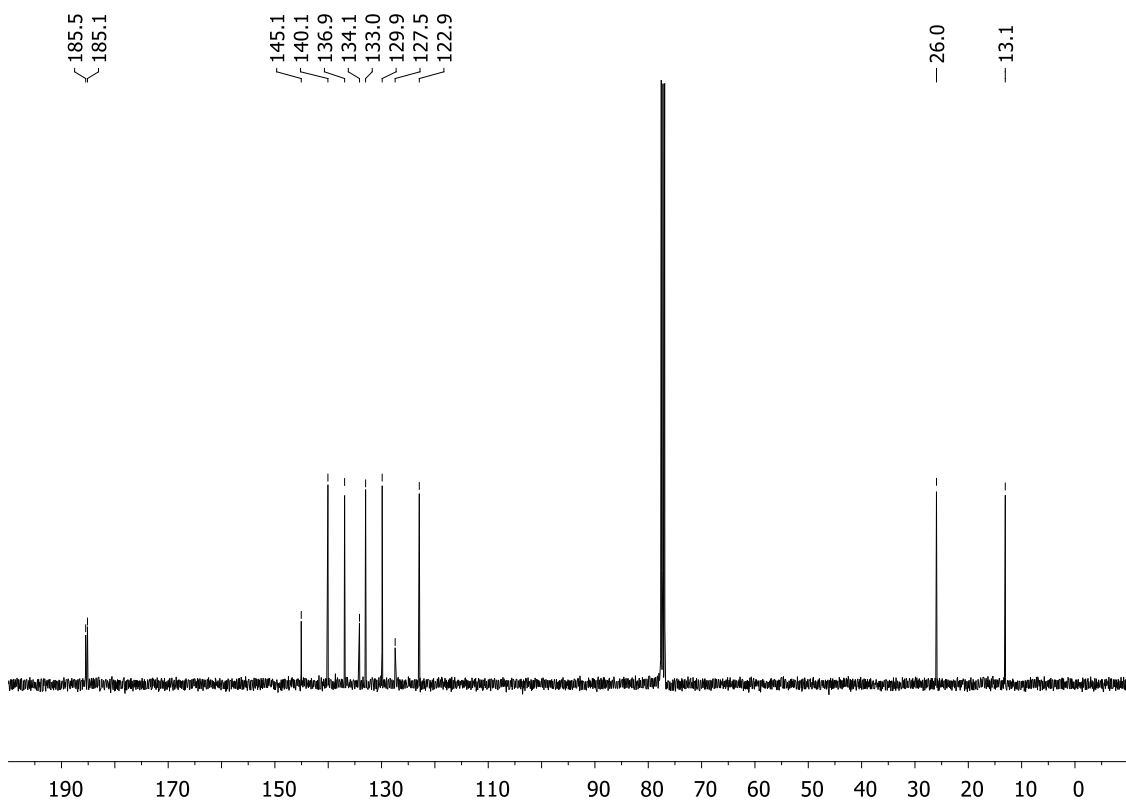


Figure 139. ¹³C NMR spectrum (100 MHz, CDCl₃) of compound **153**.

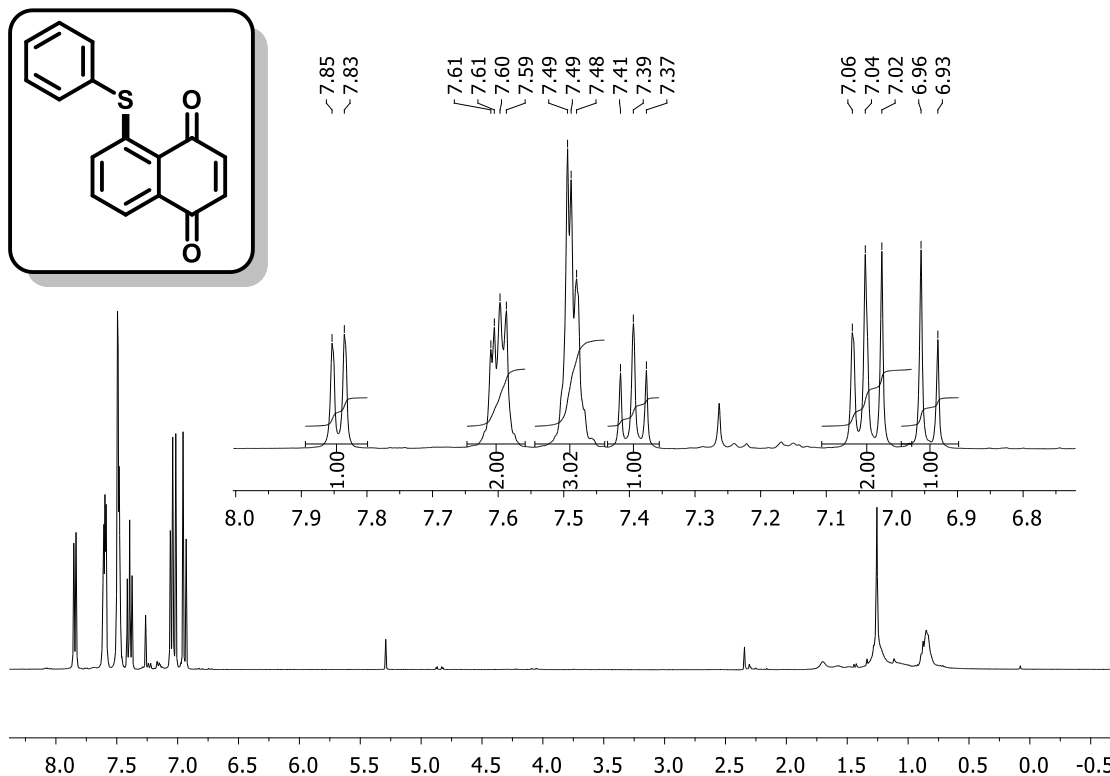


Figure 140. ¹H NMR spectrum (400 MHz, CDCl₃) of compound **154**.

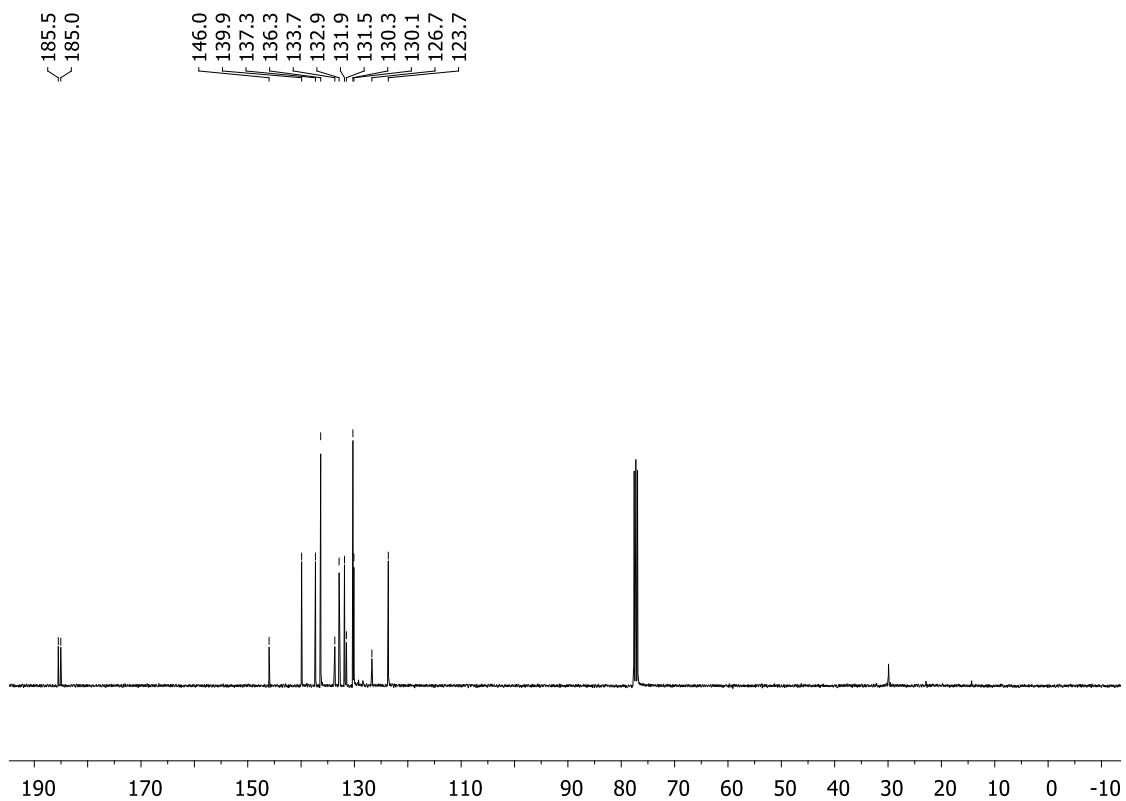


Figure 141. ¹³C NMR spectrum (100 MHz, CDCl₃) of compound **154**.

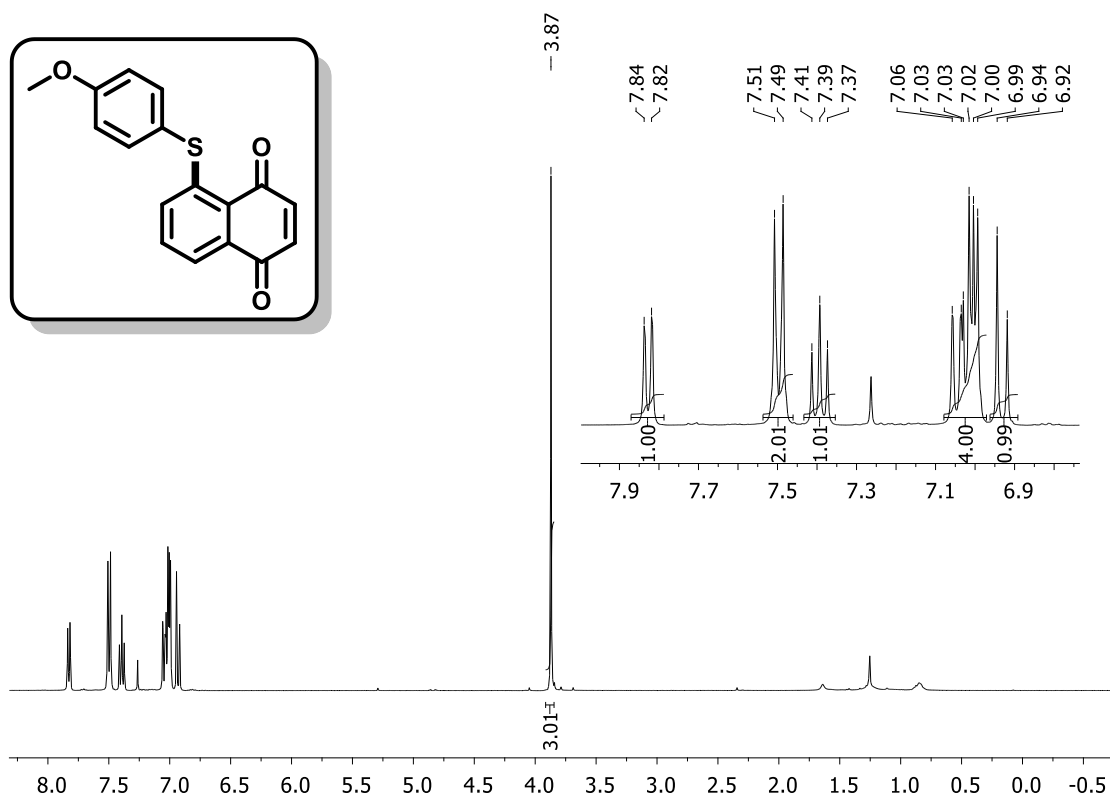


Figure 142. ¹H NMR spectrum (400 MHz, CDCl₃) of compound 155.

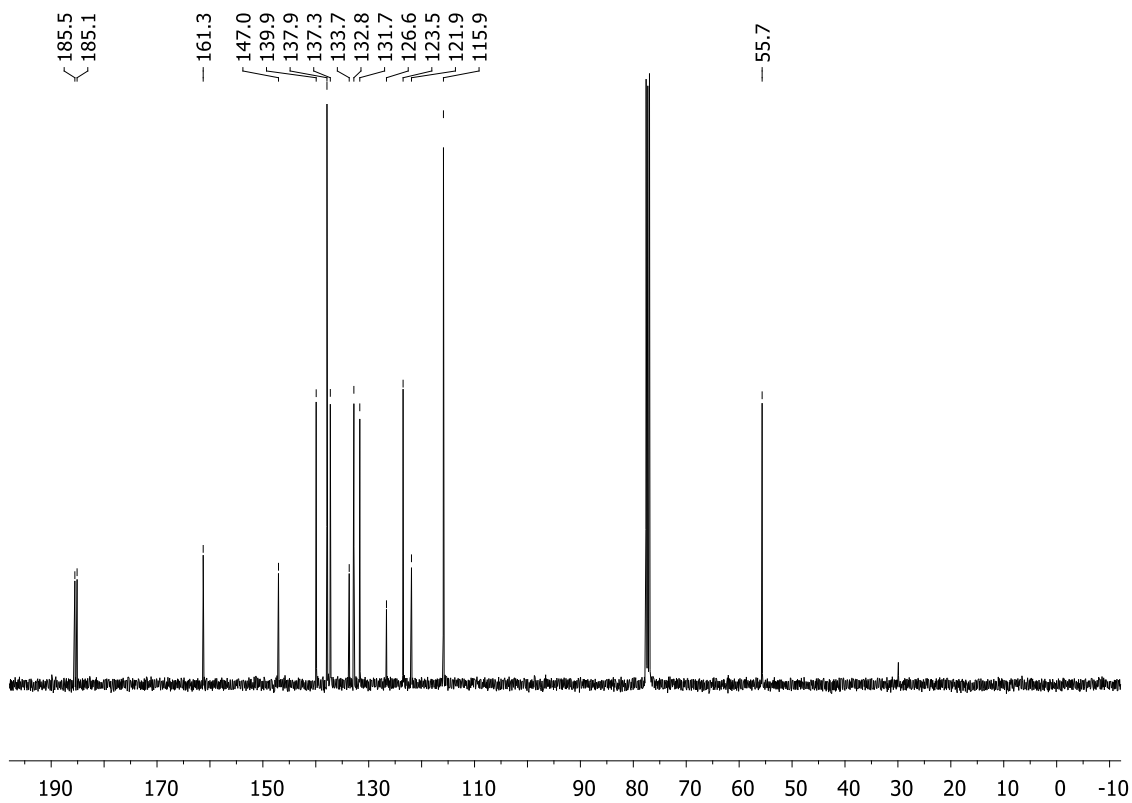


Figure 143. ¹³C NMR spectrum (100 MHz, CDCl₃) of compound 155.

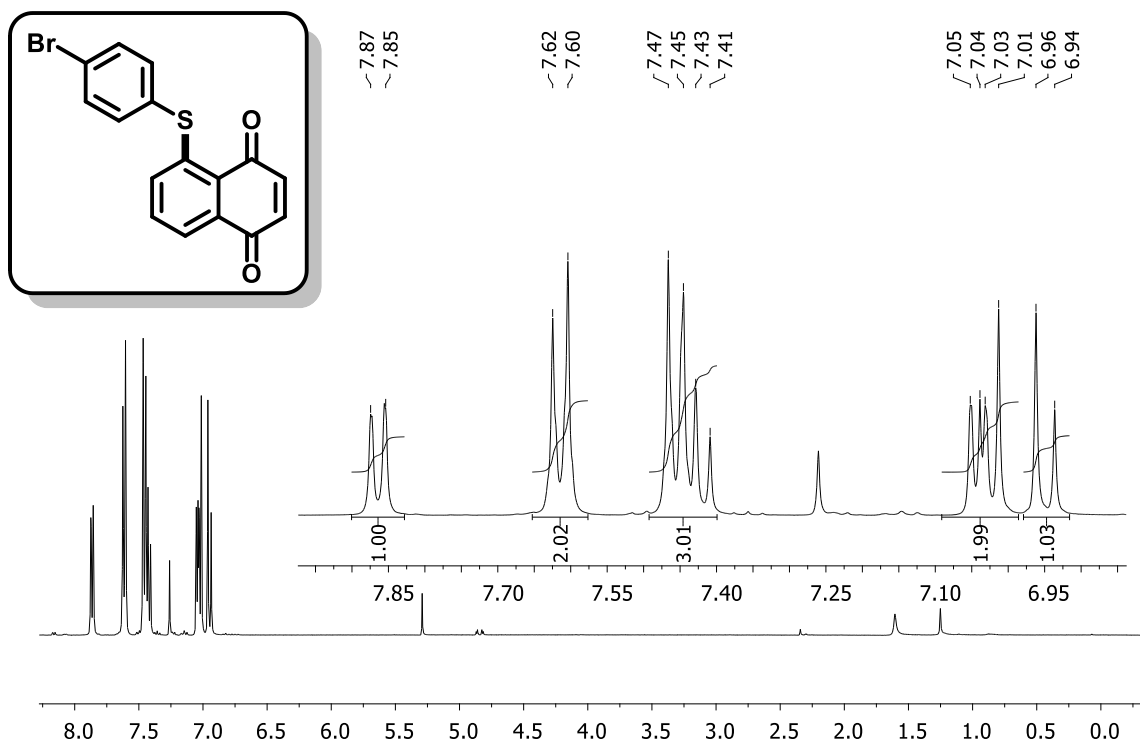


Figure 144. ¹H NMR spectrum (400 MHz, CDCl₃) of compound 156.

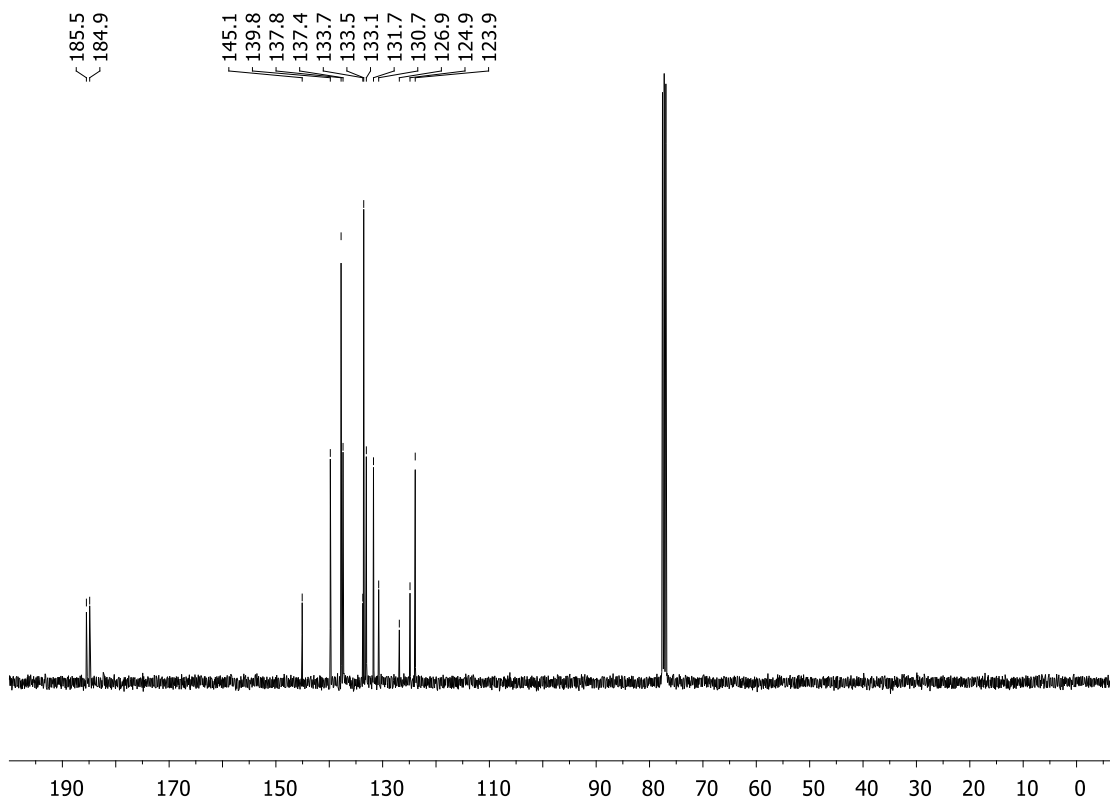


Figure 145. ¹³C NMR spectrum (100 MHz, CDCl₃) of compound 156.

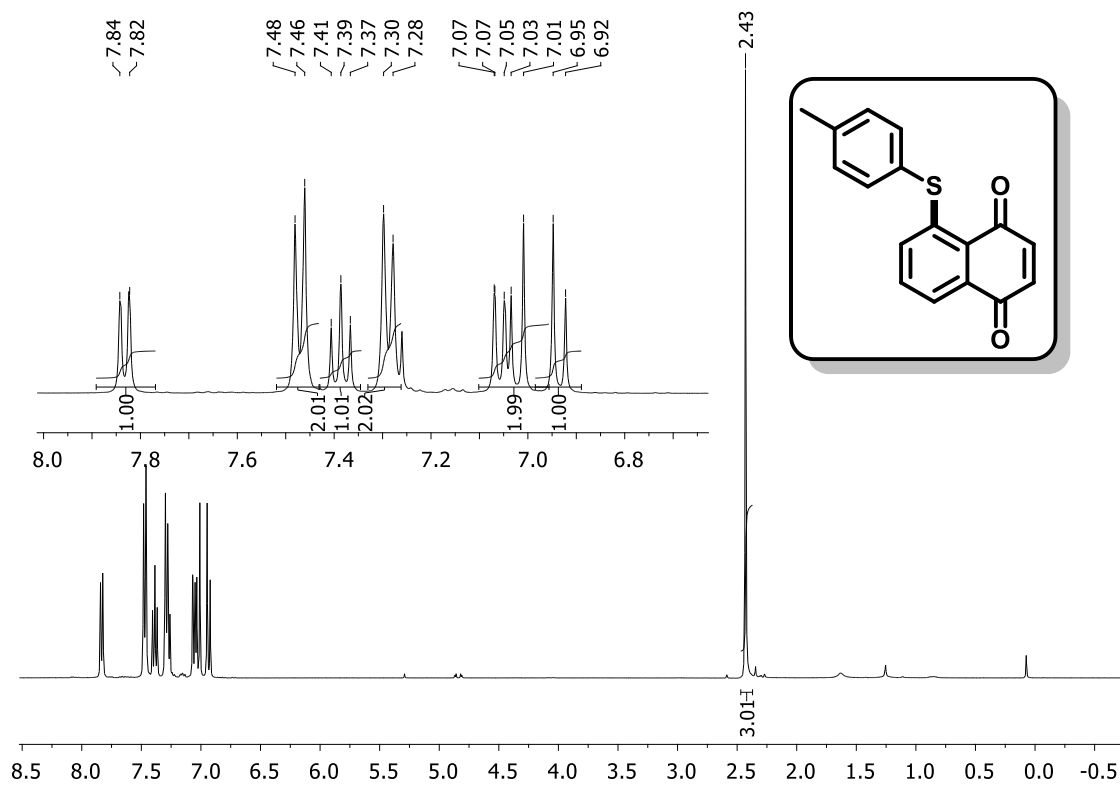


Figure 146. ¹H NMR spectrum (400 MHz, CDCl₃) of compound 157.

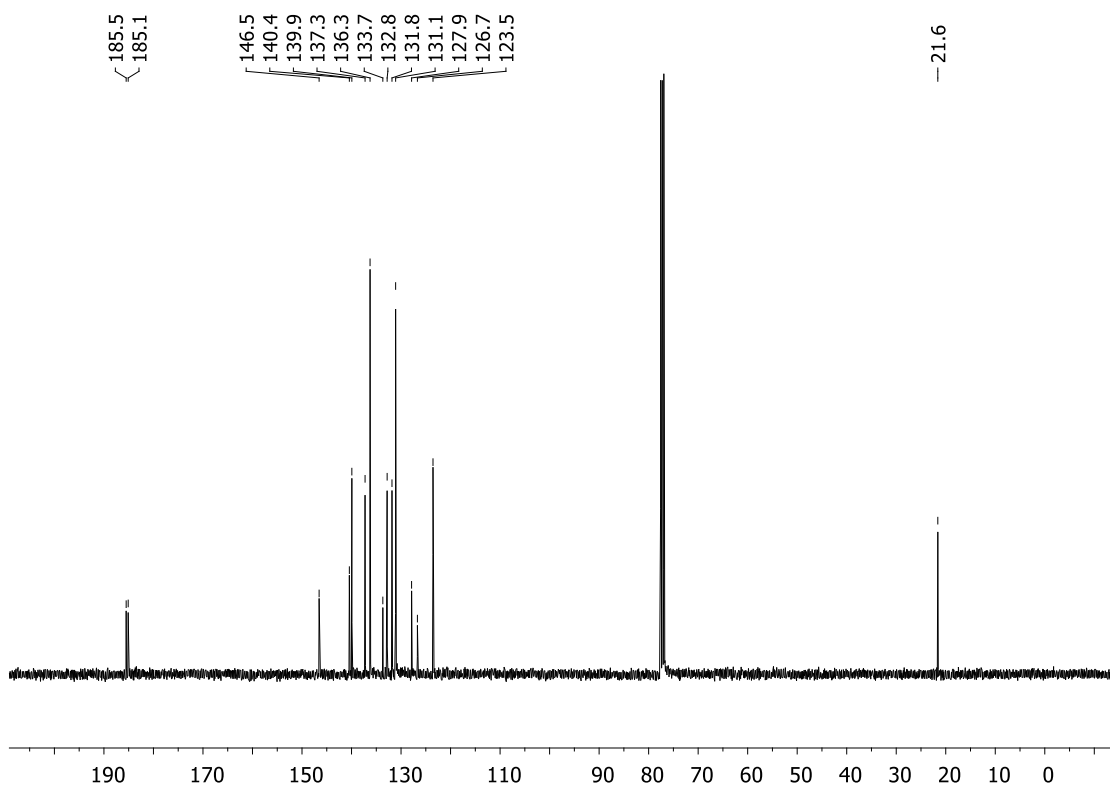


Figure 147. ¹³C NMR spectrum (100 MHz, CDCl₃) of compound 157.

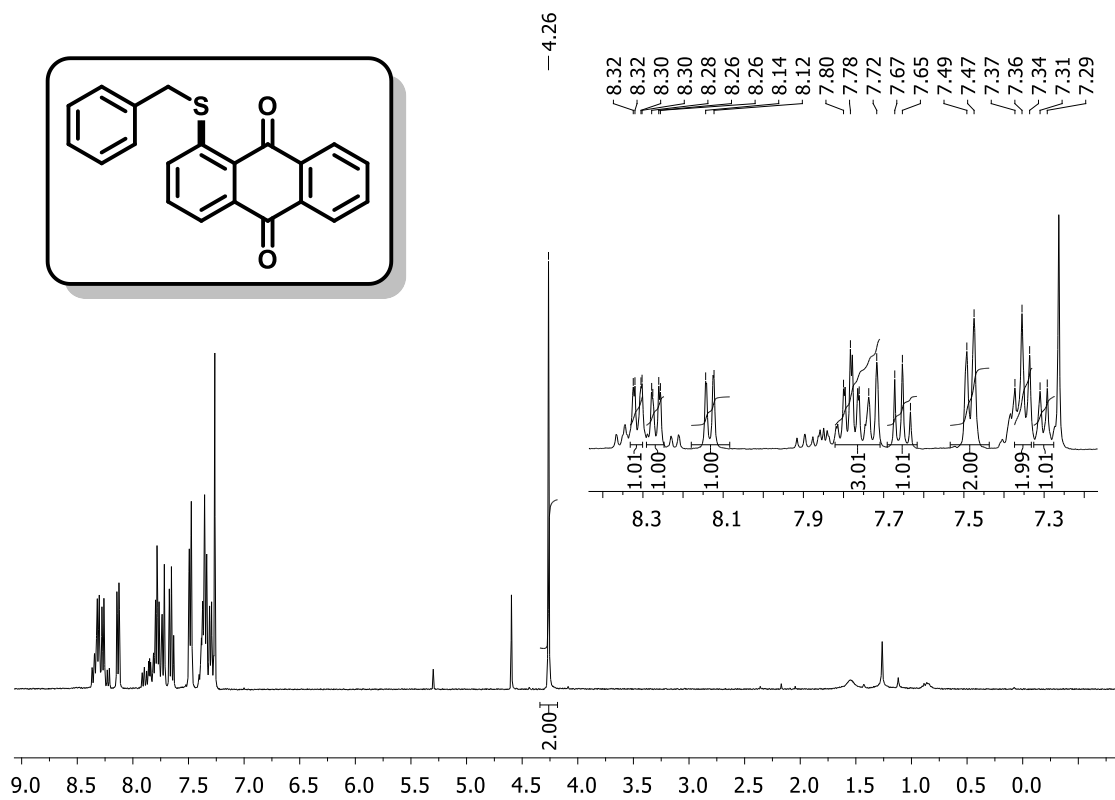


Figure 148. ¹H NMR spectrum (400 MHz, CDCl₃) of compound **158**.

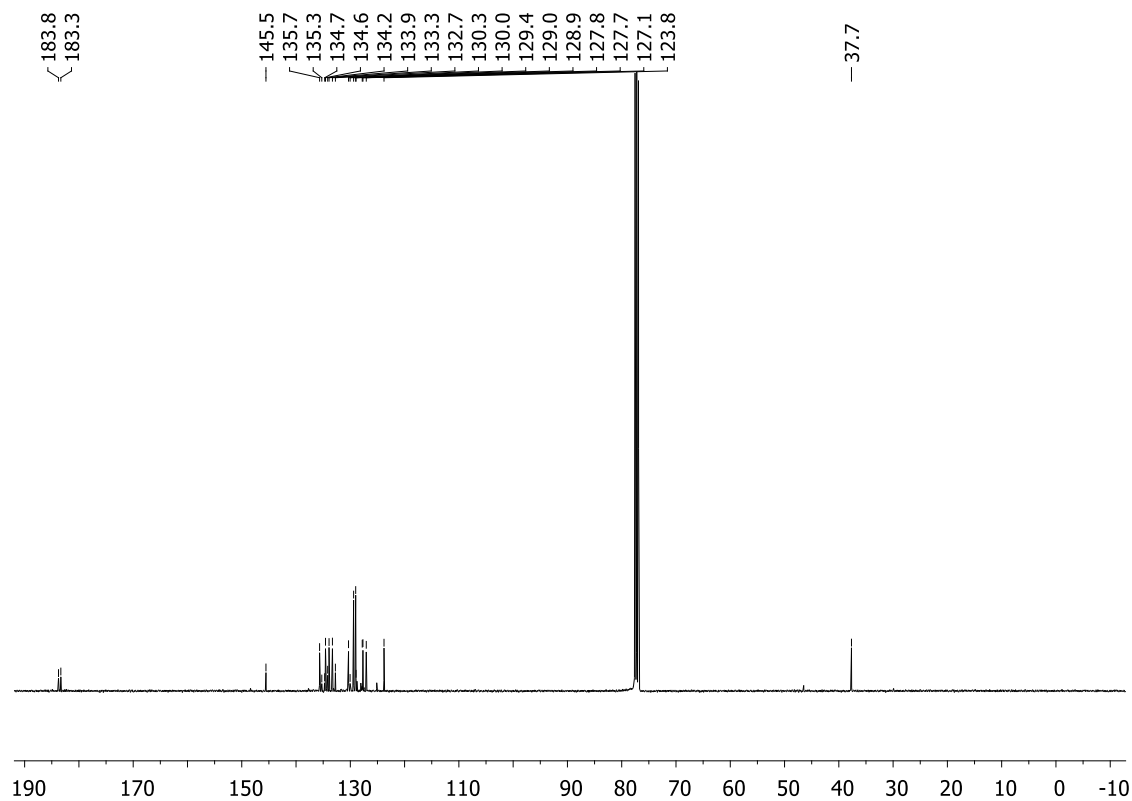


Figure 149. ¹³C NMR spectrum (100 MHz, CDCl₃) of compound **158**.

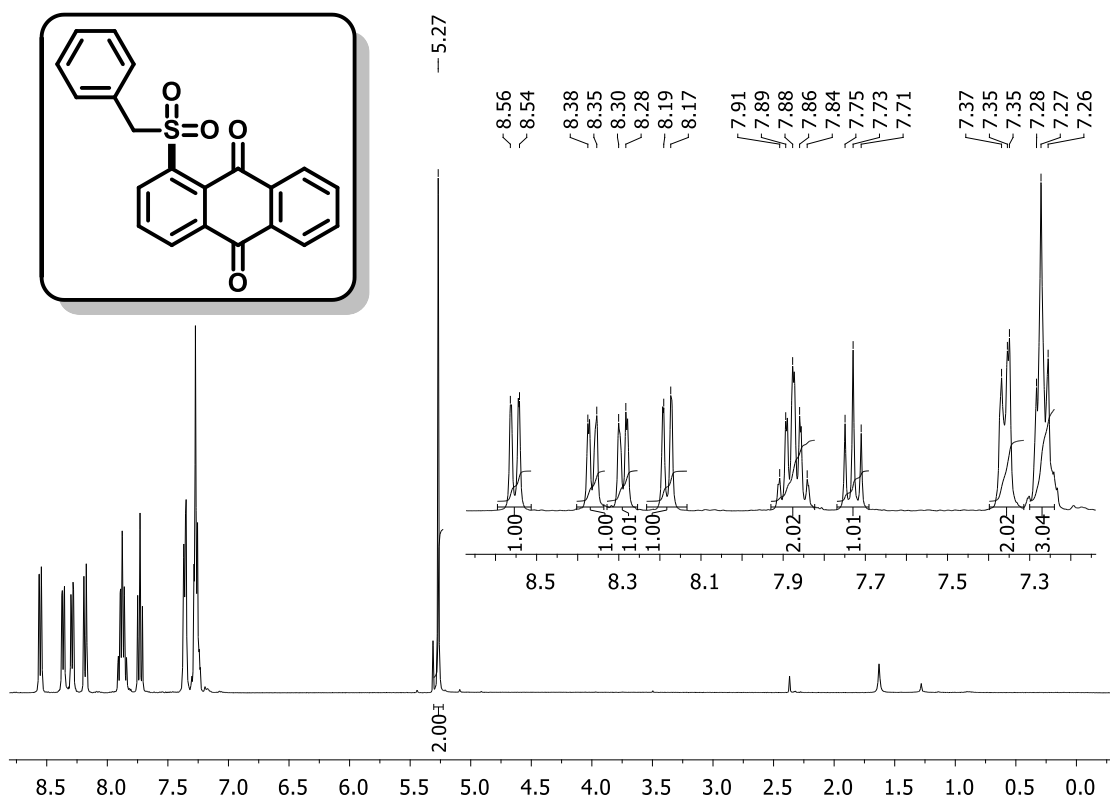


Figure 150. ¹H NMR spectrum (400 MHz, CDCl₃) of compound 159.

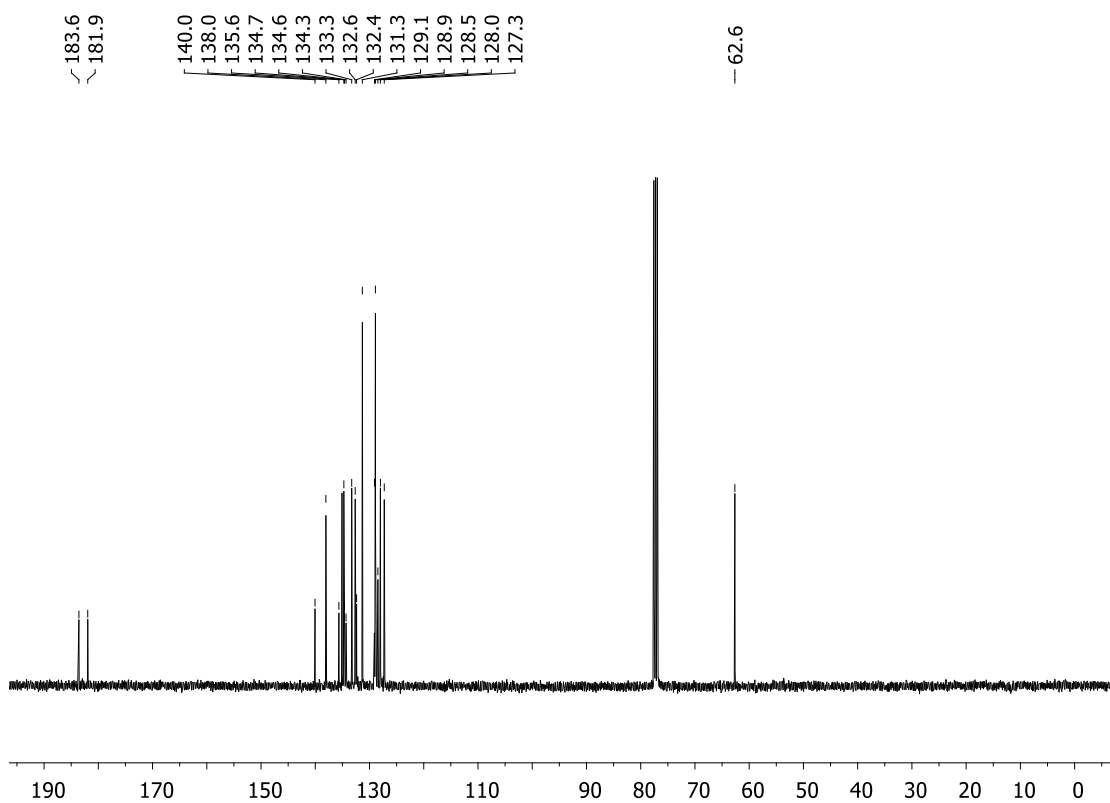


Figure 151. ¹³C NMR spectrum (100 MHz, CDCl₃) of compound 159.